The neurobiological effects of ocean acidification on a cephalopod

Thesis submitted by

Jodi Thea Thomas

(Bachelor of Science with Honours, University of Otago)

Thesis submitted for the degree of

Doctor of Philosophy

ARC Centre of Excellence for Coral Reef Studies
James Cook University

April 2022

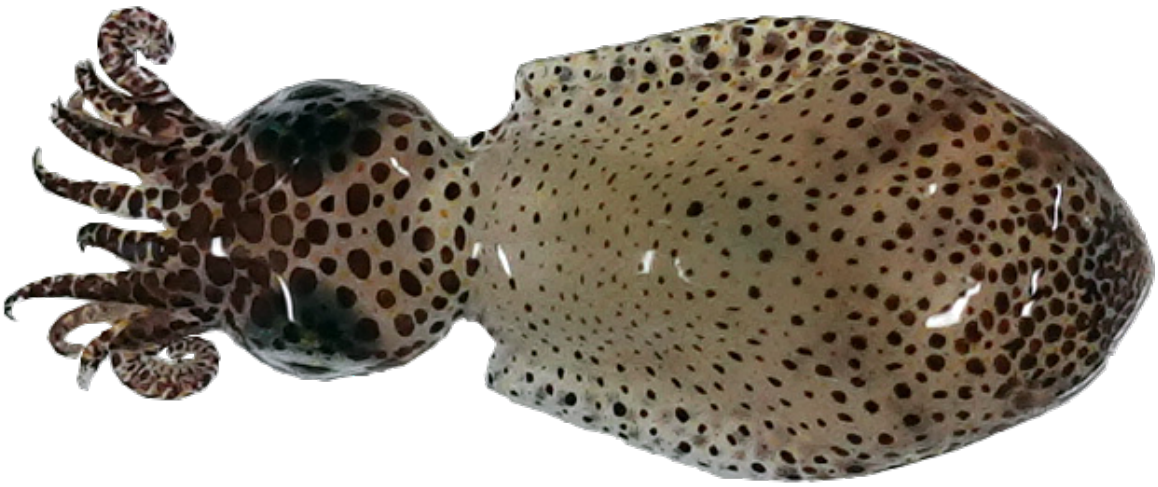

Two-toned pygmy squid *Idiosepius pygmaeus*. Photograph by Jodi Thomas.

Acknowledgments

Thank you to my supervisors, Phil Munday and Sue-Ann Watson. I am so grateful for the opportunities this PhD has provided, and for the freedom you have both given me to work independently and take this PhD in the directions I wanted. Thank you for your continual support and enthusiasm for my research.

A massive thank you to the technical staff at the Marine and Aquaculture Research Facilities Unit at James Cook University; Ben Lawes, Simon Wever and Andrew Thompson. Your work to keep the tank facilities running smoothly, and your constant advice, support, and chats made my experimental work possible. Thank you to my amazing volunteers, Annam Raza and Natalie Swinhoe, for your help with animal collection and bag filter cleaning. You were both an absolute pleasure to work with, and I am incredibly grateful for your time. Mike Jarrold, thank you for being my go-to person for all tank facilities/experimental work questions. Thank you to Blake Spady for your collaboration with my experimental work, it was greatly appreciated and made it possible to finish those experiments with the sample sizes needed. Thank you to the Breakwater Marina, Townsville for permission to collect animals within their premises.

I am so grateful for the opportunity to be a (virtual) visiting research student in the Marine Climate Change Unit (MCCU) at Okinawa Institute of Science and Technology Graduate University, Japan. Tim Ravasi, thank you so much for your collaboration and generous support, both finiancially and scientifically. Thank you to all the lab members for being so welcoming, I feel privileged to be included as a member of the MCCU. Thank you to Yoko Shintani for your amazing organisation and administration. In particular, I am incredibly grateful for the tuition and mentorship I have received from Roger Huerlimann. Thank you for generously sharing so much of your knowledge, time and enthusiasm with me.

Thank you to Celia Schunter for your collaboration. Your advice throughout my molecular research has undoubtedly improved the quality of my work. Jenni Donelson, I am so incredibly grateful for your support, both scientifically and personally, throughout my PhD. Your celebration of my succeses and inclusion in your lab group has been so important to me.

To my flatmates (and honorary flatmates) in Townsville, thank you for your amazing friendship. To my partner, Nathan Connell, thank you for all of your support; from moving

across the ditch with me, to being my assistant squid collector and keeping my spirits high through the difficult times. And lastly to my whānau, thank you for your lifelong support and ongoing interest and enthusiasm in my research.

I would like to acknowledge and pay my respects to the Traditional Owners of the land and waters where my research has been carried out; the Bindal and Wulgurukaba People of Thul Garrie Waja and Gurrumbilbarra Country (Townsville) where my research was conducted, and the Barada Barna People where a large portion of my writing was done.

Statement of the Contribution of Others

Throughout my PhD, I was supported by an Australian Government Research Training Program Scholarship (Prestige Research Training Program Stipend) and a Commonwealth Supported by Research Training Program Fee Offset.

Chapter 1: Prepared as thesis chapter only. General Introduction.
Contributions: I wrote the first draft of the chapter. Philip Munday and Sue-Ann Watson provided constructive review and editorial comments.

Chapter 2: **Thomas, J.T.**, Munday, P.L. and Watson, S.-A. (2020). Toward a mechanistic understanding of marine invertebrate behaviour at elevated CO_2. *Frontiers in Marine Science*. **7**, 345. URL https://doi.org/10.3389/fmars.2020.00345
Contributions: I reviewed the literature, synthesised current knowledge and wrote the first draft of the manuscript. Philip Munday and Sue-Ann Watson provided constructive review and editorial comments. Funding for this project was provided by the Australian Research Council Centre of Excellence for Coral Reef Studies (to Philip Munday, Sue-Ann Watson, myself).

Chapter 3: **Thomas, J.T.**, Spady, B.L., Munday, P.L. and Watson, S.-A. (2021). The role of ligand-gated chloride channels in behavioural alterations at elevated CO_2 in a cephalopod. *Journal of Experimental Biology*. **224**, jeb242335. URL https://doi.org/10.1242/jeb.242335
Contributions: Philip Munday, Sue-Ann Watson and I contributed to the original conception and design of the project. Philip Munday and Sue-Ann Watson provided supervision throughout the project. I carried out project administration and management. Blake Spady and I collected animals from the field, with assistance from Annam Raza. I carried out maintenance of the sewater systems, with assistance from Natalie Swinhoe and technical support from Ben Lawes, Simon Wever and Andrew Thompson. Blake Spady and I performed carbonate chemistry measurements, with assistance from Michael Jarrold. I undertook animal husbandry and performed the experiments. I carried out all data curation, data analysis, sta-

tistical analysis, and data visualisation. I interpreted the results and wrote the first draft of the manuscript. Blake Spady, Philip Munday and Sue-Ann Watson provided constructive review and editorial comments. Funding for this project was provided by the Australian Research Council Centre of Excellence for Coral Reef Studies (to Philip Munday, Sue-Ann Watson) and an Australian Government Research Training Program Scholarship (to myself). James Cook University provided laboratory space and funding for technicians at the Marine and Aquaculture Research Facilities Unit.

Chapter 4: **Thomas, J.T.**, Huerlimann R., Schunter C., Watson, S.-A., Munday, P.L. and Ravasi T. (in preparation). Neurobiological mechanisms underlying effects of elevated CO_2 in a cephalopod.

Contributions: Philip Munday, Sue-Ann Watson, Timothy Ravasi, Celia Schunter and I contributed to the original conception and design of the project. Philip Munday, Sue-Ann Watson and Timothy Ravasi provided supervision, and Roger Huerlimann provided mentorship, throughout the project. Yoko Shintani and I carried out project administration and management. I dissected all squid and extracted RNA from all samples, with laboratory support from Carolyn Smith-Keune and Paul O'Brien. I carried out bioinformatic analyses with tuition, support and advice from Roger Huerlimann, and advice from Celia Schunter. Bioinformatic analyses were carried out on the high-performance computing cluster at Okinawa Institute of Science and Technology (OIST), Japan, with technical support provided by the Scientific Computing and Data Analysis section of Research Support Division at OIST. I carried out statistical analyses with advice from Roger Huerlimann and Celia Schunter. I created all data visualisation and carried out data curation. I interpreted the results and wrote the first draft of the manuscript. All co-authors provided constructive review and editorial comments. Funding for this project was provided by the Okinawa Institute of Science and Technology Graduate University (to Timothy Ravasi, Roger Huerlimann, myself), the Australian Research Council Centre of Excellence for Coral Reef Studies (to Philip Munday, Sue-Ann Watson), an Australian Government Research Training Program Scholarship (to myself), and The Company of Biologists Limited Travelling Fellowship (to myself, not used due to COVID19 travel restrictions). Additional resources were provided by Celia Schunter (access to OmicsBox subscription).

Chapter 5: Prepared as thesis chapter only. Correlated transcriptomic and behavioural responses: Identifying mechanisms underpinning behavioural responses to elevated CO_2 in a cephalopod.

Contributions: Philip Munday, Sue-Ann Watson and I contributed to the original conception and design of the project. Philip Munday and Sue-Ann Watson provided supervision

throughout the project. I carried out project administration and management. I undertook statistical analyses with advice from Philip Munday and Sue-Ann Watson. Some of the statistical analyses were carried out on the high-performance computing cluster at OIST, Japan. I created all data visualisation and carried out data curation. I interpreted the results and wrote the first draft of the manuscript. Philip Munday and Sue-Ann Watson provided constructive review and editorial comments. Funding for this project was provided by the Okinawa Institute of Science and Technology Graduate University (to myself), the Australian Research Council Centre of Excellence for Coral Reef Studies (to Philip Munday, Sue-Ann Watson), and an Australian Government Research Training Program Scholarship (to myself).

Chapter 6: Prepared as thesis chapter only. General Discussion.
Contributions: I wrote the first draft of the chapter. Philip Munday and Sue-Ann Watson provided constructive review and editorial comments.

General Abstract

The uptake of anthropogenic carbon dioxide (CO_2) by the ocean is causing seawater CO_2 levels to rise, changing ocean chemistry in a process known as ocean acidification (OA). OA can affect a variety of physiological processes, life history traits and behaviours of fish and marine invertebrates. As invertebrates comprise the vast majority of marine diversity, are essential for key ecosystem processes and support human livelihoods, OA-induced effects of marine invertebrates could have far-reaching ecological, social and economic consequences. The nervous system forms the fundamental link between the environment and an organism's physiology and behaviour, likely coordinating responses to OA. However, the nervous system's role in biological responses to elevated CO_2 has been little explored, especially for marine invertebrates. Research to date has focused on the mechanistic underpinnings of OA-induced behavioural alterations in fish. In marine invertebrates, the neurobiological impacts of OA remain poorly understood, and may differ to those in fishes. This thesis investigates the neurobiological impacts of, and the mechanistic neurobiological underpinnings of biological responses to, OA in a marine invertebrate with a complex nervous system, a cephalopod mollusc.

In Chapter 2, I review the potential mechanisms underlying OA-induced behavioural alterations in marine invertebrates. I highlight that OA likely induces behavioural alterations through a range of neurobiological mechanisms, including disrupted sensation, an altered context within which information is processed, and disturbed $GABA_A$ receptor functioning, all of which need further experimental testing. I propose potential novel mechanisms, including disrupted functioning of ligand-gated chloride channels, which are similar to the $GABA_A$ receptor, and which invertebrates possess a larger variety of compared to fish. Non-targeted approaches, including omics technologies, are highlighted as an important next step to test existing hypotheses, and potentially develop novel hypotheses for the mechanistic underpinnings of OA-induced behavioural alterations.

Disrupted functioning of $GABA_A$ receptors is the prominent mechanistic explanation for OA-induced behavioral alterations in fish. The GABA hypothesis may also apply to marine molluscs, however evidence to date relies exclusively on one pharmacological agent. In Chapter 3, I used both a specific (gabazine) and non-specific (picrotoxin) $GABA_A$ receptor

antagonist to test the role of GABA-, and other (glutamate-, acetylcholine- and dopamine-) gated chloride channels in behavioural alterations at elevated CO_2 in the two-toned pygmy squid, *Idiosepius pygmaeus*. Elevated CO_2 altered a range of conspecific-directed behaviours and activity, and both antagonists had different behavioral effects at elevated, compared to current-day, CO_2 conditions. The results provide robust support for the GABA hypothesis within a cephalopod, and the first pharmacological evidence for OA-induced disruption of ligand-gated chloride channels other than the $GABA_A$ receptor, underlying behavioural alterations in any marine animal.

In Chapter 4, I evaluated the transcriptomic response of the central nervous system (CNS) and eyes of *I. pygmaeus* to elevated CO_2. As a reference for gene expression quantification, I created a *de novo* transcriptome assembly from long read PacBio ISO-sequencing data. The squid CNS and eyes both responded to elevated CO_2 with gene expression changes in three main areas; neurotransmission, immune function, and oxidative stress. Widespread changes in neurotransmission, including genes involved in GABAergic, glutamatergic, cholinergic, and monoaminergic neurotransmission, provide further support for multiple mechanisms underpinning OA-induced behavioural alterations. From these results, I propose a novel mechanistic model explaining how neurotransmission, immune function and oxidative stress could interact in the nervous system to drive behavioural and physiological responses to OA in marine invertebrates.

In Chapter 5, I use a novel approach to assess the potential mechanisms underlying behavioral changes at elevated CO_2 in *I. pygmaeus* by directly correlating the transcriptomic response of the CNS and eyes with behavioural changes at elevated CO_2 in the same individuals. First, I used a network approach to cluster transcriptome-wide gene expression for the CNS and eyes (separately). The gene expression profile of each gene cluster was then correlated with CO_2 treatment levels (current-day or elevated) and OA-affected, visually-mediated behaviours in the same individuals, using Canonical Correlation Analysis. Altered neurogenesis in both the CNS and eyes was identified as a potential key driver of OA-induced behavioural changes. From the results, I propose a mechanism by which disrupted visual detection and visual output from the eyes, in combination with disrupted neurogenesis and neurotransmission (including GABAergic signaling) in the CNS, may drive altered behavioural responses at elevated CO_2 in *I. pygmaeus*, and possibly other marine invertebrates.

Overall, this thesis highlights that OA likely induces a suite of changes in both the peripheral and central nervous systems of marine invertebrates, with a complex assortment of mechanisms underpinning OA-induced responses. This complexity could explain the variability in OA-induced biological responses, with different mechanisms potentially being predominant in different taxa and resulting in different behavioural responses. Experimental work assessing the novel mechanisms proposed in my thesis will be a potentially important direction

for future research to gain a more thorough understanding of the mechanistic complexities of OA-induced biological responses. A mechanistic neurobiological understanding will help develop cause-effect relationships to identify which animals will be most vulnerable to rising CO_2 levels in the ocean, and how this may affect marine diversity and ecosystem function.

Contents

Acknowledgments iii

Statement of the Contribution of Others v

General Abstract ix

Contents xiii

List of Tables xvii

List of Figures xix

1 General Introduction 1

1.1 The nervous system and environmental change 2

1.2 Ocean acidification and its effects on marine invertebrates 2

1.3 The mechanistic neurobiological underpinnings of biological responses to ocean acidification 3

1.4 Thesis aims and outline 7

2 Toward a mechanistic understanding of marine invertebrate behaviour at elevated CO_2 11

2.1 Abstract 12

2.2 Introduction 13

2.3 Mechanisms for elevated CO_2-induced behavioural changes 17

2.3.1 Altered sensory stimuli at elevated CO_2 17

2.3.2 Physical changes of sensory organs 19

2.3.3 Altered behavioural choices 20

2.3.4 Altered functioning of the $GABA_A$ receptor 21

2.4 The GABA hypothesis in marine invertebrates 21

2.4.1 $GABA_A$-like receptor subtypes and variability in elevated CO_2-induced behavioural alterations . . . 27
2.4.2 Pharmacological considerations . . . 28
2.4.3 Marine invertebrate acid-base regulatory mechanisms and the GABA hypothesis . . . 29
2.4.4 The effects of altered $GABA_A$-like receptor functioning . . . 30
2.5 Alternative mechanisms for behavioural change at elevated CO_2 . . . 32
2.6 Directions for future research . . . 34
2.7 Conclusion . . . 36

3 The role of ligand-gated chloride channels in behavioural alterations at elevated CO_2 in a cephalopod 39
3.1 Abstract . . . 40
3.2 Introduction . . . 41
3.3 Methods . . . 45
3.3.1 Animal collection . . . 45
3.3.2 CO_2 treatment systems . . . 48
3.3.3 Drug treatment and behavioural trials . . . 48
3.3.4 Behavioural analysis . . . 51
3.3.5 Statistical analysis . . . 52
3.4 Results . . . 54
3.4.1 Space use . . . 54
3.4.2 Soft mirror touch . . . 54
3.4.3 Aggressive mirror touch . . . 57
3.4.4 Activity . . . 59
3.5 Discussion . . . 61
3.5.1 Behavioural change in response to elevated CO_2 . . . 61
3.5.2 Behavioural change in response to drug treatment . . . 64
3.5.3 Conclusion . . . 68

4 Neurobiological mechanisms underlying effects of elevated CO_2 in a cephalopod 71
4.1 Abstract . . . 72
4.2 Introduction . . . 73
4.3 Methods . . . 76
4.3.1 Study species . . . 76
4.3.2 CO_2 treatment and sample collection . . . 76
4.3.3 RNA extraction . . . 77
4.3.4 RNA sequencing . . . 78

4.3.5 RNA-seq read pre-processing . . . 78
4.3.6 ISO-sequencing . . . 78
4.3.7 *de novo* transcriptome assembly . . . 78
4.3.8 Transcriptome annotation . . . 79
4.3.9 Read mapping and counting . . . 79
4.3.10 Statistical analyses . . . 80
4.4 Results . . . 81
4.4.1 Transcriptome assembly and annotation . . . 81
4.4.2 Differential expression analysis . . . 81
4.4.3 Gene set enrichment analysis . . . 88
4.5 Discussion . . . 90
4.5.1 *de novo* transcriptome assembly . . . 92
4.5.2 Effects of elevated CO_2 on gene expression . . . 92
4.5.3 Conclusion . . . 100

5 Correlated transcriptomic and behavioural responses: Identifying mechanisms underpinning behavioural responses to elevated CO_2 in a cephalopod 103
5.1 Abstract . . . 104
5.2 Introduction . . . 105
5.3 Methods . . . 107
5.3.1 CO_2 treatment and experimental design . . . 107
5.3.2 Behavioural data . . . 107
5.3.3 Gene count data . . . 109
5.3.4 Statistical analysis . . . 109
5.4 Results . . . 112
5.4.1 Genes in the CNS potentially driving altered activity at elevated CO_2 112
5.4.2 Genes in the eyes potentially driving altered activity at elevated CO_2 117
5.4.3 Genes potentially driving an altered number of exploratory interactions at elevated CO_2 . . . 117
5.5 Discussion . . . 123
5.5.1 Potential drivers of elevated CO_2-induced behavioural changes . . . 124
5.5.2 Proposed mechanism . . . 129
5.5.3 Conclusion . . . 130

6 General Discussion 131
6.1 Summary . . . 132
6.1.1 OA likely affects multiple types of neurotransmission, underpinning behavioural responses . . . 134

6.1.2 OA-induced disruption of adult neurogenesis may drive behavioural alterations . . . 135
6.1.3 Neurobiological impacts of OA may also drive non-behavioural responses . . . 136
6.1.4 Complex interactions between the neurobiological impacts of OA . 136
6.2 Future Directions . . . 137
6.2.1 The role of multiple types of neurotransmission in behavioural and physiological responses to OA . . . 137
6.2.2 The role of oxidative stress in behavioural responses to OA . . . 139
6.2.3 The role of adult neurogenesis in behavioural responses to OA . . . 139
6.2.4 Further exploration of the molecular mechanisms underlying biological responses to OA . . . 140
6.2.5 Sex-specific responses to ocean acidification . . . 141
6.2.6 Ecologically relevant mechanistic studies . . . 142
6.2.7 Adaptation of the nervous system as ocean acidification progresses 143
6.3 Concluding Remarks . . . 143

References **145**

A Chapter 2 Appendices **219**

B Chapter 3 Appendices **239**

C Chapter 4 Appendices **247**

D Chapter 5 Appendices **279**

List of Tables

2.1 Summary of publications that have mechanistically tested whether LGIC-mediated neurotransmission is altered in marine invertebrates at elevated CO_2. 25

3.1 Summary of the varying types of different drug effects across CO_2 treatments and how they suggest altered receptor function at elevated CO_2. 46
3.2 Experimental seawater carbonate chemistry. 49
3.3 Summary of the CO_2 effect in sham-treated squid, and the type of different drug effect across CO_2 treatments 55

4.1 Table of DEGs and their function in the CNS and eyes, ordered by log2 fold-change (LFC). 83

5.1 Eyes-specific CO_2 treatment hub genes. 118
5.2 Hub genes identified for CO_2 treatment in both the CNS and eyes. 119

List of Figures

1.1 Consequences of OA-induced responses. 4
1.2 The two-toned pygmy squid (*Idiosepius pygmaeus*). 8

2.1 Elevated CO_2 could induce behavioural alterations through a range of neurobiological mechanisms. 16
2.2 Potential reversal in function of varying LGICs at elevated CO_2 in marine invertebrates. 22
2.3 Future directions for neurobiological mehanistic research in marine invertebrates. 35

3.1 Diagram of behavioural trial set-up. 50
3.2 Effects of CO_2 and drug treatment on space use. 56
3.3 Effects of CO_2 and drug treatment on measures of soft mirror touching behaviour. 58
3.4 Effects of CO_2 and drug treatment on measures of aggressive mirror touching behaviour. 60
3.5 Effects of CO_2 and drug treatment on activity measures. 62
3.6 Evidence within molluscs that elevated CO_2 results in a suite of changes within the nervous system. 69

4.1 Experimental design overview. 77
4.2 Differential expression results. 82
4.3 Diagram outlining the role of DEGs in neurotransmission and behaviour at elevated CO_2 in *I. pygmaeus*. 87
4.4 Diagram outlining the role of DEGs in the immune response to elevated CO_2 in the nervous tissue of *I. pygmaeus*. 88
4.5 Diagram outlining the role of DEGs in the oxidative stress response to elevated CO_2 in the nervous tissue of *I. pygmaeus*. 89
4.6 Enrichment map displaying the gene set enrichment analysis (GSEA) results in both the CNS and eyes. 91

4.7 Proposed mechanistic model outlining the effects of elevated CO_2 on, and the interactions between, the three top functions found to be affected by elevated CO_2 in the nervous tissue of *I. pygmaeus*; neurotransmission, immune function and oxidative stress. 98

5.1 Experimental design overview. 108
5.2 Venn diagram depicting the number of hub genes identified for CO_2 treatment and behavioural traits in the CNS and eyes. 113
5.3 Functional categories significantly enriched in those genes in the CNS identified as potentially driving altered activity at elevated CO_2. 115
5.4 Potential molecular drivers of OA-induced behavioural changes in the CNS and eyes of *I. pygmaeus*, and a proposed mechanism by which elevated CO_2 could alter behaviour. 125

6.1 Overview of the results from the chapters in this thesis. 133

Chapter 1

General Introduction

1.1 The nervous system and environmental change

The nervous system forms the fundamental link between the environment and an organism's physiology and behaviour (Kelley *et al.*, 2018; O'Donnell, 2018). Sense organs detect the environment, and this information collected by the sense organs is sent to the central nervous system (CNS) for higher order processing. In the CNS, the information is interpreted and outputs are sent to effectors to create a response. Effectors can be muscles, which produce behavioural responses. Outputs from the nervous system can also release or regulate the release of hormones, which have downstream effects on target organs (Brown, 2001). Thus, the nervous system mediates an organism's response, both behaviourally and physiologically, to environmental change (Brown, 2001; Kelley *et al.*, 2018). Human activity is drastically altering the environments animals inhabit, for example climate change, habitat destruction, species overexploitation, pollution and the introduction of invasive species (Vitousek *et al.*, 1997; Pereira *et al.*, 2010; Steffen *et al.*, 2015). The nervous system also coordinates responses to anthropogenic environmental change (Kelley *et al.*, 2018; O'Donnell, 2018). Thus, the neurobiological impacts of human-induced environmental change are key to understanding how animals will respond as environmental change progresses, yet the role of the neurobiological mechanisms in biological responses to environmental change has been little explored (Kelley *et al.*, 2018).

1.2 Ocean acidification and its effects on marine invertebrates

For marine animals, a particularly important aspect of human-induced environmental change is ocean acidification. Human activity is resulting in unprecedented amounts of carbon dioxide (CO_2) being released into the atmosphere, with emissions projected to continue increasing into the future (Bindoff *et al.*, 2019). Approximately one third of the anthropogenic CO_2 released into the atmosphere is absorbed by the ocean, and the partial pressure of CO_2 (pCO_2) in the surface ocean is increasing at approximately the same rate as CO_2 in the atmosphere (Bindoff *et al.*, 2019). As seawater pCO_2 rises, there is an accompanying increase in bicarbonate and hydrogen ion concentrations and a decrease in carbonate ion concentrations. The increase in hydrogen ions lowers pH (moving towards more acidic conditions on the pH scale) and thus the rise in seawater pCO_2, and accompanying changes in ocean chemistry, are together known as ocean acidification (OA) (Doney *et al.*, 2009).

Research initially focused on the responses of calciferous marine invertebrates to OA due to the concern that changes in carbonate saturation states would disrupt their ability to form

shells and skeletons (Kleypas *et al.*, 1999; Feely *et al.*, 2004; Kurihara *et al.*, 2004; Orr *et al.*, 2005). However, it is now known that OA can affect not only calcification, but a wide variety of physiological processes, life history traits and behaviours of marine invertebrates (Pörtner *et al.*, 2004; Kroeker *et al.*, 2010; Clements and Hunt, 2015; Nagelkerken and Munday, 2015, Chapter 2). Invertebrates are vital components of marine ecosystems, comprising over 92% of marine species, are essential to the function of ecosystem processes, and support the livelihoods of humans across the globe (Bertness *et al.*, 2001; Chen, 2021). Consequently, any effects of OA on marine invertebrates could have far-reaching ecological, social and economic consequences (Figure 1.1). The responses of marine invertebrates to OA are variable, with some taxa and life stages more sensitive than others (Clements and Hunt, 2015; Kroeker *et al.*, 2013). This variability can have flow-on effects, altering species interactions and subsequent community and ecosystem dynamics (Zarnetske *et al.*, 2012; Kroeker *et al.*, 2014; Sanford *et al.*, 2014). Marine invertebrates include phyla as diverse as Cnidaria (including jellyfish and corals), Mollusca (including squid and mussels), and Arthropoda (including barnacles and crabs), separated by long evolutionary histories. This enormous phylogenetic variation may account for a large component of the variability in the responses to OA.

1.3 The mechanistic neurobiological underpinnings of biological responses to ocean acidification

Research has focused on the biological responses of marine invertebrates to elevated CO_2 with much less known about the mechanisms underlying these responses. A mechanistic understanding of the responses to OA is especially useful for developing cause-effect relationships, gaining insight into why some taxa are more sensitive than others and helping improve predictions of how marine invertebrates, and ultimately ecosystems, will respond as climate change progresses (Cooke *et al.*, 2013). As the nervous system mediates an animal's response to environmental change, understanding the neurobiological impacts of OA is key to gaining insight into the mechanistic underpinnings of OA-induced responses (Figure 1.1).

To date, the relatively few studies assessing the neurobiological underpinnings of OA-induced responses have focused on those mechanisms underlying OA-induced behavioural alterations. The majority of research has assessed the GABA hypothesis, proposed by Nilsson *et al.* (2012) in two coral reef fish species, which has become the prominent mechanistic hypothesis for behavioural changes at elevated CO_2. The GABA hypothesis suggests that acid-base regulatory mechanisms at elevated CO_2 alter gradients of HCO_3^- and Cl^- ions across neuronal membranes, disrupting the function of $GABA_A$ receptors (ligand-gated ion channels permeable to HCO_3^- and Cl^- ions (ligand-gated Cl^- channels)), consequently dis-

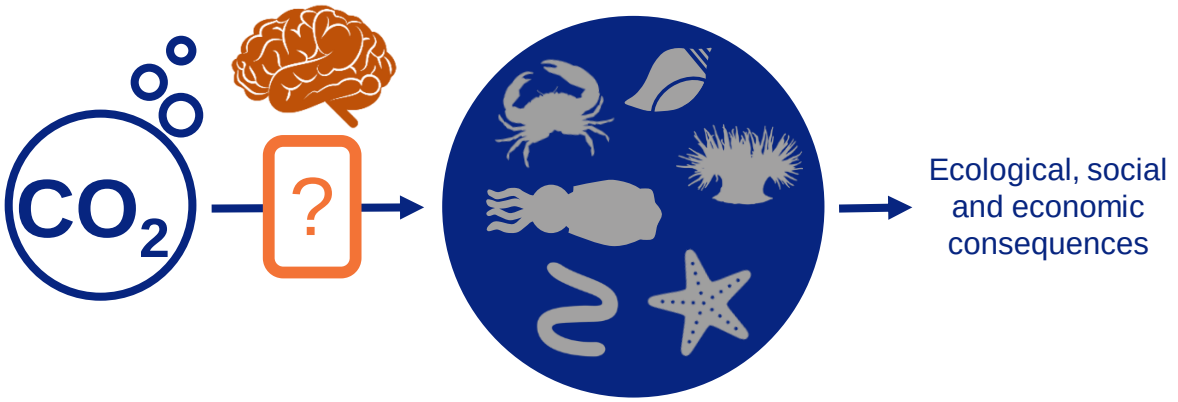

Figure 1.1. Consequences of OA-induced responses. Any effects of OA on marine invertebrates could have ecological, social and economic consequences. A neurobiological mechanistic understanding will help to improve predictions of how marine invertebrates, and ultimately ecosystems, will respond as OA progresses. Icons from NounProject.com (brain by Clockwise, worm by Deemak Daksina, anemone by Vega Asensio, crab by Ed Harrison, starfish by Stanislav Levin), remaining icons by Jodi Thomas.

rupting behaviour (Nilsson *et al.*, 2012). In fish, experimental pharmacological studies using $GABA_A$ receptor antagonists and agonists have supported the GABA hypothesis (Nilsson *et al.*, 2012; Hamilton *et al.*, 2013; Chivers *et al.*, 2014; Chung *et al.*, 2014; Lai *et al.*, 2015; Ou *et al.*, 2015; Lopes *et al.*, 2016; Munday *et al.*, 2016). Measurements of extra- and intracellular HCO_3^- ion concentrations in the brain, accompanied with behavioural measurements and a theoretical analysis of $GABA_A$ receptor function at elevated CO_2 have also supported the GABA hypothesis in fish (Heuer *et al.*, 2016, and reviewed in Heuer *et al.* (2019)).

In marine invertebrates, pharmacological studies exclusively using the $GABA_A$ receptor antagonist gabazine (Heaulme *et al.*, 1986) have supported the GABA hypothesis in a gastropod and bivalve mollusc (Watson *et al.*, 2014; Clements *et al.*, 2017), but not a crustacean (Charpentier and Cohen, 2016). Extra-cellular measurements of HCO_3^- and Cl^- ion concentrations have also supported the GABA hypothesis in a gastropod mollusc (Zlatkin and Heuer, 2019), as well as crustaceans (de la Haye *et al.*, 2012; Charpentier and Cohen, 2016). However, the pharmacological profile of receptors in invertebrates commonly differs to their counterparts in vertebrates, like fish (Rauh *et al.*, 1990), and have not been characterized as extensively as in vertebrates. For example, crustacean $GABA_A$-like receptors may be insensitive to gabazine (El Manira and Clarac, 1991; Jackel *et al.*, 1994; Pearstein *et al.*, 1996). Furthermore, both extra- and intra-cellular measurements are required to determine whether ionic gradients across neuronal membranes are altered at elevated CO_2, consequently disturbing $GABA_A$ receptor function. Thus, the marine invertebrate studies to date have provided a useful starting point to understand the mechanistic underpinnings of elevated CO_2-induced

behavioural changes, but the conclusions that can be drawn from using gabazine alone, and measurements only done in extra-cellular fluids, are limited.

OA may also disrupt the function of other receptors, similar to the $GABA_A$ receptor. In fish, disrupted functioning of glycine receptors, which are also ligand-gated Cl^- channels and thus function similarly to $GABA_A$ receptors, has been suggested to also underlie behavioural changes at elevated CO_2 (Tresguerres and Hamilton, 2017). Invertebrates possess a wider variety of ligand-gated Cl^- channels than vertebrates (Wolstenholme, 2012), including glutamate- (Vassilatis *et al.*, 1997; Kehoe and Vulfius, 2000), acetylcholine- (Kehoe, 1972; Schmidt and Calabrese, 1992; Putrenko *et al.*, 2005; van Nierop *et al.*, 2005), dopamine- (Carpenter *et al.*, 1977), serotonin- (Gerschenfeld and Tritsch, 1974; Ranganathan *et al.*, 2000) and histamine- (Gisselmann *et al.*, 2002; Zheng *et al.*, 2002) gated Cl^- channels. These ligand-gated Cl^- channels in marine invertebrates may also be disrupted by elevated CO_2 due to their functional similarity to $GABA_A$ receptors. However, the involvement of ligand-gated Cl^- channels, which are similar to $GABA_A$ receptors, in OA-induced behavioural alterations is yet to be experimentally tested in marine fish or invertebrates. Despite research focusing on the effects of elevated CO_2 on ligand-gated Cl^- channel function, OA could potentially disturb behaviour via a range of different mechanisms, all of which have been little explored to date and require further experimental testing (Briffa *et al.*, 2012, Chapter 2). As this research is in its infancy, it is also likely that unidentified mechanisms are also involved. Furthermore, the effects of OA on the nervous system likely underpins not only behavioural, but also physiological, responses.

Targeted approaches, like pharmacological studies, test specific hypotheses, which leaves potentially unidentified mechanisms unexplored. Thus, using untargeted approaches, like omics technologies, is important to provide a more holistic approach, testing existing hypotheses, potentially leading to the development of novel mechanistic hypotheses, and capturing the potential interactions between mechanisms. Transcriptomics, a powerful non-targeted approach that assesses all of the genes expressed in the selected tissue(s) (Wang *et al.*, 2009), is a key technique used to investigate the mechanistic basis of animal responses to the environment (Aubin-horth and Renn, 2009; Harris and Hofmann, 2014). For example, integrating transcriptomic data from the brains of two honeybee species with measures of anti-parasitic behaviours identified molecular signatures for resistance to the parasitic *Varroa* mite, which is devastating honeybee populations worldwide (Diao *et al.*, 2018). Transcriptomics has also widely been used to assess the broad responses of marine animals to OA (reviewed in Strader *et al.* (2020)). However, very little research has assessed the transcriptomic response of nervous tissue to OA.

Recent studies in fish have assessed the transcriptomic response of nervous tissue alongside behavioural experiments to investigate the mechanistic basis of OA-induced behavioural

alterations. A range of experiments have assessed the response of spiny damselfish brains to elevated CO_2. Short-term and developmental exposure of damselfish to elevated CO_2 triggered changes in brain expression of genes involved in GABAergic neurotransmission, but inter-generational exposure mostly returned the brain molecular response to baseline levels (Schunter *et al.*, 2018). From this transcriptional work, it has been proposed that a self-amplifying cycle is triggered, explaining how small alterations can lead to large behavioural responses. A switch in function of some $GABA_A$ receptors, from inhibitory to excitatory, is suggested to initiate the cycle, which is amplified by changes in expression of genes intended to suppress the excitation that instead further increase the excitation. This overexcitation of neurons increases the metabolic production of CO_2, also feeding into the vicious cycle (Schunter *et al.*, 2019). A clear molecular signature of parental behavioural tolerance to CO_2, which was mainly driven by circadian rhythm genes, was identified in the brains of juvenile damselfish (Schunter *et al.*, 2016), and a follow up study identified this as a maternal contribution (Monroe *et al.*, 2021). Fathers were found to have a greater role in changes in expression of histone binding genes, and both parents contributed to changes in expression of neuroplasticity genes (Monroe *et al.*, 2021). In the spiny damselfish and orange clownfish, brain transcriptional responses to OA were altered by diel CO_2 fluctuations. This differential response was largely related to changes in circadian rhythm genes and highlights the importance of using ecologically relevant CO_2 treatment conditions in laboratory experiments (Schunter *et al.*, 2021). In European sea bass exposed to elevated CO_2, reduced responses of the olfactory nerve to odourants and altered olfactory-mediated behaviour was associated with differential expression in olfactory nervous tissue, of genes involved in olfactory receptors, excitatory neurotransmission and synaptic plasticity (Porteus *et al.*, 2018). In ocean-phase salmon, exposure to elevated CO_2 disrupted olfactory-mediated behaviour, altered odour signalling in the olfactory bulb, and resulted in differential expression of genes involved in GABAergic signalling and ion balance regulation, in olfactory nervous tissue (Williams *et al.*, 2019). Thus, transcriptomics can be used to test pre-existing hypotheses, such as the GABA hypothesis, but also allows for the development of novel hypotheses, such as the involvement of circadian rhythm genes and neuroplasticity, to explain OA-induced responses.

In marine invertebrates, little research to date has utilised transcriptomics to assess the mechanisms underpinning responses to OA. Two transcriptomic studies assessing the whole-body response of pteropod molluscs to OA identified changes in expression of genes involved in nervous system functioning. In the Mediterranean pteropod (*Heliconoides inflatus*) 22% of transcripts upregulated at elevated CO_2 play roles in nervous system function, including those involved in GABAergic, glycinergic, cholinergic and glutamatergic neurotransmission (Moya *et al.*, 2016). In the Antarctic pteropod (*Limacina helicina antarctica*), acetylcholine

receptors also showed changes in expression at elevated CO_2 (Johnson and Hofmann, 2017). However, studies using whole-body measurements cannot determine the tissue specificity of transcripts responding to OA. For example, it cannot be determined whether the differential expression of genes involved in acid-base regulation and ion transport in the whole body of *H. inflatus* were restricted to specific tissues, including the nervous system (Moya *et al.*, 2016). Furthermore, due to the heterogeneity and complexity of gene expression, measurements at the whole-body level may mask transcriptomic responses in specific tissues, such as the nervous system. Thus, to understand the neurobiological mechanisms underlying responses to OA, rather than the general whole-body molecular response, assessing the transcriptomic response of the nervous tissue from a marine invertebrate will be important. Furthermore, transcriptomic studies that directly correlate changes in gene expression to phenotypic changes at elevated CO_2 will be useful to more directly assess the mechanisms underlying OA-induced responses, but such studies are lacking.

1.4 Thesis aims and outline

The objective of this thesis is to investigate the neurobiological impacts of OA on a marine invertebrate, and to determine the mechanistic neurobiological underpinnings of OA-induced biological responses in a marine invertebrate. To do this, I used a cephalopod mollusc, the two-toned pygmy squid *Idiosepius pygmaeus*. Cephalopods have a complex nervous system and behaviours rivalling those of fish (Hanlon and Messenger, 2018) making them a useful taxon to study the neurobiological effects of elevated CO_2. Furthermore, as cephalopods including squid accumulate extracellular HCO_3^- to compensate for a pH drop when exposed to increased seawater CO_2 levels (Hu *et al.*, 2014; Gutowska *et al.*, 2010) the GABA hypothesis may also apply to cephalopods. *I. pygmaeus* is a tropical squid that inhabits shallow, inshore waters of the Indo-Pacific, including Northern and Northeastern Australia (Reid, 2005) (Figure 1.2). *I. pygmaeus* grows to a maximum mantle length of 2 cm (Reid, 2005), has a short lifespan of up to 80 days (Jackson, 1988), is diurnal (Moynihan, 1983), and can be caught year-round from coastal waters around Townville, Australia (Jackson, 1992), all of which makes this species amenable for laboratory studies. Furthermore, previous work in this species has indicated OA can alter a range of behaviours, including defensive and predatory behaviours, and activity levels (Spady *et al.*, 2014, 2018), as well as reproduction and embryonic development (Spady *et al.*, 2019). For this thesis, I focused on the eyes and CNS of *I. pygmaeus* (Figure 1.2). This allowed me to evaluate the effect of OA on peripheral sensation, as well as higher order processing occurring in the CNS. I chose the eyes because cephalopods, including squid, are highly visual animals with many visually-mediated behaviours (Chung *et al.*, 2022; Mather, 2006; Muntz, 1999).

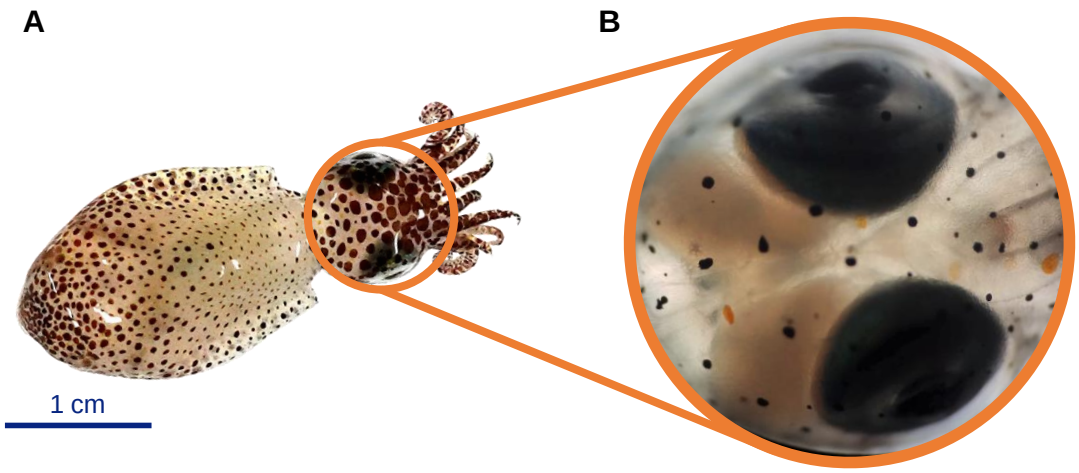

Figure 1.2. The two-toned pygmy squid (*Idiosepius pygmaeus*). **A** Whole animal, and **B** microscope image showing the two eyes (black) and the CNS sitting behind and between the eyes. Images by Jodi Thomas.

As a clear mechanistic understanding of behavioural responses to elevated CO_2 is lacking in marine invertebrates, Chapter 2 is a literature review of the potential mechanisms underlying OA-induced behavioural alterations in marine invertebrates. In this review, I explore a range of mechanisms by which OA could induce behavioural alterations in marine invertebrates, which are not necessarily mutually exclusive and all of which have been little explored and require further experimental testing. I propose potential novel mechanisms, and outline major knowledge gaps for future research to address. These knowledge gaps identified in Chapter 2 guide the following data chapters.

In Chapter 3, I pharmacologically test the role of GABA-, and other ligand-, gated Cl^- channels in behavioural changes at elevated CO_2 in *I. pygmaeus*. To do this, I exposed squid to current-day or elevated CO_2 conditions, followed by treatment with sham, gabazine (specific $GABA_A$ receptor antagonist) or picrotoxin (non-specific $GABA_A$ receptor antagonist) and then a behavioural trial. This chapter provides the first marine invertebrate study to use a drug other than gabazine to test the GABA hypothesis. As picrotoxin is structurally unrelated to gabazine, and the action of picrotoxin is better known in molluscs, using both gabazine and picrotoxin allows for a more robust test of the GABA hypothesis compared to using one drug alone. Using both drugs also provides the first opportunity to pharmacologically test the role of other ligand-gated Cl^- channels, similar to the $GABA_A$ receptor, in OA-induced behavioural alterations of any marine animal.

It is likely that other, unidentified mechanisms are also involved in OA-induced behavioural changes of marine organisms, and the nervous system coordinates not only behaviour but also physiology. Thus, in Chapter 4 I assess the transcriptomic response of a

marine invertebrate nervous system to OA, developing a more holistic view of the impacts of OA on the nervous system and allowing the development of potential novel mechanistic hypotheses for behavioural and physiological responses to OA. As a reference for gene quantification, I used long read PacBio ISO-sequencing data to create an annotated transcriptome assembly with accompanying quality and completeness metrics. I then used differential expression and gene set enrichment analyses to evaluate the transcriptomic response of the CNS and eyes of *I. pygmaeus* exposed to elevated compared to current-day CO_2 conditions.

Finally, in Chapter 5, I use a novel approach to more directly assess the potential mechanisms underlying behavioral changes at elevated CO_2 in *I. pygmaeus*. Firstly, I used a network approach to cluster transcriptome-wide gene expression in the CNS and eyes, separately. Then, I used Canonical Correlation Analysis to correlate the gene expression profile of each gene cluster with CO_2 treatment level (current-day or elevated) and OA-affected, visually-mediated behaviours in the same individuals. This is the first study to directly correlate gene expression with CO_2 treatment conditions (current-day or elevated) and behaviour of the same individuals to assess the mechanisms underpinning behavioural responses to OA.

Together, these four chapters explore the mechanisms underlying the biological responses to OA in marine invertebrates, using a cephalopod mollusc. This thesis highlights that OA likely induces a suite of changes in both the peripheral and central nervous systems, with a complex assortment of multiple mechanisms underpinning the responses to OA. This complexity in the mechanisms could explain the variability in biological responses to OA, with different mechanisms potentially being predominant in different taxa and resulting in different behavioural responses. Overall, my thesis advances our understanding of the mechanisms underlying behavioural and physiological responses of marine invertebrates to OA. This understanding will help to improve predictions of how marine animals, and ultimately ecosystems, will respond as OA progresses.

Chapter 2

Toward a mechanistic understanding of marine invertebrate behaviour at elevated CO_2

A version of this chapter is published:
Thomas, J.T., Munday, P.L. and Watson, S.-A. (2020). Toward a mechanistic understanding of marine invertebrate behaviour at elevated CO_2. *Frontiers in Marine Science*. **7**, 345. URL https://doi.org/10.3389/fmars.2020.00345

Difference between this chapter and published paper:
Minor formatting and editorial changes.

2.1 Abstract

Elevated carbon dioxide (CO_2) levels can alter ecologically important behaviours in a range of marine invertebrate taxa, however, a clear mechanistic understanding of these behavioural changes is lacking. The majority of mechanistic research on the behavioural effects of elevated CO_2 has been done in fish, focusing on disrupted functioning of the $GABA_A$ receptor (a ligand-gated ion channel). Yet, elevated CO_2 could induce behavioural alterations through a range of mechanisms that disturb different components of the neurobiological pathway that produces behaviour, including disrupted sensation, altered behavioural choices and disturbed ligand-gated ion channel-mediated neurotransmission. Here, I review the potential mechanisms by which elevated CO_2 may affect marine invertebrate behaviours. Marine invertebrate acid-base physiology and pharmacology is discussed in relation to altered $GABA_A$ receptor functioning. Alternative mechanisms for behavioural change at elevated CO_2 are considered and important topics for future research have been identified. A mechanistic understanding will be important to determine why there is variability in elevated CO_2-induced behavioural alterations across marine invertebrate taxa, why some, but not other, behaviours are affected within a species and to identify which marine invertebrates will be most vulnerable to rising CO_2 levels.

2.2 Introduction

Human activity is resulting in unprecedented amounts of carbon dioxide (CO_2) being released into the atmosphere. Since the Industrial Revolution, atmospheric CO_2 levels have increased by over 45%, from approximately 280 ppm (Joos and Spahni, 2008) to over 410 ppm today (Dlugokencky and Tans, 2019), higher than any time in the past several million years (Masson-Delmotte *et al.*, 2013). In the worst case scenario, following the business-as-usual representative concentration pathway (RCP) 8.5, atmospheric CO_2 levels will increase to over 900 ppm by the end of this century. Even if substantial efforts are made to curb global CO_2 emissions to keep warming below 2°C, atmospheric CO_2 levels will still likely exceed 600 ppm by 2100 (Betts and McNeall, 2018). The ocean has absorbed 20-30% of anthropogenic CO_2 emissions since the mid-1980s (Bindoff *et al.*, 2019), causing a reduction in seawater pH referred to as ocean acidification. Furthermore, CO_2 in the surface ocean is increasing at the same rate as in the atmosphere (Bindoff *et al.*, 2019), therefore, marine organisms will need to cope with higher CO_2 levels as well as declining seawater pH. Finally, due to a decrease in the ocean's buffering capacity as CO_2 content rises, natural CO_2 fluctuations in the ocean are projected to amplify dramatically at future higher CO_2 levels (Shaw *et al.*, 2013; McNeil and Sasse, 2016). Natural diel (Hofmann *et al.*, 2011; Santos *et al.*, 2011; Shaw *et al.*, 2012) and seasonal CO_2 fluctuations (McNeil *et al.*, 2007; Feely *et al.*, 2008) will be amplified by up to 3 times in the future (McNeil and Sasse, 2016; Gallego *et al.*, 2018), meaning that marine organisms will experience elevated CO_2 levels for certain periods of time (daily or seasonally) much earlier than predictions based on atmospheric CO_2 alone.

Elevated CO_2 has been found to affect a range of processes in marine organisms, including altering calcification (Ries *et al.*, 2009; Kroeker *et al.*, 2013), growth and survival (Fabry *et al.*, 2008; Kurihara *et al.*, 2008), and behaviour (Briffa *et al.*, 2012; Clements and Hunt, 2015; Nagelkerken and Munday, 2015). Projected future CO_2 levels were first found to alter animal behaviour in orange clownfish (*Amphiprion percula*) larvae reared in a partial pressure of CO_2 (pCO_2) of ~1,050 µatm (Munday *et al.*, 2009). In laboratory experiments, the olfactory discriminatory abilities of 11-day-old clownfish larvae were tested in a two-channel flume. Most strikingly, larvae reared in control seawater (~390 µatm pCO_2) avoided the side of the flume with chemical cues from pungent tree leaves compared to the seawater control side. However, larvae reared in elevated CO_2 spent nearly all their time in the side with these odours. Larval clownfish reared in ~1,050 µatm CO_2 were also unable to discriminate between the odour of parents and non-parents, whereas control larvae avoided the odour of their parents (Munday *et al.*, 2009). Elevated CO_2 has since been found to affect a variety of behavioural traits in a wide spectrum of fishes, including tropical and temperate reef species, eels, salmon and sharks (Munday *et al.*, 2019). Behavioural alterations at elevated CO_2 have

also been demonstrated in a variety of marine invertebrates, including cnidaria, polychaetes, echinoderms, arthropods and molluscs, from a range of environments, including the intertidal zone, coastal and offshore waters, and the deep-sea (Clements and Hunt, 2015; Nagelkerken and Munday, 2015; Wang and Wang, 2019). Marine invertebrates exhibit alterations in a range of behaviours at elevated CO_2, including activity levels (Rosa and Seibel, 2008; Ellis *et al.*, 2009; Spady *et al.*, 2014), feeding rates (Saba *et al.*, 2012; Vargas *et al.*, 2014), settlement and metamorphosis behaviours (Albright *et al.*, 2010; Doropoulos *et al.*, 2012; Guo *et al.*, 2015), burrowing behaviours (Green *et al.*, 2013; Clements and Hunt, 2014), shelter selection (de la Haye *et al.*, 2011), predatory behaviours (behaviours related to finding and eating prey) (Kim *et al.*, 2015; Queirós *et al.*, 2015; Spady *et al.*, 2018) and predator avoidance (Bibby *et al.*, 2007; Manríquez *et al.*, 2013, 2014a; Spady *et al.*, 2014; Watson *et al.*, 2014). Behavioural categorisation is often ambiguous as one behaviour may actually include multiple behaviours or decision-making processes. For example, predator avoidance behaviours include multiple decisions such as mode of avoidance (including crypticity versus escape), flight-initiation distance and mode of escape (Lima and Dill, 1990). In this review, I use the behavioural category that was reported in the corresponding research paper.

Since the review by Clements and Hunt (2015) at least 61 additional papers have assessed the impact of elevated CO_2 on marine invertebrate behaviours (Appendix A: Table A.1). Research has continued to focus on molluscs, arthropods and echinoderms, however cnidarian settlement and metamorphosis (Foster *et al.*, 2015; Olsen *et al.*, 2015; Viyakarn *et al.*, 2015; Fabricius *et al.*, 2017; Yuan *et al.*, 2018b), the settlement behaviour and swimming activity of a bryozoan (Pecquet *et al.*, 2017), and settlement of an annelid (Nelson *et al.*, 2020) have also been studied. In addition to continuing to assess the impact of elevated CO_2 on the range of behaviours previously studied (above), a few new behaviours have also been investigated. For example, the first study assessing the effect of elevated CO_2 on marine invertebrate reproductive behaviour was recently published (Borges *et al.*, 2018). Exposure of male amphipods (*Gammarus locusta*) to elevated CO_2 (800 µatm pCO_2) for two generations disrupted the chemosensory detection of potential mates (Borges *et al.*, 2018). A light/dark test on swimming crabs (*Portunus trituberculatus*) exposed to control (485 µatm pCO_2) or elevated (750 µatm and 1,500 µatm pCO_2) CO_2 was the first to assess the impact of elevated CO_2 on anxiety-like behaviour in a marine invertebrate. Crabs exposed to elevated CO_2 levels spent significantly more time in the dark zone (Ren *et al.*, 2018).

There appears to be large variability in behavioural responses to elevated CO_2, across taxonomic groups, the same behaviour can respond differently to elevated CO_2, and within a species, some behaviours but not others can be affected (Nagelkerken and Munday, 2015, Appendix A: Table A.1). As the phylogenetic variation among invertebrate taxa is enormous, it may account for a large component of the variability in behavioural responses across tax-

onomic groups, some taxa may be more tolerant to elevated CO_2 than others. At the same time, various behaviours are likely associated with different processes, such as specific circuits in the nervous system. These processes may be affected differently by elevated CO_2, accounting for the effects of elevated CO_2 on some, but not all, behaviours within a species. It must also be noted that variability may be due to differences in experimental techniques and conditions.

Animal behaviour is, to a large extent, the functional output of the nervous system (Simmons and Young, 1999), therefore, behavioural changes induced by elevated CO_2 are likely caused by neurobiological mechanisms. In the nervous system, simplistically, the pathway that produces behaviour involves sensory receptors that detect environmental stimuli (e.g. chemical cues, light waves) and internal stimuli (e.g. spatial orientation of the body). The received information is transduced into electrical impulses and neurotransmission relays these electrical impulses between neurons. Neurotransmission must be rapid to produce timely behavioural responses, and this is achieved via ligand-gated ion channel (LGIC) mediated neurotransmission (Dent, 2010). LGICs are transmembrane protein complexes that, upon binding of a specific neurotransmitter, allow ion flow which results in excitation or inhibition of neuronal firing depending on the ion charge and direction of flow (Tovar and Westbrook, 2012). When the sensory information arrives at higher centres of the nervous system, this information is processed and a behavioural output is produced (Blom, 1978; Kreher *et al.*, 2008) (Figure 2.1).

Elevated CO_2 could induce behavioural alterations through a range of mechanisms in the nervous system that disturb different components of the pathway that produces behaviour (Briffa *et al.*, 2012) (Figure 2.1). 1) Sensation may be disrupted via changes to sensory stimuli at elevated CO_2, such as structural alteration of chemical cues, disturbed transmission of acoustic cues and altered sensory output from animals experiencing behavioural changes (Roggatz *et al.*, 2016; Nagelkerken *et al.*, 2019). 2) Alternatively, elevated CO_2 may disrupt sensation via physical change to sensory organs or structural alteration of sensory receptors (Maneja *et al.*, 2011; Briffa *et al.*, 2012; Bignami *et al.*, 2013). 3) Morphological and respiratory changes at elevated CO_2 may alter the context within which decision making is carried out, influencing behavioural responses (Bibby *et al.*, 2007; Chan *et al.*, 2011; Peng *et al.*, 2017; Rich *et al.*, 2018). 4) Elevated CO_2 may alter ion gradients across neuronal membranes, due to acid-base regulation to prevent acidosis at elevated CO_2, which may disrupt LGIC-mediated neurotransmission via the γ-aminobutyric acid type A receptor ($GABA_A$ receptor) (Nilsson *et al.*, 2012). These mechanisms are not necessarily mutually exclusive and may interact to alter behaviour at elevated CO_2.

Despite the growth in literature demonstrating elevated CO_2-induced behavioural alterations in marine invertebrates, the mechanisms responsible for these behavioural alterations

are still poorly understood. Due to the diversity of invertebrate nervous and neurobiological systems, it is likely that a suite of different processes underlie these behavioural changes. Here, I discuss the potential mechanisms by which elevated CO_2 may alter marine invertebrate behaviour, 1) disturbed sensation, 2) altered context within which behavioural choices are made and 3) disrupted LGIC-mediated neurotransmission. Since the prominent hypothesis for altered LGIC-mediated transmission is the GABA hypothesis proposed in fish by Nilsson *et al.* (2012), here I discuss evidence for the GABA hypothesis in marine invertebrates and propose research to expand our understanding of the GABA hypothesis in marine invertebrates. I demonstrate that the effects of altered $GABA_A$ receptor function are likely to be widespread, including non-behavioural effects. Finally, I identify other neurobiological mechanisms that should be affected if the GABA hypothesis is correct, propose alternative neurobiological mechanisms by which behaviour could be altered by elevated CO_2 and suggest techniques to be utilised for future study of elevated CO_2-induced behavioural alterations.

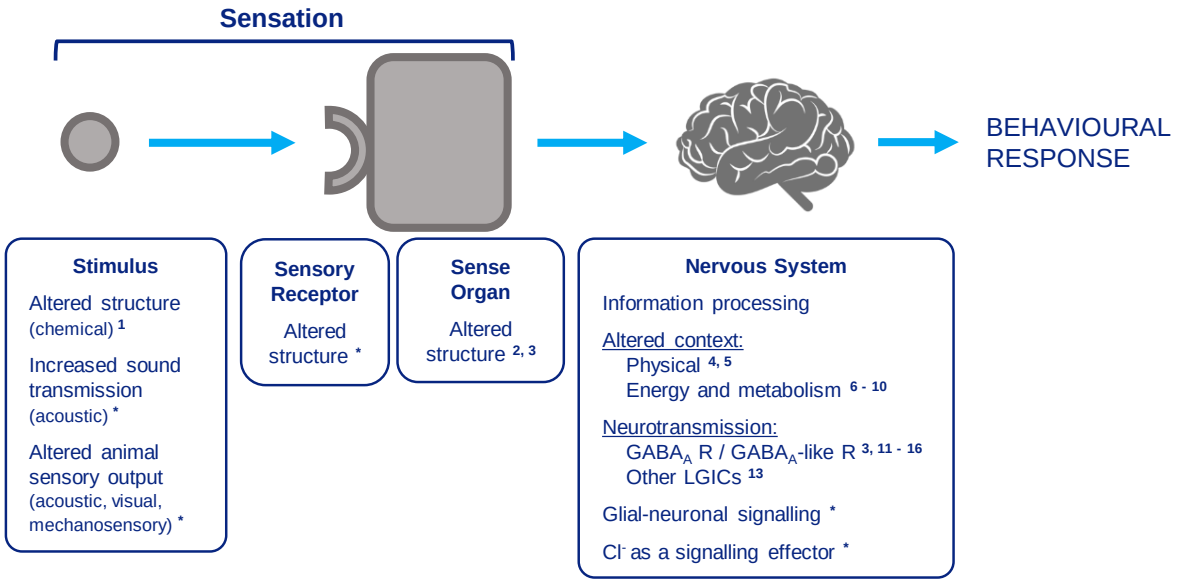

Figure 2.1. Elevated CO_2 could induce behavioural alterations through a range of neurobiological mechanisms. Simplistic pathway of how the nervous system produces behaviours and potential ways elevated CO_2 could alter marine invertebrate behaviour. An external or internal stimulus is detected by sensory receptors located on a sense organ. A physical stimulus binding to a receptor, e.g. a chemical cue binding to the corresponding receptor (chemoreception), is depicted. However, stimuli and receptors may range from photoreceptors detecting light energy to stretch receptors detecting body movement or hair cells detecting vibrations. *(see next page)*

Figure 2.1 ***(previous page).*** The detected sensory information is then transduced into electrical impulses that are relayed between neurons to higher centres of the nervous system. Here, the information is processed which includes using external and internal contextual factors to make behavioural choices. The information is transmitted between neurons to the motor system and a behavioural response is produced. Throughout this process, neurotransmission is used to relay the electrical impulses from neuron to neuron. Elevated CO_2 may alter behaviour by interfering at multiple points along this pathway. Sensation may be disrupted by changes to sensory stimuli at elevated CO_2 through structural change of chemical cues, increased sound transmission and altered sensory output from animals. Sensation may also be disrupted on the receiving end via altered structure of sensory receptors or physical change to sensory organs. Elevated CO_2 may change the context within which decision-making is carried out, thus influencing behavioural choices. The change in ion gradients across neuronal membranes, due to acid-base regulation at elevated CO_2, may disrupt LGIC-mediated neurotransmission, glial-neuronal signalling and the role of Cl^- as a signalling effector. Numbers represent references providing evidence for each mechanism in marine invertebrates, while a * indicates this mechanism is based on theory with no experimental evidence in marine invertebrates. 1 Roggatz *et al.* (2016), 2 Maneja *et al.* (2011), 3 de la Haye *et al.* (2012), 4 Bibby *et al.* (2007), 5 Chan *et al.* (2011), 6 Dissanayake and Ishimatsu (2011), 7 Li and Gao (2012), 8 Peng *et al.* (2017), 9 Wang *et al.* (2018b), 10 Rich *et al.* (2018), 11 Watson *et al.* (2014), 12 Charpentier and Cohen (2016), 13 Moya *et al.* (2016), 14 Clements *et al.* (2017), 15 Ren *et al.* (2018), 16 Zlatkin and Heuer (2019).

2.3 Mechanisms for elevated CO_2-induced behavioural changes

2.3.1 Altered sensory stimuli at elevated CO_2

Elevated CO_2 may influence behaviour by altering an animal's ability to sense the environment (Briffa *et al.*, 2012; Draper and Weissburg, 2019). A range of sensory stimuli may be disrupted at elevated CO_2 via differing mechanisms, thereby affecting associated behaviours (Figure 2.1). Structural alteration of chemical cues at elevated CO_2 may affect chemoreception; the detection of chemical cues by binding to sensory receptors, e.g. odour molecules binding to olfactory receptors (Tierney and Atema, 1988). Impaired chemo-responsive behaviour was first shown to be due to structural alteration of the chemical cue at low pH in a freshwater system (Brown *et al.*, 2002) and the same mechanism has since been demonstrated in a marine invertebrate, the shore crab *Carcinus maenas*. Near-future pH levels altered the structure and charge of signalling molecules that mediate egg ventilation behaviour in the shore crab *C. maenas* and the threshold of signalling molecule concentration required to induce egg ventilation behaviour in this species increased when tested at pH 7.7 compared to pH 8.1 (Roggatz *et al.*, 2016). Receptor alteration, such as change in ionization state, could

also conceivably occur at low pH disrupting chemoreception (Tierney and Atema, 1988), and may be an additional explanation for behavioural changes observed in the shore crab (Roggatz *et al.*, 2016). However, to date receptor structure has never been directly tested at different CO_2 levels in conjunction with a behavioural assay.

Changes in ocean chemistry associated with rising CO_2 levels will directly affect acoustic cues, potentially altering auditory driven behaviours. Sound absorption, in the low frequency range of ~0.01 – 10 kHz, is reduced by decreasing pH due to shifts in the chemical reactions of sound absorbing compounds (e.g. magnesium sulphate, boric acid and carbonate ions) in seawater (Hester *et al.*, 2008). Sound absorption (decibels per kilometre) is predicted to decrease by over 20% and almost 40% with a pH drop from 8.1 to 7.95 and 7.8, respectively (Hester *et al.*, 2008). Thus, as CO_2 levels rise, transmission of low-frequency sounds will increase and ecologically relevant acoustic cues, within this affected frequency range, will be transmitted further at elevated CO_2 levels. For example, compared to off reef-locations, oyster reefs have higher acoustic energy levels within the frequency range of 1.5 – 20 kHz. This acoustic signature of reefs is used as a settlement cue by larval oysters (Lillis *et al.*, 2013). As CO_2 levels rise, oyster larvae may thus be able to detect appropriate settlement habitats from greater distances, however it remains unknown whether the magnitude of change is sufficient to be of biological relevance. Elevated CO_2 will also increase the transmission of abiotic sounds produced naturally (e.g. waves, raindrops) and by human activity (e.g. shipping, sonar and construction) (Ilyina *et al.*, 2010). This will create a noisier environment in which it is harder for marine invertebrates to detect ecologically relevant sounds, such as those used for communication (Popper *et al.*, 2001; Buscaino *et al.*, 2011) as well as navigation and habitat selection for settlement (Jeffs *et al.*, 2003; Stanley *et al.*, 2009; Vermeij *et al.*, 2010; Lillis *et al.*, 2013). In a coral reef fish, predatory behaviour decreased when exposed to boat noise or elevated CO_2 (925 µatm pCO_2), however there was no additive effect when these stressors co-occurred (McCormick *et al.*, 2018). Studies in marine invertebrates to determine how increased transmission of biologically relevant cues and background noise will interact as CO_2 levels rise, and if this will be biologically relevant will be important.

Behavioural changes induced by elevated CO_2 may alter the sensory output of an animal, affecting whether and how this animal is sensed by other animals (Draper and Weissburg, 2019). For example, increased activity of a prey animal could enhance how much or how often sound, visual and mechanosensory cues are produced, strengthening predatory sensory detection of the prey and increasing the chance of predation (Draper and Weissburg, 2019). Elevated CO_2 reduced the intensity and frequency of snaps produced by snapping shrimp (Rossi *et al.*, 2016). As these snaps are commonly present in the soundscapes used by marine invertebrate larvae as settlement cues (Stanley *et al.*, 2009; Vermeij *et al.*, 2010; Lillis *et al.*, 2013), altered snapping behaviour of snapping shrimp at elevated CO_2 may in turn

alter marine invertebrate settlement behaviour.

2.3.2 Physical changes of sensory organs

Sensation may also be disrupted by physical change of sensory organs at elevated CO_2. Due to lower saturation states of seawater with respect to calcium carbonate at elevated CO_2, animals can have difficulty maintaining calcium carbonate structures (Orr *et al.*, 2005) which may damage sensory organ structures (Briffa *et al.*, 2012). Alternatively, active acid-base regulation to maintain a steady internal pH may alter the concentrations of ions that are fundamental for the formation of calcified sensory organs (Grosell, 2019). For example, many marine invertebrates use statocysts, which contain mineralised statoliths, to detect gravity to maintain orientation (Cohen, 1960; Clarke, 1978; Spangenberg, 1986), as well as vibrational stimuli for hearing in cephalopods (Mooney *et al.*, 2010). Statocysts are also involved in motor programs that underlie hunting behaviour in molluscs (Levi *et al.*, 2004). Statolith size was reduced and morphology altered in cephalopods exposed to ~1,300 µatm (Zakroff *et al.*, 2019), 2,200 µatm (Kaplan *et al.*, 2013) and 4,000 µatm (Maneja *et al.*, 2011) pCO_2. Abalone exposed to ~700 and ~1,000 µatm pCO_2 also exhibited decreased statolith size compared to control conditions (Manríquez *et al.*, 2014b). Conversely, statolith size was increased, and chemical composition altered, in squid exposed to 850 and 1,500 µatm pCO_2 (Lacoue-Labarthe *et al.*, 2011). Cuttlefish exposed to 4,000 µatm pCO_2 exhibited reduced statolith calcification, altered statolith microstructure and decreased prey capture efficiency compared to squid in control conditions (700 µatm pCO_2) (Maneja *et al.*, 2011). Furthermore, computer modelling showed that an increased statolith mass, similar to that seen in the otoliths of fish exposed to 2,500 µatm pCO_2, would alter cephalopod hearing below 10 Hz (Zhang *et al.*, 2015). However, squid exposed to ~1,300 µatm pCO_2 had smaller statoliths with an altered morphology (Zakroff *et al.*, 2019) but no impairment in swimming orientation (Zakroff *et al.*, 2018). Therefore, elevated CO_2-induced alteration of statoliths may disturb hearing but not gravity detection in cephalopods, impacting auditory-driven behavioural outputs but not the ability to maintain orientation.

Decapod crustaceans possess calcified antennules, housing chemoreceptors, which are used for long range chemoreception. Rapid antennule flicking is used to gather chemical cue information, much in the way sniffing increases our ability to determine smells (Schmitt and Ache, 1979; Koehl, 2005). Hermit crabs with disrupted chemo-sensory responses at extremely high levels of CO_2 (c. >12,000+ µatm pCO_2) showed no damage to their antennules (de la Haye *et al.*, 2012), suggesting that other mechanisms must be responsible for the observed response.

2.3.3 Altered behavioural choices

The physiological and ecological context, including external factors (e.g. presence of predators or temperature) and internal factors (e.g. hunger or reproductive state) can influence behavioural choices (Palmer and Kristan Jr, 2011). Elevated CO_2 may alter both external and internal factors, changing contextual modulation of behavioural choice and resulting in altered behavioural output. Physical changes induced by elevated CO_2 may alter an animal's behavioural choice. For example, predator-induced shell thickening observed in control periwinkles (*Littorina littorea*) did not occur in periwinkles exposed to extremely high levels of CO_2 (c. >12,000+ µatm). However, predator avoidance behaviour increased at elevated CO_2 conditions, compared to control, which suggests behavioural compensation for the lack of morphological defence at extremely high levels of CO_2 (Bibby *et al.*, 2007). In another example, the swimming performance of larval sand dollars (*Dendraster excentricus*) was maintained at elevated CO_2 (~1,000 µatm pCO_2) despite impaired arm and body morphology, likely due to a behavioural change in ciliary beat patterns (Chan *et al.*, 2011). By contrast, both predator cue-induced byssal thread production and protective clustering behaviour was decreased in mussels exposed to elevated CO_2 (1,100 µatm pCO_2) (Kong *et al.*, 2019), indicating no behavioural compensation for the lack of morphological defence at elevated CO_2.

The influence of elevated CO_2 on respiration, energy turnover and mode of metabolism (Pörtner *et al.*, 2004) may also alter behavioural choice. Depressed metabolism at elevated CO_2 levels may reduce energy production, reducing the energy available to meet other demands and constraining performance of some behaviours. For example, metabolic scope and swimming ability were reduced in shrimp exposed to ~1,000 µatm pCO_2 (Dissanayake and Ishimatsu, 2011) and oxygen consumption rate and digging depth were decreased in razor clams exposed to 1,900 and 3,000 µatm pCO_2 (Peng *et al.*, 2017). Increased metabolism can indicate an increased energy demand at elevated CO_2 and may decrease the energy available for other costly processes. For example, crabs exposed to 1,200 and 2,300 µatm pCO_2 exhibited an increased metabolic rate but a decreased feeding rate (Wang *et al.*, 2018a). Alternatively, organisms may alter behaviours to meet the high energy demand. For example, respiration and feeding rate were increased in a copepod exposed to 1,000 µatm pCO_2 (Li and Gao, 2012) and a sea urchin exposed to 1,300 µatm pCO_2 (Rich *et al.*, 2018). However, other studies show a change in metabolism with no associated behavioural change at 750 and 1,200 µatm pCO_2 in an echinoderm (Carey *et al.*, 2016) and at 1,500 µatm pCO_2 in a mollusc (Benítez *et al.*, 2018), or no metabolic change but altered behaviour at 960 µatm pCO_2 in a mollusc (Watson *et al.*, 2014) and at 1,000, 2,000 and 3,000 µatm pCO_2 in a crustacean (Menu-Courey *et al.*, 2018). Therefore, it seems that altered metabolism in elevated CO_2

may be responsible for some instances of altered behaviours, but not others.

2.3.4 Altered functioning of the $GABA_A$ receptor

Elevated CO_2 has been found to alter a range of behaviours across different sensory modalities, as well as behaviours that involve higher order processing, such as decision making (de la Haye *et al.*, 2011) and anxiety-like behaviours (Ren *et al.*, 2018). This suggests that not only sensory detection, but also other neuronal processes are altered by elevated CO_2. Neurotransmission is crucial to all components of the pathway producing behaviour, from relaying electrical signals from sensory receptors to (and between) higher-order neurons for information processing, to motor neurons for the production of a behavioural response. Therefore, altered neurotransmission at elevated CO_2 may underlie a variety of behavioural disturbances.

The prominent hypothesis for altered neurotransmission at elevated CO_2 is the GABA hypothesis, proposed to occur in fish (Nilsson *et al.*, 2012; Heuer and Grosell, 2014) and also suggested to apply to marine invertebrates (Watson *et al.*, 2014). In vertebrates, γ-aminobutyric acid (GABA) acts on the GABA type A receptor ($GABA_A$ receptor), a ligand-gated ion channel permeable to chloride (Cl^-) and bicarbonate (HCO_3^-) ions, as the main inhibitory neurotransmitter in the central nervous system (DeFeudis, 1975; Bormann *et al.*, 1987). Under normal conditions, binding of GABA opens the $GABA_A$ receptor channel allowing a net influx of negative charge resulting in hyperpolarization and inhibition of neuronal firing. Nilsson *et al.* (2012) proposed that the change in HCO_3^- and Cl^- gradients across the neuronal membrane, due to acid-base regulation at increased CO_2 levels, results in a net efflux of negative charge from the $GABA_A$ receptor upon GABA binding (Figure 2.2A). This could cause depolarisation and excitation of neurons, thereby altering behavioural responses. Pharmacological studies administering $GABA_A$ receptor antagonists and agonists (Chivers *et al.*, 2014; Chung *et al.*, 2014; Hamilton *et al.*, 2013; Nilsson *et al.*, 2012), and measurements of brain ion gradients (Heuer *et al.*, 2016) have supported this hypothesis in fish.

2.4 The GABA hypothesis in marine invertebrates

GABA is the main inhibitory neurotransmitter in the invertebrate peripheral and central nervous systems (Lummis, 1990; Lunt, 1991), acting on the ionotropic GABA receptor ($GABA_A$-like receptor), which is also permeable to Cl^- and HCO_3^- ions (Kaila and Voipio, 1987). Thus, the GABA hypothesis likely applies to marine invertebrates. The GABA hypothesis has been tested in marine arthropods and molluscs using pharmacological studies (Watson *et al.*, 2014; Charpentier and Cohen, 2016; Clements *et al.*, 2017), measurement of ion concentrations

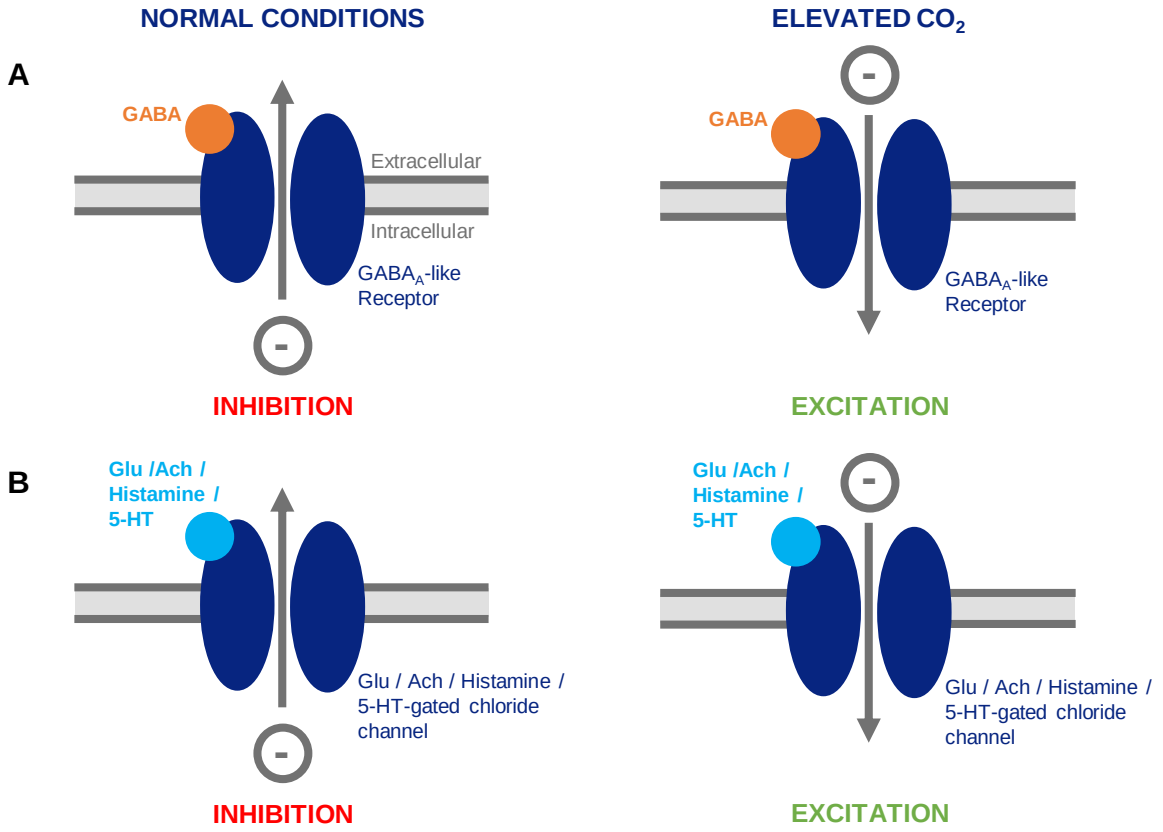

Figure 2.2. Potential reversal in function of varying LGICs at elevated CO_2 in marine invertebrates. A change in HCO_3^- and Cl^- gradients across the neuronal membrane, due to acid-base regulation at elevated CO_2, was proposed to reverse the net flow of negative charge through the $GABA_A$ receptor (Nilsson *et al.*, 2012) and likely applies to the marine invertebrate $GABA_A$-like receptor. Under normal conditions the net influx of negative charge is primarily carried by Cl^-, while at elevated CO_2 the net efflux of negative charge may be primarily carried by HCO_3^- (see Heuer *et al.* (2019) for a detailed explanation). **B** A range of invertebrates also possess glutamate, acetylcholine, histamine and serotonin-gated chloride channels. The flow of Cl^- through these channels may be similarly altered at elevated levels of CO_2. Research is needed to determine whether these receptors are also permeable to HCO_3^- which could also contribute to the reversal of the net movement of negative charge. A net influx of negative charge will result in hyperpolarisation and inhibition of neuronal firing, while a net efflux of negative charge will cause depolarisation and excitation. Glu = glutamate, ACh = acetylcholine, 5-HT = serotonin.

(de la Haye *et al.*, 2012; Charpentier and Cohen, 2016) and molecular studies (Moya *et al.*, 2016; Ren *et al.*, 2018) (Table 2.1).

One method of assessing the GABA hypothesis involves administering the $GABA_A$ receptor antagonist gabazine (SR-95531) (Heaulme *et al.*, 1986). If $GABA_A$ receptor functioning is altered at elevated CO_2, gabazine administration should reverse elevated CO_2-induced behavioural alterations by inhibiting channel opening and thus blocking the altered ion flow

(Nilsson *et al.*, 2012). Indeed, impaired escape behaviour caused by exposure to 961 µatm pCO_2 was restored to control levels by gabazine in the jumping conch snail (*Gibberulus gibbosus*) (Watson *et al.*, 2014). In the soft shell clam (*Mya arenaria*), burrowing behaviours altered by CO_2 sediment levels representing present day variation were restored by gabazine (Clements *et al.*, 2017). By contrast, in Asian shore crab larvae (*Hemigrapsus sanguineus*), the loss of chemical cue-induced photosensitive behaviour at elevated CO_2 conditions (1,380 µatm pCO_2) was not restored by gabazine (Charpentier and Cohen, 2016). These contrasting results initially appear to suggest that the GABA hypothesis applies to some, but not other, marine invertebrate taxa. However, crustacean $GABA_A$-like receptors are commonly insensitive to gabazine (El Manira and Clarac, 1991; Jackel *et al.*, 1994; Pearstein *et al.*, 1996; Barry, 2002), meaning that gabazine may be inadequate for testing the GABA hypothesis in crustaceans.

It is interesting to note that the action of gabazine differed across control animals; gabazine significantly altered the behaviour of control crab larvae (Charpentier and Cohen, 2016), had a non-significant trend of altering the behaviour of control snails (Watson *et al.*, 2014), and did not alter control clam burrowing behaviour (Clements *et al.*, 2017). As gabazine also blocks ion flow under normal conditions, preventing inhibition, over-excitation and behavioural alterations should occur in control animals. As gabazine does not appear to affect crustacean $GABA_A$-like receptors, the behavioural change observed in crabs held at control CO_2 levels may be through the action of gabazine on a different pathway, such as a different receptor type. Characterising the pharmacology of gabazine in the studied species and using a range of $GABA_A$ receptor drugs will be important to confirm the GABA hypothesis is actually being tested (see Pharmacological considerations).

Mechanistic support for the GABA hypothesis in marine invertebrates also comes from recent studies indicating changes in ion concentration and altered behaviour in the same species at elevated CO_2 (Table 2.1). Hermit crabs (*Pagurus bernhardus*) exhibited impaired chemosensory responses to a food odour and increased haemolymph Cl^- concentration ($[Cl^-]$) at extremely high (12,061 µatm pCO_2) compared to control (373 µatm pCO_2) conditions (de la Haye *et al.*, 2012). Asian shore crab larvae had altered chemical cue-induced photosensitive behaviour and increased extracellular osmolality, but similar extracellular $[Cl^-]$ at elevated CO_2 (1,380 µatm pCO_2) compared to controls (461 µatm pCO_2) (Charpentier and Cohen, 2016). However, the $[Cl^-]$ measurements were very close to the limit of detection, which may be why no difference was observed. The increased extracellular osmolality was suggested to be due to an increase in HCO_3^- concentration ($[HCO_3^-]$), however $[HCO_3^-]$ was not directly measured. In a more recent study, the California sea hare (*Aplysia californica*) exposed to elevated CO_2 (1,200 and 3,000 µatm pCO_2) showed a reduced antipredator response and increased haemolymph $[HCO_3^-]$ compared to control (400 µatm pCO_2) (Zlatkin

and Heuer, 2019). Together, these studies support the hypothesis of altered [HCO_3^-] and [Cl^-] underlying altered $GABA_A$-like receptor function and behavioural change at elevated CO_2.

Table 2.1. Summary of publications that have mechanistically tested whether LGIC-mediated neurotransmission is altered in marine invertebrates at elevated CO_2.

Species and life stage	pCO_2 (µatm) and exposure time	CO_2 Behavioural Effect	Mechanistic test	Outcome of mechanistic test	Reference
Pharmacological studies					
Hemigrapsus sanguineus Asian shore crab (Third stage larvae)	Control: 461 Treatment: 1,380 12 hours	Lost predator chemical-cue induced photosensitive behaviour	Gabazine (0.1, 1, 10 µM for 1 - 3 hours)	*Control:* 1 and 10 µM gabazine loss of chemical cue-induced photosensitive behaviour. 0.1 µM gabazine no effect. *CO_2 Treatment:* 10 µM gabazine no effect.	Charpentier and Cohen (2016)
Gibberulus gibberulus gibbosus Jumping conch snail (Adult)	Control: 405 Treatment: 961 5-7 days	Reduced jumping response to a predator	Gabazine (4 mg/L for 30 minutes)	*Control:* Gabazine had a non-significant trend of decreasing number of jumps. *CO_2 Treatment:* Gabazine restored number of jumps to control levels.	Watson *et al.* (2014)
Mya arenaria Soft shell clam (Juvenile)	Control: 1,480 Treatment: 9,532 (in sediment porewater) Clams placed on sediment surface and allowed to burrow for 20 minutes.	Decreased proportion of clams burrowing	Gabazine (5 mg/L for 30 minutes)	*Control:* No effect *CO_2 Treatment:* Gabazine increased proportion of clams burrowing to control levels	Clements *et al.* (2017)
Studies measuring ion concentration					
Hemigrapsus sanguineus Asian shore crab (Third stage larvae for $[Cl^-]$, stage 1 larvae for osmolality)	Control: 461 Treatment: 1,380 12 hours	Lost predator chemical cue-induced photosensitive behaviour	Extracellular $[Cl^-]$ Extracellular osmolality	No difference between control and treatment Increased at treatment compared to control	Charpentier and Cohen (2016)

Table 2.1 continued.

Species and life stage	pCO_2 (µatm) and exposure time	CO_2 Behavioural Effect	Mechanistic test	Outcome of mechanistic test	Reference
Pagurus bernhardus Hermit crab (Life stage not stated)	Control: 373 Treatment: 12,061 5 days	Decreased antennular flicking rates, longer to locate odour and less time in contact with odour	Haemolymph [Cl^-]	Increased at treatment compared to control	de la Haye *et al.* (2012)
Aplysia californica California sea hare (Adult)	Control: 400 Treatment: 1,200 and 3,000 4 – 11 days	No effect on self-righting behaviour, decreased time of tail withdrawal reflex	Haemolymph [HCO_3^-]	Increased in both treatments compared to control	Zlatkin and Heuer (2019)
Molecular studies					
Heliconoides inflatus Mediterranean pteropod (Life stage not stated)	Control: 382 and 410 Treatment: 617 and 720 3 days	Not tested	Whole body transcriptomic analysis	Upregulated transcripts at elevated CO_2: - 1 $GABA_A$ receptor subunit - 1 Glycine receptor subunit - 14 transcripts of acetylcholine receptor subunits (1 specified as nicotinic) - 1 Glutamate receptor subunit - 1 Glutamate transporter - 1 Voltage-gated potassium channel Downregulated transcripts at elevated CO_2: - 1 Voltage-dependent calcium channel subunit	Moya *et al.* (2016)
Portunus trituberculatus Swimming crab (Phase I juvenile)	Control: 485 Treatment: 750 and 1,500 0, 3, 6, 12, 24, 48 and 72 hours	Shoal average speed significantly higher compared to control: - 3 and 6 hours (750 µatm pCO_2) - 6 and 12 hours (1,500 µatm pCO_2)	Real-time PCR of the gene encoding the $GABA_A$ receptor associated-protein from whole crabs	mRNA levels upregulated compared to control: - 6 hours (750 µatm pCO_2) - 3 hours (1,500 µatm pCO_2)	Ren *et al.* (2018)

Molecular studies also provide support for the GABA hypothesis in marine invertebrates (Table 2.1). Transcriptomic analysis of the Mediterranean pteropod (*Heliconoides inflatus*) exposed to elevated CO_2 (617 – 720 µatm pCO_2) for three days showed upregulation of the transcript encoding a $GABA_A$ receptor subunit (Moya *et al.*, 2016). However, RNA was extracted from the whole animal, potentially masking differential expression within the nervous system, and behavioural assays were not carried out. Ren *et al.* (2018) isolated the gene encoding the $GABA_A$ receptor associated-protein (GABARAP) in a crab (*Portunus trituberculatus*). Real-time PCR found that GABARAP mRNA levels were significantly upregulated by 4.34 fold after six hours at 750 µatm pCO_2 and by 2.89 fold after three hours at 1,500 µatm pCO_2, compared to control (485 µatm pCO_2). Showing a similar trend, average speed of the crab shoal's movement was significantly higher after three and six hours at 750 µatm pCO_2, and six and 12 hours at 1,500 µatm pCO_2, compared to control. The increase in the GABARAP gene was suggested to assist more $GABA_A$ receptors to cluster on neuronal membranes, which may exaggerate the impaired function of $GABA_A$ receptors at elevated CO_2 and lead to the altered behaviour (Ren *et al.*, 2018).

2.4.1 $GABA_A$-like receptor subtypes and variability in elevated CO_2-induced behavioural alterations

Inter- and intra-species variation in the behavioural effects of elevated CO_2 may be due to the presence and variability of $GABA_A$-like receptor subtypes in invertebrates. The ion permeable pore of $GABA_A$-like receptors is made up of 5 subunits (Olsen and Sieghart, 2008). There is large variation in gene structure and the number of genes encoding $GABA_A$-like receptor subunits between invertebrate species. For example, 5 GABA R-like genes have been found in the sea-squirt *Ciona intestinalis*, 12 in the fruitfly *Drosophila melanogaster* and 39 in the roundworm *Caenorhabditis elegans* (Tsang *et al.*, 2007). Differing subunit composition forms $GABA_A$-like receptor subtypes (Olsen and Sieghart, 2008) which vary in a range of functional properties including GABA binding affinity, and Cl^- and HCO_3^- permeability (Lee and Maguire, 2014). Differences in $GABA_A$-like receptor subunits may account for the variability in behavioural alterations at elevated CO_2 observed between invertebrate species. Furthermore, subunit composition can vary between regions in the nervous system and cell types (Lee and Maguire, 2014). As different behaviours are driven by different nervous system regions, this may explain why some behaviours, but not others, are disrupted by elevated CO_2 within a species.

2.4.2 Pharmacological considerations

Studies using gabazine have provided a useful starting point to understand the mechanisms underlying behavioural alterations at elevated CO_2 in marine invertebrates. However, the pharmacological profile of invertebrate $GABA_A$-like receptors differs from that of vertebrate $GABA_A$ receptors (Rauh *et al.*, 1990), and have not been characterized as extensively as in vertebrates. The majority of invertebrate research has been in non-marine invertebrates, with invertebrate $GABA_A$-like receptor pharmacology being best studied in insects due to their potential target for insecticides (Hosie *et al.*, 1995; Bloomquist, 2003). Gabazine inhibits a cloned planthopper $GABA_A$-like receptor subunit expressed in a cell line (Narusuye *et al.*, 2007) and two cloned fruit fly $GABA_A$-like receptor subunits expressed in *Xaenopus laevis* oocytes (Hosie and Sattelle, 1996). Gabazine also inhibits $GABA_A$-like receptors in native neurons of locusts (Janssen *et al.*, 2010) and moths (Satoh *et al.*, 2005), but not in cockroaches (Aydar and Beadle, 1999). The few studies in other diverse invertebrates are conflicting, gabazine inhibits $GABA_A$-like receptors in a freshwater hydrozoan (Concas *et al.*, 1998), only weakly antagonizes GABA responses in a terrestrial nematode (Duittoz and Martin, 1991) and has no effect on crustaceans, including a freshwater crayfish (El Manira and Clarac, 1991; Pearstein *et al.*, 1996) and a marine lobster (Jackel *et al.*, 1994). These non-marine examples are more taxonomically relevant to marine invertebrates than comparisons with evolutionarily divergent marine vertebrate taxa. They indicate the wide variability in invertebrate $GABA_A$-like receptor responses to gabazine. As $GABA_A$-like receptor pharmacology can differ by subunit composition (Lee and Maguire, 2014; Sieghart, 2015) and there is large variation in subunit genes between invertebrates (Tsang *et al.*, 2007) it will be useful to characterize the pharmacology of gabazine on $GABA_A$-like receptors in the studied marine invertebrate species.

It is also important to note that antagonists are commonly not completely specific. For example, in insects gabazine partially, and bicuculline (a $GABA_A$ receptor antagonist) fully, inhibits locust nicotinic acetylcholine receptors (Jackson *et al.*, 2002), and the $GABA_A$ receptor antagonist bicuculline inhibits and the $GABA_A$ receptor agonist muscimol activates a model of insect GABA-gated cation channels (Gisselmann *et al.*, 2004). Less research has studied the off-target effects of GABA drugs in marine invertebrates, though bicuculline and picrotoxin both inhibit acetylcholine-gated chloride channels in the California sea hare (*Aplysia californica*) (Yarowsky and Carpenter, 1978a). To ensure the low affinity, alternative effects of drugs do not occur, careful consideration of concentration administered must be made. Using a range of $GABA_A$ receptor drugs with differing side effects will provide further evidence for or against the role of $GABA_A$-like receptors in behavioural alterations at elevated CO_2.

2.4.3 Marine invertebrate acid-base regulatory mechanisms and the GABA hypothesis

Acid-base regulatory mechanisms in marine invertebrates indicate that extra- and intracellular [HCO_3^-] and [Cl^-] will alter at elevated CO_2, providing theoretical support for the GABA hypothesis. Such mechanisms have best been studied in crustaceans (see reviews by Henry and Wheatly (1992); Wheatly and Henry (1992)). The primary mechanism to maintain extracellular pH (pH_e) is via ion exchange with the external water environment (Cameron, 1985; Wheatly and Henry, 1992; Pörtner *et al.*, 1998), including HCO_3^- influx in exchange for Cl^- efflux (Truchot, 1983; Wheatly and Henry, 1992). Indeed, in many marine invertebrates $[HCO_3^-]_e$ in the blood/haemolymph increases upon exposure to elevated seawater CO_2. Exposure to pCO_2 of 15 and 30 mm Hg (~20,000 and 40,000 µatm pCO_2) increased haemolymph [HCO_3^-] and decreased haemolymph [Cl^-] compared to control conditions in the blue crab (*Callinectes sapidus*) (Cameron and Iwama, 1987). At a pCO_2 of 45 mm Hg (~60,000 µatm pCO_2) in the same species, haemolymph [HCO_3^-] also increased, however haemolymph [Cl^-] increased (Cameron and Iwama, 1987), and 12,061 µatm pCO_2 increased haemolymph [Cl^-] compared to control (373 µatm pCO_2) in a hermit crab (*Pagurus bernhardus*) (de la Haye *et al.*, 2012). In palemonid shrimps, exposure to 0.3 kPa CO_2 (~3,000 µatm pCO_2) decreased haemolymph [Cl^-] in the high shore *Palaemonidae elegans*, but increased haemolymph [Cl^-] in the subtidal *Palaemonidae serratus* (Dissanayake *et al.*, 2010). Thus, changes in both $[HCO_3^-]_e$ and $[Cl^-]_e$ at elevated CO_2 support the role of compensatory acid-base regulation as a key part of the GABA hypothesis, although studies at CO_2 levels more relevant to future scenarios, such as ~1,000 µatm CO_2, would be valuable.

Intracellular pH (pH_i) is also regulated via ion exchange (Walsh and Milligan, 1989), including Na^+ dependent Cl^-/HCO_3^- exchange (Roos and Boron, 1981), as seen in muscle fibres of the sipunculid worm (Pörtner *et al.*, 2000), crayfish (Galler and Moser, 1986) and barnacle (Boron, 1977; Boron *et al.*, 1981), as well as in crayfish neurons (Moody Jr, 1981) and the squid giant axon (Russell and Boron, 1976; Boron and Russell, 1983). This suggests that $[HCO_3^-]_i$ increases and $[Cl^-]_i$ decreases in order to maintain pH_i. To date, neural $[HCO_3^-]_i$ has not been measured in a marine invertebrate exposed to elevated CO_2. However, in a sipunculid worm (*Sipunculus nudus*) muscle $[HCO_3^-]_i$ significantly increased over 96 hours in 1% CO_2 (~10,000 µatm pCO_2) in air (Pörtner *et al.*, 1998). A net efflux of Cl^- is observed from the squid giant axon at a pH_i of 6.5 reached by intracellular acid administration (Boron and Russell, 1983), and in crayfish isolated abdominal ganglia the resting $[Cl^-]_i$ (35 mM) decreased by 3 – 5 mM when exposed to Ringer's solution equilibrated with 5% CO_2 (~10,000 µatm pCO_2) (Moody Jr, 1981). Therefore, changes in $[HCO_3^-]_i$ and $[Cl^-]_i$ occur in marine invertebrates exposed to extremely high levels of CO_2. Again, studies using CO_2 levels more

relevant to future scenarios will be important to understand the theory underlying the GABA hypothesis.

It is unknown whether the above changes in $[Cl^-]_{i/e}$ and $[HCO_3^-]_{i/e}$ are sufficient to alter $GABA_A$-like receptor functioning. For elevated CO_2 to disrupt GABA functioning, it is not simply altered $[HCO_3^-]$ and $[Cl^-]$, but a difference in ion gradients across neuronal membranes that will alter ion flow through the $GABA_A$-like receptor, i.e. $[Cl^-]_i$ and $[HCO_3^-]_i$ within neurons must change by a different amount to $[Cl^-]_e$ and $[HCO_3^-]_e$ present in the fluid bathing the neurons (Nilsson and Lefevre, 2016). A useful way to determine whether the changes in $[HCO_3^-]$ and $[Cl^-]$ can alter ion flow through the $GABA_A$-like receptor is by determining the GABA reversal potential (E_{GABA}) and comparing it to the neuronal resting membrane potential (see Heuer *et al.* (2019); Tresguerres and Hamilton (2017) for a detailed explanation). This approach has previously been employed to demonstrate that altered $[Cl^-]$ and $[HCO_3^-]$ at elevated CO_2 could change $GABA_A$ receptor function in the spiny damselfish (*Acanthochromis polyacanthus*) (Heuer *et al.*, 2016).

Calculating E_{GABA} requires knowledge of the HCO_3^-/Cl^- permeability ratio of the $GABA_A$-like receptor, and $[HCO_3^-]_i$, $[Cl^-]_i$, $[HCO_3^-]_e$ and $[Cl^-]_e$ at both control and elevated CO_2 conditions. The HCO_3^-/Cl^- permeability ratio is estimated to be between 0.2 – 0.6 in crayfish muscle fibres (Kaila and Voipio, 1987; Kaila *et al.*, 1989; Farrant and Kaila, 2007), indicating that the $GABA_A$-like receptor is more permeable to Cl^- than it is to HCO_3^-. However, this permeability ratio is unknown for other invertebrates. It is important to ensure ion concentration measurements are taken in the correct fluids. In most marine invertebrates no blood brain barrier is present (Cserr and Bundgaard, 1984) and measuring extracellular ion concentration in the haemolymph may be adequate. However, structural organisation of nervous tissue may provide some regulation of the neuronal microenvironment (Cserr and Bundgaard, 1984). Cephalopods have a blood brain barrier separating the blood from the brain (Cserr and Bundgaard, 1984) and extracellular measurements should be made in the brain interstitial fluid that bathes the neurons. It is also vital intracellular measurements are done on neuronal cytoplasm, as pH_i regulatory mechanisms can differ between different cell types (Wheatly and Henry, 1992). Studies measuring these parameters and calculating E_{GABA} in a marine invertebrate exposed to elevated CO_2 will be useful to understand if altered $[Cl^-]$ and $[HCO_3^-]$ could change $GABA_A$-like receptor function.

2.4.4 The effects of altered $GABA_A$-like receptor functioning

Altered $GABA_A$-like receptor functioning is likely to disrupt behaviours due to the role of $GABA_A$-like receptor-mediated neurotransmission in invertebrate sensation and a range of behavioural outputs. In molluscs, GABA is present in the olfactory, chemoreceptive (Nezlin and Voronezhskaya, 1997; Ito *et al.*, 2001; Kobayashi *et al.*, 2008), nociceptive (Kava-

liers *et al.*, 1999), visual and vestibular (Yamoah and Kuzirian, 1994) systems. $GABA_A$-like receptor signalling mediates molluscan nociception (Kavaliers *et al.*, 1999) and visual-vestibular interaction (Alkon *et al.*, 1993), while mollusc photoreceptors respond to $GABA_A$-like receptor signalling (Yamoah and Kuzirian, 1994). $GABA_A$-like receptor-mediated signalling is important for feeding and prey-capture behaviours in molluscs (Arshavsky *et al.*, 1993; Norekian and Satterlie, 1993; Romanova *et al.*, 1996; Jing *et al.*, 2003; Norekian and Malyshev, 2005) and a cnidarian (Pierobon *et al.*, 1995; Concas *et al.*, 1998; Pierobon *et al.*, 2004), and GABAergic neurons are associated with effectors of feeding in a sea urchin (Bisgrove and Burke, 1987). $GABA_A$-like receptor signalling mediates swimming of larval sea urchins (Katow *et al.*, 2013), the righting response in a sea urchin (Shelley *et al.*, 2019) and locomotion of a mollusc (Romanova *et al.*, 1996). GABA mediates settling and metamorphosis, including associated behavioural changes in a range of molluscs (Morse *et al.*, 1979, 1980; García-Lavandeira *et al.*, 2005; Stewart *et al.*, 2011; Biscocho *et al.*, 2018), an echinoderm (Pearce and Scheibling, 1990) and a urochordate (Danqing *et al.*, 2006). GABA is thought to mimic ligands from the environment (Morse *et al.*, 1979) which may be detected by the $GABA_A$-like receptor (Stewart *et al.*, 2011) to initiate settlement and metamorphosis. Internal $GABA_A$-like receptor mediated neurotransmission is also suggested to regulate metamorphosis (Biscocho *et al.*, 2018). Thus altered $GABA_A$-like receptor function will likely affect a variety of behaviours in a range of marine invertebrates.

Neural processes other than behaviour may also be affected by altered $GABA_A$-like receptor functioning. In vertebrates, GABA can act as a trophic factor (a molecule supporting cell survival) through the $GABA_A$ receptor, influencing cell proliferation, migration and differentiation (Owens and Kriegstein, 2002; Sernagor *et al.*, 2010). In a fish, the three-spined stickleback (*Gasterosteus aculeatus*), genes involved in neurogenesis and neuroplasticity were upregulated after exposure to ~1,000 µatm pCO_2 compared to control (~330 µatm pCO_2) (Lai *et al.*, 2017). Similarly, GABA induces cellular differentiation and proliferation in abalone larvae (Morse *et al.*, 1980). Thus, elevated CO_2 may alter neurogenesis in marine invertebrates.

GABA can also have effects in non-neural tissue, playing an important role in the vertebrate immune system (Barragan *et al.*, 2015; Wu *et al.*, 2017). Invertebrate GABA also appears to play an immunomodulatory role. The $GABA_A$-like receptor associated protein is implicated in the immune response of the abalone (Bai *et al.*, 2012), GABA in the immune response of an oyster (Li *et al.*, 2016a) and mussel (Nguyen *et al.*, 2018), and a homologue of the glutamic acid decarboxylase (a rate limiting enzyme in GABA production) in immune regulation of an oyster (Li *et al.*, 2016b). Thus, altered $GABA_A$-like receptor functioning at elevated CO_2 may have widespread effects.

Cross-talk between neurotransmitter receptors may also result in widespread effects of

altered $GABA_A$-like receptor functioning. Different types of neurotransmitters can be co-released from the same nerve terminal, resulting in simultaneous activation of their specific receptors, co-localised at the same post-synaptic site. This simultaneous activation can result in cross-talk between the receptors, modulating signal transmission. For example, negative cross-talk occurs when two different neurotransmitters simultaneously bind to their specific receptors, resulting in a current smaller than the sum of the currents of these two neurotransmitters acting separately (Li *et al.*, 2003). Cross-talk involving $GABA_A$ receptors is well documented in mammals. For example, $GABA_A$ receptor activation suppresses the function of a dopamine receptor (de la Mora *et al.*, 1997) and negative cross-talk occurs in both directions between $GABA_A$ receptors and glycine Rs (Trombley *et al.*, 1999; Li *et al.*, 2003) and $GABA_A$ receptors and the adenosine-triphosphate receptor P2X (Karanjia *et al.*, 2006; Toulmé *et al.*, 2007). Neurotransmitter cross-talk is yet to be studied in an invertebrate, but co-release of neurotransmitters occurs in the marine invertebrate nervous system, such as proctolin and GABA in crabs (Blitz *et al.*, 1999), and dopamine and GABA in the California sea hare (*Aplysia californica*) (Díaz-Ríos *et al.*, 2002; Díaz-Ríos and Miller, 2005; Svensson *et al.*, 2014). Furthermore, GABA has been found to post-synaptically increase dopamine currents in *A. californica* (Svensson *et al.*, 2014). If cross-talk is present between invertebrate $GABA_A$-like receptors and other neurotransmitter Rs, altered functioning of the $GABA_A$-like receptor at elevated CO_2 may alter cross-talk mechanisms. Thus, altered $GABA_A$-like receptor function at elevated CO_2 would not only alter the GABAergic pathway, but other pathways as well.

2.5 Alternative mechanisms for behavioural change at elevated CO_2

If elevated CO_2 does alter HCO_3^- and Cl^- gradients across neuronal membranes, it is likely that functioning of LGICs other than the $GABA_A$-like/$GABA_A$ receptor, that are also permeable to these ions, will also be disrupted (Figure 2.2). In vertebrates, altered glycine receptor functioning at elevated CO_2 has been suggested due to its similarity to the $GABA_A$ receptor (Tresguerres and Hamilton, 2017). Many invertebrates lack glycine receptors (Tsang *et al.*, 2007), however invertebrates possess a larger variety of ligand-gated ion channels (LGICs) than vertebrates (Dent, 2010). Glutamate-gated chloride channels have been found in molluscs (Kehoe and Vulfius, 2000; Kehoe *et al.*, 2009) and crustaceans (Marder and Paupardin-Tritsch, 1978), and are suggested to be the invertebrate equivalent of vertebrate glycine Rs (Vassilatis *et al.*, 1997; Kehoe and Vulfius, 2000). There is also evidence for acetylcholine-gated chloride channels in molluscs (Kehoe, 1972). Moya *et al.* (2016) found a range of ner-

vous system transcripts differentially expressed at elevated CO_2 in a pteropod (*Heliconoides inflatus*), including genes encoding for the LGICs (and associated proteins) of cholinergic, GABAergic, glutamatergic and glycinergic-like synapses (Moya *et al.*, 2016) (Table 2.1). Thus, altered [Cl^-] can conceivably disrupt functioning of a range of LGICs (Figure 2.2). Furthermore, taxa specific differences in the presence of specific LGICs (Dent, 2010) may explain the variability of the effects of elevated CO_2 on marine invertebrate behaviour.

Elevated CO_2 may not only disrupt neurotransmission, but also neuronal-glial and glial-glial signalling. Glia are non-neuronal cells present in the vertebrate and invertebrate nervous system (Pentreath, 1989; Laming *et al.*, 2000). Initially thought to be restricted to supporting neurons, the role of glia is now understood to include active participation in nervous system functioning, thus contributing to behaviour (Laming *et al.*, 2000; Jackson and Haydon, 2008). Like many other cell types, glial cells regulate pH_i via ion exchange, including HCO_3^-/Cl^- exchange (Deitmer and Rose, 1996). $GABA_A$ receptors are present in vertebrate glial cells (Butt and Jennings, 1994; Fraser *et al.*, 1994). Less research has been carried out on invertebrate glia, with no research on the presence of $GABA_A$-like receptors on marine invertebrate glial cells. However, leech glial cells reportedly respond to GABA (unpublished work reported in Deitmer and Rose (1996)). If marine invertebrates are found to express $GABA_A$-like receptors, elevated CO_2 may also affect information processing through glial cells. Furthermore, fluxes in H^+ ions have been found to contribute to neuron-glia signalling (Deitmer and Rose, 1996; Laming *et al.*, 2000), which may be disrupted by exposure to elevated CO_2 (and the resultant increase in H^+ ions).

Changes in [Cl^-] due to acid-base regulatory mechanisms at elevated CO_2 may affect LGIC-mediated neurotransmission through a different mechanism, as well as having alternative effects on the nervous system. Cl^- has a role as a signalling effector, with changes in $[Cl^-]_i$ affecting a range of processes including gene expression, protein activity and cell proliferation (Valdivieso and Santa-Coloma, 2019). Mammalian work has supported the role of Cl^- as a signalling effector in the nervous system, including $[Cl^-]_i$ regulation of $GABA_A$ receptor expression (Succol *et al.*, 2012) and growth of neuronal processes (Nakajima and Marunaka, 2016). The role of Cl^- as a signalling anion has also been observed in bacterial cells, suggesting a conserved function (Valdivieso and Santa-Coloma, 2019). Thus, invertebrate Cl^- is also likely to act as a signalling effector. If altered [Cl^-]i has similar effects in marine invertebrates, elevated CO_2 may impact nervous system functioning not only by altered $GABA_A$-like receptor function but also changes in $GABA_A$-like receptor expression, as well as altered growth of neuronal projections. Thus, altered $[Cl^-]_i$ at elevated CO_2 may

have effects additional to altered LGIC function, having widespread consequences.

2.6 Directions for future research

Mechanistic studies have used targeted approaches to assess the GABA hypotheses in marine invertebrates. These approaches will also be useful to assess potential alternative mechanisms by which elevated CO_2 may alter marine invertebrate behaviour (Figure 2.3). The GABA hypothesis has been pharmacologically assessed by administering the $GABA_A$ receptor antagonist gabazine to marine invertebrates (Watson *et al.*, 2014; Clements *et al.*, 2017). Likewise, the administration of pharmacological agents targeting different LGICs will be useful to assess whether altered functioning of alternative LGICs may underlie behavioural changes at elevated CO_2 conditions. Due to the diversity of invertebrates and the potential for off-target effects, it will be important to use a range of pharmacological agents, particularly those shown to work in the invertebrate taxa being studied. Furthermore, pilot studies to determine the optimal drug concentration to use will be important. For example, Charpentier and Cohen (2016) tested three gabazine concentrations. Measurement of ion concentrations at control and elevated levels of CO_2 in conjunction with behavioural tests has been carried out in crabs (de la Haye *et al.*, 2012; Charpentier and Cohen, 2016) and a mollusc (Zlatkin and Heuer, 2019). Future studies in other invertebrate taxa, with measurements made within the correct intra- and extra-cellular fluids, as well as determining the HCO_3^- /Cl^- permeability ratio will be important to calculate E_{GABA} at elevated CO_2 to theoretically assess the GABA hypothesis. Real-time PCR, measuring the expression level of a specific gene, has been employed to assess the GABA hypothesis in a crab (Ren *et al.*, 2018) and will also be useful to assess alternative mechanisms, e.g. measuring the expression of genes encoding for alternative LGIC subunits, and genes involved in neuronal growth and proliferation.

These targeted approaches, however, may leave potentially relevant information unexplored. Omic technologies, such as transcriptomics and proteomics, provide a non-targeted approach in which *a priori* hypotheses are not required (Figure 2.3). Thus, data from omic approaches could unveil patterns leading to the development of novel hypotheses. For example, transcriptomics and proteomics have already been employed in fish nervous tissue, providing support for the GABA hypothesis as well as new avenues to pursue (Schunter *et al.*, 2016; Porteus *et al.*, 2018; Schunter *et al.*, 2018; Williams *et al.*, 2019).

In marine invertebrates exposed to control and elevated CO_2 levels, transcriptomic studies so far have analysed the whole animal and have focused on pteropods (Koh *et al.*, 2015; Maas *et al.*, 2015; Moya *et al.*, 2016; Thabet *et al.*, 2017) and sea urchins (Evans *et al.*, 2013; Padilla-Gamiño *et al.*, 2013; Todgham and Hofmann, 2008; Clark *et al.*, 2019). Likewise, proteomic studies have analysed the whole body of tubeworm larvae (Mukherjee *et al.*, 2013), oyster larvae (Dineshram *et al.*, 2012, 2013), barnacle larvae (Wong *et al.*, 2011),

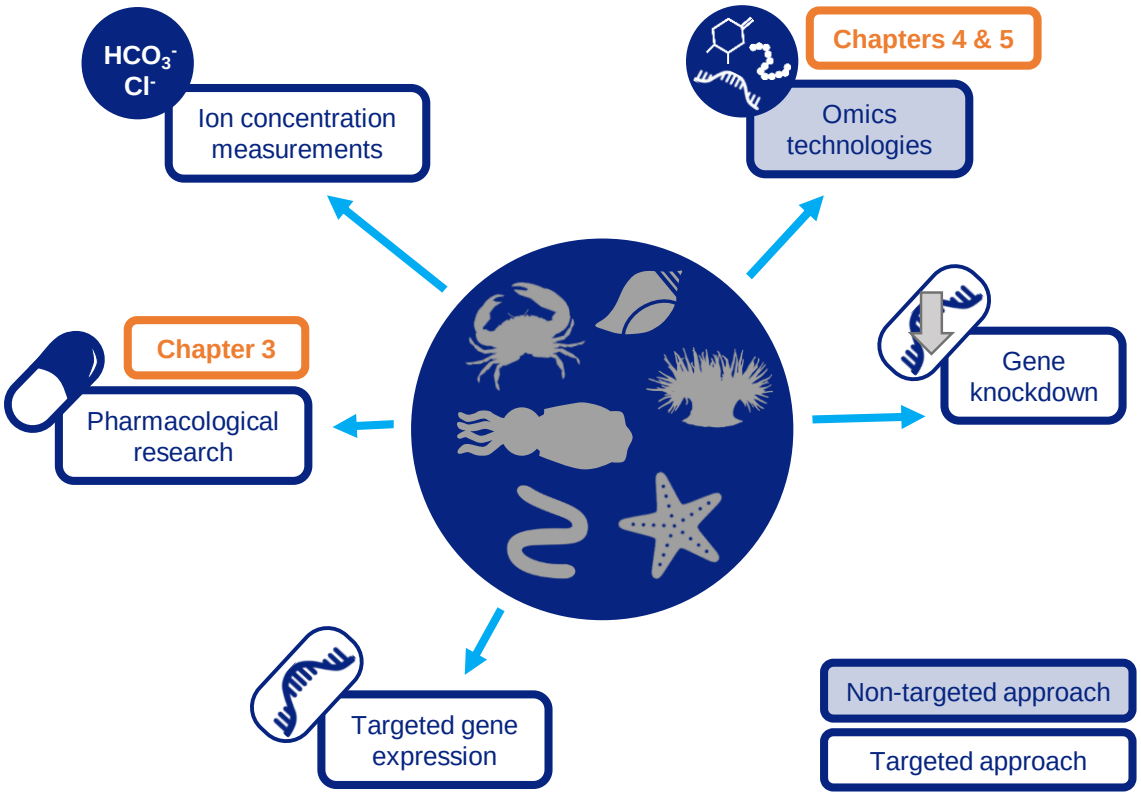

Figure 2.3. Future directions for neurobiological mehanistic research in marine invertebrates. Conceptual diagram illustrating the techniques that will be useful for future research to assess the neurobiological mechanisms underlying behavioural change at elevated CO_2 in marine invertebrates. Targeted approaches will test specific hypotheses and include pharmacological research administering drugs that target a specific receptor, measuring the expression of specific genes, measuring the concentration of HCO_3^- and Cl^- ions in the relevant intra- and extra-cellular fluids, and knocking down the expression of specific genes. Omic techniques such as transcriptomics, proteomics and epigenomics will provide a non-targeted approach which does not require *a priori* hypotheses and will likely lead to the development of new hypotheses. These knowledge gaps guided the data chapters in this thesis; Chapter 3 addressed the knowledge gap in pharmacological research and Chapter 4 and Chapter 5 used transcriptomics as a non-targeted, holistic approach. Icons from NounProject.com (worm by Deemak Daksina, anemone by Vega Asensio, crab by Ed Harrison, starfish by Stanislav Levin), remaining icons by Jodi Thomas.

sea snail larvae (Di *et al.*, 2019) and clam larvae (Timmins-Schiffman *et al.*, 2019), and a metabolomics study analysed the whole body of a crab (Trigg *et al.*, 2019) exposed to control or elevated CO_2. To understand the neurobiological mechanisms underlying behavioural changes, rather than the general molecular response to elevated CO_2, it will be important to carry out omic techniques on the nervous tissue, as measurements at the whole body level may mask differential expression in the nervous system due to the heterogeneity and complexity of gene/protein expression. This is exemplified by Liu *et al.* (2019) who found region-specific

regulation of neuropeptides in the nervous tissue of crabs (*Callinectes sapidus*) exposed to elevated CO_2.

Omic technologies will provide a powerful, holistic approach to explore neurobiological mechanisms underlying behavioural change, potentially leading to the development of novel hypotheses. However, omic approaches can only determine correlational, and not causative, links between expression and behaviour. Gene knockdown, in which the expression of a specific gene is reduced, will be a promising avenue for future research to determine a causative link between gene expression and behavioural change at elevated CO_2. Gene knockdown is yet to be used in elevated CO_2 behavioural research, however gene knockdown of a heat shock protein assessed the stress tolerance of the white leg shrimp (*Litopenaeus vannamei*) to high CO_2 (Aishi *et al.*, 2019).

2.7 Conclusion

There is large variability in the effects of elevated CO_2 on marine invertebrate behaviour, which is likely due to the incredible diversity of marine invertebrates. Elevated CO_2 likely alters behaviour via a range of mechanisms that disrupt the nervous system pathway producing behaviour, from sensory input to behavioural output. These mechanisms are not necessarily mutually exclusive, and interactions between mechanisms may account for the diversity in responses. Many of these mechanisms are based on theory and lack solid experimental evidence. Mechanistic research addressing these gaps will be important, for example linking altered sensation at elevated CO_2 to behavioural change. Mechanistic fish research has focused on altered neurotransmission via disrupted $GABA_A$ receptor functioning at elevated CO_2. The GABA hypothesis, as well as altered functioning of other LGICs, likely applies to marine invertebrates. Further research into the ionic properties of the $GABA_A$-like receptor and other LGICs, including whether they are also permeable to HCO_3^-, and measuring intra- and extra-cellular ion levels in the relevant fluids at near-future CO_2 levels will be beneficial for advancing our understanding of this mechanism. The diversity of LGIC subtypes between invertebrate species, and even between nervous system regions, may explain the variability in behavioural responses. Investigating the presence of LGICs on invertebrate glial cells, other modes of neuronal-glial and glial-glial transmission, and the role of Cl^- as a signalling effector in invertebrates will help us understand the wider impact elevated CO_2 may have on nervous system functioning.

The interconnectivity of the nervous system, such as receptor cross-talk, suggests that even disruption of one component or pathway will have widespread effects. This will make understanding the neurobiological mechanisms underlying elevated CO_2-induced behavioural change extremely complex. Omics approaches will be useful in providing an untargeted,

holistic approach to understand the response of the nervous system to elevated CO_2, provide support or opposition for proposed mechanisms, and likely provide new avenues to explore. Exploring the mechanisms underlying behavioural change at elevated CO_2 will help us to understand the variability in behavioural responses to elevated CO_2 and predict which marine invertebrates are likely to be the most vulnerable to rising CO_2 levels.

Chapter 3

The role of ligand-gated chloride channels in behavioural alterations at elevated CO_2 in a cephalopod

A version of this chapter is published:
Thomas, J.T., Spady, B.L., Munday, P.L. and Watson, S.-A. (2021). The role of ligand-gated chloride channels in behavioural alterations at elevated CO_2 in a cephalopod. *Journal of Experimental Biology*. **224**, jeb242335. URL https://doi.org/10.1242/jeb.242335

Difference between this chapter and published paper:
Minor formatting changes. A diagram of the behavioural trial set-up (page 50) and a paragraph discussing acid-base regulation in cephalopods (page 66) have been added.

Data availability:
All raw data and scripts accompanying this chapter are available at https://doi.org/10.25903/y6kz-hm11

3.1 Abstract

Projected future carbon dioxide (CO_2) levels in the ocean can alter marine animal behaviours. Disrupted functioning of γ-aminobutyric acid type A ($GABA_A$) receptors (ligand-gated chloride channels) is suggested to underlie CO_2-induced behavioural changes in fish. However, the mechanisms underlying behavioural changes in marine invertebrates are poorly understood. I pharmacologically tested the role of GABA-, glutamate-, acetylcholine- and dopamine-gated chloride channels in CO_2-induced behavioural changes in a cephalopod, the two-toned pygmy squid (*Idiosepius pygmaeus*). I exposed squid to current-day (~450 µatm) or elevated (~1,000 µatm) CO_2 for seven days. Squid were treated with sham, the $GABA_A$ receptor antagonist gabazine, or the non-specific $GABA_A$ receptor antagonist picrotoxin, before measurement of conspecific-directed behaviours and activity levels upon mirror exposure. Elevated CO_2 increased conspecific-directed attraction and aggression, as well as activity levels. For some CO_2-affected behaviours (time spent in a zone closest to the mirror, active time and distance moved), both gabazine and picrotoxin had a different effect at elevated compared to current-day CO_2, providing robust support for the GABA hypothesis within cephalopods. In another behavioural trait (latency to the first soft mirror touch), picrotoxin but not gabazine had a different effect in elevated compared to current-day CO_2, providing the first pharmacological evidence, in fish and marine invertebrates, for altered functioning of ligand-gated chloride channels, other than the $GABA_A$ receptor, underlying CO_2-induced behavioural changes. For some other behaviours (proportion of squid that touched the mirror aggressively, number of aggressive mirror touches and average speed), both gabazine and picrotoxin had a similar effect in elevated and current-day CO_2, suggesting altered function of ligand-gated chloride channels was not responsible for these CO_2-induced changes. Multiple mechanisms may be involved, which could explain the variability in the CO_2 and drug treatment effects across behaviours.

3.2 Introduction

Anthropogenic carbon dioxide (CO_2) emissions are being absorbed by the oceans at an increasing rate, resulting in reduced seawater pH referred to as ocean acidification (Bindoff *et al.*, 2019). Elevated CO_2 levels are known to alter a range of behaviours in a variety of fishes (Munday *et al.*, 2019). Elevated CO_2-induced behavioural alterations also occur in some marine invertebrates, including in cnidarians, polychaetes, echinoderms, arthropods and molluscs, across a variety of behavioural traits (reviewed in Clements and Hunt (2015); Nagelkerken and Munday (2015) and Chapter 2). The behavioural effects of elevated CO_2 are variable. Elevated CO_2 may affect some, but not other, behaviours within the same species. For example, in the blue mussel elevated CO_2 decreased predator cue-induced defensive behaviours (Kong *et al.*, 2019) and feeding rates (Gu *et al.*, 2019; Meseck *et al.*, 2020), but did not alter a startle response behaviour (Clements *et al.*, 2021). The effects of elevated CO_2 on the same behaviour may also be variable among taxa. For example, within molluscs elevated CO_2 increased locomotion speed in two species of squid (Spady *et al.*, 2014, 2018) but reduced speed in a third squid species (Zakroff *et al.*, 2018), a sea hare (Horwitz *et al.*, 2020), and two whelk species (Queirós *et al.*, 2015; Fonseca *et al.*, 2020). A mechanistic understanding of behavioural change at elevated CO_2 is important to determine why there is such variability in behavioural alterations and to identify which animals will be most vulnerable to rising CO_2 levels. However, the mechanisms underlying behavioural change at elevated CO_2 across the diverse range of marine invertebrates are poorly understood (Chapter 2).

The prominent mechanistic explanation for elevated CO_2-induced behavioural alterations is the GABA hypothesis, first demonstrated in two species of tropical coral reef fish (Nilsson *et al.*, 2012). In vertebrates, the γ-aminobutyric acid type A receptor ($GABA_A$ receptor) is a ligand-gated ion channel (LGIC)/ionotropic receptor selectively permeable to chloride (Cl^-) and bicarbonate (HCO_3^-) ions (Krnjević, 1974; Bormann *et al.*, 1987). Under normal conditions, binding of the neurotransmitter GABA opens the $GABA_A$ receptor channel, which usually allows a net influx of negative charge resulting in hyperpolarisation and inhibition of neuronal firing. At elevated CO_2 conditions, Nilsson *et al.* (2012) proposed that alterations in Cl^- and HCO_3^- ion gradients across the neuronal membrane, due to acid-base regulation, could alter the function of $GABA_A$ receptors. The change in ion gradients was suggested to reverse the net flow of negative ions, resulting in a net efflux of negative charge from some $GABA_A$ receptors, switching their function from inhibitory to excitatory, thus influencing behavioural responses (see Heuer *et al.* (2019) for a detailed explanation). Pharmacological studies have supported the GABA hypothesis in fish; administration of the $GABA_A$ receptor antagonist gabazine (SR-95531) (Heaulme *et al.*, 1986) attenuated CO_2-induced behavioural alterations (Nilsson *et al.*, 2012; Chivers *et al.*, 2014; Chung *et al.*, 2014; Lai *et al.*, 2015;

Lopes *et al.*, 2016; Regan *et al.*, 2016) and the $GABA_A$ receptor agonist muscimol (Andrews and Johnston, 1979) produced opposite effects in elevated and control CO_2 exposed fish (Hamilton *et al.*, 2013). Recently, the GABA hypothesis has been further refined by the proposal that altered functioning of some $GABA_A$ receptors initiates a vicious self-amplifying cycle, explaining how relatively small changes in ion gradients can result in large behavioural alterations (Schunter *et al.*, 2019).

Invertebrate GABA also binds to Cl^- and HCO_3^- permeable ionotropic $GABA_A$ receptors (referred to as $GABA_A$-like receptors throughout this manuscript to differentiate invertebrate from vertebrate $GABA_A$ receptors) (Kaila and Voipio, 1987; Lunt, 1991). Therefore, the GABA hypothesis should theoretically apply to invertebrates as well. Administration of the $GABA_A$ receptor antagonist gabazine has been used to test the GABA hypothesis in several marine invertebrates. In a gastropod mollusc, the jumping conch snail (*Gibberulus gibberulus gibbosus*), impaired escape behaviour at elevated CO_2 levels (961 µatm) was restored to control levels by gabazine (Watson *et al.*, 2014). In a bivalve mollusc, the soft-shell clam (*Mya arenaria*), burrowing behaviours altered at elevated sediment CO_2 levels (9,532 µatm) were also restored to control levels by gabazine (Clements *et al.*, 2017). In contrast, gabazine did not restore lost chemical-cue induced photosensitive behaviour at elevated CO_2 (1,380 µatm) in Asian shore crab larvae (*Hemigrapsus sanguineus*) (Charpentier and Cohen, 2016). Electrophysiological studies have shown crustacean $GABA_A$-like receptors to be insensitive to gabazine (El Manira and Clarac, 1991; Jackel *et al.*, 1994; Pearstein *et al.*, 1996) and thus gabazine may not have tested the GABA hypothesis in *H. sanguineus*. However, as pharmacological sensitivity of receptors can vary between differing cell types (Lee and Maguire, 2014) and only specific neurons were tested in these electrophysiological studies, it is possible that other crustacean cell types are sensitive to gabazine. Thus, systemic gabazine administration by Charpentier and Cohen (2016) could have tested the GABA hypothesis. If this is the case, it suggests the GABA hypothesis may apply to some, but not other, invertebrate taxa.

To date, pharmacological studies assessing the GABA hypothesis in marine invertebrates have exclusively used gabazine. This has provided a useful starting point to understand elevated CO_2-induced behavioural changes. However, gabazine's action in the invertebrate taxa studied to date is not well characterised. The pharmacological profile of invertebrate $GABA_A$-like receptors differs from that of vertebrate $GABA_A$ receptors (Lunt, 1991; Walker *et al.*, 1996). Furthermore, the invertebrates span an enormous amount of phylogenetic variation and invertebrate LGICs can differ across taxa (Tsang *et al.*, 2007; Wolstenholme, 2012). Thus, the action of $GABA_A$ receptor antagonists, such as gabazine, may differ between invertebrates and vertebrates and also among invertebrate taxa. The use of $GABA_A$ receptor drugs shown to work in the taxa of interest, and interpreting the results appropriately based

on the abundance or scarcity of research into the drug's action in the studied taxa, will be important to further assess the GABA hypothesis. Furthermore, using other $GABA_A$ receptor antagonists that are structurally unrelated to gabazine, such as picrotoxin, can increase our confidence in the evidence for the GABA hypothesis (Tresguerres and Hamilton, 2017).

Elevated CO_2 may also alter the functioning of other LGICs that are permeable to HCO_3^- and Cl^- ions. Altered glycine receptor functioning at elevated CO_2 levels has been suggested as another potential mechanism in fish due to its similarity to the $GABA_A$ receptor (Tresguerres and Hamilton, 2017). Glycine Rs are typically not found in invertebrates, however glutamate (Glu)-gated Cl^- channels are suggested to be the invertebrate equivalent of glycine Rs (Vassilatis *et al.*, 1997; Kehoe and Vulfius, 2000), so may respond to elevated CO_2 similarly. Invertebrates also possess a larger range of ligand-gated Cl^- channels than vertebrates (Wolstenholme, 2012), including acetylcholine (ACh)- (Kehoe1972, Yarowsky1978b, Schmidt1992, Putrenko2005, Nierop2005), dopamine (DA)- (Carpenter *et al.*, 1977), serotonin- (Gerschenfeld and Tritsch, 1974; Ranganathan *et al.*, 2000) and histamine- (Gisselmann *et al.*, 2002; Zheng *et al.*, 2002) gated Cl^- channels. Genes encoding for the LGICs (and associated proteins) of GABAergic, glycinergic-like, glutamatergic and cholinergic synapses were found to be differentially expressed in pteropod molluscs (*Heliconoides inflatus*) exposed to elevated CO_2 levels (617 – 720 µatm) compared with current-day controls (380 - 410 µatm) (Moya *et al.*, 2016). Therefore, a range of ligand-gated Cl^- channels could play a role in CO_2-induced behavioural disturbances in marine invertebrates, indicating a complex assortment of responsible mechanisms.

Elevated CO_2 has been shown to affect activity, defensive and predatory behaviours in cephalopod molluscs (Spady *et al.*, 2014, 2018). Cephalopods are a valuable taxa in which to investigate the mechanisms of CO_2-induced behavioural effects because of their well-developed nervous system and complex behaviours rivalling those of fishes (Hanlon and Messenger, 2018). In this study, male two-toned pygmy squid *Idiosepius pygmaeus* were exposed to current-day (~450 µatm) or elevated (~1,000 µatm) CO_2 levels for seven days followed by sham or treatment with the $GABA_A$ receptor antagonist gabazine or the non-specific $GABA_A$ receptor antagonist picrotoxin. After CO_2 and drug treatment, conspecific attraction, exploratory and aggressive behaviours, and activity levels were measured while squid were exposed to a mirror.

The pharmacological profile of gabazine in molluscs is not well characterised (Appendix B: Table B.1). The only study using electrophysiological methods to investigate gabazine's action in a mollusc demonstrated that gabazine inhibits both ionotropic $GABA_A$ receptor hyperpolarisations (inhibition) and depolarisations (excitation) (Vehovszky *et al.*, 1989). However, there was no evidence for what ion(s) these ionotropic $GABA_A$ receptors were permeable to. Molluscs possess both hyperpolarising and depolarising GABA-gated Cl^- channels

($GABA_A$-like receptors) (Rubakhin *et al.*, 1996). It is also suggested that excitatory GABA-gated cation channels may be present in molluscs (Yarowsky and Carpenter, 1978a; Norekian, 1999; Miller, 2019), as seen in other invertebrates (Beg and Jorgensen, 2003; Gisselmann *et al.*, 2004). Therefore, gabazine likely inhibited ionotropic GABA receptor hyperpolarisations by antagonising $GABA_A$-like receptors, but gabazine's action on ionotropic GABA R depolarisations may have been due to gabazine's action on GABA-gated cation channels. Furthermore, as the action of gabazine has not been tested on other molluscan receptors, the specificity of gabazine within molluscs is unknown. To the best of my knowledge, no studies have assessed the action of gabazine on cephalopod receptors, but $GABA_A$-like receptors are present in squid (Conti *et al.*, 2013). In the current study, gabazine administration was used to test the functioning of $GABA_A$-like receptors in *I. pygmaeus*, though GABA-gated cation channels and other closely related LGICs may have also been antagonised by gabazine.

Picrotoxin is a relatively non-specific $GABA_A$ receptor antagonist, inhibiting $GABA_A$ as well as glycine Rs in vertebrates (both ligand-gated Cl^- channels) (Dibas *et al.*, 2002; Lynch, 2004; Wang *et al.*, 2006; Masiulis *et al.*, 2019). In molluscs, picrotoxin's action has been better studied than that of gabazine (Appendix B: Table B.2). Similar to in vertebrates, picrotoxin antagonises molluscan $GABA_A$-like receptors (Yarowsky and Carpenter, 1978a,b; Rubakhin *et al.*, 1996; Jing *et al.*, 2003; Wu *et al.*, 2003) as well as Glu-gated Cl^- channels (suggested to be the invertebrate equivalent of glycine Rs (Vassilatis *et al.*, 1997)) (Piggott *et al.*, 1977). However, molluscs possess a larger range of ligand-gated Cl^- channels than vertebrates (Wolstenholme, 2012) and picrotoxin also inhibits molluscan ACh- (Yarowsky and Carpenter, 1978b) and DA- (Magoski and Bulloch, 1999) gated Cl^- channels. As far as I am aware, no studies have assessed the action of picrotoxin on cephalopod ligand-gated Cl^- channels. However, local injection of GABA and picrotoxin into the optic lobe of a cuttlefish had opposite effects on locomotion (Chichery and Chichery, 1985) suggesting picrotoxin acted on an unidentified type of $GABA_A$ receptor. In the current study, picrotoxin administration was used to investigate the functioning of $GABA_A$-like receptors as well as Glu-, ACh- and DA- gated Cl^- channels in *I. pygmaeus*.

This study aimed to: 1) determine if elevated CO_2 alters a range of conspecific-directed behaviours and activity levels in *I. pygmaeus*, (2) provide robust evidence for or against the GABA hypothesis within a cephalopod mollusc, and (3) determine whether ligand-gated Cl^- channels other than the $GABA_A$-like receptor (Glu-, ACh- and DA- gated Cl^- channels) could also underlie CO_2-induced behavioural changes in *I. pygmaeus*. If the behavioural effect of drug treatment at elevated CO_2 conditions is different to the behavioural effect of drug treatment at current-day CO_2 conditions this would suggest that altered function of the drugs target receptor(s) underlies the CO_2-induced behavioural change. The behavioural effect of drug treatment could differ across CO_2 in five ways; opposite, removed, added, diminished

or enhanced, with each of these suggesting a slightly different change in receptor function at elevated CO_2 (see Table 3.1 for definitions and explanations). As the common target of gabazine and picrotoxin is the $GABA_A$-like receptor, if both gabazine and picrotoxin alter behaviour in a similar manner across CO_2 conditions this would suggest altered function of the $GABA_A$-like receptor underlies the CO_2-induced behavioural change, supporting the GABA hypothesis. As gabazine and picrotoxin are structurally unrelated, and picrotoxin's action within molluscs has been better studied, this would provide more robust support for the GABA hypothesis than previous marine invertebrate pharmacological studies. As picrotoxin antagonises Glu-, ACh- and DA- gated Cl^- channels, but gabazine does not, if picrotoxin, but not gabazine, has a different effect on behaviour across CO_2 conditions this would suggest altered function of these picrotoxin-sensitive ligand-gated Cl^- channels underlies the CO_2-induced behavioural change.

3.3 Methods

3.3.1 Animal collection

Male two-toned pygmy squid (*Idiosepius pygmaeus*) were collected between August – October 2019 (picrotoxin experiment) and November – December 2019 (gabazine experiment) by dip net from the inshore waters around the Townsville breakwater complex (19°15'S, 146°50'E) (Queensland Government General Fisheries Permit number 199144). Males were identified by visual inspection of the testis at the tip of the mantle and transported immediately to the experimental facilities. Only males were used due to the potential for sex-specific responses to elevated CO_2 (Spady *et al.*, 2014; Ellis *et al.*, 2017) and $GABA_A$ receptor antagonists (Peričić *et al.*, 1986; Manev *et al.*, 1987). Squid were acclimated in groups at current-day seawater conditions for 1 - 6 days before transferral to treatment tanks set at either current-day current-day (~450 µatm) or elevated (~1,000 µatm) seawater CO_2, consistent with end of century projections under Representative Concentration Pathway (RCP) 8.5 (Collins *et al.*, 2013). Squid were randomly assigned to tanks within their CO_2 treatment. Treatment tanks (matte white colour, 40 x 30 x 30 cm) held squid individually for seven days, which is approximately 10% of the total lifespan and 25% of the adult lifespan of male *I. pygmaeus* (Jackson, 1988). Squid were provided with PVC pipes for shelter and fed glass shrimp (*Acetes sibogae australis*) daily *ad libitum*. Glass shrimp were collected from the same location as squid and housed at current-day conditions. This study followed the animal ethics guidelines at James Cook University (JCU animal ethics number A2644).

Table 3.1. Summary of the varying types of different drug effects across CO_2 treatments and how they suggest altered receptor function at elevated CO_2. The examples in this table all refer to inhibitory $GABA_A$-like receptors ($GABA_A$-like receptors). However, these explanations similarly refer to all receptors investigated in this study; gabazine tested the functioning of inhibitory and excitatory $GABA_A$-like receptors (and possibly GABA-gated cation channels) and picrotoxin tested the functioning of inhibitory and excitatory $GABA_A$-like receptors, and Glu-, ACh- and DA-gated Cl^- channels.

Drug effect in elevated versus current-day CO_2 treatments	Definition	Suggested change in ion flow and receptor function at elevated CO_2	Example for how the different drug effect at elevated compared with current-day CO_2 suggests a change in receptor function
Opposite	Drug treatment increases the measured behaviour at current-day CO_2 but decreases the behaviour at elevated CO_2 (or vice versa).	Reversal in ion flow through the receptor channel resulting in a switch in function of the target receptor(s).	A behaviour is supressed by $GABA_A$-like receptor-induced inhibition and generated by $GABA_A$-like receptor-induced excitation. At current-day CO_2, there is a net influx of negative charge through the $GABA_A$-like receptor having an inhibitory effect on the behaviour. Drug treatment at current-day CO_2 antagonises the $GABA_A$-like receptor-induced inhibition and suppression of the behaviour is removed, resulting in an increase in the measured behaviour. At elevated CO_2, ion flow reverses and there is a net efflux of negative charge through the $GABA_A$-like receptor resulting in excitation. Thus, the measured behaviour is higher at elevated compared to current-day CO_2. Drug treatment at elevated CO_2 antagonises the $GABA_A$-like receptor-induced excitation and generation of the behaviour is decreased, resulting in a decrease in the measured behaviour.
Removed	Drug treatment increases or decreases the behaviour at current-day CO_2 but has no effect at elevated CO_2.	Reduction in ion flow through the receptor channel resulting in a loss of function of the target receptor(s).	The ion gradient across the neuronal membrane is decreased at elevated compared to current-day CO_2. At current-day CO_2, ligand binding produces a flow of ions through the $GABA_A$-like receptor having an inhibitory effect which alters behaviour. Therefore, drug treatment at current-day CO_2 antagonises the $GABA_A$-like receptor-induced inhibition and has a behavioural effect. However, at elevated CO_2, ligand binding results in a very small, or no, flow of ions through the $GABA_A$-like receptor and produces very weak or no inhibition. This very weak (or absence of) $GABA_A$-like receptor-induced inhibition has no effect on behaviour and thus drug treatment has no behavioural effect at elevated CO_2.

Table 3.1 continued.

Drug effect in elevated versus current-day CO_2 treatments	Definition	Suggested change in ion flow and receptor function at elevated CO_2	Example for how the different drug effect at elevated compared with current-day CO_2 suggests a change in receptor function
Added	Drug treatment has no effect at current-day CO_2 but increases or decreases the behaviour at elevated CO_2.	Increased ion flow through the receptor channel resulting in a gain of function of the target receptor(s).	The ion gradient across the neuronal membrane is increased at elevated compared to current-day CO_2. At current-day CO_2, ligand binding results in a very small, or no, flow of ions through the $GABA_A$-like receptor producing very weak or no inhibition. This very weak (or absence of) $GABA_A$-like receptor-induced inhibition has no effect on behaviour and thus drug treatment has no behavioural effect at current-day CO_2. However, at elevated CO_2 ligand binding produces a flow of ions through the $GABA_A$-like receptor resulting in inhibition which affects behaviour. Therefore, drug treatment at elevated CO_2 antagonises the $GABA_A$-like receptor-induced inhibition and has a behavioural effect.
Diminished	Drug treatment causes a smaller increase or decrease in behaviour at elevated CO_2 compared with current-day CO_2.	Reduction in ion flow through the receptor channel resulting in a decreased function of the target receptor(s) (direction of ion flow remains the same).	The ion gradient across the $GABA_A$-like receptor is smaller at elevated compared to current-day CO_2. Therefore, ligand binding produces a smaller flow of ions through the $GABA_A$-like receptor and a weaker inhibitory effect at elevated compared to current-day CO_2, although the direction of ion flow remains the same at both CO_2 conditions. Drug treatment antagonises the strong inhibition at current-day CO_2 and the weaker inhibition at elevated CO_2. Consequently, drug treatment has a large behavioural effect at current-day CO_2 and a smaller behavioural effect at elevated CO_2.
Enhanced	Drug treatment causes a larger increase or decrease in behaviour at elevated CO_2 compared with current-day CO_2.	Increased ion flow through the receptor channel resulting in an enhanced function of the target receptor(s) (direction of ion flow remains the same).	The ion gradient across the $GABA_A$-like receptor is larger at elevated compared to current-day CO_2. Therefore, ligand binding produces a larger flow of ions through the $GABA_A$-like receptor and a stronger inhibitory effect at elevated compared to current-day CO_2, although the direction of ion flow remains the same at both CO_2 conditions. Drug treatment antagonises the weak inhibition at current-day CO_2 and the stronger inhibition at elevated CO_2. Consequently, drug treatment has a small behavioural effect at current-day CO_2 and a larger behavioural effect at elevated CO_2.

3.3.2 CO_2 treatment systems

Experiments were carried out in four interconnected 8,000 L recirculating seawater systems, each with a 3,000 L sump, at James Cook University's research aquarium in Townsville, Australia. Two untreated seawater systems were used for duplicated current-day CO_2 treatments, and a custom-built pH control system dosed CO_2 into the 3,000 L sumps of two seawater systems to create duplicated elevated CO_2 treatments.

An inline pH sensor (Tophit CPS471D, Endress+Hauser, Reinach, Switzerland) measured pH continuously and communicated via a transmitter (Liquiline CM442, Endress+Hauser, Reinach, Switzerland) with the computerised controller (OMNI C40 BEMS, Innotech, Brisbane, Australia) to regulate CO_2 dosing to maintain the desired pH. The four systems were interconnected by water exchange of approximately 20 L per hour to maintain similar water quality in each system.

Daily measurements of pH_{NBS} (Ecotrode plus on an 888 Titrando, Metrohm AG, Switzerland), and temperature (Comark C26, Norfolk, UK) were taken from each of the four systems. Dosing set points were adjusted as required to maintain the target pCO_2 in the two elevated CO_2 systems. Weekly measurements of salinity by a conductivity sensor (HQ40d, Hach, Loveland, CO, USA), total alkalinity by Gran titration (888 Titrando, Metrohm AG, Switzerland), and pH on the total scale (pH_T) by spectrophotometry (Spectronic 200E, ThermoScientific, Madison, USA) using m-cresol purple as an indicator dye (Dickson and Millero, 1987; Dickson *et al.*, 2007) were taken from each of the four systems. Titration calibrations remained within 1% of certified reference material from Prof. A.G. Dickson (Scripps Institution of Oceanography, batch no. 136) throughout the experiments. Daily pH_T values were estimated by comparing pH_{NBS} and pH_T values. pCO_2 values were calculated in CO_2SYS version 2.1 (`https://cdiac.ess-dive.lbl.gov/ftp/co2sys/CO2SYS_calc_XLS_v2.1/`) using the constants K1, K2 from Mehrbach *et al.* (1973) and refit by Dickson and Millero (1987), and $KHSO_4$ from Dickson *et al.* (2007). An overview of carbonate chemistry parameters are in Table 3.2. Temperature, salinity, alkalinity and current-day pH were chosen to be similar to the natural conditions where the squid were collected.

3.3.3 Drug treatment and behavioural trials

After CO_2 treatment, squid underwent drug treatment for 30 minutes. In both the gabazine and picrotoxin experiments, squid were individually placed in 100 mL aerated seawater from their CO_2 treatment containing sham or drug treatment, squid were randomly assigned to sham or drug treatment. I am not aware of any evidence that differences in CO_2 levels or seawater pH relevant to ocean acidification experiments affect the action of gabazine or picrotoxin. Gabazine experiment: sham = 0.4% distilled water (current-day CO_2, n = 22,

Table 3.2. Experimental seawater carbonate chemistry. Details are shown for duplicate current-day and elevated CO_2 treatment systems in the gabazine and picrotoxin experiments. Values are mean ± standard deviation.

CO_2 Treatment System	Temperature (°C)	Salinity	pH_{total}	Alkalinity (µmol/kg SW)	pCO_2 (µatm)
Gabazine Experiment					
Current-day 1	26.1 ± 0.2	34.9 ± 0.2	8.02 ± 0.03	2390 ± 114	450 ± 37
Current-day 2	26.2 ± 0.2	34.7 ± 0.3	7.99 ± 0.03	2385 ± 110	483 ± 43
Elevated 1	26.0 ± 0.2	35.0 ± 0.1	7.72 ± 0.02	2404 ± 113	1014 ± 83
Elevated 2	26.1 ± 0.3	35.1 ± 0.1	7.72 ± 0.02	2405 ± 120	1006 ± 54
Picrotoxin Experiment					
Current-day 1	26.0 ± 0.1	34.6 ± 0.2	8.09 ± 0.13	2619 ± 48	413 ± 55
Current-day 2	26.1 ± 0.1	34.6 ± 0.2	8.10 ± 0.05	2623 ± 44	401 ± 59
Elevated 1	26.0 ± 0.2	35.2 ± 0.4	7.73 ± 0.03	2648 ± 46	1075 ± 88
Elevated 2	26.1 ± 0.1	35.5 ± 0.5	7.73 ± 0.02	2655 ± 50	1066 ± 48

elevated CO_2, n = 22), or gabazine = 4 mg/L (10.86 µM) gabazine (SR-95531, batch no. 0000035110, Sigma-Aldrich, St Louis, USA) and 0.4% distilled water (current-day CO_2, n = 24, elevated CO_2, n = 23). Picrotoxin experiment: sham = 0.2% absolute ethanol (current-day CO_2, n = 27, elevated CO_2, n = 26), picrotoxin = 100 µM picrotoxin (batch no. 16C/230903, Tocris Bioscience, Bristol, UK) and 0.2% absolute ethanol (current-day CO_2, n = 26, elevated CO_2, n = 26). The dose of gabazine was chosen based on *in vivo* studies in fish (Nilsson *et al.*, 2012; Hamilton *et al.*, 2013; Chivers *et al.*, 2014) and another mollusc (Watson *et al.*, 2014) that showed bath application of 4 mg/L for 30 minutes reversed the behavioural effect of elevated CO_2. The dose of picrotoxin was chosen based on *in vivo* studies in a mollusc (Biscocho *et al.*, 2018) and barnacle (Rittschof *et al.*, 1986), which showed altered behaviour after 100 µM picrotoxin treatment. Distilled water and ethanol were used to dissolve gabazine and picrotoxin, respectively.

Immediately after drug treatment, squid were placed in the middle of a matte white acrylic tank (30 x 30 x 15 cm) with a mirror taking up the entire area of one wall. The tank was filled with water from their CO_2 treatment to a depth of 3 cm (to limit vertical movement for tracking). The tank was illuminated by an LED strip hung approximately 5 cm to the side of the arena walls, around the entire tank. The behavioural trial was filmed with a digital camera (Canon PowerShot G15 or G16) placed on white Corflute® directly above the tank, 70 cm from the water surface (Figure 3.1). Filming was at 30 frames per second (fps) and started before squid were placed in the behavioural arena to minimize disturbance. Filming continued for the 15 minute behavioural trial and stopped after 16 minutes to eliminate possible disturbances when approaching the camera. Squid mantle length (ML) was measured at the conclusion of each behavioural trial, gabazine experiment ML = 9.99 ± 0.99 mm (mean ± standard deviation), picrotoxin experiment ML = 9.54 ± 0.94 mm.

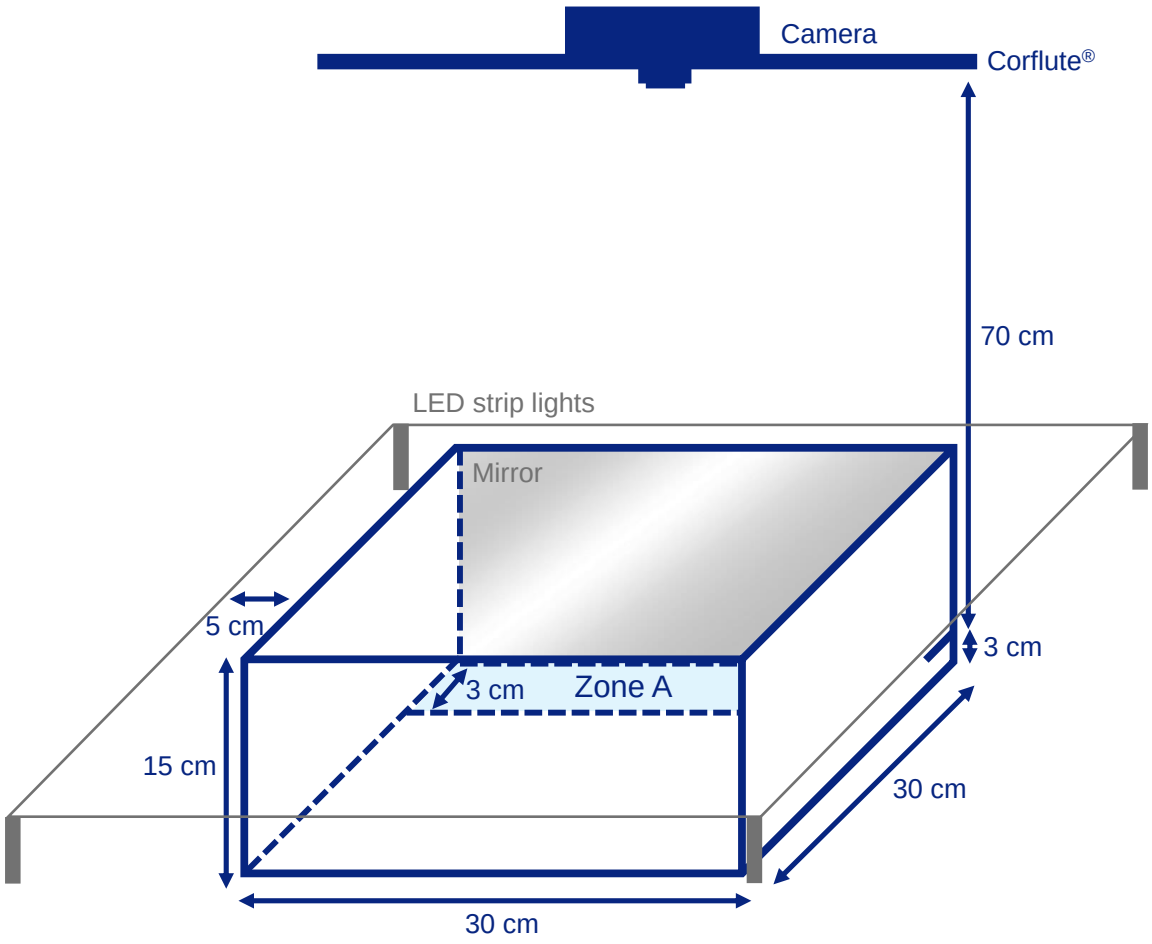

Figure 3.1. Diagram of behavioural trial set-up. The squid were placed in a matte white acrylic tank (30 x 30 x 15 cm) with a mirror taking up the entire area of one wall and filled with seawater to a depth of 3 cm. LED strip lights hung approximately 5 cm to the side of the arena walls, around the entire tank. A camera placed on white Corflute® directly above the tank, 70 cm from the water surface, filmed each behavioural trial. A 3 cm wide zone along the full length of the mirror (Zone A) was created in the tracking software when measuring space use.

3.3.4 Behavioural analysis

For each experiment, the squid's interaction with the mirror was analysed across the 15 minutes following introduction into the behavioural arena. Other cephalopod species appear to recognise their mirror image as a conspecific (Shashar *et al.*, 1996; Palmer *et al.*, 2006; Ikeda and Matsumoto, 2007). Therefore, a mirror was used to analyse visual conspecific-directed behaviours while controlling for possible confounding factors of using a live conspecific, such as size, movement and chemical cues. Furthermore, using a mirror image limited the senses that influenced behaviour to vision only. This reduced the potential of altered sensation as a mechanism underlying any elevated CO_2-induced behavioural changes (Chapter 2), which allowed me to focus on central mechanisms, such as altered LGIC function.

Videos were analysed with the observer blinded to treatment. LoliTrack tracking software (version 4.2.1, Loligo Systems) was used across the 15 minute videos with the framerate subsampled to 15 fps. A 3 cm wide zone along the full length of the mirror (Zone A) was created in LoliTrack to determine space use:

- Time spent in Zone A (seconds) (only for squid that did enter Zone A)
- Number of visits to Zone A

The following information was determined from the videos, at 30 fps, using QuickTime video software (QuickTime version 7.7.5, Apple Inc.): Mirror touching was categorized into two groups. Soft mirror touches were exploratory and defined as only the arm tips touching the mirror. Aggressive mirror touches occurred when the arms splayed upon coming in contact with the mirror, usually at high speed and accompanied by flashing body colour. Other parts of the squid's body coming in contact with the mirror (e.g. mantle) were not counted as mirror touches. Mirror touching measures determined were:

- Proportion of squid that touched the mirror softly/aggressively
- Latency to the first soft/aggressive mirror touch (only for squid that touched the mirror)
- Number of soft/aggressive mirror touches – squid's arms had to detach from the mirror completely between mirror touches before a successive touch was counted (only for squid that touched the mirror)

LoliTrack was also used across the 15 minute videos at 15 fps for measures of activity:

- Time spent active (seconds)
- Total distance moved (centimeters)

- Average speed (cm/s)

Squid that inked in the behavioural trial (gabazine experiment sham: current-day CO_2, n = 8, elevated CO_2, n = 7 and gabazine: current-day CO_2, n = 10, elevated CO_2, n = 7, and picrotoxin experiment sham: current-day CO_2, n = 6, elevated CO_2, n = 5 and picrotoxin: current-day CO_2, n = 6, elevated CO_2, n = 2) were excluded from the tracking analysis because LoliTrack could not distinguish between the squid and the ink. Furthermore, squid that were in very close proximity to the mirror for an extended period of time, e.g. attached to the mirror, were also excluded from the tracking analysis because LoliTrack could not distinguish between the squid and the squid's mirror image. A total of 38 squid (gabazine experiment) and 25 squid (picrotoxin experiment) were excluded from the tracking analysis in LoliTrack. Therefore, sample sizes for tracked data are as follows: gabazine experiment sham: current-day CO_2, n = 12, elevated CO_2, n = 13 and gabazine: current-day CO_2, n = 12, elevated CO_2, n = 16, and picrotoxin experiment sham: current-day CO_2, n = 19, elevated CO_2, n = 21 and picrotoxin: current-day CO_2, n = 18, elevated CO_2, n = 22.

3.3.5 Statistical analysis

Bayesian modelling was carried out in R (v4.0.2) (R Core Team, 2020), using RStudio (v1.3.1093) (RStudio Team, 2020) to test the effects of CO_2 and drug treatment on each behaviour. The Bayesian models were fit using the package brms (v2.13.5) (Bürkner, 2017), which uses RStan (v2.21.2) (Stan Development Team, 2020) to interface with the statistical modelling platform Stan.

All count data were modelled against a negative binomial distribution with a log link, binomial data were modelled against a Bernoulli distribution with a logit link, and continuous data were modelled with a linear model (Gaussian distribution with an identity link) or against a gamma distribution with a log link. The models were fit using the no u-turn MCMC sampler which ran with 10,000 iterations, a warm-up of 3,000 and thinning of 5 for each of 4 chains. Default, weakly informative priors were used. For two response variables in the picrotoxin experiment, number of visits to Zone A and the latency to the first aggressive mirror touch, acceptable MCMC diagnostics were maintained by adjusting the MCMC sampler to run with 120,000 iterations, a warm-up of 40,000 and thinning of 80 for each of 4 chains, Stan was forced to take smaller steps by increasing adapt_delta from the default of 0.8 to 0.99, and the priors were specified. See Appendix B: Table B.3 and Table B.4 for the distribution and link function, and the priors used for each response variable (behaviour).

Variable selection was used to choose a model with the best subset of explanatory variables for each response variable (behaviour). A set of six biologically plausible candidate

models were fit for each response variable, with each model hypothesized *a priori* to represent a particular aspect of biology that could affect the response variable. All models included the interaction of CO_2 (fixed factor with two levels, current-day and elevated) and drug (fixed factor with two levels, sham and gabazine/picrotoxin). The six models tested: 1) only the interaction of CO_2 and drug, 2) the effect of squid size by including mantle length in centimeters (continuous), 3) the effect of the methods used for behavioural testing by including the behavioural tank used (fixed factor with two levels - behavioural trials were carried out in two different tanks of the same dimensions) and the time of day the behavioural test was carried out (continuous), 4) the effect of drug lot by including the drug test number (fixed factor with three levels in the gabazine experiment or seven levels in the picrotoxin experiment – gabazine solution was made up directly before the trial and the same solution was used for up to three separate trials, while picrotoxin solution was always only used for one trial but all picrotoxin solutions were made up at the start of the day and up to seven picrotoxin solutions were used across one day), 5) the effect of housing conditions by including the number of days squid were acclimated at current-day seawater conditions before transferal to treatment tanks (fixed factor with 6 levels - squid were acclimated for 1 - 6 days) and the day squid underwent the behavioural trial (continuous), 6) the effect of the duplicate seawater systems by including system (fixed factor - two levels for current-day CO_2 and two levels for elevated CO_2). Leave-one-out cross-validation information criterion (LOOIC) values, which have the same purpose as the frequentist Akaike Information Criterion (AIC) values, were calculated for each model. All LOOIC values were considered reliable due to less than 14.5% of the Pareto k diagnostic values being larger than 0.7. The chosen model for each response variables had a LOOIC within 1 of the best model. See Appendix B: Table B.3 and Table B.4 for the explanatory variables included in the model for each response variable.

All chosen models followed the nominated distribution, tested with Q-Q plots and the Kolmogorov-Smirnov test, showed no over- or under-dispersion, no outliers and the residuals showed no patterns. MCMC diagnostics for each of the chosen models suggested that the chains were well mixed and converged on a stable posterior. MCMC diagnostics included trace plots for visual inspection of chain mixing, $\hat{R} < 1.05$, autocorrelation factor < 0.2 and effective sample size > 50%. Posterior probability checks suggest that the priors did not influence the data.

If the drug effect at elevated CO_2 was found to be different to the drug effect at current-day CO_2 this was considered support for altered function of the drugs target receptor(s) underlying the CO_2-induced behavioural change. The drug effects could differ across CO_2 in five ways, an opposite, removed, added, diminished or enhanced drug effect, with each effect suggesting a slightly different change in receptor function at elevated CO_2 (see Table 3.1 for definitions and explanations of each of these effects).

3.4 Results

A summary of the effects of elevated CO_2 on squid behaviour (in sham-treated individuals) and the drug effect across CO_2 treatments is shown in Table 3.3.

3.4.1 Space use

There was very strong evidence (95.9%) in the gabazine experiment and evidence (83.6%) in the picrotoxin experiment that elevated CO_2 increased the time that sham-treated squid spent in Zone A (for those squid that entered Zone A at least once) (gabazine: 1.74-fold increase 386 to 670 s, picrotoxin: 1.29-fold increase 409 to 529 s) (Figure 3.2A,B,E,F). There was also strong evidence (93.3%) that gabazine had a different effect at current-day and elevated CO_2 conditions. Specifically, there was no evidence of a gabazine effect at current-day CO_2 (64.4%), however there was very strong evidence (97.5%) that gabazine decreased the time spent in Zone A at elevated CO_2 (0.54-fold decrease 670 s to 363 s) (Figure 3.2A,B). The time spent in Zone A by gabazine-treated squid at elevated CO_2 was very similar to sham-treated squid at current-day CO_2 (386 and 363 s, respectively) (Figure 3.2A). There was also evidence (80.8%) that picrotoxin had a different effect at current-day and elevated CO_2. Specifically, there was strong evidence (91.8%) that picrotoxin increased the time spent in Zone A at current-day CO_2 (1.41-fold increase 409 to 577 s), but no evidence of a picrotoxin effect at elevated CO_2 (60.6%) (Figure 3.2E,F).

There was very strong evidence (99.9%) that elevated CO_2 decreased the number of times squid visited Zone A in the gabazine experiment (0.24-fold decrease 15 to 3.6 visits) (Figure 3.2C,D). There was also very strong evidence (98.8%) that gabazine had a different effect at current-day and elevated CO_2. Specifically, gabazine decreased the number of visits at current-day CO_2 (97.7% confidence, 0.37-fold decrease 15 to 5.6 visits), but increased the number of visits at elevated CO_2 (86.5% confidence, 1.63-fold increase 3.6 to 5.8 visits). In contrast, there was no evidence (56.7%) that CO_2 affected the number of visits to Zone A by sham-treated squid in the picrotoxin experiment (Figure 3.2G,H). However, there was evidence (80.9%) that picrotoxin had a different effect at current-day and elevated CO_2 (Figure 3.2H).

3.4.2 Soft mirror touch

In the gabazine experiment, there was no evidence (62.2%) for an effect of CO_2 on the proportion of sham-treated squid that explored by softly touching the mirror, nor was there any evidence (63.2%) that gabazine had a different effect at current-day and elevated CO_2 conditions (Figure 3.3A,B). However, in the picrotoxin experiment there was strong evidence (94.4%)

Table 3.3. Summary of the CO_2 effect in sham-treated squid, and the type of different drug effect across CO_2 treatments. Evidence: Very strong = probability of an effect ≥ 95%, strong = probability of an effect ≥ 90%, evidence = probability of an effect ≥ 80%, some evidence = probability of an effect ≥ 75%. CO_2 effect in sham treated squid, Direction: ↑ = increase in behaviour at elevated compared to current-day CO_2, ↓ = decrease in behaviour at elevated compared to current-day CO_2. Different drug effect across CO_2 conditions, Type: Opposite, Removed, Added, Diminished as described in Table 3.1.

	CO_2 effect in sham-treated squid				**Different drug effect across CO_2 conditions**			
	Gabazine		**Picrotoxin**		**Gabazine**		**Picrotoxin**	
	Evidence	**Direction**	**Evidence**	**Direction**	**Evidence**	**Type**	**Evidence**	**Type**
Space Use								
Time in Zone A (s)	Very strong	↑	Strong	↑	Strong	Added	Evidence	Removed
No. of visits to Zone A	Very strong	↓	None	-	Very strong	Opposite	Evidence	Removed
Soft mirror touch								
Proportion of squid that touch mirror softly	None	-	Strong	↑	None	-	None	-
Latency to first soft mirror touch (s)	Some evidence	↓	Very strong	↓	None	-	Very strong	Opposite
No. of soft mirror touches	Strong	↑	Some evidence	↑	Some evidence	Diminished	None	-
Aggressive mirror touch								
Proportion of squid that touch mirror aggressively	Evidence	↑	Very strong	↑	None	-	None	-
Latency to first aggressive mirror touch (s)	Some evidence	↑	Evidence	↑	Strong	Diminished	None	-
No. of aggressive mirror touches	Very strong	↑	Strong	↑	None	-	None	-
Activity measures								
Active time (s)	Evidence	↑	Evidence	↑	Some evidence	Added	Some evidence	Removed
Total distance moved (cm)	Strong	↑	Evidence	↑	Some evidence	Added	Some evidence	Diminished
Average speed (cm/s)	Evidence	↑	Evidence	↑	None	-	None	-

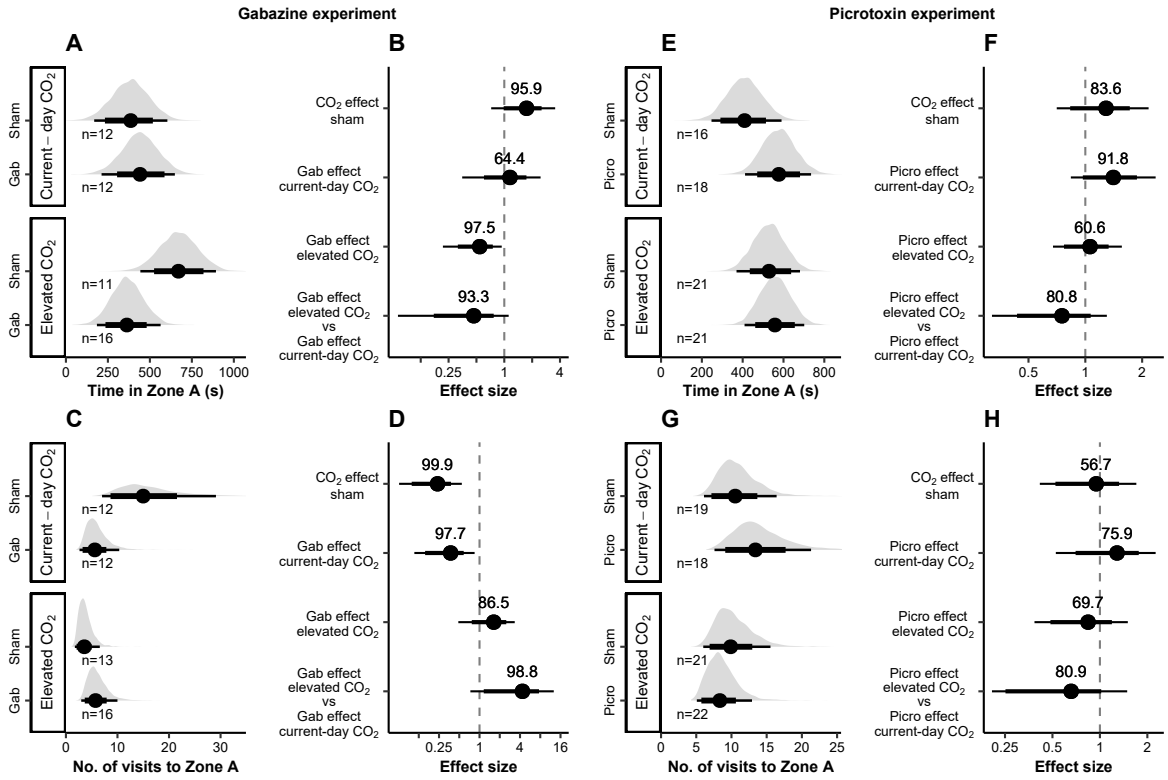

Figure 3.2. Effects of CO_2 and drug treatment on space use. A - D gabazine experiment, **E - H** picrotoxin experiment. **A, E** partial plots of the time squid spent in Zone A, **B, F** caterpillar plots for the effect of CO_2 and drug treatment on the time squid spent in Zone A, **C, G** partial plots of the number of times squid visited Zone **A, D, H** caterpillar plots for the effect of CO_2 and drug treatment on the number of times squid visited Zone A. Partial plots: point represents the Bayesian posterior median value ± 80% (thick lines) and 95% (thin lines) highest posterior density interval (HPDI), overlaid with the distribution of Bayesian posterior values. Caterpillar plots: point represents the median effect size (odds ratio for proportion data, fold change for others) ± 80% (thick lines) and 95% (thin lines) HPDI. The dashed vertical line indicates an effect size of 1 (no effect) and the numbers above each point are the percent probability of this effect (increase or decrease) occurring.

that elevated CO_2 increased the proportion of sham-treated squid that softly touched the mirror (2.44 odds ratio, increase 29% to 50%) (Figure 3.3G,H). There is no evidence (60.8%) that picrotoxin had a different effect at current-day and elevated CO_2, with strong evidence (96.9% and 92.2%, respectively) that picrotoxin increased the proportion of squid softly touching the mirror at both current-day CO_2 (2.88 odds ratio, increase 29% to 54%) and elevated CO_2 (2.31 odds ratio, increase 50% to 70%) (Figure 3.3G,H).

There was some evidence (77.9%) in the gabazine experiment and very strong evidence (99%) in the picrotoxin experiment that elevated CO_2 decreased the latency to the first soft mirror touch (gabazine: 0.67-fold decrease 107.7 to 72.5 s, picrotoxin: 0.3-fold decrease 257.3 to 75.8 s) (Figure 3.3C,D,I,J). However, there was no evidence (60.3%) for a different

effect of gabazine across CO_2 conditions. Gabazine increased the latency at both current-day CO_2 (83.2% confident, 1.66-fold increase 107.7 to 178.6 s) and elevated CO_2 (89.8% confident, 2.03-fold increase 72.5 to 146.8 s). In contrast, there was very strong evidence (99.1%) that picrotoxin had a different effect across CO_2 treatments. Picrotoxin decreased the latency at current-day CO_2 (88.4% confident, 0.55-fold decrease 257.3 to 140.5 s), whereas picrotoxin increased the latency at elevated CO_2 (98.8% confident, 2.69-fold increase 75.8 to 203.2 s) (Figure 3.3I,J).

In the gabazine experiment there was strong evidence (93.2%), and in the picrotoxin experiment some evidence (78.9%), that elevated CO_2 increased the number of soft mirror touches per individual (gabazine: 2.02-fold increase 13.3 to 27.0 touches, picrotoxin: 1.53-fold increase 32.1 to 49.1 touches) (Figure 3.3E,F,K,L). There was some evidence (78.9%) that gabazine had a smaller effect at elevated compared to current-day CO_2. Specifically, gabazine increased the number of soft touches by a median of 2.48-fold at current-day CO_2 (97.1% confidence, increase 13.3 to 33.0 touches) and 1.44-fold at elevated CO_2 (78.7% confidence, increase 27.0 to 38.8 touches) (Figure 3.3E,F). By contrast, there was no evidence (62.4%) that picrotoxin had a different effect across CO_2 conditions. Picrotoxin decreased the number of soft touches both at current-day CO_2 (86.7% confident, 0.54-fold decrease 32.1 to 17.5 touches) and at elevated CO_2 (82.5% confident, 0.68-fold decrease 49.1 to 33.4 touches) (Figure 3.3K,L).

3.4.3 Aggressive mirror touch

There was evidence (83.2%) in the gabazine experiment and very strong evidence (97.2%) in the picrotoxin experiment that elevated CO_2 increased the proportion of sham-treated squid that touched the mirror aggressively (gabazine: 1.82 odds ratio, increase 31% to 45%, picrotoxin: 3.01 odds ratio, increase 25% to 50%) (Figure 3.4A, B and G, H). In both experiments, there was no evidence (65% and 70.7%, respectively) that drug treatment had a different effect at current-day and elevated CO_2 conditions (Figure 3.4A,B,G,H).

In the gabazine experiment there was some evidence (76.5%), and in the picrotoxin experiment there was evidence (86%), that elevated CO_2 increased the latency to the first aggressive mirror touch (gabazine: 1.6-fold increase 30.8 to 48.9 s, picrotoxin: 1.85-fold increase 108.1 to 201.8 s) (Figure 3.4C,D,I,J). There was also strong evidence (94.2%) that the effect of gabazine was smaller at elevated compared to current-day CO_2. Specifically, gabazine increased the latency by a median of 7.6-fold at current-day CO_2 (99.8% confident, increase 30.8 to 235.3 s) and 2.03-fold at elevated CO_2 (91.3% confident, increase 48.9 to 97.9 s) (Figure 3.4 C,D). There was no evidence (55.5%) that picrotoxin had a different effect across CO_2 conditions (Figure 3.4I,J).

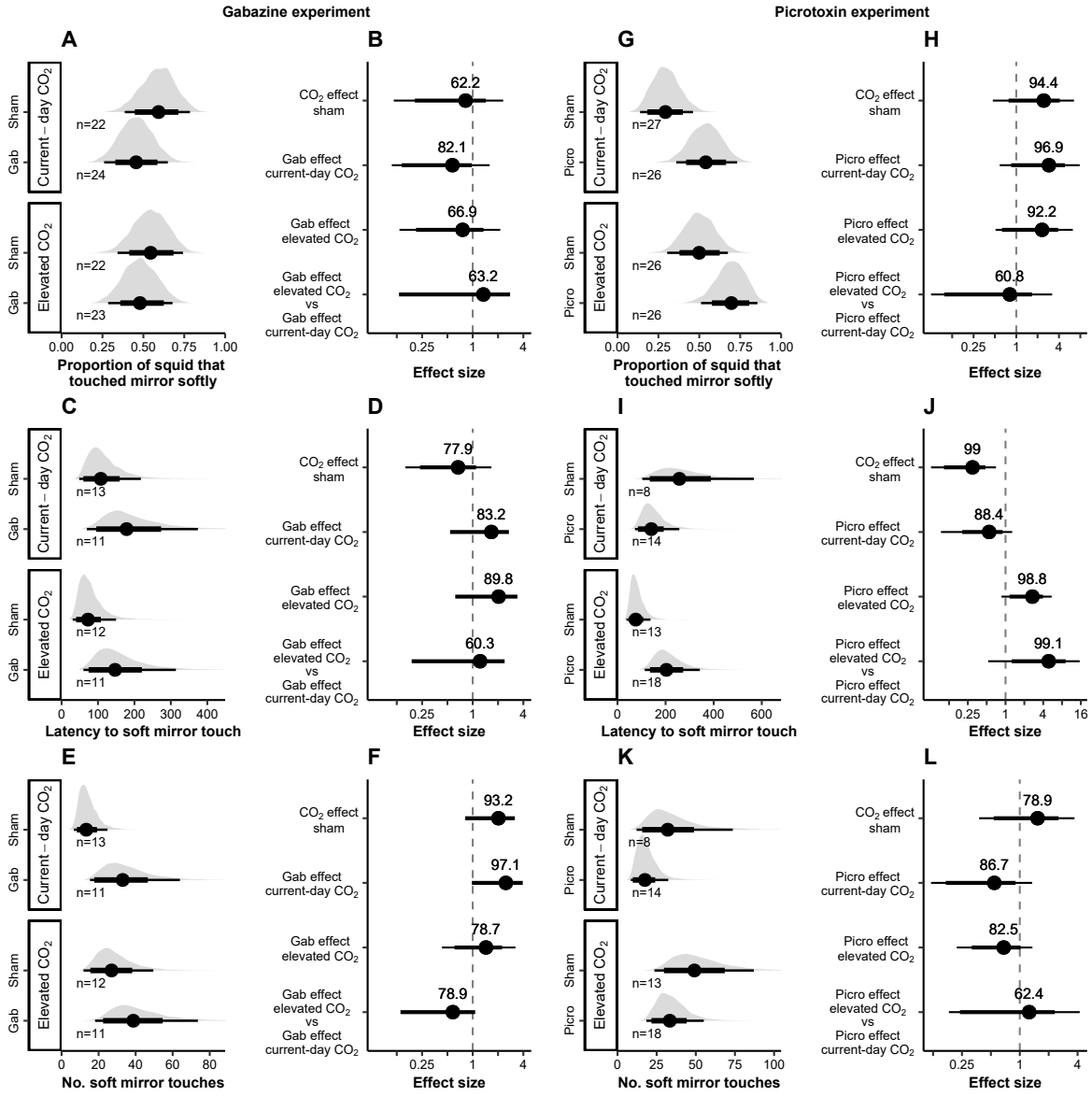

Figure 3.3. Effects of CO_2 and drug treatment on measures of soft mirror touching behaviour. **A - F** gabazine experiment, **G - L** picrotoxin experiment. **A, G** partial plots of the proportion of squid that touched the mirror softly, **B, H** caterpillar plots for the effect of CO_2 and drug treatment on the proportion of squid that touched the mirror softly, **C, I** partial plots of the latency from introduction to the first soft mirror touch (seconds), **D, J** caterpillar plots for the effect of CO_2 and drug treatment on the latency from introduction to the first soft mirror touch (seconds), **E, K** partial plots of the total number of soft mirror touches per individual, **F, L** caterpillar plots for the effect of CO_2 and drug treatment on the total number of soft mirror touches per individual. Partial and caterpillar plot symbols as per Figure 3.2.

In both the gabazine and picrotoxin experiment, there was strong evidence (97.3% and 93.3%, respectively) that elevated CO_2 increased the number of aggressive mirror touches per individual (gabazine: 2.5-fold increase 11.9 to 29.6 touches, picrotoxin: 1.79-fold increase 9.7 to 17.4 touches) (Figure 3.4E, F and K, L). However, there was no evidence (68.6% and 64.9%, respectively) that gabazine or picrotoxin had a different effect across CO_2 conditions (Figure 3.4E,F,K,L). There was strong evidence (95.6% and 93.8%, respectively) that picrotoxin increased the number of aggressive touches both at current-day CO_2 (2.16-fold increase 9.7 to 21 touches) and at elevated CO_2 (1.77-fold increase 17.4 to 30.8 touches) (Figure 3.4K,L).

3.4.4 Activity

Elevated CO_2 increased the time squid spent active in both experiments (gabazine: 87.8% confident, 1.41-fold increase 161.5 to 228.2 s, picrotoxin: 86.6% confident, 1.23-fold increase 258.4 to 316.1 s) (Figure 3.5A,B,G,H). There was some evidence that drug treatment had a different effect at current-day and elevated CO_2 in both experiments. Gabazine had a larger effect at elevated compared to current-day CO_2 (78.9% confident, 1.40-fold); there was no evidence (50.7%) at current-day CO_2, but there was evidence (88.7%) at elevated CO_2 (1.40-fold increase 228.2 to 319 s) that gabazine increased active time (Figure 3.5A,B). Conversely, picrotoxin had a smaller effect at elevated compared to current-day CO_2 (79.5% confident, 0.8-fold); there was strong evidence (91.6%) at current-day CO_2 (1.46-fold increase 316.1 to 333.9 s), but no evidence (63.5%) at elevated CO_2, that picrotoxin increased active time (Figure 3.5G,H).

The total distance moved by squid throughout the behavioural trial was also increased by elevated CO_2 in both experiments (gabazine: 90.3% confident, 1.57-fold increase 360.0 to 566.6 s, picrotoxin: 88.9% confident, 1.36-fold increase 613.5 to 833.9 s) (Figure 3.5C,D,I,J). There was some evidence (76.9%) that gabazine had a larger effect at elevated compared to current-day CO_2. Specifically, there was no evidence (57.8%) at current-day CO_2, but strong evidence (90.7%) at elevated CO_2 (1.54-fold increase 566.6 to 872.2 s) that gabazine increased active time (Figure 3.5C,D). Conversely, there was some evidence (75.3%) that picrotoxin had a smaller effect at elevated compared to current-day CO_2. Specifically, picrotoxin increased distance moved by a median of 1.46-fold at current-day CO_2 (93.4% confident, increase 613.5 to 892.8 s) and 1.17-fold at elevated CO_2 (78.9% confident, increase 833.9 s to 976 s) (Figure 3.5I,J).

Squid average speed across the behavioural trial was also higher at elevated compared to current-day CO_2 (gabazine: 86.8% confident, 1.12-fold increase 2.07 to 2.32 cm/s, picrotoxin: 87.4% confident, 1.10-fold increase 2.21 to 2.42 cm/s) (Figure 3.5E,F,K,L). There

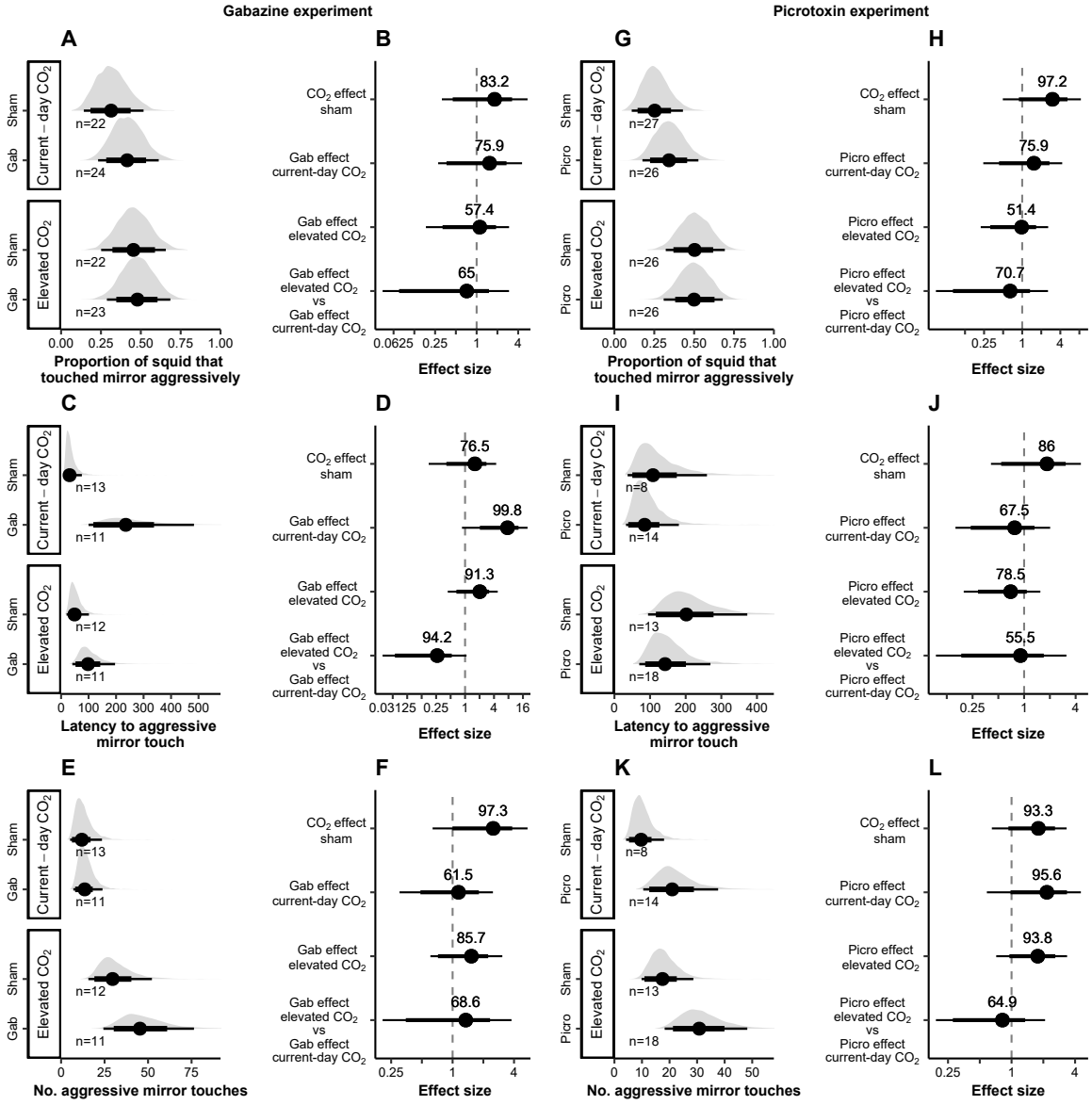

Figure 3.4. Effects of CO_2 and drug treatment on measures of aggressive mirror touching behaviour. A - F gabazine experiment, **G - L** picrotoxin experiment. **A, G** partial plots of the proportion of squid that touched the mirror aggressively, **B, H** caterpillar plots for the effect of CO_2 and drug treatment on the proportion of squid that touched the mirror aggressively, **C, I** partial plots of the latency from introduction to the first aggressive mirror touch (seconds), **D, J** caterpillar plots for the effect of CO_2 and drug treatment on the latency from introduction to the first aggressive mirror touch (seconds), **E, K** partial plots of the total number of aggressive mirror touches per individual, **F, L** caterpillar plots for the effect of CO_2 and drug treatment on the total number of aggressive mirror touches per individual. Partial and caterpillar plot symbols as per Figure 3.2.

was no evidence (55.9%) that gabazine had a different effect across CO_2 conditions, with no evidence (71.2% and 66.6%, respectively) of gabazine having an effect at either current-day or elevated CO_2 (Figure 3.5E,F). There was also no evidence (54.4%) that picrotoxin had a different effect at current-day compared to elevated CO_2, there was strong evidence (95.2% and 98.3%, respectively) that picrotoxin increased squid average speed at both current-day CO_2 (1.14-fold increase 2.21 to 2.53 cm/s) and elevated CO_2 (1.16-fold increase 2.42 to 2.81 cm/s) (Figure 3.5K,L).

3.5 Discussion

Elevated CO_2 levels can alter marine invertebrate behaviour (reviewed in Clements and Hunt (2015); Nagelkerken and Munday (2015) and Chapter 2), however, little is known about how elevated CO_2 levels might affect conspecific-directed behaviours or the mechanisms involved in altered marine invertebrate behaviour at elevated CO_2. Here, I found that elevated CO_2 increased male two-toned pygmy squid *Idiosepius pygmaeus* conspecific attraction and aggression, and activity levels in the presence of the squid's mirror image, compared to squid in current-day CO_2 conditions. Treatment with gabazine and picrotoxin had a different effect at elevated compared to current-day CO_2 conditions in some behaviours, providing robust support for the GABA hypothesis within a cephalopod, and indicating altered functioning of gluatame (Glu)-, acetylcholine (ACh)- and dopamine (DA)- gated chloride (Cl^-) channels may also underlie CO_2-induced behavioural changes. However, gabazine and picrotoxin had a similar effect in both current-day and elevated CO_2 conditions for other CO_2-affected behavioural traits, suggesting other mechanisms may also be involved.

3.5.1 Behavioural change in response to elevated CO_2

For the majority of the measured behaviours, the effect of elevated CO_2 was consistent across the gabazine and picrotoxin experiments. However, for two behavioural traits there was evidence for an effect of CO_2 in one experiment and not the other (see Table 3.3). Behaviour is notoriously difficult to measure due to its complexity (Niepoth and Bendesky, 2020), and behavioural effects are known to be influenced by subtle environmental changes, even when in controlled laboratory conditions (Crabbe *et al.*, 1999). There are many potential explanations for why the CO_2 effect was not the same between experiments for the number of times squid visited the zone closest to the mirror (Zone A) and the proportion of squid that touched the mirror softly. For example, the gabazine experiment was carried out at a later date than the picrotoxin experiment. This may have altered factors including the natural environmental conditions squid were exposed to before capture, such as temperature or turbidity, and

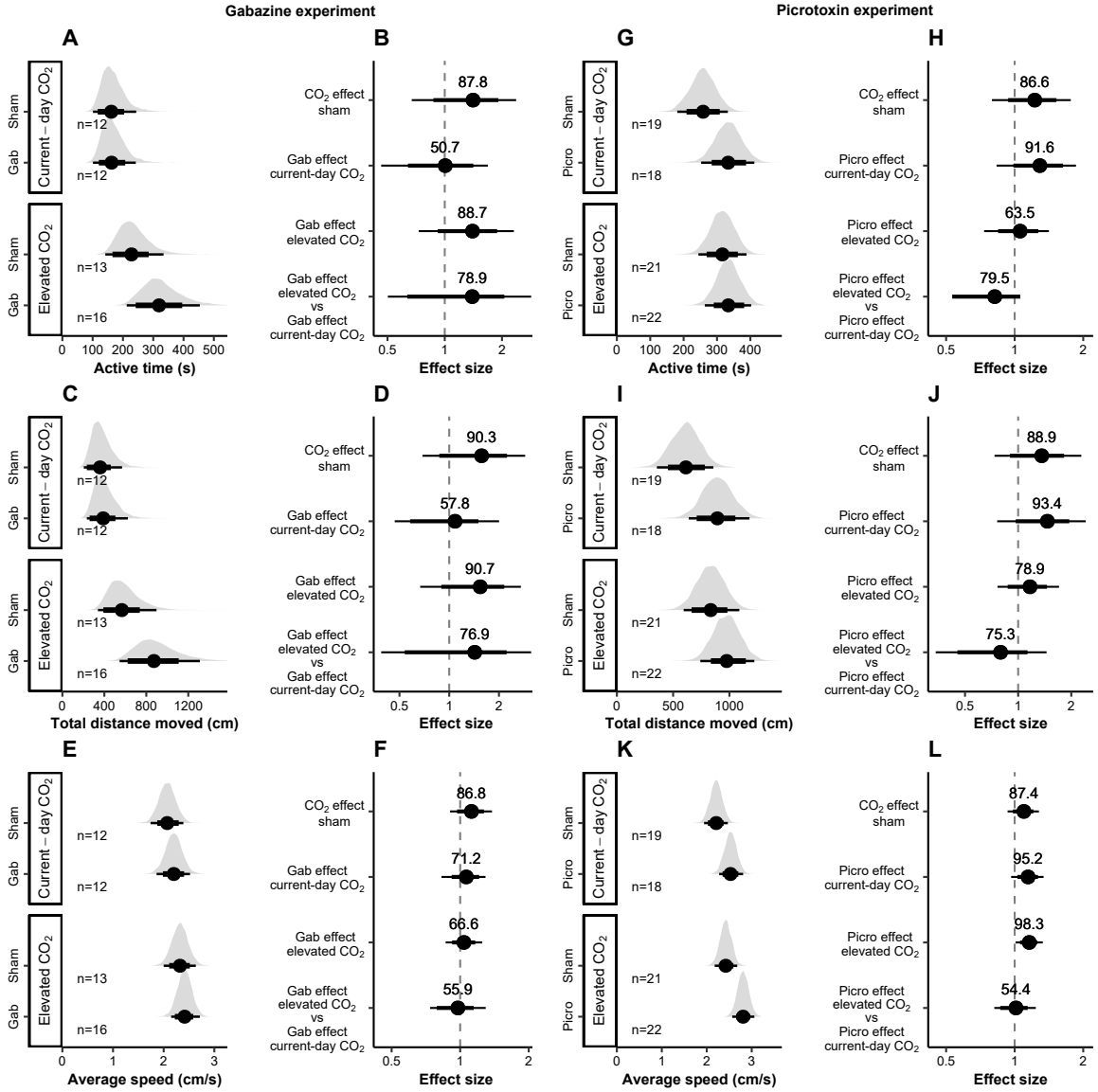

Figure 3.5. Effects of CO_2 and drug treatment on activity measures. **A - F** gabazine experiment, **G - L** picrotoxin experiment. **A, G** partial plots of the time squid spent active, **B, H** caterpillar plots for the effect of CO_2 and drug treatment on the time squid spent active, **C, I** partial plots of the total distance moved by squid, **D, J** caterpillar plots for the effect of CO_2 and drug treatment on the total distance moved by squid, **E, K** partial plots of squid average speed, **F, L** caterpillar plots for the effect of CO_2 and drug treatment on squid average speed. Partial and caterpillar plot symbols as per Figure 3.2.

the age of the squid captured. Nevertheless, nine out of the 11 behaviours measured showed a consistent response to CO_2 across the two experiments, suggesting the reliability of these results.

Squid exposed to elevated CO_2 spent more time in the zone closest to the mirror, tended to remain in this zone rather than move in and out of it, exhibited a decreased latency until the first soft mirror touch, and an increased number of soft mirror touches compared to squid at current-day CO_2 conditions. These results suggest that elevated CO_2 conditions may increase the exploratory behaviours of the squid directed towards their mirror image and an increased attraction of squid to conspecifics. This contrasts with the elevated CO_2-induced loss of conspecific chemical cue attraction in larval banded coral shrimp (Lecchini *et al.*, 2017). These opposing results may be due to the differing baseline behaviours of the studied species. Larval shrimp are attracted to conspecific chemical cues as a signal for settlement (Lecchini *et al.*, 2017), whereas adult *I. pygmaeus* are solitary and individuals are thought to avoid each other (Moynihan, 1983). Differences may also be due to the differing senses and taxa tested. Furthermore, coral shrimp were offered a binary choice (conspecific versus heterospecific chemical cues). However in the experiments here, squid did not have a choice of different cues, only whether to interact with the mirror image or not.

Elevated CO_2 also increased the proportion of squid that aggressively touched the mirror and the number of aggressive mirror touches, suggesting elevated CO_2 may increase conspecific-directed aggression in *I. pygmaeus*. All measures of activity (time spent active, distance moved and average speed) were also increased with exposure to elevated CO_2. This is consistent with increased activity levels in male *I. pygmaeus* at elevated CO_2 (626 and 956 µatm) when measured by mean number of line crosses (Spady *et al.*, 2014). In the bigfin reef squid (*Sepioteuthis lessoniana*), active time, total distance moved and average speed were also higher at elevated CO_2 conditions (935 µatm) (Spady *et al.*, 2018). In contrast, activity decreased at elevated CO_2 levels in para-larvae of the longfin inshore squid (*Doryteuthis pealeii*) (Zakroff *et al.*, 2018). Differences between studies may be due to the different species used, or differences in the timing of CO_2 treatment. *I. pygmaeus* and *S. lessoniana* were exposed to elevated CO_2 levels as adults (Spady *et al.*, 2014, 2018, this study)) whereas *D. pealeii* were exposed to elevated CO_2 for the duration of egg development (Zakroff *et al.*, 2018), in which there is already high CO_2 levels within the egg (Hu and Tseng, 2017).

It is unknown how CO_2-induced increases in conspecific attraction, aggression, and activity levels in *I. pygmaeus* may translate to changes in the wild. More conspecific interactions, particularly aggressive ones, could increase the prevalence of injuries in elevated CO_2 conditions. Increased activity levels may adversely affect the finely tuned energy budgets of squid (Rodhouse, 1998) and increase detection by predators (Draper and Weissburg, 2019).

3.5.2 Behavioural change in response to drug treatment

Within marine invertebrates, the GABA hypothesis has been assessed in gastropod molluscs (Watson *et al.*, 2014; Moya *et al.*, 2016; Zlatkin and Heuer, 2019), a bivalve mollusc (Clements *et al.*, 2017) and decapod crustaceans (de la Haye *et al.*, 2012; Charpentier and Cohen, 2016; Ren *et al.*, 2018). Here, I test the GABA hypothesis for the first time in a cephalopod, and assess whether Glu-, ACh- and DA- gated Cl^- channels may also be involved in the CO_2-induced behavioural changes, by administration of both gabazine and picrotoxin to male *I. pygmaeus* exposed to current-day or elevated CO_2 conditions.

Behavioural effects of gabazine and picrotoxin

The effects of both gabazine and picrotoxin treatment at current-day CO_2 on specific behavioural traits in the current study suggests that receptors in *I. pygmaeus* are sensitive to gabazine and picrotoxin. Furthermore, the concentrations used did not cause any obvious convulsions, which can be produced by the excitotoxic effects of $GABA_A$ receptor antagonists when administered systemically (Hinton and Johnston, 2018). The concentrations used are based on previous *in vivo* studies showing behavioural change with no convulsant effects reported (Rittschof *et al.*, 1986; Nilsson *et al.*, 2012; Hamilton *et al.*, 2013; Chivers *et al.*, 2014; Watson *et al.*, 2014; Biscocho *et al.*, 2018). There is no evidence for an effect of gabazine at current-day CO_2 on all activity measures, also indicating no convulsant effects. Picrotoxin increased all measures of activity levels at current-day CO_2. This is likely due to the action of picrotoxin on the neural circuits underlying locomotion, rather than causing excitotoxicity. At a synapse within the central pattern generator for pteropod mollusc swimming, pre-synaptic release of ACh causes post-synaptic inhibition via an increase in Cl^- permeability (Panchin *et al.*, 1995; Panchin and Sadreyev, 1997), and picrotoxin antagonizes inhibition at this synapse (Arshavsky *et al.*, 1985). Furthermore, picrotoxin has been shown to affect cephalopod mollusc locomotion (Chichery and Chichery, 1985). Receptors that are sensitive to picrotoxin but not gabazine, such as ACh-gated Cl^- channels, may be involved in the generation of mollusc swimming behaviour explaining the effect of picrotoxin, but not gabazine, on *I. pygmaeus* activity. Thus, the behavioural effects of gabazine and picrotoxin in *I. pygmaeus* are likely not convulsive side effects but rather due to the action of these drugs on the underlying neural circuits.

The effect of gabazine and picrotoxin at current-day CO_2 on some, but not other, behavioural traits is likely due to different neural circuits underlying different behaviours. Only those behaviours in which the drug's target receptor(s) play an important role in are affected by drug administration. Both gabazine and picrotoxin affected multiple measures of space use and soft mirror touching behaviour at current-day CO_2, suggesting that both gabazine-

sensitive receptors ($GABA_A$-like receptors and possibly also GABA-gated cation channels) and picrotoxin-sensitive ligand-gated Cl^- channels may be important in different aspects of squid attraction and exploratory behaviour towards their mirror image/conspecific. Interestingly, gabazine and picrotoxin mostly had opposite effects on these behavioural traits which may be due to the different target receptors of gabazine and picrotoxin. Gabazine and picrotoxin also affected various measures of aggressive mirror touching behaviour, suggesting that $GABA_A$-like receptors (and possibly also GABA-gated cation channels) and/or picrotoxin-sensitive ligand-gated Cl^- channels may also be important for producing conspecific-directed aggressive behaviours. As far as I am aware, no research has assessed what receptor(s) are involved in conspecific-directed behaviours in marine invertebrates. However, vertebrate $GABA_A$ receptors have also been found to be involved in mammalian conspecific-directed behaviours; $GABA_A$ receptor agonist administration into the rat brain increased social approach and conspecific-directed aggressive behaviours, while antagonising $GABA_A$ receptors decreased conspecific-directed aggressive behaviours (Depaulis and Vergnes, 1985).

Drug treatment effects across CO_2 conditions

Both gabazine and picrotoxin had a different effect across CO_2 treatments on a behavioural measure of space use, and on two activity measures. Gabazine had an added effect across CO_2 on the time spent in the zone closest to the mirror (Zone A), active time and distance moved by the squid. Picrotoxin had a removed effect across CO_2 on the time in Zone A and active time, and a diminished effect across CO_2 on distance moved. The different effect of both gabazine and picrotoxin across CO_2 provides strong evidence for the GABA hypothesis in *I. pygmaeus*. Furthermore, as the different effect of gabazine and picrotoxin across CO_2 were in different directions (added effect versus removed or diminished effect, respectively) this suggests that it is not just the common target receptor, the $GABA_A$-like receptors, but the target receptors of both gabazine and picrotoxin that are affected by elevated CO_2. Thus, altered functioning of GABA-, Glu-, ACh- and DA-gated Cl^- channels (and possibly also GABA-gated cation channels) may underlie the CO_2-induced increase in the time spent in Zone A and the active time and distance moved by squid.

Gabazine had an opposite effect across CO_2 treatments on the number of visits to Zone A, decreasing the number of visits at current-day CO_2 but increasing visits at elevated CO_2. This suggests that a reversal in the flow of ions through, and a switch in function of, the $GABA_A$-like receptor may underlie the elevated CO_2-induced decrease in the number of visits to Zone A.

For the latency to the first soft mirror touch, gabazine had a similar effect across CO_2 (increased the latency at both current-day and elevated CO_2), whereas picrotoxin had an op-

posite effect across CO_2 (decreased the latency at current-day CO_2 and increased the latency at elevated CO_2). This suggests that altered functioning of ligand-gated Cl^- channels, other than $GABA_A$-like receptors, underlies the CO_2-induced decrease in the latency to the first soft mirror touch. In molluscs, Glu-, ACh- and DA-gated Cl^- channels are all antagonised by picrotoxin (Piggott *et al.*, 1977; Yarowsky and Carpenter, 1978b; Magoski and Bulloch, 1999). Serotonin-gated Cl^- channels exist in nematodes (Ranganathan *et al.*, 2000) and possibly also molluscs (Gerschenfeld and Tritsch, 1974), but it is unknown whether serotonin-gated Cl^- channels are picrotoxin-sensitive. The results here cannot distinguish which specific ligand-gated Cl^- channels are involved in the behavioural effects of elevated CO_2, but they do suggest that ligand-gated Cl^- channels other than the $GABA_A$-like receptor underlie this particular CO_2-induced behavioural change. Furthermore, the opposite effect of picrotoxin across CO_2 suggests there is a reversal in ion flow through, and a switch in function of, these ligand-gated Cl^- channels. This finding agrees with previous suggestions that other ligand-gated Cl^- channels, such as vertebrate glycine receptors or invertebrate Glu-gated Cl^- channels, are likely involved due to their similarity to the $GABA_A$ receptor (Tresguerres and Hamilton, 2017, Chapter 2). My results also agree with molecular work showing altered expression of genes encoding for the LGICs (and associated proteins) of glycinergic-like, glutamatergic and cholinergic synapses at elevated CO_2 in a pteropod mollusc (Moya *et al.*, 2016). However, this result does not necessarily preclude the possibility of $GABA_A$-like receptors also being involved in the CO_2-induced decrease in the latency to the first soft mirror touch. If gabazine acts on GABA-gated cation channels, the influence of these GABA-gated cation channels could potentially mask the effect of $GABA_A$-like receptors.

In fish, altered HCO_3^- and Cl^- ion gradients across $GABA_A$ receptors was suggested to underlie altered functioning of these receptors at elevated CO_2 (Nilsson *et al.*, 2012). A similar mechanism may result in the altered function of ligand-gated Cl^- channels in *I. pygmaeus* exposed to elevated CO_2. Cephalopods can actively increase extracellular [HCO_3^-] in response to elevated environmental CO_2 levels. The cuttlefish *Sepia officinalis* exposed to elevated CO_2 (0.6 kPa ~6,000 µatm pCO_2) increased blood [HCO_3^-], partially compensating the drop in extracellular pH (Gutowska *et al.*, 2010). Exposure of the squid *Sepioteuthis lessoniana* to elevated CO_2 (1,600 and 4,100 µatm pCO_2) resulted in full compensation of extracellular pH, accompanied by an increase in blood [HCO_3^-] (Hu *et al.*, 2014). Although Cl^- levels in response to elevated seawater CO_2 have not been measured in cephalopods, a Na^+-driven HCO_3^-/Cl^- exchanger has been isolated from the squid *Loligo pealei* (Virkki *et al.*, 2003) suggesting the potential for altered [Cl^-] as part of acid-base regulation. Thus, altered ligand-gated Cl^- channel functioning observed in *I. pygmaeus* here may be due to altered HCO_3^- and Cl^- ion gradients across these receptors resulting from acid-base regulatory mechanisms at elevated CO_2. Future research measuring both extra- and intra-cellular mea-

surements of [HCO_3^-] and [Cl^-] in squid, and particularly in *I. pygmaeus*, will be useful to determine whether ionic gradients across neuronal membranes are altered at elevated CO_2, consequently disturbing ligand-gated Cl^- channel function.

In two CO_2-affected behavioural traits, the number of soft mirror touches and the latency to the first aggressive mirror touch, gabazine had a diminished effect whereas picrotoxin had a similar effect across CO_2 conditions. This suggests that receptors sensitive to gabazine, but not picrotoxin, may underlie the elevated CO_2-induced change of these behavioural traits, for example GABA-gated cation channels. This suggests the potentially widespread nature of the mechanisms underlying CO_2-induced behavioural changes. However, the lack of evidence for a different effect of picrotoxin across CO_2 conditions does not necessarily rule out the involvement of $GABA_A$-like receptors. For example, if the $GABA_A$-like receptors are the only ligand-gated Cl^- channels involved in these particular behavioural changes, the influence of other ligand-gated Cl^- channels could mask the effect of the $GABA_A$-like receptors.

A range of other CO_2-affected behavioural traits showed no evidence of gabazine nor picrotoxin having a different effect across CO_2 conditions. This suggests that $GABA_A$-like receptors as well as other gabazine-sensitive (possibly GABA-gated cation channels) and picrotoxin-sensitive (Glu-, ACh- and DA- gated Cl^- channels) receptors are not involved in the mechanisms underlying the elevated CO_2-induced change of these specific behavioural traits. Therefore, other mechanisms may be involved in these behavioural alterations.

Overall, the results here suggest that elevated CO_2 alters behaviour via multiple mechanisms in male *I. pygmaeus*, with different mechanisms underlying the changes of different behavioural traits at elevated CO_2 (Figure 3.6). It is possible that elevated CO_2 results in a suite of changes within the nervous system, including, but not limited to, altered functioning of GABA-, Glu-, ACh- and DA-gated Cl^- channels as well as possibly GABA-gated cation channels. As different neural circuits produce different behaviours, only some of the elevated CO_2-induced changes within the nervous system may result in the alteration of a particular behavioural trait. This can potentially explain the variability in the effects of elevated CO_2 among behaviours.

The complexity of the mechanisms underlying CO_2-induced behavioural changes is further increased by the fact that receptors can vary in subunit composition, and therefore pharmacological sensitivity, between differing subcellular, cellular and tissue locations (Lee and Maguire, 2014). For example, $GABA_A$ receptors are composed of 5 subunits and there are 19 different subunit genes identified in humans, α1–6, β1– 3, γ1–3, δ, ε, ϑ, π and ρ1-3 (Simon *et al.*, 2004). These subunits can combine in various ways to form $GABA_A$ receptor subtypes that differ in location, the functions (including behaviours) they are involved in, and their pharmacological profile (see Olsen and Sieghart (2009) for more detail). For example, vertebrate $GABA_A$ receptors made up of ρ subunits ($GABA_A$-ρ Rs), which are part of the

$GABA_A$ receptor family but sometimes called $GABA_C$ Rs (Olsen and Sieghart, 2008), are less sensitive to gabazine than $GABA_A$ receptors not composed of ρ subunits (Woodward *et al.*, 1993; Feigenspan and Bormann, 1994; Zhang *et al.*, 2008). Furthermore, $GABA_A$ (α1β2γ2) and $GABA_A$-ρ2 Rs are 10-fold more sensitive to picrotoxin than $GABA_A$-ρ1 Rs (Naffaa *et al.*, 2017). $GABA_A$ receptor subunits have been less studied in molluscs, though molluscan $GABA_A$ receptor-like α and β subunits have been identified (Harvey *et al.*, 1991; Moroz *et al.*, 2006; Stewart *et al.*, 2011) and $GABA_A$ receptor-like α, β, γ and ρ subunit sequences have been predicted in molluscs (for example GenBank BioProject PRJNA551489 and PRJNA625562). Picrotoxin antagonised $GABA_A$-like receptor hyperpolarisations in some neurons, but had no effect on ionotropic $GABA_A$ receptors of another neuron within the same mollusc species (Norekian and Satterlie, 1993; Norekian and Malyshev, 2005). Therefore, $GABA_A$ receptor-like subtypes that have differing pharmacological sensitivities are likely present in molluscs. Systemic drug administration allowed us to determine what receptors may be involved in the elevated CO_2-induced behavioural changes, but it cannot address the heterogeneity of receptor subtypes between different subcellular locations, cell types and tissues.

3.5.3 Conclusion

I found that elevated CO_2 increased conspecific-directed attraction and aggression as well as activity levels in male two-toned pygmy squid. Previous studies exclusively using gabazine have provided evidence for altered $GABA_A$-like receptor functioning as a mechanism for elevated CO_2-induced behavioural changes in a gastropod and bivalve mollusc. The study here now also supports the GABA hypothesis in a cephalopod mollusc. Furthermore, I have provided more robust support for the GABA hypothesis in molluscs by using both gabazine and picrotoxin, which is structurally unrelated to, and has a better studied molluscan pharmacological profile than, gabazine. Therefore, altered $GABA_A$-like receptor functioning may be a common mechanism underlying behavioural change at elevated CO_2 across marine molluscs. The use of both gabazine and picrotoxin also showed, for the first time in any marine invertebrate taxa, that altered functioning of ligand-gated Cl^- channels other than the $GABA_A$-like receptor may be involved in elevated CO_2-induced behavioural changes. I propose that elevated CO_2 leads to a suite of changes within the nervous system. As different neural circuits underlie different behaviours, and these different neural circuits may have various sensitivities to elevated CO_2, this can potentially explain the variability in the behavioural effects of elevated CO_2, both among behaviours and among species. The use of model animals will be important for future research to assess the complexities of the mechanisms underlying elevated CO_2-induced behavioural change. For example, an antipredator response was re-

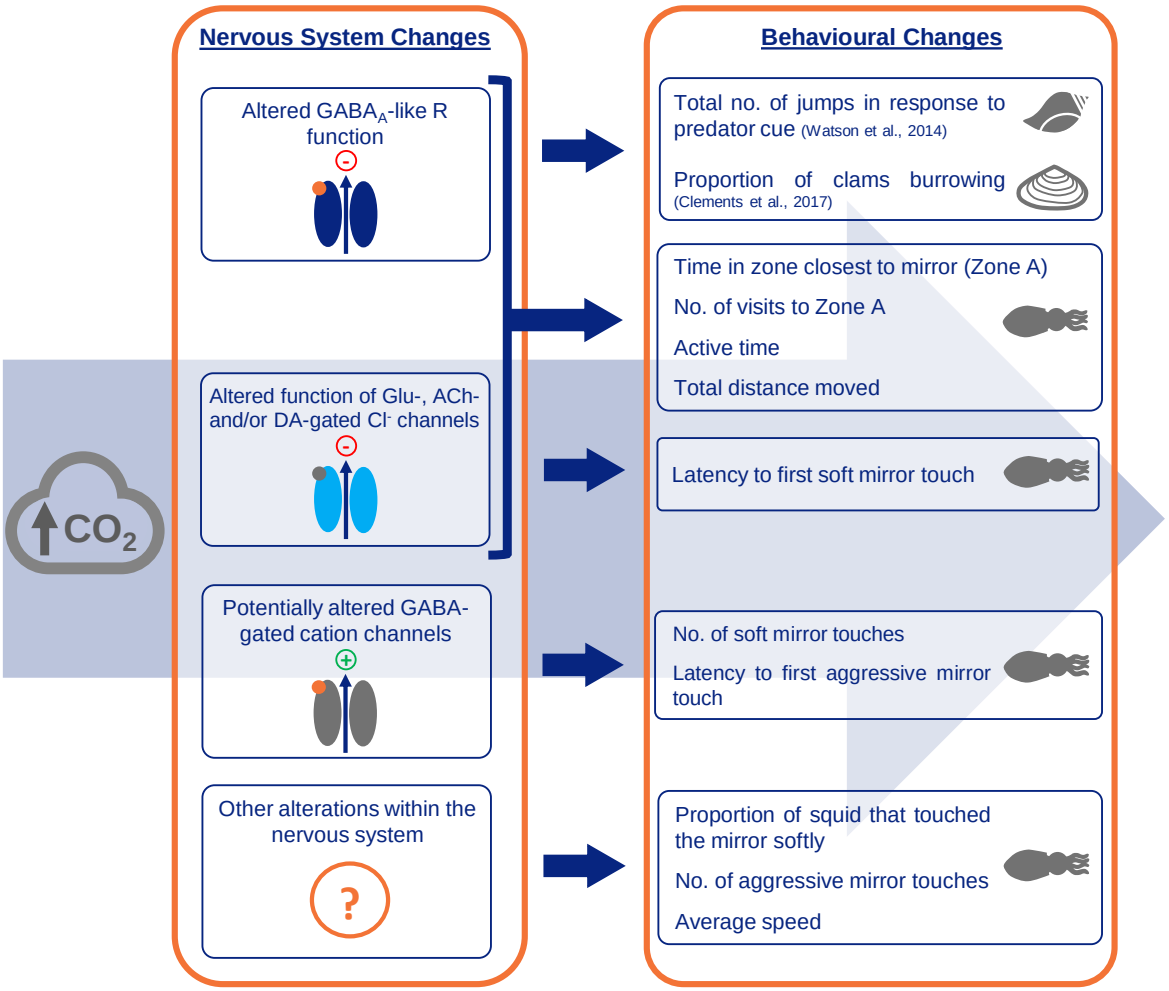

Figure 3.6. Evidence within molluscs that elevated CO_2 results in a suite of changes within the nervous system. Each change (or group of changes) likely alters different behavioural traits. The mechanisms underlying elevated CO_2-induced behavioural change were tested using gabazine in the jumping conch snail and soft-shell clam, and both gabazine and picrotoxin in the two-toned pygmy squid (this study).

cently shown to be altered at elevated CO_2 levels in *Aplysia californica* (Zlatkin and Heuer, 2019), a well-studied model organism for neurobiological work. Drug administration in a species whose pharmacological profile is well known, as well as other techniques such as gene knockdown and transcriptomics, will be important to understand the complexities of the mechanisms underlying behavioural change at elevated CO_2.

Chapter 4

Neurobiological mechanisms underlying effects of elevated CO_2 in a cephalopod

A version of this chapter is in preparation for publication:
Thomas, J.T., Huerlimann R., Schunter C., Watson, S.-A., Munday, P.L. and Ravasi T. (in preparation). Neurobiological mechanisms underlying effects of elevated CO_2 in a cephalopod.

Data availability:
All sequencing data can be found at NCBI BioProject PRJNA798187 (this is embargoed until publication).
All remaining data and scripts accompanying this chapter are available at https://doi.org/10.25903/ha66-mm11 (this is embargoed until publication).

4.1 Abstract

The nervous system is central to coordinating behavioural and physiological responses to environmental change, likely including rising seawater carbon dioxide (CO_2) levels. However, the neurobiological mechanisms underlying the responses to elevated CO_2 remain understudied in marine invertebrates. Here, I evaluated the transcriptomic response of the central nervous system (CNS) and eyes of two-toned pygmy squid (*Idiosepius pygmaeus*) exposed to elevated (~1,000 µatm) CO_2 for seven days compared with current-day (~450 µatm) controls. As a reference for gene expression quantification, I assembled a high quality, annotated *de novo* transcriptome of *I. pygmaeus* CNS and eye tissues using long read PacBio ISO-sequencing data. There were a small number of significantly differentially expressed genes, and widespread small but coordinated expression changes of genes belonging to the same functional categories, between control and elevated CO_2 conditions. Both the squid CNS and eyes responded to elevated CO_2 with expression changes in three top functions: neurotransmission, immune function, and oxidative stress. My results support both previous and novel mechanistic hypotheses for behavioural and physiological responses to elevated CO_2 and I propose a novel mechanistic model explaining how changes in neurotransmission, immune function and oxidative stress might interact in the nervous tissue of *I. pygmaeus* to drive behavioural and physiological responses to elevated CO_2. Molecular signatures for various different types of neurotransmission, including neurotransmission mediated by $GABA_A$-like receptors, suggests altered functioning of widespread neurotransmission is a likely mechanism for elevated CO_2-induced behavioural change. I suggest alterations in the neuroendocrine-immune axis may disturb the immune response, and oxidative damage may disrupt neurotransmission and the immune response at elevated CO_2. This study highlights the importance of considering neurobiological mechanisms in not only behavioural, but also physiological, responses to environmental change, and the potential complex interactions involved.

4.2 Introduction

As human-induced environmental changes progress, establishing how animals respond to projected future environmental conditions, and why these responses occur, is critical (Fuller *et al.*, 2010). A mechanistic understanding of the observed biological responses is especially useful for developing cause-effect relationships, gaining insight into why some individuals or species are more sensitive to environmental change than others, and improving predictions of how organisms and populations will respond over the timescales at which environmental change is occurring (Cooke *et al.*, 2013). The nervous system forms the fundamental link between the environment and an organism's behaviour and physiology (Brown, 2001; Kelley *et al.*, 2018; O'Donnell, 2018). Therefore, a neurobiological understanding is key to gaining insight into the mechanistic underpinnings of an organism's response to environmental change. However, the role of the neurobiological mechanisms in biological responses to environmental change has been little explored (Kelley *et al.*, 2018).

The uptake of anthropogenic CO_2 by the ocean is causing seawater CO_2 levels to rise, decreasing seawater pH and altering the concentration of carbonate ions, a process called ocean acidification (OA) (Bindoff *et al.*, 2019). These chemical changes can fundamentally affect marine organisms and the ecosystems they inhabit (Doney *et al.*, 2009). OA was first shown to disturb the calcification of calcifying marine invertebrates (Kleypas *et al.*, 1999; Riebesell *et al.*, 2000; Feely *et al.*, 2004; Kurihara *et al.*, 2004), but has since been shown to affect a range of biological responses in marine invertebrates, including a variety of physiological impacts (Pörtner *et al.*, 2004; Kroeker *et al.*, 2010) and behavioural alterations (Clements and Hunt, 2015; Nagelkerken and Munday, 2015, Chapter 2). However, sensitivity to OA can vary between taxa and life stages (Kroeker *et al.*, 2013; Clements and Hunt, 2015), which can have flow-on effects, altering species interactions and subsequent community and ecosystem dynamics (Zarnetske *et al.*, 2012; Kroeker *et al.*, 2014; Sanford *et al.*, 2014).

Despite many studies assessing the physiological and behavioural responses of marine invertebrates to OA, the neurobiological underpinnings of these responses remain poorly understood. The work that has addressed the neurobiological impacts of OA has focused on a mechanistic understanding of elevated CO_2-induced behavioural alterations. The prominent mechanistic hypothesis for behavioural change at elevated CO_2 is the GABA hypothesis, which was first proposed in fish and suggests acid-base regulatory mechanisms at elevated CO_2 alter ionic gradients across neuronal membranes, consequently disturbing $GABA_A$ receptor function and causing behavioural alterations (Nilsson *et al.*, 2012). A range of research has supported the GABA hypothesis in fish (reviewed in (Heuer *et al.*, 2019)), and more recently pharmacological studies have also supported the GABA hypothesis in molluscs (Watson *et al.*, 2014; Clements *et al.*, 2017, Chapter 3), but not a crustacean (Charpentier and

Cohen, 2016). It has also been suggested that elevated CO_2 may alter behaviour via disruption of other ligand-gated ion channels that are similar to the $GABA_A$ receptor (Tresguerres and Hamilton, 2017, Chapter 2), and there is support for this hypothesis in a tropical squid (Chapter 3). Behavioural responses to elevated CO_2 may also occur through a range of other neurobiological mechanisms, such as altered sensation and information processing, that have been little explored to date (Briffa *et al.*, 2012, Chapter 2).

The neurobiological mechanisms underlying behavioural changes at elevated CO_2 identified so far are not necessarily mutually exclusive and may also interact (Chapter 2). As this research is in its infancy, it is likely that other, yet to be identified, neurobiological mechanisms could contribute to behavioural changes at elevated CO_2. Furthermore, neurobiological mechanisms are likely also involved in physiological responses to elevated CO_2. Transcriptomics explores all of the genes expressed in the chosen tissue(s), allowing a holistic view that can capture the potential interactions of these elevated CO_2 neurobiological impacts, and test both existing hypotheses about the mechanisms of behavioural alterations at elevated CO_2, and lead to the development of novel mechanistic hypotheses. Therefore, transcriptomics is a powerful tool with which to explore an organism's response to environmental change.

Indeed, transcriptomics has widely been taken up by the OA research community to understand the response of marine animals to elevated CO_2 (Strader *et al.*, 2020). However, there is very little research assessing the transcriptomic response of nervous tissue to elevated CO_2. Recently, a few transcriptomic studies in the nervous system of fish have investigated the mechanisms underlying elevated CO_2-induced behavioural alterations. Two intergenerational experiments assessed the molecular response of the spiny damselfish brain to elevated CO_2 dependent on the behavioural tolerance of the parent fish to elevated CO_2. The brains of juvenile fish were found to show a clear molecular signature of parental behavioural tolerance to CO_2, which was mainly driven by circadian rhythm genes (Schunter *et al.*, 2016). Short-term and developmental exposure to elevated CO_2 triggered a self-amplifying cycle of altered GABAergic neurotransmission in juveniles, but intergenerational exposure to elevated CO_2 mostly returned the brain molecular response to baseline levels (Schunter *et al.*, 2018). From this transcriptional work, it has been proposed that a self-amplifying cycle is initiated by the disturbance of some $GABA_A$ receptors, explaining how small alterations can lead to large behavioural responses (Schunter *et al.*, 2019). In European sea bass, olfactory ability was reduced at elevated CO_2 which was associated with suppressed transcription of genes in the olfactory system involved in cell excitability and synaptic plasticity (Porteus *et al.*, 2018). In ocean-phase salmon, differential expression (DE) of genes involved in GABA signalling and ion balance regulation in the olfactory system was associated with disrupted olfactory-mediated behaviour at elevated CO_2 (Williams *et al.*, 2019). Recently, diel CO_2 variation has been shown to alter the brain transcriptional responses of two coral

reef fishes, indicating the importance of using ecologically relevant CO_2 treatment conditions in laboratory experiments (Schunter *et al.*, 2021). Thus, transcriptomics can be used to test pre-existing hypotheses, such as the GABA hypothesis, but also allows the development of novel hypotheses, such as the involvement of circadian rhythm genes and synaptic plasticity, to explain elevated CO_2-induced responses.

In marine invertebrates, two transcriptomic studies assessing the whole body response of pteropod molluscs to elevated CO_2 identified altered expression of nervous system genes. In *Heliconoides inflatus*, 22% of the transcripts upregulated at elevated CO_2 were involved in nervous system function, including transcripts involved in GABAergic, glycinergic, cholinergic and glutamatergic neurotransmission (Moya *et al.*, 2016). Neural genes, including acetylcholine receptors, also showed altered expression at elevated CO_2 in *Limacina helicina antarctica* (Johnson and Hofmann, 2017). However, whole body measurements cannot determine if non-tissue-specific transcripts are responding to elevated CO_2 in a system-wide manner, or only within specific tissues. For example, Moya *et al.* (2016) found DE of a range of genes involved in acid-base regulation and ion transport in *H. inflatus*, but as whole animals were used it is unknown whether these alterations were animal wide or restricted to specific tissues, including the nervous system. Furthermore, due to the heterogeneity and complexity of gene expression, measurements at the whole body level may mask transcriptomic responses in specific tissues, such as the nervous system.

Here, I investigated the transcriptomic response of the central and peripheral nervous system of a cephalopod, the two-toned pygmy squid (*Idiosepius pygmaeus*), to elevated CO_2. Cephalopods have complex nervous systems and behaviours rivalling those of fishes (Hanlon and Messenger, 2018), making them a useful taxon to investigate the neurobiological impacts of elevated CO_2. *I. pygmaeus* is an ideal species to use as previous research in this species has shown that elevated CO_2 alters a range of behaviours (Spady *et al.*, 2014, 2018, Chapter 3) and reproduction (Spady *et al.*, 2019). In this study, I exposed male *I. pygmaeus* to current-day (~450 µatm) or elevated (~1,000 µatm) CO_2 levels for 7 days, followed by dissection and RNA extraction from the central nervous system (CNS) and eyes (peripheral sense organ). A *de novo* transcriptome assemby was created and annotated, providing a reference to determine the molecular response of the CNS and eyes to elevated CO_2. Using the eyes and CNS allowed investigating the impact of elevated CO_2 on peripheral sensation and higher order processing. I used the eyes because cephalopods, including squid, are highly visual animals with many visually-guided behaviours (Muntz, 1999; Mather, 2006; Chung *et al.*, 2022). Furthermore, elevated CO_2 disrupted visually-guided behaviour in the same squid used in this study (Chapter 3), and elevated CO_2-induced visual impairment in a fish was due to disrupted $GABA_A$ receptor function in the eye (Chung *et al.*, 2014). The aim of this study was to 1) identify key genes and processes involved in the cephalopod nervous system's response to

elevated CO_2, and 2) provide an essential step towards identifying potential neurobiological mechanisms that may underlie behavioural and physiological responses to elevated CO_2.

4.3 Methods

4.3.1 Study species

The two-toned pygmy squid (*Idiosepius pygmaeus*) is a diurnal, tropical squid inhabiting shallow, inshore waters of the Indo-Pacific, including Northern and Northeastern Australia (Moynihan, 1983; Reid, 2005). They are a small, short-lived squid growing to a maximum mantle length of 2 cm (Reid, 2005) with a lifespan of up to 80 days (Jackson, 1988).

4.3.2 CO_2 treatment and sample collection

The central nervous system (CNS) and eyes of 20 male *I. pygmaeus* were collected after CO_2 treatment and behavioural testing (current-day CO_2, n = 10, elevated CO_2, n = 10), as explained in Chapter 3 (sham-treated squid from the picrotoxin experiment in Chapter 3 were used here) (Figure 4.1). Briefly, squid were collected from the wild between August – October 2019 (19°15'11"S 146°49'24"E) (Queensland Government General Fisheries Permit number 199144). Squid were acclimated in groups at current-day seawater conditions for 1 - 6 days before transferral to individual treatment tanks set at either current-day (~450 µatm) or elevated (~1,000 µatm) CO_2. Diel CO_2 variation is common in coastal habitats (Hannan *et al.*, 2020). However, the coastal waters where I collected *I. pygmaeus* show little daily variation in seawater pCO_2 levels; average daily range 20.3 ± 8.6 µatm CO_2 (mean ± SD) (Appendix C: Water sampling methods and Figure C.1). Thus, the experimental CO_2 levels used here are ecologically relevant to the population of *I. pygmaeus* used. After 7 days of current-day or elevated CO_2 treatment, squid underwent sham treatment by being individually placed in 100 mL of aerated seawater from their CO_2 treatment containing 0.2% ethanol for 30 minutes, as part of the experiment in Chapter 3. Visually-guided behaviour was then tested for 15 minutes by placing squid individually in a tank (30 × 30 × 15 cm) filled to 3 cm depth with seawater from their CO_2 treatment and with a mirror taking up the entire area of one wall. The behavioural results from this experiment are reported in Chapter 3. Immediately after each behavioural trial, squid were euthanised with AQUI-S (1:1000). The head was separated from the mantle, rinsed in distilled water, and blotted dry. The skin, tentacles, beak, and buccal mass were removed and the eyes and central nervous system (CNS, containing the oesophagus running through the middle) were dissected and snap frozen in liquid nitrogen within 4.18 ± 0.55 minutes after euthanasia. Tissues were then

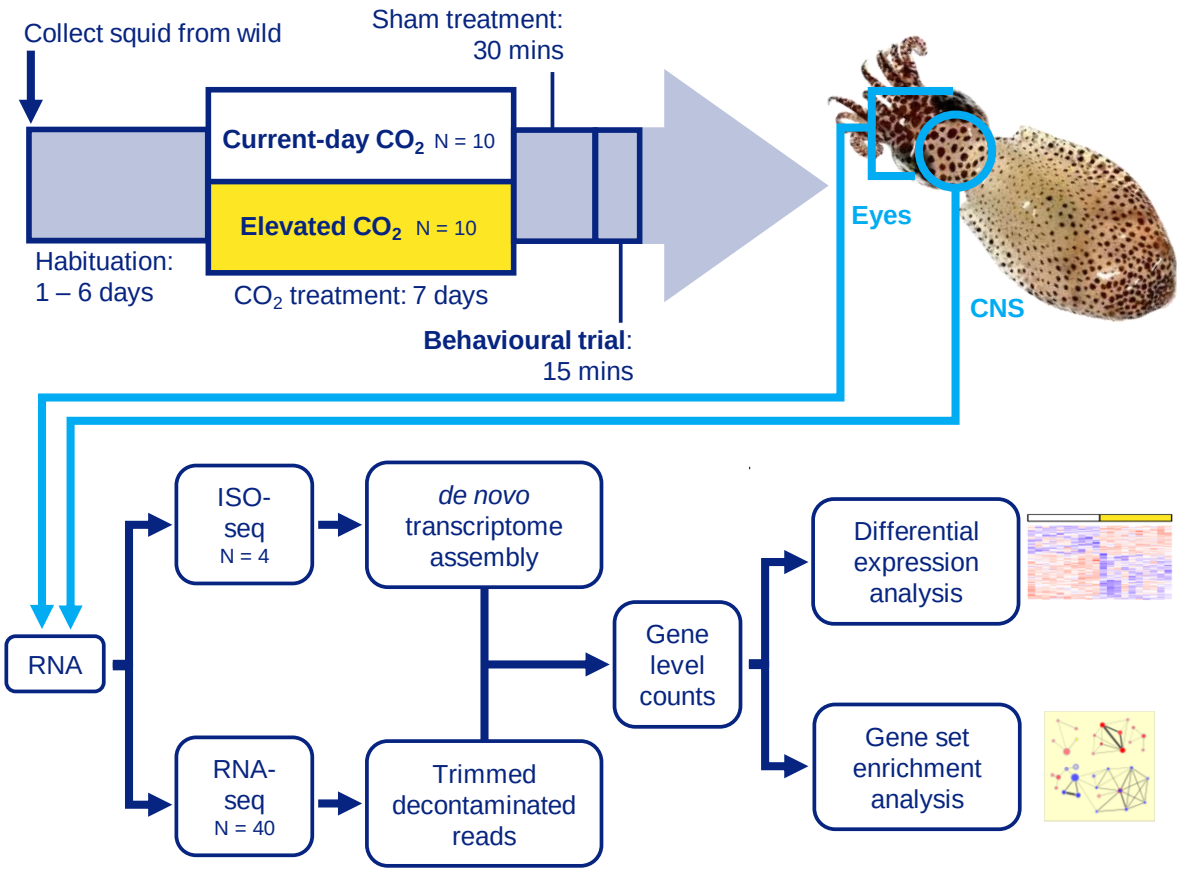

Figure 4.1. Experimental design overview. RNA was used from the CNS, and both eyes combined for each squid exposed to either current-day or elevated CO_2 conditions. Long read PacBio ISO-sequencing data from four samples, one of each tissue type and CO_2 level, was used to create a *de novo* transcriptome assembly. After trimming and decontamination removal, RNA-sequencing data from 40 samples, ten of each tissue type and CO_2 level, was mapped against the *de novo* transcriptome assembly producing gene level counts. The gene level counts were used for differential expression and gene set enrichment analyses. *Idiosepius pygmaeus* photograph by Jodi Thomas.

transferred to -80°C for storage.

4.3.3 RNA extraction

Total RNA was extracted from the CNS, and both eyes combined for each squid (current-day CO_2, n = 10, elevated CO_2, n = 10 for each tissue) (Figure 4.1). Each tissue sample was homogenised in RLT-Plus Buffer (Qiagen) with sterile zirconia/silica beads (1 mm diameter, BioSpec Products) in a Mini-BeadBeater 96 (BioSpec Products) for a total of 2 minutes. Total RNA was extracted using an AllPrep DNA/RNA Mini Kit (Qiagen). RNA integrity of all 40 samples was measured on an Agilent 2200 TapeStation (High Sensitivity RNA ScreenTape,

Agilent) (Appendix C: TapeStation electropherograms).

4.3.4 RNA sequencing

The Sequencing Section (SQC), Okinawa Institute of Science and Technology Graduate University (OIST), Japan carried out library preparation and sequencing on all 40 RNA samples. RNA was quantified by Qubit Flex Fluorometer (Qubit RNA BR assay kit, Thermo Fisher Scientific Inc.). The NEBNext® Poly(A) mRNA Magnetic Isolation Module (New England BioLabs Inc.) was followed according to the manufacturers protocol to isolate mRNA. One library was prepared for each sample, using the NEBNext® Ultra II Directional RNA Library Prep Kit for Illumina® (New England BioLabs Inc.) following the manufacturers protocol, using ten PCR cycles. Libraries were sequenced on two lanes of a NovaSeq6000 with a S2 flow cell paired end to the length of 150 bp.

4.3.5 RNA-seq read pre-processing

For a detailed workflow of the bioinformatic and statistical analyses, see Appendix C: Figure C.2. Raw reads were inspected with FastQC (v0.11.9) (Andrews, 2010) and MultiQC (v1.9) (Ewels *et al.*, 2016) and trimmed with Fastp (v0.21.1) (Chen *et al.*, 2018) using a sliding window of 4 bp, a mean Phred score of 30 and reads < 30 bp were trimmed. Kraken2 (v2.0.9) (Wood *et al.*, 2019) was used with a confidence of 0.3 to remove any contamination using the NCBI bacterial and archaeal reference libraries (downloaded 08/2020).

4.3.6 ISO-sequencing

Library preparation and sequencing was carried out by the SQC, OIST, Japan on four samples that were also used for RNA-seq, one of each tissue type and CO_2 level. RNA from the eyes was purified with oligo d(T) beads due to carry over of pigmentation (NEBNext® Poly(A) mRNA Magnetic Isolation Module, New England BioLabs Inc.). RNA was quantified by Qubit 4 Fluorometer (Qubit RNA HS Assay Kit, Life Technologies). One library was prepared for each sample following the Iso-Seq™ Express Template Preparation for Sequel® and Sequel II Systems protocol with standard size selection (86 µL ProNex® Beads). Libraries were sequenced on one SMRTcell of a PacBio Sequel II.

4.3.7 *de novo* transcriptome assembly

The ISO-seq data was processed using the PacBio isoseq3 pipeline. The raw subreads were compiled into circular consensus sequence (ccs) reads by ccs (v4.2.0) with the minimum

number of full passes set at three and the minimum predicted accuracy of a read at 0.9. Lima (v1.11.0) was used to classify the ccs reads as full-length (FL) (by the presence of both 5' and 3' primers) and remove index sequences with '–peek-guess'. The resulting FL reads from each tissue/barcode were combined and isoseq3 refine (v3.3.0) was used to remove concatemers and polyA tails, producing full-length non-concatemer (FLNC) reads. The FLNC reads were then clustered by isoform using isoseq3 cluster (v3.3.0), using the ccs quality values ('–use-qvs') to obtain a consensus sequence for each isoform. Redundancy removal was performed using CD-HIT-EST (v4.6) (Li and Godzik, 2006; Fu *et al.*, 2012) to collapse contigs with at least 99% identity. TransDecoder (v5.5.0) (Brian and Papanicolaou, n.d.) was used to identify candidate coding regions/open reading frames (ORFs). The single best ORF per contig was chosen based on blast homology to known proteins in the NCBI nr database subset for mollusca (nr_mollusca, downloaded 01/2021) using BLASTp from BLAST+ (v2.10.0+) with max_target_seqs 1 and an e-value cut-off of 1^{-5}, and then based on ORF length (minimum 100 amino acids). The entire transcript was retained for each identified ORF.

The quality and completeness of the transcriptome was assessed before and after redundancy removal, and for the final transcriptome assembly (after ORF identification by TransDecoder). Quality was assessed using Transrate (v1.0.3) (Smith-Unna *et al.*, 2016) and completeness using Benchmarking Universal Single-Copy Orthologs (BUSCO v4.1.2) (Manni *et al.*, 2021), using the lineage mollusca_odb10.2019-11-20. Quality and completeness were also assessed by blasting the transcriptome against nr_mollusca (e-value cut-off of 1^{-5}, '-max_target_seqs 1', BLASTx from BLAST+ (v2.10.0+) (Camacho *et al.*, 2009)), and mapping the trimmed, decontaminated RNA-seq reads to the transcriptome assembly (local alignment, Bowtie2 (v2.4.1) (Langmead and Salzberg, 2012)).

4.3.8 Transcriptome annotation

The transcriptome was blasted against the entire NCBI nr database (downloaded 01/2021) using BLASTx from BLAST+ (v2.10.0+) (Camacho *et al.*, 2009) with an e-value cut-off of 1^{-5}, outfmt 14, and '-num-alignments' and '-max_hsps' both set at 20. Functional annotation was carried out in OmicsBox (v1.4.12) (BioBam Bioinformatics, 2019) using BLAST2GO mapping (Goa version 2020.10, all default settings) (Götz *et al.*, 2008), followed by BLAST2GO annotation (all default settings) (Götz *et al.*, 2008) and InterProScan (v5.50-84.0, all default settings) (Jones *et al.*, 2014a). The InterProScan GOs were then merged with the annotations.

4.3.9 Read mapping and counting

The trimmed and decontaminated RNA-seq reads were mapped against the transcriptome assembly using salmon (v1.3.0) (Patro *et al.*, 2017). Correction for sequence-specific bi-

ases and fragment-level GC biases was used, the quantification step was skipped, and the flags '–validateMappings' and '–hardFilter' were also used. Corset (v1.09) (Davidson and Oshlack, 2014) was run on the salmon equivalence class files from all 40 samples to cluster the transcripts to gene-level and produce gene-level counts. In corset, I provided the four groups/treatments (eyes current-day CO_2, eyes elevated CO_2, CNS current-day CO_2 and CNS elevated CO_2), the log likelihood ratio test was switched off to prevent differentially expressed transcripts being split into different clusters, and the links between contigs were removed if the link was supported by less than 10 reads.

4.3.10 Statistical analyses

All statistical analyses were carried out in R (v4.0.4) (R Core Team, 2021) using RStudio (v 1.4.1106) (RStudio Team, 2021).

Differential expression analysis

DESeq2 (v1.30.1) (Love *et al.*, 2014) using the Wald test was used to compare gene expression between current-day and elevated CO_2 conditions for the CNS and eyes separately. Genes with an adjusted p-value (padj, Benjamini-Hochberg method) < 0.05 were reported as differentially expressed (DE). Three genes in the eyes were removed due to not showing clear DE upon inspection of the normalised counts across CO_2 levels. Log2 fold change estimates were shrunk with the ashr method (Stephens, 2016) to increase their accuracy. Heatmaps of the top 100 genes (by padj value) were created using the 'manhattan' distance method followed by the 'average' hierarchical clustering method on the regularised log transformed data scaled to Z-scores by row.

Gene set enrichment analysis

Gene set enrichment analysis (GSEA) was run in clusterProfiler (v3.18.1) (Yu *et al.*, 2012) for each tissue separately to determine if sets of genes from the same gene ontology (GO) term/functional category showed significant, concordant differences between current-day and elevated CO_2 conditions. Unweighted GSEA was run using the DESeq2 log2 fold-change values of all genes and the annotated GO terms as the 'gene sets'. A minimum and maximum gene set size of 15 and 500, respectively, was used. GSEA determines if genes from the same functional category are significantly more likely to occur at the top or bottom of the log2 fold-change list and therefore whether these functional categories are up- or down-regulated at elevated CO_2, respectively. P-values were adjusted for multiple comparisons using the Benjamini-Hochberg method and a significance threshold of padj < 0.05 was used.

The GSEA results were imported into Cytoscape (v3.8.2) (Shannon *et al.*, 2003) where EnrichmentMap (v3.3.1) (Merico *et al.*, 2010) was used to create a network to visualise the functional enrichment results. All significant functional categories were included in the network as a circular node. Functional categories with > 0.25 similarity were linked by edges. Similar functional categories were manually grouped into clusters and labelled.

4.4 Results

4.4.1 Transcriptome assembly and annotation

The *de novo* transcriptome assembly for *Idiosepius pygmaeus* was created from a total of 138.6 million PacBio ISO-sequencing subreads and resulted in 49,981 transcripts that were clustered into 27,420 'genes'. The transcriptome assembly had an N50 of 3,163 bp, 70.4% complete BUSCOs and an 82.1 ± 5.5% overall alignment rate of the RNA-seq reads (Appendix C: Table C.1). A total of 69% of the transcripts received a functional annotation (Appendix C: Table C.2). The species distribution of the top blast hits was dominated by cephalopod species (Appendix C: Figure C.3). Final mapping of RNA-seq reads against the transcriptome assembly had a 73.6 ± 6.9% mapping rate (Appendix C: Table C.3).

4.4.2 Differential expression analysis

I compared gene expression between current-day and elevated CO_2 conditions for the CNS and eyes separately. There was more variance in the eyes than the CNS (Figure 4.2A). The top 100 genes (sorted by adjusted p-value) in each tissue show strong clustering by CO_2 level (Figure 4.2C,D). In the CNS, I identified 25 differentially expressed genes (DEGs) between current-day and elevated CO_2 conditions; 14 upregulated and 11 downregulated with elevated CO_2. Sixteen of these DEGs had a match to a known gene. In the eyes, there were eight DEGs; five upregulated and three downregulated at elevated CO_2 compared to current-day CO_2 conditions, seven of which resulted in a match to a known gene. Two genes were significantly upregulated with elevated CO_2 in both the CNS and eyes (Figure 4.2B and Table 4.1).

In both tissues, the DEGs play roles in three top functions; neurotransmission (33% of the annotated DEGs), immune function (43% of the annotated DEGS) and oxidative stress (29% of the annotated DEGs). Four DEGs in the CNS (*folh1*, *syvn1-b*, *slc2a13*, *celsr3*) and three in the eyes (*maoa*, *slc18a2*, *cbs*) play a role in neurotransmission and regulating a range of resultant behaviours. One DEG in the CNS (*znf271*) and one in the eyes (*pglyrp2*) also regulate behaviour via unknown mechanisms (Table 4.1 and Figure 4.3). Six DEGs in the

CNS (*psenen*, *syvn1-b*, *map4k5*, *tf*, *nme6*, *map1l3ca/b*) and three in the eyes (*pglyrp2*, *cbs*, *maoa*) are involved in the innate immune response (Table 4.1 and Figure 4.4). DEGs in both tissues are also involved in the oxidative stress response; *tf* and *cyb561d2* in the CNS, and *cbs* in the eyes are involved in regulating reactive oxygen species (ROS) and antioxidant production, while *ykt6* in both tissues, and *syvn1-b* and *chrac1* in the CNS deal with oxidative-stress induced damages (Table 4.1 and Figure 4.5). Three DEGs in the CNS (*nme6*, *chrac1*, *znf271*) and one in the eyes (*gtf2e2*) are also involved in regulating transcription (Table 4.1).

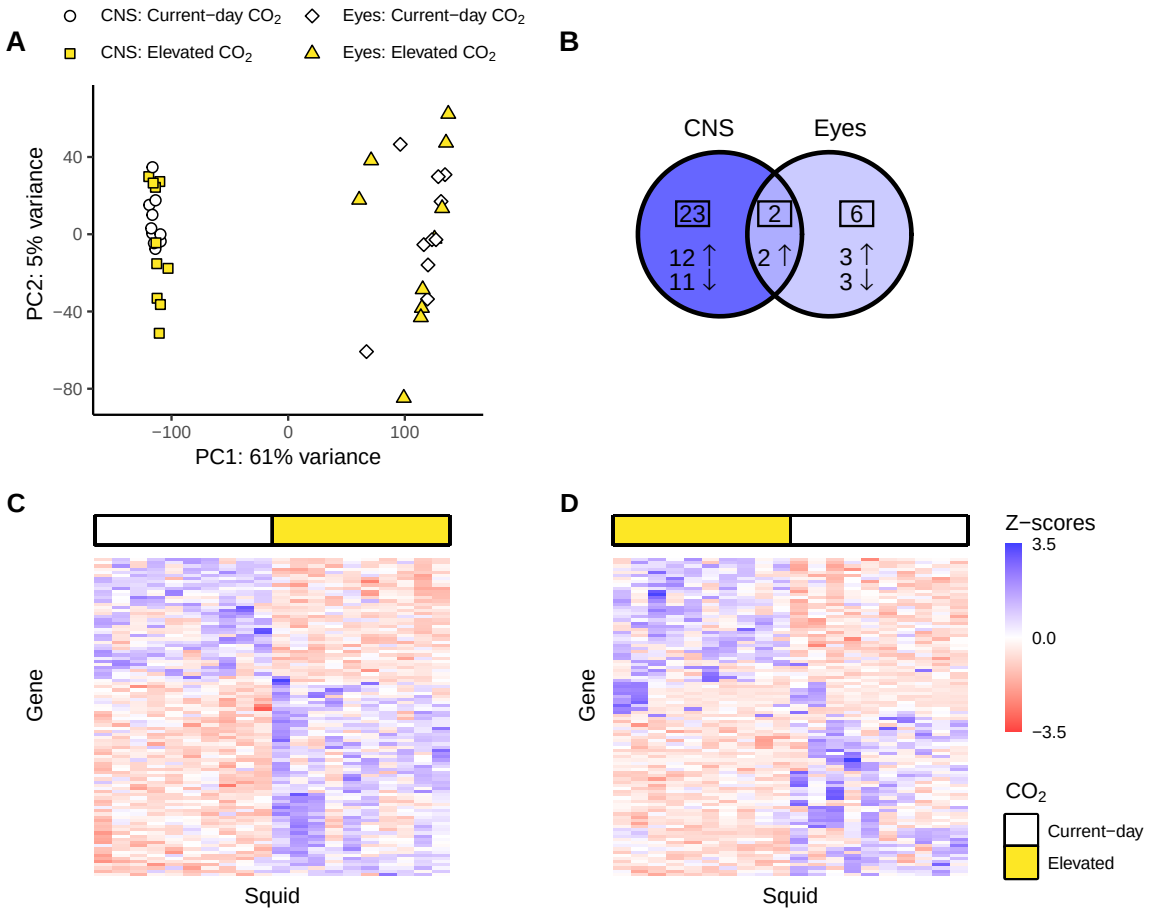

Figure 4.2. Differential expression results. **A** PC1 and PC2 axes from the principal components analysis of all genes for the 40 samples. **B** Venn diagram comparing the DEGs between current-day and elevated CO_2 levels in the CNS and eyes. **C, D** heatmap of the top 100 genes (by adjusted p-value) in the CNS and eyes, respectively. Distance was calculated using the 'manhattan' method followed by hierarchical clustering using the 'average' method. Expression level is represented by Z-scores. ○= CNS current-day, ● = CNS elevated CO2, ◇ = Eyes current-day, △ = Eyes elevated CO_2, ↑ = upregulated at elevated CO_2 conditions, ↓ = down-regulated at elevated CO_2 conditions.

Table 4.1. Table of DEGs and their function in the CNS and eyes, ordered by log2 fold-change (LFC). Genes in red and blue are upregulated and downregulated at elevated CO_2, respectively. DEGs in both tissues are in bold. Ticks in columns on the right depict which of the three top functions the DEGs are involved in. NT = neurotransmission, I = immune, OS = oxidative stress, padj = adjusted p-value.

Gene	Annotation	Putative function in CNS/eyes	Reference	padj	LFC	NT	I	OS
			CNS					
fam204a	**protein FAM204A isoform X1**	**Poorly characterised.**		**0.004**	**1.34**			
prickle3	prickle-like protein 3 isoform X4	Required for mitochondrial membrane ATP synthase function. Involved in the planar cell polarity pathway and visual function.	Yu *et al.* (2020)	0.034	0.96			
map4k5/ map4k3	mitogen-activated protein kinase kinase kinase kinase 5-like isoform X4 / 3-like isoform X3	May mediate the immune response via activation of the JNK pathway.	Chuang *et al.* (2016)	0.039	0.92		✓	
ykt6	**synaptobrevin homolog YKT6**	**Essential for lysosomal function.** **Essential for autophagy (fusing of the autophagosome and lysosome for degradation).**	**Cuddy *et al.* (2019)** **Nair *et al.* (2011); Bas *et al.* (2018); Matsui *et al.* (2018); Takáts *et al.* (2018)**	**0.039**	**0.89**			✓
znf271	zinc finger protein 271-like	Potential transcription factor. Associated with zebrafish activity levels.	Zhan and Desiderio (2003) Seifinejad *et al.* (2019)	0.039	0.86			
chrac1	chromatin accessibility complex protein 1	Histone-fold protein. Involved in the repair of DNA double-strand breaks	Narlikar *et al.* (2002); Kukimoto *et al.* (2004) Lan *et al.* (2010)	0.046	0.75			✓
nme6	nucleoside diphosphate kinase 6-like	Synthesises nucleoside triphosphates. May have an anti-viral and anti-bacterial role in invertebrates, including in molluscs.	Lacombe *et al.* (2000); Tsuiki *et al.* (2000) Chakrabarty (1998); Clavero-Salas *et al.* (2007); Jin *et al.* (2011); Quintero-Reyes *et al.* (2012); Ji *et al.* (2013); Duan *et al.* (2015)	0.039	0.63		✓	

Table 4.1 continued.

Gene	Annotation	Putative function in CNS/eyes	Reference	padj	LFC	NT	I	OS
folh1	putative N-acetylated-alpha-linked acidic dipeptidase isoform X4	Synthesises glutamate.	Robinson *et al.* (1987)	0.039	0.58	✓		
tf	transferrin-like protein	Iron sequestration as part of the molluscan innate immune response, including in squid.	Lambert *et al.* (2005); Ong *et al.* (2006); Herath *et al.* (2015); Salazar *et al.* (2015); Li *et al.* (2019)	0.039	0.48		✓	✓
		Binds iron, decreasing the amount of iron available for ROS production.	Dean (2010)					
syvn1-b	E3 ubiquitin-protein ligase synoviolin B-like	Increases pro-inflammatory cytokine production via activating NF-KB.	Lu *et al.* (2019)	0.039	0.27	✓	✓	✓
		An E3 ubiquitin ligase playing a critical role in ERAD, ubiquitinating misfolded and unfolded proteins for degradation, which protects cells from ER stress-induced apoptosis.	Bordallo *et al.* (1998); Kaneko *et al.* (2002); Carvalho *et al.* (2006); Xie *et al.* (2009); Baldridge and Rapoport (2016); Nomura *et al.* (2016)					
		Plays a critical role in $GABA_A\alpha1$ receptor subunit degradation.	Crider *et al.* (2014); Jiao *et al.* (2017)					
cyb561d2	cytochrome b561 domain-containing protein 2	Reduces Fe^{3+} to Fe^{2+}. Regenerates the antioxidant ascorbate.	Mizutani *et al.* (2007) Recuenco *et al.* (2013)	0.039	-0.46			✓
map1l3ca/b	microtubule-associated proteins 1A/1B light chain 3A/B	Key molecular marker of autophagy, which plays an important role in the molluscan immune response.	Moreau *et al.* (2015); Klionsky *et al.* (2016); Han *et al.* (2019); Picot *et al.* (2019)	0.045	-0.54		✓	
slc2a13	proton myo-inositol cotransporter	Transports myo-inositol into neurons and glia, which has a range of roles including membrane excitability, vesicular trafficking, intracellular calcium signaling, and neurotransmission.	Uldry *et al.* (2001, 2004); Shaldubina *et al.* (2007); MacFarlane and Di Fiore (2018)	0.003	-0.56	✓		
celsr3	cadherin EGF LAG seven-pass G-type receptor 3	Mediates glutamatergic synapse formation.	Thakar *et al.* (2017)	0.039	-0.8	✓		

Table 4.1 continued.

Gene	Annotation	Putative function in CNS/eyes	Reference	padj	LFC	NT	I	OS
psenen	gamma-secretase subunit PEN-2	Indispensable component of the gamma-secretase protein complex involved in Notch signalling which plays an important role in both the adaptive and innate immune responses, including via regulating NF-KB signalling.	Palaga *et al.* (2003); Osipo *et al.* (2008); Radtke *et al.* (2013)	0.039	-0.8		✓	
		Potentially involved in the invertebrate immune response.	Fuess *et al.* (2016)					
mccc2	methylcrotonoyl-CoA carboxylase beta chain, mitochondrial	Leucine and isovaleric acid catabolism.	Chu and Cheng (2007)	0.034	-0.81			
9 unannotated genes: 4 upregulated, 5 downregulated								
		Eyes						
maoa	probable flavin-containing monoamine oxidase A	Degrades monoamine neurotransmitters, including in scallops and squid.	Yagodina (2009, 2010); Zhou *et al.* (2011); Ng *et al.* (2015)	0.005	2.29	✓	✓	
		Associated with anxiety-like, depressive-like, aggression and activity behaviours.	Cases *et al.* (1995); Scott *et al.* (2008); Wang *et al.* (2017a); Bellot *et al.* (2021); Mentis *et al.* (2021)					
		Potential key role in molluscan immune response.	Zhou *et al.* (2011); Liu *et al.* (2018); Sun *et al.* (2021)					
slc18a2	synaptic vesicular amine transporter	Packages monoamine neurotransmitters into vesicles prior to exocytosis.	Ng *et al.* (2015)	0.012	2.04	✓		
		Associated with anxiety-like, depressive-like, aggression and activity behaviours.	Fukui *et al.* (2007); Simon *et al.* (2009); Lohr *et al.* (2014); Branco *et al.* (2020)					
		Required for the release of GABA from some neurons.	Tritsch *et al.* (2012)					
fam204a	**protein FAM204A isoform X1**	**Poorly characterised.**		**0.012**	**1.47**			
ykt6	**synaptobrevin homolog YKT6**	**Essential for lysosomal function.** **Essential for autophagy (fusing of the autophagosome and lysosome for degradation).**	**Cuddy *et al.* (2019)** **Nair *et al.* (2011); Bas *et al.* (2018); Matsui *et al.* (2018); Takáts *et al.* (2018)**	**<0.001**	**1.26**			✓

Table 4.1 continued.

Gene	Annotation	Putative function in CNS/eyes	Reference	padj	LFC	NT	I	OS
cbs	cystathionine beta-synthase	The main producer of H_2S, a gaseous neurotransmitter, in the nervous system and in molluscs.	Julian *et al.* (2002); Hu *et al.* (2010)	0.038	0.89	✓	✓	✓
		Role in long-term potentiation and memory.	Régnier *et al.* (2012); Chen *et al.* (2017)					
		H_2S regulates the release of both pro- and anti-inflammatory cytokines, likely via NF-KB, p38 and JNK pathways.	Hu *et al.* (2010); Zhang and Bian (2014)					
		May play a role in the immune iron-withholding strategy due to its critical role in body iron homeostasis.	Qian *et al.* (2014); Zhou *et al.* (2018)					
		Required for regulating cellular iron retention, which may alter iron availability for ROS production.	Dean (2010); Zhou *et al.* (2018)					
		Catalyses the first and rate limiting step of the transsulfuration pathway, which produces cysteine, the rate-limiting substrate for synthesis of the antioxidant glutathione.	Vitvitsky *et al.* (2006); Hu *et al.* (2010); Beard Jr. and Bearden (2011)					
		H_2S has powerful antioxidant effects via multiple pathways.	Shefa *et al.* (2018a)					
		Cbs-produced H_2S inhibits ROS-triggered ER stress.	Lu *et al.* (2012), Xie *et al.* (2012)					
gtf2e2	transcription initiation factor IIE subunit beta	One of two components of the general transcription factor IIE, which are both essential for transcription initiation by RNA polymerase II.	Gregory Peterson *et al.* (1991); Sumimoto *et al.* (1991)	0.022	-0.99			
pglyrp2	N-acetylmuramoyl-L-alanine amidase	Recognises peptidoglycans, a component of bacterial cell walls.	Schleifer and Kandler (1972)	0.002	-2.9		✓	
		Identified in cephalopods, where it binds to and degrades bacterial peptidoglycan.	Goodson *et al.* (2005); Troll *et al.* (2010); Schleicher and Nyholm (2011); Cornet *et al.* (2014)					
		Knock-out in adult mice alters anxiety-like behaviour.	Arentsen *et al.* (2018)					
1 unannotated gene: downregulated								

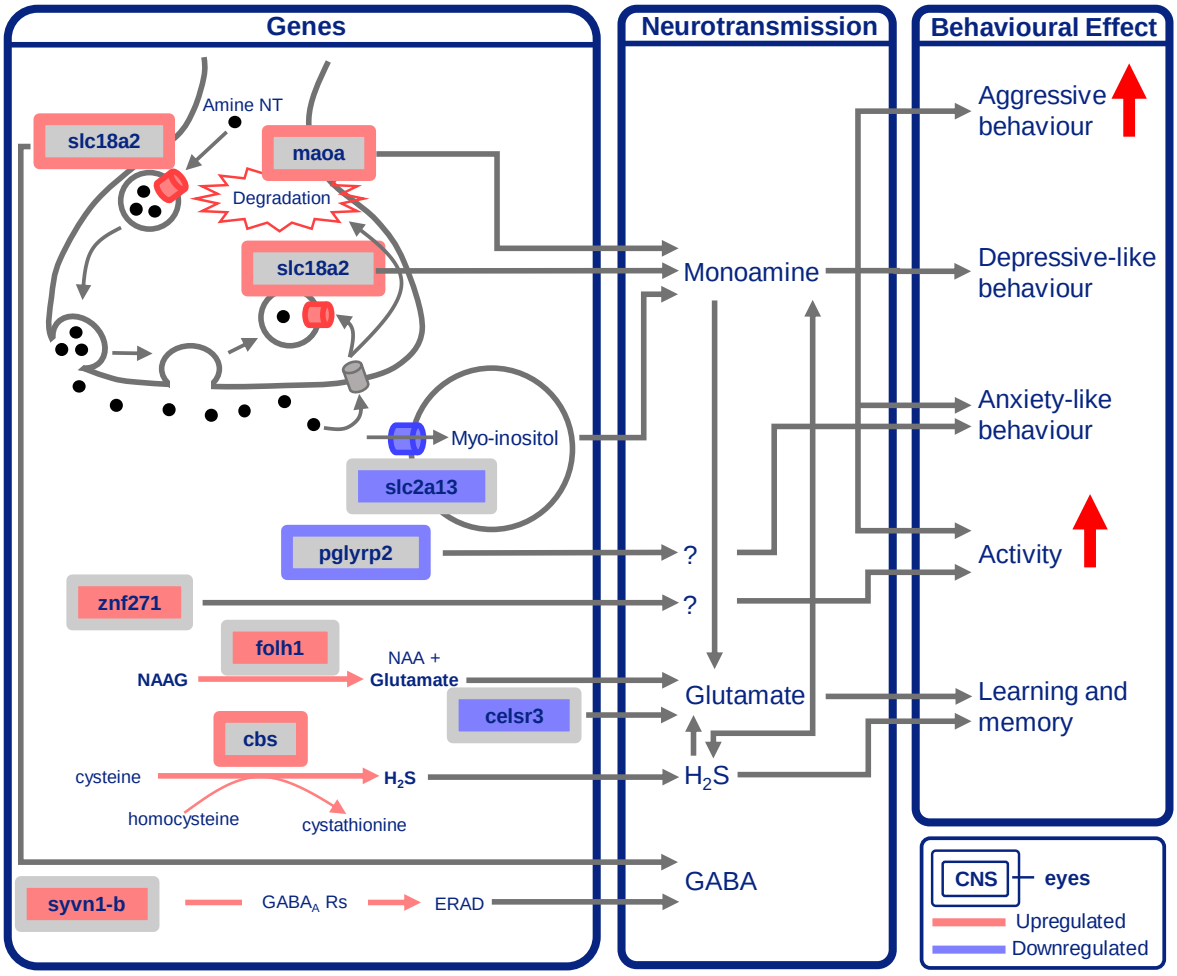

Figure 4.3. Diagram outlining the role of DEGs in neurotransmission and behaviour at elevated CO_2 in *I. pygmaeus*. Only behavioural effects that occur as a consequence of changes in the corresponding genes' expression are depicted, however changes in gene expression could also have other effects via altered neurotransmission. For example, altered *syvn1-b* expression has not been directly linked to any behavioural changes, however it could have many effects via altered GABAergic neurotransmission, which is known to regulate a variety of molluscan behaviours (Chapter 2). For each gene label, colouration of the inner label area represents significant up- or down-regulation (red and blue, respectively) at elevated CO_2 in the CNS. Colouration of the label border represents significant up- or down-regulation (red and blue, respectively) at elevated CO_2 in the eyes. Genes found not significant (padj > 0.05) are coloured grey for the corresponding tissue type. Red arrows represent the increase in aggression and activity I found in the same squid used in this study (Chapter 3). ? = unknown signalling mechanism, ERAD = endoplasmic reticulum associated degradation, H_2S = hydrogen sulphide, NAA = N-acetylaspartic acid, NAAG = N-acetyl-aspartyl-glutamate, NT = neurotransmitter, Rs = receptors.

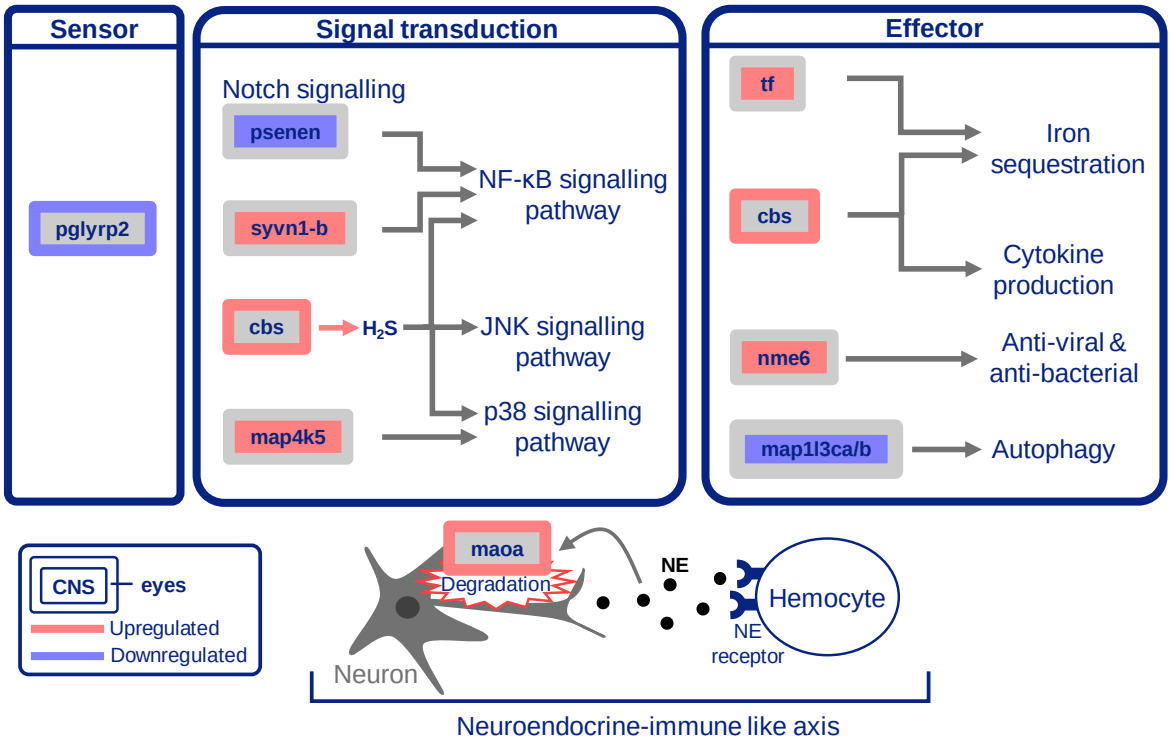

Figure 4.4. Diagram outlining the role of DEGs in the immune response to elevated CO_2 in the nervous tissue of *I. pygmaeus*. There were DEGs involved in all three levels of the innate immune response. DEGs from the CNS and eyes are represented by colouration of the inner label area and label border, respectively. Red and blue represent DEGs upregulated and downregulated at elevated CO_2, respectively. Genes found not significant (padj > 0.05) are coloured grey for the corresponding tissue type. H_2S = hydrogen sulphide, NE = norepinephrine.

4.4.3 Gene set enrichment analysis

Gene set enrichment analysis (GSEA) identified ninety-nine significant Gene Ontology (GO) terms/functional categories in the CNS, indicating small, coordinated changes in expression of the genes belonging to each of these functional categories. There were 75 upregulated and 24 downregulated functional categories in the CNS at elevated CO_2. There were 17 significant functional categories in the eyes, 12 upregulated and 5 downregulated at elevated CO_2 (Figure 4.6 and Appendix C: Figure C.4). The majority of significant functional categories from both tissues belong to 15 different clusters (manually assigned): 'DNA', 'apoptosis/repair', 'ER' (endoplasmic reticulum), 'protein-related' ('kinase activity' and 'ubiquitin'), 'cell cycle', 'epigenetic', 'transcription', 'RNA', 'ribosome/translation', 'cytoskeleton', 'adhesion', 'mRNA splicing', 'GPCR' (G-protein coupled receptor), 'ion transport' and 'ion channel'. These clusters of functional categories further group into the three top functions the DEGs are involved in: neurotransmission, immune function and oxidative

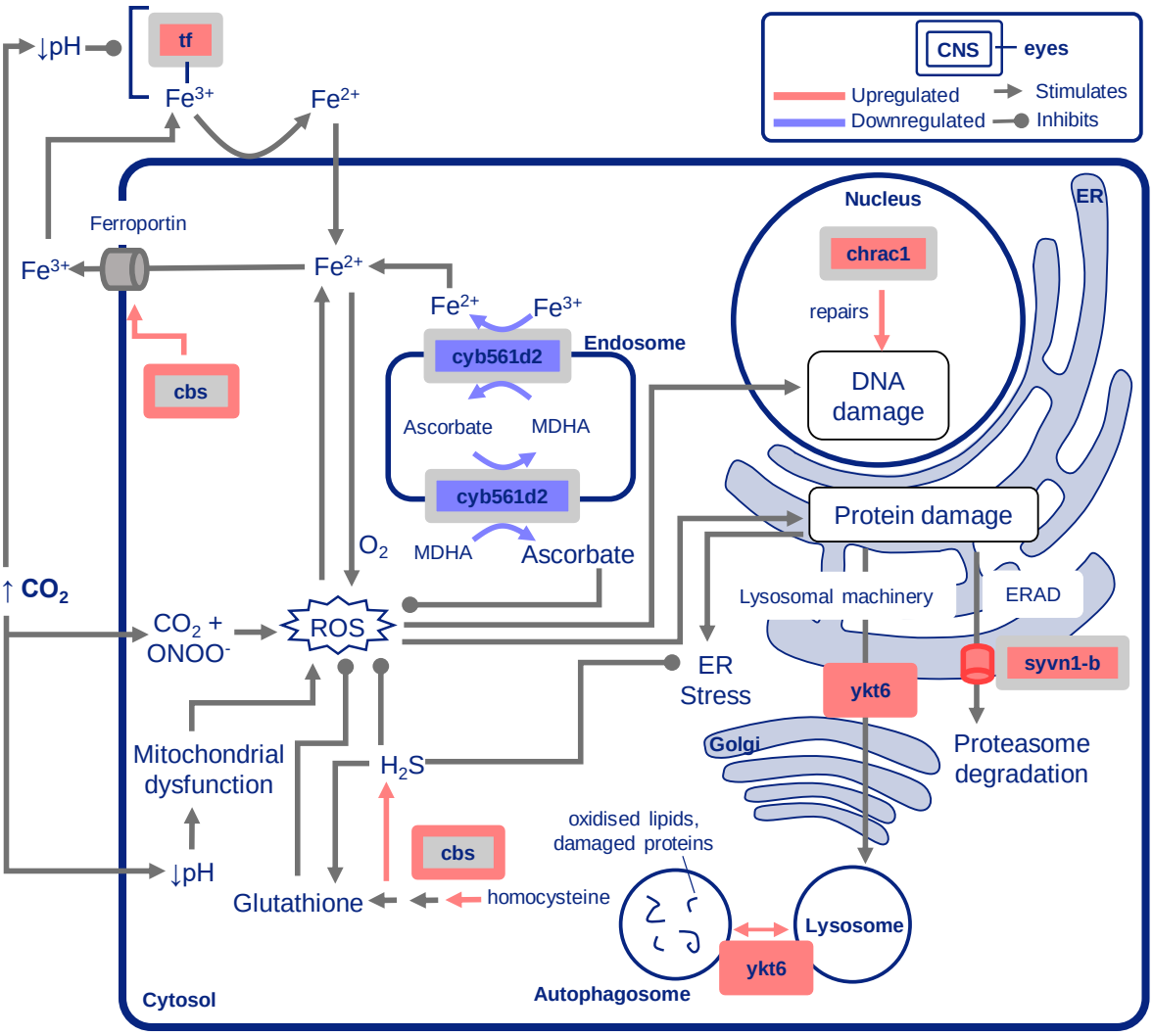

Figure 4.5. Diagram outlining the role of DEGs in the oxidative stress response to elevated CO_2 in the nervous tissue of *I. pygmaeus*. DEGs from the CNS and eyes are represented by colouration of the inner label area and label border, respectively. Red and blue represent DE genes upregulated and downregulated at elevated CO_2, respectively. Genes found not significant (padj > 0.05) are coloured grey for the corresponding tissue type. CO_2 = carbon dioxide, ER = endoplasmic reticulum, ERAD = endoplasmic reticulum associated degradation, H_2S = hydrogen sulphide, ROS = reactive oxygen species.

stress (Figure 4.6).

The 'ion channel', 'ion transport' and 'GPCR' clusters of functional categories are all related to neurotransmission. A cluster of nine ion channel-related functional categories were downregulated in the CNS, and two ion channel-related functional categories were upregulated in the eyes. The core enrichment genes, which is the subset of genes that contributes most to the enrichment result, in the ion channel-related functional categories of both tissues include 13 glutamate receptor-related transcripts, one glycine receptor subunit, two $GABA_A$

receptor transcripts and 18 acetylcholine (ACh) receptor-related transcripts (Appendix C: Table C.4). The 'ion transport' cluster contains seven K^+ and Ca^{2+} ion transport-related functional categories which were downregulated in the CNS and contain core enrichment genes for neurotransmission, including maintenance of membrane potential, action potential generation and neurotransmitter release (Appendix C: Table C.5). Furthermore, the functional categories 'G protein-coupled receptor activity' and 'G protein-coupled receptor signalling pathway' were also downregulated in the CNS, and included the core enrichment genes for five serotonin, three dopamine, three $GABA_B$ and eight metabotropic glutamate receptor transcripts (Appendix C: Table C.6). Functional categories related to immune function, including 'cell adhesion' and 'integrin complex', which are mediators of the phagocytic immune response, were upregulated in the CNS. The cytoskeleton is also important for phagocytosis and three cytoskeleton-related functional categories were upregulated in the CNS ('motor activity', 'actin binding', and 'microtubule cytoskeleton'), and two downregulated in the eyes ('cytoskeleton' and 'intermediate filament cytoskeleton organisation'). Functional categories related to oxidative stress-induced damage were also significantly upregulated at elevated CO_2. This includes upregulation of functional categories related to ER protein damage control, 'endoplasmic reticulum', 'endoplasmic reticulum membrane' and seven ubiquitin-related functional categories in the CNS, and 'proteasome complex' in both tissues. Furthermore, the functional categories 'damaged DNA binding' and 'DNA repair' as well as 'regulation of apoptotic process' were all upregulated in the CNS (Figure 4.6).

4.5 Discussion

I used transcriptomics to investigate the molecular response of the central nervous system (CNS) and eyes (peripheral sense organ) of *Idiosepius pygmaeus* to elevated CO_2. The CNS and eyes of *I. pygmaeus* responded to elevated CO_2 with significant differential expression (DE) of a small number of genes, however, widespread small but coordinated changes of genes belonging to particular functional categories were found between CO_2 conditions. Both tissues responded to elevated CO_2 with expression changes in three top functions; neurotransmission, immune fucntion and oxidative stress, suggesting that the peripheral and central nervous systems of *I. pygmaeus* respond to elevated CO_2 in a similar way. However, elevated CO_2 resulted in a larger number of differentially expressed genes (DEGs), and a larger number of significant functional categories with small coordinated changes in gene expression, in the CNS, compared to the eyes.

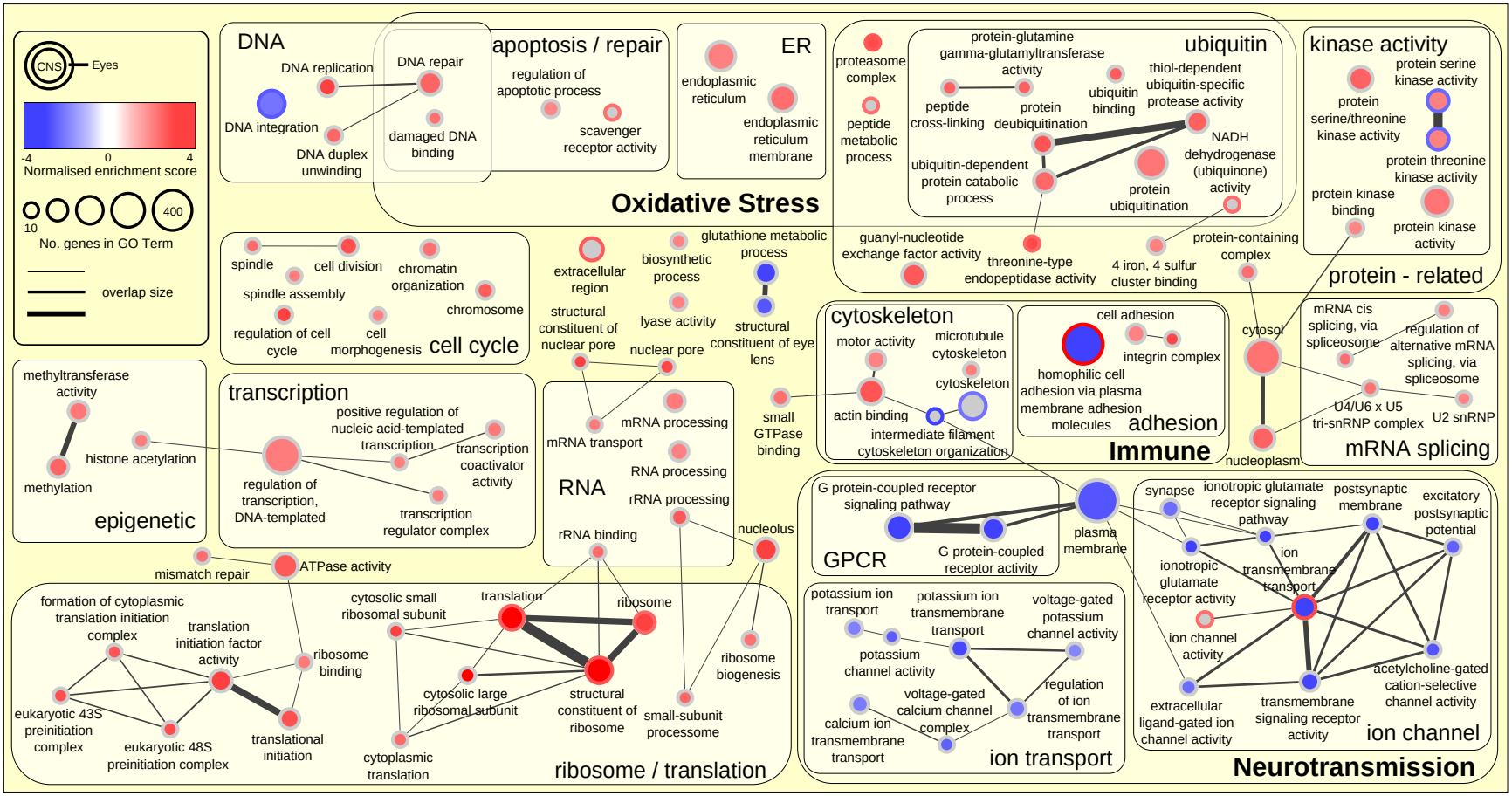

Figure 4.6. Enrichment map displaying the gene set enrichment analysis (GSEA) results in both the CNS and eyes. *(see next page)*

Figure 4.6 *(previous page).* Significant GO terms/functional categories are represented by a circular node. Results from the CNS and eyes are represented by colouration of the inner node area and node border, respectively. Red represents functional categories upregulated at elevated CO_2 and blue represents functional categories downregulated at elevated CO_2. Colour intensity represents the normalised enrichment score and node size the number of core enrichment genes in each functional category. Functional categories found not significant (padj > 0.05) are coloured grey for the corresponding tissue type. The nodes from functional categories with a similarity > 0.25 are connected by an edge, with edge width increasing with increasing similarity (increasing number of genes shared by the functional categories). Similar functional categories were manually grouped into clusters and assigned a label. These clusters were also organised into larger groups of neurotransmission, immune and oxidative stress.

4.5.1 *de novo* transcriptome assembly

To provide a reference for gene quantification, I created a *de novo* transcriptome assembly of *I. pygmaeus* CNS and eye tissue using PacBio long-read ISO-seq data. This transcriptome will be made publicly available upon publication of this chapter as a research paper, joining the 41 other publicly available cephalopod transcriptome shotgun assembly (TSA) records on the National Centre for Biotechnology Information (NCBI) database (searched 5th November 2021). No transcriptome assemblies from the *Idiosepius* genus are publicly available on NCBI, however there is one published transcriptome assembly from the head and dorsal adhesive gland of *Xipholeptos notoides*, which was originally classified in the *Idiosepius* genus (Reid and Strugnell, 2018). Many of the cephalopod transcriptome assemblies published on NCBI are not annotated nor contain accompanying quality and completeness metrics. Thus, my *I. pygmaeus* annotated cephalopod transcriptome assembly that has accompanying quality and completeness metrics will provide a valuable resource to other researchers. Particularly as cephalopod genomics and transcriptomics research progresses and *Idiosepius* are being identified as potential important model organisms (Albertin *et al.*, 2012).

4.5.2 Effects of elevated CO_2 on gene expression

While there were relatively few DEGs in the nervous system of *I. pygmaeus*, elevated CO_2-induced behavioural changes were observed in the same squid individuals (Chapter 3). Behavioural alterations have been found to occur in fish in which relatively small numbers of DEGs were found in the nervous tissue (Porteus *et al.*, 2018; Williams *et al.*, 2019; Schunter *et al.*, 2021). Thus, subtle gene expression changes may still have noticeable phenotypic effects. Furthermore, phenotypic effects can occur independently of changes in gene expression. For example, proteomic variation can also be achieved by alternative splicing, and I

identified significant upregulation of four functional categories involved in mRNA splicing in the CNS of *I. pygmaeus*. RNA editing can also result in proteomic variation, and is pervasive in squid, particularly in the nervous system, and can respond to the physical environment (Marden, 2008; Garrett and Rosenthal, 2012; Alon *et al.*, 2015).

Both the CNS and eyes responded to elevated CO_2 across the same three top functions: neurotransmission, immune function and oxidative stress, suggesting that both the peripheral and central nervous systems have a similar response to elevated CO_2. However, there was a larger response to elevated CO_2 in the CNS than in the eyes of *I. pygmaeus*. RNA was extracted from the whole eye, which contains not only neuronal cells but also other tissue types such as the lens, cornea and connective tissue. These multiple tissue types may have influenced the results, increasing the variance in gene expression from whole eye samples and thus decreasing the power by which changes in gene expression could be detected.

Neurotransmission

The results here suggest that elevated CO_2 disrupts a range of different types of neurotransmission in *I. pygmaeus* (Figure 4.3 and Figure 4.7). Altered HCO_3^- and Cl^- concentrations, due to acid-base regulation at elevated CO_2, is suggested to alter the function of $GABA_A$ receptors; the major hypothesis for altered behaviour at elevated CO_2 in fish (Nilsson *et al.*, 2012). In the CNS, I found significant upregulation of *syvn1-b*, which plays a critical role in $GABA_A\alpha1$ receptor subunit degradation (Crider *et al.*, 2014; Jiao *et al.*, 2017), and downregulation of multiple ion channel-related functional categories that contain core enrichment genes for two $GABA_A$ receptor transcripts. This suggests there may be fewer $GABA_A$ receptors present in the CNS of *I. pygmaeus* at elevated CO_2, which is opposite to the upregulation of $GABA_A$ receptor transcripts observed at elevated CO_2 in the brain of a coral reef fish (Schunter *et al.*, 2018). Recent pharmacological work also supports the GABA hypothesis in molluscs (Watson *et al.*, 2014; Clements *et al.*, 2017), including in *I. pygmaeus* (Chapter 3).

Changes in HCO_3^- and Cl^- ion gradients at elevated CO_2 may also alter the function of other, typically inhibitory, ligand-gated Cl^- channels similar to the $GABA_A$ receptor (Tresguerres and Hamilton, 2017, Chapter 2). Indeed, a recent pharmacological study showed altered GABA-, glutamate, acetylcholine (ACh)- and dopamine-gated Cl^- channels may underlie behavioural alterations at elevated CO_2 in *I. pygmaeus* (Chapter 3). Here, there was differential expression of genes involved in GABAergic, glutamatergic and monoaminergic (dopamine, serotonin (5-HT), norepinephrine, and epinephrine) neurotransmission (Figure 4.3). Furthermore, the enrichment of ion channel functional categories in both tissues includes core enrichment genes for GABA, glutamate, and ACh receptors. Elevated CO_2 also upregulated GABAergic, glycinergic, cholinergic and glutamatergic transcripts in the

whole body of a pteropod mollusc (Moya *et al.*, 2016) and glutamatergic transcripts in the non-nervous tissue of oysters (Ertl *et al.*, 2016; Wang *et al.*, 2020). Multiple glutamate pathway genes, and a gene for an ACh receptor subunit, were also differentially expressed in the olfactory system, and associated with impaired olfaction, of fish exposed to elevated CO_2 (Porteus *et al.*, 2018). Molluscs possess GABA, glutamate, ACh- and dopamine-gated Cl^- channels (Gerschenfeld and Tritsch, 1974; Carpenter *et al.*, 1977; Yarowsky and Carpenter, 1978a; van Nierop *et al.*, 2005). Furthermore, cephalopods including squid can actively increase extracellular [HCO_3^-] in response to elevated environmental CO_2 levels (Gutowska *et al.*, 2010; Hu *et al.*, 2014). Although Cl^- levels in response to elevated seawater CO_2 have not been measured in cephalopods, a Na^+-driven HCO_3^-/Cl^- exchanger has been isolated from a squid (Virkki *et al.*, 2003) suggesting the potential for altered [Cl^-] as part of acid-base regulation. Thus, the results here support the hypothesis that elevated CO_2 alters not only $GABA_A$ receptors, but also other ligand gated Cl^- channels, possibly via altered HCO_3^- and Cl^- ion concentrations due to acid-base regulatory mechanisms at elevated CO_2 (Nilsson *et al.*, 2012; Tresguerres and Hamilton, 2017, Chapter 3).

As well as acting on molluscan inhibitory ligand-gated Cl^- channels, glutamate, ACh and monoamine neurotransmitters also act on excitatory cation channels. Thus, the alterations in glutamatergic, cholinergic and monoaminergic neurotransmission found in *I. pygmaeus* may also contribute to changes in excitatory neurotransmission. Furthermore, the enrichment of functions related to ion channels in both tissues includes core enrichment genes for excitatory cation channels, including glutamate NMDA and kainate receptors, and nicotinic ACh receptors. I also found CNS upregulation of GPCR-related functional categories, which contain core enrichment genes for the excitatory metabotropic glutamate, dopamine 1-like, and 5-HT_2 and 5-HT_4 receptors. Thus, excitatory cation channels and excitatory GPCRs may be altered in *I. pygmaeus* at elevated, compared to current-day, CO_2 conditions. This may be a compensatory response to elevated CO_2-induced changes in typically inhibitory ligand-gated Cl^- channels, to maintain a balance between excitatory and inhibitory neurotransmission required for proper neurological functioning (Mele *et al.*, 2016; Samardzic *et al.*, 2018).

There were also molecular signatures for altered K^+ and Ca^{2+} channels at elevated CO_2 in *I. pygmaeus*, which may have widespread effects on neurotransmission. In the CNS of *I. pygmaeus*, there was significant downregulation of a cluster of ion transport-related functional categories including core enrichment genes for ion channels that act to maintain cellular levels of K^+ and Ca^{2+}, and are important for neurotransmission, including action potential regulation and neurotransmitter release. Furthermore, many of the core enrichment genes within the ion channel cluster of functional categories are cation channels permeable to K^+ and Ca^{2+} ions (Di Cosmo *et al.*, 2006; Dani, 2015; Wollmuth, 2018). Thus, elevated CO_2-induced disruption of K^+ and Ca^{2+} channels in the nervous system could affect the functioning of ligand-

gated cation channels permeable to K^+ and Ca^{2+}, and have a potentially more widespread effect on neurotransmission due to the critical role of K^+ and Ca^{2+} in neurotransmission and action potential regulation (Rusakov, 2006; Catterall, 2021). As suggested by Tresguerres and Hamilton (2017), elevated CO_2-induced changes in HCO_3^- concentrations could regulate K^+ channel activity (Kaila *et al.*, 1997; Ma *et al.*, 2012; Jones *et al.*, 2014b), potentially explaining the alterations in K^+ channels observed here in *I. pygmaeus*. Disruption of Ca^{2+} channels may be due to elevated CO_2-induced oxidative stress (discussed below in Oxidative stress) which can increase intracellular 'free' Ca^{2+} levels (Halliwell and Gutteridge, 2015).

Overall, I have found molecular signatures for elevated CO_2-induced alterations in a variety of different types of neurotransmission in *I. pygmaeus*, including monoaminergic, glutamatergic, GABAergic and cholinergic neurotransmission that is mediated by ligand-gated Cl^- and cation channels, GPCRs and K^+ and Ca^{2+} ion channels playing critical roles in the general process of neurotransmission. The elevated CO_2-induced disruptions to neurotransmission may be explained by four potential mechanisms. 1) Altered HCO_3^- and Cl^- concentrations could disrupt ligand-gated Cl^- channel function, 2) changes in excitatory neurotransmission may occur to compensate for disruption of typically inhibitory ligand-gated Cl^- channels, 3) elevated CO_2-induced changes in HCO_3^- concentrations could regulate K^+ channel activity, and 4) oxidative stress-induced changes in Ca^{2+} at elevated CO_2 could disrupt Ca^{2+} channel functioning (Figure 4.3 and Figure 4.7).

These changes in neurotransmission at elevated CO_2 may contribute to behavioural alterations. Altered glutamatergic neurotransmission may disrupt learning and memory due to glutamate's key role in long term potentiation (LTP), the main mechanism underlying learning and memory in vertebrates (Bliss and Collingridge, 1993; Peng *et al.*, 2011), and molluscs (Roberts and Glanzman, 2003). Two genes involved in glutamatergic neurotransmission were differentially expressed in *I. pygmaeus*' CNS, *folh1* (upregulated) and *celsr3* (downregulated). Overexpression of *folh1* altered memory performance in mice (Zink *et al.*, 2020) and *celsr3* knock-out mice exhibit fewer glutamatergic synapses and impaired learning and memory behaviours (Thakar *et al.*, 2017). *Cbs*, which was upregulated at elevated CO_2 here and in the brains of fish from behaviourally tolerant parents (Schunter *et al.*, 2016), is the main producer of hydrogen sulphide (H_2S), a gaseous neurotransmitter in the vertebrate brain and in molluscs (Julian *et al.*, 2002; Hu *et al.*, 2010; Shefa *et al.*, 2018a). H_2S has a range of roles, including facilitating LTP (Abe and Kimura, 1996; Kimura, 2000; Régnier *et al.*, 2012; Chen *et al.*, 2017). Thus, altered gaseous neurotransmission via H_2S may also contribute to changes in learning and memory.

Altered monoaminergic neurotransmission may also contribute to behavioural disturbances. Key regulators of monoaminergic neurotransmission, *maoa* and *slc18a2*, were upregulated at elevated CO_2 in the eyes of *I. pygmaeus*. Indeed, expression changes of *slc18a2*

and *maoa* alter aggression, depressive-like, anxiety-like, and activity behaviours in mammals (*slc18a2*: (Fukui *et al.*, 2007; Lohr *et al.*, 2014; Branco *et al.*, 2020), *maoa*: (Cases *et al.*, 1995; Scott *et al.*, 2008; Wang *et al.*, 2017a; Mentis *et al.*, 2021)) and activity in invertebrates (Simon *et al.*, 2009; Bellot *et al.*, 2021). Altered levels of the monoamines dopamine and 5-HT were correlated with behaviours affected by elevated CO_2 in two fish (Paula *et al.*, 2019). *Slc2a13*, which was downregulated at elevated CO_2 here and in the non-nervous tissue of an oyster (Ertl *et al.*, 2016), codes for a cotransporter that moves myo-inositol into neurons and glia (Uldry *et al.*, 2001, 2004). Altered intracellular myo-inositol levels, via monoamine signalling, are also thought to cause depression and anxiety (Einat and Belmaker, 2001; Shaldubina *et al.*, 2007). Furthermore, these changes in neurotransmission likely do not occur in isolation. Monoamine neurotransmitters can regulate glutamatergic signalling (Nicola *et al.*, 2000; Simon *et al.*, 2009). There is also potential cross-talk between CBS-produced H_2S and monoamines (Skrajny *et al.*, 1992; Talaei *et al.*, 2011; London *et al.*, 2019), and H_2S promotes glutamate uptake (Lu *et al.*, 2008). Thus, elevated CO_2-induced changes in glutamatergic, H_2S and monoaminergic neurotransmission, and their interactions, may contribute to behavioural alterations, including increased aggression and activity levels that were observed in the squid from this experiment (Chapter 3) (Figure 4.3).

Immune response

Elevated CO_2 alters the molluscan immune response, with most research focusing on bivalves (Bibby *et al.*, 2008; Li *et al.*, 2015; Liu *et al.*, 2016; Wu *et al.*, 2016; Su *et al.*, 2018)). Recently, the immune response of a cephalopod was also found to be altered at elevated CO_2 (Culler-Juarez and Onthank, 2021). Molluscs, including cephalopods, rely on an innate immune response that consists of three levels, 1) sensor molecules that recognise and interact with pathogens to trigger 2) signal transduction pathways, resulting in 3) activation and production of immune effectors, such as phagocytosis and antimicrobial peptides, that kill, neutralise or remove pathogens (Castillo *et al.*, 2015). Here, I found changes in gene expression related to all three levels of the innate immune response in both the CNS and eyes of *I. pygmaeus* at elevated CO_2 (Figure 4.4). A gene coding for the peptidoglycan recognition protein was downregulated at elevated CO_2 in the eyes of *I. pygmaeus* here (*pglyrp2*), and also in the gills of a mussel (Castillo *et al.*, 2017) and non-nervous tissue of an oyster (Ertl *et al.*, 2016). I also found differential expression of genes that regulate the immune signal transduction pathways NF-KB, JNK and p38 (Guha and Mackman, 2001), which are also implicated in the molluscan immune response (Goodson *et al.*, 2005; Canesi *et al.*, 2006; De Zoysa *et al.*, 2010; Salazar *et al.*, 2015). Gene expression changes also suggest a range of immune effectors, including iron sequestration (*tf* and *cbs*), autophagy (*map1l3ca/b*), con-

trolling the pool of available nucleoside triphosphates (*nme6*), and phagocytosis ('cell adhesion' and multiple cytoskeleton functional categories), may be altered at elevated CO_2 in *I. pygmaeus*. Previous research has also indicated altered phagocytosis in molluscs at elevated CO_2; adhesion capacity of hemocytes was decreased in a clam and expression of integrin (involved in cell adhesion for phagocytosis) was decreased in one oyster species (Ivanina *et al.*, 2014) but increased in another oyster (Ertl *et al.*, 2016). Furthermore, the phagocytic rate and cytoskeleton component abundance was decreased, and the expression of cytoskeleton genes was upregulated, in a clam at elevated CO_2 (Su *et al.*, 2018). Therefore, elevated CO_2 may alter all three levels of the innate immune response in *I. pygmaeus*.

Cross-talk between the neuroendocrine and immune systems coordinates appropriate physiological and behavioural responses to environmental change (Demas *et al.*, 2011). In molluscs, neuronal release of norepinephrine regulates hemocyte-mediated immune responses through a neuroendocrine-immune axis-like pathway (Liu *et al.*, 2017). Thus, upregulation of *maoa* and *slc18a2* in *I. pygmaeus*, which regulate norepinephrine signalling, may mediate changes in the immune response at elevated CO_2. Indeed, changes in *maoa* expression and activity in molluscs appears to play a key role in immune functioning via norepinephrine (Zhou *et al.*, 2011; Liu *et al.*, 2018; Sun *et al.*, 2021). Immune-derived factors, such as cytokines, can also feedback to alter the nervous system and behaviour (Adamo, 2006; Dantzer and Kelley, 2007). Thus, elevated CO_2-induced disruption of the immune system could feedback to alter the nervous system and behaviour. Of particular relevance to my results, H_2S, which is produced by *cbs* (upregulated in the eyes of *I. pygmaeus* here), is suggested to modulate behaviour via regulating pro-inflammatory mediators, such as cytokines (Gong *et al.*, 2010; Li *et al.*, 2021). Furthermore, knock out of the immune sensor molecule *pglyrp2* in adult mice, which was upregulated in the eyes of *I. pygmaeus* here, altered anxiety-like behaviour (Arentsen *et al.*, 2018). Thus, *I. pygmaeus*' nervous system may respond to elevated CO_2 to mediate changes in the immune system through a neuroendocrine-immune axis, and these immune changes may also feedback on the nervous system to alter behaviours at elevated CO_2 (Figure 4.7).

Oxidative stress

Oxidative stress occurs when there is an imbalance between the production of reactive oxygen species (ROS) and protection by antioxidant mechanisms (Halliwell and Gutteridge, 2015). Elevated CO_2 induces oxidative stress in molluscs, increasing ROS and altering antioxidant defences, which induces oxidative damage such as DNA damage, lipid peroxidation and apoptosis (Tomanek *et al.*, 2011; Wang *et al.*, 2016; Cao *et al.*, 2018a,b; Zhang *et al.*, 2021). Here, I found molecular signatures for oxidative stress in *I. pygmaeus* nervous tissue at ele-

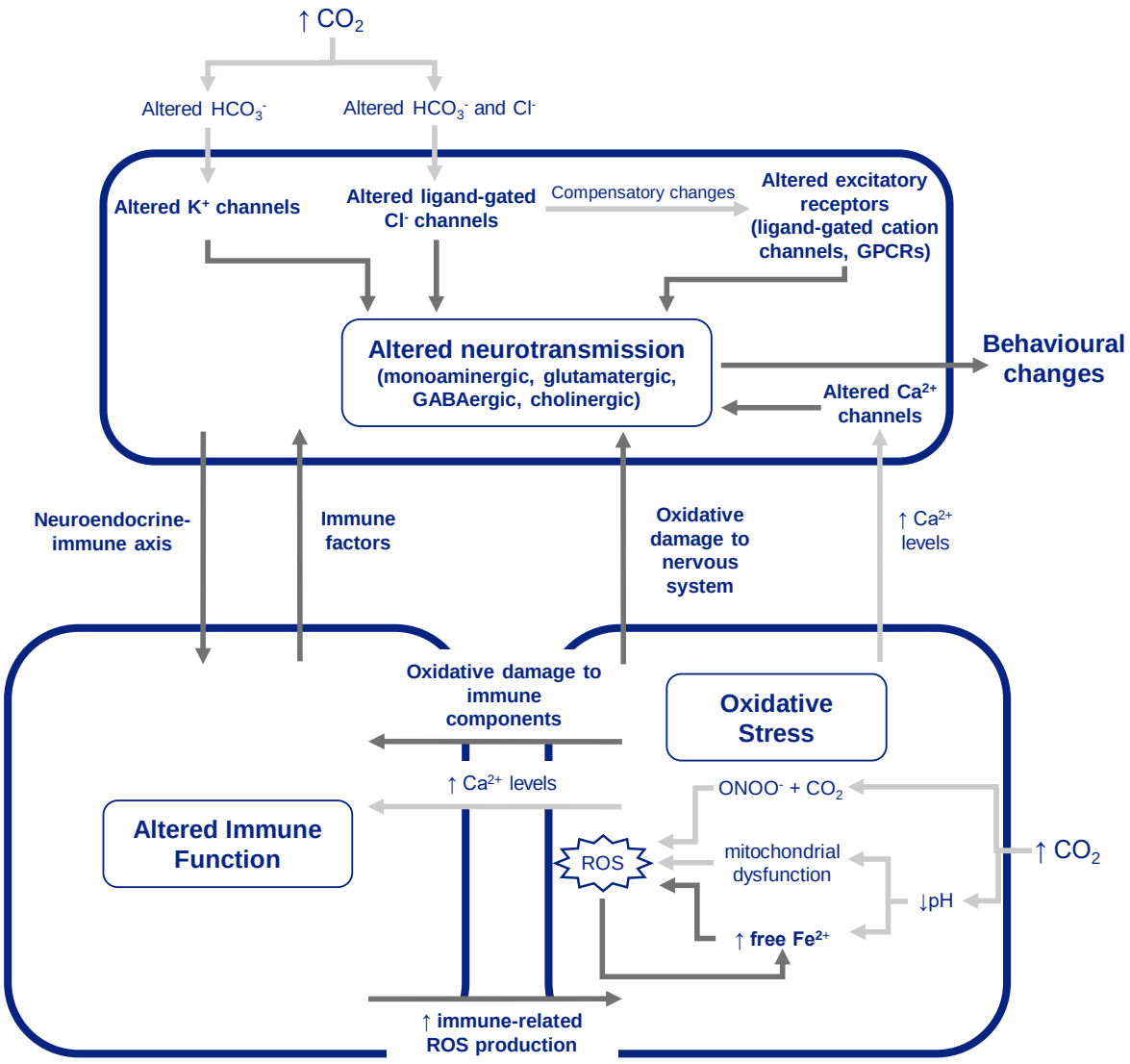

Figure 4.7. Proposed mechanistic model outlining the effects of elevated CO_2 on, and the interactions between, the three top functions found to be affected by elevated CO_2 in the nervous tissue of *I. pygmaeus*; neurotransmission, immune function and oxidative stress. The mechanisms in bold and arrows in dark grey are those pathways that there was some some evidence for in *I. pygmaeus*. CO_2 = carbon dioxide, $ONOO^-$ = peroxynitrite, ROS = reactive oxygen species.

vated CO_2. In the nervous system of *I. pygmaeus*, there was differential expression of genes involved in production of the antioxidants glutathione and ascorbate, and H_2S which has an antioxidant role (Shefa *et al.*, 2018b) (Figure 4.5). I also found significant upregulation of genes and functional categories involved in cellular clearance, including the endoplasmic reticulum associated degradation (ERAD) pathway and lysosomal system, and repair of DNA damage, suggesting oxidative damage may have occurred in the nervous system of *I. pygmaeus* at elevated CO_2. DNA damage was also observed at elevated CO_2 in an oyster (Cao *et al.*, 2018a) and a mussel (Nardi *et al.*, 2018). Despite no molecular markers of apoptosis being differentially expressed, there was upregulation of the functional category 'regulation of apoptotic process' in the CNS. Increased apoptosis at elevated CO_2 was observed in a sea snail (Zhang *et al.*, 2021) and an oyster (Cao *et al.*, 2018a). Thus, cellular clearance and DNA repair mechanisms may have been upregulated to deal with oxidative damage at elevated CO_2, which potentially caused apoptosis in the nervous system of *I. pygmaeus*.

Tomanek *et al.* (2011) proposed three mechanisms by which elevated CO_2 could induce oxidative stress; 1) cellular CO_2 reacts with peroxynitrite ($ONOO^-$) to form reactive species, and in organisms with a limited acid/base regulatory capacity a decreased pH at elevated CO_2 could 2) negatively affect the mitochondrial electron transport chain leading to electron slip and ROS production, and 3) release free Fe^{2+} ions, catalysing the production of ROS through Fentons reaction (Figure 4.5 and Figure 4.7). In *I. pygmaeus*, DE of *tf*, *cyb561d2* and *cbs* may work together to decrease Fe^{2+} availability for ROS production in a response to counteract acidosis-induced release of Fe^{2+} irons, supporting mechanism three above (Figure 4.5). *Cyb561d1*, which has a similar function to *cyb561d2* in reducing Fe^{3+} (Su and Asard, 2006), was also downregulated at elevated CO_2 in the olfactory bulb of a fish (Porteus *et al.*, 2018). However, extracellular pH was maintained in a gastropod mollusc exposed to 1,000 µatm CO_2 for 4 - 11 days (Zlatkin and Heuer, 2019) and a squid after 20 hours in 1,600 and 4,100 µatm CO_2 (Hu *et al.*, 2014). Thus, it is likely that pH was maintained in *I. pygmaeus* after 7 days at 1,000 µatm CO_2, and there would likely not be an acidosis-induced release of free Fe^{2+} ions. However, oxidative stress itself can increase iron levels (Halliwell and Gutteridge, 2015), and this increased iron could then catalyse ROS production creating a self-amplifying cycle of oxidative stress. Thus, if elevated CO_2 induces oxidative stress by another mechanism(s), differential expression of *tf*, *cyb561d2* and *cbs* may be a response to, rather than the mechanism producing, oxidative stress (Figure 4.7).

Oxidative stress potentially interacts with the immune system and neurotransmission

Previous research has shown elevated CO_2-induced disruption of both the immune and oxidative stress systems in molluscs (Ertl *et al.*, 2016; Sun *et al.*, 2017; Cao *et al.*, 2018b),

which may be due to cross-talk between these two systems. Oxidative stress may alter the immune response by damaging immune components, such as the cytoskeleton and hemocytes (Sun *et al.*, 2017; Cao *et al.*, 2018b), and increasing Ca^{2+} levels which could disturb calcium-dependent immune processes, such as phagocytosis (Sun *et al.*, 2017). The reverse is also possible, elevated CO_2-induced disruption of the immune system could increase immune-related ROS production (Terahara and Takahashi, 2008). Elevated CO_2 could also disturb iron sequestration (as part of an altered immune response), consequently altering the availability of free iron to catalyse ROS production and potentially leading to oxidative stress (Figure 4.7).

The nervous system is particularly vulnerable to oxidative stress (Halliwell, 2006; Valko *et al.*, 2007), and oxidative stress in the nervous system can inactivate receptors, enzymes and ion channels resulting in disrupted neurotransmission and neuronal function (Lebel and Bondy, 1991; Halliwell, 2006; Bouayed *et al.*, 2009; Halliwell and Gutteridge, 2015). This oxidative damage-induced disruption of neurotransmission may consequently disturb downstream processes controlled by the nervous system. Indeed, many studies have shown a link between oxidative stress in the nervous system and changes in anxiety and aggressive behaviours, as well as depression (Rammal *et al.*, 2010; Bouayed, 2011; Bhatt *et al.*, 2020). As I found molecular signatures of oxidative damage in the nervous system of *I. pygmaeus* at elevated CO_2, oxidative damage could be a mechanism contributing to altered neurotransmission, and potentially behavioural disturbances, at elevated CO_2 (Figure 4.7).

4.5.3 Conclusion

Here, I have created a *de novo* annotated cephalopod transcriptome assembly with accompanying quality and completeness metrics, providing a valuable resource for other researchers. Using this resource, a small number of DEGs and small but widespread and coordinated expression changes of genes in the CNS and eyes of *I. pygmaeus* exposed to elevated CO_2, were identified. Changes in gene expression in both tissues show elevated CO_2 affected three top functions; neurotransmission, immune function and oxidative stress. The results here support previous findings that elevated CO_2 alters neurotransmission, and agree with suggestions that multiple types of neurotransmission are altered. Furthermore, my results support a growing number of studies demonstrating that elevated CO_2 induces alterations in both the immune and oxidative stress systems, and I also show molecular signatures for alterations in the immune and oxidative stress systems in the nervous system. Altered iron homeostasis was identified as a possible mechanism for oxidative stress at elevated CO_2, although altered iron homeostasis may be a consequence of oxidative stress. I propose a mechanistic model showing how cross-talk between changes in neurotransmission, immune function and oxidative

stress may drive behavioural and physiological responses to elevated CO_2. The findings here highlight that the mechanisms underlying biological responses to elevated CO_2 are likely not occurring in isolation. Furthermore, elevated CO_2-induced alterations in the nervous system likely drives not only behavioural, but also physiological, responses. Moving forward, causative research is now required to evaluate the findings. For example, knockdown studies of specific genes in model animals will determine their importance in elevated CO_2-induced changes. Pharmacological studies targeting receptors and neurotransmitter pathways, other than only $GABA_A$ receptors, will be important to determine their role in both behavioural and physiological responses to elevated CO_2. Furthermore, experiments exploring the link between neuroendocrine-immune crosstalk and oxidative stress-induced damage in the nervous system, to behavioural change at elevated CO_2 could provide a fruitful avenue for future research.

Chapter 5

Correlated transcriptomic and behavioural responses: Identifying mechanisms underpinning behavioural responses to elevated CO_2 in a cephalopod

Data availability:
All data and scripts accompanying this chapter are available at https://doi.org/10.25903/7dcz-th66 (this is embargoed until publication).

5.1 Abstract

Rising carbon dioxide (CO_2) levels in the ocean can affect marine invertebrate behaviours. Given the vital role of marine invertebrates in marine ecosystems, and the importance of behaviour in an individual's survival, these behavioural changes may have widespread consequences. However, the mechanisms underlying marine invertebrate behavioural changes remain poorly understood. Here, I directly correlated gene expression with CO_2 treatment levels and behavioural responses of the same individuals to more directly assess the molecular mechanisms underlying behavioural changes at elevated CO_2. I used a network approach to cluster transcriptome-wide gene expression from the central nervous system (CNS) and eyes of two-toned pygmy squid (*Idiosepius pygmaeus*). The gene expression profile of each gene cluster was then correlated with CO_2 treatment levels (current-day: ~450 µatm, elevated: ~1,000 µatm) and visually-mediated behavioural responses previously shown to be altered at elevated CO_2, using Canonical Correlation Analysis. This analysis identified altered neurogenesis in both the CNS and eyes as a potential main driver of elevated CO_2-induced behavioural changes. From the results, I propose a mechanism by which alterations in visual detection and visual information output from the eyes, in combination with disrupted neurogenesis and neurotransmission (including GABAergic signalling) in the CNS, may drive behavioural changes at elevated CO_2. My findings suggest that elevated CO_2 disturbs both the peripheral visual and central nervous systems leading to behavioural alterations via multiple mechanisms.

5.2 Introduction

Nearly one third of all anthropogenic carbon dioxide (CO_2) emissions are being absorbed by the ocean, resulting in increasing seawater CO_2 levels and decreasing pH, a process known as ocean acidification (OA) (Bindoff *et al.*, 2019). OA can affect a variety of physiological processes, life history traits and behaviours of marine invertebrates (reviewed in Kroeker *et al.* (2013); Melzner *et al.* (2020) and Chapter 2), with some taxa being more sensitive than others (Melzner *et al.*, 2009; Wittmann and Pörtner, 2013). Invertebrates are vital components of marine ecosystems, comprising over 92% of life in the ocean, are essential to the function of ecosystem processes, and support the livelihoods of human societies across the globe (Bertness *et al.*, 2001; Chen, 2021). Animal behaviour influences an individual's own fitness, complex interactions with other individuals and species, and key ecological processes that shape the structure of marine communities and ecosystems (Nagelkerken and Munday, 2015). Consequently, behavioural effects of elevated CO_2 on marine invertebrates could potentially have wide-ranging ecological, social and economic consequences.

A mechanistic understanding of OA-induced behavioural changes is important to understand the variability in these behavioural alterations and improve predictions of how marine invertebrates, and ultimately marine ecosystems, will respond to global change. However, the mechanistic underpinnings of behavioural alterations at elevated CO_2 in marine invertebrates are poorly understood (Chapter 2). The majority of mechanistic work has been done in fish, focusing on disrupted functioning of $GABA_A$ receptors (Nilsson *et al.*, 2012; Heuer *et al.*, 2019; Schunter *et al.*, 2019). Pharmacological work has also supported the GABA hypothesis in marine molluscs (Watson *et al.*, 2014; Clements *et al.*, 2017, Chapter 3), but not a crustacean (Charpentier and Cohen, 2016). Extra-cellular measurements of HCO_3^- and Cl^- ion concentrations have supported the theory behind the GABA hypothesis in a gastropod mollusc (Zlatkin and Heuer, 2019), as well as crustaceans (de la Haye *et al.*, 2012; Charpentier and Cohen, 2016). Other targeted approaches have indicated additional mechanisms may also underlie behavioural changes at elevated CO_2 in marine invertebrates, including altered sensation and information processing (reviewed in Briffa *et al.* (2012) and Chapter 2). However, targeted approaches like these only provide a limited view and leave potentially relevant information unexplored.

Transcriptomics provides a non-targeted, holistic approach to identify how environmental change affects marine organisms. Indeed, in fish, transcriptomics alongside behavioural testing has been used to explore hypotheses for the mechanisms underlying OA-induced behavioural changes. For example, a molecular signature of parental behavioural tolerance to elevated CO_2, defined by differential expression of circadian rhythm genes, was found in the brain of juvenile damselfish (Schunter *et al.*, 2016). The association of circadian rhythm

genes with parental behavioural tolerance was found to be primarily a maternal contribution, whereas fathers had a greater role in the association of histone binding gene expression, and both mothers and fathers contributed to neuroplasticity related changes in gene expression (Monroe *et al.*, 2021). Recent work in two coral reef fish, the spiny damselfish and orange clownfish, showed brain transcriptional responses to elevated CO_2 were altered by diel CO_2 fluctuations, and this differential response was largely related to changes in circadian rhythm genes (Schunter *et al.*, 2021). In European sea bass at elevated CO_2, differential expression of genes involved in olfactory receptors, excitatory neurotransmission and synaptic plasticity were associated with altered olfactory-mediated behaviour and reduced responses of the olfactory nerve to odourants (Porteus *et al.*, 2018). Furthermore, exposure of ocean-phase coho salmon to elevated CO_2 caused differential expression of genes involved in GABAergic signalling and ion balance regulation in the olfactory system, and these patterns were associated with disrupted olfactory-mediated behaviour and altered odour signalling in the olfactory bulb (Williams *et al.*, 2019). Thus, transcriptomics can provide support for existing hypotheses, such as the GABA hypothesis, but also allows for the development of novel hypotheses, such as the involvement of circadian rhythm genes and neuroplasticity, to explain behavioural alterations at elevated CO_2.

In marine invertebrates, little research has utilised transcriptomics to assess the mechanisms underpinning OA-induced behavioural alterations. Two transcriptomic studies using the whole body of pteropod molluscs identified altered expression of nervous system genes at elevated CO_2, including those involved in GABAergic, glycinergic, cholinergic and glutamatergic signalling (Moya *et al.*, 2016; Johnson and Hofmann, 2017). A transcriptomic study in the central nervous system (CNS) and eyes of a tropical squid also identified expression changes in neurotransmission, immune function, and oxidative stress related genes, at elevated CO_2 (Chapter 4). However, studies that directly correlate changes in gene expression to behavioural changes at elevated CO_2, and thus provide a more direct assessment of the molecular mechanisms underpinning OA-induced behavioural changes, are lacking.

Here, I correlated patterns of gene expression with CO_2 treatment levels and OA-affected behaviors in two-toned pygmy squid (*Idiosepius pygmaeus*) to provide a more direct assessment of the potential mechanisms underlying OA-induced behavioural changes. As cephalopods have a complex nervous system and behaviours rivalling those of fishes (Hanlon and Messenger, 2018), they are a useful taxon to investigate the mechanistic underpinnings of behavioural alterations at elevated CO_2. *I. pygmaeus* is an ideal species for this research as OA-induced behavioural alterations have previously been reported (Spady *et al.*, 2014, 2018, Chapter 3), and a *de novo* reference transcriptome has recently been assembled for this species (Chapter 4). In this study, I first used weighted gene co-expression network analysis to cluster transcriptome-wide gene expression into modules of genes within the CNS

and eyes, separately. Using a network approach to cluster genes into modules allows for the correlation of behavioural traits with a small number of gene modules, rather than each individual gene. Canonical correlation analysis was then used to correlate the expression profile of each gene module with CO_2 treatment levels (~450 µatm or ~1,000 µatm) and visually-mediated behavioral responses previously shown to be altered at elevated CO_2 in the same individuals. Cephalopods, including squid, are highly visual animals with many visually-guided behaviours (Muntz, 1999; Mather, 2006; Chung *et al.*, 2022). Therefore, I focused on the eyes and visually-mediated behaviours to assess the mechanisms in the peripheral visual system underlying relevant behavioural changes. The CNS was included to assess whether higher order processing mechanisms were also involved in behavioural alterations. The overall aim of this study was to determine potential drivers of behavioural change at elevated CO_2 in a cephalopod mollusc, a marine invertebrate with a complex nervous system.

5.3 Methods

5.3.1 CO_2 treatment and experimental design

Male two-toned pygmy squid (*Idiosepius pygmaeus*) were exposed to either current-day (~450 µatm) or elevated (~1,000 µatm) CO_2 as described in Chapter 3 (picrotoxin experiment, sham-treated squid used) (Figure 5.1). Briefly, wild-caught squid (19°15'11"S 146°49'24"E), were acclimated in groups at current-day seawater conditions (~450 µatm CO_2) for 1 - 6 days. Squid were then transferred to individual treatment tanks at either current-day (~450 µatm) or elevated (~1,000 µatm) CO_2 for seven days. After CO_2 treatment, squid underwent sham treatment (30 minutes in 100 mL aerated seawater from their CO_2 treatment containing 0.2% ethanol) as part of the experiment described in Chapter 3, followed by a behavioural trial. Visually-mediated behaviour was tested for 15 minutes by placing squid individually in a tank (30 × 30 × 15 cm) filled to 3 cm deep with seawater from their CO_2 treatment and with a mirror taking up the entire length of one wall. Immediately after the behavioural trial, squid were euthanised with AQUI-S (1:1000) and the eyes and central nervous system (CNS, containing the oesophagus running through the middle) were dissected and snap frozen (within 4.18 ± 0.55 minutes of euthanisation (mean ± SD)) and stored at -80°C.

5.3.2 Behavioural data

Behavioural data from Chapter 3 was used here. Three aspects of squid behaviour shown to be altered by elevated CO_2 were used: activity, exploratory conspecific-directed behaviours, and aggressive conspecific-directed behaviours. For activity I measured: (i) total time spent ac-

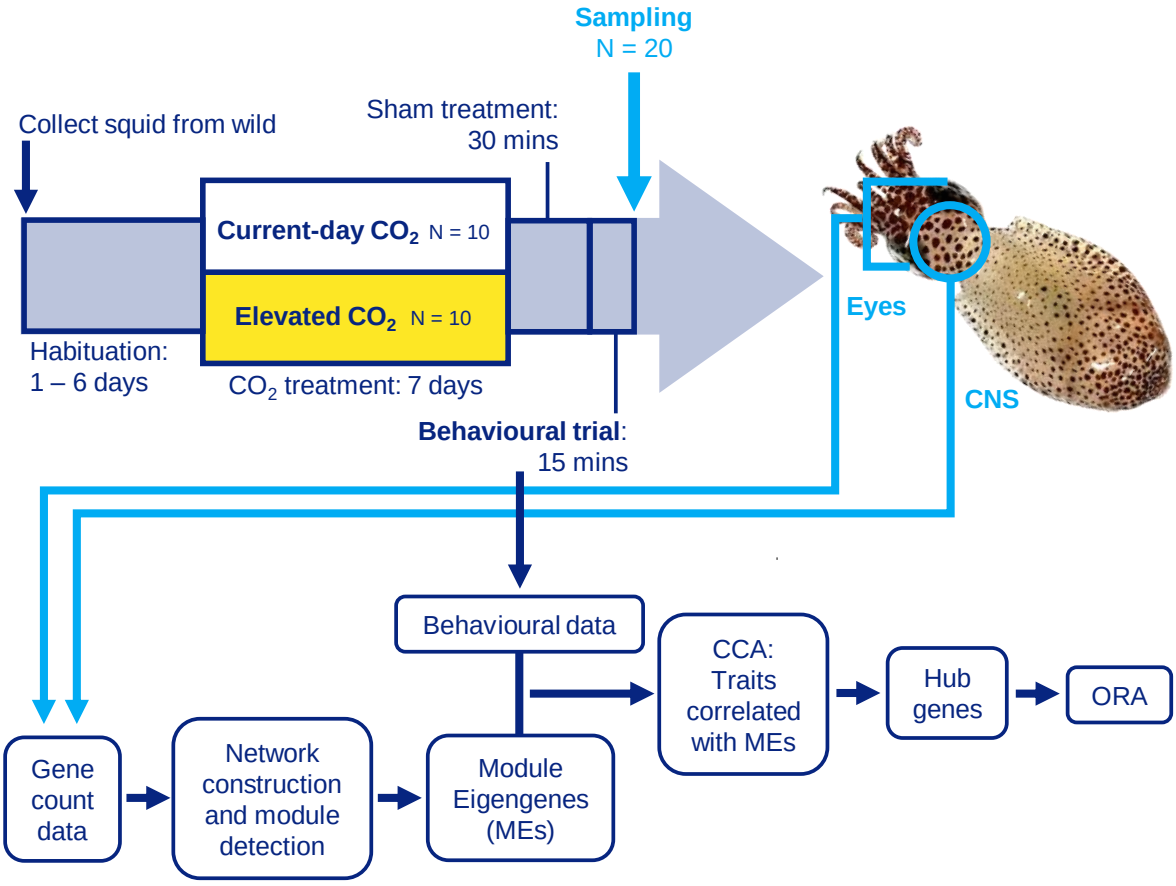

Figure 5.1. Experimental design overview. Gene count data from the CNS, and both eyes combined, of each squid exposed to either current-day or elevated CO_2 conditions was used from Chapter 4. A co-expression network was constructed and modules detected using WGCNA, and module eigengenes (MEs) were calculated for each module. MEs were correlated with the behavioural data of the same squid from Chapter 3, using Canonical Correlation Analysis (CCA). Hub genes for CO_2 treatment and each behavioural trait were identified and over-representation analysis (ORA) was used on large sets of hub genes to determine functional enrichment. *Idiosepius pygmaeus* photograph by Jodi Thomas.

tive (s), (ii) total distance moved (cm) and, (iii) average speed (cm/s). For visually-mediated exploratory conspecific-directed behaviour I measured: (i) the total time (s) spent in Zone A (3 cm closest to the mirror), (ii) whether any exploratory interactions occurred (i.e. whether the squid touched the mirror softly) (yes/no) and, (iii) the number of exploratory interactions (i.e the total number of soft mirror touches). For visually-mediated aggressive conspecific-directed behaviour I measured: (i) whether any aggressive interactions occurred (i.e. whether the squid touched the mirror aggressively) (yes/no) and, (ii) the number of aggressive interactions (i.e. the total number of aggressive mirror touches). The behavioural analysis is described in detail and the behavioural results are reported in Chapter 3. Three behaviours recorded in Chapter 3 were not used in the current study. The number of visits to Zone

A was not included because it was unaffected by elevated CO_2, and the latency to first soft/aggressive mirror touch had a large proportion of zeroes in the data making these two behaviours inappropriate for correlation analysis.

5.3.3 Gene count data

Gene count data from Chapter 4 was used here. Briefly, RNA-sequencing was carried out on the total RNA from the CNS, and both eyes combined from each of 20 squid (current-day CO_2, n = 10, elevated CO_2, n = 10 for each tissue). After trimming and contamination removal, RNA-seq reads were mapped against the *de novo* reference transcriptome for *I. pygmaeus* CNS and eye tissue from Chapter 4. Corset (v1.09) (Davidson and Oshlack, 2014) was used to cluster transcripts to gene-level and produce gene-level counts. Behavioural and gene count data are from the same individual squid.

5.3.4 Statistical analysis

To analyse the correlation between gene expression and behavioural traits of squid across CO_2 treatments, I employed weighted gene co-expression network analysis (WGCNA) and canonical correlation analysis (CCA) on the CNS and eyes, separately (Figure 5.1). All statistical analyses were carried out in R (v4.0.4) (R Core Team, 2021), primarily using RStudio (v1.4.1106) (RStudio Team, 2021).

Gene co-expression network construction and module detection

The gene-level counts for all 20 samples from each tissue were normalised, transcripts with low read counts were removed ($\leq$10 counts in $\geq$ 90% samples) and the remaining count data was variance stabilised in DESeq2 (v1.30.1) (Love *et al.*, 2014). This count data was then used in the WGCNA package (v1.70-3) (Langfelder and Horvath, 2008) for co-expression network construction and module detection. No genes were identified as outliers, using 'goodSamplesGenes'. To detect sample outliers, a sample dendrogram was created using hierarchical clustering with the 'average' method. Three and two obvious sample outliers were identified and removed from the analysis in the CNS and eyes, respectively (Appendix D: Figure D.1). Soft thresholding power was evaluated and powers of 14 and 13 were chosen for the CNS and eyes, respectively, to approximate a scale free topology (Appendix D: Figure D.2 and Figure D.3). The following co-expression network construction and module detection steps were carried out on a high-performance computing cluster at Okinawa Institute of Science and Technology, Japan to allow multiple threads for a full network analysis occurring in one block. A signed correlation network adjacency was calculated using

Pearson correlation and the chosen soft thresholding power. The adjacency was transformed into a signed topological overlap matrix (TOM) and the corresponding dissimilarity was calculated (1-TOM). A cluster dendrogram of genes was created using hierarchical clustering with the 'average' method and the dissimilarity TOM. Modules were detected using dynamic tree cut with the hybrid method, a minimum cluster size of 30, an intermediate sensitivity to cluster splitting (deepSplit = 2) and the Partitioning Around Medoids (PAM)-like step set to not respect the dendrogram (pamRespectsDendro = FALSE). Modules with a correlation of ≥ 0.70 were then merged (Appendix D: Figure D.4, Table D.1 and Table D.2). Eigengenes were calculated for each final module, which is the first principal component in the corresponding module used to represent the gene expression profiles of that module. These module eigengenes (MEs) allow gene modules to be correlated with external traits (Langfelder and Horvath, 2008).

Module eigengene correlation with behavioural traits

Regularised canonical correlation analysis (CCA) using package CCA (v1.2.1) (González *et al.*, 2008) was used to explore the correlations between the two sets of variables from the same individual squid: ME set = MEs from each module, traits set = CO_2 level (current-day or elevated) and behavioural traits (active time (s), distance (cm), speed (cm/s), time in Zone A (s), whether any exploratory interactions occurred (yes/no), the number of exploratory interactions, whether any aggressive interactions occurred (yes/no), and the number of aggressive interactions). CCA is a multivariate method that is similar to principal components analysis (PCA), but instead of finding new axes (principle components) that maximise the variance in the dataset, CCA finds new axes (canonical functions) that maximise the correlation between the variables in the two datasets (González *et al.*, 2008).

The canonical loadings and cross-loadings were calculated for the first four canonical functions (CF) in the CNS and eyes, separately. The first four CFs were chosen for interpretation as they explained a reasonable amount of variance between the traits set and MEs set; the CFs with a canonical correlation > 0.6 were chosen (Sherry and Henson, 2005). For each CF, the canonical loadings represent the correlation of each variable from one set to the entire set of variables in the same set. For example, the canonical loading of CO_2 treatment for CF 1 is the correlation of CO_2 treatment to the entire traits set at CF 1. For each CF, the canonical cross-loadings represent the correlation of each variable from one set to the entire set of variables in the other set. For example, the canonical cross-loading of CO_2 treatment at CF 1 is the correlation of CO_2 treatment to the entire ME set at CF 1. Heatmaps of all canonical loadings and cross-loadings for all variables of each set were created for each of the four CFs (Appendix D: Figure D.5 and Figure D.6). If the canonical loading and cross-loading

of a given variable from both the ME set and traits set were ≥ 0.3 for the same CF, this ME and trait were considered correlated. For example, if ME brown had a canonical loading of ≥ 0.3 for CF 1 it was considered correlated with CF 1 of the ME set. If CO_2 treatment had a canonical loading of ≥ 0.3 for CF 1 it was considered correlated with CF 1 of the traits set. Furthermore, if both ME brown and CO_2 treatment had a cross-loading ≥ 0.3 for CF 1, ME brown was considered correlated to CO_2 treatment. A cut-off value of 0.3 is commonly used (Lambert and Durand, 1975; Kabir *et al.*, 2014) and was a clear cut-off for my data.

Biplots were created for each two-way combination of the four CFs (Appendix D: Figure D.7 - Figure D.18). These biplots show where the MEs lie in space in relation to the traits. MEs and traits within the same or opposite quarters of the biplot, and sitting on or outside the biplot inner ring with a radius of 0.5, were considered positively or negatively correlated, respectively. If MEs and traits were considered correlated by both the canonical loadings/cross-loadings heatmap and biplots they were identified as modules of interest for the given trait(s).

Module membership vs gene significance

The Pearson correlation of module membership (MM) and gene significance (GS) was used to check the modules of interest identified by CCA. MM is the Pearson correlation between an individual gene's expression and the ME, with higher values indicating the gene is more highly connected to the given module. GS is the Pearson correlation between the individual gene's expression and a given trait, with higher values indicating a more biologically relevant gene (Langfelder and Horvath, 2008). A correlation of GS and MM imply that genes more highly connected within a given module also tend to be more highly correlated with the given trait, providing another measure for the importance of this module with the given trait. All modules of interest initially identified by CCA that had a MM vs GS correlation (R-value) > 0.2, a commonly used threshold for evidence of a weak correlation (Evans, 1996), were chosen as the final modules of interest (Appendix D: Figure D.19).

Identification of hub genes

MM and GS values were used as a gene screening method to identify biologically relevant, highly interconnected hub genes (Fuller *et al.*, 2007; Horvath and Dong, 2008; Langfelder and Horvath, 2008), i.e. to find genes correlated with CO_2 treatment and each behavioural trait. Hub genes were defined as those genes within the final modules of interest with a very strong correlation with the module (MM > 0.8) and a moderate correlation with the given trait (GS > 0.4). The Pearson correlation (R-value) between the normalised expression of each hub gene and the given trait was calculated and genes with a very weak correlation (R <

0.2) were excluded, resulting in the final list of hub genes. All hub genes for CO_2 treatment were compared across tissues to identify hub genes for CO_2 treatment that are CNS-specific, eyes-specific or found in both tissues. Hub genes for CO_2 treatment that are also a hub gene for one or more behavioural traits were identified as potential drivers of behavioural change at elevated CO_2.

Functional enrichment analysis

Over-representation analysis (ORA) was run in clusterProfiler (v3.18.1) (Yu *et al.*, 2012) using the hypergeometric test. The gene ontology (GO) terms of the CNS-specific CO_2 treatment hub genes that were also hub genes for one or more activity traits in the CNS, and the CNS-specific CO_2 treatment hub genes that were also hub genes for all three activity traits in the CNS, were compared to the entire set of genes in the CNS. This determined if any GO terms/functional categories were significantly over-represented within the list of hub genes. All other groups of CO_2 treatment hub genes had 25 or fewer genes and thus ORA was not run. P-values were adjusted for multiple comparisons using the Benjamini-Hochberg method and a significance threshold of padj < 0.05 was used.

5.4 Results

I identified 230 and 25 hub genes for CO_2 treatment in the CNS and eyes, respectively, with 14 CO_2 treatment hub genes shared by both tissues. Of these CO_2 treatment hub genes in the CNS, eyes and both tissues, 169, 6 and 10 genes were also identified as hub genes for one or more behavioural traits, respectively, indicating these genes as potential drivers of behavioural change at elevated CO_2 (Figure 5.2).

5.4.1 Genes in the CNS potentially driving altered activity at elevated CO_2

In the CNS, 159 hub genes were shared by CO_2 treatment and one or more activity traits, and 87 of these were hub genes for all three activity traits (Figure 5.2), implicating these genes in the CNS as potential drivers of altered activity at elevated CO_2. All of these shared hub genes were correlated with CO_2 treatment and the activity trait(s) in the same direction, with the majority of hub genes positively correlated with both CO_2 treatment and the activity trait(s) (Appendix D: Table D.3). The 159 hub genes shared by CO_2 treatment and one or more activity traits, and the 87 hub genes shared by CO_2 treatment and all three activity traits, were significantly enriched for four and 13 GO terms, respectively. These GO

terms include functions related to the cell cycle; '3'-5' DNA helicase activity' and 'chromosome' related to DNA replication, and 'actin filament binding', 'myosin complex', 'myofibril', 'motor activity' and 'ruffle membrane' related to mitosis/cytokinesis and cell migration (actin and myosin are key orchestrators of cell movement (Bressan and Saghatelyan, 2021)). 'Protein kinase binding' may also be involved in the cell-division cycle, as phosphorylation

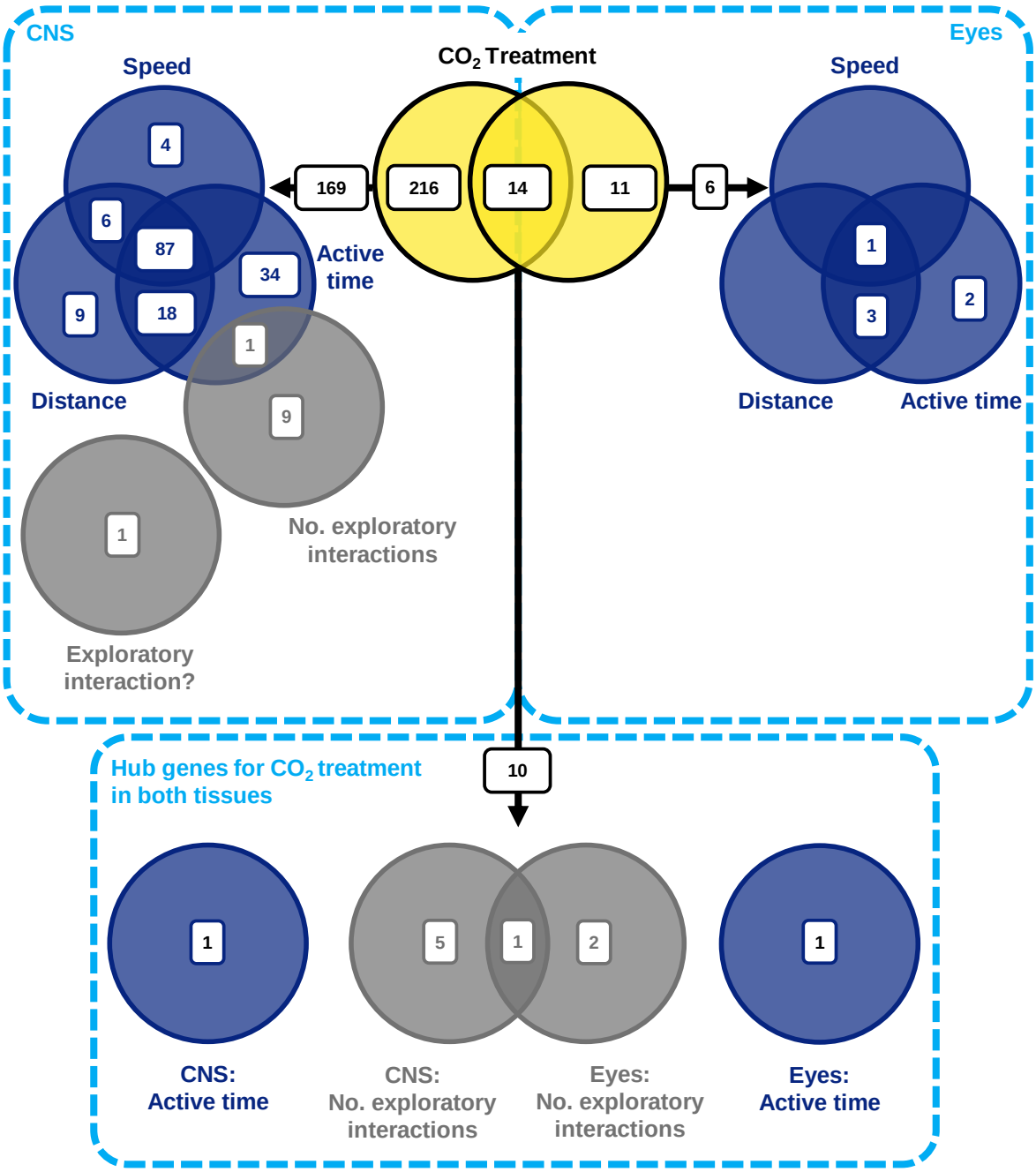

Figure 5.2. Venn diagram depicting the number of hub genes identified for CO_2 treatment and behavioural traits in the CNS and eyes. *(see next page)*

Figure 5.2 ***(previous page).*** The yellow venn diagram in the centre depicts the number of hub genes for CO_2 treatment that are CNS-specific (left) and eyes-specific (right), and the overlap represents the number of CO_2 treatment hub genes shared by both tissues. CNS-specific and eyes-specific CO_2 treatment hub genes also identified as a hub gene for one or more behavioural traits in the CNS or eyes are on the left and right, respectively. Hub genes for CO_2 treatment found in both tissues, that are also a hub gene for a behavioural trait in one or both tissues, are shown at the bottom centre. CO_2 treatment hub genes shared with activity traits (active time, distance and speed) and exploratory conspecific-directed behaviours (number of exploratory interactions and whether any exploratory interactions occurred) are in blue and grey, respectively. Exploratory interaction? = whether any exploratory interactions occurred (yes/no).

coordinates the cell cycle phases. GO terms involved in protein synthesis and folding were also significantly enriched in the shared hub genes; 'endoplasmic reticulum lumen', 'protein disulphide isomerase activity', and 'nuclear pore' (Figure 5.3).

The majority of CNS-specific hub genes shared by CO_2 treatment and one or more activity traits are involved in the cell cycle. Full names and functions of genes can be found in Appendix D: Table D.3 and Table D.4. Genes involved in the G1 growth phase (*cdt1*), regulation of G1 to S-phase (DNA replication) transition (*snd1*), DNA replication, including the initiation of DNA replication (*psf2*, *cdt1*, *mcm5*, *dbf4*) and elongation (*mcm5* and *spt16*), the mitotic phase, including chromosome condensation (*ncaph*, *smc4*) and chromosome alignment and segregration (*ttk*, *incenp*, *bub1*), mitotic checkpoint signalling (*ttk*), spindle assembly checkpoint signalling (*bub3*) and cytokinesis, including three myosin genes (*zip*, *myh9/10*, *myl9*) and an actin binding protein (*anln*), were all positively correlated with CO_2 treatment and activity traits. Hub genes positively correlated with CO_2 treatment and activity also include regulators of the cell cycle, including transcription factors (*foxm1*), initiators of translation (*eif3b*), and kinases which phosphorylate targets to regulate cell cycle progression (*ccnb3*, *melk*, *ttk*, *bub1*, *dbf4*). Genes involved in both cell proliferation (*ttk*, *eif3b*, *foxm1*, *melk*, *dbf4*, *srrt*, *tk1*, *tgfb1i1*, *pa2g4*, *ttc3*) and cell cycle-related apoptosis (*anb32a*, *eif3b*, *melk*) were also positively correlated with CO_2 treatment and activity traits. Genes involved in cell differentiation (*eif3b*, *rac1*, *ptpr*, *tbc1d1*, *tgfb1i1*, *itga4*, *pa2g4*, *slc4a11*), including specifically neuronal differentiation (*ttc3*), neural stem cell self-renewal (*srrt*), neural progenitor proliferation (*melk*), and neurogenesis (*ncaph*, *adgrb3*) were also all positively correlated with CO_2 treatment and activity traits. Only a few cell cycle genes were negatively correlated with CO_2 treatment and behavioural traits, including an anti-proliferative gene (*btg1*) and a gene whose loss of expression promotes cell growth (*nit1*).

Many of the CNS-specific hub genes shared by CO_2 treatment and activity traits are involved in cell migration and adhesion. Cell migration genes, including those that interact

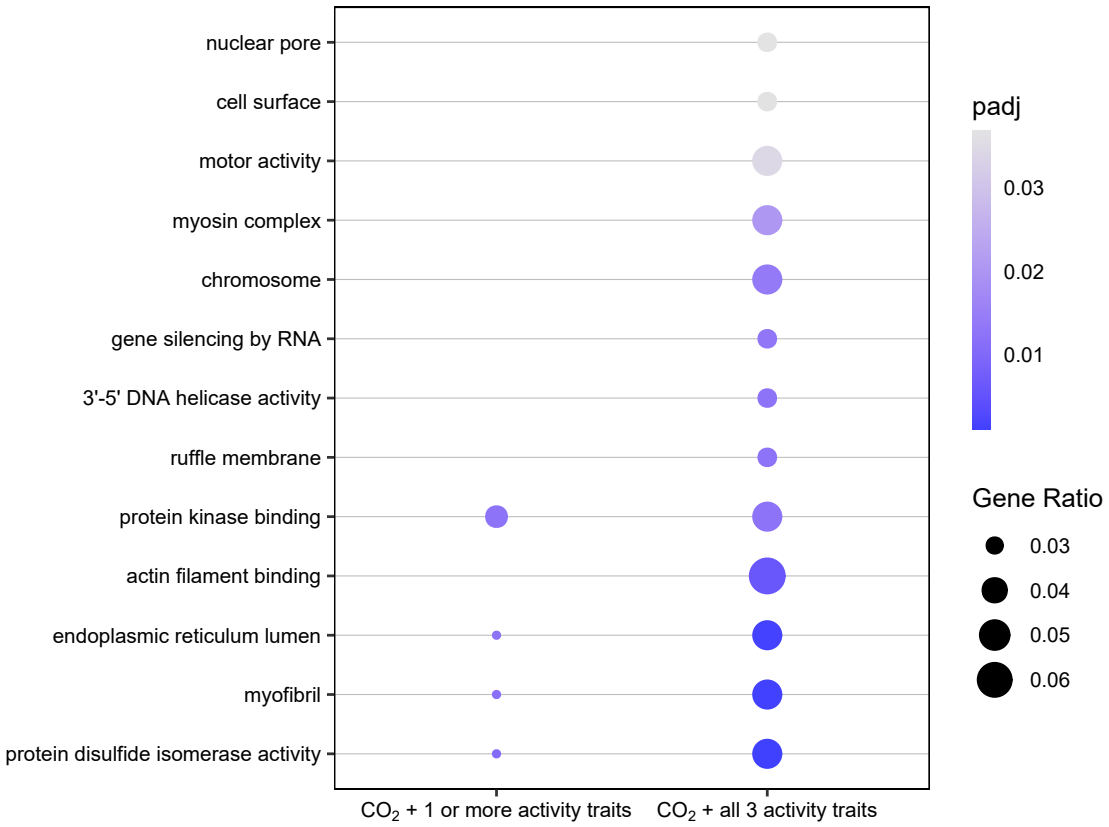

Figure 5.3. Functional categories significantly enriched in those genes in the CNS identified as potentially driving altered activity at elevated CO_2. Results from over-representation analysis of CNS-specific CO_2 treatment hub genes shared by one or more activity traits (159 genes), and CNS-specific CO_2 treatment hub genes shared by all three activity traits (87 genes). padj = adjusted p-value.

with actin (*arpc5*, *anln*), the myosin subunit *myl9*, and a molecular guide for cellular migration (*slit3*), were all positively correlated with CO_2 treatment and activity. Furthermore, genes involved in cell adhesion, including the integrins *itga4* and *itga9*, *slc4a11* which acts in synergy with integrins, a protocadherin (*pcdh1*), and an actin filament binding protein (*vcl*), were also positively correlated with CO_2 treatment and activity traits. Genes with a role specifically in neuron migration and adhesion, and the related processes of neurite (dendrite and axon) outgrowth and branching, dendritic spine formation, and synapse formation (*rac1*, *ptpr*, *adgrb3*, *apbb1*) were also positively correlated with CO_2 treatment and activity. One gene involved in neurite growth and branching (*futsch*) was negatively correlated with CO_2 treatment and activity traits.

A large number of the CNS-specific shared hub genes are involved in protein synthesis and turnover, with the majority positively correlated with CO_2 treatment and activity traits. These hub genes shared by CO_2 treatment and activity include those involved in transcription

(*polr1a*, *spt16*, *bptf*, *arpc5*), RNA splicing (*melk*, *snrpa*, *ecd*, *prpf40a*) and RNA processing (*cstf1*, *exosc10*). Many of the CNS-specific hub genes shared by CO_2 treatment and activity traits are involved in translation, including three components of the 60S (*rpl23a*, *rpl4*, *rpl7l*) and a component of the 40S (*rps27a*) ribosomal subunits, a gene required for 60S ribosomal subunit biogenesis (*nop58*), two components of the eukaryotic translation initiation factor 3 complex (*eif3b*, *eif3d*), and a subunit of the elongation factor-1 complex (*eef1g*). Protein folding and quality control genes include three protein disulphide isomerase enzyme genes (*pdia3*, *pdia4* and *pdia5*), an ER chaperone that plays a key role in protein folding and degradation of misfolded proteins (*hspa5*), and a glucosidase subunit (*ganab*). Protein translocation genes included three subunits of the oligosaccharyl transferase complex (*stt3a*, *rpn1*, *rpn2*), a gene involved in vesicular protein trafficking (*tmed2*), and three components of the nuclear pore (*nup160*, *nup155*, *nup205*). CNS-specific hub genes shared by CO_2 treatment and activity traits that play a role in protein turnover included E3 ubiquitin ligases which promote proteasome degradation (*cblb*, *ttc3*), and a subunit for the 26S proteasome (*rpn1*).

A few of the CNS-specific hub genes shared by CO_2 treatment and activity traits also play a role in neurotransmission. *Phf24*, which is a key modulator of $GABA_B$ receptor signalling (Gaillard *et al.*, 2014; Numakura *et al.*, 2021), and *rac1*, which plays a crucial role in regulating $GABA_A$ receptor signalling, and is necessary for full $GABA_A$ receptor activity (Meyer *et al.*, 2000; Smith *et al.*, 2014; Wang *et al.*, 2017a) were positively correlated with CO_2 treatment and activity. *Aldh5a1*, which is involved in the final degradation step of the neurotransmitter GABA (Kim *et al.*, 2009), was negatively correlated with CO_2 treatment and activity traits. Furthermore, *tmed2*, which is involved in G-protein coupled receptor (GPCR) trafficking was positively correlated with CO_2 treatment and activity traits, while *futsch*, which regulates synaptic microtubule cytoskeleton and neurotransmitter release (Lepicard *et al.*, 2014), and *dgkq*, which regulates synaptic vesicle endocytosis and supports synaptic neurotransmission (Goldschmidt *et al.*, 2016), were negatively correlated with CO_2 treatment and activity traits.

A range of genes involved in cellular stress responses were identified as hub genes for CO_2 treatment and activity traits in the CNS. *Scl4a11*, which regulates the oxidative stress response, was positively correlated with CO_2 treatment and activity traits. Genes involved in DNA repair were mostly positively correlated with CO_2 treatment and activity traits (*spt16*, *foxm1*, *bptf*, *arpc5*), while *nit1*, whose loss of expression promotes resistance to DNA damage stress, was negatively correlated. A heat shock protein, *hspa5*, which is a key repressor of the unfolded protein response, and genes that induce apoptosis in response to DNA damage (*apbb5*) and ER stress (*tmem214-b*), were positively correlated with CO_2 treatment and activity traits.

Genes involved in the immune response were also identified as hub genes for CO_2 treat-

ment and activity traits in the CNS. This includes *tf*, which sequesters iron so it is unavailable for pathogens (which need iron for survival and proliferation) and is a key component of the molluscan innate immune response, including in squid (Lambert *et al.*, 2005; Ong *et al.*, 2006; Herath *et al.*, 2015; Salazar *et al.*, 2015; Li *et al.*, 2019). Genes involved in cell adhesion as part of the immune response (*itga4*, *itga9*, *rac1*, *ptpr*) were also positively correlated with CO_2 treatment and activity traits.

5.4.2 Genes in the eyes potentially driving altered activity at elevated CO_2

Of the 11 eyes-specific CO_2 treatment hub genes, six transcripts belonging to three different genes were also hub genes for one or more activity traits (Figure 5.2, Table 5.1), implicating these genes in the eyes as potential drivers of altered activity at elevated CO_2. All of these shared hub genes were positively correlated with CO_2 treatment, but negatively correlated with the activity trait(s). Notably, *chrna10*, a subunit for the nicotinic acetylcholine (ACh) receptor, was the only hub gene shared by CO_2 treatment and all three activity traits in the eyes (Table 5.1). Protein crumbs, *crb*, which is essential for photoreceptor cell morphogenesis during eye development (Izaddoost *et al.*, 2002; Pellikka *et al.*, 2002) and the maintenance of retinal tissue integrity (Johnson *et al.*, 2002; van de Pavert *et al.*, 2004; Chartier *et al.*, 2012), and an uncharacterized protein D2-like, were hub genes shared by CO_2 treatment and one or two activity traits (Table 5.1). Furthermore, *gid-4* was positively correlated with CO_2 treatment in both tissues and negatively correlated with active time in the eyes (Table 5.2). *Gid-4* is a subunit of the CTLH E3 ubiquitin-protein ligase complex in mammals that is critical for maintaining normal cell proliferation (Lampert *et al.*, 2018), and may also play a role in cellular metabolism (Leal-Esteban *et al.*, 2018; Liu *et al.*, 2020; Maitland *et al.*, 2021).

5.4.3 Genes potentially driving an altered number of exploratory interactions at elevated CO_2

Ten, zero and eight hub genes were shared by CO_2 treatment and the number of exploratory interactions in the CNS, eyes and both tissues, respectively (Figure 5.2), suggesting these genes are potential drivers of the altered number of exploratory interactions at elevated CO_2. All of the hub genes shared by CO_2 treatment and number of exploratory interactions have an opposite correlation with these two traits; hub genes positively correlated with CO_2 treatment were negatively correlated with the exploratory interactions, and vice versa.

Table 5.1. Eyes-specific CO_2 treatment hub genes. For each of these CO_2 treatment hub genes, those genes also identified as a hub gene for one or more behavioural traits in the eyes are indicated in the columns on the right (active time, distance, speed, no. exploratory interactions). The numbers in each column are the gene significance (GS) for the corresponding trait (-1 to 1). Positive GS = positive correlation between gene expression and trait (in red), negative GS = negative correlation between gene expression and trait (in blue). The larger the GS absolute value the more biologically relevant the gene is. Dist. = distance, No. EI = number of exploratory interactions.

			Eyes				
Gene	**Annotation**	**Putative function**	**CO_2 treat-ment**	**Active time**	**Dist.**	**Speed**	**No. EI**
chrna10	neuronal acetylcholine receptor subunit alpha-10-like isoform X1	Subunit of the nicotinic acetylcholine receptor.	0.48	-0.56	-0.5	-0.46	
chrna10	neuronal acetylcholine receptor subunit alpha-10-like isoform X1	Subunit of the nicotinic acetylcholine receptor.	0.42	-0.51	-0.43		
crb	protein crumbs-like isoform X1	Essential for photoreceptor cell morphogenesis during eye development, and the maintenance of retinal tissue integrity.	0.55	-0.54	-0.47		
-	protein D2-like	Uncharacterised.	0.45	-0.47	-0.42		
crb	protein crumbs-like isoform X1	Essential for photoreceptor cell morphogenesis during eye development, and the maintenance of retinal tissue integrity.	0.56	-0.4			
crb	protein crumbs-like isoform X2	Essential for photoreceptor cell morphogenesis during eye development, and the maintenance of retinal tissue integrity.	0.53	-0.44			
-	protein D2-like	Uncharacterised.	0.56				
flot1	flotillin-1 isoform X1/2/4	May act as a scaffolding protein within caveolar membranes, functionally participating in formation of caveolae or caveolae-like vesicles.	0.47				
-	protein D2-like	Uncharacterised.	-0.47				
-	protein D2-like	Uncharacterised.	-0.54				

1 unannotated gene: negative correlation with CO_2 treatment

Table 5.2. Hub genes identified for CO_2 treatment in both the CNS and eyes. For each of these CO_2 treatment hub genes, those genes also identified as a hub gene for a behavioural trait in the CNS or eyes are indicated in the columns on the right (active time, distance, speed, no. exploratory interactions). The numbers in each column are the gene significance (GS) for the corresponding trait (-1 to 1). Positive GS = positive correlation between gene expression and trait (in red), negative GS = negative correlation between gene expression and trait (in blue). The larger the GS absolute value the more biologically relevant the gene is. Dist. = distance, No. EI = number of exploratory interactions.

			CNS					Eyes				
Gene	**Annotation**	**Putative function**	**CO_2 treat-ment**	**Active time**	**Dist.**	**Speed**	**No. EI**	**CO_2 treat-ment**	**Active time**	**Dist.**	**Speed**	**No. EI**
ndufab1	acyl carrier protein, mitochondrial	Carrier of the growing fatty acid chain in fatty acid biosynthesis. Non-catalytic subunit of the mitochondrial membrane respiratory chain NADH dehydrogenase (Complex I).	0.57	-0.41				0.56				
/	/											
sc16a	protein transport protein Sec16A isoform X2	Acts as a molecular scaffold playing a key role in the organization of the endoplasmic reticulum exit sites (ERES), involved in protein trafficking.										
gid-4	glucose-induced degradation protein 4 homolog	Subunit of the CTLH E3 ubiquitin-protein ligase complex in mammals that is critical for maintaining normal cell proliferation. May also play a role in cellular metabolism.	0.53					0.5	-0.45			
gmppa	mannose-1-phosphate guanyltransferase alpha-A-like isoform X1/2	Part of the pathway synthesising GDP-alpha-D-mannose biosynthesis, which is itself part of nucleotide-sugar biosynthesis.	0.56				-0.54	0.54				
srp72	signal recognition particle subunit	Recognises and targets specific proteins to the endoplasmic reticulum.	0.6					0.53				

Table 5.2 continued.

			CNS					Eyes				
Gene	**Annotation**	**Putative function**	**CO_2 treatment**	**Active time**	**Dist.**	**Speed**	**No. EI**	**CO_2 treatment**	**Active time**	**Dist.**	**Speed**	**No. EI**
	SRP72-like	Possibly participates in the elongation arrest function (slowing of translation).										
vhl	von Hippel-Lindau disease tumor suppressor-like	Involved in the ubiquitination and subsequent proteasomal degradation via the von Hippel-Lindau ubiquitination complex. Involved in transcriptional repression.	0.52					0.43				
derl1	derlin-1-like	Component of endoplasmic reticulum-associated protein degradation (ERAD) pathway.	0.42					0.43				
zranb1	ubiquitin thioesterase zranb1-B	Deubiquitinating enzyme with a range of roles, including regulating cell morphology, cytoskeletal organisation and cell migration. In the eyes, may be important for photoreceptor cell development and maintenance and is potentially involved in retinal neurodegeneration.	-0.58				0.47	-0.52				0.46
vhl	von Hippel-Lindau disease tumor suppressor-like	Involved in the ubiquitination and subsequent proteasomal degradation via the von Hippel-Lindau ubiquitination complex. Involved in transcriptional repression.	-0.51				0.45	-0.5				
ndufab1	acyl carrier protein, mitochondrial	Carrier of the growing fatty acid chain in fatty acid biosynthesis. Non-catalytic subunit of the mitochondrial membrane respiratory chain NADH dehydrogenase (Complex I).	-0.55				0.43	-0.53				

Table 5.2 continued.

			CNS					Eyes				
Gene	**Annotation**	**Putative function**	**CO_2 treat-ment**	**Active time**	**Dist.**	**Speed**	**No. EI**	**CO_2 treat-ment**	**Active time**	**Dist.**	**Speed**	**No. EI**
gmppa	mannose-1-phosphate guanyltransferase alpha-A-like isoform X1/2	Part of the pathway synthesising GDP-alpha-D-mannose biosynthesis, which is itself part of nucleotide-sugar biosynthesis.	-0.66				0.46	-0.7				
chrna10	neuronal acetylcholine receptor subunit alpha-10 isoform X1	Subunit of the nicotinic acetylcholine receptor.	-0.68				0.5	-0.65				
srp72	signal recognition particle subunit SRP72-like	Recognises and targets specific proteins to the endoplasmic reticulum. Possibly participates in the elongation arrest function (slowing of translation).	-0.54					-0.53				0.42
cdk10	cyclin-dependent kinase 10	Protein kinase that controls a range of fundamental cellular processes including cell proliferation, neurogenesis, development, ciliogenesis and actin cytoskeleton organization. Essential for cell cycle progression.	-0.56					-0.58				0.49
acot8	acyl-coenzyme A thioesterase 8-like	Catalyses the hydrolysis of acyl-CoAs into free fatty acids and coenzyme A (CoASH), regulating their respective intracellular levels.	-0.57					-0.62				

Genes in both tissues potentially driving altered number of exploratory interactions at elevated CO_2

Zranb1, coding for a deubiquitinating enzyme with a range of roles, including regulating cell morphology, cytoskeletal organisation and cell migration (Bai *et al.*, 2011), was negatively correlated with CO_2 treatment and positively correlated with the number of exploratory interactions in both tissues (Table 5.2). In the eyes, *zranb1* may be important for photoreceptor cell development and maintenance (Esquerdo-Barragán *et al.*, 2019) and is potentially involved in retinal neurodegeneration (Wang *et al.*, 2018a). Furthermore, a transcript for cyclin dependent kinase 10, *cdk10*, was negatively correlated with CO_2 treatment in both tissues and positively correlated with the number of exploratory interactions in the eyes (Table 5.2). Another *cdk10* transcript was positively correlated with CO_2 treatment and negatively correlated with the number of exploratory interactions in the CNS (Appendix D: Table D.3). *Cdk10* is a protein kinase that plays pivotal roles in controlling a range of fundamental cellular processes including cell proliferation and neurogenesis (reviewed in Guen *et al.* (2017)).

Chrna10, *gmppa*, *ndufab1* and *vhl* were all negatively correlated with CO_2 in both tissues and positively correlated with the number of exploratory interactions in the CNS (Table 5.2). Another transcript for the nicotinic ACh receptor, *chrna10*, was a hub gene for CO_2 treatment and all three activity traits in the eyes (Table 5.1). Another *gmppa* transcript was positively correlated with CO_2 treatment in both tissues and negatively correlated with the number of exploratory interactions in the CNS (Table 5.1). *Gmppa* may act as a regulatory subunit of *gmppb* (synthesises GDP-mannose, an essential mannose donor used for glycosylation) (Koehler *et al.*, 2013). Furthermore, another transcript for *ndufab1*, coding for a non-catalytic subunit of the mitochondrial membrane respiratory chain NADH hydrogenase, was positively correlated with CO_2 treatment in both tissues and negatively correlated with active time in the CNS (Table 5.2). *Vhl* is involved in ubiquitination and subsequent proteasomal degradation of target proteins. *Srp72*, a subunit of the signal recognition particle that mediates targeting of newly synthesised proteins emerged from the ribosome to the ER (Keenan *et al.*, 2001; Koch *et al.*, 2003; Gao *et al.*, 2017), was negatively correlated with CO_2 in both tissues and positively correlated with the number of exploratory interactions in the eyes (Table 5.2).

Genes in the CNS potentially driving altered number of exploratory interactions at elevated CO_2

Ten of the CNS-specific CO_2 treatment hub genes are also hub genes for the number of exploratory interactions in the CNS, and seven of these are annotated (Appendix D: Table D.3). Three of these genes were positively correlated with CO_2 treatment and negatively correlated with the number of exploratory interactions in the CNS: *cdk10*, as mentioned above,

trub2, and *snrnp200*. *Trub2* codes for an enzyme contributing to pseudouridinylation (a common post-transcriptional modification converting uridine to pseudouridine) of mitochondrial RNA, playing an essential role in oxidative phosphorylation (the major pathway for ATP production) (Arroyo *et al.*, 2016; Antonicka *et al.*, 2017). *Snrnp200* codes for an essential component of the spliceosome, an enzyme that excises introns and ligates exons to form mature mRNA (Kambach *et al.*, 1999; Patel and Bellini, 2008). A transcript for *snrnp200* was also negatively correlated with CO_2 treatment and positively correlated with number of exploratory interactions in the CNS. A further three genes were negatively correlated with CO_2 treatment and positively correlated with number of exploratory interactions in the CNS: *bcar3*, *psap*, and *derl1*. *Bcar3* promotes cell proliferation, migration and redistribution of actin fibres, *psap* acts as a neurotrophic and myelinotrophic factor (i.e. supports the growth and survival of neurons and myelin, the insulating layer around nerves that allows rapid transmission of electrical signals), and *derl1* is a component of the endoplasmic reticulum associated degradation (ERAD) pathway, moving misfolded proteins into the cytosol for degradation. Another transcript for *derl1* was also negatively correlated with CO_2 treatment and positively correlated with whether the squid had an exploratory interaction (Appendix D: Table D.3). The transcript identified as a CNS-specific hub gene for CO_2 treatment and shared with the number of exploratory interactions as well as active time was not annotated.

5.5 Discussion

This study identified patterns of gene expression in the CNS and eyes of the two-toned pygmy squid *Idiosepius pygmaeus* that were correlated with CO_2 treatment conditions and visually-mediated behavioural responses in the same individuals, identifying potential molecular drivers of behavioural change at elevated CO_2. Neurogenesis was identified in both the CNS and eyes as a potential key driver of behavioural changes at elevated CO_2. Collectively, the results here suggest multiple mechanisms may underlie elevated CO_2-induced behavioural alterations in this species.

There was a larger response to CO_2 treatment in the CNS than the eyes, consistent with previous findings in *I. pygmaeus* (Chapter 4). This may be influenced by the multiple tissue types within the whole eye from which RNA was extracted. The presence of multiple tissue types may have increased the variance in gene expression from whole eye samples and thus decreased the power by which changes in gene expression could be detected. However, a larger number of genes also responded to elevated CO_2 in the more centrally located olfactory bulbs, compared to the peripheral sensory olfactory rosettes in ocean-phase coho salmon (Williams *et al.*, 2019). In contrast, a similar number of genes responded to elevated CO_2 in the olfactory bulbs and sensory olfactory epithelium of European sea bass (Porteus *et al.*,

2018), suggesting the difference in the response of the peripheral and central nervous systems to elevated CO_2 may be species-specific.

5.5.1 Potential drivers of elevated CO_2-induced behavioural changes

In this study, I identified hub genes correlated with both CO_2 treatment and behavioural traits as potential drivers of behavioural change at elevated CO_2. Interestingly, CNS-specific hub genes were consistently correlated with CO_2 treatment and activity traits in the same direction, whereas eyes-specific hub genes were correlated with CO_2 treatment and activity traits in opposite directions, i.e. were positively correlated with CO_2 treatment but negatively correlated with activity traits . This might reflect an opposing effect of each tissue on activity at elevated CO_2, or perhaps the tendency for the CNS and eyes to use opposing gene expression to control activity under normal conditions.

Neurogenesis

Notably, *cdk10*, which plays an important role in neurogenesis (Yeh *et al.*, 2013), was identified as a potential driver of an altered number of exploratory interactions at elevated CO_2 in both the CNS and eyes. Furthermore, potential drivers of altered activity at elevated CO_2 in the CNS were enriched for functions related to the cell cycle and cell migration, and also included genes involved in stem cell renewal, cell differentiation, cell adhesion, neurite outgrowth and branching, and synaptogenesis. A gene involved in cell proliferation, *gid-4*, was also identified in the eyes as a potential driver of the OA-induced alteration in activity (Figure 5.4). Adult neurogenesis is a multi-step process in which new neurons are generated and integrated into existing neural circuits (Sailor *et al.*, 2017). Neurogenesis requires re-entering and exiting the cell cycle (Ohnuma and Harris, 2003) to create new cells that differentiate into immature neurons and migrate to their final destination (Kaneko *et al.*, 2017). Here, the new neurons are incorporated into existing circuits by outgrowth and branching of the neuron's dendrites and axons (collectively known as neurites) to form new connections with other neurons (synaptogenesis) (Toni *et al.*, 2007). Thus, my results suggest neurogenesis in both the CNS and eyes as a potential main driver of elevated CO_2-induced behavioural change.

Previous research shows mixed effects of elevated CO_2 on neurogenesis in the fish nervous system. Two genes involved in neurogenesis (*NeuroD*, *dcx*) were upregulated in the brain of a three-spined stickleback, but not in an anemone fish nor a damselfish, exposed to elevated CO_2 for 43 days, 10 months, or four days, respectively (Lai *et al.*, 2017). In a transcriptomic study in which Asian seabass were exposed to elevated CO_2 for seven days, differentially expressed genes in the brain were functionally enriched for neurogenesis (Wang *et al.*, 2021). In spiny damselfish, a neurite growth-regulating factor (*rtn4*) was downregu-

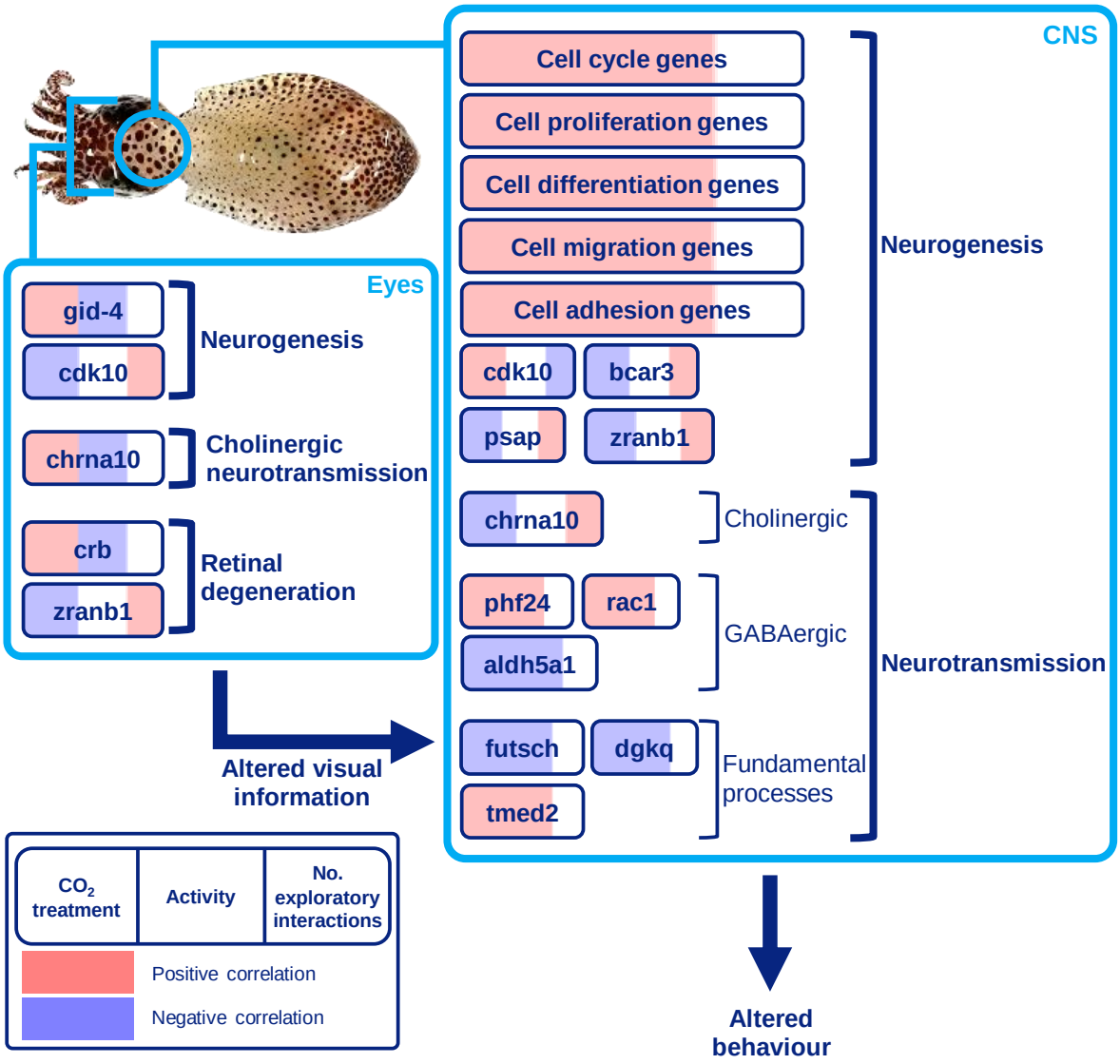

Figure 5.4. Potential molecular drivers of OA-induced behavioural changes in the CNS and eyes of *I. pygmaeus*, and a proposed mechanism by which elevated CO_2 could alter behaviour. Retinal degeneration, as well as altered neurogenesis and cholinergic neurotransmission in the eyes, may disrupt visual information detected and sent to the CNS. Disrupted visual inputs to the CNS, in combination with altered neurogenesis and neurotransmission in the CNS may disturb higher order processing, resulting in behavioural alterations.

lated after developmental exposure (from hatching for 5 months) to elevated CO_2 (Schunter *et al.*, 2018). However, the neurogenesis gene *dcx* was not altered in the olfactory bulbs of European sea bass after four years exposure to elevated CO_2 (Mazurais *et al.*, 2020). In the gilthead seabream, expression of a gene involved in cell proliferation (*pcna*) and a gene involved in neurogenesis and neuronal differentiation (*bdnf*) were down- and up-regulated in the brain, respectively, after four weeks exposure to elevated CO_2 conditions. However, the four week exposure to elevated CO_2 did not affect *pcna* expression in the gilthead seabream

olfactory bulb (Costa *et al.*, 2022a). Elevated CO_2 has also been shown to affect neurogenesis in another mollusc; in a Mediterranean pteropod, transcripts involved in neuronal cell adhesion (*bcan*, *cntn5*, *faxc*, *ncan*, *nxpe2*, *nxpe3*, *tenm1*), and neuronal differentiation and survival (*ntrk2*, *fkrp*, *nmnat3*, *samd8*, *ttll7*, *tppp2*) were upregulated after three days exposure to elevated CO_2 (Moya *et al.*, 2016).

Neurogenesis allows constant modification and refinement of neuronal circuits, contributing to neuroplasticity (the ability of the nervous system to change) (Fuchs and Flügge, 2014). Synaptic plasticity, which is the changing of synaptic strength over time, also contributes to neuroplasticity (Citri and Malenka, 2008), and appears to also be affected by elevated CO_2. In the European sea bass olfactory system, genes involved in synaptic plasticity (*grpr*, *camk2ga*, *nptxr*, *gria1b*, *map2k2a*, *tmub1*) were differentially expressed after 2 - 7 days exposure to elevated CO_2 (Porteus *et al.*, 2018). In spiny damselfish, a range of genes involved in cytoskeleton plasticity, which is related to synaptic plasticity, were upregulated after acute (four days) exposure to elevated CO_2 (Schunter *et al.*, 2018). Also in spiny damselfish, a molecular signature of parental behavioural tolerance to elevated CO_2 was seen in the brain expression profile of offspring, including genes involved in synaptic plasticity and neurite growth (*amigo1*, *gfra2*, *cdk5r1*, *mpdz*, *igsf9b*) (Monroe *et al.*, 2021). However, the expression of genes involved in synaptic plasticity were not altered after four weeks exposure to elevated CO_2 in the olfactory epithelium (*gria4a*) and olfactory bulb (*gria4a*, *grm4*) of the gilthead seabream (Costa *et al.*, 2022a). A transcript related to synaptic plasticity (*d2*) was also upregulated after three days exposure to elevated CO_2 in a pteropod mollusc (Moya *et al.*, 2016). Thus, altered neuroplasticity, due to changes in neurogenesis and/or synaptic plasticity, appears to be a common response to elevated CO_2, but this response may be taxa-specific and/or dependent on CO_2 exposure duration.

Neuroplasticity is an important mechanism by which animals can respond and adapt their behaviour to changing environments (Kania *et al.*, 2017). Indeed, adult neurogenesis is influenced by the environment, including in cephalopods (Bertapelle *et al.*, 2017), and changes in neurogenesis can have functional outcomes, including behavioural effects. It is thought that environmentally-induced changes in neurogenesis may act to fine-tune the nervous system to the environment and produce adaptive behaviours (reviewed in Opendak and Gould (2015); LaDage (2015)). Of particular interest *apbb1*, which plays a role in neurogenesis and spatial memory (Chow *et al.*, 2015), was identified as a potential driver of elevated CO_2-induced behavioural change in the CNS of *I. pygmaeus*. Thus, changes in neurogenesis at elevated CO_2 may coordinate responses, including behavioural adjustments, to cope with this environmental change. However, it is yet to be determined whether these changes are adaptive or maladaptive.

Protein synthesis

My results also identified genes involved in protein synthesis as potential drivers of behavioural change at elevated CO_2 in both tissues, and functional categories involved in protein synthesis were enriched in those hub genes in the CNS identified as potential drivers of altered activity at elevated CO_2. Genes and proteins related to protein synthesis were upregulated at elevated CO_2 in oysters (Tomanek *et al.*, 2011; Ertl *et al.*, 2016; Cao *et al.*, 2018b), but downregulated in a pteropod mollusc (Maas *et al.*, 2015; Moya *et al.*, 2016). Here, changes in protein synthesis could potentially be a response to deal with the changed protein demand required due to alterations in neurogenesis.

Neurotransmission

The GABA hypothesis is the predominant mechanistic explanation for elevated CO_2-induced behavioural changes in fish. This hypothesis proposes that altered HCO_3^- and Cl^- ion gradients across neuronal membranes, due to acid-base regulatory mechanisms, alter $GABA_A$ receptor function leading to behavioural alterations at elevated CO_2 (Nilsson *et al.*, 2012). Pharmacological work has also supported this hypothesis in marine molluscs (Watson *et al.*, 2014; Clements *et al.*, 2017), including in *I. pygmaeus* (Chapter 3). Furthermore, recent transcriptomic studies show expression changes in transcripts related to GABAergic signalling in the fish nervous system (Schunter *et al.*, 2018; Williams *et al.*, 2019), the whole-body of a pteropod mollusc (Moya *et al.*, 2016), and the nervous system of *I. pygmaeus* (Chapter 4). Here, I identified genes involved in GABAergic neurotransmission (*phf24*, *rac1*, *aldh5a1*) in the CNS as potential drivers of behavioural change at elevated CO_2 (Figure 5.4).

OA-induced disruption of $GABA_A$ receptor function has been suggested to drive altered neurogenesis in fish (Lai *et al.*, 2017) due to the role of vertebrate $GABA_A$ receptors in cell proliferation and neuronal differentiation (Owens and Kriegstein, 2002; Tozuka *et al.*, 2005; Sernagor *et al.*, 2010). In molluscs, GABA also induces cellular differentiation and proliferation (Morse *et al.*, 1980). Thus, the molecular signatures for altered neurogenesis identified in the CNS of *I. pygmaeus* here may be driven by changes in GABAergic neurotransmission within the CNS. However, in the eyes of *I. pygmaeus* genes involved in neurogenesis, but not GABAergic neurotransmission, were identified as potential drivers of OA-induced behavioural change. This suggests that a mechanism other than altered GABAergic neurotransmission may be driving altered neurogenesis in the eyes. Costa *et al.* (2022b) suggested alterations within the thyroid-system might drive disrupted neurogenesis in fish at elevated CO_2. However, I found no genes involved in the thyroid-system as potential drivers of OA-induced behavioural change in the eyes or CNS of *I. pygmaeus*. As neurogenesis is not only regulated via internal cues, such as neurotransmitters and hormones, but also via environ-

mental conditions (Cayre *et al.*, 2002), changes in neurogenesis within *I. pygmaeus* may be a consequence of OA itself.

Recent studies suggest that not only GABAergic, but also other types of neurotransmission, may be altered at elevated CO_2 levels (Moya *et al.*, 2016; Johnson and Hofmann, 2017; Porteus *et al.*, 2018, Chapter 3, Chapter 4). Here, I identified *chrna10*, a gene coding for a nicotinic acetylcholine receptor (nAChR) subunit, as a potential driver of behavioural change in both the eyes and CNS of *I. pygmaeus*. *Chrna10*, as well as other genes coding for nAChR subunits (*chrna1*, *chrna3*, *chrna5*, and *chrnb1*), were within the ion channel functional category that was significantly affected by elevated CO_2 treatment in the same individuals (Chapter 4). Genes coding for nAChRs were differentially expressed at elevated, compared to current-day, CO_2 levels in the European sea bass (*chrna7*) (Porteus *et al.*, 2018), and the pteropod molluscs *Heliconoides inflatus* (*chrna6*, *chrnd*, *chrnb3*, β-type LnAChR J) (Moya *et al.*, 2016) and *Limacina helicina antarctica* (*chrnb3*) (Johnson and Hofmann, 2017). Furthermore, here I identified genes involved in processes required for a range of different types of neurotransmission as potential regulators of behavioural change in *I. pygmaeus*. This includes *tmed2*, which is involved in GPCR trafficking, *dgkq*, which supports synaptic neurotransmission (Goldschmidt *et al.*, 2016), and *futsch*, which regulates neurotransmitter release (Lepicard *et al.*, 2014). These results suggest that changes in GABAergic and cholinergic neurotransmission, and processes that regulate a variety of different types of neurotransmission may drive behavioural changes at elevated CO_2 (Figure 5.4).

Immune function

Elevated CO_2 alters the immune response in molluscs (Bibby *et al.*, 2008; Li *et al.*, 2015; Liu *et al.*, 2016; Wu *et al.*, 2016; Su *et al.*, 2018), including squid (Culler-Juarez and Onthank, 2021). In Chapter 4, I found changes in gene expression related to all three levels of the innate immune response in the nervous system of *I. pygmaeus* at elevated CO_2. As immune-derived factors, such as cytokines, can feedback to alter the nervous system and behaviour (Adamo, 2006; Dantzer and Kelley, 2007), I suggested in Chapter 4 that OA-induced disturbances to immune function could disturb behaviour. Indeed, here I identified genes involved in the immune response as potential drivers of OA-induced behavioural changes in the CNS of *I. pygmaeus*. This includes the integrins *itga4* and *itga9*, which are cell adhesion molecules that play a key role in invertebrate immune responses (Johansson, 1999; Terahara *et al.*, 2006). The functional categories ‘cell adhesion’ and ‘integrin complex’ were also significantly affected by elevated CO_2 treatment in the CNS of the same individuals (Chapter 4). *Tf*, a key component of the molluscan innate immune response (Lambert *et al.*, 2005; Ong *et al.*, 2006; Herath *et al.*, 2015; Salazar *et al.*, 2015; Li *et al.*, 2019), was identified here as a potential

driver of behavioural change in the CNS of *I. pygmaeus*, and was also differentially expressed in the CNS of the same individuals after elevated CO_2 exposure (Chapter 4).

Oxidative stress

Oxidative stress, which occurs when there is an imbalance between reactive oxygen species (ROS) production and antioxidant defence mechanisms (Halliwell and Gutteridge, 2015), can occur at elevated CO_2 conditions in molluscs. OA has been found to increase ROS levels and alter antioxidant defences, resulting in oxidative damage such as DNA damage, lipid peroxidation and apoptosis in molluscs (Tomanek *et al.*, 2011; Wang *et al.*, 2016; Cao *et al.*, 2018a,b; Zhang *et al.*, 2021). In Chapter 4, I found molecular signatures for OA-induced oxidative stress and damage in *I. pygmaeus* nervous tissue. As oxidative damage in the nervous system can disrupt neurotransmission and neuronal function (Halliwell, 2006; Halliwell and Gutteridge, 2015), I suggested oxidative damage in nervous tissue could alter behaviour at elevated CO_2 (Chapter 4). Indeed, here I identified a gene that regulates oxidative stress (*slc4a11*) and genes involved in oxidative damage, including DNA damage and repair (*apbb1*, *spt16*, *foxm1*, *bptf*, *arpc5*), as potential drivers of OA-induced behavioural changes.

My results suggest that oxidative stress-induced damage at elevated CO_2 could potentially disrupt retinal function. Two genes, *crb* and *zranb1* identified here as potential drivers of OA-induced behavioural changes in the eyes of *I. pygmaeus*, are involved in oxidative-stress induced retinal degeneration (Chartier *et al.*, 2012; Wang *et al.*, 2018a). In particular, *crb* prevents photoreceptor degeneration by limiting the production of ROS and the resultant oxidative damage (Chartier *et al.*, 2012). Research investigating the effect of elevated CO_2 on visual function is scarce, however eye defects have been observed at elevated CO_2 in fish larvae (Frommel *et al.*, 2012, 2016; Wang *et al.*, 2017b). Therefore, eye damage could potentially occur at elevated CO_2, possibly via oxidative stress, which could contribute to visually-mediated behavioural alterations. However, more research is required to assess the effect, and underlying mechanisms, of elevated CO_2 on vision.

5.5.2 Proposed mechanism

A combination of multiple changes within the eyes and CNS of *I. pygmaeus* may drive alterations in visually-mediated behaviours at elevated CO_2 (Figure 5.4). In the eyes of *I. pygmaeus*, I identified genes involved in retinal degeneration as potential drivers of elevated CO_2-induced behavioural change. Thus, at elevated CO_2 squid visual detection may potentially be disrupted. In the eyes, genes involved in neurogenesis and cholinergic neurotransmission were also identified as potential drivers of behavioural change, indicating potential disturbances of neural circuitry structure and function, and signal transmission. Together,

these changes in the eyes may disrupt the visual information detected and sent to the CNS. In the CNS, disrupted visual inputs from the eyes, in combination with altered neurogenesis and neurotransmission, may disturb higher order processing, leading to behavioural changes (Figure 5.4). This mechanism shows parallels to a mechanism proposed to drive olfactory-mediated behavioural disturbances in a fish; Porteus *et al.* (2018) proposed that at elevated CO_2 conditions, fish sense less olfactory information, and less olfactory information is sent to higher brain centres. In combination with decreased synaptic plasticity, this was suggested to lead to changes in olfactory-mediated behaviours at elevated CO_2 (Porteus *et al.*, 2018).

5.5.3 Conclusion

Previous research has identified differentially expressed genes in the nervous system associated with behavioural changes at elevated CO_2 in fish, and now in a marine invertebrate as well (Chapter 4). This has increased our understanding of the response of the nervous system to elevated CO_2, and provided hypotheses for the potential mechanisms underlying behavioural changes at elevated CO_2 in marine animals. Here, I correlate gene expression with CO_2 treatment levels and behaviour in any marine animal, allowing a more direct assessment of the molecular mechanisms underlying behavioural change at elevated CO_2. The results identify altered neurogenesis in the CNS and eyes as a potential main driver of elevated CO_2-induced behavioural changes. I also identified genes involved in various types of neurotransmission, immune function and oxidative stress as potential drivers of behavioural change, supporting my results from Chapter 4. I propose a mechanism involving a combination of multiple changes within the eyes and CNS of *I. pygmaeus* may drive alterations in visually-mediated behaviours at elevated CO_2. As research in this field progresses, it appears that elevated CO_2 induces changes in both the peripheral and central nervous systems, leading to behavioural alterations via multiple mechanisms. These mechanisms may occur in both marine fish and invertebrates. Furthermore, unlike the downstream effects of acid-base regulation at high CO_2 on the function of $GABA_A$ receptors, alterations in sensory detection and neuroplasticity may be independent of internal acid-base chemistry. This raises the potentially widespread susceptibility of marine animals to elevated CO_2, but also the possibility of different mechanisms being predominant in different taxa.

Chapter 6

General Discussion

6.1 Summary

Human-induced environmental change is drastically altering the environments in which animals live (Vitousek *et al.*, 1997; Pereira *et al.*, 2010; Steffen *et al.*, 2015). In particular, ocean acidification (OA) is a serious emerging threat to marine animals, ecosystems, and the services they provide (Doney *et al.*, 2009; Bindoff *et al.*, 2019). Establishing a mechanistic understanding of marine animal responses to OA is critical to improve predictions of how marine animals will respond as seawater CO_2 levels rise (Fuller *et al.*, 2010; Cooke *et al.*, 2013). The nervous system forms the fundamental link between an animal and its environment, coordinating physiological and behavioural responses to environmental change (Kelley *et al.*, 2018; O'Donnell, 2018). Thus, a neurobiological understanding of OA is key, yet to date has been little explored. My thesis provides novel explorations into the neurobiological impacts of, and the mechanistic neurobiological underpinnings of biological responses to, OA in a marine invertebrate with a complex nervous system, a cephalopod mollusc. Together, the chapters in this thesis present evidence that a complex assortment of mechanisms underpin OA-induced responses. I have found support for previous mechanistic hypothesis, and from my results proposed novel mechanistic hypotheses, providing a foundation from which future research can develop.

As so little is known about the mechanistic basis of OA-induced behavioural responses in marine invertebrates, I started this thesis with a literature review in Chapter 2. In this review, I highlighted that OA likely induces behavioural alterations through a range of mechanisms, which are not necessarily mutually exclusive and all of which have been little explored and require further experimental testing. I proposed potential novel mechanisms and outlined major knowledge gaps, which guided the following chapters. I highlighted the importance of using multiple pharmacological agents, in particular those shown to work in the taxa being studied, to more robustly test the GABA hypothesis in marine invertebrates. I also suggested that using drugs that target other ligand-gated Cl^- channels would allow testing whether other receptors, similar to the $GABA_A$ receptor, are also involved in OA-induced behavioural alterations. These knowledge gaps informed Chapter 3. In Chapter 2, I also highlighted that non-targeted approaches, such as omics technologies, will be important to provide a more holistic view of the neurobiological impacts of OA and potentially lead to the development of novel mechanistic hypotheses for OA-induced behavioural alterations. Thus, in Chapter 4 and Chapter 5, I used transcriptomics as a more holistic approach, which resulted in my proposal of novel hypotheses for the mechanistic basis of physiological and behavioural responses to OA. Together, Chapter 3, Chapter 4 and Chapter 5 provide evidence that a complex assortment of mechanisms underpin biological responses to OA (Figure 6.1).

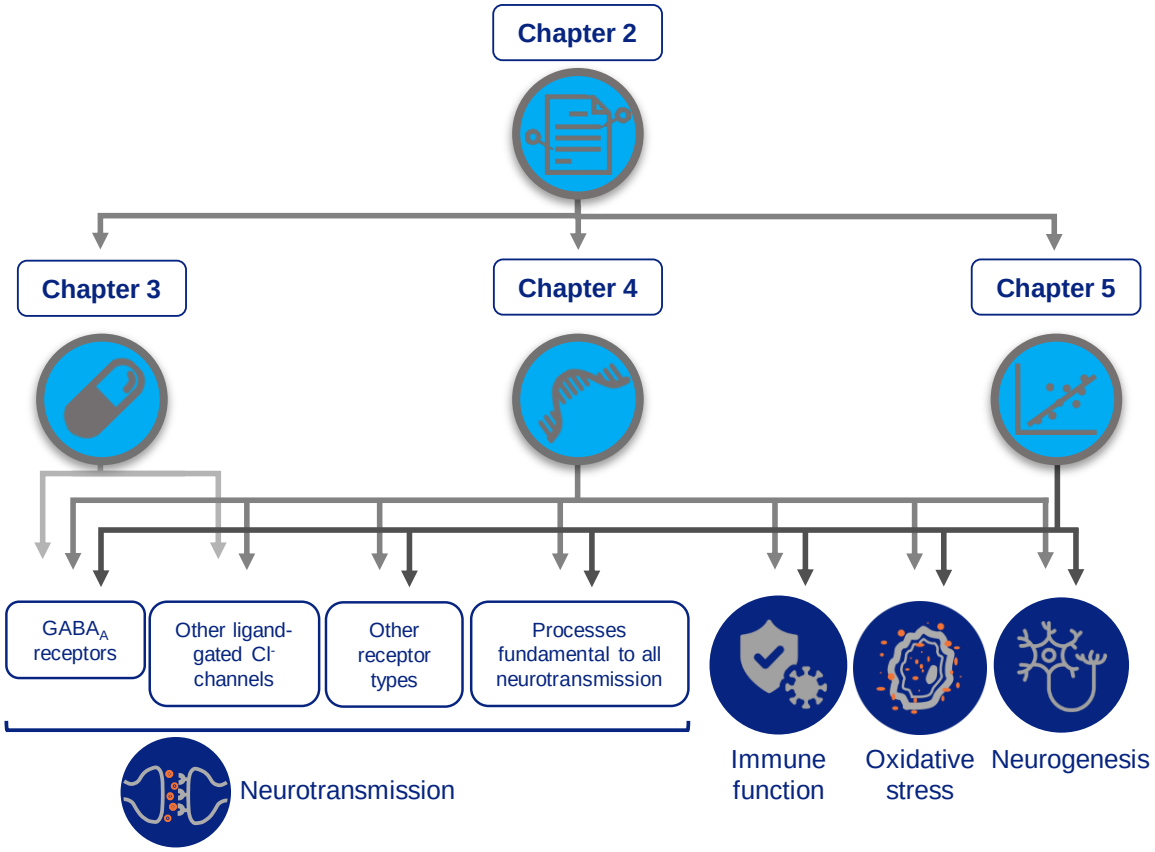

Figure 6.1. Overview of the results from the chapters in this thesis. Chapter 2 outlined major knowledge gaps and proposed novel mechanisms, guiding the data chapters. Chapter 3 demonstrated pharmacological evidence for altered functioning of $GABA_A$ receptors and other ligand-gated Cl^- channels underlying OA-induced behavioural alterations. Chapter 4 identified molecular signatures for OA-induced disruption to various different types of neurotransmission, including neurotransmission mediated by $GABA_A$ receptors, other ligand-gated Cl^- channels, ligand-gated cation channels and GPCRs, as well as Ca^{2+} and K^+ channels fundamental for neurotransmission. Chapter 4 also identified molecular signatures for altered immune function and oxidative stress at elevated CO_2. Chapter 5 identified genes involved in neurogenesis as potential key drivers of OA-induced behavioural changes. Furthermore, Chapter 4 also identified molecular signatures for altered neurogenesis at elevated CO_2, supporting the results from Chapter 5. Chapter 5 also found genes involved in GABAergic neurotransmission, GPCR function, synaptic processes fundamental to neurotransmission, immune function and oxidative stress as potential drivers of behavioural change at elevated CO_2, supporting the results from Chapter 4. Icons from NounProject.com (immune function by Adrien Coquet, neuron by tezar tantular), remaining icons by Jodi Thomas.

6.1.1 OA likely affects multiple types of neurotransmission, underpinning behavioural responses

To date, mechanistic research has focused on the GABA hypothesis, which proposes OA-induced disruption of $GABA_A$ receptor functioning underpins behavioural alterations (Nilsson *et al.*, 2012). However, the nervous system is enormously complex and it's likely other mechanisms are also involved. Indeed, in Chapter 3, Chapter 4 and Chapter 5 I found evidence that GABAergic and other different types of neurotransmission are potentially affected by elevated CO_2 conditions.

In Chapter 3, I used both a specific (gabazine) and non-specific (picrotoxin) $GABA_A$ receptor antagonist, providing the first marine invertebrate study to use a drug other than gabazine to test the GABA hypothesis. As picrotoxin is structurally unrelated to gabazine, and the action of picrotoxin is better known in molluscs, using both gabazine and picrotoxin provided more robust evidence for the GABA hypothesis in marine molluscs, as well as evidence for the GABA hypothesis in a cephalopod mollusc. Using both drugs also provided pharmacological evidence that other ligand-gated Cl^- channels, similar to the $GABA_A$ receptor, may also be involved in OA-induced behavioural alterations. The results from this chapter also suggest that mechanisms other than altered functioning of gabazine- and picrotoxin-sensitive receptors are likely involved in behavioural responses to elevated CO_2. Thus, Chapter 3 highlighted the complexity of the mechanisms underlying OA-induced behavioural changes, with $GABA_A$ receptors, receptors similar to the $GABA_A$ receptor, as well as other mechanisms likely not linked to the theory behind the GABA hypothesis, found to be involved in behavioural alterations at elevated CO_2.

In Chapter 4 and Chapter 5, I used modern transcriptomic methods to investigate the response of a marine invertebrate nervous system to OA. Furthermore, in Chapter 5 I correlated gene expression with OA-affected behaviours in order to more directly assess the mechanistic basis for OA-induced behavioural responses. Together, these chapters develop a more holistic view of the neurobiological impacts of elevated CO_2. The results from both Chapter 4 and Chapter 5 support the GABA hypothesis. By looking at both the eyes (peripheral sense organ) and central nervous system (CNS), I found molecular signatures for altered functioning of $GABA_A$ receptors at elevated CO_2 in both the peripheral and central nervous systems, implicating the importance of $GABA_A$ receptor function in both peripheral sensing and central processing for OA-induced biological responses. Chapter 4 also found molecular signatures for disruption to monoaminergic, glutamatergic, and cholinergic neurotransmission, including neurotransmission mediated by ligand-gated Cl^- channels, ligand-gated cation channels and G-protein coupled receptors (GPCRs). These results support Chapter 3, that not only $GABA_A$ receptor, but also other ligand-gated Cl^- channel, functioning is affected by OA.

Molecular signatures for altered ligand-gated cation channels and GPCRs in Chapter 4, and GPCRs in Chapter 5, also support my suggestion in Chapter 3 that mechanisms not linked to the theory behind the GABA hypothesis, i.e. disruption of nervous system processes other than receptors permeable to HCO_3^- and Cl^- ions, are also involved. Furthermore, molecular signatures for OA-induced disruption of K^+ and Ca^{2+} channels in Chapter 4, and synaptic processes in Chapter 5, suggest widespread effects of OA on neurotransmission due to the fundamental role of these ions and processes in neurotransmission. Overall, Chapter 4 and Chapter 5 suggest elevated CO_2 disrupts a wide range of different types of neurotransmission.

6.1.2 OA-induced disruption of adult neurogenesis may drive behavioural alterations

Lai *et al.* (2017) suggested that OA-induced disruption of adult neurogenesis within the fish nervous system is another potential mechanism for behavioural alterations at elevated CO_2. However, the effects of elevated CO_2 on neurogenesis within fish nervous tissue are variable (Lai *et al.*, 2017; Schunter *et al.*, 2018; Mazurais *et al.*, 2020; Wang *et al.*, 2021; Costa *et al.*, 2022a), and this mechanism remains unexplored in marine invertebrates. In Chapter 5, I demonstrated correlation of changes in expression of genes involved in neurogenesis with CO_2 treatment and OA-disrupted behaviours. These results provide more direct evidence for altered neurogenesis as a potential driver of behavioural changes at elevated CO_2. In Chapter 4, I also identified small, coordinated changes in expression of genes belonging to functional categories related to neurogenesis in the nervous system of squid exposed to current-day versus elevated CO_2 conditions. Thus, the results from Chapter 4 also support the proposal in Chapter 5 that altered neurogenesis is a potential driver of behavioural responses to OA. Transcripts involved in neurogenesis were also differentially expressed after exposure to elevated CO_2 in another mollusc; the whole-body of a pteropod mollusc (Moya *et al.*, 2016). Thus, OA-induced disturbance of neurogenesis may occur in marine fish and invertebrates, suggesting this mechanism may be applicable to a wide range of animals.

OA-induced disruption of neurogenesis has been suggested to be a downstream consequence of altered $GABA_A$ receptor function (Lai *et al.*, 2017) and alterations in the thyroid-system (Costa *et al.*, 2022a). However, neurogenesis is not only regulated via internal cues, such as neurotransmitters and hormones, but also via environmental conditions (Cayre *et al.*, 2002). Furthermore, environmentally influenced changes in neurogenesis are thought to fine-tune the nervous system to the environment and produce adaptive behaviours (Opendak and Gould, 2015). Thus, in Chapter 5 I propose that changes in neurogenesis may be a consequence of OA itself, and that altered neurogenesis may coordinate behavioural responses to cope with this environmental change. However, it is yet to be determined whether these

changes are adaptive or maladaptive.

6.1.3 Neurobiological impacts of OA may also drive non-behavioural responses

In Chapter 2, I propose that the neurobiological impacts of OA likely have widespread impacts, affecting not only behaviour, but also physiology. In particular, I suggest that as GABAergic neurotransmission plays an important role in the molluscan immune response (Bai *et al.*, 2012; Li *et al.*, 2016a,b; Nguyen *et al.*, 2018), altered $GABA_A$ receptor functioning at elevated CO_2 may also affect immune function. Indeed, the results from Chapter 4 support this proposal; I found changes in gene expression related to all three levels of the innate immune response in the nervous tissue of *Idiosepius pygmaeus*. An altered immune response may be due to disrupted GABAergic neurotransmission, which I found molecular signatures for in the same individual squid. OA-induced disturbance of norepinephrine, which mediates a neuroendocrine-immune axis-like pathway in molluscs (Liu *et al.*, 2017), may also contribute to altered immune function as suggested by upregulation of *maoa* in *I. pygmaeus*. *Maoa* codes for the enzyme monoamine oxidase A which degrades monoamine neurotransmitters and plays a key role in molluscan immune function via regulation of norepinephrine signalling (Zhou *et al.*, 2011; Liu *et al.*, 2018; Sun *et al.*, 2021). In Chapter 4 I also found molecular signatures for oxidative stress within the nervous system of *I. pygmaeus* at elevated CO_2 conditions, which supports a growing number of molluscan studies demonstrating that elevated CO_2 induces alterations in both the immune and oxidative stress systems (Ertl *et al.*, 2016; Sun *et al.*, 2017; Cao *et al.*, 2018b). Oxidative stress may disrupt the immune response by damaging immune components, such as the cytoskeleton and hemocytes (Sun *et al.*, 2017; Cao *et al.*, 2018b), and increasing Ca^{2+} levels which could disturb calcium-dependent immune processes, such as phagocytosis (Sun *et al.*, 2017). These mechanisms are not necessarily mutually exclusive, disruption of GABAergic and norepinephrine signalling, as well as oxidative damage and oxidative stress-induced Ca^{2+} increases, may all contribute to OA-induced disturbance of immune function.

6.1.4 Complex interactions between the neurobiological impacts of OA

The neurobiological impacts of OA may not only directly drive behavioural and physiological responses, but the downstream effects of OA may also feedback onto the nervous system, indirectly altering behaviour and physiology further. In Chapter 4, I found molecular signatures for OA-induced disruption of immune function and oxidative stress in the nervous system of *I. pygmaeus*. Immune-derived factors, such as cytokines, can feedback to alter the

nervous system and behaviour (Adamo, 2006; Dantzer and Kelley, 2007). Between elevated and current-day CO_2 levels, I found differential expression of genes thought to regulate behaviour via immune factors in the nervous tissue of *I. pygmaeus*. Thus, the nervous system of *I. pygmaeus* may respond to elevated CO_2 to mediate changes in the immune system through a neuroendocrine-immune axis (as discussed above), and these immune changes may also feedback on the nervous system to alter behaviours at elevated CO_2. Oxidative damage in the nervous system can disrupt neurotransmission and neuronal function (Halliwell, 2006; Halliwell and Gutteridge, 2015) and I found molecular signatures of oxidative damage in the nervous system of *I. pygmaeus* at elevated CO_2 (Chapter 4). Furthermore, oxidative stress increases intracellular 'free' Ca^{2+} levels (Halliwell and Gutteridge, 2015), Ca^{2+} ions play a fundamental role in neurotransmission (Rusakov, 2006), and I found OA-induced changes in expression of genes for Ca^{2+} channels in *I. pygmaeus* nervous tissue (Chapter 4). Thus, OA-induced oxidative stress in the nervous system may feedback to disrupt neurotransmission, via oxidative damage and altered Ca^{2+} levels, further altering behaviour and physiology. Indeed, in Chapter 5 I identified genes involved in immune function and oxidative stress as potential molecular drivers of behavioural changes at elevated CO_2. Overall, Chapter 4 and Chapter 5 show the potential complexity of the interactions between the mechanisms underlying biological responses to OA, highlighting the need for integrative research, rather than studying behavioural and physiological mechanisms in isolation.

6.2 Future Directions

The exploratory work in this thesis forms a foundation for future research into the mechanistic basis of biological responses to OA, especially in invertebrates. In particular, experimental work assessing the novel mechanisms proposed in my thesis will be a potentially important direction for future research to gain a more thorough understanding of the complexities of the mechanisms underlying OA-induced biological responses. For example, the transcriptomic results from Chapter 4 and Chapter 5 provide correlational evidence for the mechanistic basis of OA-induced biological responses. Thus, causative studies are a critical next step.

6.2.1 The role of multiple types of neurotransmission in behavioural and physiological responses to OA

In Chapter 4, I found molecular signatures for disturbance of $GABA_A$ receptors at elevated CO_2 in both the peripheral and central nervous systems, and in Chapter 5 I identified genes involved in GABAergic signalling in the CNS as potential molecular drivers of behavioural change at elevated CO_2. The systemic administration of gabazine and picrotoxin (Chapter 3)

provided additional support for altered functioning of $GABA_A$-like receptors causing OA-induced behavioural alterations. However, as gabazine and picrotoxin cross the blood brain barrier (BBB) (Hinton and Johnston, 2018), I could not differentiate between central and peripheral $GABA_A$-like receptors. Using quaternary salts of bicuculline, such as bicuculline methiodide, which antagonise the $GABA_A$ receptor but do not cross the BBB (Hinton and Johnston, 2018), in combination with drugs that do cross the BBB will be useful to experimentally determine the relative importance of peripheral and central $GABA_A$ receptors in OA-induced behavioural alterations.

In Chapter 4, I also identified molecular signatures for OA-induced disruption of multiple types of neurotransmission, including GABAergic, monoaminergic, glutamatergic, and cholinergic neurotransmission, mediated by ligand-gated Cl^- channels, ligand-gated cation channels, and GPCRs. I also identified genes involved in GABAergic and cholinergcic signalling as potential drivers of behavioural change et elevated CO_2 in Chapter 5. Chapter 3 provided experimental, pharmacological evidence for altered functioning of $GABA_A$ receptors, as well as other ligand-gated Cl^- channels, underpinning behavioural disturbances at elevated CO_2. Experimental studies determining the behavioural effects, at elevated versus current-day CO_2 conditions, of a range of drugs that target other types of neurotransmission identified in Chapter 4 and Chapter 5 will be important to test a causative link between these other types of neurotransmission and OA-induced behavioural alterations. Furthermore, to test the proposal that altered neurotransmission at elevated CO_2 drives not only behavioural changes, but also physiological responses, physiological measures should also be tested after CO_2 and drug treatment. For example, immune function could be measured after exposure to either current-day or elevated CO_2 conditions, followed by administration of $GABA_A$ receptor agonists/antagonists (as GABAergic neurotransmission plays an important role in the molluscan immune response (Bai *et al.*, 2012; Li *et al.*, 2016a,b; Nguyen *et al.*, 2018)), or drugs acting on norepinephrine signalling, such as norepinephrine reuptake inhibitors and agonists/antagonists of α- and β-adrenergic receptors (as norepinephrine mediates a molluscan neuroendocrine-immune axis-like pathway, via these receptors (Lacoste *et al.*, 2001; Zhou *et al.*, 2013; Liu *et al.*, 2017)).

Gene knockdown, in which the expression of a specific gene is reduced, will be a promising avenue for future research to determine a causative link between gene expression and biological responses to OA. A particularly useful gene knockdown technique is RNA interference (RNAi) in which introduction of double-stranded RNA (dsRNA) degrades target mRNA (Scherer and Rossi, 2003). RNAi has successfully been used to assess gene function in vertebrates and invertebrates, including under *in vivo* conditions in molluscs (Jiang *et al.*, 2006). Thus, RNAi could be used to knockdown expression of key genes identified in Chapter 4 and Chapter 5. For example, animals exposed to current-day or elevated CO_2 conditions,

and injected with dsRNA targeting *maoa* or a sham injection, could be tested for measures of aggressive behaviour, activity levels, and immune function. *Maoa* plays important roles in aggressive behaviour, activity levels and molluscan immune function (Scott *et al.*, 2008; Liu *et al.*, 2018; Mentis *et al.*, 2021) and was differentially expressed between CO_2 treatment levels in Chapter 4. This experiment would test the causative role of *maoa* in behavioural and physiological responses to OA.

6.2.2 The role of oxidative stress in behavioural responses to OA

In Chapter 4, I proposed oxidative stress-induced damage as a potential mechanism underlying OA-induced behavioural responses, with support from correlational molecular evidence in Chapter 5. Developing a cause-effect relationship between OA-induced oxidative stress and behavioural alterations would be an exciting avenue for future research. Elevated CO_2 alters the levels of antioxidants and reactive oxygen species, inducing oxidative damage such as DNA damage, lipid peroxidation and apoptosis in the non-nervous tissue of molluscs (Tomanek *et al.*, 2011; Wang *et al.*, 2016; Cao *et al.*, 2018a,b; Zhang *et al.*, 2021). Similar studies measuring indicators of oxidative damage in the nervous tissue, as well as behaviours of the same individuals exposed to elevated CO_2, will be useful to test for a correlation between neurobiological oxidative damage and OA-induced behavioural responses. Furthermore, experimentally inducing oxidative stress, followed by measures of behaviours previously shown to be altered by OA, will determine whether oxidative stress can induce behavioural alterations in the study species. For example, hydrogen peroxide administration has been used to demonstrate a cause-effect relationship between this oxidising agent and anxiety-like behaviours in mice (Bouayed and Soulimani, 2019). The administration of antioxidants to animals held at either current-day or elevated CO_2 levels, followed by behavioural tests and measures of oxidative damage (to check the effect of prior antioxidant administration) could be used to test for a causative role of oxidative damage in behavioural responses to elevated CO_2. Together, these proposed experiments would provide a strong test for the role of oxidative stress within the nervous system, in OA-induced behavioural alterations.

6.2.3 The role of adult neurogenesis in behavioural responses to OA

OA-induced disruption of adult neurogenesis has recently been suggested as another potential mechanism for OA-induced behavioural responses in fish (Lai *et al.*, 2017), and in Chapter 5 I found more direct evidence for this hypothesis in the nervous system of *I. pygmaeus*. However, all evidence for OA-induced alterations of neurogenesis relies on measures of mRNA levels (Moya *et al.*, 2016; Lai *et al.*, 2017; Schunter *et al.*, 2018; Wang *et al.*, 2021, Chap-

ter 4 and Chapter 5). Thus, experimental studies are now needed to determine whether these changes in gene expression translate to phenotypic effects of neurogenesis, and to test for a cause-effect relationship between neurogenesis and OA-induced behavioural responses. Firstly, an *in vivo* 5-bromo-2'-deoxyuridine (BrdU) cell proliferation assay, in combination with behavioural measures of the same individuals, exposed to either current-day or elevated CO_2 levels would be useful to test for a correlation between altered neurogenesis and OA-induced behavioural responses. *In vivo* BrdU injection specifically labels dividing cells, which can later be immunohistologically detected in the nervous tissue by the use of an antibody targeted to the BrdU-containing DNA, thus measuring neurogenesis (Cameron, 2006). Secondly, determining the behavioural effect of neurogenesis inhibition in animals exposed to elevated versus current-day CO_2 levels, will test for a cause-effect relationship between neurogenesis and OA-induced behavioural disturbances. Neurogenesis inhibition has previously been achieved by administration of a drug that is selectively cytotoxic for dividing cells, and was used to investigate the causative role of neurogenesis in learning and memory behaviours (Shors *et al.*, 2001).

6.2.4 Further exploration of the molecular mechanisms underlying biological responses to OA

In Chapter 4 and Chapter 5, I explored the effects of elevated CO_2 on mRNA levels within the entire CNS and eyes of *I. pygmaeus*. However, the complexity and heterogeneity of the nervous system means that measurements at the tissue level (e.g. whole CNS or eye) could mask changes in gene expression in one brain region or cell type, leaving fine scale changes in gene expression undetected. Future work using single-cell sequencing would provide higher resolution to explore the mechanistic complexities of biological responses to OA. As the neural circuitry of the tail-withdrawal reflex in the model organism *Aplysia californica* (the California sea hare, a mollusc) is relatively simple (Walters *et al.*, 1983), and this behaviour is altered by OA (Zlatkin and Heuer, 2019), single-cell sequencing of the cells within this neural circuit would provide an excellent opportunity to develop a finer scale understanding of the mechanisms underlying OA-induced behavioural alterations.

A quantitative change in mRNA levels, as measured in Chapter 4 and Chapter 5, is not the only molecular mechanism by which phenotypic change can occur in response to the environment. Alternative splicing and RNA editing are other mechanisms that can also produce phenotypic variation, and are promising avenues for future research to assess the molecular mechanisms underpinning OA-induced responses. Alternative splicing is the process in which different exons are excluded or included in the final mRNA, resulting in a variety of alternative mRNA strands made up of different combinations of exons. Consequently, a range

of functionally different proteins can be produced from the same gene (Marden, 2008). The role of alternative splicing in phenotypic responses to environmental change has been much less studied than quantifying mRNA levels. However, studies to date suggest alternative splicing as a promising molecular mechanism producing phenotypic variation in response to the environment (Huang *et al.*, 2016; Tan *et al.*, 2019; Xing *et al.*, 2019; Chan *et al.*, 2022). Furthermore, in Chapter 4 functional categories involved in mRNA splicing were significantly upregulated in the CNS after elevated CO_2 exposure, and in Chapter 5 I identified multiple genes involved in RNA splicing as potential drivers of behavioural change at elevated CO_2 in *I. pygmaeus*. RNA editing is the process in which point mutations are generated within RNA. For example, the editing of adenosine to inosine (which is interpreted as guanosine) on an mRNA strand (A-to-I editing). If this editing changes the way a codon is interpreted, it results in a functionally different protein (Rosenthal, 2015). As RNA editing is particularly pervasive in cephalopods, including squid, especially in the nervous system (Alon *et al.*, 2015; Rosenthal, 2015), and can respond to the environment (Garrett and Rosenthal, 2012), exploring the role of RNA editing in cephalopod responses to OA is a particularly exciting avenue for future research to pursue.

Changes in mRNA levels do not always translate into altered protein levels, reflecting phenotypic change. Correlational studies between mRNA and protein levels are not very abundant, but most report only a weak mRNA-protein correlation (reviewed in Maier *et al.* (2009)). Using both transcriptomes and proteomes from the same individual fish, Schunter *et al.* (2016) analysed the molecular response of transgenerational exposure to elevated CO_2 and found both similarities and differences between the mRNA and proteins differentially expressed. Thus, it cannot be assumed that the mRNA levels measured in Chapter 4 and Chapter 5 here correlate with protein levels. Protein analyses, such as proteomics, Western blotting and immunohistochemistry would be an interesting avenue for future research to investigate whether the alterations in gene expression measured across CO_2 conditions within this thesis translate into changes in protein levels.

6.2.5 Sex-specific responses to ocean acidification

In this thesis, all experiments were done using male *I. pygmaeus*. In fish and marine invertebrates, physiological, reproductive and biochemical responses to OA can be sex-specific (Ellis *et al.*, 2017). Recent work in a sea urchin has shown that behavioural responses to OA can also be sex-specific (Marčeta *et al.*, 2020). Thus, the results presented in this thesis can only be attributed to male *I. pygmaeus*. As far as I am aware, no research to date has assessed the role of sex in the mechanisms underlying biological responses to OA. Future work in females is needed to determine whether the behavioural reponses to OA, and the

mechanisms underlying these CO_2-induced responses, may be similar or different to those measured in male *I. pygmaeus*. As non-destructively determining the sex of marine animals is often difficult, sex has commonly been neglected in OA studies (Ellis *et al.*, 2017). The sex of *I. pygmaeus* can easily be determined by visual inspection of live animals. Thus, *I. pygmaeus* is a useful species to determine the role of sex in the mechanisms underpinning biological responses to OA, which will be important to accurately determine the impact of OA at the population level.

6.2.6 Ecologically relevant mechanistic studies

Natural fluctuations in CO_2 levels are present in some habitats. For example, diel CO_2 cycles are common in shallow coastal waters (Hofmann *et al.*, 2011; Santos *et al.*, 2011; Shaw *et al.*, 2012; Hannan *et al.*, 2020), and these fluctuations are projected to amplify by up to three times by the end of this century (McNeil and Sasse, 2016). Furthermore, recent research in fish has shown brain transcriptional responses to OA were altered by diel CO_2 fluctuations (Schunter *et al.*, 2021). The experimental CO_2 levels used in this thesis are ecologically relevant to the population of *I. pygmaeus* used, because despite these squid inhabiting a coastal environment, I found very little daily variation in seawater pCO_2 levels at the site of squid collection (Appendix C: Water sampling methods and Figure C.1). However, marine invertebrates can experience extreme CO_2 fluctuations, e.g. those living in the intertidal zone (Menge and Branch, 2001; Wolfe *et al.*, 2020). It will be interesting to determine whether marine invertebrates that naturally experience extreme CO_2 fluctuations also respond to elevated stable, versus diel-cycling, CO_2 conditions with changes in expression of circadian rhythm genes, as determined in two coral reef fish species (Schunter *et al.*, 2021). Furthermore, OA is not occurring in isolation. A variety of other marine environmental parameters are projected to also change as climate change progresses, e.g. ocean warming and deoxygenation (Bindoff *et al.*, 2019). Multi-stressor experiments are increasingly being used to gain a more holistic and ecologically relevant understanding of how animals may respond to future ocean conditions (Riebesell and Gattuso, 2015; Boyd *et al.*, 2018). Indeed, it has been observed that animal responses to OA alone can be different to those when animals are exposed to OA in combination with other stressors, and this varies between taxa (Gao *et al.*, 2020). Furthermore, the effects of a single stressor can generally not be extrapolated to multiple stressors, as interactions can be additive, antagonistic or synergistic (Riebesell and Gattuso, 2015). Adding to this complexity, other environmental parameters also experience fluctuations. For example, shallow water coastal habitats can also experience daily temperature and oxygen cycles (McCabe *et al.*, 2010; Baumann *et al.*, 2015; Kline *et al.*, 2015). Moving forward, introducing multi-stressor mechanistic studies, with ecologically relevant

treatment regimes, will be vital to examine the mechanistic basis for responses to conditions that more closely resemble the future ocean. Mechanistic studies in increasing ecologically relevant scenarios will enable more accurate predictions of how marine animals will respond as human-induced environmental change progresses.

6.2.7 Adaptation of the nervous system as ocean acidification progresses

This thesis has contributed to our understanding of the neurobiological mechanisms underlying the acute behavioural responses of a marine invertebrate to OA. However, it is yet to be determined whether the nervous system could adapt as climate change progresses. Research in marine invertebrates has assessed the long-term and transgenerational responses of physiological processes and life history traits to OA, finding both positive and negative carryover effects of parental exposure to OA. A range of potential mechanisms have been proposed to underlie these transgenerational responses (reviewed in Lee *et al.* (2020)). However, the potential for behavioural adaptation, and the underlying mechanisms in the nervous system, have been little explored. In the brains of juvenile damselfish, a transgenerational molecular signature of behaviourally tolerant versus sensitive parents suggests that fish may behaviourally adapt to OA (Schunter *et al.*, 2016). Future research assessing the longer-term and transgenerational responses of the nervous system and behaviour of marine invertebrates to OA will be important to determine how they will fare in a rapidly changing ocean.

6.3 Concluding Remarks

This thesis provides novel insights into the neurobiological impacts of, and the mechanistic basis for biological responses to, elevated CO_2 in a marine invertebrate. Using pharmacological experiments, I have demonstrated more robust support for the GABA hypothesis in marine molluscs, and experimental evidence for the involvement of other ligand-gated Cl^- channels in OA-induced behavioural responses. I also used modern transcriptomic methods to investigate the response of a marine invertebrate nervous system to OA. These data chapters have revealed that OA likely induces a suite of changes in both the peripheral and central nervous systems, with a complex assortment of mechanisms underpinning OA-induced behavioral and physiological responses. I found support for previous mechanistic hypotheses, and from my results proposed novel mechanistic hypotheses, providing a foundation from which future research can develop. Overall, my thesis advances our mechanistic understanding of biological responses to OA, enabling the development of improved predictions for how marine animals will respond as OA progresses. This thesis also highlights the importance of considering the nervous system, and its role in coordinating both behavioural and physiolog-

ical responses, to the wider field of research exploring biological responses to anthropogenic environmental change.

References

Abe, K. and Kimura, H. (1996). The possible role of hydrogen sulfide as an endogenous neuromodulator. *Journal of Neuroscience*. **16**(3), 1066–1071. URL https://doi.org/10.1523/JNEUROSCI.16-03-01066.1996.

Adamo, S. A. (2006). Comparative psychoneuroimmunology: Evidence from the insects. *Behavioral and Cognitive Neuroscience Reviews*. **5**(3), 128–140. URL https://doi.org/10.1177/1534582306289580.

Aishi, K., Sinnasamy, S., MacRae, T. H., Muhammad, T. S. T., Lv, A., Sun, J., Chen, S., Shi, H., Pau, T. M., and Abdullah, M. D.-D. (2019). *Hsp70* knockdown reduced the tolerance of *Litopenaeus vannamei* post larvae to low pH and salinity. *Aquaculture*. **512**, 734346. URL https://doi.org/10.1016/j.aquaculture.2019.734346.

Albertin, C. B., Bonnaud, L., Brown, C. T., Crookes-Goodson, W. J., da Fonseca, R. R., Di Cristo, C., Dilkes, B. P., Edsinger-Gonzales, E., Freeman, R. M., Hanlon, R. T., Koenig, K. M., Lindgren, A. R., Martindale, M. Q., Minx, P., Moroz, L. L., Nödl, M.-T., Nyholm, S. V., Ogura, A., Pungor, J. R., Rosenthal, J. J. C., Schwarz, E. M., Shigeno, S., Strugnell, J. M., Wollesen, T., Zhang, G., and Ragsdale, C. W. (2012). Cephalopod genomics: A plan of strategies and organization. *Standards in Genomic Sciences*. **7**(1), 175–188. URL https://doi.org/10.4056/sigs.3136559.

Albright, R., Mason, B., Miller, M., and Langdon, C. (2010). Ocean acidification compromises recruitment success of the threatened Caribbean coral *Acropora palmata*. *Proceedings of the National Academy of Sciences*. **107**(47), 20400–20404. URL https://doi.org/10.1073/pnas.1007273107.

Alkon, D., Anderson, M., Kuzirian, A., Rogers, D., Pass, D., Collin, C., Nelson, T., Kapetanovic, I., and Matzel, L. (1993). GABA-mediated synaptic interaction between the visual and vestibular pathways of *hermissenda*. *Journal of Neurochemistry*. **61**(2), 556–566. URL https://doi.org/10.1111/j.1471-4159.1993.tb02159.x.

Alon, S., Garrett, S. C., Levanon, E. Y., Olson, S., Graveley, B. R., Rosenthal, J. J., and Eisenberg, E. (2015). The majority of transcripts in the squid nervous system are extensively recoded by A-to-I RNA editing. *Elife*. **4**, e05198. URL https://doi.org/10.7554/eLife.05198.001.

Andrews, P. and Johnston, G. (1979). GABA agonists and antagonists. *Biochemical Pharmacology*. **28**(18), 2697–2702. URL https://doi.org/10.1016/0006-2952(79)90549-5.

Andrews, S. (2010). FastQC: A quality control tool for high throughput sequence data. URL https://www.bioinformatics.babraham.ac.uk/projects/fastqc/.

Antonicka, H., Choquet, K., Lin, Z.-Y., Gingras, A.-C., Kleinman, C. L., and Shoubridge, E. A. (2017). A pseudouridine synthase module is essential for mitochondrial protein synthesis and cell viability. *EMBO Reports*. **18**(1), 28–38. URL https://doi.org/10.15252/embr.201643391.

Arentsen, T., Khalid, R., Qian, Y., and Diaz Heijtz, R. (2018). Sex-dependent alterations in motor and anxiety-like behavior of aged bacterial peptidoglycan sensing molecule 2 knockout mice. *Brain, Behavior, and Immunity*. **67**, 345–354. URL https://doi.org/10.1016/j.bbi.2017.09.014.

Arroyo, J. D., Jourdain, A. A., Calvo, S. E., Ballarano, C. A., Doench, J. G., Root, D. E., and Mootha, V. K. (2016). A genome-wide CRISPR death screen identifies genes essential for oxidative phosphorylation. *Cell Metabolism*. **24**(6), 875–885. URL https://doi.org/10.1016/j.cmet.2016.08.017.

Arshavsky, Y. I., Beloozerova, I., Orlovsky, G., Panchin, Y. V., and Pavlova, G. (1985). Control of locomotion in marine mollusc *Clione limacina* III. On the origin of locomotory rhythm. *Experimental Brain Research*. **58**(2), 273–284. URL https://doi.org/10.1007/BF00235309.

Arshavsky, Y. I., Deliagina, T., Gamkrelidze, G., Orlovsky, G., Panchin, Y. V., Popova, L., and Shupliakov, O. (1993). Pharmacologically induced elements of the hunting and feeding behavior in the pteropod mollusk *Clione limacina*. I. Effects of GABA. *Journal of Neurophysiology*. **69**(2), 512–521. URL https://doi.org/10.1152/jn.1993.69.2.512.

Aubin-horth, N. and Renn, S. C. (2009). Genomic reaction norms: Using integrative biology to understand molecular mechanisms of phenotypic plasticity. *Molecular Ecology*. **18**(18), 3763–3780. URL https://doi.org/10.1111/j.1365-294X.2009.04313.x.

Aydar, E. and Beadle, D. (1999). The pharmacological profile of GABA receptors on cultured insect neurones. *Journal of Insect Physiology*. **45**(3), 213–219. URL https://doi.org/10.1016/S0022-1910(98)00114-0.

Bai, R., You, W., Chen, J., Huang, H., and Ke, C. (2012). Molecular cloning and expression analysis of $GABA_A$ receptor-associated protein (GABARAP) from small abalone, *Haliotis diversicolor*. *Fish and Shellfish Immunology*. **33**(4), 675–682. URL https://doi.org/10.1016/j.fsi.2012.05.003.

Bai, S. W., Herrera-Abreu, M. T., Rohn, J. L., Racine, V., Tajadura, V., Suryavanshi, N., Bechtel, S., Wiemann, S., Baum, B., and Ridley, A. J. (2011). Identification and characterization of a set of conserved and new regulators of cytoskeletal organization, cell morphology and migration. *BMC Biology*. **9**(1), 54. URL https://doi.org/10.1186/1741-7007-9-54.

Baldridge, R. D. and Rapoport, T. A. (2016). Autoubiquitination of the Hrd1 ligase triggers protein retrotranslocation in ERAD. *Cell*. **166**(2), 394–407. URL https://doi.org/10.1016/j.cell.2016.05.048.

Barragan, A., Weidner, J. M., Jin, Z., Korpi, E., and Birnir, B. (2015). GABAergic signalling in the immune system. *Acta Physiologica*. **213**(4), 819–827. URL https://doi.org/10.1111/apha.12467.

Barry, M. J. (2002). Progress toward understanding the neurophysiological basis of predator-induced morphology in *Daphnia pulex*. *Physiological and Biochemical Zoology*. **75**(2), 179–186. URL https://doi.org/10.1086/339389. pMID: 12024293.

Bas, L., Papinski, D., Licheva, M., Torggler, R., Rohringer, S., Schuschnig, M., and Kraft, C. (2018). Reconstitution reveals Ykt6 as the autophagosomal SNARE in autophagosome–vacuole fusion. *Journal of Cell Biology*. **217**(10), 3656–3669. URL https://doi.org/10.1083/jcb.201804028.

Baumann, H., Wallace, R. B., Tagliaferri, T., and Gobler, C. J. (2015). Large natural pH, CO_2 and O_2 fluctuations in a temperate tidal salt marsh on diel, seasonal, and interannual time scales. *Estuaries and Coasts*. **38**(1), 220–231. URL https://doi.org/10.1007/s12237-014-9800-y.

Beard Jr., R. S. and Bearden, S. E. (2011). Vascular complications of cystathionine β-synthase deficiency: Future directions for homocysteine-to-hydrogen sulfide research. *American Journal of Physiology-Heart and Circulatory Physiology*. **300**(1), H13–H26. URL https://doi.org/10.1152/ajpheart.00598.2010.

Beg, A. A. and Jorgensen, E. M. (2003). EXP-1 is an excitatory GABA-gated cation channel. *Nature neuroscience*. **6**(11), 1145–1152. URL https://doi.org/10.1038/nn1136.

Bellot, M., Faria, M., Gómez-Canela, C., Raldúa, D., and Barata, C. (2021). Pharmacological modulation of behaviour, serotonin and dopamine levels in *Daphnia magna* exposed to the monoamine oxidase inhibitor deprenyl. *Toxics*. **9**(8), 187. URL https://doi.org/10.3390/toxics9080187.

Benítez, S., Lagos, N. A., Osores, S., Opitz, T., Duarte, C., Navarro, J. M., and Lardies, M. A. (2018). High pCO_2 levels affect metabolic rate, but not feeding behavior and fitness, of farmed giant mussel *Choromytilus chorus*. *Aquaculture Environment Interactions*. **10**, 267–278. URL https://doi.org/10.3354/aei00271.

Bertapelle, C., Polese, G., and Di Cosmo, A. (2017). Enriched environment increases PCNA and PARP1 levels in *Octopus vulgaris* central nervous system: First evidence of adult neurogenesis in lophotrochozoa. *Journal of Experimental Zoology Part B: Molecular and Developmental Evolution*. **328**(4), 347–359. URL https://doi.org/10.1002/jez.b.22735.

Bertness, M. D., Gaines, S. D., and Hay, M. E. (2001). *Marine Community Ecology*. Sinauer Associates, Sunderland, Massachusetts.

Betts, R. A. and McNeall, D. (2018). How much CO_2 at 1.5°C and 2°C? *Nature Climate Change*. **8**(7), 546–553. URL https://doi.org/10.1038/s41558-018-0199-5.

Bhatt, S., Nagappa, A. N., and Patil, C. R. (2020). Role of oxidative stress in depression. *Drug Discovery Today*. **25**(7), 1270–1276. URL https://doi.org/10.1016/j.drudis.2020.05.001.

Bibby, R., Cleall-Harding, P., Rundle, S., Widdicombe, S., and Spicer, J. (2007). Ocean acidification disrupts induced defences in the intertidal gastropod *Littorina littorea*. *Biology Letters*. **3**(6), 699–701. URL https://doi.org/10.1098/rsbl.2007.0457.

Bibby, R., Widdicombe, S., Parry, H., Spicer, J., and Pipe, R. (2008). Effects of ocean acidification on the immune response of the blue mussel *Mytilus edulis*. *Aquatic Biology*. **2**(1), 67–74. URL https://doi.org/10.3354/ab00037.

Bignami, S., Enochs, I. C., Manzello, D. P., Sponaugle, S., and Cowen, R. K. (2013). Ocean acidification alters the otoliths of a pantropical fish species with implications for sensory function. *Proceedings of the National Academy of Sciences*. **110**(18), 7366–7370. URL https://doi.org/10.1073/pnas.1301365110.

Bindoff, N. L., Cheung, W. W., Kairo, J. G., Arístegui, J., Guinder, V. A., Hallberg, R., Hilmi, N., Jiao, N., Karim, M. S., Levin, L., O'Donoghue, S., Cuicapusa, S. R. P., Rinkevich, B., Suga, T., Tagliabue, A., and Williamson, P. (2019). Changing ocean, marine ecosystems, and dependent communities. In *IPCC Special Report on the Ocean and Cryosphere in a Changing Climate* (eds. H.O. Pörtner, D. Roberts, V. Masson-Delmotte, P. Zhai, M. Tignor, E. Poloczanska, K. Mintenbeck, A. Alegría, M. Nicolai, A. Okem, J. Petzold, B. Rama, and N. Weyer). pp. 447 – 587. Cambridge University Press, Cambridge, UK and New York, NY, USA. URL https://doi.org/10.1017/9781009157964.007.

BioBam Bioinformatics (2019). OmicsBox - Bioinformatics made easy (Version 1.4.12). URL https://www.biobam.com/omicsbox.

Biscocho, D., Cook, J. G., Long, J., Shah, N., and Leise, E. M. (2018). GABA is an inhibitory neurotransmitter in the neural circuit regulating metamorphosis in a marine snail. *Developmental Neurobiology*. **78**(7), 736–753. URL https://doi.org/10.1002/dneu.22597.

Bisgrove, B. W. and Burke, R. D. (1987). Development of the nervous system of the pluteus larva of *Strongylocentrotus droebachiensis*. *Cell and Tissue Research*. **248**(2), 335–343. URL https://doi.org/10.1007/BF00218200.

Bliss, T. V. P. and Collingridge, G. L. (1993). A synaptic model of memory: Long-term potentiation in the hippocampus. *Nature*. **361**(6407), 31–39. URL https://doi.org/10.1038/361031a0.

Blitz, D. M., Christie, A. E., Coleman, M. J., Norris, B. J., Marder, E., and Nusbaum, M. P. (1999). Different proctolin neurons elicit distinct motor patterns from a multifunctional neuronal network. *Journal of Neuroscience*. **19**(13), 5449–5463. URL https://doi.org/10.1523/JNEUROSCI.19-13-05449.1999.

Blom, F. (1978). Sensory input behavioural output relationships in the feeding activity of some Lepidopterous larvae. *Entomologia Experimentalis et Applicata*. **24**(3), 258–263. URL https://doi.org/10.1111/j.1570-7458.1978.tb02781.x.

Bloomquist, J. R. (2003). Chloride channels as tools for developing selective insecticides. *Archives of Insect Biochemistry and Physiology: Published in Collaboration with the Entomological Society of America*. **54**(4), 145–156. URL https://doi.org/10.1002/arch.10112.

Bordallo, J., Plemper, R. K., Finger, A., and Wolf, D. H. (1998). Der3p/Hrd1p Is required for endoplasmic reticulum-associated degradation of misfolded lumenal and integral membrane proteins. *Molecular Biology of the Cell*. **9**(1), 209–222. URL https://doi.org/10.1091/mbc.9.1.209.

Borges, F. O., Sampaio, E., Figueiredo, C., Rosa, R., and Grilo, T. F. (2018). Hypercapnia-induced disruption of long-distance mate-detection and reduction of energy expenditure in a coastal keystone crustacean. *Physiology and Behavior*. **195**, 69–75. URL https://doi.org/10.1016/j.physbeh.2018.07.023.

Bormann, J., Hamill, O. P., and Sakmann, B. (1987). Mechanism of anion permeation through channels gated by glycine and gamma-aminobutyric acid in mouse cultured spinal neurones. *The Journal of Physiology*. **385**(1), 243–286. URL https://doi.org/10.1113/jphysiol.1987.sp016493.

Boron, W. and Russell, J. (1983). Stoichiometry and ion dependencies of the intracellular-pH-regulating mechanism in squid giant axons. *The Journal of General Physiology*. **81**(3), 373–399. URL https://doi.org/10.1085/jgp.81.3.373.

Boron, W. F. (1977). Intracellular pH transients in giant barnacle muscle fibers. *American Journal of Physiology-Cell Physiology*. **233**(3), C61–C73. URL https://doi.org/10.1152/ajpcell.1977.233.3.C61.

Boron, W. F., McCormick, W. C., and Roos, A. (1981). pH regulation in barnacle muscle fibers: Dependence on extracellular sodium and bicarbonate. *American Journal of Physiology-Cell Physiology*. **240**(1), C80–C89. URL https://doi.org/10.1152/ajpcell.1981.240.1.C80.

Bouayed, J. (2011). Relationship between oxidative stress and anxiety: Emerging role of antioxidants within therapeutic or preventive approaches. In *Anxiety Disorders* (ed. V. Kalinin). pp. 27–38. InTech, Rijeka, Croatia.

Bouayed, J., Rammal, H., and Soulimani, R. (2009). Oxidative stress and anxiety: Relationship and cellular pathways. *Oxidative Medicine and Cellular Longevity*. **2**, 623654. URL https://doi.org/10.4161/oxim.2.2.7944.

Bouayed, J. and Soulimani, R. (2019). Evidence that hydrogen peroxide, a component of oxidative stress, induces high-anxiety-related behaviour in mice. *Behavioural Brain Research*. **359**, 292–297. URL https://doi.org/10.1016/j.bbr.2018.11.009.

Boyd, P. W., Collins, S., Dupont, S., Fabricius, K., Gattuso, J.-P., Havenhand, J., Hutchins, D. A., Riebesell, U., Rintoul, M. S., Vichi, M., Biswas, H., Ciotti, A., Gao, K., Gehlen, M., Hurd, C. L., Kurihara, H., McGraw, C. M., Navarro, J. M., Nilsson, G. E., Passow, U., and Pörtner, H.-O. (2018). Experimental strategies to assess the biological ramifications of multiple drivers of global ocean change—A review. *Global Change Biology*. **24**(6), 2239–2261. URL https://doi.org/10.1111/gcb.14102.

Branco, R. C., Burkett, J. P., Black, C. A., Winokur, E., Ellsworth, W., Dhamsania, R. K., Lohr, K. M., Schroeder, J. P., Weinshenker, D., Jovanovic, T., and Miller, G. W. (2020). Vesicular monoamine transporter 2 mediates fear behavior in mice. *Genes, Brain and Behavior*. **19**(5), e12634. URL https://doi.org/10.1111/gbb.12634.

Bressan, C. and Saghatelyan, A. (2021). Intrinsic mechanisms regulating neuronal migration in the postnatal brain. *Frontiers in Cellular Neuroscience*. **14**(462). URL https://doi.org/10.3389/fncel.2020.620379.

Brian, H. and Papanicolaou, A. (n.d.). Transdecoder (find coding regions within transcripts). URL http://transdecoder.github.io.

Briffa, M., de la Haye, K., and Munday, P. L. (2012). High CO_2 and marine animal behaviour: Potential mechanisms and ecological consequences. *Marine Pollution Bulletin*. **64**(8), 1519–1528. URL https://doi.org/10.1016/j.marpolbul.2012.05.032.

Brown, A. G. (2001). The nervous system and the internal and external environments — homeostasis and interactions. In *Nerve Cells and Nervous Systems: An Introduction to Neuroscience* (ed. A.G. Brown). pp. 197–213. Springer, London. URL https://doi.org/10.1007/978-1-4471-0237-3_15.

Brown, G. E., Adrian, Jr, J. C., Lewis, M. G., and Tower, J. M. (2002). The effects of reduced pH on chemical alarm signalling in ostariophysan fishes. *Canadian Journal of Fisheries and Aquatic Sciences*. **59**(8), 1331–1338. URL https://doi.org/10.1139/f02-104.

Bürkner, P.-C. (2017). brms: An R package for Bayesian multilevel models using Stan. *Journal of Statistical Software*. **80**(1), 1–28. URL https://doi.org/10.18637/jss.v080.i01.

Buscaino, G., Filiciotto, F., Gristina, M., Bellante, A., Buffa, G., Di Stefano, V., Maccarrone, V., Tranchida, G., Buscaino, C., and Mazzola, S. (2011). Acoustic behaviour of the European spiny lobster *Palinurus elephas*. *Marine Ecology Progress Series*. **441**, 177–184. URL https://doi.org/10.3354/meps09404.

Butt, A. M. and Jennings, J. (1994). Response of astrocytes to γ-aminobutyric acid in the neonatal rat optic nerve. *Neuroscience Letters*. **168**(1-2), 53–56. URL https://doi.org/10.1016/0304-3940(94)90414-6.

Camacho, C., Coulouris, G., Avagyan, V., Ma, N., Papadopoulos, J., Bealer, K., and Madden, T. L. (2009). BLAST+: Architecture and applications. *BMC Bioinformatics*. **10**(1), 1–9. URL https://doi.org/10.1186/1471-2105-10-421.

Cameron, H. A. (2006). Quantitative analysis of *in vivo* cell proliferation. *Current Protocols in Neuroscience*. **37**(1), 3.9.1–3.9.15. URL https://doi.org/10.1002/N0471142301.ns0309s37.

Cameron, J. N. (1985). Compensation of hypercapnic acidosis in the aquatic blue crab, *Callinectes sapidus*: The predominance of external sea water over carapace carbonate as the proton sink. *Journal of Experimental Biology*. **114**(1), 197–206. URL https://doi.org/10.1242/jeb.114.1.197.

Cameron, J. N. and Iwama, G. K. (1987). Compensation of progressive hypercapnia in channel catfish and blue crabs. *Journal of Experimental Biology*. **133**(1), 183–197. URL https://doi.org/10.1242/jeb.133.1.183.

Campanati, C., Yip, S., Lane, A., and Thiyagarajan, V. (2015). Combined effects of low pH and low oxygen on the early-life stages of the barnacle *Balanus amphitrite*. *ICES Journal of Marine Science*. **73**(3), 791–802. URL https://doi.org/10.1093/icesjms/fsv221.

Canesi, L., Betti, M., Ciacci, C., Lorusso, L., Pruzzo, C., and Gallo, G. (2006). Cell signalling in the immune response of mussel hemocytes. *Invertebrate Survival Journal*. **3**(1), 40–49.

Cao, R., Liu, Y., Wang, Q., Zhang, Q., Yang, D., Liu, H., Qu, Y., and Zhao, J. (2018a). The impact of ocean acidification and cadmium on the immune responses of Pacific oyster, *Crassostrea gigas*. *Fish and Shellfish Immunology*. **81**, 456–462. URL https://doi.org/10.1016/j.fsi.2018.07.055.

Cao, R., Wang, Q., Yang, D., Liu, Y., Ran, W., Qu, Y., Wu, H., Cong, M., Li, F., Ji, C., and Zhao, J. (2018b). CO_2-induced ocean acidification impairs the immune function of the Pacific oyster against *Vibrio splendidus* challenge: An integrated study from a cellular and proteomic perspective. *Science of The Total Environment*. **625**, 1574–1583. URL https://doi.org/10.1016/j.scitotenv.2018.01.056.

Carey, N., Harianto, J., and Byrne, M. (2016). Sea urchins in a high-CO_2 world: Partitioned effects of body size, ocean warming and acidification on metabolic rate. *Journal of Experimental Biology*. **219**(8), 1178–1186. URL https://doi.org/10.1242/jeb.136101.

Carpenter, D., Swann, J., and Yarowsky, P. (1977). Effect of curare on responses to different putative neurotransmitters in *Aplysia* neurons. *Journal of Neurobiology*. **8**(2), 119–132. URL https://doi.org/10.1002/neu.480080204.

Carvalho, P., Goder, V., and Rapoport, T. A. (2006). Distinct ubiquitin-ligase complexes define convergent pathways for the degradation of ER proteins. *Cell*. **126**(2), 361–373. URL https://doi.org/10.1016/j.cell.2006.05.043.

Cases, O., Seif, I., Grimsby, J., Gaspar, P., Chen, K., Pournin, S., Müller, U., Aguet, M., Babinet, C., Shih, J. C., and De Maeyer, E. (1995). Aggressive behavior and altered amounts of brain serotonin and norepinephrine in mice lacking MAOA. *Science*. **268**(5218), 1763–1766. URL https://doi.org/10.1126/science.7792602.

Castillo, M. G., Salazar, K. A., and Joffe, N. R. (2015). The immune response of cephalopods from head to foot. *Fish and Shellfish Immunology*. **46**(1), 145–160. URL https://doi.org/10.1016/j.fsi.2015.05.029.

Castillo, N., Saavedra, L. M., Vargas, C. A., Gallardo-Escárate, C., and Détrée, C. (2017). Ocean acidification and pathogen exposure modulate the immune response of the edible mussel *Mytilus chilensis*. *Fish and Shellfish Immunology*. **70**, 149–155. URL https://doi.org/10.1016/j.fsi.2017.08.047.

Catterall, W. A. (2021). Membrane transport | The ion channel protein superfamily. In *Encyclopedia of Biological Chemistry III (Third Edition)* (ed. J. Jez). pp. 880–885. Elsevier, Oxford. URL https://doi.org/10.1016/B978-0-12-809633-8.21567-7.

Cayre, M., Malaterre, J., Scotto-Lomassese, S., Strambi, C., and Strambi, A. (2002). The common properties of neurogenesis in the adult brain: From invertebrates to vertebrates. *Comparative Biochemistry and Physiology Part B: Biochemistry and Molecular Biology*. **132**(1), 1–15. URL https://doi.org/10.1016/S1096-4959(01)00525-5.

Chakrabarty, A. (1998). Nucleoside diphosphate kinase: Role in bacterial growth, virulence, cell signalling and polysaccharide synthesis. *Molecular Microbiology*. **28**(5), 875–882. URL https://doi.org/10.1046/j.1365-2958.1998.00846.x.

Chan, K. Y. K., Grünbaum, D., and O'Donnell, M. J. (2011). Effects of ocean-acidification-induced morphological changes on larval swimming and feeding. *Journal of Experimental Biology*. **214**(22), 3857–3867. URL https://doi.org/10.1242/jeb.054809.

Chan, S. K. N., Suresh, S., Munday, P., Ravasi, T., Bernal, M. A., and Schunter, C. (2022). The alternative splicing landscape of a coral reef fish during a marine heatwave. *Ecology and Evolution*. **12**(3), e8738. URL https://doi.org/10.1002/ece3.8738.

Charpentier, C. L. and Cohen, J. H. (2016). Acidification and γ-aminobutyric acid independently alter kairomone-induced behaviour. *Open Science*. **3**(9), 160311. URL https://doi.org/10.1098/rsos.160311.

Chartier, F. J.-M., Hardy, É. J.-L., and Laprise, P. (2012). Crumbs limits oxidase-dependent signaling to maintain epithelial integrity and prevent photoreceptor cell death. *Journal of Cell Biology*. **198**(6), 991–998. URL https://doi.org/10.1083/jcb.201203083.

Chatzinikolaou, E., Grigoriou, P., Martini, E., and Sterioti, A. (2019). Impact of ocean acidification and warming on the feeding behaviour of two gastropod species. *Mediterranean Marine Science*. URL https://doi.org/10.12681/mms.19187.

Chen, E. Y.-S. (2021). Often overlooked: Understanding and meeting the current challenges of marine invertebrate conservation. *Frontiers in Marine Science*. **8**(1161), 690704. URL https://doi.org/10.3389/fmars.2021.690704.

Chen, H.-B., Wu, W.-N., Wang, W., Gu, X.-H., Yu, B., Wei, B., and Yang, Y.-J. (2017). Cystathionine-β-synthase-derived hydrogen sulfide is required for amygdalar long-term potentiation and cued fear memory in rats. *Pharmacology Biochemistry and Behavior*. **155**, 16–23. URL https://doi.org/10.1016/j.pbb.2017.03.002.

Chen, S., Zhou, Y., Chen, Y., and Gu, J. (2018). fastp: An ultra-fast all-in-one FASTQ preprocessor. *Bioinformatics*. **34**(17), i884–i890. URL https://doi.org/10.1093/bioinformatics/bty560.

Chichery, R. and Chichery, M.-P. (1985). Motor and behavioural effects induced by putative neurotransmitter injection into the optic lobe of the cuttlefish, *Sepia officinalis*. *Comparative Biochemistry and Physiology Part C: Comparative Pharmacology*. **80**(2), 415–419. URL https://doi.org/10.1016/0742-8413(85)90078-7.

Chivers, D. P., McCormick, M. I., Nilsson, G. E., Munday, P. L., Watson, S.-A., Meekan, M. G., Mitchell, M. D., Corkill, K. C., and Ferrari, M. C. (2014). Impaired learning of predators and lower prey survival under elevated CO_2: A consequence of neurotransmitter interference. *Global Change Biology*. **20**(2), 515–522. URL https://doi.org/10.1111/gcb.12291.

Chow, W. N. V., Cheung, H. N. M., Li, W., and Lau, K.-F. (2015). FE65: Roles beyond amyloid precursor protein processing. *Cellular and Molecular Biology Letters*. **20**(1), 66–87. URL https://doi.org/10.1515/cmble-2015-0002.

Chu, C.-H. and Cheng, D. (2007). Expression, purification, characterization of human 3-methylcrotonyl-CoA carboxylase (MCCC). *Protein Expression and Purification*. **53**(2), 421–427. URL https://doi.org/10.1016/j.pep.2007.01.012.

Chuang, H.-C., Wang, X., and Tan, T.-H. (2016). MAP4K family kinases in immunity and inflammation. In *Advances in Immunology* (ed. F.W. Alt). pp. 277–314. Academic Press. URL https://doi.org/10.1016/bs.ai.2015.09.006.

Chung, W.-S., Kurniawan, N. D., and Marshall, N. J. (2022). Comparative brain structure and visual processing in octopus from different habitats. *Current Biology*. **32**(1), 97–110.e4. URL https://doi.org/10.1016/j.cub.2021.10.070.

Chung, W.-S., Marshall, N. J., Watson, S.-A., Munday, P. L., and Nilsson, G. E. (2014). Ocean acidification slows retinal function in a damselfish through interference with $GABA_A$ receptors. *Journal of Experimental Biology*. **217**(3), 323–326. URL https://doi.org/10.1242/jeb.092478.

Citri, A. and Malenka, R. C. (2008). Synaptic plasticity: Multiple forms, functions, and mechanisms. *Neuropsychopharmacology*. **33**(1), 18–41. URL https://doi.org/10.1038/sj.npp.1301559.

Clark, M. S., Suckling, C. C., Cavallo, A., Mackenzie, C. L., Thorne, M. A., Davies, A. J., and Peck, L. S. (2019). Molecular mechanisms underpinning transgenerational plasticity in the green sea urchin *Psammechinus miliaris*. *Scientific Reports*. **9**(1), 952. URL https://doi.org/10.1038/s41598-018-37255-6.

Clarke, M. R. (1978). The cephalopod statolithan-introduction to its form. *Journal of the Marine Biological Association of the United Kingdom*. **58**(3), 701–712. URL https://doi.org/10.1017/S0025315400041345.

Clavero-Salas, A., Sotelo-Mundo, R. R., Gollas-Galván, T., Hernández-López, J., Peregrino-Uriarte, A. B., Muhlia-Almazán, A., and Yepiz-Plascencia, G. (2007). Transcriptome analysis of gills from the white shrimp *Litopenaeus vannamei* infected with white spot syndrome virus. *Fish and Shellfish Immunology*. **23**(2), 459–472. URL https://doi.org/10.1016/j.fsi.2007.01.010.

Clements, J. C., Bishop, M. M., and Hunt, H. L. (2017). Elevated temperature has adverse effects on GABA-mediated avoidance behaviour to sediment acidification in a wide-ranging marine bivalve. *Marine Biology*. **164**(3), 56. URL https://doi.org/10.1007/s00227-017-3085-1.

Clements, J. C. and Hunt, H. L. (2014). Influence of sediment acidification and water flow on sediment acceptance and dispersal of juvenile soft-shell clams (*Mya arenaria* L.). *Journal of Experimental Marine Biology and Ecology*. **453**, 62–69. URL https://doi.org/10.1016/j.jembe.2014.01.002.

Clements, J. C. and Hunt, H. L. (2015). Marine animal behaviour in a high CO_2 ocean. *Marine Ecology Progress Series*. **536**, 259–279. URL https://doi.org/10.3354/meps11426.

Clements, J. C., Ramesh, K., Nysveen, J., Dupont, S., and Jutfelt, F. (2021). Animal size and sea water temperature, but not pH, influence a repeatable startle response behaviour in a wide-ranging marine mollusc. *Animal Behaviour*. **173**, 191–205. URL https://doi.org/10.1016/j.anbehav.2020.12.008.

Clements, J. C., Woodard, K. D., and Hunt, H. L. (2016). Porewater acidification alters the burrowing behavior and post-settlement dispersal of juvenile soft-shell clams (*Mya arenaria*). *Journal of Experimental Marine Biology and Ecology*. **477**, 103–111. URL https://doi.org/10.1016/j.jembe.2016.01.013.

Cohen, M. (1960). The response patterns of single receptors in the crustacean statocyst. *Proceedings of the Royal Society of London. Series B. Biological Sciences*. **152**(946), 30–49. URL https://doi.org/10.1098/rspb.1960.0020.

Collins, M., Knutti, R., Arblaster, J., Dufresne, J.-L., Fichefet, T., Friedlingstein, P., Gao, X., Gutowski, W. J., Johns, T., and Krinner, G. (2013). Long-term climate change: Projections, commitments and irreversibility. In *Climate Change 2013: The Physical Science Basis. Contribution of Working Wroup I to the Fifth Assessment Report of the Intergovernmental Panel on Climate Change* (eds. T. Stocker, D. Qin, G.K. Plattner, M. Tignor, S. Allen, J. Boschung, A. Nauels, Y. Xia, V. Bex, and P. Midgley). pp. 1029–1136. Cambridge University Press, Cambridge, United Kingdom and New York, NY, USA.

Concas, A., Pierobon, P., Mostallino, M., Marino, G., Minei, R., and Biggio, G. (1998). Modulation of γ-aminobutyric acid GABA receptors and the feeding response by neurosteroids in *Hydra vulgaris*. *Neuroscience*. **85**(3), 979–988. URL https://doi.org/10.1016/S0306-4522(97)00515-0.

Conti, L., Limon, A., Palma, E., and Miledi, R. (2013). Microtransplantation of cellular membranes from squid stellate ganglion reveals ionotropic GABA receptors. *The Biological Bulletin*. **224**(1), 47–52. URL https://doi.org/10.1086/BBLv224n1p47.

Cooke, S. J., Sack, L., Franklin, C. E., Farrell, A. P., Beardall, J., Wikelski, M., and Chown, S. L. (2013). What is conservation physiology? Perspectives on an increasingly integrated and essential science. *Conservation Physiology*. **1**(1), cot001. URL https://doi.org/10.1093/conphys/cot001.

Cornet, V., Henry, J., Corre, E., Le Corguille, G., Zanuttini, B., and Zatylny-Gaudin, C. (2014). Dual role of the cuttlefish salivary proteome in defense and predation. *Journal of Proteomics*. **108**, 209–222. URL https://doi.org/10.1016/j.jprot.2014.05.019.

Costa, R. A., Olvera, A., Power, D. M., and Velez, Z. (2022a). Ocean acidification affects the expression of neuroplasticity and neuromodulation markers in seabream. *Biology Open*. **11**(3), bio059073. URL https://doi.org/10.1242/bio.059073.

Costa, R. A., Velez, Z., and Hubbard, P. C. (2022b). GABA receptors in the olfactory epithelium of the gilthead seabream (*Sparus aurata*). *Journal of Experimental Biology*. URL https://doi.org/10.1242/jeb.243112.

Crabbe, J. C., Wahlsten, D., and Dudek, B. C. (1999). Genetics of mouse behavior: Interactions with laboratory environment. *Science*. **284**(5420), 1670–1672. URL https://doi.org/10.1126/science.284.5420.1670.

Crider, A., Pandya, C. D., Peter, D., Ahmed, A. O., and Pillai, A. (2014). Ubiquitin-proteasome dependent degradation of $GABA_A$α1 in autism spectrum disorder. *Molecular Autism*. **5**(1), 45. URL https://doi.org/10.1186/2040-2392-5-45.

Cserr, H. F. and Bundgaard, M. (1984). Blood-brain interfaces in vertebrates: A comparative approach. *American Journal of Physiology-Regulatory, Integrative and Comparative Physiology*. **246**(3), R277–R288. URL https://doi.org/10.1152/ajpregu.1984.246.3.R277.

Cuddy, L. K., Wani, W. Y., Morella, M. L., Pitcairn, C., Tsutsumi, K., Fredriksen, K., Justman, C. J., Grammatopoulos, T. N., Belur, N. R., Zunke, F., Subramanian, A.,

Affaneh, A., Lansbury, Peter T., J., and Mazzulli, J. R. (2019). Stress-induced cellular clearance is mediated by the SNARE protein ykt6 and disrupted by α-synuclein. *Neuron*. **104**(5), 869–884.e11. URL https://doi.org/10.1016/j.neuron.2019.09.001.

Culler-Juarez, M. E. and Onthank, K. L. (2021). Elevated immune response in *Octopus rubescens* under ocean acidification and warming conditions. *Marine Biology*. **168**(9), 137. URL https://doi.org/10.1007/s00227-021-03913-z.

Dani, J. A. (2015). Neuronal nicotinic acetylcholine receptor structure and function and response to nicotine. In *International Review of Neurobiology* (ed. M. De Biasi). pp. 3–19. Academic Press. URL https://doi.org/10.1016/bs.irn.2015.07.001.

Danqing, F., Ying, H., Caihuan, K., Shiqiang, Z., and Shaojing, L. (2006). Settlement and metamorphosis of *Styela canopus* savigny larvae in response to some neurotransmitters and thyroxin. *Acta Oceanologica Sinica*. **25**(3), 90–97.

Dantzer, R. and Kelley, K. W. (2007). Twenty years of research on cytokine-induced sickness behavior. *Brain, Behavior, and Immunity*. **21**(2), 153–160. URL https://doi.org/10.1016/j.bbi.2006.09.006.

Davidson, N. M. and Oshlack, A. (2014). Corset: Enabling differential gene expression analysis for *de novo* assembled transcriptomes. *Genome Biology*. **15**(7), 1–14. URL https://doi.org/10.1186/s13059-014-0410-6.

De Zoysa, M., Nikapitiya, C., Oh, C., Whang, I., Lee, J.-S., Jung, S.-J., Choi, C. Y., and Lee, J. (2010). Molecular evidence for the existence of lipopolysaccharide-induced TNF-α factor (LITAF) and Rel/NF-KB pathways in disk abalone (*Haliotis discus discus*). *Fish and Shellfish Immunology*. **28**(5), 754–763. URL https://doi.org/10.1016/j.fsi.2010.01.024.

Dean, J. B. (2010). Hypercapnia causes cellular oxidation and nitrosation in addition to acidosis: Implications for CO_2 chemoreceptor function and dysfunction. *Journal of Applied Physiology*. **108**(6), 1786–1795. URL https://doi.org/10.1152/japplphysiol.01337.2009.

DeFeudis, F. (1975). Amino acids as central neurotransmitters. *Annual Review of Pharmacology*. **15**(1), 105–130.

Deitmer, J. W. and Rose, C. R. (1996). pH regulation and proton signalling by glial cells. *Progress in Neurobiology*. **48**(2), 73–103. URL https://doi.org/10.1016/0301-0082(95)00039-9.

Demas, G. E., Adamo, S. A., and French, S. S. (2011). Neuroendocrine-immune crosstalk in vertebrates and invertebrates: Implications for host defence. *Functional Ecology*. **25**(1), 29–39. URL https://doi.org/10.1111/j.1365-2435.2010.01738.x.

Dent, J. A. (2010). The evolution of pentameric ligand-gated ion channels. In *Insect Nicotinic Acetylcholine Receptors* (ed. S.H. Thany). Advances in Experimental Medicine and Biology. pp. 11–23. Springer-Verlag, New York. URL https://doi.org/10.1007/978-1-4419-6445-8_2.

Depaulis, A. and Vergnes, M. (1985). Elicitation of conspecific attack or defense in the male rat by intraventricular injection of a GABA agonist or antagonist. *Physiology anbehavior*. **35**(3), 447–453. URL https://doi.org/10.1016/0031-9384(85)90322-1.

Di, G., Li, Y., Zhu, G., Guo, X., Li, H., Huang, M., Shen, M., and Ke, C. (2019). Effects of acidification on the proteome during early development of *Babylonia areolata*. *FEBS Open Bio*. URL https://doi.org/10.1002/2211-5463.12695.

Di Cosmo, A., Di Cristo, C., and Messenger, J. (2006). L-glutamate and its ionotropic receptors in the nervous system of cephalopods. *Current Neuropharmacology*. **4**(4), 305–312. URL https://doi.org/10.2174/157015906778520809.

Diao, Q., Sun, L., Zheng, H., Zeng, Z., Wang, S., Xu, S., Zheng, H., Chen, Y., Shi, Y., Wang, Y., Meng, F., Sang, Q., Cao, L., Liu, F., Zhu, Y., Li, W., Li, Z., Dai, C., Yang, M., Chen, S., Chen, R., Zhang, S., Evans, J. D., Huang, Q., Liu, J., Hu, F., Su, S., and Wu, J. (2018). Genomic and transcriptomic analysis of the Asian honeybee *Apis cerana* provides novel insights into honeybee biology. *Scientific Reports*. **8**(1), 822. URL https://doi.org/10.1038/s41598-017-17338-6.

Díaz-Ríos, M. and Miller, M. W. (2005). Rapid dopaminergic signaling by interneurons that contain markers for catecholamines and GABA in the feeding circuitry of *Aplysia*. *Journal of Neurophysiology*. **93**(4), 2142–2156. URL https://doi.org/10.1152/jn.00003.2004.

Díaz-Ríos, M., Oyola, E., and Miller, M. W. (2002). Colocalization of γ-aminobutyric acid-like immunoreactivity and catecholamines in the feeding network of aplysia *californica*. *Journal of Comparative Neurology*. **445**(1), 29–46. URL https://doi.org/10.1002/cne.10152.

Dibas, M. I., Gonzales, E. B., Das, P., Bell-Horner, C. L., and Dillon, G. H. (2002). Identification of a novel residue within the second transmembrane domain that confers

use-facilitated block by picrotoxin in glycine α1 receptors. *Journal of Biological Chemistry*. **277**(11), 9112–9117. URL https://www.jbc.org/article/S0021-9258(19)36277-5/pdf.

Dickson, A. and Millero, F. J. (1987). A comparison of the equilibrium constants for the dissociation of carbonic acid in seawater media. *Deep Sea Research Part A. Oceanographic Research Papers*. **34**(10), 1733–1743. URL https://doi.org/10.1016/0198-0149(87)90021-5.

Dickson, A. G., Sabine, C. L., and Christian, J. R. (2007). *Guide to Best Practices for Ocean CO_2 Measurements. PICES Special Publication 3*. North Pacific Marine Science Organization, Sidney, Canada. URL https://doi.org/10.25607/OBP-1342.

Dineshram, R., Thiyagarajan, V., Lane, A., Ziniu, Y., Xiao, S., and Leung, P. T. (2013). Elevated CO_2 alters larval proteome and its phosphorylation status in the commercial oyster, *Crassostrea hongkongensis*. *Marine Biology*. **160**(8), 2189–2205. URL https://doi.org/10.1007/s00227-013-2176-x.

Dineshram, R., Wong, K. K., Xiao, S., Yu, Z., Qian, P. Y., and Thiyagarajan, V. (2012). Analysis of pacific oyster larval proteome and its response to high-CO_2. *Marine Pollution Bulletin*. **64**(10), 2160–2167. URL https://doi.org/10.1016/j.marpolbul.2012.07.043.

Dissanayake, A., Clough, R., Spicer, J., and Jones, M. (2010). Effects of hypercapnia on acid–base balance and osmo-/iono-regulation in prawns (Decapoda: Palaemonidae). *Aquatic Biology*. **11**(1), 27–36. URL https://doi.org/10.3354/ab00285.

Dissanayake, A. and Ishimatsu, A. (2011). Synergistic effects of elevated CO_2 and temperature on the metabolic scope and activity in a shallow-water coastal decapod (*Metapenaeus joyneri*; Crustacea: Penaeidae). *ICES Journal of Marine Science*. **68**(6), 1147–1154. URL https://doi.org/10.1093/icesjms/fsq188.

Dlugokencky, E. and Tans, P. (2019). Trends in atmospheric carbon dioxide. URL https://www.esrl.noaa.gov/gmd/ccgg/trends/global.html.

Domenici, P., Torres, R., and Manríquez, P. H. (2017). Effects of elevated carbon dioxide and temperature on locomotion and the repeatability of lateralization in a keystone marine mollusc. *Journal of Experimental Biology*. **220**(4), 667–676. URL https://doi.org/10.1242/jeb.151779.

Doney, S. C., Fabry, V. J., Feely, R. A., and Kleypas, J. A. (2009). Ocean acidification: The other CO_2 problem. *Annual Review of Marine Science*. **1**, 169–192. URL https://doi.org/10.1146/annurev.marine.010908.163834.

Doropoulos, C., Ward, S., Diaz-Pulido, G., Hoegh-Guldberg, O., and Mumby, P. J. (2012). Ocean acidification reduces coral recruitment by disrupting intimate larval-algal settlement interactions. *Ecology Letters*. **15**(4), 338–346. URL https://doi.org/10.1111/j.1461-0248.2012.01743.x.

Draper, A. M. and Weissburg, M. (2019). Impacts of global warming and elevated CO_2 on sensory behavior in predator-prey interactions: A review and synthesis. *Frontiers in Ecology and Evolution*. **7**, 72. URL https://doi.org/10.3389/fevo.2019.00072.

Duan, Y., Li, J., Zhang, Z., Li, J., Ge, Q., and Liu, P. (2015). The role of oncoprotein NM23 gene from *Exopalaemon carinicauda* is response to pathogens challenge and ammonia-N stress. *Fish and Shellfish Immunology*. **47**(2), 1067–1074. URL https://doi.org/10.1016/j.fsi.2015.08.018.

Duittoz, A. and Martin, R. (1991). Effects of the arylaminopyridazine-GABA derivatives, sr95103 and SR95531 on the Ascaris muscle GABA receptor: The relative potency of the antagonists in Ascaris is different to that at vertebrate $GABA_A$ receptors. *Comparative Biochemistry and Physiology Part C: Comparative Pharmacology*. **98**(2-3), 417–422. URL https://doi.org/10.1016/0742-8413(91)90227-K.

Einat, H. and Belmaker, R. H. (2001). The effects of inositol treatment in animal models of psychiatric disorders. *Journal of Affective Disorders*. **62**(1), 113–121. URL https://doi.org/10.1016/S0165-0327(00)00355-4.

El Manira, A. and Clarac, F. (1991). GABA-mediated presynaptic inhibition in crayfish primary afferents by non-A, non-B GABA receptors. *European Journal of Neuroscience*. **3**(12), 1208–1218. URL https://doi.org/10.1111/j.1460-9568.1991.tb00055.x.

Ellis, R. P., Bersey, J., Rundle, S. D., Hall-Spencer, J. M., and Spicer, J. I. (2009). Subtle but significant effects of CO_2 acidified seawater on embryos of the intertidal snail, *Littorina obtusata*. *Aquatic Biology*. **5**(1), 41–48. URL https://doi.org/10.3354/ab00118.

Ellis, R. P., Davison, W., Queirós, A. M., Kroeker, K. J., Calosi, P., Dupont, S., Spicer, J. I., Wilson, R. W., Widdicombe, S., and Urbina, M. A. (2017). Does sex really matter? Explaining intraspecies variation in ocean acidification responses. *Biology Letters*. **13**(2), 20160761. URL https://doi.org/10.1098/rsbl.2016.0761.

Ertl, N. G., O'Connor, W. A., Wiegand, A. N., and Elizur, A. (2016). Molecular analysis of the Sydney rock oyster (*Saccostrea glomerata*) CO_2 stress response. *Climate Change Responses*. **3**(1), 6. URL https://doi.org/10.1186/s40665-016-0019-y.

Esquerdo-Barragán, M., Brooks, M. J., Toulis, V., Swaroop, A., and Marfany, G. (2019). Expression of deubiquitinating enzyme genes in the developing mammal retina. *Molecular Vision*. **25**, 800–813. URL http://www.molvis.org/molvis/v25/800/.

Evans, J. D. (1996). *Straightforward Statistics for the Behavioral Sciences*. Thomson Brooks/Cole Publishing Co.

Evans, T. G., Chan, F., Menge, B. A., and Hofmann, G. E. (2013). Transcriptomic responses to ocean acidification in larval sea urchins from a naturally variable pH environment. *Molecular Ecology*. **22**(6), 1609–1625. URL https://doi.org/10.1111/mec.12188.

Ewels, P., Magnusson, M., Lundin, S., and Käller, M. (2016). MultiQC: Summarize analysis results for multiple tools and samples in a single report. *Bioinformatics*. **32**(19), 3047–3048. URL https://doi.org/10.1093/bioinformatics/btw354.

Fabricius, K. E., Noonan, S. H., Abrego, D., Harrington, L., and De'ath, G. (2017). Low recruitment due to altered settlement substrata as primary constraint for coral communities under ocean acidification. *Proceedings of the Royal Society B: Biological Sciences*. **284**(1862), 20171536. URL https://doi.org/10.1098/rspb.2017.1536.

Fabry, V. J., Seibel, B. A., Feely, R. A., and Orr, J. C. (2008). Impacts of ocean acidification on marine fauna and ecosystem processes. *ICES Journal of Marine Science*. **65**(3), 414–432. URL https://doi.org/10.1093/icesjms/fsn048.

Farrant, M. and Kaila, K. (2007). The cellular, molecular and ionic basis of $GABA_A$ receptor signalling. *Progress in Brain Research*. **160**, 59–87. URL https://doi.org/10.1016/S0079-6123(06)60005-8.

Feely, R. A., Sabine, C. L., Hernandez-Ayon, J. M., Ianson, D., and Hales, B. (2008). Evidence for upwelling of corrosive "acidified" water onto the continental shelf. *Science*. **320**(5882), 1490–1492. URL https://doi.org/10.1126/science.1155676.

Feely, R. A., Sabine, C. L., Lee, K., Berelson, W., Kleypas, J., Fabry, V. J., and Millero, F. J. (2004). Impact of anthropogenic CO_2 on the $CaCO_3$ system in the oceans. *Science*. **305**(5682), 362–366. URL https://doi.org/10.1126/science.1097329.

Feigenspan, A. and Bormann, J. (1994). Differential pharmacology of $GABA_A$ and $GABA_C$ receptors on rat retinal bipolar cells. *European Journal of Pharmacology: Molecular Pharmacology*. **288**(1), 97–104. URL https://doi.org/10.1016/0922-4106(94)90014-0.

Fonseca, J., Laranjeiro, F., Freitas, D., Oliveira, I., Rocha, R., Machado, J., Hinzmann, M., Barroso, C., and Galante-Oliveira, S. (2020). Impairment of swimming performance in *Tritia reticulata* (L.) veligers under projected ocean acidification and warming scenarios. *Science of The Total Environment*. **731**, 139187. URL https://doi.org/10.1016/j.scitotenv.2020.139187.

Foster, T., Gilmour, J., Chua, C., Falter, J., and McCulloch, M. (2015). Effect of ocean warming and acidification on the early life stages of subtropical *Acropora spicifera*. *Coral Reefs*. **34**(4), 1217–1226. URL https://doi.org/10.1007/s00338-015-1342-7.

Fraser, D. D., Mudrick-Donnon, L. A., and Macvicar, B. A. (1994). Astrocytic GABA receptors. *Glia*. **11**(2), 83–93. URL https://doi.org/10.1002/glia.440110203.

Froehlich, K. R. and Lord, J. P. (2020). Can ocean acidification interfere with the ability of mud snails (*Tritia obsoleta*) to sense predators? *Journal of Experimental Marine Biology and Ecology*. **526**, 151355. URL https://doi.org/10.1016/j.jembe.2020.151355.

Frommel, A. Y., Maneja, R., Lowe, D., Malzahn, A. M., Geffen, A. J., Folkvord, A., Piatkowski, U., Reusch, T. B. H., and Clemmesen, C. (2012). Severe tissue damage in atlantic cod larvae under increasing ocean acidification. *Nature Climate Change*. **2**(1), 42–46. URL https://doi.org/10.1038/nclimate1324.

Frommel, A. Y., Margulies, D., Wexler, J. B., Stein, M. S., Scholey, V. P., Williamson, J. E., Bromhead, D., Nicol, S., and Havenhand, J. (2016). Ocean acidification has lethal and sub-lethal effects on larval development of yellowfin tuna, *Thunnus albacares*. *Journal of Experimental Marine Biology and Ecology*. **482**, 18–24. URL https://doi.org/10.1016/j.jembe.2016.04.008.

Fu, L., Niu, B., Zhu, Z., Wu, S., and Li, W. (2012). CD-HIT: Accelerated for clustering the next-generation sequencing data. *Bioinformatics*. **28**(23), 3150–3152. URL https://doi.org/10.1093/bioinformatics/bts565.

Fuchs, E. and Flügge, G. (2014). Adult neuroplasticity: More than 40 years of research. *Neural Plasticity*. **2014**, 541870. URL https://doi.org/10.1155/2014/541870.

Fuess, L. E., Pinzón C, J. H., Weil, E., and Mydlarz, L. D. (2016). Associations between transcriptional changes and protein phenotypes provide insights into immune regulation in corals. *Developmental and Comparative Immunology*. **62**, 17–28. URL https://doi.org/10.1016/j.dci.2016.04.017.

Fukui, M., Rodriguiz, R. M., Zhou, J., Jiang, S. X., Phillips, L. E., Caron, M. G., and Wetsel, W. C. (2007). Vmat2 heterozygous mutant mice display a depressive-like phenotype. *The Journal of Neuroscience*. **27**(39), 10520–10529. URL https://doi.org/10.1523/jneurosci.4388-06.2007.

Fuller, A., Dawson, T., Helmuth, B., Hetem, R., Mitchell, D., and Maloney, S. (2010). Physiological mechanisms in coping with climate change. *Physiological and Biochemical Zoology*. **83**(5), 713–720. URL https://doi.org/10.1086/652242.

Fuller, T. F., Ghazalpour, A., Aten, J. E., Drake, T. A., Lusis, A. J., and Horvath, S. (2007). Weighted gene coexpression network analysis strategies applied to mouse weight. *Mammalian Genome*. **18**(6), 463–472. URL https://doi.org/10.1007/s00335-007-9043-3.

Gaillard, S., Lo Re, L., Mantilleri, A., Hepp, R., Urien, L., Malapert, P., Alonso, S., Deage, M., Kambrun, C., Landry, M., Low, S. A., Alloui, A., Lambolez, B., Scherrer, G., Le Feuvre, Y., Bourinet, E., and Moqrich, A. (2014). GINIP, a gαi-interacting protein, functions as a key modulator of peripheral $GABA_B$ receptor-mediated analgesia. *Neuron*. **84**(1), 123–136. URL https://doi.org/10.1016/j.neuron.2014.08.056.

Gallego, M., Timmermann, A., Friedrich, T., and Zeebe, R. (2018). Drivers of future seasonal cycle changes in oceanic pCO_2. *Biogeosciences*. **15**, 5315–5327. URL https://doi.org/10.5194/bg-15-5315-2018.

Galler, S. and Moser, H. (1986). The ionic mechanism of intracellular pH regulation in crayfish muscle fibres. *The Journal of Physiology*. **374**(1), 137–151. URL https://doi.org/10.1113/jphysiol.1986.sp016071.

Gao, K., Gao, G., Wang, Y., and Dupont, S. (2020). Impacts of ocean acidification under multiple stressors on typical organisms and ecological processes. *Marine Life Science and Technology*. **2**, 279–291. URL https://doi.org/10.1007/s42995-020-00048-w.

Gao, Y., Zhang, Q., Lang, Y., Liu, Y., Dong, X., Chen, Z., Tian, W., Tang, J., Wu, W., Tong, Y., and Chen, Z. (2017). Human apo-SRP72 and SRP68/72 complex structures reveal the molecular basis of protein translocation. *Journal of Molecular Cell Biology*. **9**(3), 220–230. URL https://doi.org/10.1093/jmcb/mjx010.

García, E., Hernández, J. C., Clemente, S., Cohen-Rengifo, M., Hernández, C. A., and Dupont, S. (2015). Robustness of *Paracentrotus lividus* larval and post-larval development to pH levels projected for the turn of the century. *Marine Biology*. **162**(10), 2047–2055. URL https://doi.org/10.1007/s00227-015-2731-8.

García-Lavandeira, M., Silva, A., Abad, M., Pazos, A. J., Sánchez, J. L., and Pérez-Parallé, M. L. (2005). Effects of GABA and epinephrine on the settlement and metamorphosis of the larvae of four species of bivalve molluscs. *Journal of Experimental Marine Biology and Ecology*. **316**(2), 149–156. URL https://doi.org/10.1016/j.jembe.2004.10.011.

Garrett, S. and Rosenthal, J. J. (2012). RNA editing underlies temperature adaptation in K^+ channels from polar octopuses. *Science*. **335**(6070), 848–851. URL https://doi.org/10.1126/science.1212795.

Gerschenfeld, H. and Tritsch, D. P. (1974). Ionic mechanisms and receptor properties underlying the responses of molluscan neurones to 5-hydroxytryptamine. *The Journal of Physiology*. **243**(2), 427–456. URL https://doi.org/10.1113/jphysiol.1974.sp010761.

Gisselmann, G., Plonka, J., Pusch, H., and Hatt, H. (2004). *Drosophila melanogaster* GRD and LCCH3 subunits form heteromultimeric GABA-gated cation channels. *British Journal of Pharmacology*. **142**(3), 409–413. URL https://doi.org/10.1038/sj.bjp.0705818.

Gisselmann, G., Pusch, H., Hovemann, B. T., and Hatt, H. (2002). Two cDNAs coding for histamine-gated ion channels in *D. melanogaster*. *Nature Neuroscience*. **5**(1), 11–12. URL https://doi.org/10.1038/nn787.

Glaspie, C. N., Longmire, K., and Seitz, R. D. (2017). Acidification alters predator-prey interactions of blue crab *Callinectes sapidus* and soft-shell clam *Mya arenaria*. *Journal of Experimental Marine Biology and Ecology*. **489**, 58–65. URL https://doi.org/10.1016/j.jembe.2016.11.010.

Goldschmidt, H. L., Tu-Sekine, B., Volk, L., Anggono, V., Huganir, R. L., and Raben, D. M. (2016). DGKθ catalytic activity is required for efficient recycling of presynaptic vesicles at excitatory synapses. *Cell Reports*. **14**(2), 200–207. URL https://doi.org/10.1016/j.celrep.2015.12.022.

Gong, Q.-H., Wang, Q., Pan, L.-L., Liu, X.-H., Huang, H., and Zhu, Y.-Z. (2010). Hydrogen sulfide attenuates lipopolysaccharide-induced cognitive impairment: A pro-

inflammatory pathway in rats. *Pharmacology Biochemistry and Behavior*. **96**(1), 52–58. URL https://doi.org/10.1016/j.pbb.2010.04.006.

González, I., Déjean, S., Martin, P., and Baccini, A. (2008). CCA: An R package to extend canonical correlation analysis. *Journal of Statistical Software*. **23**(12), 1–14. URL https://doi.org/10.18637/jss.v023.i12.

Goodson, M. S., Kojadinovic, M., Troll, J. V., Scheetz, T. E., Casavant, T. L., Soares, M. B., and McFall-Ngai, M. J. (2005). Identifying components of the NF-KB pathway in the beneficial *Euprymna scolopes-Vibrio fischeri* light organ symbiosis. *Applied and Environmental Microbiology*. **71**(11), 6934–6946. URL https://doi.org/10.1128/AEM.71.11.6934-6946.2005.

Götz, S., García-Gómez, J. M., Terol, J., Williams, T. D., Nagaraj, S. H., Nueda, M. J., Robles, M., Talón, M., Dopazo, J., and Conesa, A. (2008). High-throughput functional annotation and data mining with the Blast2GO suite. *Nucleic Acids Research*. **36**(10), 3420–3435. URL https://doi.org/10.1093/nar/gkn176.

Gravinese, P. M., Enochs, I. C., Manzello, D. P., and van Woesik, R. (2019). Ocean acidification changes the vertical movement of stone crab larvae. *Biology Letters*. **15**, 20190414. URL https://doi.org/10.1098/rsbl.2019.0414.

Gray, M. W., Langdon, C. J., Waldbusser, G. G., Hales, B., and Kramer, S. (2017). Mechanistic understanding of ocean acidification impacts on larval feeding physiology and energy budgets of the mussel *Mytilus californianus*. *Marine Ecology Progress Series*. **563**, 81–94. URL https://doi.org/10.3354/meps11977.

Green, M. A., Waldbusser, G. G., Hubazc, L., Cathcart, E., and Hall, J. (2013). Carbonate mineral saturation state as the recruitment cue for settling bivalves in marine muds. *Estuaries and Coasts*. **36**(1), 18–27. URL https://doi.org/10.1007/s12237-012-9549-0.

Gregory Peterson, M., Inostroza, J., Maxon, M. E., Flores, O., Admon, A., Reinberg, D., and Tjian, R. (1991). Structure and functional properties of human general transcription factor IIE. *Nature*. **354**(6352), 369–373. URL https://doi.org/10.1038/354369a0.

Grilo, T. F., Repolho, T., Rosa, R., and Cardoso, P. G. (2019). Performance and herbivory of the tropical topshell *Trochus histrio* under short-term temperature increase and high CO_2. *Marine Pollution Bulletin*. **138**, 295–301. URL https://doi.org/10.1016/j.marpolbul.2018.11.011.

Grosell, M. (2019). CO_2 and calcification processes in fish. In *Carbon Dioxide* (eds. M. Grosell, P.L. Munday, A.P. Farrell, and C.J. Brauner). Fish Physiology. pp. 133–159. Academic Press, Cambridge, San Diego, Oxford, London. URL https://doi.org/10.1016/bs.fp.2019.07.002.

Gu, H., Shang, Y., Clements, J., Dupont, S., Wang, T., Wei, S., Wang, X., Chen, J., Huang, W., and Hu, M. (2019). Hypoxia aggravates the effects of ocean acidification on the physiological energetics of the blue mussel *Mytilus edulis*. *Marine Pollution Bulletin*. **149**, 110538. URL https://doi.org/10.1016/j.marpolbul.2019.110538.

Guen, V. J., Gamble, C., Lees, J. A., and Colas, P. (2017). The awakening of the CDK10/Cyclin M protein kinase. *Oncotarget*. **8**(30), 50174–50186. URL https://doi.org/10.18632/oncotarget.15024.

Guha, M. and Mackman, N. (2001). LPS induction of gene expression in human monocytes. *Cellular Signalling*. **13**(2), 85–94. URL https://doi.org/10.1016/S0898-6568(00)00149-2.

Guo, X., Huang, M., Pu, F., You, W., and Ke, C. (2015). Effects of ocean acidification caused by rising CO_2 on the early development of three mollusks. *Aquatic Biology*. **23**(2), 147–157. URL https://doi.org/10.3354/ab00615.

Gutowska, M. A., Melzner, F., Langenbuch, M., Bock, C., Claireaux, G., and Pörtner, H.-O. (2010). Acid–base regulatory ability of the cephalopod (*Sepia officinalis*) in response to environmental hypercapnia. *Journal of Comparative Physiology B*. **180**(3), 323–335. URL https://doi.org/10.1007/s00360-009-0412-y.

Halliwell, B. (2006). Oxidative stress and neurodegeneration: Where are we now? *Journal of Neurochemistry*. **97**(6), 1634–1658. URL https://doi.org/10.1111/j.1471-4159.2006.03907.x.

Halliwell, B. and Gutteridge, J. (2015). Oxidative stress and redox regulation: Adaptation, damage, repair, senescence, and death. In *Free Radicals in Biology and Medicine. Fifth Edition* (eds. B. Halliwell and J. Gutteridge). pp. 199–283. Oxford University Press.

Hamilton, T. J., Holcombe, A., and Tresguerres, M. (2013). CO_2-induced ocean acidification increases anxiety in rockfish via alteration of $GABA_A$ receptor functioning. *Proceedings of the Royal Society B*. **281**(1775), 20132509. URL https://doi.org/10.1098/rspb.2013.2509.

Han, Z., Wang, W., Lv, X., Zong, Y., Liu, S., Liu, Z., Wang, L., and Song, L. (2019). ATG10 (autophagy-related 10) regulates the formation of autophagosome in the anti-virus immune response of pacific oyster (*Crassostrea gigas*). *Fish and Shellfish Immunology*. **91**, 325–332. URL https://doi.org/10.1016/j.fsi.2019.05.027.

Hanlon, R. T. and Messenger, J. B. (2018). *Cephalopod Behaviour*. Cambridge University Press, Cambridge. Second edition. URL https://doi.org/10.1017/9780511843600.

Hannan, K. D., Miller, G. M., Watson, S.-A., Rummer, J. L., Fabricius, K., and Munday, P. L. (2020). Diel pCO_2 variation among coral reefs and microhabitats at Lizard Island, Great Barrier Reef. *Coral Reefs*. **39**(5), 1391–1406. URL https://doi.org/10.1007/s00338-020-01973-z.

Harris, R. M. and Hofmann, H. A. (2014). Neurogenomics of behavioral plasticity. In *Ecological Genomics: Ecology and the Evolution of Genes and Genomes* (eds. C.R. Landry and N. Aubin-Horth). pp. 149–168. Springer Netherlands, Dordrecht. URL https://doi.org/10.1007/978-94-007-7347-9_8.

Harvey, R. J., Vreugdenhil, E., Zaman, S., Bhandal, N., Usherwood, P., Barnard, E., and Darlison, M. (1991). Sequence of a functional invertebrate $GABA_A$ receptor subunit which can form a chimeric receptor with a vertebrate alpha subunit. *The EMBO Journal*. **10**(11), 3239–3245. URL https://doi.org/10.1002/j.1460-2075.1991.tb04887.x.

de la Haye, K., Spicer, J., Widdicombe, S., and Briffa, M. (2011). Reduced sea water pH disrupts resource assessment and decision making in the hermit crab *Pagurus bernhardus*. *Animal Behaviour*. **82**(3), 495–501. URL https://doi.org/10.1016/j.anbehav.2011.05.030.

de la Haye, K. L., Spicer, J. I., Widdicombe, S., and Briffa, M. (2012). Reduced pH sea water disrupts chemo-responsive behaviour in an intertidal crustacean. *Journal of Experimental Marine Biology and Ecology*. **412**, 134–140. URL https://doi.org/10.1016/j.jembe.2011.11.013.

Heaulme, M., Chambon, J.-P., Leyris, R., Molimard, J.-C., Wermuth, C. G., and Biziere, K. (1986). Biochemical characterization of the interaction of three pyridazinyl-GABA derivatives with the $GABA_A$ receptor site. *Brain Research*. **384**(2), 224–231. URL https://doi.org/10.1016/0006-8993(86)91158-3.

Henry, R. P. and Wheatly, M. G. (1992). Interaction of respiration, ion regulation, and acid-base balance in the everyday life of aquatic crustaceans. *American Zoologist*. **32**(3), 407–416. URL https://doi.org/10.1093/icb/32.3.407.

Herath, H. M. L. P. B., Elvitigala, D. A. S., Godahewa, G. I., Whang, I., and Lee, J. (2015). Molecular insights into a molluscan transferrin homolog identified from disk abalone (*Haliotis discus discus*) evidencing its detectable role in host antibacterial defense. *Developmental and Comparative Immunology*. **53**(1), 222–233. URL https://doi.org/10.1016/j.dci.2015.07.013.

Hester, K. C., Peltzer, E. T., Kirkwood, W. J., and Brewer, P. G. (2008). Unanticipated consequences of ocean acidification: A noisier ocean at lower pH. *Geophysical Research Letters*. **35**(19). URL https://doi.org/10.1029/2008GL034913.

Heuer, R., Welch, M., Rummer, J., Munday, P., and Grosell, M. (2016). Altered brain ion gradients following compensation for elevated CO_2 are linked to behavioural alterations in a coral reef fish. *Scientific Reports*. **6**, 33216. URL https://doi.org/10.1038/srep33216.

Heuer, R. M. and Grosell, M. (2014). Physiological impacts of elevated carbon dioxide and ocean acidification on fish. *American Journal of Physiology-Regulatory, Integrative and Comparative Physiology*. **307**(9), R1061–R1084. URL https://doi.org/10.1152/ajpregu.00064.2014.

Heuer, R. M., Hamilton, T. J., and Nilsson, G. E. (2019). The physiology of behavioural impacts of high CO_2. In *Carbon Dioxide* (eds. M. Grosell, P.L. Munday, A.P. Farrell, and C.J. Brauner). Fish Phyisology. pp. 161–194. Academic Press, Cambridge, San Diego, Oxford, London. URL https://doi.org/10.1016/bs.fp.2019.08.002.

Hinton, T. and Johnston, G. A. (2018). Antagonists of ionotropic receptors for the inhibitory neurotransmitter GABA: Therapeutic indications. In *GABA And Glutamate: New Developments In Neurotransmission Research* (ed. J. Samadrzie). pp. 91–106. InTech, Rijeka, Croatia.

Hofmann, G. E., Smith, J. E., Johnson, K. S., Send, U., Levin, L. A., Micheli, F., Paytan, A., Price, N. N., Peterson, B., and Takeshita, Y. (2011). High-frequency dynamics of ocean pH: A multi-ecosystem comparison. *PloS One*. **6**(12), e28983. URL https://doi.org/10.1371/journal.pone.0028983.

Horvath, S. and Dong, J. (2008). Geometric interpretation of gene coexpression network analysis. *PLoS Computational Biology*. **4**(8), e1000117–e1000117. URL https://doi.org/10.1371/journal.pcbi.1000117.

Horwitz, R., Norin, T., Watson, S.-A., Pistevos, J. C., Beldade, R., Hacquart, S., Gattuso, J.-P., Rodolfo-Metalpa, R., Vidal-Dupiol, J., and Killen, S. S. (2020). Near-future ocean warming and acidification alter foraging behaviour, locomotion, and metabolic rate in a keystone marine mollusc. *Scientific Reports*. **10**(1), 1–11. URL https://doi.org/10.1038/s41598-020-62304-4.

Hosie, A., Shirai, Y., Buckingham, S., Rauh, J., Roush, R., Baylis, H., and Sattelle, D. (1995). Blocking actions of BIDN, a bicyclic dinitrile convulsant compound, on wild-type and dieldrin-resistant GABA receptor homo-oligomers of *Drosophila melanogaster* expressed in *Xenopus* oocytes. *Brain Research*. **693**(1-2), 257–260. URL https://doi.org/10.1016/0006-8993(95)00605-P.

Hosie, A. M. and Sattelle, D. B. (1996). Agonist pharmacology of two *Drosophila* GABA receptor splice variants. *British Journal of Pharmacology*. **119**(8), 1577–1585. URL https://doi.org/10.1111/j.1476-5381.1996.tb16075.x.

Hu, L.-F., Lu, M., Hon Wong, P. T., and Bian, J.-S. (2010). Hydrogen sulfide: Neurophysiology and neuropathology. *Antioxidants and Redox Signaling*. **15**(2), 405–419. URL https://doi.org/10.1089/ars.2010.3517.

Hu, M. and Tseng, Y.-C. (2017). Acid–base regulation and ammonia excretion in cephalopods: An ontogenetic overview. In *Acid-Base Balance and Nitrogen Excretion in Invertebrates: Mechanisms and Strategies in Various Invertebrate Groups with Considerations of Challenges Caused by Ocean Acidification* (eds. D. Weihrauch and M. O'Donnell). pp. 275–298. Springer, Cham. URL https://doi.org/10.1007/978-3-319-39617-0_11.

Hu, M. Y., Guh, Y.-J., Stumpp, M., Lee, J.-R., Chen, R.-D., Sung, P.-H., Chen, Y.-C., Hwang, P.-P., and Tseng, Y.-C. (2014). Branchial NH_4^+-dependent acid–base transport mechanisms and energy metabolism of squid (*Sepioteuthis lessoniana*) affected by seawater acidification. *Frontiers in Zoology*. **11**(1), 55. URL https://doi.org/10.1186/s12983-014-0055-z.

Huang, B., Zhang, L., Tang, X., Zhang, G., and Li, L. (2016). Genome-wide analysis of alternative splicing provides insights into stress adaptation of the Pacific oyster. *Marine biotechnology*. **18**(5), 598–609. URL https://doi.org/10.1007/s10126-016-9720-x.

Ikeda, Y. and Matsumoto, l. G. (2007). Mirror image reactions in the oval squid *Sepioteuthis lessoniana*. *Fisheries Science*. **73**(6), 1401–1403. URL https://doi.org/10.1111/j.1444-2906.2007.01485.x.

Ilyina, T., Zeebe, R. E., and Brewer, P. G. (2010). Future ocean increasingly transparent to low-frequency sound owing to carbon dioxide emissions. *Nature Geoscience*. **3**(1), 18. URL https://doi.org/10.1038/NGEO719.

Ito, I., Kimura, T., and Ito, E. (2001). Odor responses and spontaneous oscillatory activity in tentacular nerves of the terrestrial slug, *Limax marginatus*. *Neuroscience Letters*. **304**(3), 145–148. URL https://doi.org/10.1016/S0304-3940(01)01775-X.

Ivanina, A. V., Hawkins, C., and Sokolova, I. M. (2014). Immunomodulation by the interactive effects of cadmium and hypercapnia in marine bivalves *Crassostrea virginica* and *Mercenaria mercenaria*. *Fish and Shellfish Immunology*. **37**(2), 299–312. URL https://doi.org/10.1016/j.fsi.2014.02.016.

Izaddoost, S., Nam, S.-C., Bhat, M. A., Bellen, H. J., and Choi, K.-W. (2002). *Drosophila* Crumbs is a positional cue in photoreceptor adherens junctions and rhabdomeres. *Nature*. **416**(6877), 178–183. URL https://doi.org/10.1038/nature720.

Jackel, C., Krenz, W., and Nagy, F. (1994). Bicuculline/baclofen-insensitive GABA response in crustacean neurones in culture. *Journal of Experimental Biology*. **191**(1), 167–193. URL https://doi.org/10.1242/jeb.191.1.167.

Jackson, C., Bermudez, I., and Beadle, D. J. (2002). Pharmacological properties of nicotinic acetylcholine receptors in isolated *Locusta migratoria* neurones. *Microscopy Research and Technique*. **56**(4), 249–255. URL https://doi.org/10.1002/jemt.10028.

Jackson, F. R. and Haydon, P. G. (2008). Glial cell regulation of neurotransmission and behavior in *Drosophila*. *Neuron Glia Biology*. **4**(1), 11–17. URL https://doi.org/10.1017/S1740925X09000027.

Jackson, G. (1992). Seasonal abundance of the small tropical Sepioid *Idiosepius pygmaeus* (Cephalopoda, Idiosepiidae) at two localities off Townsville, North Queensland, Australia. *The Veliger*. **35**(4), 396–397.

Jackson, G. D. (1988). The use of statolith microstructures to analyze life history events in the small tropical cephalopod *Idiosepius pygmaeus*. *Fishery Bulletin*. **87**, 265–272.

Jakubowska, M. and Normant-Saremba, M. (2015). The effect of CO_2-induced seawater acidification on the behaviour and metabolic rate of the Baltic clam *Macoma balthica*.

Annales Zoologici Fennici. **52**(5–6), 353–367. URL https://doi.org/10.5735/086.052.0509.

Janssen, D., Derst, C., Rigo, J.-M., and Van Kerkhove, E. (2010). Cys-loop ligand-gated chloride channels in dorsal unpaired median neurons of *Locusta migratoria*. *Journal of Neurophysiology*. **103**(5), 2587–2598. URL https://doi.org/10.1152/jn.00466.2009.

Jansson, A., Lischka, S., Boxhammer, T., Schulz, K. G., and Norkko, J. (2016). Survival and settling of larval *Macoma balthica* in a large-scale mesocosm experiment at different fCO_2 levels. *Biogeosciences*. **13**, 3377–3388. URL https://doi.org/10.5194/bg-13-3377-2016.

Jeffs, A., Tolimieri, N., and Montgomery, J. C. (2003). Crabs on cue for the coast: The use of underwater sound for orientation by pelagic crab stages. *Marine and Freshwater Research*. **54**(7), 841–845. URL https://doi.org/10.1071/MF03007.

Jellison, B. M., Ninokawa, A. T., Hill, T. M., Sanford, E., and Gaylord, B. (2016). Ocean acidification alters the response of intertidal snails to a key sea star predator. *Proceedings of the Royal Society B: Biological Sciences*. **283**, 20160890. URL https://doi.org/10.1098/rspb.2016.0890.

Ji, C., Wu, H., Wei, L., Zhao, J., Wang, Q., and Lu, H. (2013). Responses of *Mytilus galloprovincialis* to bacterial challenges by metabolomics and proteomics. *Fish and Shellfish Immunology*. **35**(2), 489–498. URL https://doi.org/10.1016/j.fsi.2013.05.009.

Jiang, Y., Loker, E. S., and Zhang, S.-M. (2006). *In vivo* and *in vitro* knockdown of FREP2 gene expression in the snail *Biomphalaria glabrata* using RNA interference. *Developmental and Comparative Immunology*. **30**(10), 855–866. URL https://doi.org/10.1016/j.dci.2005.12.004.

Jiao, D., Chen, Y., Liu, Y., Ju, Y., Long, J., Du, J., Yu, C., Wang, Y., Zhao, M., and Liu, J. (2017). SYVN1, an ERAD E3 ubiquitin ligase, is involved in $GABA_A\alpha1$ degradation associated with methamphetamine-induced conditioned place preference. *Frontiers in Molecular Neuroscience*. **10**(313). URL https://doi.org/10.3389/fnmol.2017.00313.

Jin, X.-K., Li, W.-W., He, L., Lu, W., Chen, L.-L., Wang, Y., Jiang, H., and Wang, Q. (2011). Molecular cloning, characterization and expression analysis of two apoptosis genes, caspase and nm23, involved in the antibacterial response in chinese mitten crab,

Eriocheir sinensis. *Fish and Shellfish Immunology*. **30**(1), 263–272. URL https://doi.org/10.1016/j.fsi.2010.10.016.

Jing, J., Vilim, F. S., Wu, J.-S., Park, J.-H., and Weiss, K. R. (2003). Concerted GABAergic actions of *Aplysia* feeding interneurons in motor program specification. *Journal of Neuroscience*. **23**(12), 5283–5294. URL https://doi.org/10.1523/JNEUROSCI.23-12-05283.2003.

Johansson, M. W. (1999). Cell adhesion molecules in invertebrate immunity. *Developmental and Comparative Immunology*. **23**(4), 303–315. URL https://doi.org/10.1016/S0145-305X(99)00013-0.

Johnson, K., Grawe, F., Grzeschik, N., and Knust, E. (2002). *Drosophila* Crumbs is required to inhibit light-induced photoreceptor degeneration. *Current Biology*. **12**(19), 1675–1680. URL https://doi.org/10.1016/S0960-9822(02)01180-6.

Johnson, K. M. and Hofmann, G. E. (2017). Transcriptomic response of the Antarctic pteropod *Limacina helicina antarctica* to ocean acidification. *BMC Genomics*. **18**(1), 812. URL https://doi.org/10.1186/s12864-017-4161-0.

Jones, P., Binns, D., Chang, H.-Y., Fraser, M., Li, W., McAnulla, C., McWilliam, H., Maslen, J., Mitchell, A., Nuka, G., Pesseat, S., Quinn, A. F., Sangrador-Vegas, A., Scheremetjew, M., Yong, S.-Y., Lopez, R., and Hunter, S. (2014a). InterProScan 5: Genome-scale protein function classification. *Bioinformatics*. **30**(9), 1236–1240. URL https://doi.org/10.1093/bioinformatics/btu031.

Jones, R. T., Faas, G. C., and Mody, I. (2014b). Intracellular bicarbonate regulates action potential generation via KCNQ channel modulation. *The Journal of Neuroscience*. **34**(12), 4409–4417. URL https://doi.org/10.1523/jneurosci.3836-13.2014.

Joos, F. and Spahni, R. (2008). Rates of change in natural and anthropogenic radiative forcing over the past 20,000 years. *Proceedings of the National Academy of Sciences*. **105**(5), 1425–1430. URL https://doi.org/10.1073/pnas.0707386105.

Julian, D., Statile, J., Wohlgemuth, S., and Arp, A. (2002). Enzymatic hydrogen sulfide production in marine invertebrate tissues. *Comparative Biochemistry and Physiology Part A: Molecular and Integrative Physiology*. **133**, 105–115. URL https://doi.org/10.1016/S1095-6433(02)00122-8.

Kabir, A., Merrill, R. D., Shamim, A. A., Klemn, R. D. W., Labrique, A. B., Christian, P., West, Jr, K. P., and Nasser, M. (2014). Canonical correlation analysis of infant's size

at birth and maternal factors: A study in rural Northwest Bangladesh. *PLOS ONE*. **9**(4), 1–8. URL https://doi.org/10.1371/journal.pone.0094243.

Kaila, K., Lamsa, K., Smirnov, S., Taira, T., and Voipio, J. (1997). Long-lasting GABA-mediated depolarization evoked by high-frequency stimulation in pyramidal neurons of rat hippocampal slice is attributable to a network-driven, bicarbonate-dependent K^+ transient. *The Journal of Neuroscience*. **17**(20), 7662–7672. URL https://doi.org/10.1523/jneurosci.17-20-07662.1997.

Kaila, K., Pasternack, M., Saarikoski, J., and Voipio, J. (1989). Influence of GABA-gated bicarbonate conductance on potential, current and intracellular chloride in crayfish muscle fibres. *The Journal of Physiology*. **416**(1), 161–181. URL https://doi.org/10.1113/jphysiol.1989.sp017755.

Kaila, K. and Voipio, J. (1987). Postsynaptic fall in intracellular pH induced by GABA-activated bicarbonate conductance. *Nature*. **330**(6144), 163.

Kambach, C., Walket, S., and Nagai, K. (1999). Structure and assembly of the spliceosomal small nuclear ribonucleoprotein particles. *Current Opinion in Structural Biology*. **9**(2), 222–230. URL https://doi.org/10.1016/S0959-440X(99)80032-3.

Kaneko, M., Ishiguro, M., Niinuma, Y., Uesugi, M., and Nomura, Y. (2002). Human HRD1 protects against ER stress-induced apoptosis through ER-associated degradation. *FEBS Letters*. **532**(1-2), 147–152. URL https://doi.org/10.1016/S0014-5793(02)03660-8.

Kaneko, N., Sawada, M., and Sawamoto, K. (2017). Mechanisms of neuronal migration in the adult brain. *Journal of Neurochemistry*. **141**(6), 835–847. URL https://doi.org/10.1111/jnc.14002.

Kania, B. F., Wrońska, D., and Zięba, D. (2017). Introduction to neural plasticity mechanism. *Journal of Behavioral and Brain Science*. **7**(2), 41–49. URL https://doi.org/10.4236/jbbs.2017.72005.

Kaplan, M. B., Mooney, T. A., McCorkle, D. C., and Cohen, A. L. (2013). Adverse effects of ocean acidification on early development of squid (*Doryteuthis pealeii*). *PLoS One*. **8**(5), e63714. URL https://doi.org/10.1371/journal.pone.0063714.

Karanjia, R., García-Hernández, L. M., Miranda-Morales, M., Somani, N., Espinosa-Luna, R., Montano, L. M., and Barajas-López, C. (2006). Cross-inhibitory interactions between $GABA_A$ and P2X channels in myenteric neurones. *European Journal*

of Neuroscience. **23**(12), 3259–3268. URL https://doi.org/10.1111/j.1460-9568.2006.04861.x.

Katow, H., Abe, K., Katow, T., Zamani, A., and Abe, H. (2013). Development of the γ-amino butyric acid GABA-ergic signaling system and its role in larval swimming in sea urchin. *Journal of Experimental Biology*. **216**, 1704–1716. URL https://doi.org/10.1242/jeb.074856.

Kavaliers, M., Perrot-Sinal, T. S., Desjardins, D. C., Cross-Mellor, S. K., and Wiebe, J. P. (1999). Antinociceptive effects of the neuroactive steroid, 3α-hydroxy-5α-pregnan-20-one and progesterone in the land snail, *Cepaea nemoralis*. *Neuroscience*. **95**(3), 807–812. URL https://doi.org/10.1016/S0306-4522(99)00499-6.

Keenan, R. J., Freymann, D. M., Stroud, R. M., and Walter, P. (2001). The signal recognition particle. *Annual Review of Biochemistry*. **70**(1), 755–775. URL https://doi.org/10.1146/annurev.biochem.70.1.755.

Kehoe, J. (1972). Ionic mechanism of a two-component cholinergic inhibition in *Aplysia* neurones. *The Journal of Physiology*. **225**(1), 85–114. URL https://doi.org/10.1113/jphysiol.1972.sp009930.

Kehoe, J., Buldakova, S., Acher, F., Dent, J., Bregestovski, P., and Bradley, J. (2009). *Aplysia* cys-loop glutamate-gated chloride channels reveal convergent evolution of ligand specificity. *Journal of Molecular Evolution*. **69**(2), 125–141. URL https://doi.org/10.1007/s00239-009-9256-z.

Kehoe, J. and Vulfius, C. (2000). Independence of and interactions between GABA-, glutamate-, and acetylcholine-activated Cl conductances in *Aplysia* neurons. *Journal of Neuroscience*. **20**(23), 8585–8596. URL https://doi.org/10.1523/JNEUROSCI.20-23-08585.2000.

Kelley, J., Chapuis, L., Davies, W. I. L., and Collin, S. (2018). Sensory system responses to human-induced environmental change. *Frontiers in Ecology and Evolution*. **6**, 95. URL https://doi.org/10.3389/fevo.2018.00095.

Kim, T. W., Taylor, J., Lovera, C., and Barry, J. P. (2015). CO_2-driven decrease in pH disrupts olfactory behaviour and increases individual variation in deep-sea hermit crabs. *ICES Journal of Marine Science*. **73**(3), 613–619. URL https://doi.org/10.1093/icesjms/fsv019.

Kim, Y.-G., Lee, S., Kwon, O.-S., Park, S.-Y., Lee, S.-J., Park, B.-J., and Kim, K.-J. (2009). Redox-switch modulation of human SSADH by dynamic catalytic loop. *The EMBO journal*. **28**(7), 959–968. URL https://doi.org/10.1038/emboj.2009.40.

Kimura, H. (2000). Hydrogen sulfide induces cyclic AMP and modulates the NMDA receptor. *Biochemical and Biophysical Research Communications*. **267**(1), 129–133. URL https://doi.org/10.1006/bbrc.1999.1915.

Kleypas, J. A., Buddemeier, R. W., Archer, D., Gattuso, J.-P., Langdon, C., and Opdyke, B. N. (1999). Geochemical consequences of increased atmospheric carbon dioxide on coral reefs. *Science*. **284**(5411), 118–120. URL https://doi.org/10.1126/science.284.5411.118.

Kline, D. I., Teneva, L., Hauri, C., Schneider, K., Miard, T., Chai, A., Marker, M., Dunbar, R., Caldeira, K., and Lazar, B. (2015). Six month in situ high-resolution carbonate chemistry and temperature study on a coral reef flat reveals asynchronous pH and temperature anomalies. *PloS One*. **10**(6), e0127648. URL https://doi.org/10.1371/journal.pone.0127648.

Klionsky, D. J., Abdelmohsen, K., Abe, A., Abedin, M. J., Abeliovich, H., AcevedoArozena, A., ..., and Zughaier, S. M. (2016). Guidelines for the use and interpretation of assays for monitoring autophagy (3rd edition). *Autophagy*. **1**, 1–22. URL https://doi.org/10.1080/15548627.2015.1100356.

Kobayashi, S., Hattori, M., and Ito, E. (2008). The effects of GABA on the network oscillations of the procerebrum in *Limax valentianus*. *Acta Biologica Hungarica*. **59**(Supplement 2), 77–79. URL https://doi.org/10.1556/ABiol.59.2008.Suppl.12.

Koch, H.-G., Moser, M., and Müller, M. (2003). Signal recognition particle-depencent protein targeting, universal to all kingdoms of life. *Reviews of Physiology, Biochemistry and Pharmacology*. **146**, 55–94. URL https://doi.org/10.1007/s10254-002-0002-9.

Koehl, M. (2005). The fluid mechanics of arthropod sniffing in turbulent odor plumes. *Chemical Senses*. **31**(2), 93–105. URL https://doi.org/10.1093/chemse/bjj009.

Koehler, K., Malik, M., Mahmood, S., Gießelmann, S., Beetz, C., Hennings, J. C., Huebner, A., Grahn, A., Reunert, J., Nürnberg, G., Thiele, H., Altmüller, J., Nürnberg, P., Mumtaz, R., Babovic-Vuksanovic, D., Basel-Vanagaite, L., Borck, G., Brämswig, J., Mühlenberg, R., Sarda, P., Sikiric, A., Anyane-Yeboa, K., Zeharia, A., Ahmad, A., Coubes, C., Wada, Y., Marquardt, T., Vanderschaeghe, D., Van Schaftingen, E.,

Kurth, I., Huebner, A., and Hübner, C. (2013). Mutations in GMPPA cause a glycosylation disorder characterized by intellectual disability and autonomic dysfunction. *The American Journal of Human Genetics*. **93**(4), 727–734. URL https://doi.org/10.1016/j.ajhg.2013.08.002.

Koh, H. Y., Lee, J. H., Han, S. J., Park, H., Shin, S. C., and Lee, S. G. (2015). A transcriptomic analysis of the response of the arctic pteropod *Limacina helicina* to carbon dioxide-driven seawater acidification. *Polar Biology*. **38**(10), 1727–1740. URL https://doi.org/10.1007/s00300-015-1738-4.

Kong, H., Clements, J. C., Dupont, S., Wang, T., Huang, X., Shang, Y., Huang, W., Chen, J., Hu, M., and Wang, Y. (2019). Seawater acidification and temperature modulate anti-predator defenses in two co-existing *Mytilus* species. *Marine Pollution Bulletin*. **145**, 118–125. URL https://doi.org/10.1016/j.marpolbul.2019.05.040.

Kreher, S. A., Mathew, D., Kim, J., and Carlson, J. R. (2008). Translation of sensory input into behavioral output via an olfactory system. *Neuron*. **59**(1), 110–124. URL https://doi.org/10.1016/j.neuron.2008.06.010.

Krnjević, K. (1974). Chemical nature of synaptic transmission in vertebrates. *Physiological Reviews*. **54**(2), 418–540. URL https://doi.org/10.1152/physrev.1974.54.2.418.

Kroeker, K. J., Gambi, M. C., and Micheli, F. (2013). Community dynamics and ecosystem simplification in a high-CO_2 ocean. *Proceedings of the National Academy of Sciences*. **110**(31), 12721–12726. URL https://doi.org/10.1073/pnas.1216464110.

Kroeker, K. J., Kordas, R. L., Crim, R. N., and Singh, G. G. (2010). Meta-analysis reveals negative yet variable effects of ocean acidification on marine organisms. *Ecology Letters*. **13**(11), 1419–1434. URL https://doi.org/10.1111/j.1461-0248.2010.01518.x.

Kroeker, K. J., Sanford, E., Jellison, B. M., and Gaylord, B. (2014). Predicting the effects of ocean acidification on predator-prey interactions: A conceptual framework based on coastal molluscs. *The Biological Bulletin*. **226**(3), 211–222. URL https://doi.org/10.1086/BBLv226n3p211.

Kukimoto, I., Elderkin, S., Grimaldi, M., Oelgeschläger, T., and Varga-Weisz, P. D. (2004). The histone-fold protein complex CHRAC-15/17 enhances nucleosome sliding and assembly mediated by ACF. *Molecular Cell*. **13**(2), 265–277. URL https://doi.org/10.1016/S1097-2765(03)00523-9.

Kurihara, H., Matsui, M., Furukawa, H., Hayashi, M., and Ishimatsu, A. (2008). Long-term effects of predicted future seawater CO_2 conditions on the survival and growth of the marine shrimp *Palaemon pacificus*. *Journal of Experimental Marine Biology and Ecology*. **367**(1), 41–46. URL https://doi.org/10.1016/j.jembe.2008.08.016.

Kurihara, H., Shimode, S., and Shirayama, Y. (2004). Sub-lethal effects of elevated concentration of CO_2 on planktonic copepods and sea urchins. *Journal of Oceanography*. **60**(4), 743–750. URL https://doi.org/10.1007/s10872-004-5766-x.

Lacombe, M.-L. L., Munier, A., Mehus, J. G., and Lambeth, D. O. (2000). The human Nm23/nucleoside diphosphate kinases. *Journal of Bioenergetics and Biomembranes*. **32**(3), 247–258. URL https://doi.org/10.1023/A:1005584929050.

Lacoste, A., Malham, S. K., Cueff, A., and Poulet, S. A. (2001). Noradrenaline modulates hemocyte reactive oxygen species production via β-adrenergic receptors in the oyster *Crassostrea gigas*. *Developmental and Comparative Immunology*. **25**(4), 285–289. URL https://doi.org/10.1016/S0145-305X(00)00067-7.

Lacoue-Labarthe, T., Reveillac, E., Oberhänsli, F., Teyssié, J.-L., Jeffree, R., and Gattuso, J. (2011). Effects of ocean acidification on trace element accumulation in the early-life stages of squid *Loligo vulgaris*. *Aquatic Toxicology*. **105**(1-2), 166–176. URL https://doi.org/10.1016/j.aquatox.2011.05.021.

LaDage, L. D. (2015). Environmental change, the stress response, and neurogenesis. *Integrative and Comparative Biology*. **55**(3), 372–383. URL https://doi.org/10.1093/icb/icv040.

Lai, F., Fagernes, C. E., Bernier, N. J., Miller, G. M., Munday, P. L., Jutfelt, F., and Nilsson, G. E. (2017). Responses of neurogenesis and neuroplasticity related genes to elevated CO_2 levels in the brain of three teleost species. *Biology Letters*. **13**(8), 20170240. URL https://doi.org/10.1098/rsbl.2017.0240.

Lai, F., Jutfelt, F., and Nilsson, G. E. (2015). Altered neurotransmitter function in CO_2-exposed stickleback (*Gasterosteus aculeatus*): A temperate model species for ocean acidification research. *Conservation Physiology*. **3**(1), cov018. URL https://doi.org/10.1093/conphys/cov018.

Lambert, L. A., Perri, H., Halbrooks, P. J., and Mason, A. B. (2005). Evolution of the transferrin family: Conservation of residues associated with iron and anion binding. *Comparative Biochemistry and Physiology Part B: Biochemistry and Molecular Biology*. **142**(2), 129–141. URL https://doi.org/10.1016/j.cbpb.2005.07.007.

Lambert, Z. V. and Durand, R. M. (1975). Some precautions in using canonical analysis. *Journal of Marketing Research*. **12**(4), 468–475. URL https://doi.org/10.1177/002224377501200411.

Laming, P., Kimelberg, H., Robinson, S., Salm, A., Hawrylak, N., Müller, C., Roots, B., and Ng, K. (2000). Neuronal–glial interactions and behaviour. *Neuroscience and Biobehavioural Reviews*. **24**(3), 295–340. URL https://doi.org/10.1016/S0149-7634(99)00080-9.

Lampert, F., Stafa, D., Goga, A., Soste, M. V., Gilberto, S., Olieric, N., Picotti, P., Stoffel, M., and Peter, M. (2018). The multi-subunit GID/CTLH E3 ubiquitin ligase promotes cell proliferation and targets the transcription factor Hbp1 for degradation. *eLife*. **7**, e35528. URL https://doi.org/10.7554/eLife.35528.

Lan, L., Ui, A., Nakajima, S., Hatakeyama, K., Hoshi, M., Watanabe, R., Janicki, S. M., Ogiwara, H., Kohno, T., Kanno, S.-i., and Yasui, A. (2010). The ACF1 complex is required for DNA double-strand break repair in human cells. *Molecular Cell*. **40**(6), 976–987. URL https://doi.org/10.1016/j.molcel.2010.12.003.

Langfelder, P. and Horvath, S. (2008). WGCNA: An R package for weighted correlation network analysis. *BMC bioinformatics*. **9**(1), 1–13. URL https://doi.org/10.1186/1471-2105-9-559.

Langmead, B. and Salzberg, S. L. (2012). Fast gapped-read alignment with Bowtie 2. *Nature Methods*. **9**(4), 357–359. URL https://doi.org/10.1038/nmeth.1923.

Lassoued, J., Babarro, J. M., Padín, X., Comeau, L. A., Bejaoui, N., and Pérez, F. F. (2019). Behavioural and eco-physiological responses of the mussel *Mytilus galloprovincialis* to acidification and distinct feeding regimes. *Marine Ecology Progress Series*. **626**, 97–108. URL https://doi.org/10.3354/meps13075.

Leal-Esteban, L. C., Rothé, B., Fortier, S., Isenschmid, M., and Constam, D. B. (2018). Role of bicaudal C1 in renal gluconeogenesis and its novel interaction with the CTLH complex. *PLOS Genetics*. **14**(7), e1007487. URL https://doi.org/10.1371/journal.pgen.1007487.

Lebel, C. P. and Bondy, S. C. (1991). Oxygen radicals: Common mediators of neurotoxicity. *Neurotoxicology and Teratology*. **13**(3), 341–346. URL https://doi.org/10.1016/0892-0362(91)90081-7.

Lecchini, D., Dixson, D. L., Lecellier, G., Roux, N., Frédérich, B., Besson, M., Tanaka, Y., Banaigs, B., and Nakamura, Y. (2017). Habitat selection by marine larvae in changing chemical environments. *Marine Pollution Bulletin*. **114**(1), 210–217. URL https://doi.org/10.1016/j.marpolbul.2016.08.083.

Lee, V. and Maguire, J. (2014). The impact of tonic $GABA_A$ receptor-mediated inhibition on neuronal excitability varies across brain region and cell type. *Frontiers in Neural Circuits*. **8**, 3. URL https://doi.org/10.3389/fncir.2014.00003.

Lee, Y. H., Jeong, C.-B., Wang, M., Hagiwara, A., and Lee, J.-S. (2020). Transgenerational acclimation to changes in ocean acidification in marine invertebrates. *Marine Pollution Bulletin*. **153**, 111006. URL https://doi.org/10.1016/j.marpolbul.2020.111006.

Lepicard, S., Franco, B., de Bock, F., and Parmentier, M.-L. (2014). A presynaptic role of microtubule-associated protein 1/Futsch in *Drosophila*: Regulation of active zone number and neurotransmitter release. *The Journal of Neuroscience*. **34**(20), 6759–6771. URL https://doi.org/10.1523/jneurosci.4282-13.2014.

Levi, R., Varona, P., Arshavsky, Y. I., Rabinovich, M. I., and Selverston, A. I. (2004). Dual sensory-motor function for a molluskan statocyst network. *Journal of Neurophysiology*. **91**(1), 336–345. URL https://doi.org/10.1152/jn.00753.2003.

Li, F., Mu, F.-H., Liu, X.-S., Xu, X.-Y., and Cheung, S. (2020). Predator prey interactions between predatory gastropod *Reishia clavigera*, barnacle *Amphibalanus amphitrite amphitrite* and mussel *Brachidontes variabilis* under ocean acidification. *Marine Pollution Bulletin*. **152**, 110895. URL https://doi.org/10.1016/j.marpolbul.2020.110895.

Li, H.-W., Chen, C., Kuo, W.-L., Lin, C.-J., Chang, C.-F., and Wu, G.-C. (2019). The characteristics and expression profile of transferrin in the accessory nidamental gland of the bigfin reef squid during bacteria transmission. *Scientific Reports*. **9**(1), 20163. URL https://doi.org/10.1038/s41598-019-56584-8.

Li, M., Qiu, L., Wang, L., Wang, W., Xin, L., Li, Y., Liu, Z., and Song, L. (2016a). The inhibitory role of γ-aminobutyric acid GABA on immunomodulation of pacific oyster *Crassostrea gigas*. *Fish and Shellfish Immunology*. **52**, 16–22. URL https://doi.org/10.1016/j.fsi.2016.03.015.

Li, M., Wang, L., Qiu, L., Wang, W., Xin, L., Xu, J., Wang, H., and Song, L. (2016b). A glutamic acid decarboxylase (CgGAD) highly expressed in hemocytes of Pacific oys-

ter *Crassostrea gigas*. *Developmental and Comparative Immunology*. **63**, 56–65. URL https://doi.org/10.1016/j.dci.2016.05.010.

Li, S., Liu, Y., Liu, C., Huang, J., Zheng, G., Xie, L., and Zhang, R. (2015). Morphology and classification of hemocytes in *Pinctada fucata* and their responses to ocean acidification and warming. *Fish and Shellfish Immunology*. **45**(1), 194–202. URL https://doi.org/10.1016/j.fsi.2015.04.006.

Li, T., Chu, X., Xin, D., Ke, H., Wang, S., Liu, D., Chen, W., and Wang, Z. (2021). H_2S prevents peripheral immune cell invasion, increasing $[Ca^{2+}]_i$ and excessive phagocytosis following hypoxia-ischemia injury in neonatal mice. *Biomedicine and Pharmacotherapy*. **135**, 111207. URL https://doi.org/10.1016/j.biopha.2020.111207.

Li, W. and Gao, K. (2012). A marine secondary producer respires and feeds more in a high CO_2 ocean. *Marine Pollution Bulletin*. **64**(4), 699–703. URL https://doi.org/10.1016/j.marpolbul.2012.01.033.

Li, W. and Godzik, A. (2006). Cd-hit: A fast program for clustering and comparing large sets of protein or nucleotide sequences. *Bioinformatics*. **22**(13), 1658–1659. URL https://doi.org/10.1093/bioinformatics/btl158.

Li, Y., Wu, L.-J., Legendre, P., and Xu, T.-L. (2003). Asymmetric cross-inhibition between $GABA_A$ and glycine receptors in rat spinal dorsal horn neurons. *Journal of Biological Chemistry*. **278**(40), 38637–38645. URL https://doi.org/10.1074/jbc.M303735200.

Lillis, A., Eggleston, D. B., and Bohnenstiehl, D. R. (2013). Oyster larvae settle in response to habitat-associated underwater sounds. *PloS One*. **8**(10), e79337. URL https://doi.org/10.1371/journal.pone.0079337.

Lima, S. L. and Dill, L. M. (1990). Behavioral decisions made under the risk of predation: A review and prospectus. *Canadian Journal of Zoology*. **68**(4), 619–640. URL https://doi.org/10.1139/z90-092.

Liu, H., Ding, J., Köhnlein, K., Urban, N., Ori, A., Villavicencio-Lorini, P., Walentek, P., Klotz, L.-O., Hollemann, T., and Pfirrmann, T. (2020). The GID ubiquitin ligase complex is a regulator of AMPK activity and organismal lifespan. *Autophagy*. **16**(9), 1618–1634. URL https://doi.org/10.1080/15548627.2019.1695399.

Liu, S., Shi, W., Guo, C., Zhao, X., Han, Y., Peng, C., Chai, X., and Liu, G. (2016). Ocean acidification weakens the immune response of blood clam through hampering the

NF-kappa β and toll-like receptor pathways. *Fish and Shellfish Immunology*. **54**, 322–327. URL https://doi.org/10.1016/j.fsi.2016.04.030.

Liu, Y., Buchberger, A. R., DeLaney, K., Li, Z., and Li, L. (2019). Multifaceted mass spectrometric investigation of neuropeptide changes in atlantic blue crab, *Callinectes sapidus*, in response to low pH stress. *Journal of Proteome Research*. **18**, 2759–2770. URL https://doi.org/10.1021/acs.jproteome.9b00026.

Liu, Z., Wang, L., Lv, Z., Zhou, Z., Wang, W., Li, M., Yi, Q., Qiu, L., and Song, L. (2018). The cholinergic and adrenergic autocrine signaling pathway mediates immunomodulation in oyster *Crassostrea gigas*. *Frontiers in Immunology*. **9**(284), 284. URL http://dx.doi.org/10.3389/fimmu.2018.00284.

Liu, Z., Zhou, Z., Jiang, Q., Wang, L., Yi, Q., Qiu, L., and Song, L. (2017). The neuroendocrine immunomodulatory axis-like pathway mediated by circulating haemocytes in Pacific oyster *Crassostrea gigas*. *Open Biology*. **7**(1), 160289. URL https://doi.org/10.1098/rsob.160289.

Lohr, K. M., Bernstein, A. I., Stout, K. A., Dunn, A. R., Lazo, C. R., Alter, S. P., Wang, M., Li, Y., Fan, X., and Hess, E. J. (2014). Increased vesicular monoamine transporter enhances dopamine release and opposes Parkinson disease-related neurodegeneration *in vivo*. *Proceedings of the National Academy of Sciences*. **111**(27), 9977–9982. URL https://doi.org/10.1073/pnas.1402134111.

London, J., Ndiaye, F. K., Bui, L. C., Souchet, B., Daubigney, F., Magnan, C., Luquet, S., Dairou, J., Janel, N., and Rouch, C. (2019). Alterations in the serotonin and dopamine pathways by cystathionine beta synthase overexpression in murine brain. *Molecular Neurobiology*. **56**(6), 3958–3971. URL https://doi.org/10.1007/s12035-018-1323-2.

Long, W. C., Pruisner, P., Swiney, K. M., and Foy, R. J. (2019). Effects of ocean acidification on the respiration and feeding of juvenile red and blue king crabs (*Paralithodes camtschaticus* and *P. platypus*). *ICES Journal of Marine Science*. URL https://doi.org/10.1093/icesjms/fsz090.

Lopes, A. F., Morais, P., Pimentel, M., Rosa, R., Munday, P. L., Gonçalves, E. J., and Faria, A. M. (2016). Behavioural lateralization and shoaling cohesion of fish larvae altered under ocean acidification. *Marine Biology*. **163**(12), 243. URL https://doi.org/10.1007/s00227-016-3026-4.

Love, M. I., Huber, W., and Anders, S. (2014). Moderated estimation of fold change and dispersion for RNA-seq data with DESeq2. *Genome Biology*. **15**(12), 550. URL https://doi.org/10.1186/s13059-014-0550-8.

Lu, M., Hu, L.-F., Hu, G., and Bian, J.-S. (2008). Hydrogen sulfide protects astrocytes against H_2O_2-induced neural injury via enhancing glutamate uptake. *Free Radical Biology and Medicine*. **45**(12), 1705–1713. URL https://doi.org/10.1016/j.freeradbiomed.2008.09.014.

Lu, M., Zhao, F.-F., Tang, J.-J., Su, C.-J., Fan, Y., Ding, J.-H., Bian, J.-S., and Hu, G. (2012). The neuroprotection of hydrogen sulfide against MPTP-induced dopaminergic neuron degeneration involves uncoupling protein 2 rather than ATP-sensitive potassium channels. *Antioxidants and Redox Signaling*. **17**(6), 849–859. URL https://doi.org/10.1089/ars.2011.4507.

Lu, Y., Qiu, Y., Chen, P., Chang, H., Guo, L., Zhang, F., Ma, L., Zhang, C., Zheng, X., Xiao, J., Zhong, R., Han, L., Xu, X., Zhang, Y., Li, D., Zhong, G., Boyton, R., Huang, Y., He, Y., Hu, R., Wei, B., and Wang, H. (2019). ER-localized Hrd1 ubiquitinates and inactivates Usp15 to promote TLR4-induced inflammation during bacterial infection. *Nature Microbiology*. **4**(12), 2331–2346. URL https://doi.org/10.1038/s41564-019-0542-2.

Lummis, S. C. (1990). GABA receptors in insects. *Comparative Biochemistry and Physiology Part C: Comparative Pharmacology*. **95**(1), 1–8. URL https://doi.org/10.1016/0742-8413(90)90073-I.

Lunt, G. (1991). GABA and GABA receptors in invertebrates. *Seminars in Neuroscience*. **3**(3), 251–258. URL https://doi.org/10.1016/1044-5765(91)90022-G.

Lynch, J. W. (2004). Molecular structure and function of the glycine receptor chloride channel. *Physiological Reviews*. **84**(4), 1051–1095. URL https://doi.org/10.1152/physrev.00042.2003.

Ma, B.-F., Xie, M.-J., and Zhou, M. (2012). Bicarbonate efflux via $GABA_A$ receptors depolarizes membrane potential and inhibits two-pore domain potassium channels of astrocytes in rat hippocampal slices. *Glia*. **60**(11), 1761–1772. URL https://doi.org/10.1002/glia.22395.

Maas, A. E., Lawson, G. L., and Tarrant, A. M. (2015). Transcriptome-wide analysis of the response of the thecosome pteropod *Clio pyramidata* to short-term CO_2 exposure.

Comparative Biochemistry and Physiology Part D: Genomics and Proteomics. **16**, 1–9. URL https://doi.org/10.1016/j.cbd.2015.06.002.

MacFarlane, P. M. and Di Fiore, J. M. (2018). Myo-inositol effects on the developing respiratory neural control system. In *Arterial Chemoreceptors* (eds. E.B. Gauda, M.E. Monteiro, N. Prabhakar, C. Wyatt, and H.D. Schultz). Advances in Experimental Medicine and Biology. pp. 159–166. Springer, Cham. URL https://doi.org/10.1007/978-3-319-91137-3_20.

Magoski, N. S. and Bulloch, A. G. (1999). Dopamine activates two different receptors to produce variability in sign at an identified synapse. *Journal of Neurophysiology*. **81**(3), 1330–1340. URL https://doi.org/10.1152/jn.1999.81.3.1330.

Maier, T., Güell, M., and Serrano, L. (2009). Correlation of mRNA and protein in complex biological samples. *FEBS Letters*. **583**(24), 3966–3973. URL https://doi.org/10.1016/j.febslet.2009.10.036.

Maitland, M. E. R., Kuljanin, M., Wang, X., Lajoie, G. A., and Schild-Poulter, C. (2021). Proteomic analysis of ubiquitination substrates reveals a CTLH E3 ligase complex-dependent regulation of glycolysis. *The FASEB Journal*. **35**(9), e21825. URL https://doi.org/10.1096/fj.202100664R.

Maneja, R., Piatkowski, U., and Melzner, F. (2011). Effects of ocean acidification on statolith calcification and prey capture in early life cuttlefish, *Sepia officinalis*. *Journal of Shellfish Research*. **30**(3), 1011. URL https://doi.org/10.2983/035.030.0342.

Manev, H., Peričić, D., and Anić-Stojiljković, S. (1987). Sex differences in the sensitivity of CBA mice to convulsions induced by GABA antagonists are age-dependent. *Psychopharmacology*. **91**(2), 226–229. URL https://doi.org/10.1007/BF00217068.

Manni, M., Berkeley, M. R., Seppey, M., Simão, F. A., and Zdobnov, E. M. (2021). BUSCO update: Novel and streamlined workflows along with broader and deeper phylogenetic coverage for scoring of eukaryotic, prokaryotic, and viral genomes. *Molecular Biology and Evolution*. **38**(10), 4647–4654. URL https://doi.org/10.1093/molbev/msab199.

Manríquez, P. H., Jara, M. E., Mardones, M. L., Navarro, J. M., Torres, R., Lardies, M. A., Vargas, C. A., Duarte, C., Widdicombe, S., and Salisbury, J. (2013). Ocean acidification disrupts prey responses to predator cues but not net prey shell growth in *Concholepas concholepas* (loco). *PLoS One*. **8**(7), e68643. URL https://doi.org/10.1371/journal.pone.0068643.

Manríquez, P. H., Jara, M. E., Mardones, M. L., Torres, R., Navarro, J. M., Lardies, M. A., Vargas, C. A., Duarte, C., and Lagos, N. A. (2014a). Ocean acidification affects predator avoidance behaviour but not prey detection in the early ontogeny of a keystone species. *Marine Ecology Progress Series*. **502**, 157–167. URL https://doi.org/10.3354/meps10703.

Manríquez, P. H., Jara, M. E., Torres, R., Mardones, M. L., Lagos, N. A., Lardies, M. A., Vargas, C. A., Duarte, C., and Navarro, J. M. (2014b). Effects of ocean acidification on larval development and early post-hatching traits in *Concholepas concholepas* (loco). *Marine Ecology Progress Series*. **514**, 87–103. URL https://doi.org/10.3354/meps10951.

Marangon, E., Goldenberg, S. U., and Nagelkerken, I. (2019). Ocean warming increases availability of crustacean prey via riskier behavior. *Behavioral Ecology*. **31**(2), 287–291. URL https://doi.org/10.1093/beheco/arz196.

Marden, J. H. (2008). Quantitative and evolutionary biology of alternative splicing: How changing the mix of alternative transcripts affects phenotypic plasticity and reaction norms. *Heredity*. **100**(2), 111–120. URL https://doi.org/10.1038/sj.hdy.6800904.

Marder, E. and Paupardin-Tritsch, D. (1978). The pharmacological properties of some crustacean neuronal acetylcholine, gamma-aminobutyric acid, and L-glutamate responses. *The Journal of Physiology*. **280**(1), 213–236. URL https://doi.org/10.1113/jphysiol.1978.sp012381.

Marčeta, T., Matozzo, V., Alban, S., Badocco, D., Pastore, P., and Marin, M. G. (2020). Do males and females respond differently to ocean acidification? An experimental study with the sea urchin *Paracentrotus lividus*. *Environmental Science and Pollution Research*. **27**, 39516–39530. URL https://doi.org/10.1007/s11356-020-10040-7.

Masiulis, S., Desai, R., Uchański, T., Martin, I. S., Laverty, D., Karia, D., Malinauskas, T., Zivanov, J., Pardon, E., and Kotecha, A. (2019). $GABA_A$ receptor signalling mechanisms revealed by structural pharmacology. *Nature*. **565**(7740), 454–459. URL https://doi.org/10.1038/s41586-018-0832-5.

Masson-Delmotte, V., Sculz, M., Abe-Ouchi, A., Beer, J., Ganopolski, A., González Rouco, J., Jansen, E., Lambeck, K., Luterbacher, J., Naish, T., Osborn, T., Otto-Bliesner, B., Quinn, T., Ramesh, R., Rojas, M., Shao, X., and Timmermann, A. (2013). Information from paleoclimate archives. In *Climate change 2013: The physical science basis. Contribution of working group I to the fifth assessment report of the Intergovernmental Panel on Climate Change* (eds. T. Stocker, D. Qin, G.K. Plattner, M. Tignor,

S. Allen, J. Boschung, A. Nauels, Y. Xia, V. Bex, and P. Midgley). Cambridge University Press, Cambridge, New York. URL https://doi.org/10.1017/CBO9781107415324.013.

Mather, J. A. (2006). Behaviour development: A cephalopod perspective. *International Journal of Comparative Psychology*. **19**(1), 98–115. URL https://escholarship.org/uc/item/5hb932x3.

Matsui, T., Jiang, P., Nakano, S., Sakamaki, Y., Yamamoto, H., and Mizushima, N. (2018). Autophagosomal YKT6 is required for fusion with lysosomes independently of syntaxin 17. *Journal of Cell Biology*. **217**(8), 2633–2645. URL https://doi.org/10.1083/jcb.201712058.

Mazurais, D., Servili, A., Le Bayon, N., Gislard, S., Madec, L., and Zambonino-Infante, J.-L. (2020). Long-term exposure to near-future ocean acidification does not affect the expression of neurogenesis-and synaptic transmission-related genes in the olfactory bulb of European sea bass (*Dicentrarchus labrax*). *Journal of Comparative Physiology B*. **190**, 161–167.

McCabe, R., Estrade, P., Middleton, J., Melville, W., Roughan, M., and Lenain, L. (2010). Temperature variability in a shallow, tidally isolated coral reef lagoon. *Journal of Geophysical Research: Oceans*. **115**, C12011. URL https://doi.org/10.1029/2009JC006023.

McCarthy, I. D., Whiteley, N. M., Fernandez, W. S., Ragagnin, M. N., Cornwell, T. O., Suckling, C. C., and Turra, A. (2019). Elevated pCO_2 does not impair performance in autotomised individuals of the intertidal predatory starfish *Asterias rubens* (Linnaeus, 1758). *Marine Environmental Research*. p. 104841. URL https://doi.org/10.1016/j.marenvres.2019.104841.

McCormick, M. I., Watson, S.-A., Simpson, S. D., and Allan, B. J. (2018). Effect of elevated CO_2 and small boat noise on the kinematics of predator–prey interactions. *Proceedings of the Royal Society B: Biological Sciences*. **285**(1875), 20172650. URL https://doi.org/10.1098/rspb.2017.2650.

McNeil, B. I., Metzl, N., Key, R. M., Matear, R. J., and Corbiere, A. (2007). An empirical estimate of the southern ocean air-sea CO_2 flux. *Global Biogeochemical Cycles*. **21**(3), GB3011. URL https://doi.org/10.1029/2007GB002991.

McNeil, B. I. and Sasse, T. P. (2016). Future ocean hypercapnia driven by anthropogenic amplification of the natural CO_2 cycle. *Nature*. **529**(7586), 383–386. URL https://doi.org/10.1038/nature16156.

Mehrbach, C., Culberson, C., Hawley, J., and Pytkowicx, R. (1973). Measurement of the apparent dissociation constants of carbonic acid in seawater at atmospheric pressure 1. *Limnology and Oceanography*. **18**(6), 897–907. URL https://doi.org/10.4319/lo.1973.18.6.0897.

Mele, M., Leal, G., and Duarte, C. B. (2016). Role of $GABA_A$ R trafficking in the plasticity of inhibitory synapses. *Journal of Neurochemistry*. **139**(6), 997–1018. URL https://doi.org/10.1111/jnc.13742.

Melzner, F., Gutowska, M., Langenbuch, M., Dupont, S., Lucassen, M., Thorndyke, M., Bleich, M., and Pörtner, H.-O. (2009). Physiological basis for high CO_2 tolerance in marine ectothermic animals: Pre-adaptation through lifestyle and ontogeny? *Biogeosciences*. **6**(10), 2313–2331. URL https://doi.org/10.5194/bg-6-2313-2009.

Melzner, F., Mark, F. C., Seibel, B. A., and Tomanek, L. (2020). Ocean acidification and coastal marine invertebrates: Tracking CO_2 effects from seawater to the cell. *Annual Review of Marine Science*. **12**(1), 499–523. URL https://doi.org/10.1146/annurev-marine-010419-010658.

Menge, B. and Branch, G. (2001). Rocky intertidal communities. In *Marine Community Ecology* (eds. M. Bertness, S. Gaines, and M. Hay). pp. 221–251. Sinauer Associates, Sunderland, Massachusetts.

Mentis, A. A., Dardiotis, E., Katsouni, E., and Chrousos, G. P. (2021). From warrior genes to translational solutions: Novel insights into monoamine oxidases (MAOs) and aggression. *Translational Psychiatry*. **11**(1), 130. URL https://doi.org/10.1038/s41398-021-01257-2.

Menu-Courey, K., Noisette, F., Piedalue, S., Daoud, D., Blair, T., Blier, P. U., Azetsu-Scott, K., and Calosi, P. (2018). Energy metabolism and survival of the juvenile recruits of the American lobster (*Homarus americanus*) exposed to a gradient of elevated seawater pCO_2. *Marine Environmental Research*. **143**, 111–123. URL https://doi.org/10.1016/j.marenvres.2018.10.002.

Merico, D., Isserlin, R., Stueker, O., Emili, A., and Bader, G. D. (2010). Enrichment map: A network-based method for gene-set enrichment visualization and interpretation. *PloS One*. **5**(11), e13984. URL https://doi.org/10.1371/journal.pone.0013984.

Meseck, S. L., Sennefelder, G., Krisak, M., and Wikfors, G. H. (2020). Physiological feeding rates and cilia suppression in blue mussels (*Mytilus edulis*) with increased levels of dissolved carbon dioxide. *Ecological Indicators*. **117**, 106675. URL https://doi.org/10.1016/j.ecolind.2020.106675.

Meyer, D. K., Olenik, C., Hofmann, F., Barth, H., Leemhuis, J., Brünig, I., Aktories, K., and Nörenberg, W. (2000). Regulation of somatodendritic $GABA_A$ receptor channels in rat hippocampal neurons: Evidence for a role of the small GTPase Rac1. *The Journal of Neuroscience*. **20**(18), 6743–6751. URL https://doi.org/10.1523/jneurosci.20-18-06743.2000.

Meyer-Kaiser, K. S., Houlihan, E. P., Wheeler, J. D., McCorkle, D. C., and Mullineaux, L. S. (2019). Behavioral response of Eastern oyster *Crassostrea virginica* larvae to a chemical settlement cue is not impaired by low pH. *Marine Ecology Progress Series*. **623**, 13–24. URL https://doi.org/10.3354/meps13014.

Miller, M. W. (2019). GABA as a neurotransmitter in gastropod molluscs. *The Biological Bulletin*. **236**(2), 144–156. URL https://doi.org/10.1086/701377.

Mizutani, A., Sanuki, R., Kakimoto, K., Kojo, S., and Taketani, S. (2007). Involvement of 101F6, a homologue of cytochrome b561, in the reduction of ferric ions. *The Journal of Biochemistry*. **142**(6), 699–705. URL https://doi.org/10.1093/jb/mvm185.

Moccia, F., Di Cristo, C., Winlow, W., and Di Cosmo, A. (2009). $GABA_A$- and AMPA-like receptors modulate the activity of an identified neuron within the central pattern generator of the pond snail *Lymnaea stagnalis*. *Invertebrate Neuroscience*. **9**(1), 29–41. URL https://doi.org/10.1007/s10158-009-0086-x.

Monroe, A. A., Schunter, C., Welch, M. J., Munday, P. L., and Ravasi, T. (2021). Molecular basis of parental contributions to the behavioural tolerance of elevated pCO_2 in a coral reef fish. *Proceedings of the Royal Society B: Biological Sciences*. **288**(1964), 20211931. URL https://doi.org/10.1098/rspb.2021.1931.

Moody Jr, W. (1981). The ionic mechanism of intracellular pH regulation in crayfish neurones. *The Journal of Physiology*. **316**(1), 293–308. URL https://doi.org/10.1113/jphysiol.1981.sp013788.

Mooney, T. A., Hanlon, R. T., Christensen-Dalsgaard, J., Madsen, P. T., Ketten, D. R., and Nachtigall, P. E. (2010). Sound detection by the longfin squid (*Loligo pealeii*) studied with auditory evoked potentials: Sensitivity to low-frequency particle motion

and not pressure. *Journal of Experimental Biology*. **213**(21), 3748–3759. URL https://doi.org/10.1242/jeb.048348.

de la Mora, M. P., Ferré, S., and Fuxe, K. (1997). GABA-dopamine receptor-receptor interactions in neostriatal membranes of the rat. *Neurochemical Research*. **22**(8), 1051–1054. URL https://doi.org/10.1023/A:1022439212836.

Moreau, P., Moreau, K., Segarra, A., Tourbiez, D., Travers, M.-A., Rubinsztein, D. C., and Renault, T. (2015). Autophagy plays an important role in protecting Pacific oysters from OsHV-1 and *Vibrio aestuarianus* infections. *Autophagy*. **11**(3), 516–526. URL https://doi.org/10.1080/15548627.2015.1017188.

Moroz, L. L., Edwards, J. R., Puthanveettil, S. V., Kohn, A. B., Ha, T., Heyland, A., Knudsen, B., Sahni, A., Yu, F., and Liu, L. (2006). Neuronal transcriptome of *Aplysia*: Neuronal compartments and circuitry. *Cell*. **127**(7), 1453–1467. URL https://doi.org/10.1016/j.cell.2006.09.052.

Morse, D. E., Duncan, H., Hooker, N., Baloun, A., and Young, G. (1980). GABA induces behavioral and developmental metamorphosis in planktonic molluscan larvae. *Federation Proceedings*. **39**(14), 3237–3241. URL http://europepmc.org/abstract/MED/6254810.

Morse, D. E., Hooker, N., Duncan, H., and Jensen, L. (1979). γ-aminobutyric acid, a neurotransmitter, induces planktonic abalone larvae to settle and begin metamorphosis. *Science*. **204**(4391), 407–410. URL https://doi.org10.1126/science.204.4391.407.

Moura, É., Pimentel, M., Santos, C. P., Sampaio, E., Pegado, M. R., Lopes, V. M., and Rosa, R. (2019). Cuttlefish early development and behavior under future high CO_2 conditions. *Frontiers in Physiology*. **10**(975). URL https://doi.org/10.3389/fphys.2019.00975.

Moya, A., Howes, E. L., Lacoue-Labarthe, T., Forêt, S., Hanna, B., Medina, M., Munday, P. L., Ong, J., Teyssié, J., and Torda, G. (2016). Near-future pH conditions severely impact calcification, metabolism and the nervous system in the pteropod *Heliconoides inflatus*. *Global Change Biology*. **22**(12), 3888–3900. URL https://doi.org/10.1111/gcb.13350.

Moynihan, M. (1983). Notes on the behavior of *Idiosepius pygmaeus* (Cephalopoda; Idiosepiidae). *Behaviour*. **85**(1), 42–57. URL https://www.jstor.org/stable/4534254.

Mukherjee, J., Wong, K. K., Chandramouli, K. H., Qian, P.-Y., Leung, P. T., Wu, R. S., and Thiyagarajan, V. (2013). Proteomic response of marine invertebrate larvae to ocean acidification and hypoxia during metamorphosis and calcification. *The Journal of Experimental Biology*. **216**, 4580–4589. URL https://doi.org/10.1242/jeb.094516.

Munday, P. L., Dixson, D. L., Donelson, J. M., Jones, G. P., Pratchett, M. S., Devitsina, G. V., and Døving, K. B. (2009). Ocean acidification impairs olfactory discrimination and homing ability of a marine fish. *Proceedings of the National Academy of Sciences*. **106**(6), 1848–1852. URL https://doi.org/10.1073/pnas.0809996106.

Munday, P. L., Jarrold, M. D., and Nagelkerken, I. (2019). Ecological effects of elevated CO_2 on marine and freshwater fishes: From individual to community effects. In *Carbon Dioxide* (eds. M. Grosell, P.L. Munday, A.P. Farrell, and C.J. Brauner). Fish Physiology. pp. 323–368. Academic Press, Cambridge, San Diego, Oxford, London. URL https://doi.org/10.1016/bs.fp.2019.07.005.

Munday, P. L., Welch, M. J., Allan, B. J., Watson, S.-A., McMahon, S. J., and McCormick, M. I. (2016). Effects of elevated CO_2 on predator avoidance behaviour by reef fishes is not altered by experimental test water. *PeerJ*. **4**, e2501. URL https://doi.org/10.7717/peerj.2501.

Muntz, W. R. A. (1999). Visual systems, behaviour, and environment in cephalopods. In *Adaptive Mechanisms in the Ecology of Vision* (eds. S.N. Archer, M.B.A. Djamgoz, E.R. Loew, J.C. Partridge, and S. Vallerga). pp. 467–483. Springer Netherlands, Dordrecht. URL https://doi.org/10.1007/978-94-017-0619-3_15.

Naffaa, M. M., Hung, S., Chebib, M., Johnston, G. A. R., and Hanrahan, J. R. (2017). GABA-ρ receptors: Distinctive functions and molecular pharmacology. *British Journal of Pharmacology*. **174**(13), 1881–1894. URL https://doi.org/10.1111/bph.13768.

Nagelkerken, I., Doney, S. C., and Munday, P. (2019). Consequences of anthropogenic changes in the sensory landscape of marine animals. In *Oceanography and Marine Biology: An Annual Review* (eds. S.J. Hawkins, A.L. Allcock, A.E. Bates, L.B. Firth, I.P. Smith, S.E. Swearer, and P.A. Todd). CRC Press, London, New York.

Nagelkerken, I. and Munday, P. L. (2015). Animal behaviour shapes the ecological effects of ocean acidification and warming: Moving from individual to community-level responses. *Global Change Biology*. **22**(3), 974–989. URL https://doi.org/10.1111/gcb.13167.

Nair, U., Jotwani, A., Geng, J., Gammoh, N., Richerson, D., Yen, W.-L., Griffith, J., Nag, S., Wang, K., Moss, T., Baba, M., McNew, J., Jiang, X., Reggiori, F., Melia, T., and Klionsky, D. (2011). SNARE proteins are required for macroautophagy. *Cell*. **146**(2), 290–302. URL https://doi.org/10.1016/j.cell.2011.06.022.

Nakajima, K.-i. and Marunaka, Y. (2016). Intracellular chloride ion concentration in differentiating neuronal cell and its role in growing neurite. *Biochemical and Biophysical Research Communications*. **479**(2), 338–342. URL https://doi.org/10.1016/j.bbrc.2016.09.075.

Nardi, A., Benedetti, M., d'Errico, G., Fattorini, D., and Regoli, F. (2018). Effects of ocean warming and acidification on accumulation and cellular responsiveness to cadmium in mussels *Mytilus galloprovincialis*: Importance of the seasonal status. *Aquatic Toxicology*. **204**, 171–179. URL https://doi.org/10.1016/j.aquatox.2018.09.009.

Narlikar, G. J., Fan, H.-Y., and Kingston, R. E. (2002). Cooperation between complexes that regulate chromatin structure and transcription. *Cell*. **108**(4), 475–487. URL https://doi.org/10.1016/S0092-8674(02)00654-2.

Narusuye, K., Nakao, T., Abe, R., Nagatomi, Y., Hirase, K., and Ozoe, Y. (2007). Molecular cloning of a GABA receptor subunit from *Laodelphax striatella* (Fallén) and patch clamp analysis of the homo-oligomeric receptors expressed in a *Drosophila* cell line. *Insect Molecular Biology*. **16**(6), 723–733. URL https://doi.org/10.1111/j.1365-2583.2007.00766.x.

Nelson, K. S., Baltar, F., Lamare, M. D., and Morales, S. E. (2020). Ocean acidification affects microbial community and invertebrate settlement on biofilms. *Scientific Reports*. **10**(1), 1–9. URL https://doi.org/10.1038/s41598-020-60023-4.

Nezlin, L. and Voronezhskaya, E. (1997). GABA-immunoreactive neurones and interactions of GABA with serotonin and fmrfamide in a peripheral sensory ganglion of the pond snail *Lymnaea stagnalis*. *Brain Research*. **772**(1-2), 217–225.

Ng, J., Papandreou, A., Heales, S. J., and Kurian, M. A. (2015). Monoamine neurotransmitter disorders—clinical advances and future perspectives. *Nature Reviews Neurology*. **11**(10), 567–584. URL https://doi.org/10.1038/nrneurol.2015.172.

Nguyen, T. V., Alfaro, A. C., Young, T., Ravi, S., and Merien, F. (2018). Metabolomics study of immune responses of New Zealand greenshell™ mussels (*Perna canaliculus*) infected with pathogenic *Vibrio sp*. *Marine Biotechnology*. **20**(3), 396–409. URL https://doi.org/10.1007/s10126-018-9804-x.

Nicola, S. M., Surmeier, D. J., and Malenka, R. C. (2000). Dopaminergic modulation of neuronal excitability in the striatum and nucleus accumbens. *Annual Review of Neuroscience*. **23**(1), 185–215. URL https://doi.org/10.1146/annurev.neuro.23.1.185.

Niepoth, N. and Bendesky, A. (2020). How natural genetic variation shapes behavior. *Annual Review of Genomics and Human Genetics*. **21**, 10.1–10.27. URL https://doi.org/10.1146/annurev-genom-111219-080427.

van Nierop, P., Keramidas, A., Bertrand, S., van Minnen, J., Gouwenberg, Y., Bertrand, D., and Smit, A. B. (2005). Identification of molluscan nicotinic acetylcholine receptor (nAChR) subunits involved in formation of cation-and anion-selective nachrs. *Journal of Neuroscience*. **25**(46), 10617–10626. URL https://doi.org/10.1523/JNEUROSCI.2015-05.2005.

Nilsson, G. E., Dixson, D. L., Domenici, P., McCormick, M. I., Sørensen, C., Watson, S.-A., and Munday, P. L. (2012). Near-future carbon dioxide levels alter fish behaviour by interfering with neurotransmitter function. *Nature Climate Change*. **2**(3), 201–204. URL https://doi.org/10.1038/NCLIMATE1352.

Nilsson, G. E. and Lefevre, S. (2016). Physiological challenges to fishes in a warmer and acidified future. *Physiology*. **31**(6), 409–417. URL https://doi.org/10.1152/physiol.00055.2015.

Nomura, J., Hosoi, T., Kaneko, M., Ozawa, K., Nishi, A., and Nomura, Y. (2016). Neuroprotection by endoplasmic reticulum stress-induced HRD1 and chaperones: Possible therapeutic targets for Alzheimer's and Parkinson's disease. *Medical Sciences*. **4**(3), 14. URL https://doi.org/10.3390/medsci4030014.

Norekian, T. P. (1999). GABAergic excitatory synapses and electrical coupling sustain prolonged discharges in the prey capture neural network of *Clione limacina*. *Journal of Neuroscience*. **19**(5), 1863–1875. URL https://doi.org/10.1523/JNEUROSCI.19-05-01863.1999.

Norekian, T. P. and Malyshev, A. Y. (2005). Coordinated excitatory effect of GABAergic interneurons on three feeding motor programs in the mollusk *Clione limacina*. *Journal of Neurophysiology*. **93**(1), 305–315. URL https://doi.org/10.1152/jn.00722.2004.

Norekian, T. P. and Satterlie, R. A. (1993). FMRFamide and GABA produce functionally opposite effects on prey-capture reactions in the pteropod mollusk *Clione limacina*. *The Biological Bulletin*. **185**(2), 248–262. URL https://doi.org/10.2307/1542005.

Numakura, Y., Uemura, R., Tanaka, M., Izawa, T., Yamate, J., Kuramoto, T., Kaneko, T., Mashimo, T., Yamamoto, T., Serikawa, T., and Kuwamura, M. (2021). PHF24 is expressed in the inhibitory interneurons in rats. *Experimental Animals*. **70**(1), 137–143. URL https://doi.org/10.1538/expanim.20-0105.

O'Donnell, S. (2018). The neurobiology of climate change. *The Science of Nature*. **105**(1), 1–7. URL https://doi.org/10.1007/s00114-017-1538-5.

Ohnuma, S.-i. and Harris, W. A. (2003). Neurogenesis and the cell cycle. *Neuron*. **40**(2), 199–208. URL https://doi.org/10.1016/S0896-6273(03)00632-9.

Olsen, K., Paul, V. J., and Ross, C. (2015). Direct effects of elevated temperature, reduced pH, and the presence of macroalgae (*Dictyota spp.*) on larvae of the Caribbean coral *Porites astreoides*. *Bulletin of Marine Science*. **91**(2), 255–270. URL https://doi.org/10.5343/bms.2014.1050.

Olsen, R. W. and Sieghart, W. (2008). International union of pharmacology. LXX. Subtypes of γ-aminobutyric acid a receptors: Classification on the basis of subunit composition, pharmacology, and function. Update. *Pharmacological Reviews*. **60**(3), 243–260. URL https://doi.org/10.1124/pr.108.00505.

Olsen, R. W. and Sieghart, W. (2009). $GABA_A$ receptors: Subtypes provide diversity of function and pharmacology. *Neuropharmacology*. **56**(1), 141–148. URL https://doi.org/10.1016/j.neuropharm.2008.07.045.

Ong, S. T., Shan Ho, J. Z., Ho, B., and Ding, J. L. (2006). Iron-withholding strategy in innate immunity. *Immunobiology*. **211**(4), 295–314. URL https://doi.org/10.1016/j.imbio.2006.02.004.

Opendak, M. and Gould, E. (2015). Adult neurogenesis: A substrate for experience-dependent change. *Trends in Cognitive Sciences*. **19**(3), 151–161. URL https://doi.org/10.1016/j.tics.2015.01.001.

Orr, J. C., Fabry, V. J., Aumont, O., Bopp, L., Doney, S. C., Feely, R. A., Gnanadesikan, A., Gruber, N., Ishida, A., and Joos, F. (2005). Anthropogenic ocean acidification over the twenty-first century and its impact on calcifying organisms. *Nature*. **437**(7059), 681–686. URL https://doi.org/10.1038/nature04095.

Osipo, C., Golde, T. E., Osborne, B. A., and Miele, L. A. (2008). Off the beaten pathway: The complex cross talk between Notch and NF-KB. *Laboratory Investigation*. **88**(1), 11–17. URL http://dx.doi.org/10.1038/labinvest.3700700.

Ou, M., Hamilton, T. J., Eom, J., Lyall, E. M., Gallup, J., Jiang, A., Lee, J., Close, D. A., Yun, S.-S., and Brauner, C. J. (2015). Responses of pink salmon to CO_2-induced aquatic acidification. *Nature Climate Change*. **5**(10), 950. URL https://doi.org/10.1038/nclimate2694.

Owens, D. F. and Kriegstein, A. R. (2002). Is there more to GABA than synaptic inhibition? *Nature Reviews Neuroscience*. **3**(9), 715. URL https://doi.org/10.1038/nrn919.

Padilla-Gamiño, J. L., Kelly, M. W., Evans, T. G., and Hofmann, G. E. (2013). Temperature and CO_2 additively regulate physiology, morphology and genomic responses of larval sea urchins, *Strongylocentrotus purpuratus*. *Proceedings of the Royal Society of London B: Biological Sciences*. **280**(1759), 20130155. URL https://doi.org/10.1098/rspb.2013.0155.

Palaga, T., Miele, L., Golde, T. E., and Osborne, B. A. (2003). TCR-mediated notch signaling regulates proliferation and IFN-γ production in peripheral T cells. *The Journal of Immunology*. **171**(6), 3019–3024. URL https://doi.org/10.4049/jimmunol.171.6.3019.

Palmer, C. R. and Kristan Jr, W. B. (2011). Contextual modulation of behavioral choice. *Current Opinion in Neurobiology*. **21**(4), 520–526. URL https://doi.org/10.1016/j.conb.2011.05.003.

Palmer, M., Calvé, M. R., and Adamo, S. A. (2006). Response of female cuttlefish *Sepia officinalis* (Cephalopoda) to mirrors and conspecifics: Evidence for signaling in female cuttlefish. *Animal Cognition*. **9**(2), 151–155. URL https://doi.org/10.1007/s10071-005-0009-0.

Panchin, Y. V., Sadreev, R., and Arshavsky, Y. I. (1995). Control of locomotion in marine mollusc *Clione limacina* X. Effects of acetylcholine antagonists. *Experimental Brain Research*. **106**(1), 135–144. URL https://doi.org/10.1007/BF00241363.

Panchin, Y. V. and Sadreyev, R. I. (1997). Effects of acetylcholine and glutamate on isolated neurons of locomotory network of *Clione*. *NeuroReport*. **8**(13), 2897–2901.

Pansch, C., Hattich, G. S., Heinrichs, M. E., Pansch, A., Zagrodzka, Z., and Havenhand, J. N. (2018). Long-term exposure to acidification disrupts reproduction in a marine invertebrate. *PloS One*. **13**(2), e0192036. URL https://doi.org/10.1371/journal.pone.0192036.

Park, S., Ahn, I.-Y., Sin, E., Shim, J., and Kim, T. (2019). Ocean freshening and acidification differentially influences mortality and behavior of the Antarctic amphipod *Gondogeneia antarctica*. *Marine Environmental Research*. p. 104847. URL https://doi.org/10.1016/j.marenvres.2019.104847.

Patel, S. B. and Bellini, M. (2008). The assembly of a spliceosomal small nuclear ribonucleoprotein particle. *Nucleic Acids Research*. **36**(20), 6482–6493. URL https://doi.org/10.1093/nar/gkn658.

Patro, R., Duggal, G., Love, M. I., Irizarry, R. A., and Kingsford, C. (2017). Salmon provides fast and bias-aware quantification of transcript expression. *Nature Methods*. **14**(4), 417–419. URL https://doi.org/10.1038/nmeth.4197.

Paula, J. R., Repolho, T., Pegado, M. R., Thörnqvist, P.-O., Bispo, R., Winberg, S., Munday, P. L., and Rosa, R. (2019). Neurobiological and behavioural responses of cleaning mutualisms to ocean warming and acidification. *Scientific Reports*. **9**(1), 1–10. URL https://doi.org/10.1038/s41598-019-49086-0.

van de Pavert, S. A., Kantardzhieva, A., Malysheva, A., Meuleman, J., Versteeg, I., Levelt, C., Klooster, J., Geiger, S., Seeliger, M. W., Rashbass, P., Le Bivic, A., and Wijnholds, J. (2004). Crumbs homologue 1 is required for maintenance of photoreceptor cell polarization and adhesion during light exposure. *Journal of Cell Science*. **117**(18), 4169–4177. URL https://doi.org/10.1242/jcs.01301.

Pearce, C. M. and Scheibling, R. E. (1990). Induction of metamorphosis of larvae of the green sea urchin, *Strongylocentrotus droebachiensis*, by coralline red algae. *The Biological Bulletin*. **179**(3), 304–311. URL https://doi.org/10.2307/1542322.

Pearstein, E., Cattaert, D., and Clarac, F. (1996). Crayfish sensory terminals and motor neurones exhibit two distinct types of GABA receptors. *Journal of Comparative Physiology A*. **180**(1), 71–79. URL https://doi.org/10.1007/s003590050028.

Pechenik, J., Pires, A., Trudel, J., Levy, M., Dooley, T., Resnikoff, A., and Taylor, R. (2019). Impact of ocean acidification on growth, onset of competence, and perception of cues for metamorphosis in larvae of the slippershell snail, *Crepidula fornicata*. *Marine Biology*. **166**(10), 128. URL https://doi.org/10.1007/s00227-019-3576-3.

Pecquet, A., Dorey, N., and Chan, K. Y. K. (2017). Ocean acidification increases larval swimming speed and has limited effects on spawning and settlement of a robust fouling bryozoan, *Bugula neritina*. *Marine Pollution Bulletin*. **124**(2), 903–910. URL https://doi.org/10.1016/j.marpolbul.2017.02.057.

Pellikka, M., Tanentzapf, G., Pinto, M., Smith, C., McGlade, C. J., Ready, D. F., and Tepass, U. (2002). Crumbs, the *Drosophila* homologue of human CRB1/RP12, is essential for photoreceptor morphogenesis. *Nature*. **416**(6877), 143–149. URL https://doi.org/10.1038/nature721.

Peng, C., Zhao, X., Liu, S., Shi, W., Han, Y., Guo, C., Peng, X., Chai, X., and Liu, G. (2017). Ocean acidification alters the burrowing behaviour, Ca^{2+}/Mg^{2+}-ATPase activity, metabolism, and gene expression of a bivalve species, *Sinonovacula constricta*. *Marine Ecology Progress Series*. **575**, 107–117. URL https://doi.org/10.3354/meps12224.

Peng, S., Zhang, Y., Zhang, J., Wang, H., and Ren, B. (2011). Glutamate receptors and signal transduction in learning and memory. *Molecular Biology Reports*. **38**(1), 453–460. URL https://doi.org/10.1007/s11033-010-0128-9.

Pentreath, V. (1989). Invertebrate glial cells. *Comparative Biochemistry and Physiology Part A: Physiology*. **93**(1), 77–83. URL https://doi.org/10.1016/0300-9629(89)90194-1.

Pereira, H. M., Leadley, P. W., Proença, V., Alkemade, R., Scharlemann, J. P. W., Fernandez-Manjarrés, J. F., Araújo, M. B., Balvanera, P., Biggs, R., Cheung, W. W. L., Chini, L., Cooper, H. D., Gilman, E. L., Guénette, S., Hurtt, G. C., Huntington, H. P., Mace, G. M., Oberdorff, T., Revenga, C., Rodrigues, P., Scholes, R. J., Sumaila, U. R., and Walpole, M. (2010). Scenarios for global biodiversity in the 21st century. *Science*. **330**(6010), 1496–1501. URL https://doi.org/10.1126/science.1196624.

Peričić, D., Manev, H., and Geber, J. (1986). Sex related differences in the response of mice, rats and cats to administration of picrotoxin. *Life Sciences*. **38**(10), 905–913. URL https://doi.org/10.1016/0024-3205(86)90258-4Getrightsandcontent.

Picot, S., Morga, B., Faury, N., Chollet, B., Dégremont, L., Travers, M.-A., Renault, T., and Arzul, I. (2019). A study of autophagy in hemocytes of the Pacific oyster, *Crassostrea gigas*. *Autophagy*. **15**(10), 1801–1809. URL https://doi.org/10.1080/15548627.2019.1596490.

Pierobon, P., Concas, A., Santoro, G., Marino, G., Minei, R., Pannaccione, A., Mostallino, M. C., and Biggio, G. (1995). Biochemical and functional identification of GABA receptors in *Hydra vulgaris*. *Life Sciences*. **56**(18), 1485–1497. URL https://doi.org/10.1016/0024-3205(95)00111-I.

Pierobon, P., Tino, A., Minei, R., and Marino, G. (2004). Different roles of GABA and glycine in the modulation of chemosensory responses in *Hydra vulgaris*

(Cnidaria, Hydrozoa). *Hydrobiologia*. **530**(1-3), 59–66. URL https://doi.org/10.1007/s10750-004-2690-4.

Piggott, S. M., Kerkut, G., and Walker, R. (1977). The actions of picrotoxin, strychnine, bicuculline and other convulsants and antagonists on the responses to acetylcholine glutamic acid and gamma-aminobutyric acid on *Helix* neurones. *Comparative Biochemistry and Physiology Part C: Comparative Pharmacology*. **57**(2), 107–116. URL https://doi.org/10.1016/0306-4492(77)90054-5.

Popper, A. N., Salmon, M., and Horch, K. W. (2001). Acoustic detection and communication by decapod crustaceans. *Journal of Comparative Physiology A*. **187**(2), 83–89. URL https://doi.org/10.1007/s003590100184.

Porteus, C. S., Hubbard, P. C., Webster, T. M. U., van Aerle, R., Canário, A. V., Santos, E. M., and Wilson, R. W. (2018). Near-future CO_2 levels impair the olfactory system of a marine fish. *Nature Climate Change*. **8**(8), 737–746. URL https://doi.org/10.1038/s41558-018-0224-8.

Pörtner, H.-O., Bock, C., and Reipschlager, A. (2000). Modulation of the cost of pH_i regulation during metabolic depression: A (31)P-NMR study in invertebrate (*Sipunculus nudus*) isolated muscle. *Journal of Experimental Biology*. **203**(16), 2417–2428. URL https://doi.org/10.1242/jeb.203.16.2417.

Pörtner, H.-O., Langenbuch, M., and Reipschläger, A. (2004). Biological impact of elevated ocean CO_2 concentrations: Lessons from animal physiology and earth history. *Journal of Oceanography*. **60**(4), 705–718. URL https://doi.org/10.1007/s10872-004-5763-0.

Pörtner, H.-O., Reipschläger, A., and Heisler, N. (1998). Acid-base regulation, metabolism and energetics in *Sipunculus nudus* as a function of ambient carbon dioxide level. *Journal of Experimental Biology*. **201**(1), 43–55. URL https://doi.org/10.1242/jeb.201.1.43.

Putrenko, I., Zakikhani, M., and Dent, J. A. (2005). A family of acetylcholine-gated chloride channel subunits in *Caenorhabditis elegans*. *Journal of Biological Chemistry*. **280**(8), 6392–6398. URL https://doi.org/10.1074/jbc.M412644200.

Qian, Z.-M., He, X., Liang, T., Wu, K.-C., Yan, Y.-C., Lu, L.-N., Yang, G., Luo, Q. Q., Yung, W.-H., and Ke, Y. (2014). Lipopolysaccharides upregulate hepcidin in neuron via microglia and the IL-6/STAT3 signaling pathway. *Molecular Neurobiology*. **50**(3), 811–820. URL https://doi.org/10.1007/s12035-014-8671-3.

Queirós, A. M., Fernandes, J. A., Faulwetter, S., Nunes, J., Rastrick, S. P., Mieszkowska, N., Artioli, Y., Yool, A., Calosi, P., and Arvanitidis, C. (2015). Scaling up experimental ocean acidification and warming research: From individuals to the ecosystem. *Global Change Biology*. **21**(1), 130–143. URL https://doi.org/10.1111/gcb.12675.

Quintero-Reyes, I. E., Garcia-Orozco, K. D., Sugich-Miranda, R., Arvizu-Flores, A. A., Velazquez-Contreras, E. F., Castillo-Yañez, F. J., and Sotelo-Mundo, R. R. (2012). Shrimp oncoprotein nm23 is a functional nucleoside diphosphate kinase. *Journal of bioenergetics and biomembranes*. **44**(3), 325–331. URL https://doi.org/10.1007/s10863-012-9436-1.

R Core Team (2020). *R: A language and environment for statistical computing*. R Foundation for Statistical Computing. Vienna, Austria. URL https://www.R-project.org/.

R Core Team (2021). *R: A language and environment for statistical computing*. R Foundation for Statistical Computing. Vienna, Austria. URL https://www.R-project.org/.

Radtke, F., MacDonald, H. R., and Tacchini-Cottier, F. (2013). Regulation of innate and adaptive immunity by Notch. *Nature Reviews Immunology*. **13**(6), 427–437. URL https://doi.org/10.1038/nri3445.

Ragagnin, M. N., McCarthy, I. D., Fernandez, W. S., Tschiptschin, A. P., and Turra, A. (2018). Vulnerability of juvenile hermit crabs to reduced seawater pH and shading. *Marine Environmental Research*. **142**, 130–140. URL https://doi.org/10.1016/j.marenvres.2018.10.001.

Rammal, H., Bouayed, J., and Soulimani, R. (2010). A direct relationship between aggressive behavior in the resident/intruder test and cell oxidative status in adult male mice. *European Journal of Pharmacology*. **627**(1), 173–176. URL https://doi.org/10.1016/j.ejphar.2009.11.001.

Ranganathan, R., Cannon, S. C., and Horvitz, H. R. (2000). MOD-1 is a serotonin-gated chloride channel that modulates locomotory behaviour in *C. elegans*. *Nature*. **408**(6811), 470. URL https://doi.org/10.1038/35044083.

Rankin, A., Seo, K., Graeve, O., and Taylor, J. (2019). No compromise between metabolism and behavior of decorator crabs in reduced pH conditions. *Scientific Reports*. **9**, 6262. URL https://doi.org/10.1038/s41598-019-42696-8.

Rauh, J. J., Lummis, S. C., and Sattelle, D. B. (1990). Pharmacological and biochemical properties of insect GABA receptors. *Trends in Pharmacological Sciences*. **11**(8), 325–329. URL https://doi.org/10.1016/0165-6147(90)90236-2.

Recuenco, M. C., Rahman, M. M., Takeuchi, F., Kobayashi, K., and Tsubaki, M. (2013). Electron transfer reactions of candidate tumor suppressor 101F6 protein, a cytochrome b561 homologue, with ascorbate and monodehydroascorbate radical. *Biochemistry*. **52**(21), 3660–3668. URL https://doi.org/10.1021/bi301607s.

Regan, M. D., Turko, A. J., Heras, J., Andersen, M. K., Lefevre, S., Wang, T., Bayley, M., Brauner, C. J., Phuong, N. T., and Nilsson, G. E. (2016). Ambient CO_2, fish behaviour and altered GABAergic neurotransmission: Exploring the mechanism of CO_2-altered behaviour by taking a hypercapnia dweller down to low CO_2 levels. *Journal of Experimental Biology*. **219**(1), 109–118. URL https://doi.org/10.1242/jeb.131375.

Régnier, V., Billard, J.-M., Gupta, S., Potier, B., Woerner, S., Paly, E., Ledru, A., David, S., Luilier, S., Bizot, J.-C., Vacano, G., Kraus, J. P., Patterson, D., Kruger, W. D., Delabar, J. M., and London, J. (2012). Brain phenotype of transgenic mice overexpressing cystathionine β-synthase. *PLOS One*. **7**(1), e29056. URL https://doi.org/10.1371/journal.pone.0029056.

Reid, A. (2005). Family Idiosepiidae. In *Cephalopods of the World : An Annotated and Illustrated Catalogue of Cephalopod Species Known to Date. Volume 1. Chambered Nautiluses and Sepioids (Nautilidae, Sepiidae, Sepiolidae, Sepiadariidae, Idiosepiidae and Spirulidae).* (eds. P. Jereb and C. Roper). FAO species catalogue for fishery purposes. pp. 208 – 210. FAO, Rome.

Reid, A. L. and Strugnell, J. M. (2018). A new pygmy squid, *Idiosepius hallami* n. sp.(Cephalopoda: Idiosepiidae) from eastern Australia and elevation of the southern endemic 'notoides' clade to a new genus, *Xipholeptos* n. gen. *Zootaxa*. **4369**(4), 451–486. URL https://doi.org/10.11646/zootaxa.4369.4.1.

Ren, Z., Mu, C., Li, R., Song, W., and Wang, C. (2018). Characterization of a γ-aminobutyrate type A receptor-associated protein gene, which is involved in the response of *Portunus trituberculatus* to CO_2-induced ocean acidification. *Aquaculture Research*. **49**(7), 2393–2403. URL https://doi.org/10.1111/are.13699.

Rich, W. A., Schubert, N., Schläpfer, N., Carvalho, V. F., Horta, A. C., and Horta, P. A. (2018). Physiological and biochemical responses of a coralline alga and a sea urchin to climate change: Implications for herbivory. *Marine Environmental Research*. URL https://doi.org/10.1016/j.marenvres.2018.09.026.

Riebesell, U. and Gattuso, J.-P. (2015). Lessons learned from ocean acidification research. *Nature Climate Change*. **5**(1), 12–14. URL https://doi.org/10.1038/nclimate2456.

Riebesell, U., Zondervan, I., Rost, B., Tortell, P. D., Zeebe, R. E., and Morel, F. M. M. (2000). Reduced calcification of marine plankton in response to increased atmospheric CO_2. *Nature*. **407**(6802), 364–367. URL https://doi.org/10.1038/35030078.

Ries, J. B., Cohen, A. L., and McCorkle, D. C. (2009). Marine calcifiers exhibit mixed responses to CO_2-induced ocean acidification. *Geology*. **37**(12), 1131–1134. URL https://doi.org/10.1130/G30210A.1.

Rittschof, D., Maki, J., Mitchell, R., and Costlow, J. D. (1986). Ion and neuropharmacological studies of barnacle settlement. *Netherlands Journal of Sea Research*. **20**(2-3), 269–275. URL https://doi.org/10.1016/0077-7579(86)90048-7.

Roberts, A. C. and Glanzman, D. L. (2003). Learning in *Aplysia*: Looking at synaptic plasticity from both sides. *Trends in Neurosciences*. **26**(12), 662–670. URL https://doi.org/10.1016/j.tins.2003.09.014.

Robinson, M. B., Blakely, R. D., Couto, R., and Coyle, J. T. (1987). Hydrolysis of the brain dipeptide N-acetyl-L-aspartyl-L-glutamate. Identification and characterization of a novel N-acetylated alpha-linked acidic dipeptidase activity from rat brain. *Journal of Biological Chemistry*. **262**(30), 14498–14506. URL https://doi.org/10.1016/S0021-9258(18)47823-4.

Rodhouse, P. G. (1998). Physiological progenesis in cephalopod molluscs. *The Biological Bulletin*. **195**(1), 17–20. URL https://doi.org/10.2307/1542771.

Roggatz, C. C., Lorch, M., Hardege, J. D., and Benoit, D. M. (2016). Ocean acidification affects marine chemical communication by changing structure and function of peptide signalling molecules. *Global Change Biology*. **22**(12), 3914–3926. URL https://doi.org/10.1111/gcb.13354.

Romanova, E. V., Rubakhin, S., and S-rózsa, K. (1996). Behavioral changes induced by GABA-receptor agonists in *Lymnaea stagnalis* L. *General Pharmacology*. **27**(6), 1067–1071. URL https://doi.org/10.1016/0306-3623(95)00122-0.

Roos, A. and Boron, W. F. (1981). Intracellular pH. *Physiological Reviews*. **61**(2), 296–434. URL https://doi.org/10.1152/physrev.1981.61.2.296.

Rosa, R. and Seibel, B. A. (2008). Synergistic effects of climate-related variables suggest future physiological impairment in a top oceanic predator. *Proceedings of the National Academy of Sciences*. **105**(52), 20776–20780. URL https://doi.org/10.1073/pnas.0806886105.

Rosenthal, J. J. (2015). The emerging role of RNA editing in plasticity. *Journal of Experimental Biology*. **218**(12), 1812–1821. URL https://doi.org/10.1242/jeb.119065.

Ross, E. and Behringer, D. (2019). Changes in temperature, pH, and salinity affect the sheltering responses of Caribbean spiny lobsters to chemosensory cues. *Scientific Reports*. **9**, 4375. URL https://doi.org/10.1038/s41598-019-40832-y.

Rossi, T., Connell, S. D., and Nagelkerken, I. (2016). Silent oceans: Ocean acidification impoverishes natural soundscapes by altering sound production of the world's noisiest marine invertebrate. *Proceedings of the Royal Society B: Biological Sciences*. **283**(1826), 20153046. URL https://doi.org/10.1098/rspb.2015.3046.

RStudio Team (2020). *RStudio: Integrated development environment for R*. RStudio, Inc.. Boston, MA. URL http://www.rstudio.com.

RStudio Team (2021). *RStudio: Integrated development environment for R*. RStudio, Inc.. Boston, MA. URL http://www.rstudio.com.

Rubakhin, S., Szücs, A., and Rozsa, K. (1996). Characterization of the GABA response on identified dialysed *Lymnaea* neurons. *General Pharmacology*. **27**(4), 731–739. URL https://doi.org/10.1016/0306-3623(95)00123-9.

Rusakov, D. A. (2006). Ca^{2+}-dependent mechanisms of presynaptic control at central synapses. *The Neuroscientist*. **12**(4), 317–326. URL https://doi.org/10.1177/1073858405284672.

Russell, J. M. and Boron, W. F. (1976). Role of chloride transport in regulation of intracellular pH. *Nature*. **264**(5581), 73–74. URL https://doi.org/10.1038/264073a0.

Saba, G. K., Schofield, O., Torres, J. J., Ombres, E. H., and Steinberg, D. K. (2012). Increased feeding and nutrient excretion of adult Antarctic krill, *Euphausia superba*, exposed to enhanced carbon dioxide (CO_2). *PLoS One*. **7**(12), e52224. URL https://doi.org/10.1371/journal.pone.0052224.

Sailor, K. A., Schinder, A. F., and Lledo, P.-M. (2017). Adult neurogenesis beyond the niche: Its potential for driving brain plasticity. *Current Opinion in Neurobiology*. **42**, 111–117. URL https://doi.org/10.1016/j.conb.2016.12.001.

Salazar, K. A., Joffe, N. R., Dinguirard, N., Houde, P., and Castillo, M. G. (2015). Transcriptome analysis of the white body of the squid *Euprymna tasmanica* with emphasis on immune and hematopoietic gene discovery. *PLoS One*. **10**(3), e0119949. URL https://doi.org/10.1371/journal.pone.0119949.

Samardzic, J., Jadzic, D., Hencic, B., Jancic, J., and Strac, D. S. (2018). Introductory chapter: GABA/glutamate balance: A key for normal brain functioning. In *GABA And Glutamate: New Developments In Neurotransmission Research* (ed. J. Samardzic). pp. 1–9. InTech, Croatia.

Sanford, E., Gaylord, B., Hettinger, A., Lenz, E. A., Meyer, K., and Hill, T. M. (2014). Ocean acidification increases the vulnerability of native oysters to predation by invasive snails. *Proceedings of the Royal Society B: Biological Sciences*. **281**(1778), 20132681. URL https://doi.org/10.1098/rspb.2013.2681.

Santos, I. R., Glud, R. N., Maher, D., Erler, D., and Eyre, B. D. (2011). Diel coral reef acidification driven by porewater advection in permeable carbonate sands, Heron Island, Great Barrier Reef. *Geophysical Research Letters*. **38**(3), L03604. URL https://doi.org/10.1029/2010GL046053.

Satoh, H., Daido, H., and Nakamura, T. (2005). Preliminary analysis of the GABA-induced current in cultured CNS neurons of the cutworm moth, *Spodoptera litura*. *Neuroscience Letters*. **381**(1-2), 125–130. URL https://doi.org/10.1016/j.neulet.2005.02.007.

Scherer, L. J. and Rossi, J. J. (2003). Approaches for the sequence-specific knockdown of mRNA. *Nature Biotechnology*. **21**(12), 1457–1465. URL https://doi.org/10.1038/nbt915.

Schleicher, T. R. and Nyholm, S. V. (2011). Characterizing the host and symbiont proteomes in the association between the bobtail squid, *Euprymna scolopes*, and the bacterium, *Vibrio fischeri*. *PLOS One*. **6**(10), e25649. URL https://doi.org/10.1371/journal.pone.0025649.

Schleifer, K. H. and Kandler, O. (1972). Peptidoglycan types of bacterial cell walls and their taxonomic implications. *Bacteriological Reviews*. **36**(4), 407–477. URL https://doi.org/10.1128/br.36.4.407-477.1972.

Schmidt, J. and Calabrese, R. L. (1992). Evidence that acetylcholine is an inhibitory transmitter of heart interneurons in the leech. *Journal of Experimental Biology*. **171**(1), 329–347. URL https://doi.org/10.1242/jeb.171.1.329.

Schmitt, B. C. and Ache, B. W. (1979). Olfaction: Responses of a decapod crustacean are enhanced by flicking. *Science*. **205**(4402), 204–206. URL https://doi.org/10.1126/science.205.4402.204.

Schunter, C., Jarrold, M. D., Munday, P. L., and Ravasi, T. (2021). Diel pCO_2 fluctuations alter the molecular response of coral reef fishes to ocean acidification conditions. *Molecular Ecology*. **30**, 5105– 5118.. URL https://doi.org/10.1111/mec.16124.

Schunter, C., Ravasi, T., Munday, P. L., and Nilsson, G. E. (2019). Neural effects of elevated CO_2 in fish may be amplified by a vicious cycle. *Conservation Physiology*. **7**(1), coz100. URL https://doi.org/10.1093/conphys/coz100.

Schunter, C., Welch, M. J., Nilsson, G. E., Rummer, J. L., Munday, P. L., and Ravasi, T. (2018). An interplay between plasticity and parental phenotype determines impacts of ocean acidification on a reef fish. *Nature Ecology and Evolution*. **2**(2), 334. URL https://doi.org/10.1038/s41559-017-0428-8.

Schunter, C., Welch, M. J., Ryu, T., Zhang, H., Berumen, M. L., Nilsson, G. E., Munday, P. L., and Ravasi, T. (2016). Molecular signatures of transgenerational response to ocean acidification in a species of reef fish. *Nature Climate Change*. **6**, 1014–1018. URL https://doi.org/10.1038/NCLIMATE3087.

Scott, A. L., Bortolato, M., Chen, K., and Shih, J. C. (2008). Novel monoamine oxidase a knock out mice with human-like spontaneous mutation. *Neuroreport*. **19**(7), 739–743. URL https://doi.org/10.1097/WNR.0b013e3282fd6e88.

Seifinejad, A., Li, S., Mikhail, C., Vassalli, A., Pradervand, S., Arribat, Y., Pezeshgi Modarres, H., Allen, B., John, R. M., Amati, F., and Tafti, M. (2019). Molecular codes and *in vitro* generation of hypocretin and melanin concentrating hormone neurons. *Proceedings of the National Academy of Sciences of the United States of America*. **116**(34), 17061–17070. URL https://doi.org/10.1073/pnas.1902148116.

Sernagor, E., Chabrol, F., Bony, G., and Cancedda, L. (2010). GABAergic control of neurite outgrowth and remodeling during development and adult neurogenesis: General rules and differences in diverse systems. *Frontiers in Cellular Neuroscience*. **4**. URL https://doi.org/10.3389/fncel.2010.00011.

Shaldubina, A., Buccafusca, R., Johanson, R. A., Agam, G., Belmaker, R. H., Berry, G. T., and Bersudsky, Y. (2007). Behavioural phenotyping of sodium-myo-inositol co-transporter heterozygous knockout mice with reduced brain inositol. *Genes, Brain and Be-*

havior. **6**(3), 253–259. URL https://doi.org/10.1111/j.1601-183X.2006.00253.x.

Shannon, P., Markiel, A., Ozier, O., Baliga, N. S., Wang, J. T., Ramage, D., Amin, N., Schwikowski, B., and Ideker, T. (2003). Cytoscape: A software environment for integrated models of biomolecular interaction networks. *Genome Research*. **13**(11), 2498–2504. URL https://www.ncbi.nlm.nih.gov/pmc/articles/PMC403769/pdf/0132498.pdf.

Shashar, N., Rutledge, P., and Cronin, T. (1996). Polarization vision in cuttlefish in a concealed communication channel? *Journal of Experimental Biology*. **199**(9), 2077–2084. URL https://doi.org/10.1242/jeb.199.9.2077.

Shaw, E. C., McNeil, B. I., and Tilbrook, B. (2012). Impacts of ocean acidification in naturally variable coral reef flat ecosystems. *Journal of Geophysical Research: Oceans*. **117**(C3), C03038. URL https://doi.org/10.1029/2011JC007655.

Shaw, E. C., Mcneil, B. I., Tilbrook, B., Matear, R., and Bates, M. L. (2013). Anthropogenic changes to seawater buffer capacity combined with natural reef metabolism induce extreme future coral reef CO_2 conditions. *Global Change Biology*. **19**(5), 1632–1641. URL https://doi.org/10.1111/gcb.12154.

Shefa, U., Kim, D., Kim, M.-S., Jeong, N. Y., and Jung, J. (2018a). Roles of gasotransmitters in synaptic plasticity and neuropsychiatric conditions. *Neural Plasticity*. **2018**, 1824713. URL https://doi.org/10.1155/2018/1824713.

Shefa, U., Kim, M.-S., Jeong, N. Y., and Jung, J. (2018b). Antioxidant and cell-signaling functions of hydrogen sulfide in the central nervous system. *Oxidative medicine and Cellular Longevity*. **2018**, 1873962–1873962. URL https://doi.org/10.1155/2018/1873962.

Shelley, C., Dyar, A., and Schieber, M. (2019). Neurotransmitter receptor antagonism inhibits the sea urchin righting response. *The FASEB Journal*. **33**, Abstract 849.3. URL https://doi.org/10.1096/fasebj.2019.33.1_supplement.849.3.

Sherry, A. and Henson, R. K. (2005). Conducting and interpreting canonical correlation analysis in personality research: A user-friendly primer. *Journal of Personality Assessment*. **84**(1), 37–48. URL https://doi.org/10.1207/s15327752jpa8401_09.

Shors, T. J., Miesegaes, G., Beylin, A., Zhao, M., Rydel, T., and Gould, E. (2001). Neurogenesis in the adult is involved in the formation of trace memories. *Nature*. **410**(6826), 372–376. URL https://doi.org/10.1038/35066584.

Sieghart, W. (2015). Allosteric modulation of $GABA_A$ receptors via multiple drug-binding sites. In *Advances in Pharmacology* (ed. U. Rudolph). pp. 53–96. Academic Press. URL https://doi.org/10.1016/bs.apha.2014.10.002.

Simmons, P. and Young, D. (1999). *Nerve Cells and Animal Behaviour*. Cambridge University Press, Cambridge, New York, Melbourne, Madrid. 2 edition. URL https://doi.org/10.1017/CBO9780511782138.

Simon, A. F., Daniels, R., Romero-Calderón, R., Grygoruk, A., Chang, H.-Y., Najibi, R., Shamouelian, D., Salazar, E., Solomon, M., Ackerson, L. C., Maidment, N. T., DiAntonio, A., and Krantz, D. E. (2009). *Drosophila* vesicular monoamine transporter mutants can adapt to reduced or eliminated vesicular stores of dopamine and serotonin. *Genetics*. **181**(2), 525–541. URL https://doi.org/10.1534/genetics.108.094110.

Simon, J., Wakimoto, H., Fujita, N., Lalande, M., and Barnard, E. A. (2004). Analysis of the set of $GABA_A$ receptor genes in the human genome. *Journal of Biological Chemistry*. **279**(40), 41422–41435. URL https://doi.org/10.1074/jbc.M401354200.

Skrajny, B., Hannah, R. S., and Roth, S. H. (1992). Low concentrations of hydrogen sulphide alter monoamine levels in the developing rat central nervous system. *Canadian Journal of Physiology and Pharmacology*. **70**(11), 1515–1518. URL https://doi.org/10.1139/y92-215.

Small, D. P., Calosi, P., Boothroyd, D., Widdicombe, S., and Spicer, J. I. (2016). The sensitivity of the early benthic juvenile stage of the European lobster *Homarus gammarus* (L.) to elevated pCO_2 and temperature. *Marine Biology*. **163**(3), 53. URL https://doi.org/10.1007/s00227-016-2834-x.

Smith, K., Davenport, E., Wei, J., Li, X., Pathania, M., Vaccaro, V., Yan, Z., and Kittler, J. (2014). GIT1 and βPIX are essential for $GABA_A$ receptor synaptic stability and inhibitory neurotransmission. *Cell Reports*. **9**(1), 298–310. URL https://doi.org/10.1016/j.celrep.2014.08.061.

Smith-Unna, R., Boursnell, C., Patro, R., Hibberd, J. M., and Kelly, S. (2016). TransRate: Reference-free quality assessment of *de novo* transcriptome assemblies. *Genome Research*. **26**(8), 1134–1144. URL https://doi.org/10.1101/gr.196469.115.

Spady, B. L., Munday, P. L., and Watson, S.-A. (2018). Predatory strategies and behaviours in cephalopods are altered by elevated CO_2. *Global Change Biology*. **24**, 2585–2596. URL https://doi.org10.1111/gcb.14098.

Spady, B. L., Munday, P. L., and Watson, S.-A. (2019). Elevated seawater pCO_2 affects reproduction and embryonic development in the pygmy squid, *Idiosepius pygmaeus*. *Marine Environmental Research*. **153**, 104812. URL https://doi.org/10.1016/j.marenvres.2019.104812.

Spady, B. L., Watson, S.-A., Chase, T. J., and Munday, P. L. (2014). Projected near-future CO_2 levels increase activity and alter defensive behaviours in the tropical squid *Idiosepius pygmaeus*. *Biology Open*. **3**(11), 1063–1070. URL https://doi.org/10.1242/bio.20149894.

Spangenberg, D. (1986). Statolith formation in Cnidaria: Effects of cadmium on *Aurelia* statoliths. *Scanning Electron Microscopy*. pp. 1609–16. URL https://digitalcommons.usu.edu/electron/vol1986/iss4/36.

Stan Development Team (2020). *RStan: the R interface to Stan*. URL http://mc-stan.org/. r package version 2.21.2.

Stanley, J. A., Radford, C. A., and Jeffs, A. G. (2009). Induction of settlement in crab megalopae by ambient underwater reef sound. *Behavioral Ecology*. **21**(1), 113–120. URL https://doi.org/10.1093/beheco/arp159.

Steffen, W., Broadgate, W., Deutsch, L., Gaffney, O., and Ludwig, C. (2015). The trajectory of the Anthropocene: The great acceleration. *The Anthropocene Review*. **2**(1), 81–98. URL https://doi.org/10.1177/2053019614564785.

Stephens, M. (2016). False discovery rates: A new deal. *Biostatistics*. **18**(2), 275–294. URL https://doi.org/10.1093/biostatistics/kxw041.

Stewart, P., Williams, E. A., Stewart, M. J., Soonklang, N., Degnan, S. M., Cummins, S. F., Hanna, P. J., and Sobhon, P. (2011). Characterization of a $GABA_A$ receptor β subunit in the abalone *Haliotis asinina* that is upregulated during larval development. *Journal of Experimental Marine Biology and Ecology*. **410**, 53–60. URL https://doi.org/10.1016/j.jembe.2011.10.005.

Strader, M. E., Wong, J. M., and Hofmann, G. E. (2020). Ocean acidification promotes broad transcriptomic responses in marine metazoans: A literature survey. *Frontiers in Zoology*. **17**(1), 7. URL https://doi.org/10.1186/s12983-020-0350-9.

Su, D. and Asard, H. (2006). Three mammalian cytochromes b561 are ascorbate-dependent ferrireductases. *The FEBS Journal*. **273**(16), 3722–3734. URL https://doi.org/10.1111/j.1742-4658.2006.05381.x.

Su, W., Rong, J., Zha, S., Yan, M., Fang, J., and Liu, G. (2018). Ocean acidification affects the cytoskeleton, lysozymes, and nitric oxide of hemocytes: A possible explanation for the hampered phagocytosis in blood clams, *Tegillarca granosa*. *Frontiers in Physiology*. **9**(619). URL https://doi.org/10.3389/fphys.2018.00619.

Succol, F., Fiumelli, H., Benfenati, F., Cancedda, L., and Barberis, A. (2012). Intracellular chloride concentration influences the $GABA_A$ receptor subunit composition. *Nature Communications*. **3**, 738. URL https://doi.org/10.1038/ncomms1744.

Sui, Y., Zhou, K., Lai, Q., Yao, Z., and Gao, P. (2019). Effects of seawater acidification on early development of clam *Cyclina sinensis*. *Journal of Ocean University of China*. **18**(4), 913–918. URL https://doi.org/10.1007/s11802-019-3942-2.

Sumimoto, H., Ohkuma, Y., Sinn, E., Kato, H., Shimasaki, S., Horikoshi, M., and Roeder, R. G. (1991). Conserved sequence motifs in the small subunit of human general transcription factor tfiie. *Nature*. **354**(6352), 401–404. URL https://doi.org/10.1038/354401a0.

Sun, Q., Zheng, Y., Chen, X., Kong, N., Wang, Y., Zhang, Y., Zong, Y., Liu, Z., Wang, L., and Song, L. (2021). A diet rich in diatom improves the antibacterial capacity of Pacific oyster *Crassostrea gigas* by enhancing norepinephrine-regulated immunomodulation. *Invertebrate Survival Journal*. **18**(1), 56–65.

Sun, T., Tang, X., Jiang, Y., and Wang, Y. (2017). Seawater acidification induced immune function changes of haemocytes in *Mytilus edulis*: A comparative study of CO_2 and HCl enrichment. *Scientific Reports*. **7**(1), 41488. URL https://doi.org/10.1038/srep41488.

Svensson, E., Proekt, A., Jing, J., and Weiss, K. R. (2014). PKC-mediated GABAergic enhancement of dopaminergic responses: Implication for short-term potentiation at a dual-transmitter synapse. *Journal of Neurophysiology*. **112**(1), 22–29. URL https://doi.org/10.1152/jn.00794.2013.

Takáts, S., Glatz, G., Szenci, G., Boda, A., Horváth, G., Hegedűs, K., Kovács, A. L., and Juhász, G. (2018). Non-canonical role of the SNARE protein Ykt6 in autophagosome-lysosome fusion. *PLOS Genetics*. **14**(4), e1007359. URL https://doi.org/10.1371/journal.pgen.1007359.

Talaei, F., Bouma, H. R., Van der Graaf, A. C., Strijkstra, A. M., Schmidt, M., and Henning, R. H. (2011). Serotonin and dopamine protect from hypothermia/rewarming

damage through the CBS/ H_2S pathway. *PLOS One*. **6**(7), e22568. URL https://doi.org/10.1371/journal.pone.0022568.

Tan, S., Wang, W., Tian, C., Niu, D., Zhou, T., Jin, Y., Yang, Y., Gao, D., Dunham, R., and Liu, Z. (2019). Heat stress induced alternative splicing in catfish as determined by transcriptome analysis. *Comparative Biochemistry and Physiology Part D: Genomics and Proteomics*. **29**, 166–172. URL https://doi.org/10.1016/j.cbd.2018.11.008.

Terahara, K. and Takahashi, K. G. (2008). Mechanisms and immunological roles of apoptosis in molluscs. *Current Pharmaceutical Design*. **14**(2), 131–137. URL https://doi.org/10.2174/138161208783378725.

Terahara, K., Takahashi, K. G., Nakamura, A., Osada, M., Yoda, M., Hiroi, T., Hirasawa, M., and Mori, K. (2006). Differences in integrin-dependent phagocytosis among three hemocyte subpopulations of the Pacific oyster "*Crassostrea gigas*". *Developmental and Comparative Immunology*. **30**(8), 667–683. URL https://doi.org/10.1016/j.dci.2005.09.009.

Thabet, A. A., Maas, A. E., Saber, S. A., and Tarrant, A. M. (2017). Assembly of a reference transcriptome for the gymnosome pteropod *Clione limacina* and profiling responses to short-term CO_2 exposure. *Marine Genomics*. **34**, 39–45. URL https://doi.org/10.1016/j.margen.2017.03.003.

Thakar, S., Wang, L., Yu, T., Ye, M., Onishi, K., Scott, J., Qi, J., Fernandes, C., Han, X., Yates, J. R., Berg, D. K., and Zou, Y. (2017). Evidence for opposing roles of Celsr3 and Vangl2 in glutamatergic synapse formation. *Proceedings of the National Academy of Sciences*. **114**(4), E610–E618. URL https://doi.org/10.1073/pnas.1612062114.

Tierney, A. J. and Atema, T. (1988). Amino acid chemoreception: Effects of pH on receptors and stimuli. *Journal of Chemical Ecology*. **14**(1), 135–141. URL https://doi.org/10.1007/BF01022537.

Timmins-Schiffman, E., Guzmán, J. M., Thompson, R. E., Vadopalas, B., Eudeline, B., and Roberts, S. B. (2019). Dynamic response in the larval geoduck (*Panopea generosa*) proteome to elevated pCO_2. *Ecology and Evolution*. URL https://doi.org/10.1002/ece3.5885.

Todgham, A. E. and Hofmann, G. E. (2008). Transcriptomic response of sea urchin larvae *Strongylocentrotus purpuratus* to CO_2-driven seawater acidification. *Journal of Experimental Biology*. **212**, 2579–2594. URL https://doi.org/10.1242/jeb.032540.

Tomanek, L., Zuzow, M. J., Ivanina, A. V., Beniash, E., and Sokolova, I. M. (2011). Proteomic response to elevated PCO_2 level in eastern oysters, *Crassostrea virginica*: Evidence for oxidative stress. *Journal of Experimental Biology*. **214**(11), 1836–1844. URL https://doi.org/10.1242/jeb.055475.

Toni, N., Teng, E. M., Bushong, E. A., Aimone, J. B., Zhao, C., Consiglio, A., van Praag, H., Martone, M. E., Ellisman, M. H., and Gage, F. H. (2007). Synapse formation on neurons born in the adult hippocampus. *Nature Neuroscience*. **10**(6), 727–734. URL https://doi.org/10.1038/nn1908.

Toulmé, E., Blais, D., Léger, C., Landry, M., Garret, M., Séguéla, P., and Boué-Grabot, E. (2007). An intracellular motif of P2X3 receptors is required for functional cross-talk with $GABA_A$ receptors in nociceptive DRG neurons. *Journal of Neurochemistry*. **102**(4), 1357–1368. URL https://doi.org/10.1111/j.1471-4159.2007.04640.x.

Tovar, K. R. and Westbrook, G. L. (2012). Ligand-gated ion channels. In *Cell Physiology Source Book* (ed. N. Sperelakis). pp. 549–562. Academic Press, London, Waltham, San Diego. URL https://doi.org/10.1016/B978-012656976-6/50132-3.

Tozuka, Y., Fukuda, S., Namba, T., Seki, T., and Hisatsune, T. (2005). GABAergic excitation promotes neuronal differentiation in adult hippocampal progenitor cells. *Neuron*. **47**(6), 803–815. URL https://doi.org/10.1016/j.neuron.2005.08.023.

Tresguerres, M. and Hamilton, T. J. (2017). Acid–base physiology, neurobiology and behaviour in relation to CO_2-induced ocean acidification. *Journal of Experimental Biology*. **220**(12), 2136–2148. URL https://doi.org/10.1242/jeb.144113.

Trigg, S. A., McElhany, P., Maher, M., Perez, D., Busch, D. S., and Nichols, K. M. (2019). Uncovering mechanisms of global ocean change effects on the Dungeness crab (*Cancer magister*) through metabolomics analysis. *Scientific Reports*. **9**, 10717. URL https://doi.org/10.1038/s41598-019-46947-6.

Tritsch, N. X., Ding, J. B., and Sabatini, B. L. (2012). Dopaminergic neurons inhibit striatal output through non-canonical release of GABA. *Nature*. **490**(7419), 262–266. URL https://doi.org/10.1038/nature11466.

Troll, J. V., Bent, E. H., Pacquette, N., Wier, A. M., Goldman, W. E., Silverman, N., and McFall-Ngai, M. J. (2010). Taming the symbiont for coexistence: A host PGRP neutralizes a bacterial symbiont toxin. *Environmental Microbiology*. **12**(8), 2190–2203. URL https://doi.org/10.1111/j.1462-2920.2009.02121.x.

Trombley, P. Q., Hill, B. J., and Horning, M. S. (1999). Interactions between GABA and glycine at inhibitory amino acid receptors on rat olfactory bulb neurons. *Journal of Neurophysiology*. **82**(6), 3417–3422. URL https://doi.org/10.1152/jn.1999.82.6.3417.

Truchot, J. (1983). Regulation of acid–base balance. In *The Biology of Crustacea. Internal Anatomy and Physiological Regulation* (ed. L. Mantel). pp. 431–57. Academic Press, New York.

Tsang, S.-Y., Ng, S.-K., Xu, Z., and Xue, H. (2007). The evolution of $GABA_A$ receptor–like genes. *Molecular Biology and Evolution*. **24**(2), 599–610. URL https://doi.org/10.1093/molbev/msl188.

Tsuiki, H., Nitta, M., Furuya, A., Hanai, N., Fujiwara, T., Inagaki, M., Kochi, M., Ushio, Y., Saya, H., and Nakamura, H. (2000). A novel human nucleoside diphosphate (NDP) kinase, Nm23-H6, localizes in mitochondria and affects cytokinesis. *Journal of Cellular Biochemistry*. **76**(2), 254–269. URL https://doi.org/10.1002/(SICI)1097-4644(20000201)76:2<254::AID-JCB9>3.0.CO;2-G.

Uldry, M., Ibberson, M., Horisberger, J.-D., Chatton, J.-Y., Riederer, B. M., and Thorens, B. (2001). Identification of a mammalian H^+-myo-inositol symporter expressed predominantly in the brain. *The EMBO Journal*. **20**(16), 4467–4477. URL https://doi.org/10.1093/emboj/20.16.4467.

Uldry, M., Steiner, P., Zurich, M.-G., Béguin, P., Hirling, H., Dolci, W., and Thorens, B. (2004). Regulated exocytosis of an H^+/myo-inositol symporter at synapses and growth cones. *The EMBO Journal*. **23**(3), 531–540. URL https://doi.org/10.1038/sj.emboj.7600072.

Valdivieso, n. G. and Santa-Coloma, T. A. (2019). The chloride anion as a signalling effector. *Biological Reviews*. **94**(5), 1839–1856. URL https://doi.org/10.1111/brv.12536.

Valko, M., Leibfritz, D., Moncol, J., Cronin, M. T., Mazur, M., and Telser, J. (2007). Free radicals and antioxidants in normal physiological functions and human disease. *The International Journal of Biochemistry and Cell Biology*. **39**(1), 44–84. URL https://doi.org/10.1016/j.biocel.2006.07.001.

Van Colen, C., Ong, E. Z., Briffa, M., Wethey, D. S., Abatih, E., Moens, T., and Woodin, S. A. (2020). Clam feeding plasticity reduces herbivore vulnerability to ocean warming

and acidification. *Nature Climate Change*. **10**, 1–5. URL https://doi.org/10.1038/s41558-019-0679-2.

Vargas, C. A., Aguilera, V. M., San Martín, V., Manríquez, P. H., Navarro, J. M., Duarte, C., Torres, R., Lardies, M. A., and Lagos, N. A. (2014). CO_2-driven ocean acidification disrupts the filter feeding behavior in Chilean gastropod and bivalve species from different geographic localities. *Estuaries and Coasts*. **38**(4), 1163–1177. URL https://doi.org/10.1007/s12237-014-9873-7.

Vassilatis, D. K., Elliston, K. O., Paress, P. S., Hamelin, M., Arena, J. P., Schaeffer, J. M., Van der Ploeg, L. H., and Cully, D. F. (1997). Evolutionary relationship of the ligand-gated ion channels and the avermectin-sensitive, glutamate-gated chloride channels. *Journal of Molecular Evolution*. **44**(5), 501–508. URL https://doi.org/10.1007/PL00006174.

Vehovszky, A., Bokisch, A. J., Krogsgaard-Larsen, P., and Walker, R. J. (1989). Pharmacological profile of gamma-aminobutyric acid GABA receptors of identified central neurones from *Helix aspersa*. *Comparative Biochemistry and Physiology Part C: Comparative Pharmacology*. **92**(2), 391–399. URL https://doi.org/10.1016/0742-8413(89)90073-X.

Vermeij, M. J., Marhaver, K. L., Huijbers, C. M., Nagelkerken, I., and Simpson, S. D. (2010). Coral larvae move toward reef sounds. *PloS One*. **5**(5), e10660. URL https://doi.org/10.1371/journal.pone.0010660.

Virkki, L. V., Choi, I., Davis, B. A., and Boron, W. F. (2003). Cloning of a na+-driven cl/hco3 exchanger from squid giant fiber lobe. *American Journal of Physiology-Cell Physiology*. **285**(4), C771–C780. URL https://doi.org/10.1152/ajpcell.00439.2002.

Vitousek, P. M., Mooney, H. A., Lubchenco, J., and Melillo, J. M. (1997). Human domination of earth's ecosystems. *Science*. **277**(5325), 494–499. URL https://doi.org/10.1126/science.277.5325.494.

Vitvitsky, V., Thomas, M., Ghorpade, A., Gendelman, H. E., and Banerjee, R. (2006). A functional transsulfuration pathway in the brain links to glutathione homeostasis. *Journal of Biological Chemistry*. **281**(47), 35785–35793. URL https://doi.org/10.1074/jbc.M602799200.

Viyakarn, V., Lalitpattarakit, W., Chinfak, N., Jandang, S., Kuanui, P., Khokiattiwong, S., and Chavanich, S. (2015). Effect of lower pH on settlement and development of coral,

Pocillopora damicornis (Linnaeus, 1758). *Ocean Science Journal*. **50**(2), 475–480. URL https://doi.org/10.1007/s12601-015-0043-z.

Walker, R., Brooks, H., and Holden-Dye, L. (1996). Evolution and overview of classical transmitter molecules and their receptors. *Parasitology*. **113**(S1), S3–S33. URL https://doi.org/10.1017/S0031182000077878.

Waller, J. D., Wahle, R. A., McVeigh, H., and Fields, D. M. (2017). Linking rising pCO_2 and temperature to the larval development and physiology of the American lobster (*Homarus americanus*). *ICES Journal of Marine Science*. **74**(4), 1210–1219. URL https://doi.org/10.1093/icesjms/fsw154.

Walsh, P. J. and Milligan, C. L. (1989). Coordination of metabolism and intracellular acid–base status: Ionic regulation and metabolic consequences. *Canadian Journal of Zoology*. **67**(12), 2994–3004. URL https://doi.org/10.1139/z89-422.

Walters, E. T., Byrne, J. H., Carew, T. J., and Kandel, E. R. (1983). Mechanoafferent neurons innervating tail of *Aplysia*. I. Response properties and synaptic connections. *Journal of Neurophysiology*. **50**(6), 1522–1542. URL https://doi.org/10.1152/jn.1983.50.6.1522.

Wang, D.-S., Mangin, J.-M., Moonen, G., Rigo, J.-M., and Legendre, P. (2006). Mechanisms for picrotoxin block of α2 homomeric glycine receptors. *Journal of Biological Chemistry*. **281**(7), 3841–3855. URL https://doi.org/10.1074/jbc.M511022200.

Wang, J.-J., Shan, K., Liu, B.-H., Liu, C., Zhou, R.-M., Li, X.-M., Dong, R., Zhang, S.-J., Zhang, S.-H., Wu, J.-H., and Yan, B. (2018a). Targeting circular RNA-ZRANB1 for therapeutic intervention in retinal neurodegeneration. *Cell Death and Disease*. **9**(5), 540. URL https://doi.org/10.1038/s41419-018-0597-7.

Wang, L., Sun, F., Wen, Y., and Yue, G. H. (2021). Effects of ocean acidification on transcriptomes in Asian seabass juveniles. *Marine Biotechnology*. **23**, 445–455. URL https://doi.org/10.1007/s10126-021-10036-5.

Wang, Q., Cao, R., Ning, X., You, L., Mu, C., Wang, C., Wei, L., Cong, M., Wu, H., and Zhao, J. (2016). Effects of ocean acidification on immune responses of the Pacific oyster *Crassostrea gigas*. *Fish and Shellfish Immunology*. **49**, 24–33. URL https://doi.org/10.1016/j.fsi.2015.12.025.

Wang, T. and Wang, Y. (2019). Behavioral responses to ocean acidification in marine invertebrates: New insights and future directions. *Journal of Oceanology and Limnology*. pp. 1–14. URL https://doi.org/10.1007/s00343-019-9118-5.

Wang, W., Ju, Y.-Y., Zhou, Q.-X., Tang, J.-X., Li, M., Zhang, L., Kang, S., Chen, Z.-G., Wang, Y.-J., Ji, H., Ding, Y.-Q., Xu, L., and Liu, J.-G. (2017a). The small GTPase Rac1 contributes to extinction of aversive memories of drug withdrawal by facilitating $GABA_A$ receptor endocytosis in the vmPFC. *The Journal of Neuroscience*. **37**(30), 7096–7110. URL https://doi.org/10.1523/jneurosci.3859-16.2017.

Wang, X., Song, L., Chen, Y., Ran, H., and Song, J. (2017b). Impact of ocean acidification on the early development and escape behavior of marine medaka (*Oryzias melastigma*). *Marine Environmental Research*. **131**, 10–18. URL https://doi.org/10.1016/j.marenvres.2017.09.001.

Wang, X., Wang, M., Wang, W., Liu, Z., Xu, J., Jia, Z., Chen, H., Qiu, L., Lv, Z., and Wang, L. (2020). Transcriptional changes of Pacific oyster *Crassostrea gigas* reveal essential role of calcium signal pathway in response to CO_2-driven acidification. *Science of The Total Environment*. **741**, 140177. URL https://doi.org/10.1016/j.scitotenv.2020.140177.

Wang, Y., Hu, M., Wu, F., Storch, D., and Pörtner, H.-O. (2018b). Elevated pCO_2 affects feeding behavior and acute physiological response of the brown crab *Cancer pagurus*. *Frontiers in Physiology*. **9**, 1164. URL https://doi.org/10.3389/fphys.2018.01164.

Wang, Z., Gerstein, M., and Snyder, M. (2009). RNA-Seq: A revolutionary tool for transcriptomics. *Nature Reviews Genetics*. **10**(1), 57–63. URL https://doi.org/10.1038/nrg2484.

Watson, S.-A., Fields, J. B., and Munday, P. L. (2017). Ocean acidification alters predator behaviour and reduces predation rate. *Biology Letters*. **13**(2), 20160797. URL https://doi.org/10.1098/rsbl.2016.0797.

Watson, S.-A., Lefevre, S., McCormick, M. I., Domenici, P., Nilsson, G. E., and Munday, P. L. (2014). Marine mollusc predator-escape behaviour altered by near-future carbon dioxide levels. *Proceedings of the Royal Society of London B: Biological Sciences*. **281**(1774), 20132377. URL https://doi.org/10.1098/rspb.2013.2377.

Welch, M. (2015). *Where do Nitergic and GABAergic neurons lie in the metamorphic pathway of Nassarius obsoletus?* Thesis. Department of Biology, University of North Carolina at Greensboro. Greensboro, North Carolina.

Wheatly, M. G. and Henry, R. P. (1992). Extracellular and intracellular acid-base regulation in crustaceans. *Journal of Experimental Zoology*. **263**(2), 127–142. URL https://doi.org/10.1002/jez.1402630204.

Williams, C. R., Dittman, A. H., McElhany, P., Busch, D. S., Maher, M. T., Bammler, T. K., MacDonald, J. W., and Gallagher, E. P. (2019). Elevated CO_2 impairs olfactory-mediated neural and behavioral responses and gene expression in ocean-phase coho salmon (*Oncorhynchus kisutch*). *Global Change Biology*. **25**, 963–977. URL https://doi.org/10.1111/gcb.14532.

Winnebeck, E. C., Millar, C. D., and Warman, G. R. (2010). Why does insect RNA look degraded? *Journal of Insect Science*. **10**(1). URL https://doi.org/10.1673/031.010.14119. 159.

Wittmann, A. C. and Pörtner, H.-O. (2013). Sensitivities of extant animal taxa to ocean acidification. *Nature Climate Change*. **3**(11), 995–1001. URL https://doi.org/10.1038/nclimate1982.

Wolfe, K., Nguyen, H. D., Davey, M., and Byrne, M. (2020). Characterizing biogeochemical fluctuations in a world of extremes: A synthesis for temperate intertidal habitats in the face of global change. *Global Change Biology*. **26**(7), 3858–3879. URL https://doi.org/10.1111/gcb.15103.

Wollmuth, L. P. (2018). Ion permeation in ionotropic glutamate receptors: Still dynamic after all these years. *Current Opinion in Physiology*. **2**, 36–41. URL https://doi.org/10.1016/j.cophys.2017.12.003.

Wolstenholme, A. J. (2012). Glutamate-gated chloride channels. *Journal of Biological Chemistry*. **287**(48), 40232–40238. URL https://doi.org/10.1074/jbc.R112.406280.

Wong, K. K., Lane, A. C., Leung, P. T., and Thiyagarajan, V. (2011). Response of larval barnacle proteome to CO_2-driven seawater acidification. *Comparative Biochemistry and Physiology Part D: Genomics and Proteomics*. **6**(3), 310–321. URL https://doi.org/10.1016/j.cbd.2011.07.001.

Wood, D. E., Lu, J., and Langmead, B. (2019). Improved metagenomic analysis with Kraken 2. *Genome Biology*. **20**(1), 257. URL https://doi.org/10.1186/s13059-019-1891-0.

Woodward, R., Polenzani, L., and Miledi, R. (1993). Characterization of bicuculline/baclofen-insensitive (rho-like) gamma-aminobutyric acid receptors expressed in *Xenopus* oocytes. II. Pharmacology of gamma-aminobutyric acidA and gamma-aminobutyric acidB receptor agonists and antagonists. *Molecular Pharmacology*. **43**(4), 609–625.

Wu, C., Qin, X., Du, H., Li, N., Ren, W., and Peng, Y. (2017). The immunological function of GABAergic system. *Frontiers in Bioscience*. **22**, 1162–72.

Wu, F., Lu, W., Shang, Y., Kong, H., Li, L., Sui, Y., Hu, M., and Wang, Y. (2016). Combined effects of seawater acidification and high temperature on hemocyte parameters in the thick shell mussel *Mytilus coruscus*. *Fish and Shellfish Immunology*. **56**, 554–562. URL https://doi.org/10.1016/j.fsi.2016.08.012.

Wu, J.-S., Jing, J., Dıaz-Rıos, M., Miller, M. W., Kupfermann, I., and Weiss, K. R. (2003). Identification of a GABA-containing cerebral-buccal interneuron-11 in *Aplysia californica*. *Neuroscience letters*. **341**(1), 5–8. URL https://doi.org/10.1016/S0304-3940(03)00052-1.

Xie, L., Tiong, C. X., and Bian, J.-S. (2012). Hydrogen sulfide protects SH-SY5Y cells against 6-hydroxydopamine-induced endoplasmic reticulum stress. *American Journal of Physiology-Cell Physiology*. **303**(1), C81–C91. URL https://doi.org/10.1152/ajpcell.00281.2011.

Xie, W., Kanehara, K., Sayeed, A., and Ng, D. T. (2009). Intrinsic conformational determinants signal protein misfolding to the Hrd1/Htm1 endoplasmic reticulum–associated degradation system. *Molecular Biology of the Cell*. **20**(14), 3317–3329. URL https://doi.org/10.1091/mbc.e09-03-0231.

Xing, Q., Wang, J., Zhao, Q., Liao, H., Xun, X., Yang, Z., Huang, X., and Bao, Z. (2019). Alternative splicing, spatiotemporal expression of TEP family genes in Yesso scallop (*Patinopecten yessoensis*) and their disparity in responses to ocean acidification. *Fish and Shellfish Immunology*. URL https://doi.org/10.1016/j.fsi.2019.10.026.

Yagodina, O. V. (2009). Enzymological characteristic of monoamine oxidase from the visual ganglia of the Pacific squid *Todarodes pacificus*. *Doklady. Biochemistry and Biophysics*. **428**(1), 284–7. URL http://doi.org/10.1134/S1607672909050159.

Yagodina, O. V. (2010). Comparative study of substrate and inhibitory specificity of monoamine oxidase of squid optic ganglia. *Journal of Evolutionary Biochemistry and Physiology*. **46**(3), 227–234. URL https://doi.org/10.1134/S0022093010030014.

Yamoah, E. and Kuzirian, A. M. (1994). Effects of GABA on outward currents in *Hermissenda* photoreceptors. *The Biological Bulletin*. **187**(2), 265–266. URL http://doi.org/10.1086/BBLv187n2p265.

Yarowsky, P. and Carpenter, D. (1978a). A comparison of similar ionic responses to gamma-aminobutyric acid and acetylcholine. *Journal of neurophysiology*. **41**(3), 531–541. URL https://doi.org/10.1152/jn.1978.41.3.531.

Yarowsky, P. and Carpenter, D. (1978b). Receptors for gamma-aminobutyric acid GABA on *Aplysia* neurons. *Brain Research*. **144**(1), 75–94. URL https://doi.org/10.1016/0006-8993(78)90436-5.

Yeh, C.-W., Kao, S.-H., Cheng, Y.-C., and Hsu, L.-S. (2013). Knockdown of cyclin-dependent kinase 10 (cdk10) gene impairs neural progenitor survival via modulation of raf1a gene expression. *Journal of Biological Chemistry*. **288**(39), 27927–27939. URL https://doi.org/10.1074/jbc.M112.420265.

Young, C. S., Lowell, A., Peterson, B., and Gobler, C. J. (2019). Ocean acidification and food limitation combine to suppress herbivory by the gastropod *Lacuna vincta*. *Marine Ecology Progress Series*. **627**, 83–94. URL https://doi.org/10.3354/meps13087.

Yu, G., Wang, L.-G., Han, Y., and He, Q.-Y. (2012). clusterProfiler: An R package for comparing biological themes among gene clusters. *OMICS: A Journal of Integrative Biology*. **16**(5), 284–287. URL https://doi.org/10.1089/omi.2011.0118.

Yu, J., Liang, X., Ji, Y., Ai, C., Liu, J., Zhu, L., Nie, Z., Jin, X., Wang, C., and Zhang, J. (2020). PRICKLE3 linked to ATPase biogenesis manifested Leber's hereditary optic neuropathy. *The Journal of Clinical Investigation*. **130**(9). URL https://doi.org/10.1172/JCI134965.

Yuan, X., McCoy, S. J., Du, Y., Widdicombe, S., and Hall-Spencer, J. M. (2018a). Physiological and behavioral plasticity of the sea cucumber *Holothuria forskali* (Echinodermata, Holothuroidea) to acidified seawater. *Frontiers in Physiology*. **9**, 1339. URL https://doi.org/10.3389/fphys.2018.01339.

Yuan, X., Yuan, T., Huang, H., Jiang, L., Zhou, W., and Liu, S. (2018b). Elevated CO_2 delays the early development of scleractinian coral *Acropora gemmifera*. *Scientific Reports*. **8**, 2787. URL https://doi.org/10.1038/s41598-018-21267-3.

Zakroff, C., Mooney, T. A., and Berumen, M. L. (2019). Dose-dependence and small-scale variability in responses to ocean acidification during squid, *Doryteuthis*

pealeii, development. *Marine Biology*. **166**(5), 62. URL https://doi.org/10.1007/s00227-019-3510-8.

Zakroff, C., Mooney, T. A., and Wirth, C. (2018). Ocean acidification responses in paralarval squid swimming behavior using a novel 3D tracking system. *Hydrobiologia*. **808**, 83–106. URL https://doi.org/10.1007/s10750-017-3342-9.

Zarnetske, P. L., Skelly, D. K., and Urban, M. C. (2012). Biotic multipliers of climate change. *Science*. **336**(6088), 1516–1518. URL https://doi.org/doi:10.1126/science.1222732.

Zhan, X. and Desiderio, D. M. (2003). Heterogeneity analysis of the human pituitary proteome. *Clinical Chemistry*. **49**(10), 1740–1751. URL https://doi.org/10.1373/49.10.1740.

Zhang, J., Xue, F., and Chang, Y. (2008). Structural determinants for antagonist pharmacology that distinguish the ρ1 $GABA_C$ receptor from $GABA_A$ receptors. *Molecular Pharmacology*. **74**(4), 941–951. URL https://doi.org/10.1124/mol.108.048710.

Zhang, T., Qu, Y., Zhang, Q., Tang, J., Cao, R., Dong, Z., Wang, Q., and Zhao, J. (2021). Risks to the stability of coral reefs in the South China Sea: An integrated biomarker approach to assess the physiological responses of *Trochus niloticus* to ocean acidification and warming. *Science of The Total Environment*. **782**, 146876. URL https://doi.org/10.1016/j.scitotenv.2021.146876.

Zhang, X. and Bian, J.-S. (2014). Hydrogen sulfide: A neuromodulator and neuroprotectant in the central nervous system. *ACS Chemical Neuroscience*. **5**(10), 876–883. URL https://doi.org/10.1021/cn500185g.

Zhang, Y., Shi, F., Song, J., Zhang, X., and Yu, S. (2015). Hearing characteristics of cephalopods: Modeling and environmental impact study. *Integrative Zoology*. **10**, 141–151. URL https://doi.org/10.1111/1749-4877.12104.

Zheng, Y., Hirschberg, B., Yuan, J., Wang, A. P., Hunt, D. C., Ludmerer, S. W., Schmatz, D. M., and Cully, D. F. (2002). Identification of two novel *Drosophila melanogaster* histamine-gated chloride channel subunits expressed in the eye. *Journal of Biological Chemistry*. **277**(3), 2000–2005. URL https://doi.org/10.1074/jbc.M107635200.

Zhou, Y.-F., Wu, X.-M., Zhou, G., Mu, M.-d., Zhang, F.-L., Li, F.-M., Qian, C., Du, F., Yung, W.-H., Qian, Z.-M., and Ke, Y. (2018). Cystathionine β-synthase is required for

body iron homeostasis. *Hepatology*. **67**(1), 21–35. URL https://doi.org/10.1002/hep.29499.

Zhou, Z., Jiang, Q., Wang, M., Yue, F., Wang, L., Wang, L., Li, F., Liu, R., and Song, L. (2013). Modulation of haemocyte phagocytic and antibacterial activity by alpha-adrenergic receptor in scallop *Chlamys farreri*. *Fish and Shellfish Immunology*. **35**(3), 825–832. URL https://doi.org/10.1016/j.fsi.2013.06.020.

Zhou, Z., Wang, L., Gao, Y., Wang, M., Zhang, H., Wang, L., Qiu, L., and Song, L. (2011). A monoamine oxidase from scallop *Chlamys farreri* serving as an immunomodulator in response against bacterial challenge. *Developmental and Comparative Immunology*. **35**(7), 799–807. URL https://doi.org/10.1016/j.dci.2011.03.014.

Zink, C. F., Barker, P. B., Akira Sawa, M., Weinberger, D. R., Wang, M., Quillian, H., Ulrich, W. S., Chen, Q., Jaffe, A. E., Kleinman, J. E., Hyde, T. M., Prettyman, G. E., Giegerich, M., Carta, K., van Ginkel, M., and Bigos, K. L. (2020). Association of missense mutation in FOLH1 with decreased NAAG levels and impaired working memory circuitry and cognition. *American Journal of Psychiatry*. **177**(12), 1129–1139. URL https://doi.org/10.1176/appi.ajp.2020.19111152.

Zlatkin, R. L. and Heuer, R. M. (2019). Ocean acidification affects acid–base physiology and behaviour in a model invertebrate, the California sea hare (*Aplysia californica*). *Royal Society Open Science*. **6**(10), 191041. URL https://doi.org/10.1098/rsos.191041.

Appendix A

Chapter 2 Appendices

Table A.1. Summary of published papers assessing the effects of elevated CO_2 on marine invertebrate behaviour. Summary of published papers since the reviews by Clements and Hunt (2015) and Nagelkerken and Munday (2015) assessing the effects of elevated CO_2 on marine invertebrate behaviour. Papers are grouped by behaviour, then phyla. Stimulus: - = no stimulus given, Response to high CO_2 : - = no effect on behaviour measured, ↑ = increase in behaviour measured, ↓ = decrease in behaviour measured, (trend) = a non-significant trend.

Behaviour	Phylum	Specific behaviour	Stimulus	Control pCO_2 (µatm)	Elevated pCO_2 (µatm)	pCO_2 exposure time	Response to high CO_2	Life stage	Common name	Species	Reference
Feeding	Mollusc	Feeding rate	*Isochrysis galbana* cells	500	750	30 days	-	Juvenile	Giant mussel	*Choromytilus chorus*	Benítez *et al.* (2018)
					1,200		-				
		Feeding rate	Polystyrene beads	250	400	48 hours	-	Larvae	California mussel	*Mytilus californianus*	Gray *et al.* (2017)
					800		-				
					2,200		-				
		Initiation of feeding		250	400		delay				
					800		delay				
					2,200		delay				
		Feeding rate	Algal pieces	400	1,000	7 days	-	Not reported	Topshell snail	*Trochus histrio*	Grilo *et al.* (2019)
		Feeding rate	Micro-algae *Chlorella vulgaris*	∼370	∼1,100	1 day	↓	Adult	Blue mussel	*Mytilus edulis*	Gu *et al.* (2019)
						3 days	↓				
						7 days	↓				
						14 days	↓				
					∼2,700	1 day	↓				
						3 days	↓				
						7 days	↓				
						14 days	↓				

Table A.1 continued.

Behaviour	Phylum	Specific behaviour	Stimulus	Control pCO_2 (µatm)	Elevated pCO_2 (µatm)	pCO_2 exposure time	Response to high CO_2	Life stage	Common name	Species	Reference
		Feeding rate when given an optimal diet	Two microalgae cultures: *Isochrysis galbana* and *Rhodomonas lens*	500	800	2 weeks	↑	Juvenile	Mediterranean mussel	*Mytilus gallo-provincialis*	Lassoued *et al.* (2019)
					1,200		↑				
		Feeding rate when given a sub-optimal diet			800		-				
					1,200		-				
		Feeding rate	Macroalgae *Ulva spp.*	440	1,900	24 hours	↓	Not reported	Banded chink shell	*Lacuna vincta*	Young *et al.* (2019)
		Successfully reach food source	Opened mussel	394	2,045	2.5 years	↓	Adult and juvenile	Banded dye-murex	*Hexaplex trunculus*	Chatzinikolaou *et al.* (2019)
		Response time, duration, speed and path index to food source					-				
		Response time to food source		394	2,045	2.5 years	↓	Adult	Nassa mud snail	*Nassarius nitidus*	Chatzinikolaou *et al.* (2019)

Table A.1 continued.

Behaviour	Phylum	Specific behaviour	Stimulus	Control pCO_2 (µatm)	Elevated pCO_2 (µatm)	pCO_2 exposure time	Response to high CO_2	Life stage	Common name	Species	Reference
		Duration, speed, path index and success to food source					-				
		Feeding rate	Live barnacles *Amphibalanus amphitrite amphitrite*	380	950	1 month	-	Not reported	Murex snail	*Reishia clavigera*	Li *et al.* (2020)
					1,250		-				
		Suspension feeding events and time	-	500	2,140	4 weeks	↓	Adult	Peppery furrow shell	*Scrobicularia plana*	Van Colen *et al.* (2020)
	Arthropod	Feeding rate	Herring blocks	400	600	40 days	-	Stage V	American lobster	*Homarus americanus*	Menu-Courey *et al.* (2018)
					800		-				
					1,000		↑				
					2,000		↑				
					3,000		↓				
		Feeding rate	live *Artemia salina* nauplii	∼380	∼750	hatching until 48 hours after Stage IV moulting	↓	Stage IV	American lobster	*Homarus americanus*	Waller *et al.* (2017)
		Feeding rate	Squid pieces	450	1,100	5 weeks	↓	Juvenile	European lobster	*Homarus gammarus*	Small *et al.* (2016)

Table A.1 continued.

Behaviour	Phylum	Specific behaviour	Stimulus	Control pCO_2 (µatm)	Elevated pCO_2 (µatm)	pCO_2 exposure time	Response to high CO_2	Life stage	Common name	Species	Reference
					9,000		↓				
		Feeding rate	Mussels	360	1,200	2 weeks	↓	Adult	Brown crab	*Cancer pagurus*	Wang *et al.* (2018b)
					2,300		↓				
		Cirral activity	-	400	1,600	16 months	↑	Juveniles grown to maturity	Bay barnacle	*Balanus improvisus*	Pansch *et al.* (2018)
		Feeding rate	Clams	360	2,700	2 hours	↓	Adult	Japanese stone crab	*Charybdis japonica*	Wu *et al.* (2017)
		Feeding rate	Squid piece	330	770	Immediately and 3 weeks	-	Juvenile	Red and blue king crabs	*Paralithodes camtschaticus, P. platypus*	Long *et al.* (2019)
					1500		-				
		Feeding rate	Algae	430	2,200	2 days	-	Nauplii larvae	Purple acorn barnacle	*Balanus Amphitrite*	Campanati *et al.* (2015)
		Foraging activity and duration	Olfactory cues - blood-worms, crus-taceans, molluscs, visual cues - live shrimp	465	905	2.5 months	-	Not reported	Common shrimp	*Palaemon inter-medius, P. serenus*	Marangon *et al.* (2019)
		Food detection	Crustacean food	593	1,617	1 week	-	Not reported	Antarctic amphipod	*Gondogeneia antarctica*	Park *et al.* (2019)
						2 weeks	↓				

Table A.1 continued.

Behaviour	Phylum	Specific behaviour	Stimulus	Control pCO_2 (µatm)	Elevated pCO_2 (µatm)	pCO_2 exposure time	Response to high CO_2	Life stage	Common name	Species	Reference
						3 weeks 4 weeks	- ↓ (trend)				
	Echino-derm	Feeding rate	Algae/agar cubes	450	1,500	9 weeks	-	Adult	Sea urchin	*Heliocidaris erythro-gramma*	Carey *et al.* (2016)
		Feeding rate	Live algae	360	1,300	21 days	↑	Adult	Rock-boring urchin	*Echinometra lucunter*	Rich *et al.* (2018)
Predatory	Mollusc	Capture and consumption	Live conch snails	390	975	2 - 3 weeks	↓	Adult	Cone snail	*Conus marmoreus*	Watson *et al.* (2017)
		Attack	Live shrimp	440	700	5 days	↓	Adult	Two-toned pygmy squid	*Idiosepius pygmaeus*	Spady *et al.* (2018)
					900	5 days	↓				
		Attack	Live fish	440	900	28 days	↓	Adult	Bigfin reef squid	*Sepioteuthis lessoniana*	Spady *et al.* (2018)
		Attack	5 live *Gammarus sp.*	460	1,000	65 days	-	15 - 20 days post-hatching	Common cuttlefish	*Sepia officinalis*	Moura *et al.* (2019)
		Prey search	Live mussels, visually obstructed	500	1,400	6 months	↓	Juvenile	Chilean abalone	*Concholepas conc-holepas*	Domenici *et al.* (2017)
		Search time	Live barnacles *Amphibal-anus amphitrite amphitrite*	380	950	1 month	-	Not reported	Murex snail	*Reishia clavigera*	Li *et al.* (2020)

Table A.1 continued.

Behaviour	Phylum	Specific behaviour	Stimulus	Control pCO_2 (µatm)	Elevated pCO_2 (µatm)	pCO_2 exposure time	Response to high CO_2	Life stage	Common name	Species	Reference
					1,250		↑				
		Speed to prey			950		-				
					1,250		-				
		Prey preference	Live barnacles *A. Amphitrite amphitritem* and mussels *Brachidontes variabilis*		950		-				
					1,250		-				
	Arthropod	Foraging	Clams	360	2,700	2 hours	↓	Adult	Japanese stone crab	*Charybdis japonica*	Wu *et al.* (2017)
		Foraging	Mussels	360	1,200	2 weeks	↓	Adult	Brown crab	*Cancer pagurus*	Wang *et al.* (2018b)
					2,300		↓				
		Foraging	Clams	1,300	6,500	30 days	-	Not reported	Blue crab	*Callinectes sapidus*	Glaspie *et al.* (2017)
		Prey capture					↑				
Predator avoidance	Mollusc	Avoidance	Predator chemical cue	16 levels 400 - 2,600		5 days	↓	Not reported	Black turban snail	*Tegula funebralis*	Jellison *et al.* (2016)

Table A.1 continued.

Behaviour	Phylum	Specific behaviour	Stimulus	Control pCO_2 (µatm)	Elevated pCO_2 (µatm)	pCO_2 exposure time	Response to high CO_2	Life stage	Common name	Species	Reference
				10 baseline levels 540 - 3,200 (fluctuating to 3,500 - 14,800 for 6 hours each day)			↓				
		Protective	Predator in cage	350	1,100	7 days	↓	Not reported	Korean and blue mussels	*Mytilus coruscus and M. edulis*	Kong *et al.* (2019)
		Shelter-seeking	-	460	1,000	65 days	↓ (trend)	15 – 20 days post-hatching	Common cuttlefish	*Sepia officinalis*	Moura *et al.* (2019)
		Alarm response	Conspecific alarm cue (ink)				-				
		Avoidance	Mechanical	1,300	6,500	30 days	↓	Juvenile	Soft-shell clam	*Mya arenaria*	Glaspie *et al.* (2017)
		Self-righting	Placed upside down	390	975	2 - 3 weeks	-	Adult	Cone snail	*Conus marmoreus*	Watson *et al.* (2017)

Table A.1 continued.

Behaviour	Phylum	Specific behaviour	Stimulus	Control pCO_2 (µatm)	Elevated pCO_2 (µatm)	pCO_2 exposure time	Response to high CO_2	Life stage	Common name	Species	Reference
		Self-righting	Released from top of water column on side	400	1,200	4- 11 days	-	Not reported	California sea hare	*Aplysia californica*	Zlatkin and Heuer (2019)
					3,000		-				
		Tail-withdrawal reflex	Mechanical		1,200		↓				
					3,000		↓				
		Escape response type	Predator chemical cue (northern mud crab *Dys-panopeus sayi*)	410	1,200	4 weeks	altered	Adult	Mud snail	*Tritia obsoleta*	Froehlich and Lord (2020)
			Crushed con-specifics chemical cue				-				
			-				-				
		Movement vector (distance and direction)	Predator chemical cue (northern mud crab *Dys-panopeus sayi*)				movement away from cue lost				

Table A.1 continued.

Behaviour	Phylum	Specific behaviour	Stimulus	Control pCO_2 (µatm)	Elevated pCO_2 (µatm)	pCO_2 exposure time	Response to high CO_2	Life stage	Common name	Species	Reference
			Crushed con-specifics chemical cue				movement away from cue lost				
			-				-				
	Arthropod	Avoidance	Predator chemical cue	450	1,400	12 hours	↓	Stage III larvae	Asian shore crab	*Hemigrapsus sanguineus*	Charpentier and Cohen (2016)
		Avoidance	Predator chemical cue	not reported (pH = 8.1)	not reported (pH = 7.6)	98 days	-	Juvenile	Hermit crab	*Pagurus criniticor-nis*	Ragagnin *et al.* (2018)
		Avoidance	No predator cue	600	900	5 weeks	-	Not reported	Decorator crab	*Pelia tumida*	Rankin *et al.* (2019)
	Echino-derm	Defence	Mechanical	670	900	22 weeks	-	Adult	Black sea cucumber	*Holothuria forskali*	Yuan *et al.* (2018a)
					1,100		-				
		Self-righting	Placed upside down	519	1,070	30 – 120 days	-	Adult	Common starfish	*Asterias rubens*	McCarthy *et al.* (2019)
Settlement and meta-morpho-sis	Mollusc	Metamorphosis	-	450	800	24 hours	-	Trochophore larvae	Variously coloured abalone	*Haliotis di-versicolor*	Guo *et al.* (2015)
					1,500		-				
					2,000		-				

Table A.1 continued.

Behaviour	Phylum	Specific behaviour	Stimulus	Control pCO_2 (µatm)	Elevated pCO_2 (µatm)	pCO_2 exposure time	Response to high CO_2	Life stage	Common name	Species	Reference
					3,000		↓				
					800		-	Trochophore larvae	Disc abalone	*Haliotis discus hannai*	
					1,500		↓				
					2,000		↓				
					3,000		↓				
		Metamorphosis	-		800	3 days	-	Veliger larvae	Variously coloured abalone	*Haliotis diversicolor*	
					1,500		-				
					2,000		↓				
					3,000		↓				
					800		-	Veliger larvae	Disc abalone	*Haliotis discus hannai*	
					1,500		-				
					2,000		↓				
					3,000		↓				
		Settlement	-	320	500	9 - 17 days	-	Larvae	Baltic clam	*Macoma balthica*	Jansson *et al.* (2016)
					900		delay				
					1,100		delay				
					1,300		delay				
		Metamorphosis			900		↑				
					1,500		-				
		Downward swimming	Presence and absence of chemical settlement cue	~500	~2,500	Immediately prior to experiments	-	Larvae	Eastern oyster	*Crassostrea virginica*	Meyer-Kaiser *et al.* (2019)

Table A.1 continued.

Behaviour	Phylum	Specific behaviour	Stimulus	Control pCO_2 (µatm)	Elevated pCO_2 (µatm)	pCO_2 exposure time	Response to high CO_2	Life stage	Common name	Species	Reference
		Settlement		∼500	∼2,500		-				
		Metamorphosis	10mM KCl	∼400	∼1,200	10 – 14 days	delayed		Slippershell snail	*Crepidula fornicata*	Pechenik *et al.* (2019)
					∼1,400		delayed				
			Adult cues for 3 hours	∼500	∼1,400	At the same time as adult cue exposure	-				
					∼1,400	Two hours	-				
					∼1,400	14 days	-				
	Arthropod	Settlement	-	430	2,200	4 days	-	Cyprid larvae	Acorn barnacle	*Balanus amphitrite*	Campanati *et al.* (2015)
			Settlement-inducing cue		2,200		-				
		Conspecific attraction	Conspecific and heterospecific chemical cues	400	700	Duration of behavioural trial	↓	Larvae	Banded coral shrimp	*Stenopus hispidus*	Lecchini *et al.* (2017)
					1,000		↓				
	Echinoderm	Settlement	-	500	1,300	35 days	delay	Larvae	Purple sea urchin	*Paracentrotus lividus*	García *et al.* (2015)
					2,600		lost				

Table A.1 continued.

Behaviour	Phylum	Specific behaviour	Stimulus	Control pCO_2 (µatm)	Elevated pCO_2 (µatm)	pCO_2 exposure time	Response to high CO_2	Life stage	Common name	Species	Reference
	Cnidaria	Settlement choice	Settlement substrata (from control or high CO_2 field site)	~400	~800	Substrata from field sites	preferred control sub-strata	Larvae	Coral	*Acropora tenuis*	Fabricius *et al.* (2017)
		Recruitment	Field sites	~400	~800	13 months	↓	Larvae	Coral	15 coral taxa	Fabricius *et al.* (2017)
		Settlement	Crustose coralline algae	400	700	2 days	↓	Larvae	Coral	*Acropora gemmifera*	Yuan *et al.* (2018b)
					1,200		↓				
		Settlement	-	not reported (pH = 8.1)	not reported (pH = 7.9)	31 hours	↓	Larvae	Coral	*Pocillopora damicornis*	Viyakarn *et al.* (2015)
					not reported (pH = 7.6)		↓				
		Metamorphosis			not reported (pH = 7.9)		delay				
					not reported (pH = 7.6)		delay				
		Settlement	Crustose coralline algae	250	900	1 week	-	Larvae	Coral	*Acropora spicifera*	Foster *et al.* (2015)

Table A.1 continued.

Behaviour	Phylum	Specific behaviour	Stimulus	Control pCO_2 (µatm)	Elevated pCO_2 (µatm)	pCO_2 exposure time	Response to high CO_2	Life stage	Common name	Species	Reference
		Settlement	Settlement substrate	520	2,200	72 hours	-	Larvae	Coral	*Porites astreoides*	Olsen *et al.* (2015)
	Bryozoan	Settlement	-	8 levels 266 – 18,689		6 hours	delay	Larvae	Brown bryozoan	*Bugula neritina*	Pecquet *et al.* (2017)
				600	1,200	48 hours (parents) + 6 hours (larvae)	↓				
	Annelid	Settlement success	Biofilm exposed to pCO_2 for 23 days	350	1,180	24 and 48 hours	-	Larvae	Tubeworm	*Galeolaria hystrix*	Nelson *et al.* (2020)
					2,600		-				
			Biofilm exposed to pCO_2 for 60 days	350	1,180	24 and 48 hours	-				
					2,600		-				
Reproductive behaviour	Arthropod	Mate detection	Female chemical cue	350	800	2 generations	↓	Adult	Amphipod	*Gammarus locusta*	Borges *et al.* (2018)
Other chemosensory behaviours	Arthropod	Binary choice	Healthy conspecific chemical cue	not reported (pH = 8.1)	not reported (pH = 7.65)	~10 days	avoided	Juvenile	Caribbean spiny lobster	*Panulirus argus*	Ross and Behringer (2019)

Table A.1 continued.

Behaviour	Phylum	Specific behaviour	Stimulus	Control pCO_2 (µatm)	Elevated pCO_2 (µatm)	pCO_2 exposure time	Response to high CO_2	Life stage	Common name	Species	Reference
			Diseased conspecific chemical cue				attracted				
			Competitor chemical cue				-				
			Antennule flicking				↓ (trend)				
		Displacement	Dead gastropod chemical cue	not reported (pH = 8.1)	not reported (pH = 7.6)	98 days	-	Juvenile	Hermit crab	*Pagurus criniticornis*	Ragagnin *et al.* (2018)
Activity	Mollusc	Swimming speed	-	400 - 2,200		Duration of egg development	↓	Paralarvae	Longfin inshore squid	*Doryteuthis pealeii*	Zakroff *et al.* (2018)
		Other swimming measures					altered				
		Path velocity	-	400	900	48 hours	-	Larvae	Black clam	*Cyclina sinensis*	Sui *et al.* (2019)
		Time active, speed, distance	-	440	2,600 900	28 days	↓ ↑	Adult	Bigfin reef squid	*Sepioteuthis lessoniana*	Spady *et al.* (2018)
		Distance	-	390	975	2 - 3 weeks	↑	Adult	Cone snail	*Conus marmoreus*	Watson *et al.* (2017)

Table A.1 continued.

Behaviour	Phylum	Specific behaviour	Stimulus	Control pCO_2 (µatm)	Elevated pCO_2 (µatm)	pCO_2 exposure time	Response to high CO_2	Life stage	Common name	Species	Reference
		Distance	Predator chemical cue	16 levels 400 - 2,600		5 days	-	Not reported	Black turban snail	*Tegula funebralis*	Jellison *et al.* (2016)
				10 baseline levels 540 - 3,200 (fluctuating to 3,500 - 148,000 for 6 hours each day)			-				
	Arthropod	Swimming speed	-	~380	~750	hatching until 48 hours after Stage IV moulting	↑	Stage IV	American lobster	*Homarus americanus*	Waller *et al.* (2017)
		Average shoal speed	-	480	750	3 hours	↑	Phase I Juvenile	Swimming crab	*Portunus trituberculatus*	Ren *et al.* (2018)
					750	6 hours	↑				
					750	12 - 72 hours	-				
					1,500	3 hours	-				
					1,500	6 hours	↑				

Table A.1 continued.

Behaviour	Phylum	Specific behaviour	Stimulus	Control pCO_2 (µatm)	Elevated pCO_2 (µatm)	pCO_2 exposure time	Response to high CO_2	Life stage	Common name	Species	Reference
		Swimming direction	-	460	966	From hatching	altered	Stage III	Florida stone crab	*Menippe mercenaria*	Gravinese *et al.* (2019)
							-	Stage V			
		Swimming speed	-				↑	Stage III			
							-	Stage V			
					1,500	12 hours	↑				
					1,500	24 - 72 hours	-				
		Time active	Presence and absence of chemical cues	not reported (pH = 8.1)	not reported (pH = 7.65)	~10 days	-	Juvenile	Caribbean spiny lobster	*Panulirus argus*	Ross and Behringer (2019)
		Speed and distance	-	400	1,000	2 months	-	Not reported	Snapping shrimp	*Alpheus novaeze-landiae*	Rossi *et al.* (2016)
		Swimming activity	Day	593	1,617	1 – 26 days	-	Not reported	Antarctic amphipod	*Gondogeneia antarctica*	Park *et al.* (2019)
			Night				-				
	Bryozoan	Swimming speed	-	600	1,200	48 hours (parents) + 6 hours (larvae)	↑	Larvae	Brown bryozoan	*Bugula neritina*	Pecquet *et al.* (2017)
Burrowing	Mollusc	Burying	-	390	975	2 - 3 weeks	↓	Adult	Cone snail	*Conus marmoreus*	Watson *et al.* (2017)
		Digging depth	-	550	1,200	24 hours	-	Adult	Razor clam	*Sinonovacula constricta*	Peng *et al.* (2017)
					1,900		↓				
					3,000		↓				

Table A.1 continued.

Behaviour	Phylum	Specific behaviour	Stimulus	Control pCO_2 (µatm)	Elevated pCO_2 (µatm)	pCO_2 exposure time	Response to high CO_2	Life stage	Common name	Species	Reference
		Percentage buried	-	not reported (pH = 8.1)	not reported (pH = 7)	14 days	↑	Not reported	Baltic clam	*Macoma balthica*	Jakubowska and Normant-Saremba (2015)
					not reported (pH = 6)		↑				
		Percentage buried	-	not reported (pH = 6.84 - 7.37, field collected)		5 hours	↓	Juvenile	Soft-shell clam	*Mya arenaria*	Clements *et al.* (2016)
				~1,300	~8,500	20 mins	↓	Juvenile	Soft-shell clam	*Mya arenaria*	Clements *et al.* (2017)
Anxiety-like behaviour	Arthropod	Scototaxis	Visual (light/dark)	480	750	72 hours	altered	Phase I Juvenile	Swimming crab	*Portunus trituberculatus*	Ren *et al.* (2018)
					1,500		altered				
		Speed	Visual (light/dark)		750		↑				
					1,500		-				
Other behaviours	Mollusc	Lateralisation	Live mussels, visually obstructed	500	1,400	1.5 months	-	Juvenile	Chilean abalone	*Concholepas concholepas*	Domenici *et al.* (2017)

Table A.1 continued.

Behaviour	Phylum	Specific behaviour	Stimulus	Control pCO_2 (µatm)	Elevated pCO_2 (µatm)	pCO_2 exposure time	Response to high CO_2	Life stage	Common name	Species	Reference
		Repeatability of lateralisation				~6 months	lost				
	Arthropod	Snapping	-	400	1,000	2 months	↓	Not reported	Snapping shrimp	*Alpheus novaeze-landiae*	Rossi *et al.* (2016)
			Simulated aggression				-				
			Field sites	~500	700 - 5,400	Field	↓				
		Shelter-use	Day	593	1,617	1 – 26 days	↓	Not reported	Antarctic amphipod	*Gondogeneia antarctica*	Park *et al.* (2019)
			Night				-				

Appendix B

Chapter 3 Appendices

Table B.1. Studies that have investigated the mechanism of action of gabazine in molluscs. All studies in molluscs have been done in gastropod molluscs. Target receptor: ion? = unknown which ion(s) the receptor is permeable to, hyper/depolarising? = unknown whether activation of the receptor results in hyperpolarisation (inhibitory) or depolarisation (excitatory). Administration method: bath application = animal/tissue/neuron sitting in the solution. Gabazine effect: the effect of gabazine on the behaviour measured or electrophysiological recording (neurotransmitter-induced hyper or depolarisation): - = no effect, × = completely blocked, ↓ = decrease, ↑ = increase.

Target receptor	Species Common name	Life stage	Gabazine conc. (μM)	Administration method	Method of measurement	Gabazine effect	Reference
Ionotropic GABA R (Cl^-, hyper/depolarising?)	*Tritia obsoleta* Marine mud snail	Larvae	0.1, 1, 10, 100	Bath application	*In vivo* Percentage of larvae metamorphosing	-	Biscocho *et al.* (2018)
Ionotropic GABA R (ion?, hyperpolarising)	*Helix aspersa* Terrestrial snail	Not stated	10	Bath application then by micropipette	*In vitro* Electrophysiology	×	Vehovszky *et al.* (1989)
Ionotropic GABA R (ion?, depolarising)	*Helix aspersa* Terrestrial snail	Not stated	10	Bath application then by micropipette	*In vitro* Electrophysiology	↓	Vehovszky *et al.* (1989)
GABA R (type unknown)	*Nassarius obsoletus* Eastern mud snail (marine)	Larvae	1, 10 100, 1,000	Bath application	*In vivo* Percentage of larvae metamorphosing	- ↑	Welch (2015)

Table B.2. Studies that have investigated the mechanism of action of picrotoxin in molluscs. All studies are in gastropod molluscs, apart from one study in a cephalopod mollusc (Chichery and Chichery, 1985). Target receptor: ion? = unknown which ion(s) the receptor is permeable to, hyper/depolarising? = unknown whether activation of the receptor results in hyperpolarisation (inhibitory) or depolarisation (excitatory). Administration method: superfusion = continuous flow over the outside of the tissue/neuron, perfusion = continuous flow through the tissue/neuron, bath application = animal/tissue/neuron sitting in the solution. Picrotoxin effect: The effect of picrotoxin on the behaviour measured or the electrophysiological recording (neurotransmitter-induced hyper or depolarisation): - = no effect, × = completely blocked, ↓ = decrease, ↑ = increase.

Target receptor	Species Common name	Life stage	Picrotoxin conc. (µM)	Administration method	Method of measurement	Picrotoxin effect	Reference
Ionotropic GABA R (Cl^-, hyperpolarising)	*Aplysia californica* California sea hare	Not stated, 50 - 300 g	1,000	Bath application	*In vitro* Electrophysiology	↓	Jing *et al.* (2003)
	Aplysia californica California sea hare	Not stated	1,000	Perfusion	*In vitro* Electrophysiology	×	Yarowsky and Carpenter (1978a)
	Aplysia californica California sea hare	Not stated	10 1,000	Perfusion	*In vitro* Electrophysiology	↓ ×	Yarowsky and Carpenter (1978b)
	Aplysia californica California sea hare	Not stated, 150 - 300 g	1,000	Not stated	*In vitro* Electrophysiology	↓	Wu *et al.* (2003)
	Clione limacina Sea angel	Adult	1,000	Bath application	*In vitro* Electrophysiology	-	Norekian and Satterlie (1993)
Ionotropic GABA R (ion?, hyperpolarising)	*Clione limacina* Sea angel	Adult	1,000	Bath application	*In vitro* Electrophysiology	↓	Norekian and Malyshev (2005)

Table B.2 continued.

Target receptor	Species Common name	Life stage	Picrotoxin conc. (µM)	Administration method	Method of measurement	Picrotoxin effect	Reference
	Lymnaea stagnalis Pond snail	2-3 months	100	Superfusion	*In vitro* Electrophysiology	-	Moccia *et al.* (2009)
	Helix aspersa Terrestrial snail	Not stated	0.008 0.08 0.8	Bath application	*In vitro* Electrophysiology	- ↓ ↓	Piggott *et al.* (1977)
	Helix aspersa Terrestrial snail	Not stated	1,000	Bath application then applied by micropipettte	*In vitro* Electrophysiology	×	Vehovszky *et al.* (1989)
Ionotropic GABA R (Cl^-, depolarising)	*Lymnaea stagnalis* Pond snail	Adult	1,000	Bath application	*In vitro* Electrophysiology	↓ and × depending on the neuron	Rubakhin *et al.* (1996)
Ionotropic GABA R (Cl^-, hyper/depolarising?)	*Tritia obsoleta* Marine mud snail	Larvae	100	Bath application	*In vivo* Percentage of larvae metamorphosing	↑ only in 1 of 5 experiments	Biscocho *et al.* (2018)
GABA R (Na^+, depolarising)	*Aplysia californica* California sea hare	Not stated	1,000	Perfusion	*In vitro* Electrophysiology	-	Yarowsky and Carpenter (1978a)
	Aplysia californica California sea hare	Not stated	10 and 1,000	Perfusion	*In vitro* Electrophysiology	-	Yarowsky and Carpenter (1978b)
	Clione limacina Sea angel	Adult	50 and 1,000	Applied by pipette	*In vitro* Electrophysiology	-	Norekian (1999)
GABA R (K^+, depolarising)	*Aplysia californica* California sea hare	Not stated	10 and 1,000	Perfusion	*In vitro* Electrophysiology	-	Yarowsky and Carpenter (1978b)

Table B.2 continued.

Target receptor	Species Common name	Life stage	Picrotoxin conc. (µM)	Administration method	Method of measurement	Picrotoxin effect	Reference
GABA R (K^+, hyperpolarising)	*Aplysia californica* California sea hare	Not stated	10 and 1,000	Perfusion	*In vitro* Electrophysiology	- 	Yarowsky and Carpenter (1978b)
Ionotropic GABA R (ion?, depolarising)	*Helix aspersa* Terrestrial snail	Not stated	1,000	Bath application then applied by micropipettte	*In vitro* Electrophysiology	×	Vehovszky *et al.* (1989)
	Helix aspersa Terrestrial snail	Not stated	0.008 0.08 and 0.8	Bath application	*In vitro* Electrophysiology	- ↑	Piggott *et al.* (1977)
	Clione limacina Sea angel	Adult	1	Bath application	*In vitro* Electrophysiology	-	Arshavsky *et al.* (1993)
	Clione limacina Sea angel	Adult	1,000	Bath application	*In vitro* Electrophysiology	-	Norekian and Malyshev (2005)
GABA R (type unknown)	*Sepia officinalis* Common cuttlefish	Not stated, 100 - 1,500 g	<2 10	Local microinjection into the optic lobe	*In vivo* Behaviour	- General excitation or decreased spontaneous locomotion with immobilised fins	Chichery and Chichery (1985)
Ionotropic glutamate receptor (ion?, hyperpolarising)	*Helix aspersa* Terrestrial snail	Not stated	0.008 and 0.08 0.8	Bath application	*In vitro* Electrophysiology	- ↓	Piggott *et al.* (1977)
Ionotropic acetylcholine receptor (Cl^-, hyperpolarising)	*Aplysia californica* California sea hare	Not stated	1,000	Perfusion	*In vitro* Electrophysiology	×	Yarowsky and Carpenter (1978a)

Table B.2 continued.

Target receptor	Species Common name	Life stage	Picrotoxin conc. (µM)	Administration method	Method of measurement	Picrotoxin effect	Reference
Ionotropic acetylcholine receptor (ion?, hyperpolarising)	*Helix aspersa* Terrestrial snail	Not stated	0.008 0.08 and 0.8	Bath application	*In vitro* Electrophysiology	- ↓	Piggott *et al.* (1977)
Ionotropic acetylcholine receptor (Na^+, depolarising)	*Aplysia californica* California sea hare	Not stated	1,000	Perfusion	*In vitro* Electrophysiology	-	Yarowsky and Carpenter (1978a)
Ionotropic dopamine receptor (Cl^-, depolarising)	*Lymnaea stagnalis* Pond snail	~1 - 4 months old	100	Bath application	*In vitro* Electrophysiology	↓	Magoski and Bulloch (1999)

Table B.3. Explanatory variables, distribution family and link function as well as the priors used for the chosen model of each response variable in the gabazine experiment. Explanatory variables: * = interactive effect, + = additive effect. Priors: - = priors not applicable for this parameter, improper uniform = improper uniform priors were used (= uniform priors from infinity to -infinity).

Response variable	Explanatory variables	Family (link)	Intercept prior	Slope prior	sigma prior	shape prior
Time in Zone A (s)	CO2 * Drug	Gaussian (identity)	student_t(3, 316, 458.1)	improper uniform	student_t(3, 0, 458.1)	-
No. of visits to Zone A	CO2 * Drug + Mantle length	Negative binomial (log)	student_t(3, 1.4, 2.5)	improper uniform	-	gamma(0.01, 0.01)
Proportion of squid that touched mirror softly	CO2 * Drug	Binomial (logit)	student_t(3, 0, 2.5)	improper uniform	-	-
Latency to first soft mirror touch (s)	CO2 * Drug	Gamma (log)	student_t(3, 3.7, 2.5)	improper uniform	-	gamma(0.01, 0.01)
No. of soft mirror touches	CO2 * Drug + Behavioural tank + Time of test	Negative binomial (log)	student_t(3, 2.9, 2.5)	improper uniform	-	gamma(0.01, 0.01)
Proportion of squid that touched mirror aggressively	CO2 * Drug	Binomial (logit)	student_t(3, 0, 2.5)	improper uniform	-	-
Latency to first aggressive mirror touch (s)	CO2 * Drug + Behavioural tank + Time of test	Gamma (log)	student_t(3, 3.7, 2.5)	improper uniform	-	gamma(0.01, 0.01)
No. of aggressive mirror touches	CO2 * Drug	Negative binomial (log)	student_t(3, 2.9, 2.5)	improper uniform	-	gamma(0.01, 0.01)
Active time (s)	CO2 * Drug	Gamma (log)	student_t(3, 5.3, 2.5)	improper uniform	-	gamma(0.01, 0.01)
Total distance moved (cm)	CO2 * Drug	Gamma (log)	student_t(3, 6, 2.5)	improper uniform	-	gamma(0.01, 0.01)
Average speed (cm/s)	CO2 * Drug	Gaussian (identity)	student_t(3, 2.1, 2.5)	improper uniform	student_t(3, 0, 2.5)	-

Table B.4. Explanatory variables, distribution family and link function as well as the priors used for the chosen model of each response variable in the picrotoxin experiment. Explanatory variables: * = interactive effect, + = additive effect. Priors: - = priors not applicable for this parameter, improper uniform = improper uniform priors were used (= uniform priors from infinity to -infinity).

Response variable	Explanatory variables	Family (link)	Intercept prior	Slope prior	sigma prior	shape prior
Time in Zone A (s)	CO2 * Drug + Behavioural tank + Time of test	Gaussian (identity)	student_t(3, 677, 315.8)	improper uniform	student_t(3, 0, 315.8)	-
No. of visits to Zone A	CO2 * Drug + System	Negative binomial (log)	normal(0, 8)	normal(0, 2.5)	-	gamma(0.01, 0.01)
Proportion of squid that touched mirror softly	CO2 * Drug	Binomial (logit)	student_t(3, 0, 2.5)	improper uniform	-	-
Latency to first soft mirror touch (s)	CO2 * Drug	Gamma (log)	student_t(3, 4.4, 2.5)	improper uniform	-	gamma(0.01, 0.01)
No. of soft mirror touches	CO2 * Drug + Mantle length	Negative binomial (log)	student_t(3, 2.8, 2.5)	improper uniform	-	gamma(0.01, 0.01)
Proportion of squid that touched mirror aggressively	CO2 * Drug	Binomial (logit)	student_t(3, 0, 2.5)	improper uniform	-	-
Latency to first aggressive mirror touch (s)	CO2 * Drug + System	Gamma (log)	normal(0, 10)	normal(0, 2.5)	-	gamma(0.01, 0.01)
No. of aggressive mirror touches	CO2 * Drug + Number of acclimation days + Date introduced to treatment	Negative binomial (log)	student_t(3, 3.1, 2.5)	improper uniform	-	gamma(0.01, 0.01)
Active time (s)	CO2 * Drug	Gaussian (identity)	student_t(3, 297.8, 206.5)	improper uniform	student_t(3, 0, 206.5)	-
Total distance moved (cm)	CO2 * Drug	Gaussian (identity)	student_t(3, 737.1, 641.1)	improper uniform	student_t(3, 0, 641.1)	-
Average speed (cm/s)	CO2 * Drug	Gaussian (identity)	student_t(3, 2.4, 2.5)	improper uniform	student_t(3, 0, 2.5)	-

Appendix C

Chapter 4 Appendices

Water sampling methods.

To evaluate the magnitude of natural diel CO_2 fluctuations and the ecological relevance of the experimental CO_2 treatment levels used in my study, water samples were taken from the same location where two-toned pygmy squid (*Idiosepius pygmaeus*) were collected. *I. pygmaeus* were collected from August - October 2019, and water samples from August - September 2021, from coastal waters around the Townsville breakwater complex. All water samples were collected with 250 mL borosilicate glass bottles. Bottles were dipped into the water upside down and at approximately 25 cm deep the bottle was inverted several times to allow water to enter and remove all air bubbles, and the lid was screwed on underwater. Each sample was taken in pairs; one was placed directly in the dark for storage until lab measurements, and the other was used immediately for measurements of water temperature (Comark C26, Norfolk, UK) and pH_{NBS} (Seven2Go™ pro Conductivity Meter with an InLab Expert Go-ISM pH electrode, Metler Toledo). Three pairs of water samples were taken in immediate succession at each location and sampling time. All lab measurements were taken within 2.13 ± 1 hour (mean ± SD) of water sample collection. Total alkalinity was measured by Gran titration (888 Titrando, Metrohm AG, Switzerland) and salinity was measured with a conductivity sensor (HQ40d, Hach, Loveland, CO, USA). CO_2 values were calculated in CO_2SYS v.2.1 (`https://cdiac.ess-dive.lbl.gov/ftp/co2sys/CO2SYS_calc_XLS_v2.1/`) using the constants K1, K2 from Mehrbach *et al.* (1973) and refit by Dickson and Millero (1987) and $KHSO_4$ from Dickson *et al.* (2007).

To determine any spatial variation within the breakwater marina complex, three pairs of water samples were taken from each of three different locations (19°15'06.3"S 146°49'22.4"E; 19°15'08.1"S 146°49'27.6"E; 19°15'11.8"S 146°49'21.6"E), both before first light (approximately 5:30) and mid-afternoon (approximately 13:30). CO_2 levels were consistent across

these three locations, therefore all subsequent sampling was done from one location (19°15'06.3"S 146°49'22.4"E). To determine the best time for afternoon sampling to capture maximum change in CO_2 levels, three pairs of water samples were collected at each of three time points; 12:30, 13:30 and 14:30. These time points were chosen based on previous research that found minimum CO_2 was reached between 12:30 and 14:20 at Lizard Island, Great Barrier Reef (Hannan *et al.*, 2020). CO_2 levels were consistent across these three time points, therefore all subsequent sampling was done at 13:30. After these initial checks were completed, water sampling was carried out to determine any diel CO_2 variation. Three pairs of water samples were taken before first light (approximately 5:00) and at 13:30 across five days of differing tidal heights, all from the same location. Figure C.1 shows the diel CO_2 variation. All raw data from water sampling can be found at https://doi.org/10.25903/ha66-mm11 (this is embargoed until publication, access for thesis examination can be found at https://cloudstor.aarnet.edu.au/plus/s/sV1Qv1exuwXdiOd).

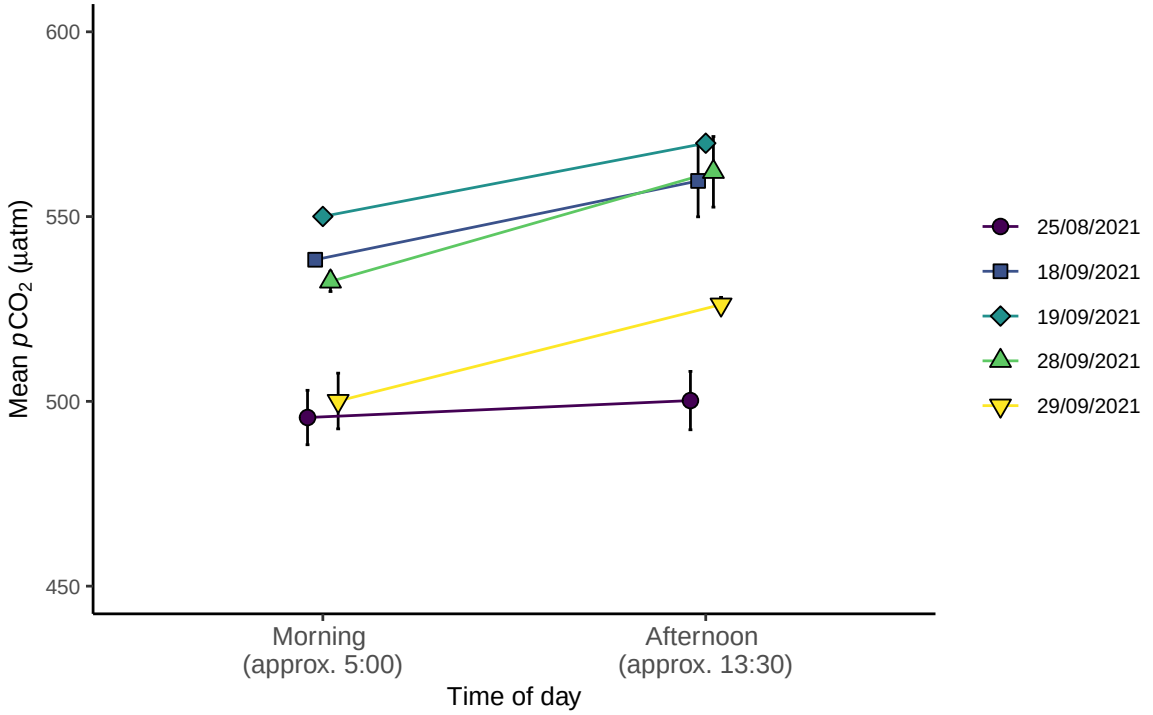

Figure C.1. Diel CO_2 variation at the site *I. pygmaeus* were collected. Water samples were taken to measure CO_2 levels before first light at approximately 5:00 (morning) and at approximately 13:30 (afternoon) across five days. Points represent the mean ± standard deviation.

TapeStation electropherograms for each of the 40 RNA samples used for RNA-sequencing.

Each sample is labelled by its individual ID and the tissue type. RNA integrity of all 40 samples was measured on an Agilent 2200 TapeStation (High Sensitivity RNA ScreenTape, Agilent), without the sample denaturation step due to denaturation removing the 28S peak, likely due to a 'hidden break' as reported in some other animals (Winnebeck *et al.*, 2010). All central nervous system (CNS) RNA had an equivalent RNA integrity (RIN_e) $\geq$ 8.5 (mean 9.3, SD 0.3). For the eye samples, a RIN_e value could not be obtained due to the TapeStation being unable to detect the lower marker, likely due to carry over of pigment into the eye RNA samples. A Femto Pulse system (Ultra Sensitivity RNA Kit, Agilent) did obtain RNA Quality Scores (RQN): eye RQN $\geq$ 4.8 (mean 6.5, SD 1.3). The four samples also used for ISO-sequencing are outlined in thick black. CNS samples used for ISO-seq had RIN_e values of 9.4 and 9.5. Before ISO-seq, RNA from the eyes was purified with oligo d(T) beads due to carry over of pigmentation (NEBNext® Poly(A) mRNA Magnetic Isolation Module, New England BioLabs Inc.), followed by integrity assessment on a Femto Pulse system (Ultra Sensitivity RNA Kit, Agilent). After purification, eyes samples had an RQN of 6.1 and 8.6.

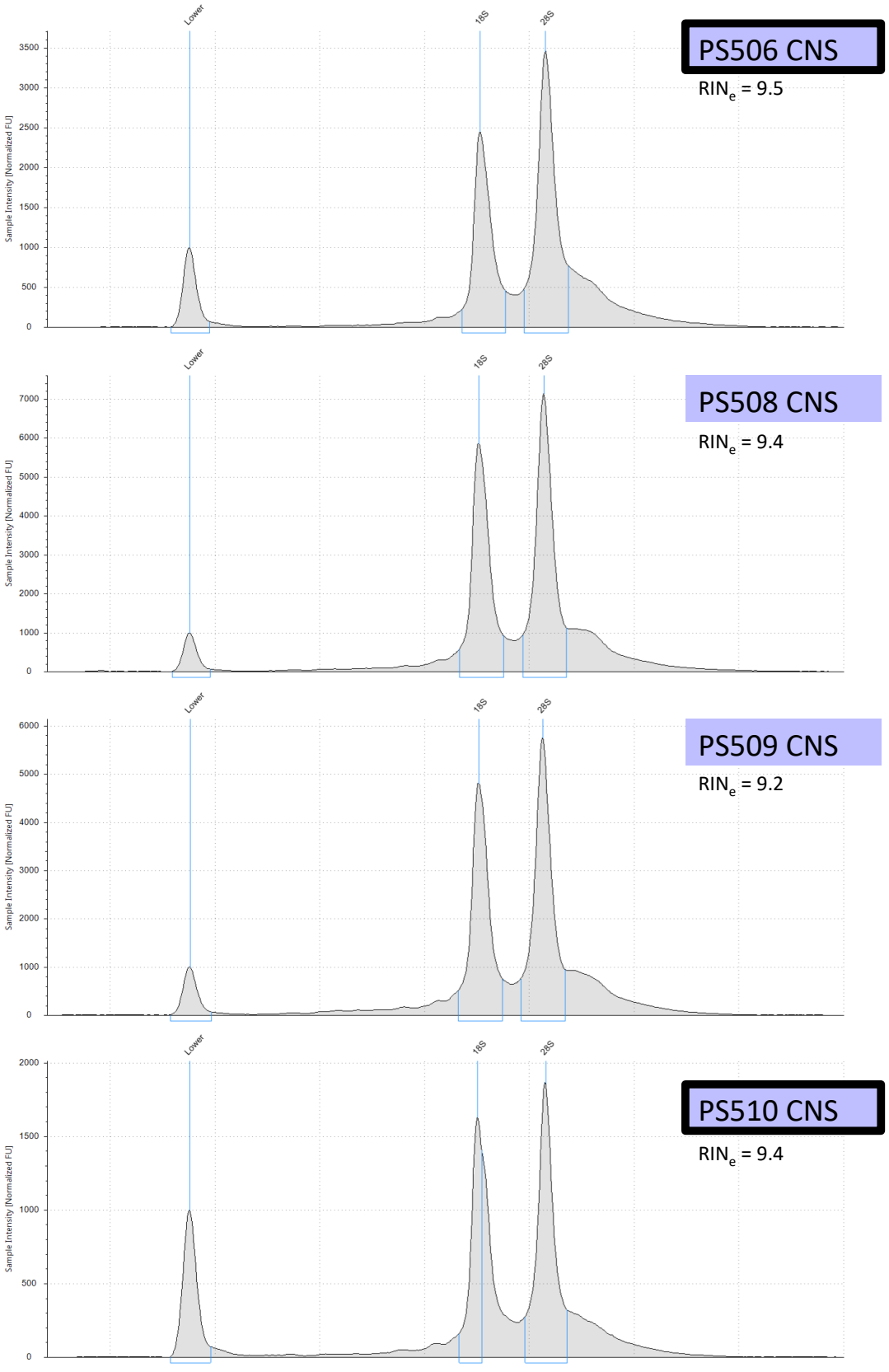
Lower
18S
28S
Sample Intensity [Normalized FU]
PS506 CNS
RIN$_e$ = 9.5
PS508 CNS
RIN$_e$ = 9.4
PS509 CNS
RIN$_e$ = 9.2
PS510 CNS
RIN$_e$ = 9.4

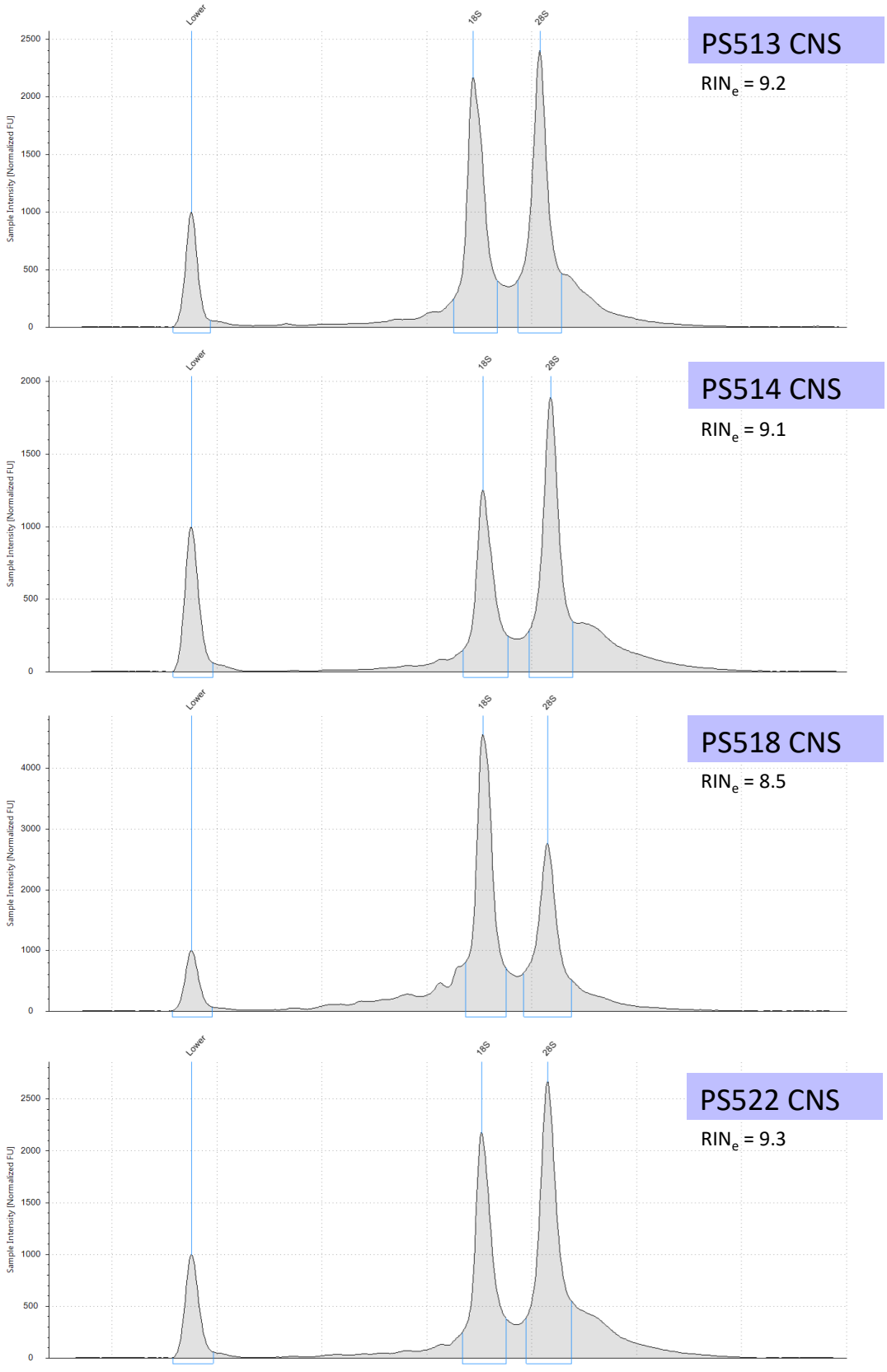
PS513 CNS
RIN$_e$ = 9.2
PS514 CNS
RIN$_e$ = 9.1
PS518 CNS
RIN$_e$ = 8.5
PS522 CNS
RIN$_e$ = 9.3
Lower
18S
28S
Sample Intensity [Normalized FU]

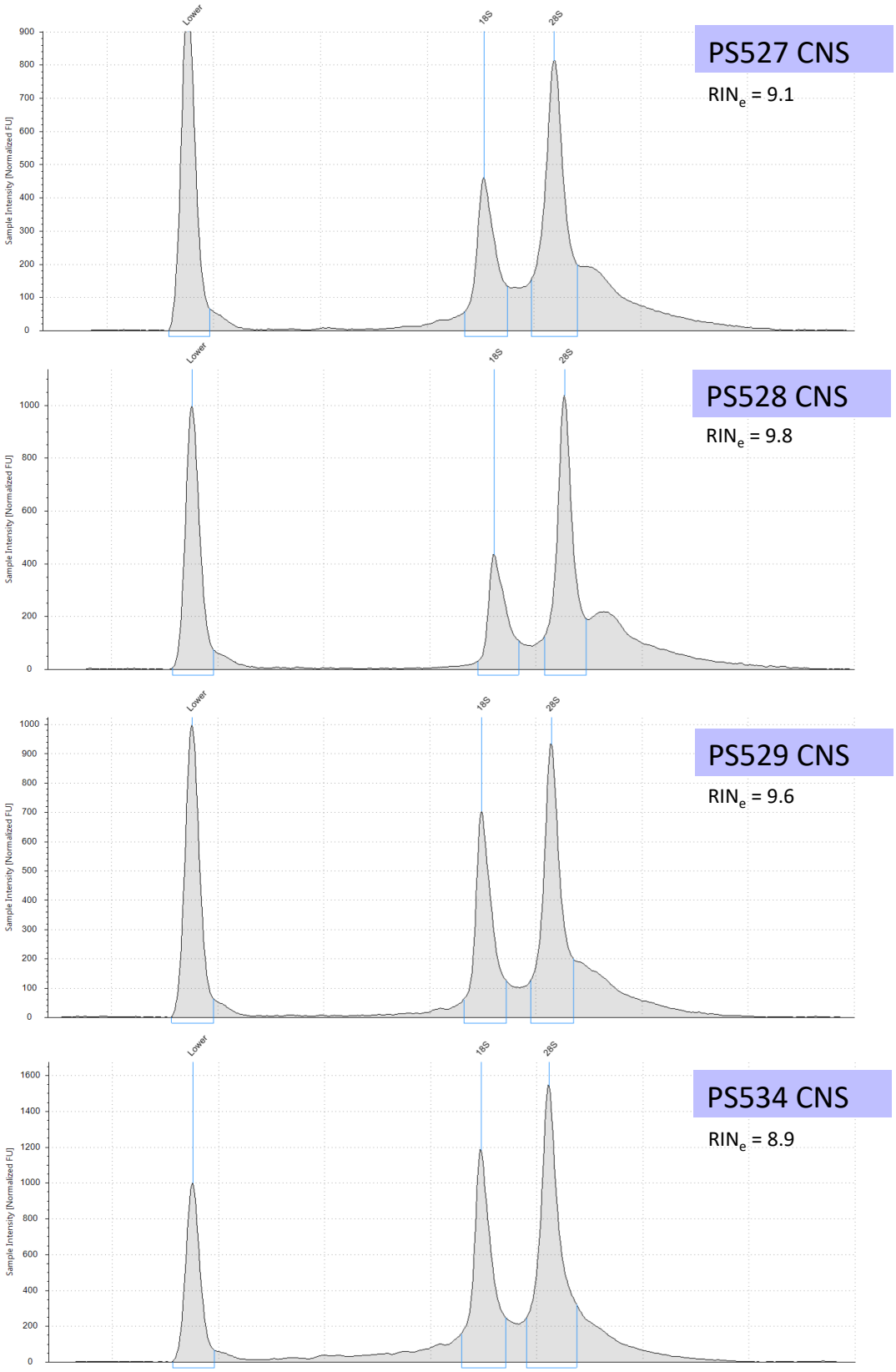
Lower
18S
28S
Sample Intensity [Normalized FU]
PS527 CNS
RIN$_e$ = 9.1
PS528 CNS
RIN$_e$ = 9.8
PS529 CNS
RIN$_e$ = 9.6
PS534 CNS
RIN$_e$ = 8.9

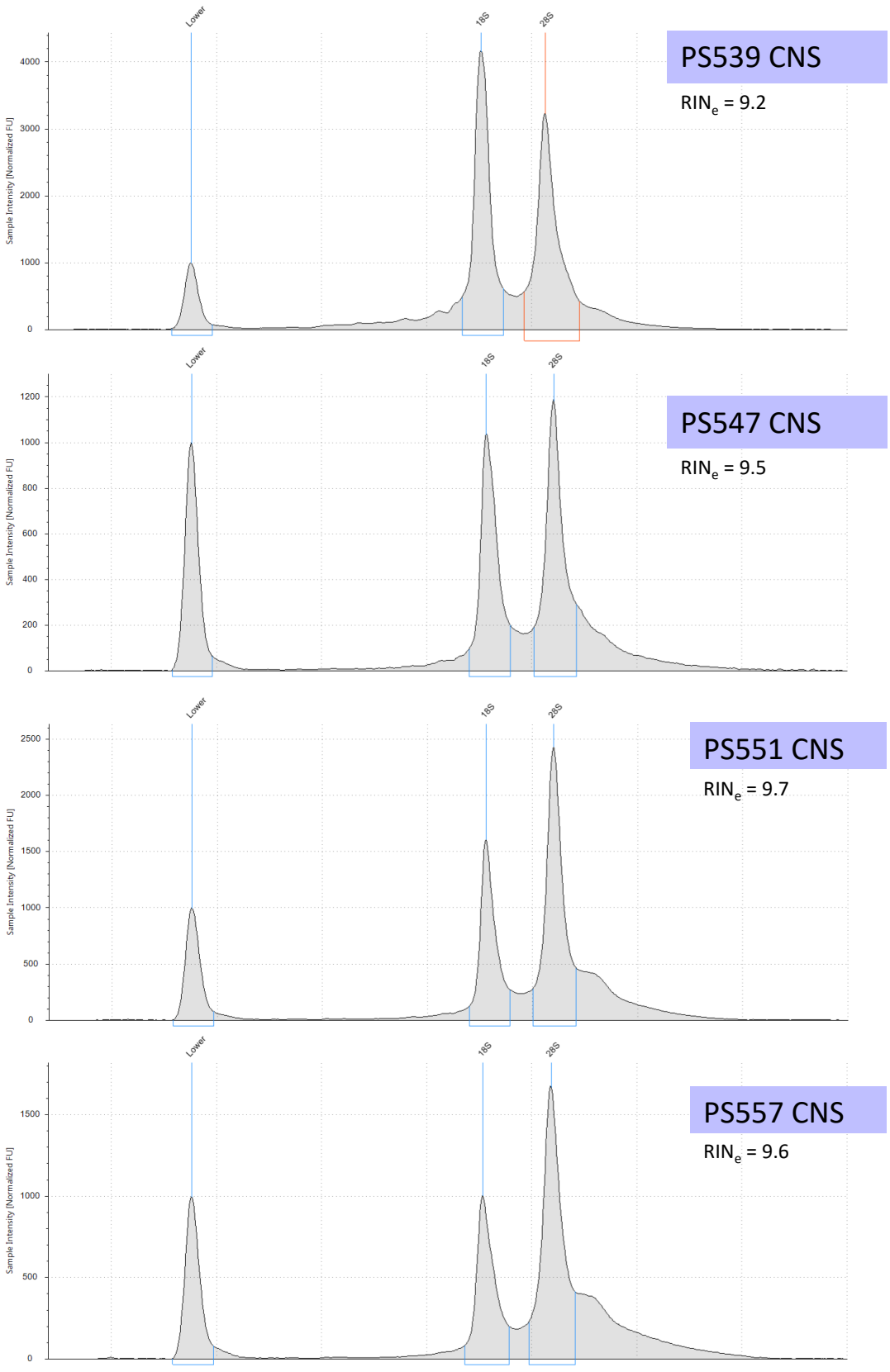
Lower
18S
28S
Sample Intensity [Normalized FU]
PS539 CNS
RIN$_e$ = 9.2
PS547 CNS
RIN$_e$ = 9.5
PS551 CNS
RIN$_e$ = 9.7
PS557 CNS
RIN$_e$ = 9.6

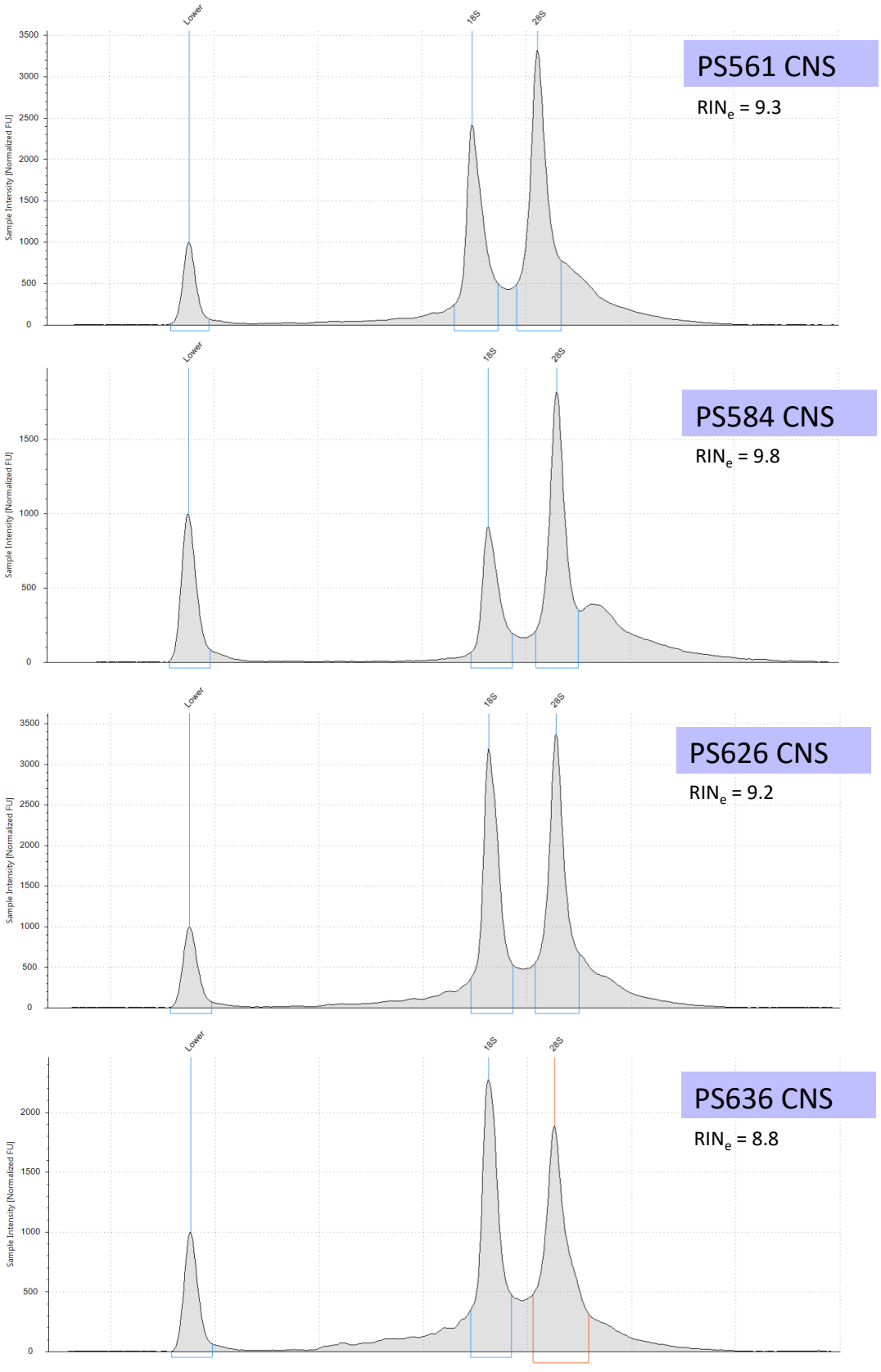
Lower
18S
28S
Sample Intensity (Normalized FU)
PS561 CNS
RIN$_e$ = 9.3
PS584 CNS
RIN$_e$ = 9.8
PS626 CNS
RIN$_e$ = 9.2
PS636 CNS
RIN$_e$ = 8.8

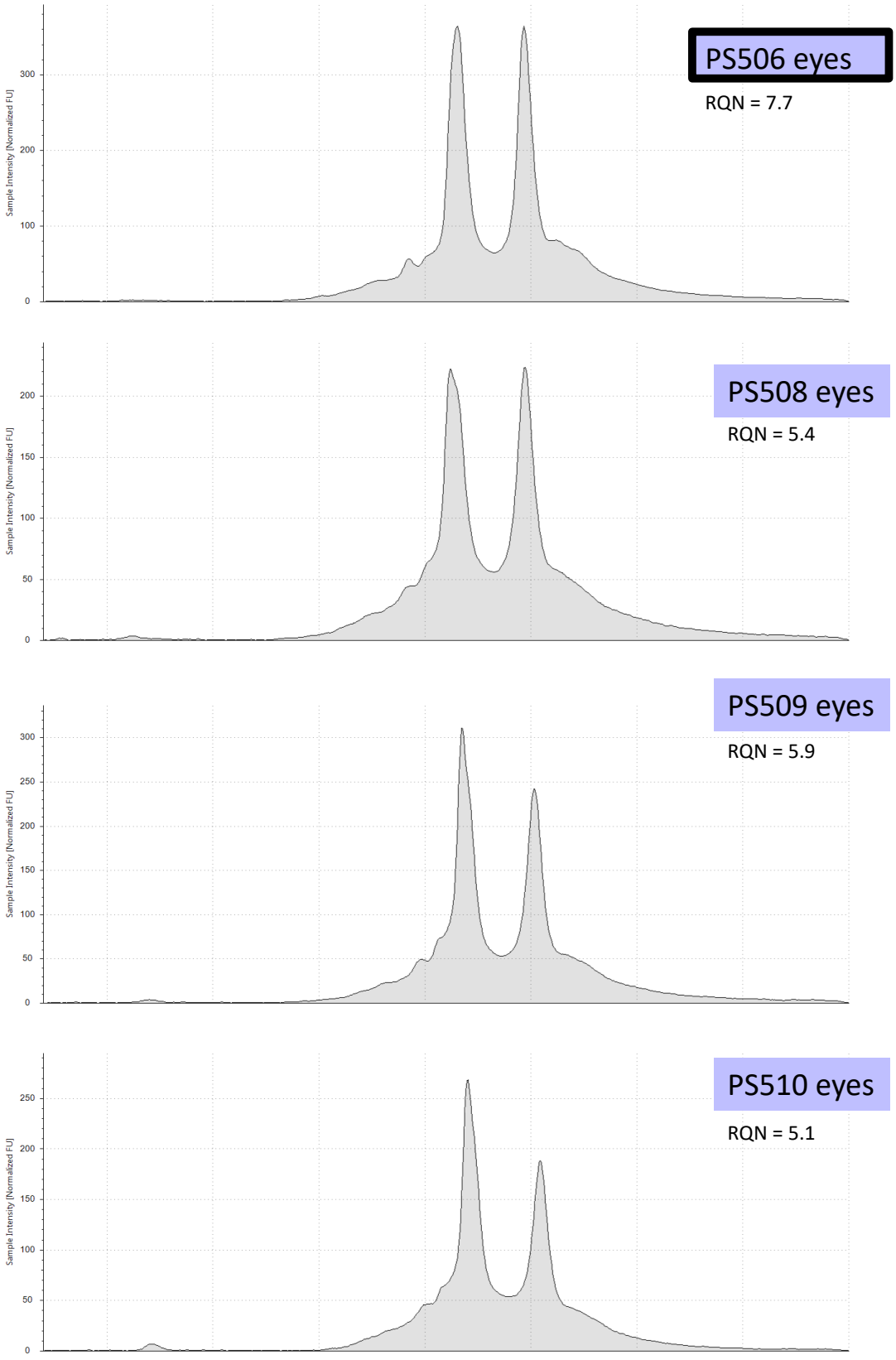
PS506 eyes
RQN = 7.7
PS508 eyes
RQN = 5.4
PS509 eyes
RQN = 5.9
PS510 eyes
RQN = 5.1
Sample Intensity (Normalized FU)

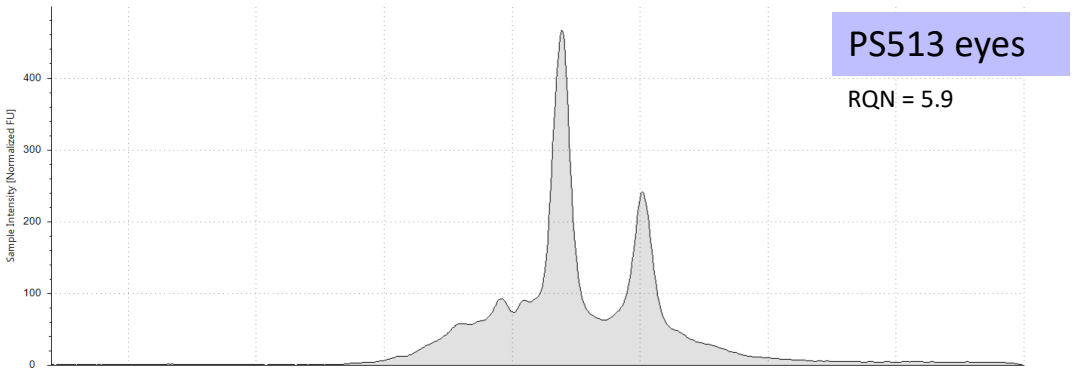
PS513 eyes
RQN = 5.9
Sample Intensity [Normalized FU]
0
100
200
300
400

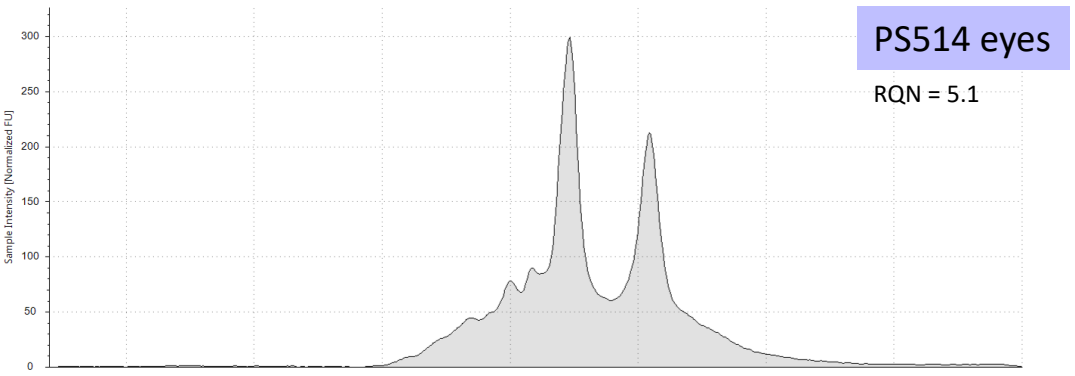
PS514 eyes
RQN = 5.1
Sample Intensity [Normalized FU]
0
50
100
150
200
250
300

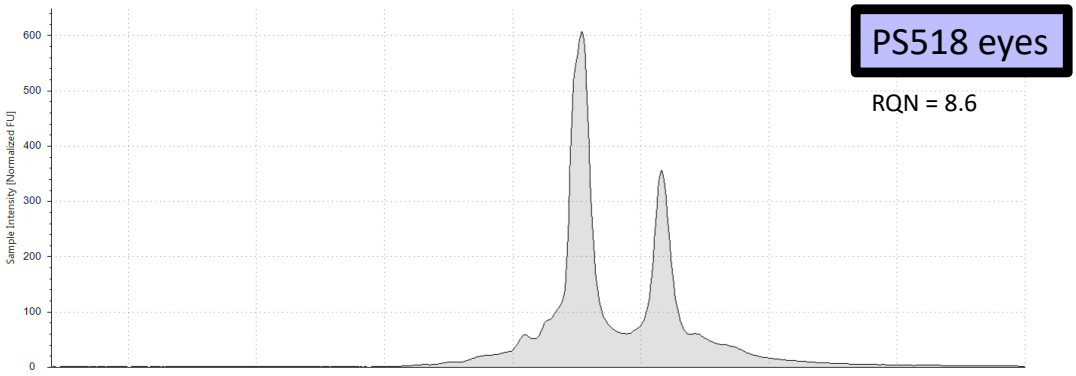
PS518 eyes
RQN = 8.6
Sample Intensity [Normalized FU]
0
100
200
300
400
500
600

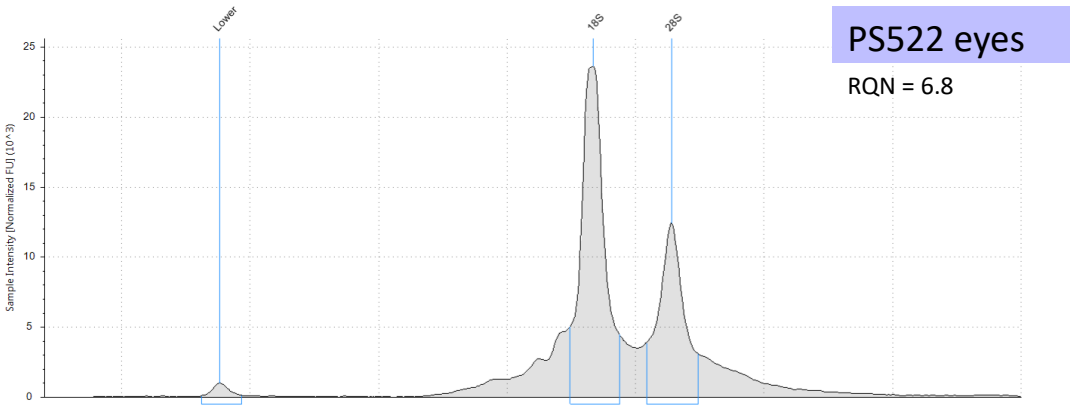
PS522 eyes
RQN = 6.8
Lower
18S
28S
Sample Intensity [Normalized FU] (10^3)
0
5
10
15
20
25

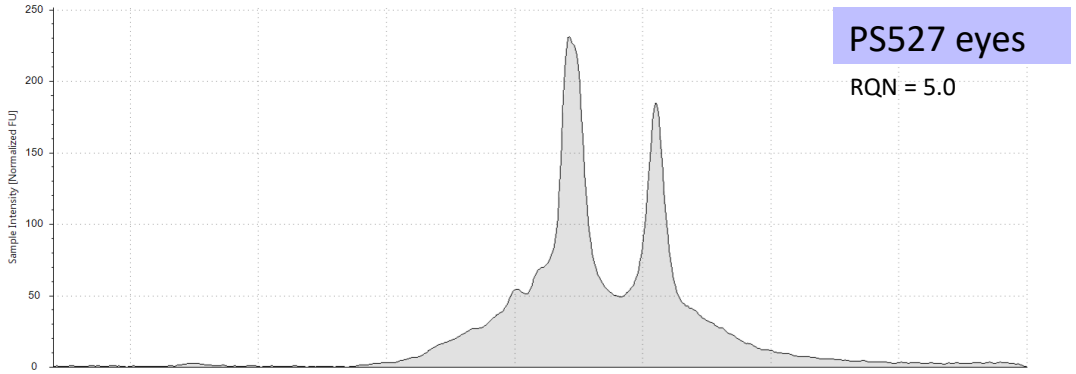
PS527 eyes
RQN = 5.0
Sample Intensity [Normalized FU]
250
200
150
100
50
0

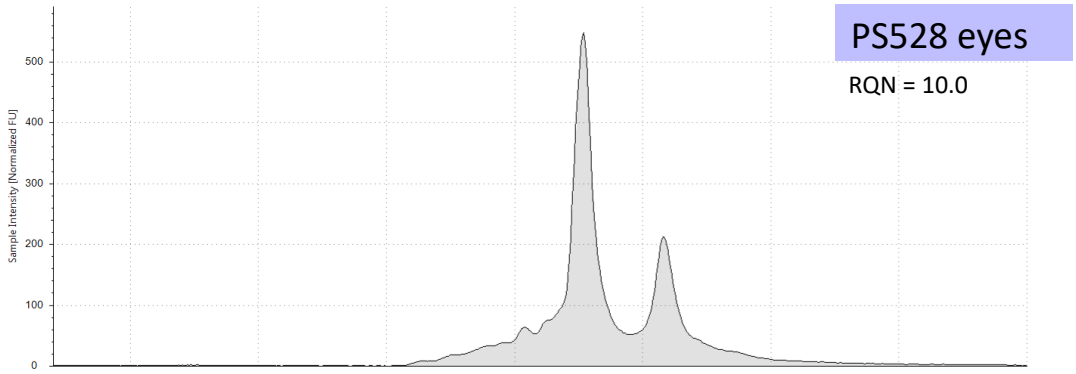
PS528 eyes
RQN = 10.0
Sample Intensity [Normalized FU]
500
400
300
200
100
0

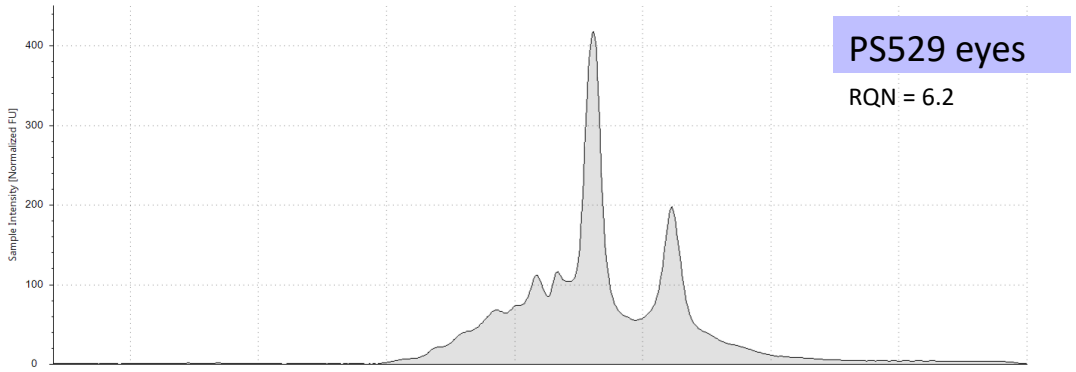
PS529 eyes
RQN = 6.2
Sample Intensity [Normalized FU]
400
300
200
100
0

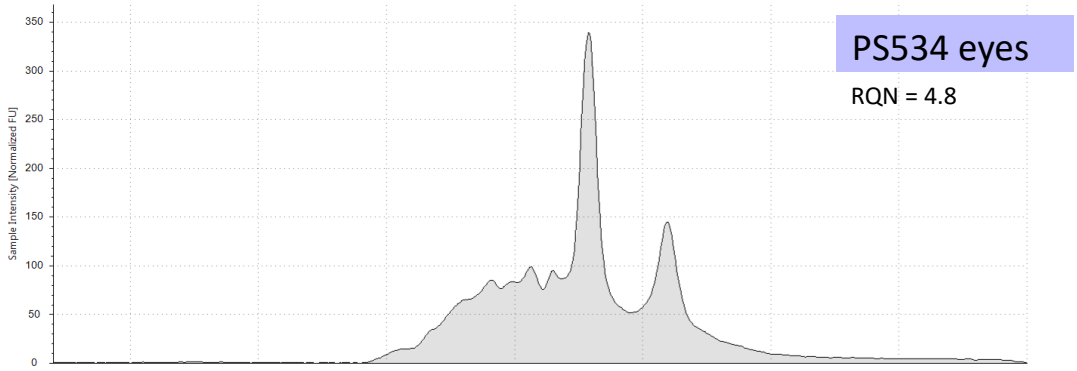
PS534 eyes
RQN = 4.8
Sample Intensity [Normalized FU]
350
300
250
200
150
100
50
0

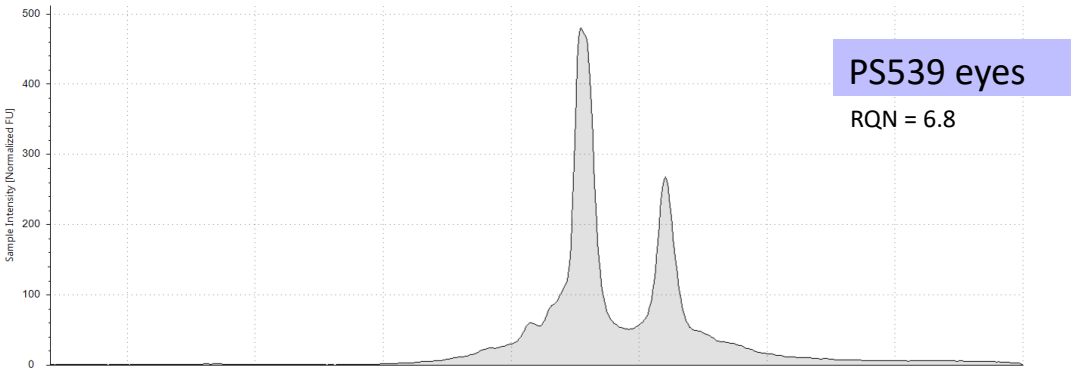
Sample Intensity [Normalized FU]
500
400
300
200
100
0
PS539 eyes
RQN = 6.8

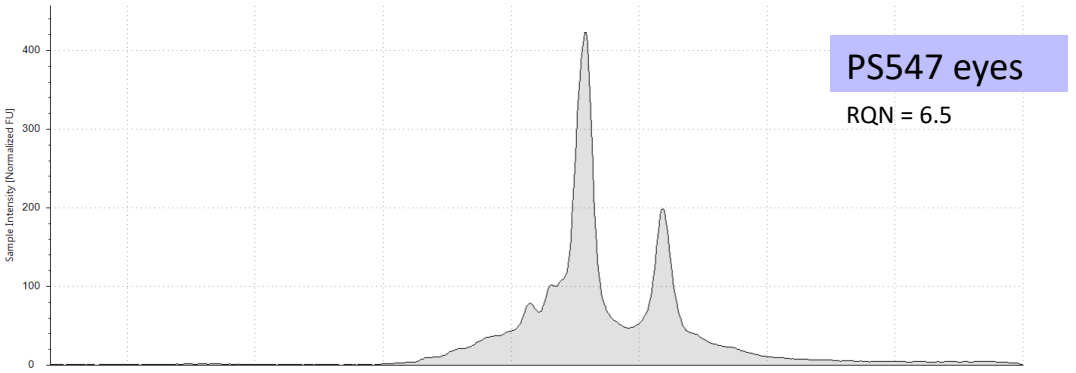
Sample Intensity [Normalized FU]
400
300
200
100
0
PS547 eyes
RQN = 6.5

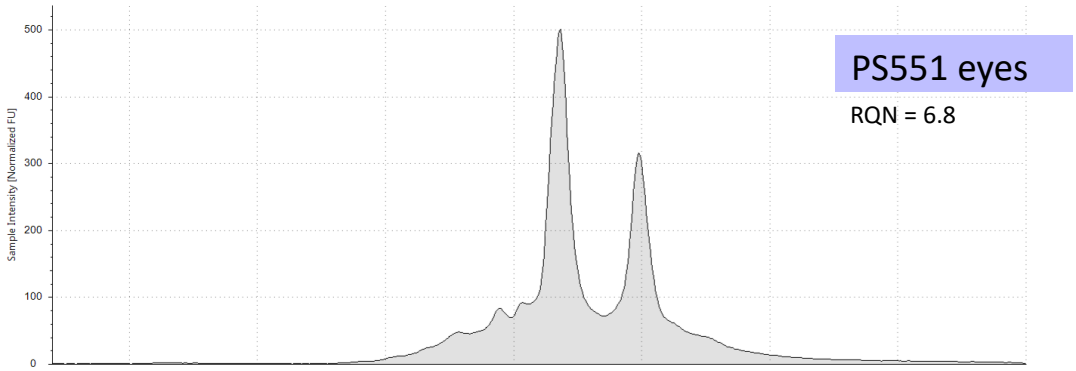
Sample Intensity [Normalized FU]
500
400
300
200
100
0
PS551 eyes
RQN = 6.8

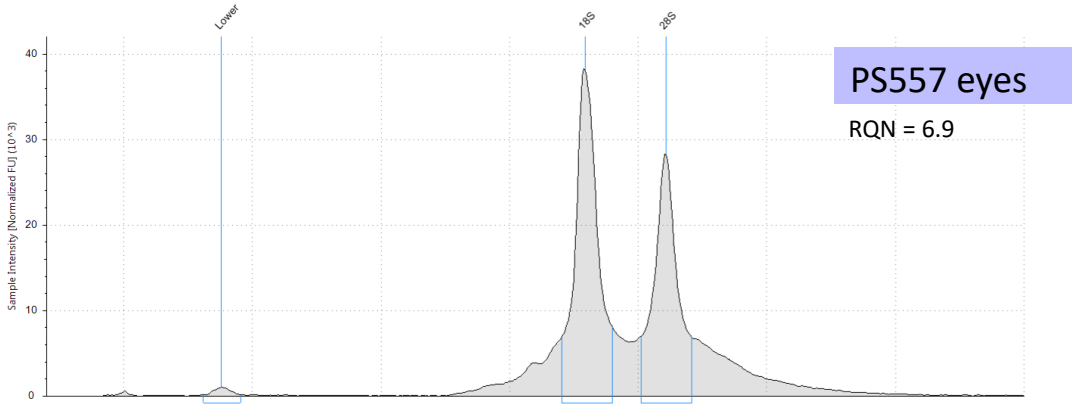
Lower
18S
28S
Sample Intensity [Normalized FU] (10^3)
40
30
20
10
0
PS557 eyes
RQN = 6.9

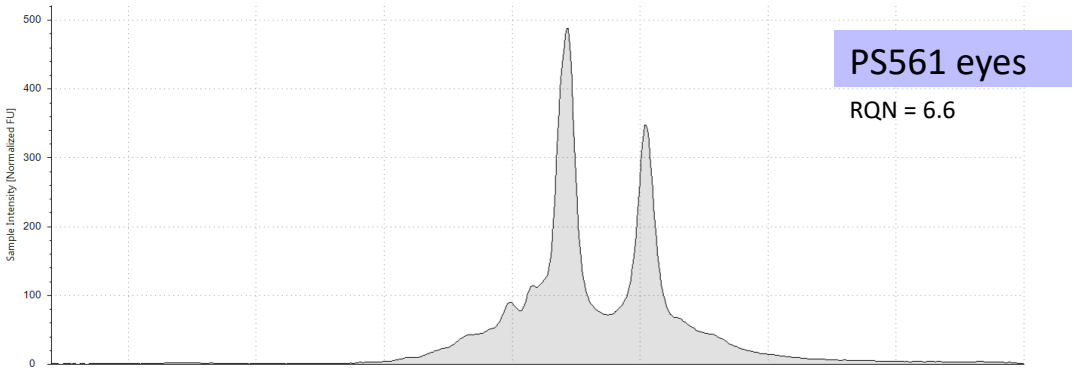
PS561 eyes
RQN = 6.6
Sample Intensity [Normalized FU]
500
400
300
200
100
0

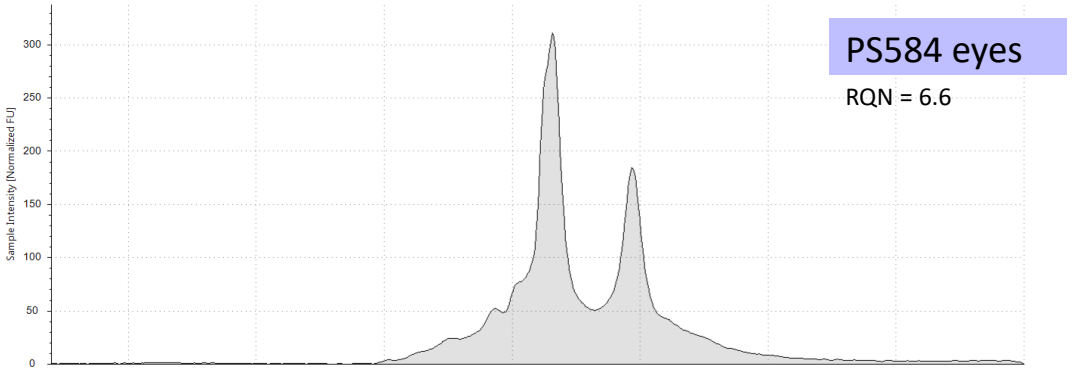
PS584 eyes
RQN = 6.6
Sample Intensity [Normalized FU]
300
250
200
150
100
50
0

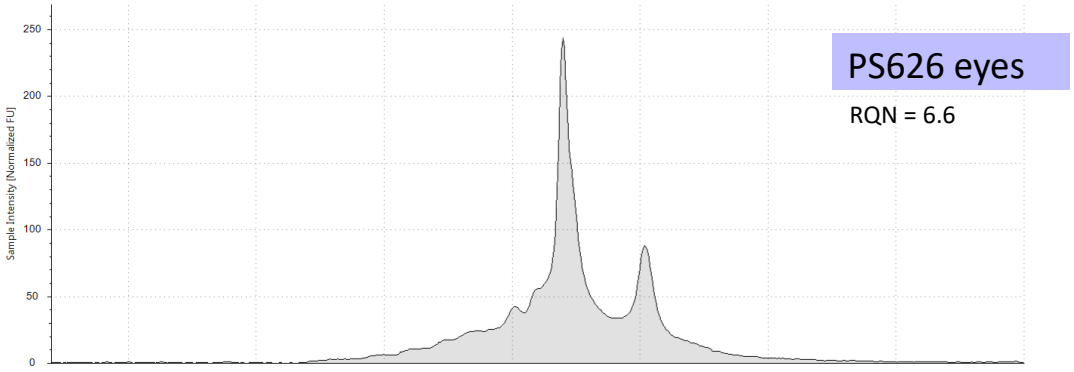
PS626 eyes
RQN = 6.6
Sample Intensity [Normalized FU]
250
200
150
100
50
0

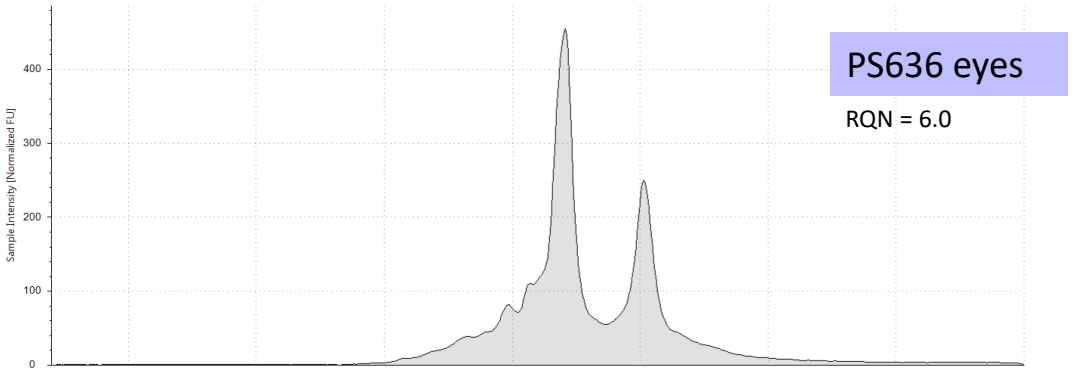
PS636 eyes
RQN = 6.0
Sample Intensity [Normalized FU]
400
300
200
100
0

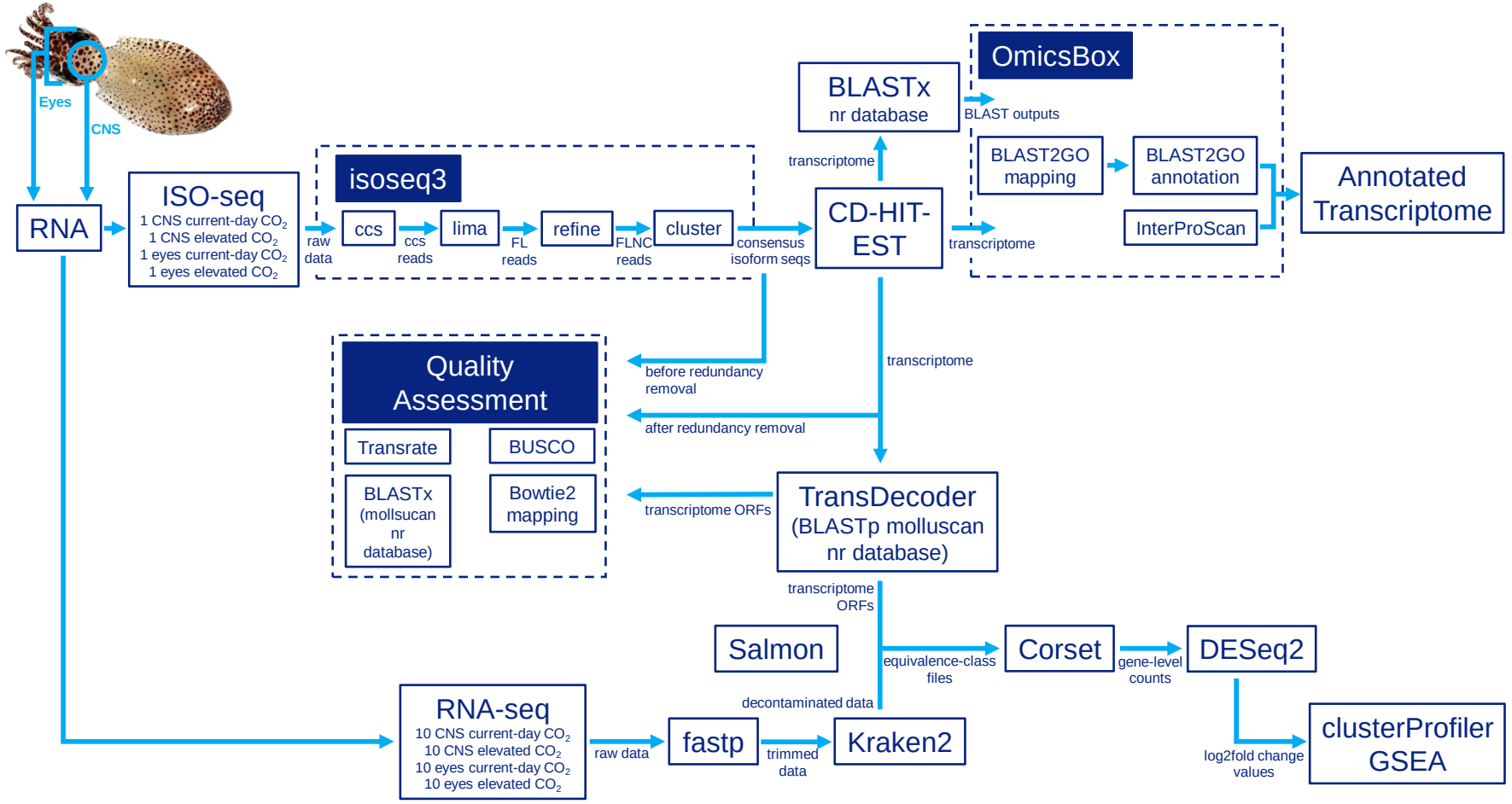

Figure C.2. Detailed workflow from tissue sampling to bioinformatics analyses and statistical analyses. ccs = circular consensus sequence, DE = differentially expressed, FL = full length, FLNC = full-length non-concatemer, GSEA = gene set enrichment analysis, ISO-seq = PacBio long read ISO-sequencing, ORF = open reading frame, RNA-seq = RNA sequencing, seqs = sequences.

Table C.1. Quality and completeness measures of the transcriptome assembly. The PacBio Sequel II produced a total of 138.6 million subreads which were used to create the *de novo* transcriptome assembly. Before redundancy removal = ISO-seq data processed with the isoseq3 pipeline. After redundancy removal = ISO-seq data processed with the isoseq3 pipeline followed by redundancy removal with CD-HIT-EST. Final transcriptome assembly = ISO-seq data processed with the isoseq3 pipeline, followed by redundancy removal with CD-HIT-EST and only the transcripts containing an ORF, as identified by TransDecoder, were retained. bp = base pairs.

		Before redundancy removal	After redundancy removal	Final transcriptome assembly
Transrate	**No. contigs**	229334	85481	49981
	Smallest contig length	51	51	299
	Largest contig length	10554	10554	10554
	No. bases	546681269	217542313	142604702
	Mean contig length	2383.47	2544.65	2853.18
	No. contigs <200 bp	520	169	0
	No. contigs >1,000 bp	218222	81717	48921
	No. contigs >10,000 bp	5	5	5
	No. contigs containing an ORF	128721	43780	43487
	Mean % of the contig covered by the ORF	41.86	34.87	47.9
	N90	1538	1623	1855
	N70	2126	2278	2562
	N50	2657	2870	3163
	N30	3283	3549	3856
	N10	4379	4716	5029
	Proportion bases G or C	0.35	0.34	0.37
	No. bases N	0	0	0
	Proportion bases N	0	0	0
BUSCO	**Complete BUSCOs (C)**	3805	3781	3766
		71.86%	71.40%	70.40%
	Complete and single-copy BUSCOs (S)	821	1391	1392
		15.51%	26.30%	26.20%
	Complete and duplicated BUSCOs (D)	2984	2390	2374
		56.36%	45.10%	44.20%
	Fragmented BUSCOs (F)	51	49	50

Table C.1 continued.

		Before redundancy removal	After redundancy removal	Final transcriptome assembly
		0.96%	0.90%	1.10%
	Missing BUSCOs (M)	1439	1465	1479
		27.18%	27.70%	28.50%
	Total BUSCO groups searched	5295	5295	5295
Bowtie2 mapping:	**Mean**	91.85%	91.85%	82.10%
Overall alignment	**Minimum**	86.63%	86.67%	72.93%
	Maximum	95.04%	95.07%	89.42%
	Mean (CNS samples)	89.37%	89.38%	76.88%
	Mean (eyes samples)	94.32%	94.32%	87.33%
Bowtie2 mapping:	**Mean**	87.73%	87.53%	77.12%
Total concordant alignment	**Minimum**	81.85%	80.92%	66.54%
	Maximum	91.95%	91.74%	85.84%
	Mean (CNS samples)	84.70%	84.32%	71.03%
	Mean (eyes samples)	90.76%	90.74%	83.21%
Blastx to nr database	**No. proteins any hit**	150375	52367	46515
subset for mollusca	**% of transcriptome with any hit**	65.57	61.26	93.07

Table C.2. Annotation measures of the transcriptome assembly.

		Final transcriptome assembly
Blastx to nr database	No. transcripts $\geq$ 1 blast hit % transcriptome $\geq$ 1 blast hit	46,311 93
BLAST2GO mapping	No. transcripts succesful GO mapping % transcripts succesful GO mapping	13,221 73
Complete Annotation	No. transcripts with complete annotation % transcripts with complete annotation	34,347 69

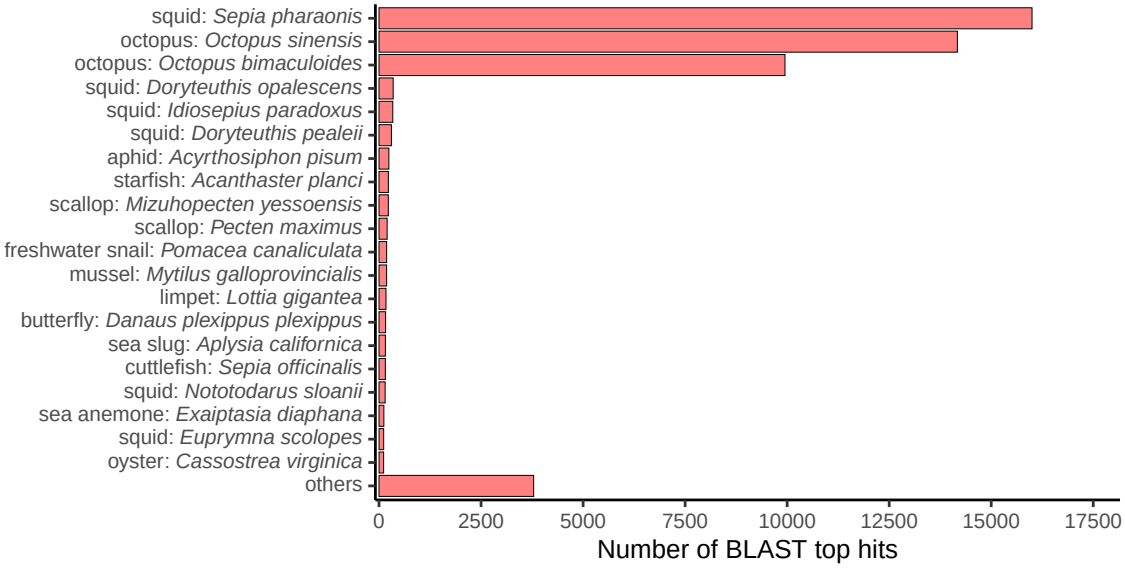

Figure C.3. Species distribution for the top blast hits of the annotated transcriptome assembly. The top 29 species are shown. Others = the remaining 936 species grouped together.

Table C.3. RNA-sequencing information for each sample. CNS = central nervous system, eyes = both eyes combined from the same individual, % mapping rate is mapping of the trimmed and decontaminated RNA-seq reads against the final transcriptome assembly, SD = standard deviation.

Sample ID	CO_2 Treatment	No. raw reads	No. reads after trimming and decontamination	% Mapping rate
PS506_CNS	Current-day	102139439	83323155	66.68%
PS506_eyes	Current-day	129110309	105557471	80.19%
PS508_CNS	Current-day	110779545	90371514	65.78%
PS508_eyes	Current-day	121705839	100798440	81.51%
PS509_CNS	Elevated	106147892	80132801	66.41%
PS509_eyes	Elevated	92031181	74985091	80.86%
PS510_CNS	Elevated	87217004	71030689	65.55%
PS510_eyes	Elevated	93132849	76180212	82.64%
PS513_CNS	Current-day	96318278	77505546	62.75%
PS513_eyes	Current-day	120073036	88786117	80.61%
PS514_CNS	Current-day	100874118	79625419	63.86%
PS514_eyes	Current-day	105947686	80633114	79.24%
PS518_CNS	Current-day	93632224	77006330	63.67%
PS518_eyes	Current-day	125427413	103231592	80.42%
PS522_CNS	Elevated	125785668	101021105	61.51%
PS522_eyes	Elevated	102772897	82672385	82.93%
PS527_CNS	Elevated	95046094	78238706	63.62%
PS527_eyes	Elevated	100839899	81990702	78.53%
PS528_CNS	Elevated	100739627	83947119	71.27%
PS528_eyes	Elevated	123262918	103640293	81.33%
PS529_CNS	Current-day	91326387	76678162	65.06%
PS529_eyes	Current-day	119554860	100130525	78.77%
PS534_CNS	Current-day	95139757	76615235	67.31%
PS534_eyes	Current-day	117198920	97221144	80.02%
PS539_CNS	Elevated	101306635	70136432	68.26%
PS539_eyes	Elevated	95044179	79247609	80.00%
PS547_CNS	Elevated	95437419	73571670	70.61%
PS547_eyes	Elevated	144223366	118214271	78.54%
PS551_CNS	Current-day	103427279	84367088	69.67%
PS551_eyes	Current-day	116654316	95952400	79.16%
PS557_CNS	Current-day	92862187	73022082	67.71%
PS557_eyes	Current-day	102809092	85449238	78.58%
PS561_CNS	Current-day	106613800	85482402	68.82%
PS561_eyes	Current-day	89919652	74277911	81.86%
PS584_CNS	Elevated	201511022	164079389	70.56%
PS584_eyes	Elevated	104998922	85722187	80.40%
PS626_CNS	Elevated	110020976	88819227	69.51%
PS626_eyes	Elevated	87134097	68250602	78.86%
PS636_CNS	Elevated	93625133	77083466	73.16%
PS636_eyes	Elevated	129384378	102326531	77.28%
Mean		108279407	87433134	73.59%
SD		20100481	16838289	6.93%
Mean CNS		105497524	84602877	67.09%
SD CNS		23596334	19577787	3.07%
Mean eyes		111061290	90263392	80.09%

Table C.3 continued.

Sample ID	CO_2 Treatment	No. raw reads	No. reads after trimming and decontamination	% Mapping rate
SD eyes		15355582	12951661	1.45%

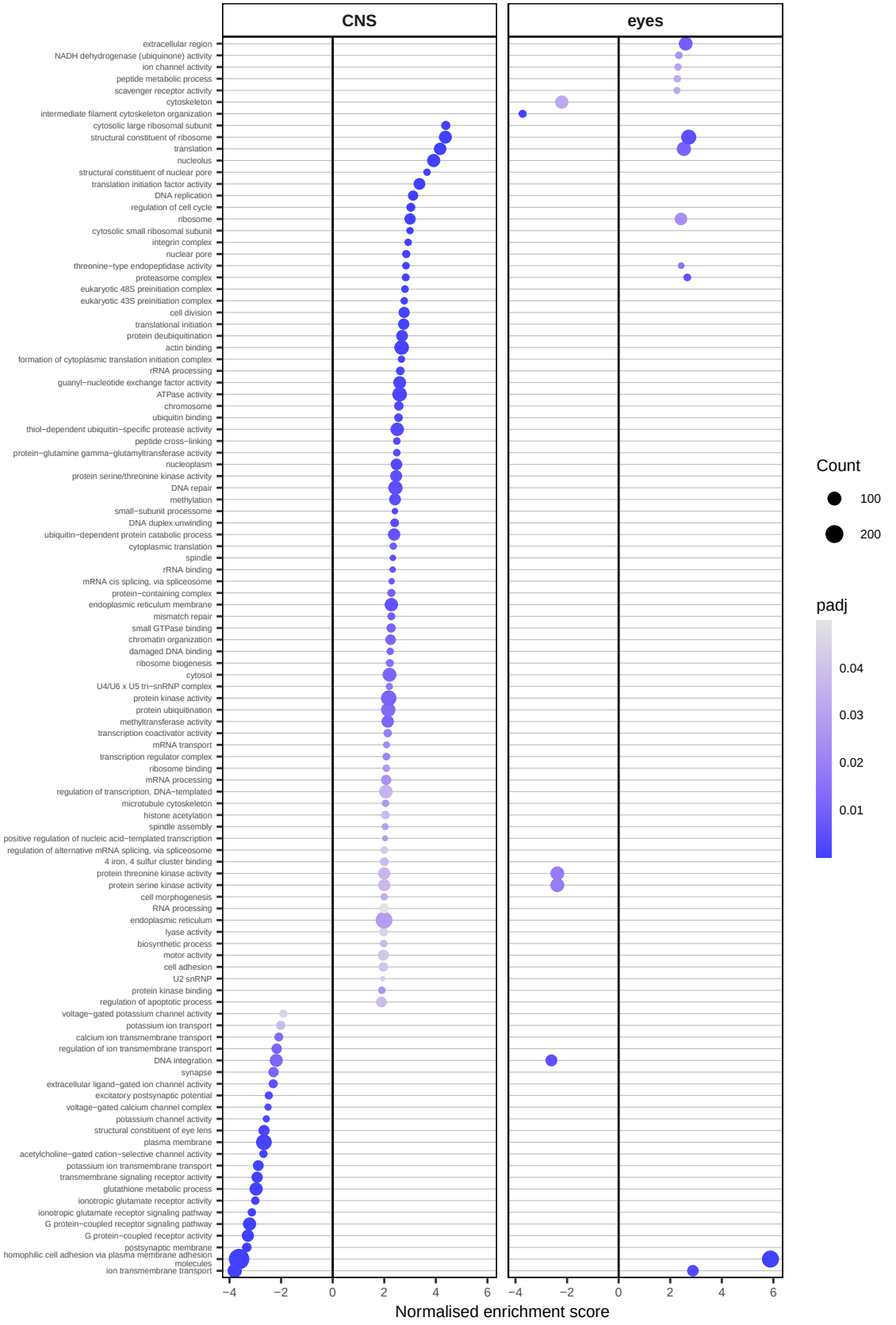

Figure C.4. *(see next page)*

Figure C.4 *(previous page)*. Dotplot showing the results from gene set enrichment analysis (GSEA) using GO terms/functional categories in the CNS and eyes CNS = central nervous system, padj = adjusted p-value, count = number of core enrichment genes in the GO term/functional category.

Table C.4. All core enrichment genes from the cluster of GO terms/functional categories related to ion channels that were found significant with gene set enrichment analysis in both the CNS and eyes. The ion channel cluster includes the GO terms 'ionotropic glutamate receptor signaling pathway', 'ionotropic glutamate receptor activity', 'postsynaptic membrane', 'excitatory postsynaptic potential', 'ion transmembrane transport', 'acetylcholine-gated cation-selective channel activity', 'transmembrane signaling receptor activity', 'extracellular ligand-gated ion channel activity', 'synapse', and 'ion channel activity'. Gene = gene ID in the transcriptome, annotation = annotation of the corresponding gene, ordered alphabetically.

Gene	Annotation
5283.7784	-
3318	-
5283.946	-
5661.1	acetylcholine receptor subunit alpha-like 1 isoform X1
5661	acetylcholine receptor subunit alpha-like isoform X2
5283.4488	acetylcholine receptor subunit beta-like 1 isoform X2
5283.4489	acetylcholine receptor subunit beta-like 1 isoform X2
5283.7592	cyclic nucleotide-gated cation channel alpha-3
5283.7592	cyclic nucleotide-gated cation channel alpha-3-like
6610	cyclic nucleotide-gated cation channel beta-3-like isoform X1
6610.2	cyclic nucleotide-gated cation channel beta-3-like isoform X2
6610	cyclic nucleotide-gated cation channel beta-3-like isoform X7
5283.9458	cyclic nucleotide-gated olfactory channel-like
5283.946	cyclic nucleotide-gated olfactory channel-like
7253.3	Cys-loop ligand-gated ion channel
7253.4	cys-loop ligand-gated ion channel-like isoform X2
7253	cys-loop ligand-gated ion channel-like isoform X2
7253.3	cys-loop ligand-gated ion channel-like isoform X2
7253.6	cys-loop ligand-gated ion channel-like isoform X3
5283.9038	gamma-aminobutyric acid receptor alpha-like
3318	gamma-aminobutyric acid receptor alpha-like
5283.8285	glutamate receptor 1-like
5283.8285	glutamate receptor 4
7335	glutamate receptor ionotropic, kainate 2-like isoform X1
7335.3	glutamate receptor ionotropic, kainate 2-like isoform X1
2901	glutamate receptor ionotropic, kainate 2-like isoform X1
6740	glutamate receptor ionotropic, kainate 2-like isoform X1
6740.2	glutamate receptor ionotropic, kainate 2-like isoform X1
7335.6	glutamate receptor ionotropic, kainate 2-like isoform X1
7335.1	glutamate receptor ionotropic, kainate 2-like isoform X1
6740.3	glutamate receptor ionotropic, kainate 2 isoform X1
1742	glutamate receptor ionotropic, NMDA 2B-like
4067	glutamate receptor ionotropic, NMDA 3A-like
3215.2	glutamate receptor ionotropic, NMDA 3A-like isoform X2
2499	glycine receptor subunit alphaZ1-like
5283.8285	GRIA4 protein
5283.2592	HCN channel protein
5283.2593	HCN channel protein
7253.3	Hypothetical predicted protein
5283.5377	neuronal acetylcholine receptor subunit alpha-10-like
6426.1	neuronal acetylcholine receptor subunit alpha-10-like

Table C.4 continued.

Gene	Annotation
6426.7	neuronal acetylcholine receptor subunit alpha-10-like
5283.7784	neuronal acetylcholine receptor subunit alpha-10-like
6426.1	neuronal acetylcholine receptor subunit alpha-10-like
3136	neuronal acetylcholine receptor subunit alpha-10-like
6426.6	neuronal acetylcholine receptor subunit alpha-10-like
6426.5	neuronal acetylcholine receptor subunit alpha-10-like
5283.10464	neuronal acetylcholine receptor subunit alpha-10-like
5283.2323	neuronal acetylcholine receptor subunit alpha-10-like isoform X3
5283.8846	neuronal acetylcholine receptor subunit alpha-3-like
5283.8847	neuronal acetylcholine receptor subunit alpha-3-like
878	neuronal acetylcholine receptor subunit alpha-5-like
5283.10467	neuronal acetylcholine receptor subunit alpha-6-like
4605.3	piezo-type mechanosensitive ion channel component 1-like isoform X1
5283.2593	potassium/sodium hyperpolarization-activated cyclic nucleotide-gated channel 2-like
5283.2593	potassium/sodium hyperpolarization-activated cyclic nucleotide-gated channel 3-like isoform X2
5283.2593	potassium/sodium hyperpolarization-activated cyclic nucleotide-gated channel 3-like isoform X4
6010.2	sideroflexin-1
5283.2593	voltage-activated ion channel, putative

Table C.5. All core enrichment genes from the cluster of GO terms/functional categories related to ion transport that were found significant with gene set enrichment analysis in the CNS (no ion transport GO terms found significant in the eyes). The ion transport cluster includes the GO terms 'potassium channel activity', 'potassium ion transmembrane transport', 'voltage-gated potassium channel activity', 'regulation of ion transmembrane transport', 'voltage-gated calcium channel complex', and 'calcium ion transmembrane transport'. Gene = gene ID in the transcriptome, annotation = annotation of the corresponding gene, ordered alphabetically.

Gene	Annotation
6427.3	-
5283.946	-
6093.6	ATP-binding cassette sub-family C member 9-like isoform X1
6093.4	ATP-binding cassette sub-family C member 9-like isoform X1
6093.4	ATP-binding cassette sub-family C member 9-like isoform X2
6093.4	ATP-binding cassette sub-family C member 9-like isoform X3
6093.1	ATP-binding cassette sub-family C member 9 isoform X1
6093	ATP-binding cassette sub-family C member 9 isoform X1
5283.394	CACNA1G
5283.7244	CACNA1G
1506	calcium-activated potassium channel slowpoke isoform X15
1506.1	calcium-activated potassium channel subunit alpha-1 isoform X10
1506.1	calcium-activated potassium channel subunit alpha-1 isoform X8
1506	calcium-activated potassium channel subunit alpha-1 isoform X8
7412	calcium channel beta subunit
5283.10202	calcium uniporter protein, mitochondrial-like
5283.7592	cyclic nucleotide-gated cation channel alpha-3
5283.7592	cyclic nucleotide-gated cation channel alpha-3-like
5283.946	cyclic nucleotide-gated olfactory channel-like
1329	G protein-activated inward rectifier potassium channel 2-like
5187.3	G protein-activated inward rectifier potassium channel 3-like
5283.7191	G protein-activated inward rectifier potassium channel 3-like
5283.7192	G protein-activated inward rectifier potassium channel 3-like
5187.7	G protein-activated inward rectifier potassium channel 3-like
5283.2593	HCN channel protein
5496.1	muscle calcium channel subunit alpha-1-like isoform X1
5496	muscle calcium channel subunit alpha-1-like isoform X3
1933	muscle calcium channel subunit alpha-1-like isoform X4
5283.11306	Na+/K+ ATPase beta subunit
206	neuronal calcium sensor 1
7325.1	plasma membrane calcium-transporting ATPase 2-like isoform X1
7325.6	plasma membrane calcium-transporting ATPase 2-like isoform X1
7325.1	plasma membrane calcium-transporting ATPase 2 isoform X1
7325.5	plasma membrane calcium-transporting ATPase 2 isoform X1
7325.2	plasma membrane calcium-transporting ATPase 2 isoform X1
7107	potassium channel Kv1
5283.986	potassium channel subfamily K member 1-like
5283.4027	potassium channel subfamily K member 4-like
5283.1287	potassium channel subfamily T member 2-like isoform X1
5283.1286	potassium channel subfamily T member 2-like isoform X1
5283.5242	potassium channel subfamily T member 2-like isoform X1
5283.1287	potassium channel subfamily T member 2-like isoform X2

Table C.5 continued.

Gene	Annotation
5283.524	potassium channel subfamily T member 2-like isoform X2
5283.5241	potassium channel subfamily T member 2-like isoform X2
5283.5239	potassium channel subfamily T member 2-like isoform X3
5283.5241	potassium channel subfamily T member 2-like isoform X5
7032	potassium intermediate/small conductance calcium-activated channel subfamily N member 3
7032.1	potassium intermediate/small conductance calcium-activated channel subfamily N member 3
7109.1	potassium voltage-gated channel protein Shab-like
5283.2059	potassium voltage-gated channel protein Shaker-like
5283.2058	potassium voltage-gated channel protein Shaker-like
5283.206	potassium voltage-gated channel protein Shaker-like
5283.2159	potassium voltage-gated channel protein Shal-like
5283.2158	potassium voltage-gated channel protein Shal-like
5283.216	potassium voltage-gated channel protein Shal-like isoform X1
5283.2157	potassium voltage-gated channel protein Shal-like isoform X1
7066.1	potassium voltage-gated channel protein Shaw-like
7066	potassium voltage-gated channel protein Shaw-like
6752.2	potassium voltage-gated channel protein Shaw-like isoform X1
6752	potassium voltage-gated channel protein Shaw-like isoform X1
6752.1	potassium voltage-gated channel protein Shaw-like isoform X1
995	potassium voltage-gated channel subfamily A member 1-like
7109	potassium voltage-gated channel subfamily B member 2 isoform X6
7109.1	potassium voltage-gated channel subfamily B member 2 isoform X6
5283.1038	potassium voltage-gated channel subfamily H member 4
5283.1038	potassium voltage-gated channel subfamily H member 4 isoform X1
1571	potassium voltage-gated channel subfamily H member 6 isoform X1
1768	potassium voltage-gated channel subfamily H member 7-like isoform X1
5283.1038	potassium voltage-gated channel subfamily H member 8-like
3824	potassium voltage-gated channel subfamily KQT member 1-like isoform X1
3824.1	potassium voltage-gated channel subfamily KQT member 1-like isoform X1
5283.2593	potassium/sodium hyperpolarization-activated cyclic nucleotide-gated channel 2-like
5283.2593	potassium/sodium hyperpolarization-activated cyclic nucleotide-gated channel 3-like isoform X2
5283.2593	potassium/sodium hyperpolarization-activated cyclic nucleotide-gated channel 3-like isoform X4
7109.1	probable serine/threonine-protein kinase DDB_G0282963
5283.11306	probable sodium/potassium-transporting ATPase subunit beta-3
6905	putative Na+/K+-ATPase alpha subunit
5283.4923	riboflavin-binding protein-like
5283.324	ryanodine receptor-like isoform X11
5283.324	ryanodine receptor-like isoform X12
5283.324	ryanodine receptor-like isoform X15
5283.324	ryanodine receptor-like isoform X17
5283.324	ryanodine receptor-like isoform X2
5283.324	ryanodine receptor-like isoform X7
5283.324	ryanodine receptor 2
5283.324	ryanodine receptor 2-like isoform X10
1483	short transient receptor potential channel 3-like
1418	short transient receptor potential channel 3-like isoform X1
7032.1	small conductance calcium-activated potassium channel protein-like
7032.2	small conductance calcium-activated potassium channel protein 2 isoform X1

Table C.5 continued.

Gene	Annotation
7032.1	small conductance calcium-activated potassium channel protein 2 isoform X1
7381.7	sodium channel
5283.2924	sodium channel protein 1 brain
5283.2924	sodium channel protein 1 brain-like
5283.2922	sodium channel protein 1 brain-like
5283.2924	sodium channel protein 1 brain-like isoform X1
5283.2924	sodium channel protein 1 brain isoform X1
5283.2924	sodium channel protein para isoform X2
5283.2922	sodium channel protein para isoform X2
7381.6	sodium channel protein type 4 subunit alpha A-like isoform X1
5283.2924	sodium channel protein type 4 subunit alpha B-like
7381.2	sodium channel protein type 4 subunit alpha B-like isoform X1
7381.3	sodium channel protein type 4 subunit alpha B-like isoform X1
7381.1	sodium channel protein type 4 subunit alpha B-like isoform X1
7381.5	sodium channel protein type 4 subunit alpha B-like isoform X1
7381.4	sodium channel protein type 4 subunit alpha B-like isoform X1
5283.9598	sodium/potassium-transporting ATPase subunit beta-like
5283.9595	sodium/potassium-transporting ATPase subunit beta-like
5283.9596	sodium/potassium-transporting ATPase subunit beta-like
5283.96	sodium/potassium-transporting ATPase subunit beta-like
4619	sodium/potassium-transporting ATPase subunit beta-like
5283.9599	sodium/potassium-transporting ATPase subunit beta-like
4619.1	sodium/potassium-transporting ATPase subunit beta-like
5283.9594	sodium/potassium-transporting ATPase subunit beta-like
5283.9214	sodium/potassium/calcium exchanger 2-like isoform X2
7433.2	sodium/potassium/calcium exchanger 4-like
7433	sodium/potassium/calcium exchanger 4-like
7433.3	sodium/potassium/calcium exchanger 4-like
7433.1	sodium/potassium/calcium exchanger 4-like
5283.9214	sodium/potassium/calcium exchanger Nckx30C
5283.9214	sodium/potassium/calcium exchanger Nckx30C-like
5283.9213	sodium/potassium/calcium exchanger Nckx30C-like
6396.2	solute carrier family 12 member 4-like isoform X1
6396.3	solute carrier family 12 member 4-like isoform X1
6396.1	solute carrier family 12 member 4-like isoform X2
6396.9	solute carrier family 12 member 4-like isoform X2
3790	transient-receptor-potential-like protein
3790	transient-receptor-potential-like protein isoform X1
3790.1	transient-receptor-potential-like protein isoform X1
5283.3687	transient receptor potential-gamma protein-like
5811.9	transient receptor potential cation channel subfamily M member-like 2 isoform X1
6627	trimeric intracellular cation channel type 1B.1-like
7122.2	TWiK family of potassium channels protein 18-like
7122.1	TWiK family of potassium channels protein 18-like
7122	TWiK family of potassium channels protein 18-like
6244	two pore potassium channel protein sup-9-like
5283.2593	voltage-activated ion channel, putative
6427.3	voltage-dependent calcium channel
6427.2	voltage-dependent calcium channel
1684.1	voltage-dependent calcium channel
6427.3	voltage-dependent calcium channel type A subunit alpha-1-like
6427	voltage-dependent calcium channel type A subunit alpha-1-like

Table C.5 continued.

Gene	Annotation
6427.3	voltage-dependent calcium channel type A subunit alpha-1-like isoform X6
1684	voltage-dependent calcium channel type A subunit alpha-1 isoform X2
5283.3939	voltage-dependent T-type calcium channel subunit alpha-1G-like
5283.394	voltage-dependent T-type calcium channel subunit alpha-1G-like isoform X2
5283.7246	voltage-dependent T-type calcium channel subunit alpha-1G-like isoform X2
5283.7243	voltage-dependent T-type calcium channel subunit alpha-1H-like
5283.7245	voltage-dependent T-type calcium channel subunit alpha-1H-like
5283.7242	voltage-dependent T-type calcium channel subunit alpha-1I-like
5283.7244	voltage-dependent T-type calcium channel subunit alpha-1I-like
5283.10568	voltage-gated potassium channel subunit beta-2-like isoform X1
5283.10569	voltage-gated potassium channel subunit beta-2-like isoform X1
7381.5	voltage-gated sodium channel invertebrate type 1

Table C.6. All core enrichment genes from the cluster of GO terms/functional categories related to GPCR (G-protein coupled receptors) that were found significant with gene set enrichment analysis in the CNS (no GPCR GO terms found significant in the eyes). The GPCR cluster includes the GO terms 'G protein-coupled receptor activity' and 'G protein-coupled receptor signaling pathway'. Gene = gene ID in the transcriptome, annotation = annotation of the corresponding gene, ordered alphabetically.

Gene	Annotation
5283.11228	-
6174	-
5283.7636	-
5283.406	-
3985	5-hydroxytryptamine receptor-like
396	5-hydroxytryptamine receptor 1D-like
5283.11786	5-hydroxytryptamine receptor 2C-like
5283.11785	5-hydroxytryptamine receptor 2C-like
5283.1508	5-hydroxytryptamine receptor 4-like
5283.9162	adhesion G-protein coupled receptor D1-like
5283.9162	adhesion G-protein coupled receptor D2-like
252.1	adhesion G protein-coupled receptor A3-like
6594	adhesion G protein-coupled receptor L2-like isoform X1
6594	adhesion G protein-coupled receptor L2 isoform X1
2554	allatostatin-A receptor
1650	alpha-2A adrenergic receptor
5283.10427	cadherin EGF LAG seven-pass G-type receptor 1-like
5283.1043	cadherin EGF LAG seven-pass G-type receptor 1-like
5283.10428	cadherin EGF LAG seven-pass G-type receptor 1-like
5596.4	cadherin EGF LAG seven-pass G-type receptor 1 isoform X3
5596.1	cadherin EGF LAG seven-pass G-type receptor 1 isoform X3
5596.3	cadherin EGF LAG seven-pass G-type receptor 2 isoform X1
5596.2	cadherin EGF LAG seven-pass G-type receptor 2 isoform X5
5283.11833	calcitonin gene-related peptide type 1 receptor-like isoform X1
5283.2398	cAMP-dependent protein kinase catalytic subunit beta
5283.2398	cAMP-dependent protein kinase catalytic subunit isoform X5
5283.2397	cAMP-dependent protein kinase catalytic subunit isoform X5
5283.903	cardioacceleratory peptide receptor-like isoform X1
5283.5948	catalytic subunit of protein kinase A
2171	cholecystokinin receptor type A-like
3084	cholecystokinin receptor type A-like
5283.8548	corticotropin-releasing factor receptor 2-like
6072	CX3C chemokine receptor 1 isoform X1
5283.11354	dopamine receptor 1-like
5283.11353	dopamine receptor 1-like
3912.1	dopamine receptor 1-like
3716	FMRFamide receptor-like
1567	FMRFamide receptor-like
3871	FMRFamide receptor-like
5415.1	FMRFamide receptor-like
6899.1	frizzled-9
6899.1	frizzled-9-like
6899.1	Frizzled 10A
6899	Frizzled 10A
6899.1	frizzled 9/10

Table C.6 continued.

Gene	Annotation
5283.9573	G-protein coupled receptor 143-like
5283.9574	G-protein coupled receptor 143-like
1827	G-protein coupled receptor 161-like
4382	G-protein coupled receptor Mth-like
5283.11232	GABR1 protein
5283.11232	gamma-aminobutyric acid type B receptor subunit 1-like
5283.11229	gamma-aminobutyric acid type B receptor subunit 1-like
5283.8308	Gamma-aminobutyric acid type B receptor subunit 2
5283.10141	gonadotropin-releasing hormone receptor
5283.2535	growth hormone secretagogue receptor type 1-like
5283.732	guanine nucleotide-binding protein subunit beta-5
5283.2425	Hypothetical predicted protein
5283.4222	leucine-rich repeat-containing G-protein coupled receptor 5-like
5283.4293	leucine-rich repeat-containing G-protein coupled receptor 5-like
5283.4294	leucine-rich repeat-containing G-protein coupled receptor 5-like
5283.10762	lissencephaly-1 homolog
5283.10762	lissencephaly-1 homolog B
5283.4221	lutropin-choriogonadotropic hormone receptor isoform X3
5283.11295	melatonin receptor type 1A-like
5283.11297	melatonin receptor type 1A-like
5283.7577	metabotropic glutamate receptor 1-like
5283.757	metabotropic glutamate receptor 1-like
5283.7573	metabotropic glutamate receptor 1-like
5283.7569	metabotropic glutamate receptor 1-like
5283.7574	metabotropic glutamate receptor 1-like
1651	metabotropic glutamate receptor 3
5283.7578	metabotropic glutamate receptor 5-like
5283.7575	metabotropic glutamate receptor 5-like
6075	neuropeptide FF receptor 1-like
6075.1	neuropeptide FF receptor 1-like
1357	octopamine receptor Oamb-like
1357.1	octopamine receptor Oamb-like
2184.1	octopamine receptor Oamb isoform X1
2664	orexin receptor type 2-like
5283.9529	orexin receptor type 2-like
3932.1	parathyroid hormone/parathyroid hormone-related peptide receptor isoform X3
6072	PREDICTED: uncharacterized protein LOC106880461
4782	prolactin-releasing peptide receptor-like
5283.2398	protein kinase A
5283.2397	protein kinase A
1909.1	pyrokinin-1 receptor-like
5283.1602	regulator of G-protein signaling 4-like
5283.1599	regulator of G-protein signaling 4-like
5283.1146	retinochrome
5283.8098	retinochrome
5283.1143	retinochrome
5283.1145	retinochrome
5283.1142	retinochrome
5283.7855	rhodopsin
5283.7636	S-antigen protein-like
3932	secretin receptor-like isoform X1
6876.2	somatostatin receptor type 2-like

Table C.6 continued.

Gene	Annotation
5629	somatostatin receptor type 3-like
5984	thyrotropin-releasing hormone receptor-like
5629	thyrotropin-releasing hormone receptor-like
5283.1199	type-1 angiotensin II receptor isoform X1
5283.1602	unnamed protein product

Appendix D

Chapter 5 Appendices

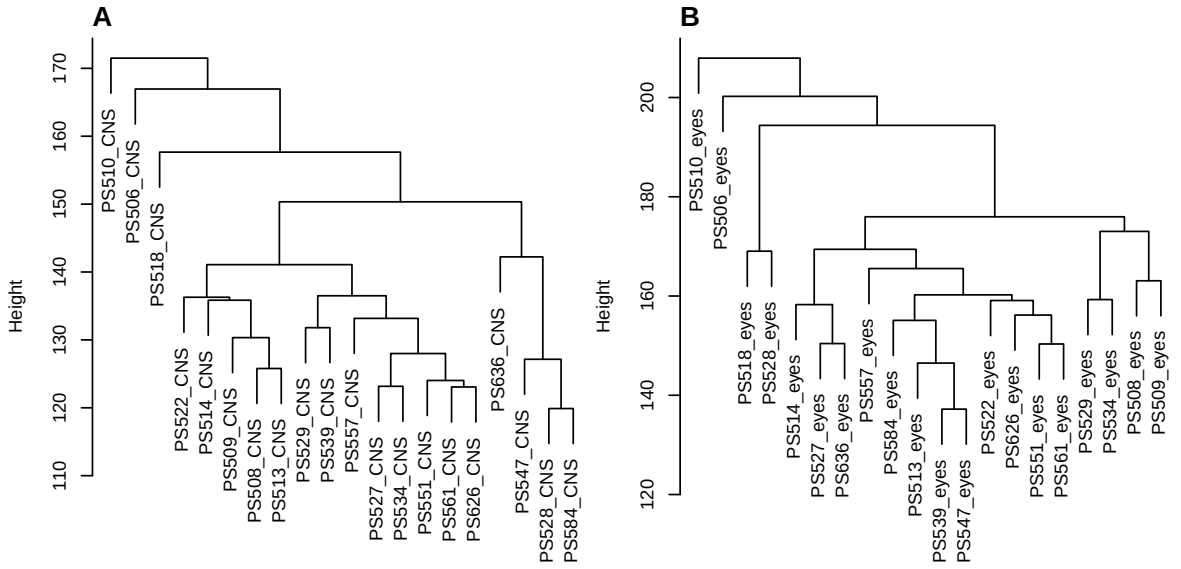

Figure D.1. Sample dendrograms created using hierarchical clustering with the 'average' method was used to detect sample outliers. Three and two outliers were detected in the **A** CNS and **B** eyes, respectively. PS510_CNS, PS506_CNS, PS518_CNS, PS510_eyes and PS506_eyes were removed as they were sample outliers.

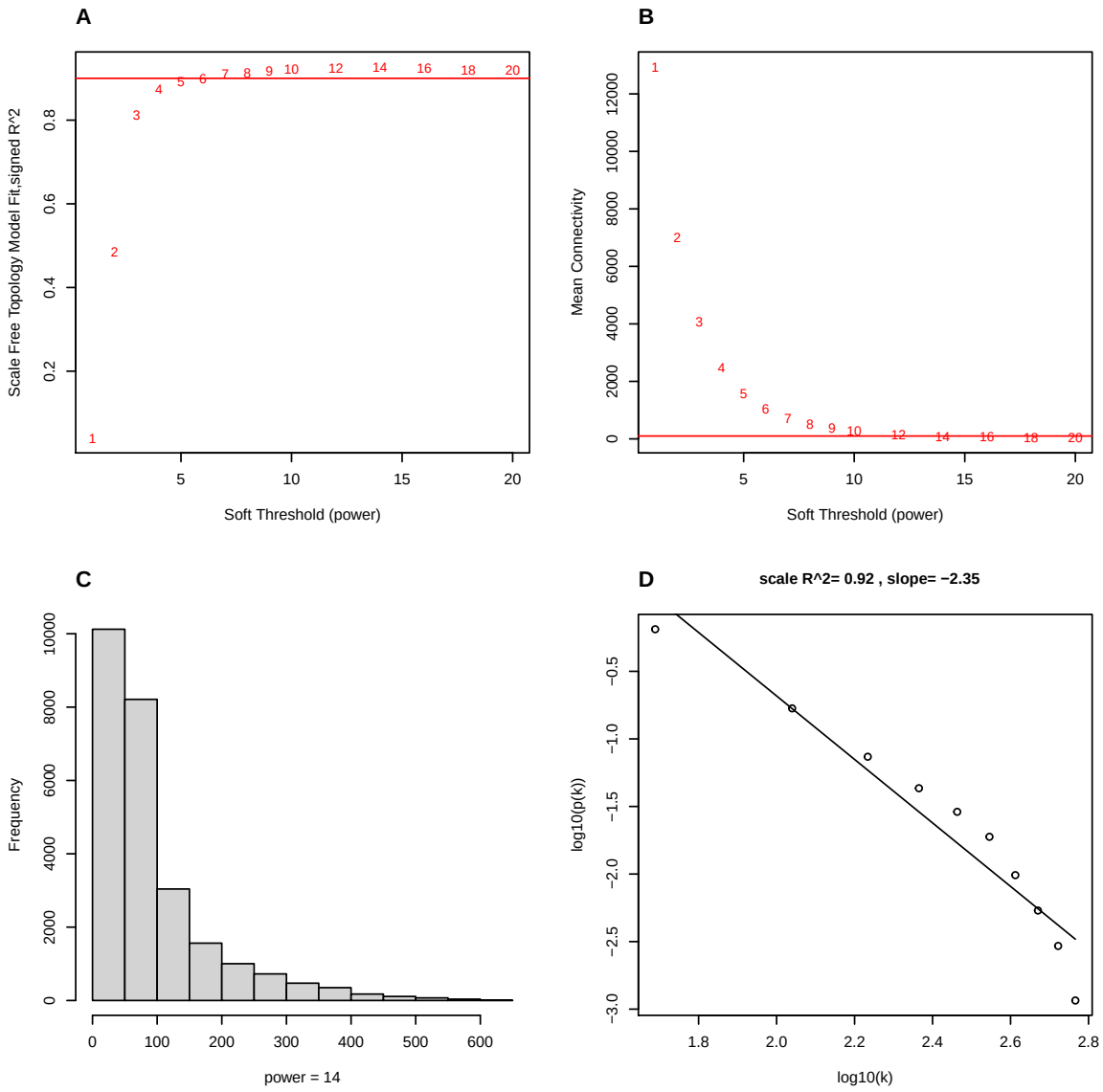

Figure D.2. Choosing and checking the soft threshold power for network construction using the CNS samples. A Scale-free topology fit index as a function of the soft-threshold power shows the network reaches approximately a scale free topology ($R^2 > 0.9$) when the soft threshold power is 7, however **B** mean connectivity as a function of the soft threshold power shows mean connectivity remains high and mean connectivity only drops below 100 at a soft threshold power of 14. **C** and **D** were used to check the chosen soft threshold power of 14 approximates a scale free topology.

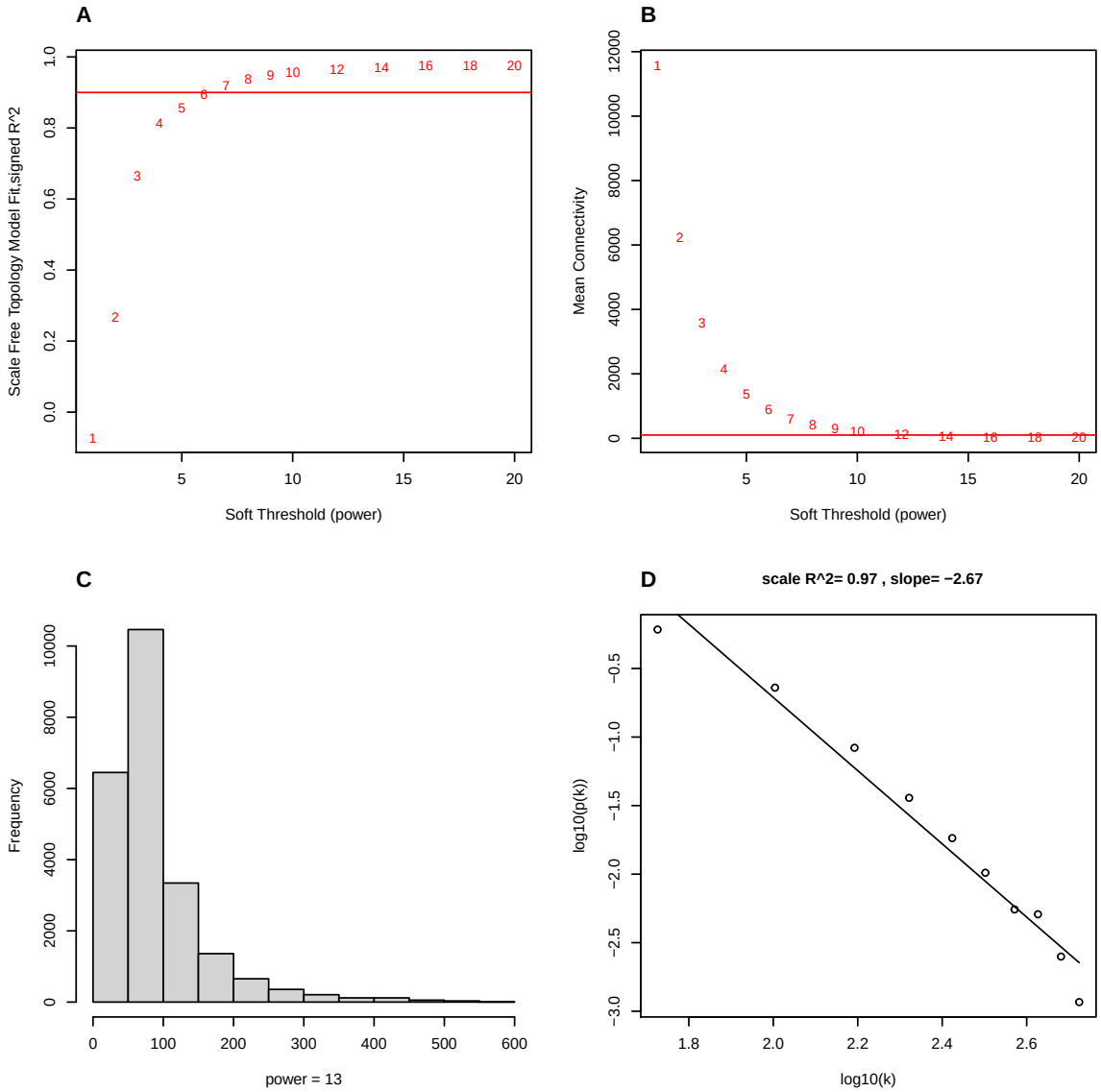

Figure D.3. Choosing and checking the soft threshold power for network construction using the eyes samples. A Scale-free topology fit index as a function of the soft-threshold power shows the network reaches approximately a scale free topology ($R^2 > 0.9$) when the soft threshold power is 7, however **B** mean connectivity as a function of the soft threshold power shows mean connectivity remains high and mean connectivity only drops below 100 at a soft threshold power of 13. **C** and **D** were used to check the chosen soft threshold power of 13 approximates a scale free topology.

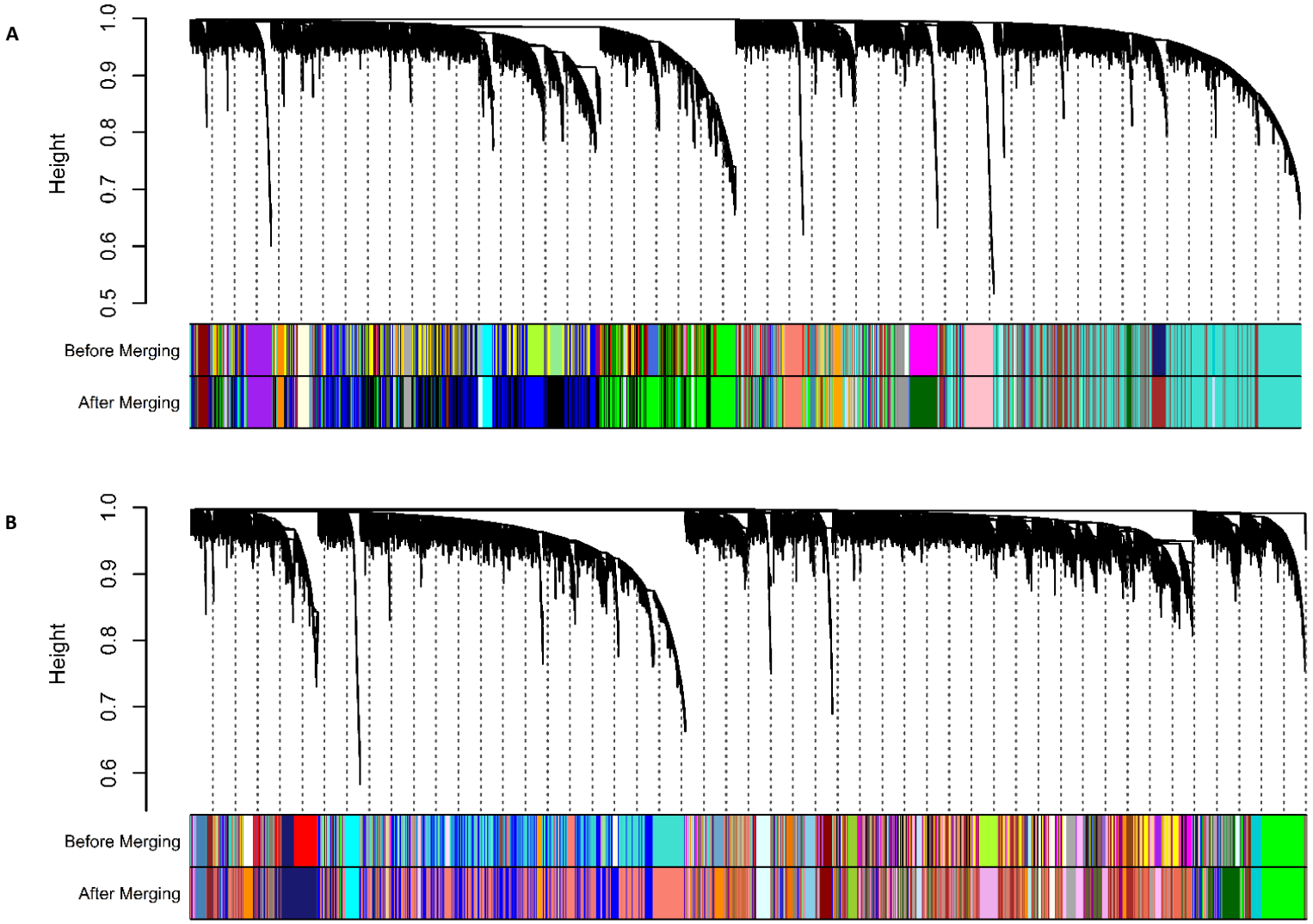

Figure D.4. Cluster dendrogram with co-expression network modules before and after merging modules. *(see next page)*

Figure D.4 ***(previous page).*** In the **A** CNS and **B** eyes. Each line in the cluster dendrogram is a gene and each module is represented by a different colour.

Table D.1. Modules detetcted in the CNS. Twenty seven modules were detected in the CNS. The modules were each labelled with a unique colour, and the number of genes within each module are shown.

Module	Number of genes
turquoise	5654
black	3917
blue	3346
green	3099
brown	2839
darkgreen	896
orange	738
pink	728
purple	597
grey60	508
lightcyan	500
cyan	475
salmon	423
lightsteelblue1	395
lightyellow	266
darkred	249
darkgrey	211
darkorange	177
saddlebrown	151
steelblue	139
paleturquoise	128
darkolivegreen	108
skyblue3	85
plum1	73
orangered4	70
mediumpurple3	62
lightcyan1	50

Table D.2. Modules detetcted in the eyes. Thirty eight modules were detected in the eyes. The modules were each labelled with a unique colour, and the number of genes within each module are shown.

Module	Number of genes
salmon	4278
blue	3442
coral2	1916
brown	1470
midnightblue	1248
darkolivegreen	1155
darkgrey	1078
green	1017
plum1	929
darkorange	688
darkgreen	682
plum2	632
sienna3	540
darkmagenta	448
cyan	327
darkred	304
lightcyan	301
darkturquoise	236
orange	214
skyblue	202
steelblue	196
paleturquoise	188
violet	186
yellowgreen	173
orangered4	151
lightsteelblue1	127
floralwhite	119
darkorange2	116
brown4	112
bisque4	108
thistle2	94
palevioletred3	90
navajowhite2	81
maroon	78
lavenderblush3	63
honeydew1	60
darkseagreen4	55
antiquewhite4	52

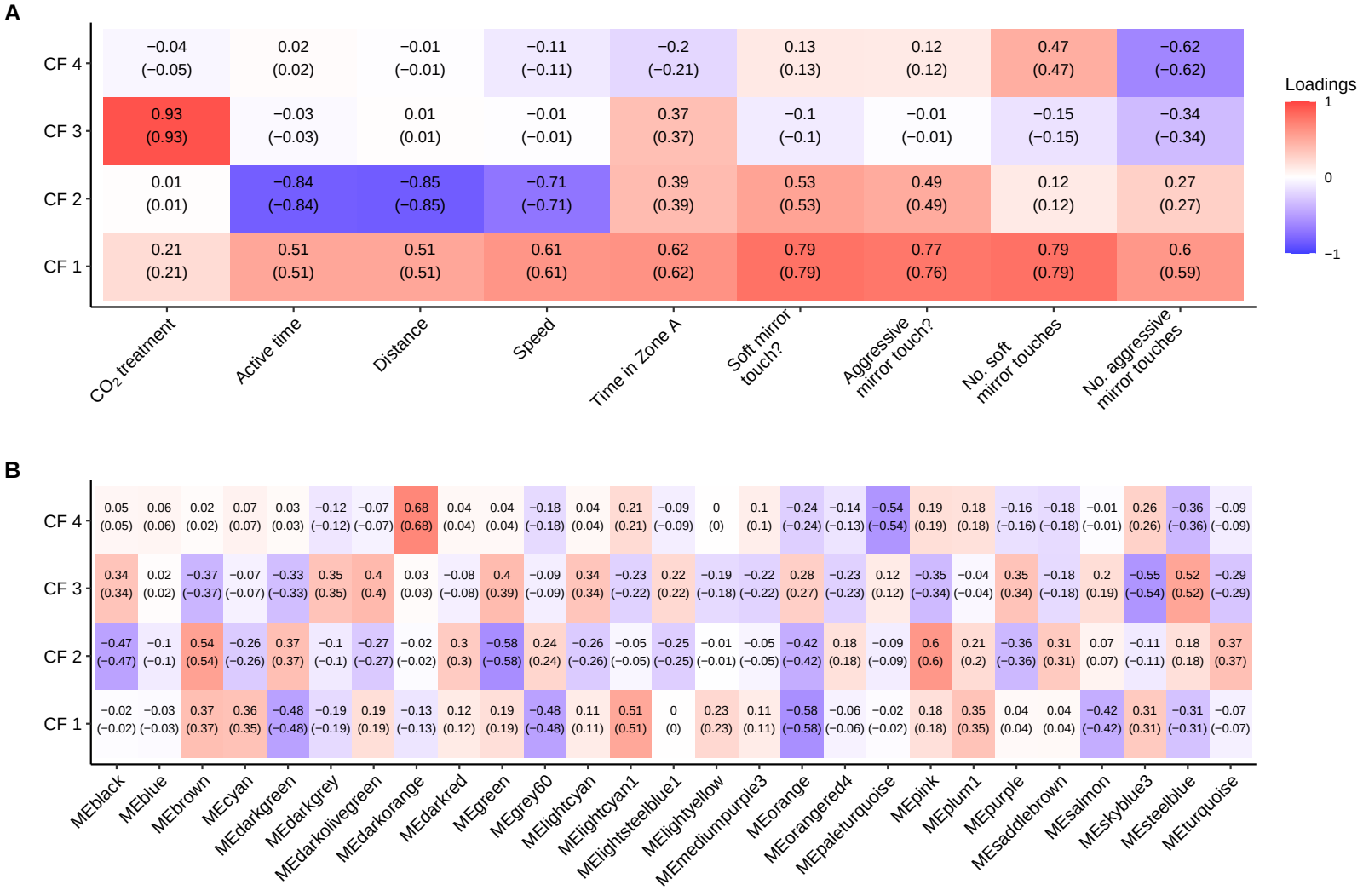

Figure D.5. Canonical loadings and cross loadings for the CNS samples. *(see next page)*

Figure D.5 ***(previous page).*** Canonical loadings and cross loadings for each canonical function (CF) of each variable in the **A** traits set and **B** module eigengenes (MEs) set, in the CNS. Canonical loadings are shown above canonical cross-loadings, which are in brackets. Colouration depicts canonical loadings. Soft mirror touch? = whether any soft mirror touches occurred (yes/no), Aggressive mirror touch? = whether any aggressive mirror touches occurred (yes/no).

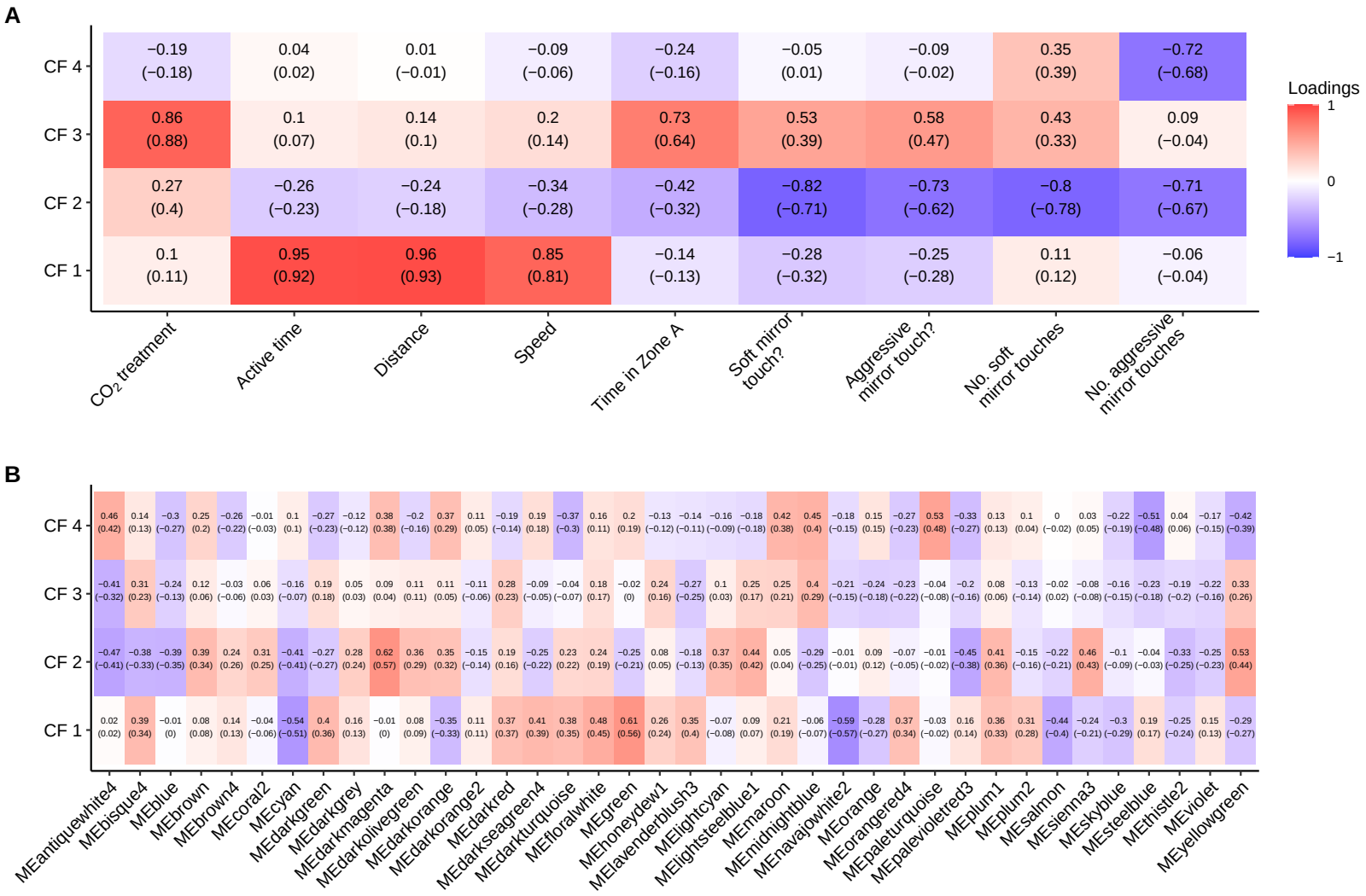

Figure D.6. Canonical loadings and cross loadings for the eyes samples. *(see next page)*

Figure D.6 ***(previous page).*** Canonical loadings and cross loadings for each canonical function (CF) of each variable in the **A** traits set and **B** module eigengenes (MEs) set, in the eyes. Canonical loadings are shown above canonical cross-loadings, which are in brackets. Colouration depicts canonical loadings. Soft mirror touch? = whether any soft mirror touches occurred (yes/no), Aggressive mirror touch? = whether any aggressive mirror touches occurred (yes/no).

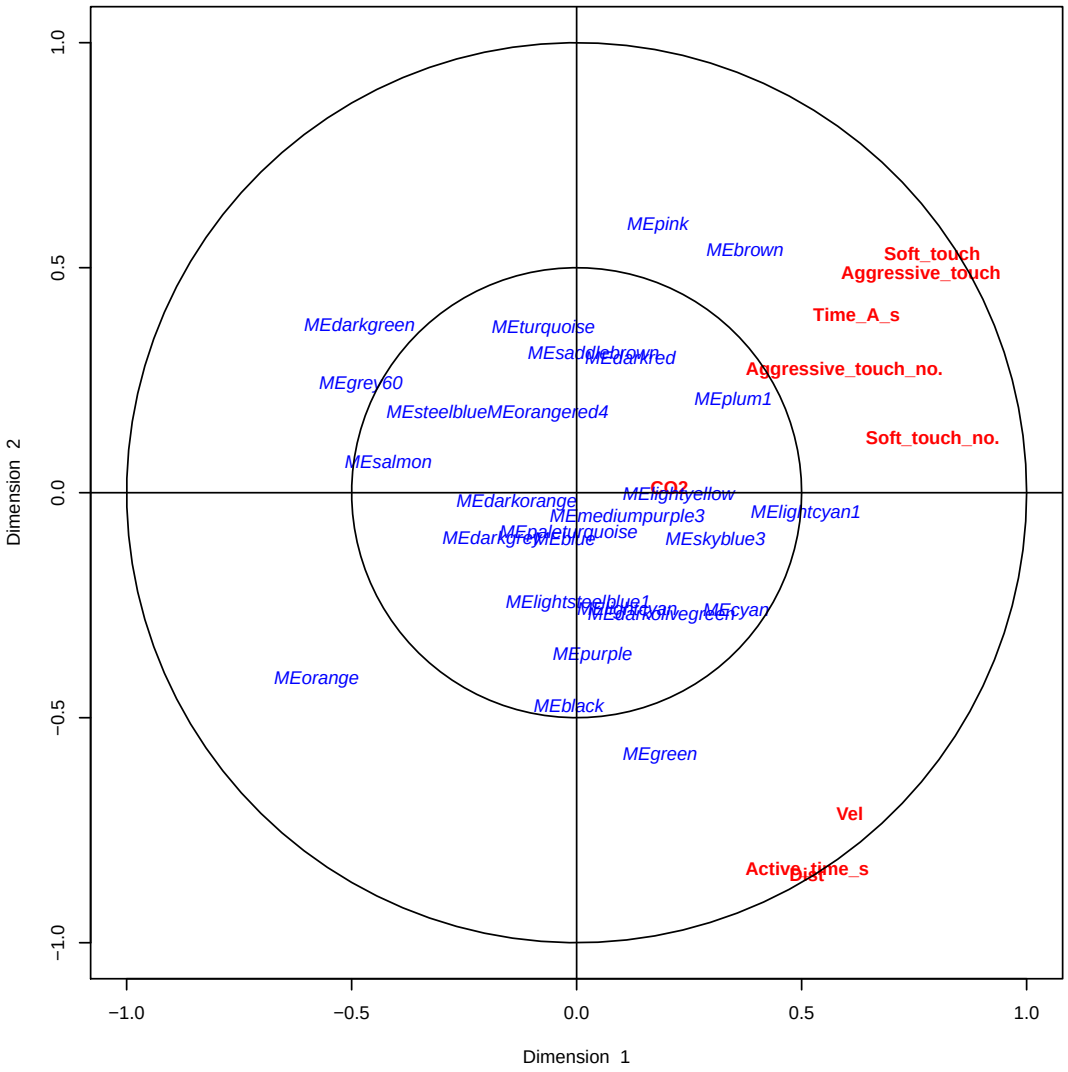

Figure D.7. Canonical correlation analysis biplot depicting where the module eigengenes (MEs) lie in space in relation to the traits for the CNS, for canonical functions (dimensions) 1 and 2. Variables from the MEs set and the traits set are in blue and red, respectively. The inner ring is set at a radius of 0.5. CO2 = CO_2 treatment, Active_time_s = time spent active (s), Dist = total distance moved (cm), Vel = average speed (cm/s), Time_A_s = time spent in Zone A (3 cm closes to mirror) (s), Soft_touch_no. = number of soft mirror touches, Soft_touch = whether any soft mirror touches occurred (yes/no), Aggressive_touch_no. = number of aggressive mirror touches = Aggressive_touch = whether any aggressive mirror touches occurred (yes/no), ME = module eigengene.

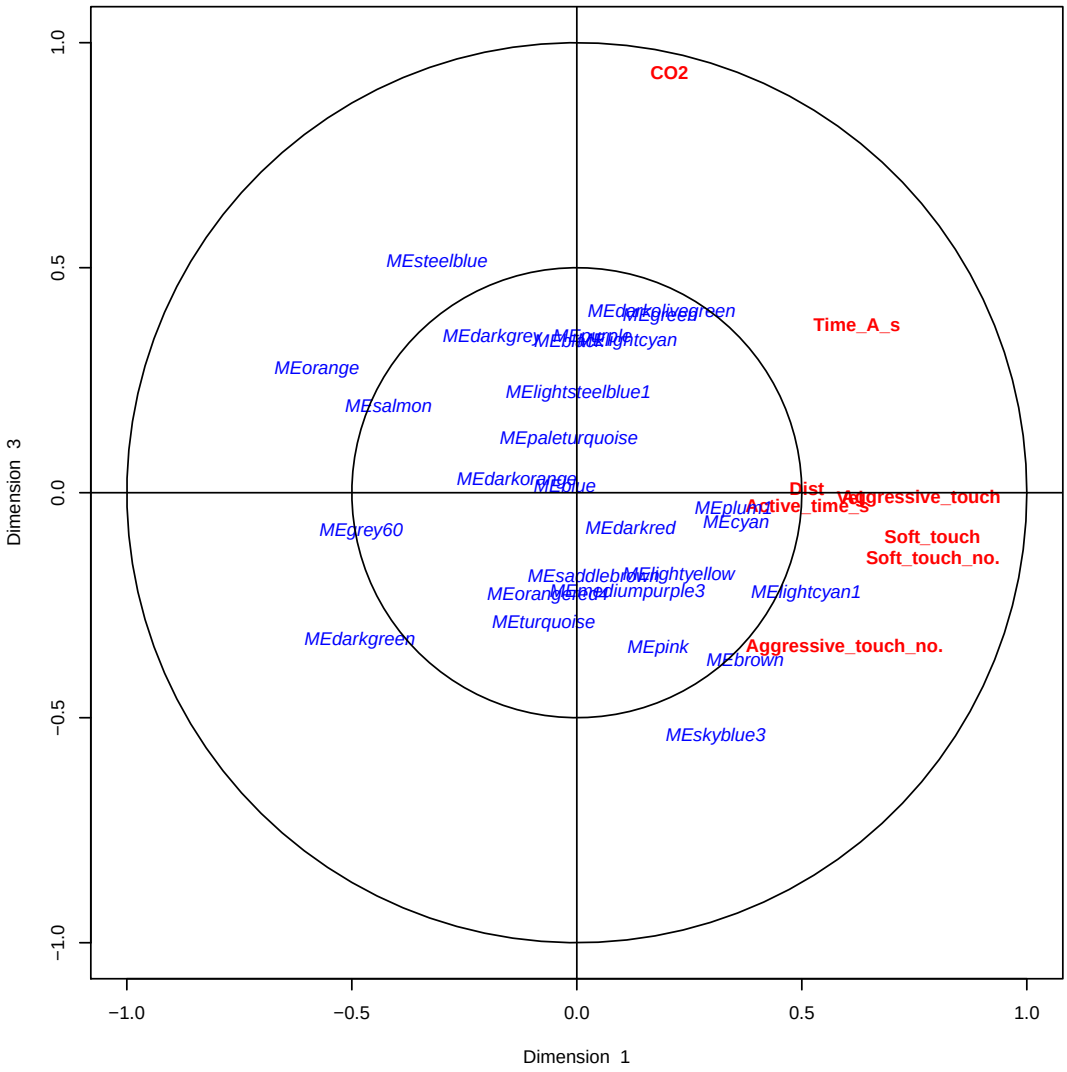

Figure D.8. Canonical correlation analysis biplot depicting where the module eigengenes (MEs) lie in space in relation to the traits for the CNS, for canonical functions (dimensions) 1 and 3. Variables from the MEs set and the traits set are in blue and red, respectively. The inner ring is set at a radius of 0.5. CO2 = CO_2 treatment, Active_time_s = time spent active (s), Dist = total distance moved (cm), Vel = average speed (cm/s), Time_A_s = time spent in Zone A (3 cm closes to mirror) (s), Soft_touch_no. = number of soft mirror touches, Soft_touch = whether any soft mirror touches occurred (yes/no), Aggressive_touch_no. = number of aggressive mirror touches = Aggressive_touch = whether any aggressive mirror touches occurred (yes/no), ME = module eigengene.

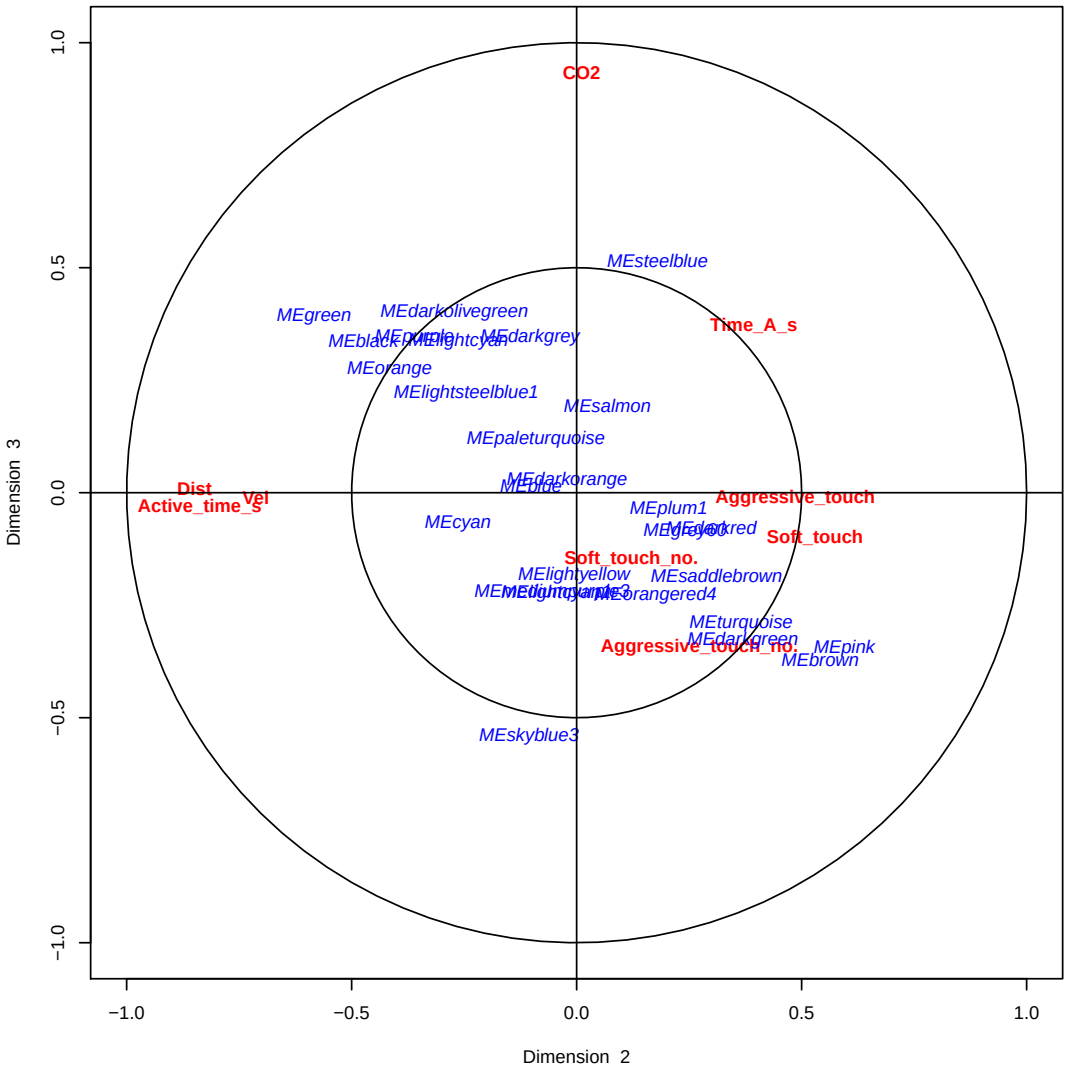

Figure D.9. Canonical correlation analysis biplot depicting where the module eigengenes (MEs) lie in space in relation to the traits for the CNS, for canonical functions (dimensions) 2 and 3. Variables from the MEs set and the traits set are in blue and red, respectively. The inner ring is set at a radius of 0.5. CO2 = CO_2 treatment, Active_time_s = time spent active (s), Dist = total distance moved (cm), Vel = average speed (cm/s), Time_A_s = time spent in Zone A (3 cm closes to mirror) (s), Soft_touch_no. = number of soft mirror touches, Soft_touch = whether any soft mirror touches occurred (yes/no), Aggressive_touch_no. = number of aggressive mirror touches = Aggressive_touch = whether any aggressive mirror touches occurred (yes/no), ME = module eigengene.

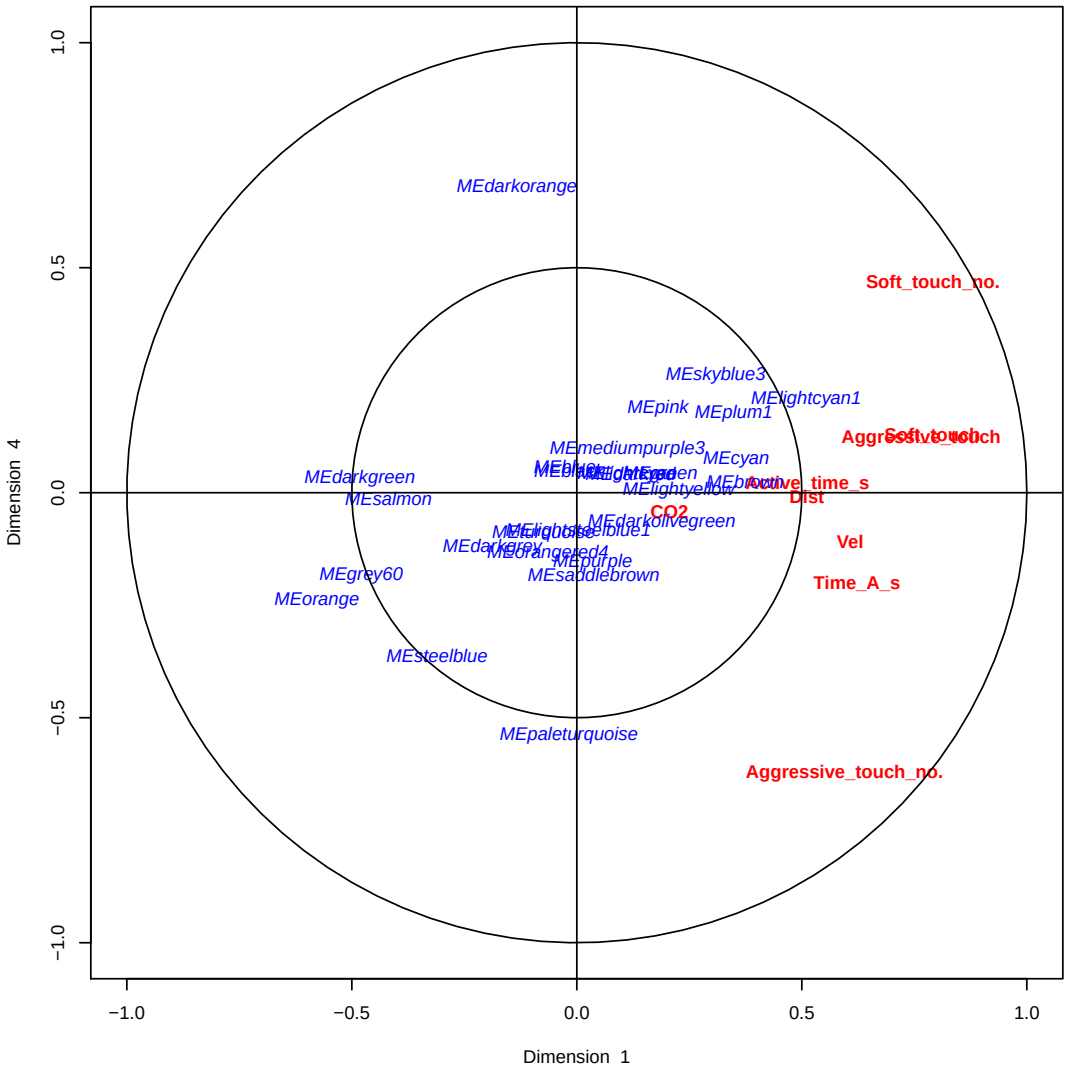

Figure D.10. Canonical correlation analysis biplot depicting where the module eigengenes (MEs) lie in space in relation to the traits for the CNS, for canonical functions (dimensions) 1 and 4. Variables from the MEs set and the traits set are in blue and red, respectively. The inner ring is set at a radius of 0.5. CO2 = CO_2 treatment, Active_time_s = time spent active (s), Dist = total distance moved (cm), Vel = average speed (cm/s), Time_A_s = time spent in Zone A (3 cm closes to mirror) (s), Soft_touch_no. = number of soft mirror touches, Soft_touch = whether any soft mirror touches occurred (yes/no), Aggressive_touch_no. = number of aggressive mirror touches = Aggressive_touch = whether any aggressive mirror touches occurred (yes/no), ME = module eigengene.

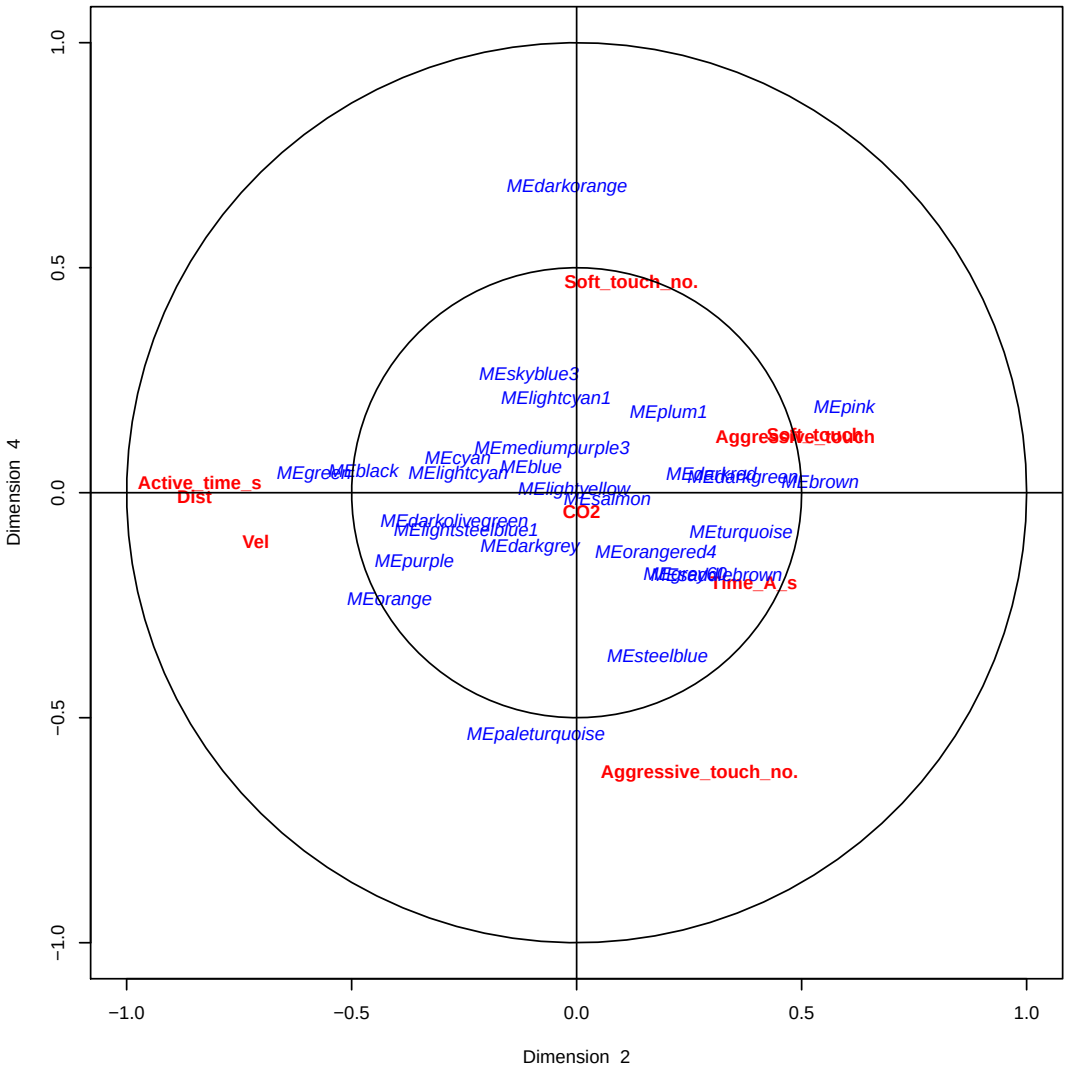

Figure D.11. Canonical correlation analysis biplot depicting where the module eigengenes (MEs) lie in space in relation to the traits for the CNS, for canonical functions (dimensions) 2 and 4. Variables from the MEs set and the traits set are in blue and red, respectively. The inner ring is set at a radius of 0.5. CO2 = CO_2 treatment, Active_time_s = time spent active (s), Dist = total distance moved (cm), Vel = average speed (cm/s), Time_A_s = time spent in Zone A (3 cm closes to mirror) (s), Soft_touch_no. = number of soft mirror touches, Soft_touch = whether any soft mirror touches occurred (yes/no), Aggressive_touch_no. = number of aggressive mirror touches = Aggressive_touch = whether any aggressive mirror touches occurred (yes/no), ME = module eigengene.

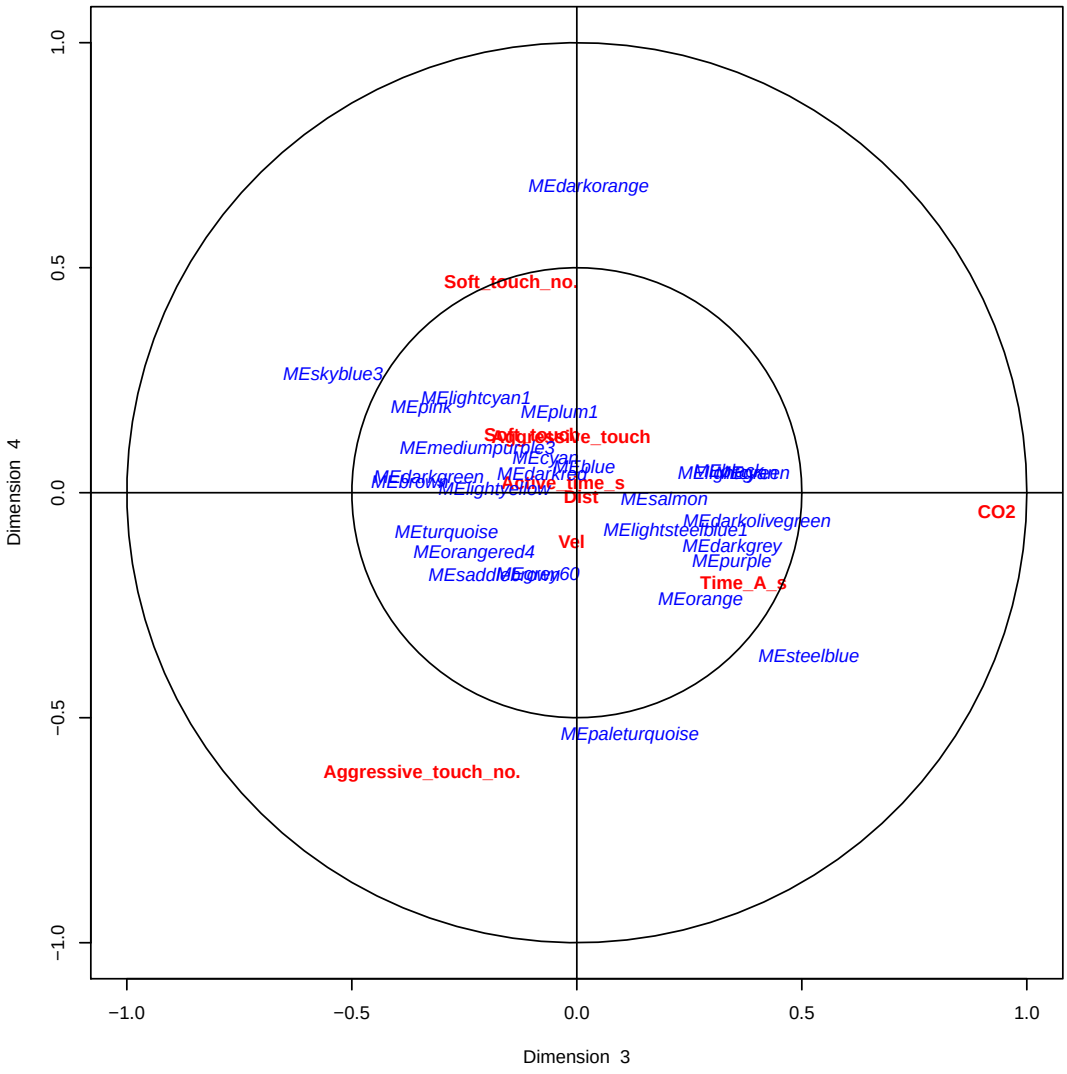

Figure D.12. Canonical correlation analysis biplot depicting where the module eigengenes (MEs) lie in space in relation to the traits for the CNS, for canonical functions (dimensions) 3 and 4. Variables from the MEs set and the traits set are in blue and red, respectively. The inner ring is set at a radius of 0.5. CO2 = CO_2 treatment, Active_time_s = time spent active (s), Dist = total distance moved (cm), Vel = average speed (cm/s), Time_A_s = time spent in Zone A (3 cm closes to mirror) (s), Soft_touch_no. = number of soft mirror touches, Soft_touch = whether any soft mirror touches occurred (yes/no), Aggressive_touch_no. = number of aggressive mirror touches = Aggressive_touch = whether any aggressive mirror touches occurred (yes/no), ME = module eigengene.

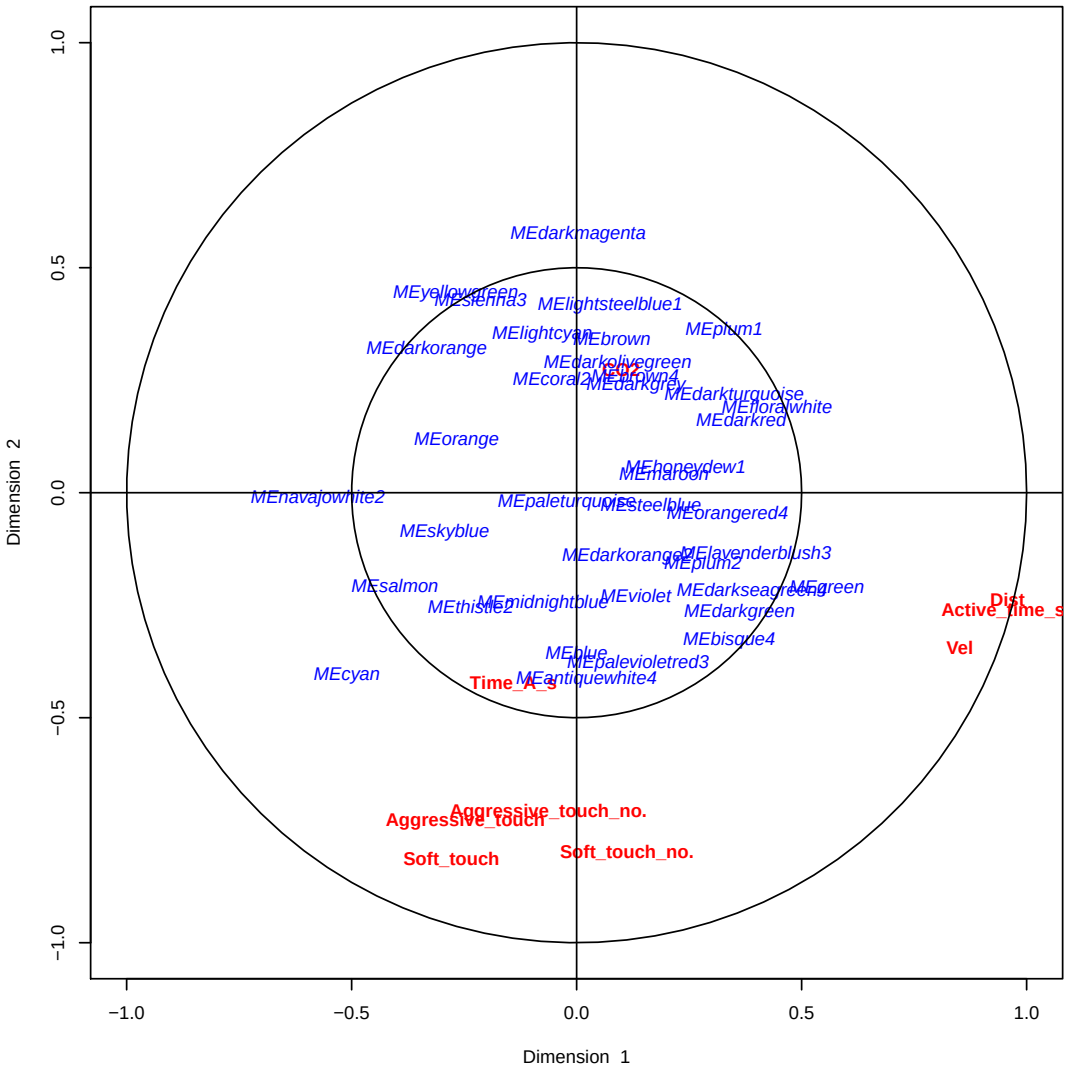

Figure D.13. Canonical correlation analysis biplot depicting where the module eigengenes (MEs) lie in space in relation to the traits for the eyes, for canonical functions (dimensions) 1 and 2. Variables from the MEs set and the traits set are in blue and red, respectively. The inner ring is set at a radius of 0.5. CO2 = CO_2 treatment, Active_time_s = time spent active (s), Dist = total distance moved (cm), Vel = average speed (cm/s), Time_A_s = time spent in Zone A (3 cm closes to mirror) (s), Soft_touch_no. = number of soft mirror touches, Soft_touch = whether any soft mirror touches occurred (yes/no), Aggressive_touch_no. = number of aggressive mirror touches = Aggressive_touch = whether any aggressive mirror touches occurred (yes/no), ME = module eigengene.

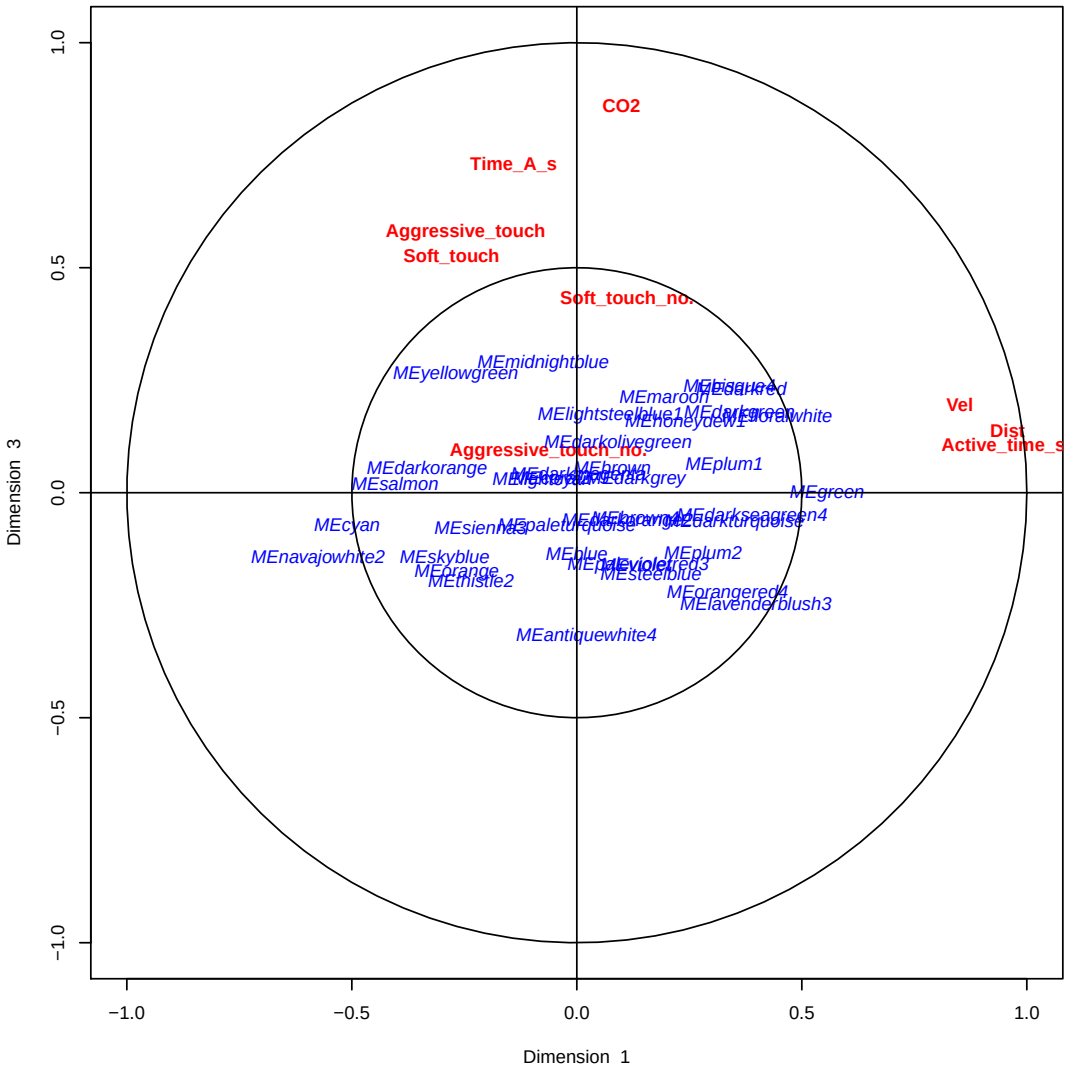

Figure D.14. Canonical correlation analysis biplot depicting where the module eigengenes (MEs) lie in space in relation to the traits for the eyes, for canonical functions (dimensions) 1 and 3. Variables from the MEs set and the traits set are in blue and red, respectively. The inner ring is set at a radius of 0.5. CO2 = CO_2 treatment, Active_time_s = time spent active (s), Dist = total distance moved (cm), Vel = average speed (cm/s), Time_A_s = time spent in Zone A (3 cm closes to mirror) (s), Soft_touch_no. = number of soft mirror touches, Soft_touch = whether any soft mirror touches occurred (yes/no), Aggressive_touch_no. = number of aggressive mirror touches = Aggressive_touch = whether any aggressive mirror touches occurred (yes/no), ME = module eigengene.

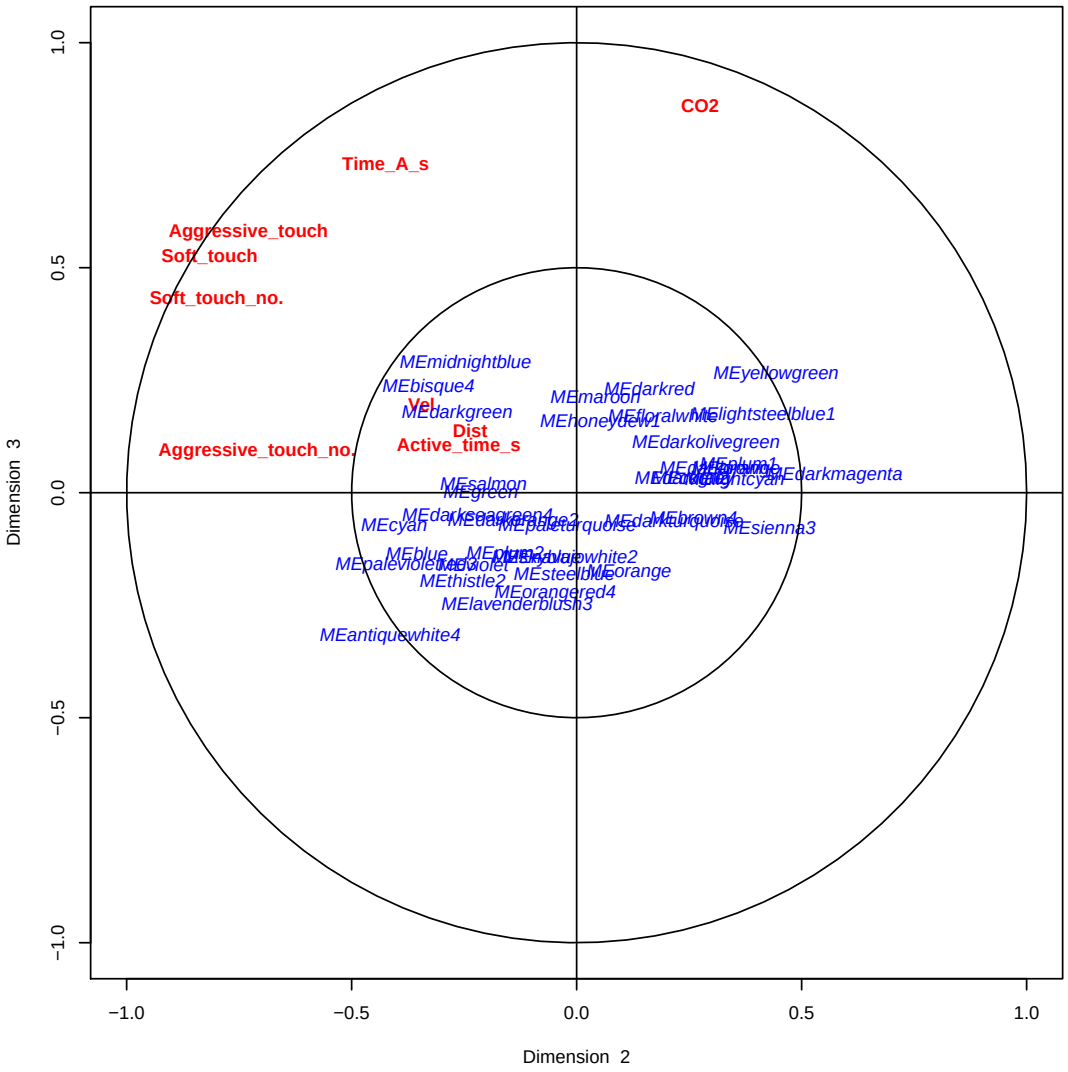

Figure D.15. Canonical correlation analysis biplot depicting where the module eigengenes (MEs) lie in space in relation to the traits for the eyes, for canonical functions (dimensions) 2 and 3. Variables from the MEs set and the traits set are in blue and red, respectively. The inner ring is set at a radius of 0.5. CO2 = CO_2 treatment, Active_time_s = time spent active (s), Dist = total distance moved (cm), Vel = average speed (cm/s), Time_A_s = time spent in Zone A (3 cm closes to mirror) (s), Soft_touch_no. = number of soft mirror touches, Soft_touch = whether any soft mirror touches occurred (yes/no), Aggressive_touch_no. = number of aggressive mirror touches = Aggressive_touch = whether any aggressive mirror touches occurred (yes/no), ME = module eigengene.

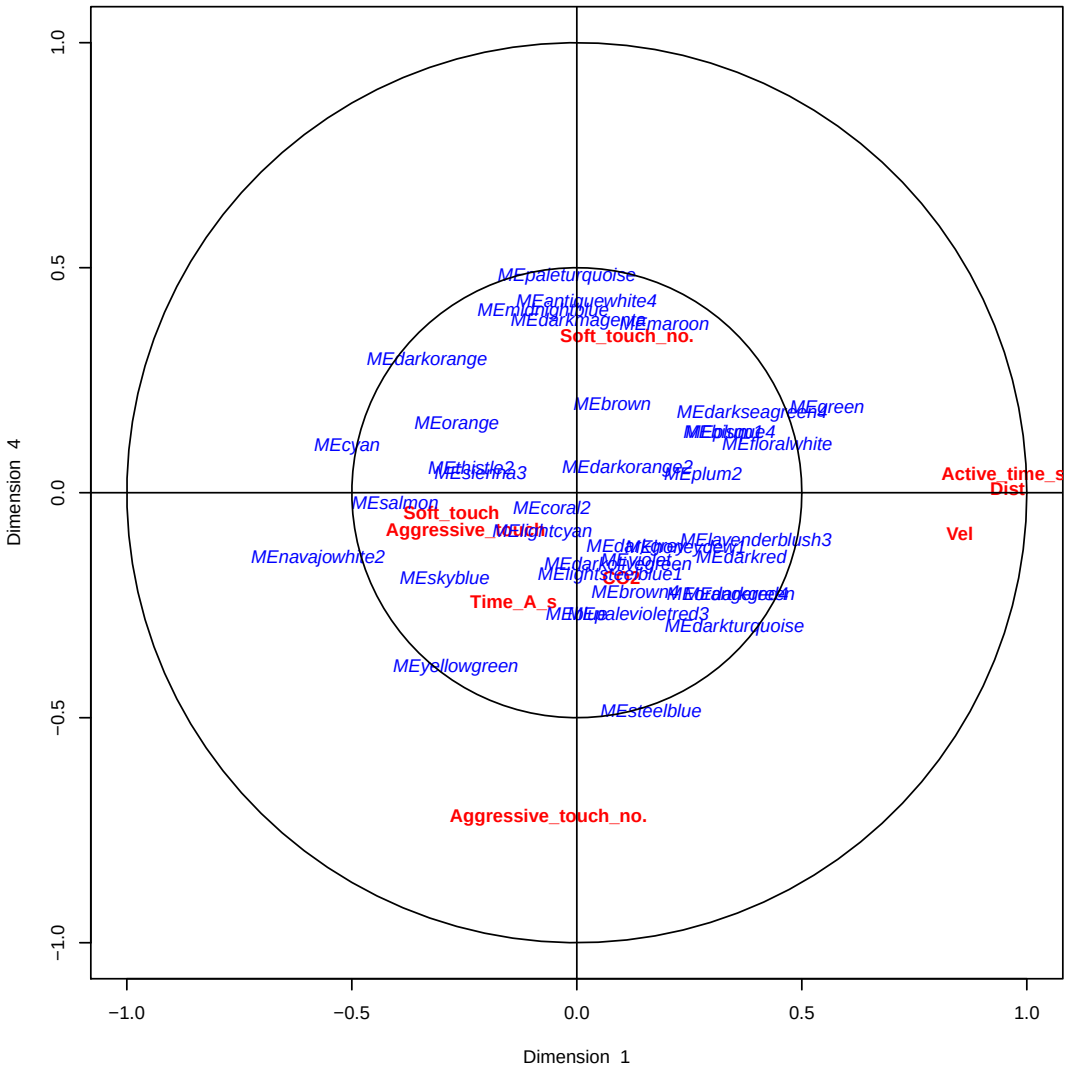

Figure D.16. Canonical correlation analysis biplot depicting where the module eigengenes (MEs) lie in space in relation to the traits for the eyes, for canonical functions (dimensions) 1 and 4. Variables from the MEs set and the traits set are in blue and red, respectively. The inner ring is set at a radius of 0.5. CO2 = CO_2 treatment, Active_time_s = time spent active (s), Dist = total distance moved (cm), Vel = average speed (cm/s), Time_A_s = time spent in Zone A (3 cm closes to mirror) (s), Soft_touch_no. = number of soft mirror touches, Soft_touch = whether any soft mirror touches occurred (yes/no), Aggressive_touch_no. = number of aggressive mirror touches = Aggressive_touch = whether any aggressive mirror touches occurred (yes/no), ME = module eigengene.

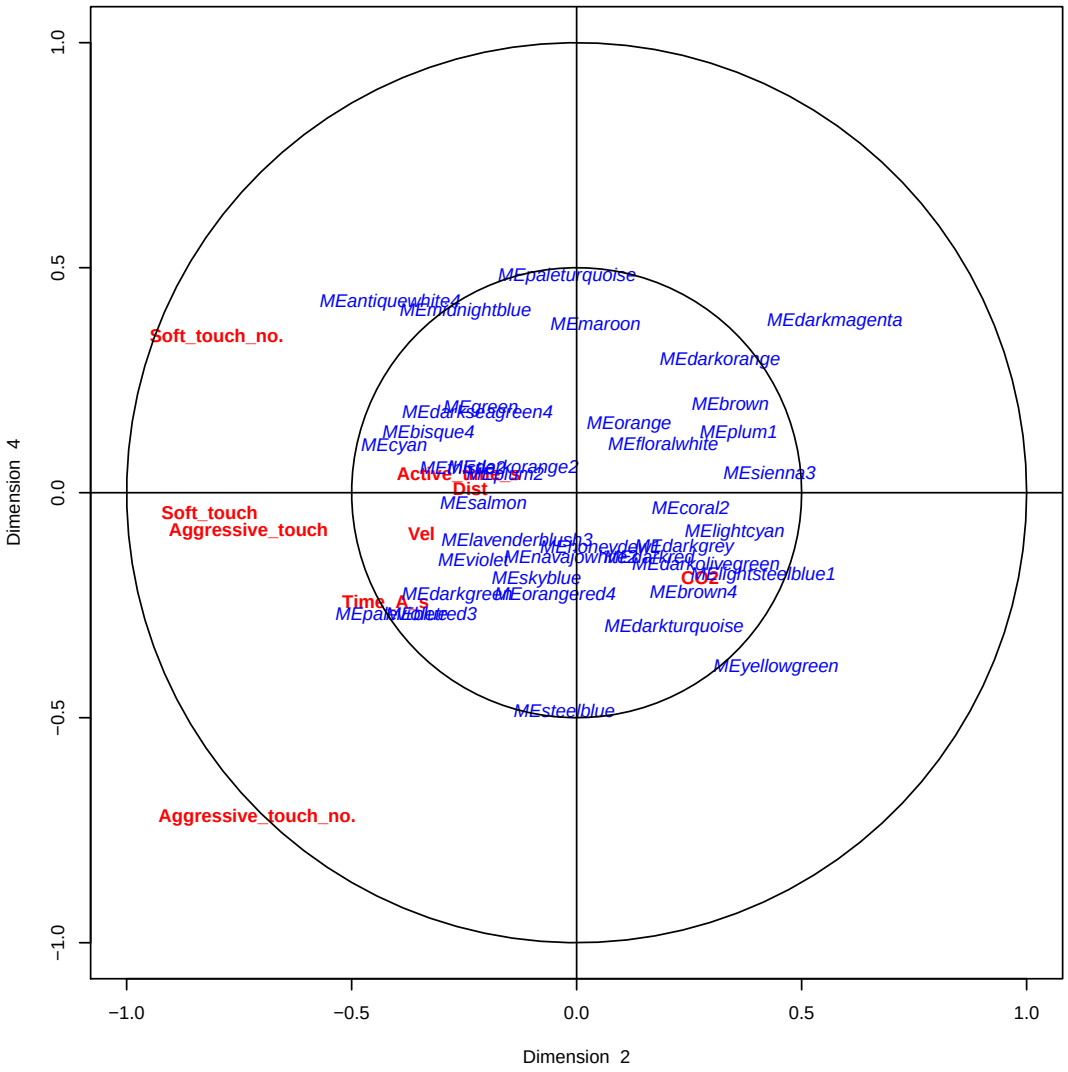

Figure D.17. Canonical correlation analysis biplot depicting where the module eigengenes (MEs) lie in space in relation to the traits for the eyes, for canonical functions (dimensions) 2 and 4. Variables from the MEs set and the traits set are in blue and red, respectively. The inner ring is set at a radius of 0.5. CO2 = CO_2 treatment, Active_time_s = time spent active (s), Dist = total distance moved (cm), Vel = average speed (cm/s), Time_A_s = time spent in Zone A (3 cm closes to mirror) (s), Soft_touch_no. = number of soft mirror touches, Soft_touch = whether any soft mirror touches occurred (yes/no), Aggressive_touch_no. = number of aggressive mirror touches = Aggressive_touch = whether any aggressive mirror touches occurred (yes/no), ME = module eigengene.

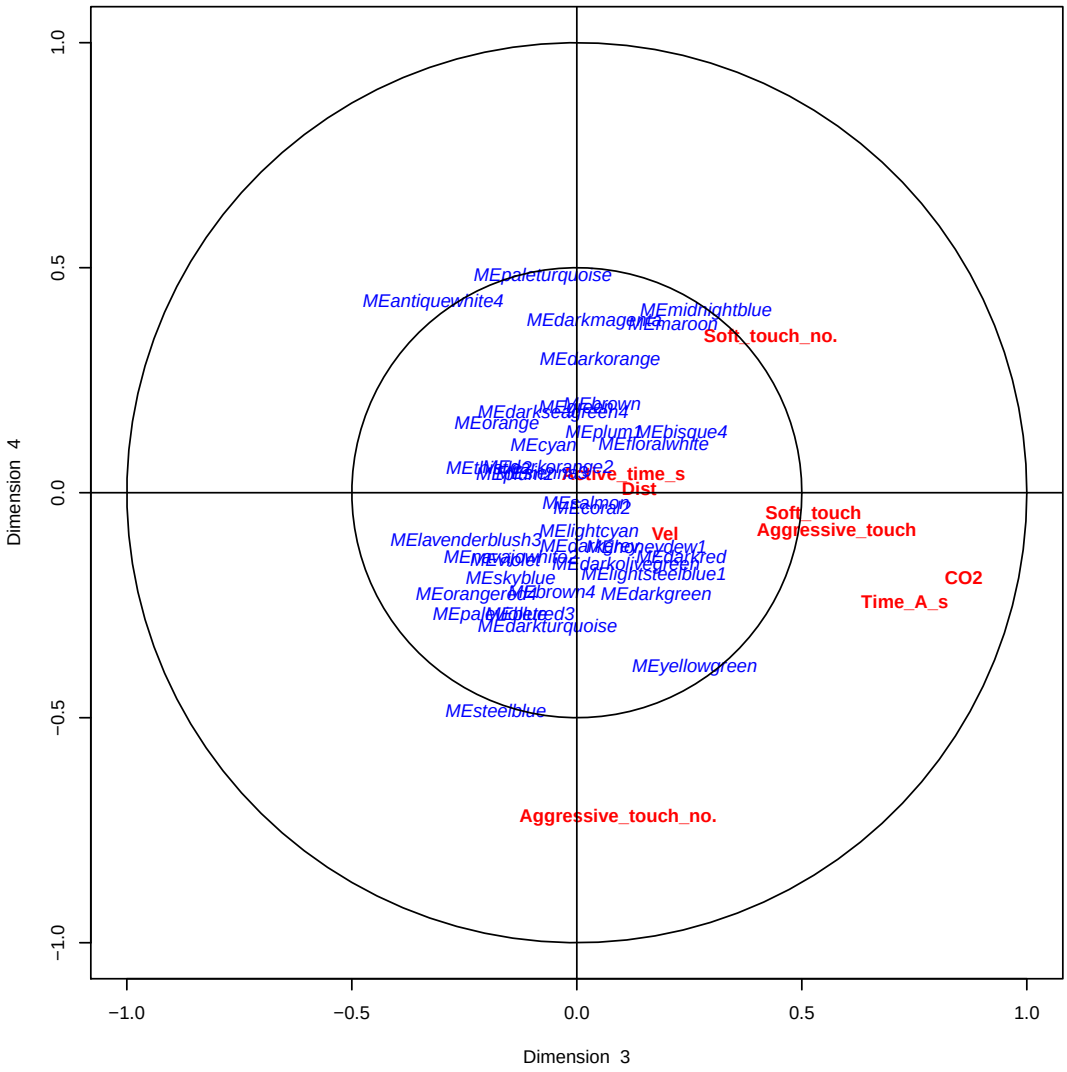

Figure D.18. Canonical correlation analysis biplot depicting where the module eigengenes (MEs) lie in space in relation to the traits for the eyes, for canonical functions (dimensions) 3 and 4. Variables from the MEs set and the traits set are in blue and red, respectively. The inner ring is set at a radius of 0.5. CO2 = CO_2 treatment, Active_time_s = time spent active (s), Dist = total distance moved (cm), Vel = average speed (cm/s), Time_A_s = time spent in Zone A (3 cm closes to mirror) (s), Soft_touch_no. = number of soft mirror touches, Soft_touch = whether any soft mirror touches occurred (yes/no), Aggressive_touch_no. = number of aggressive mirror touches = Aggressive_touch = whether any aggressive mirror touches occurred (yes/no), ME = module eigengene.

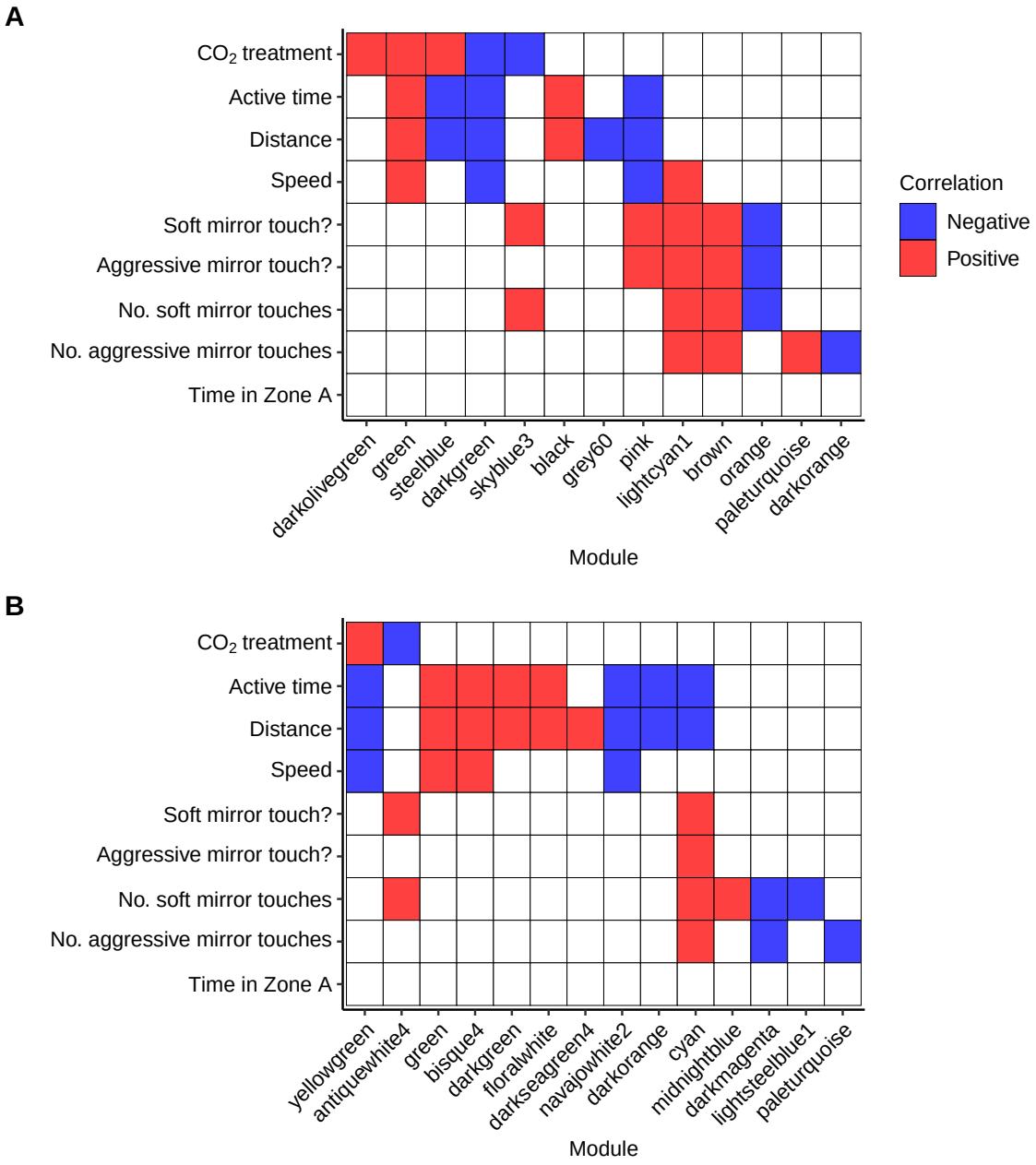

Figure D.19. Final modules of interest. In the **A** CNS and **B** eyes. Red = positive correlation between the trait and module eigengene, blue = negative correlation between the trait and module eigengene. Soft mirror touch? = whether any soft mirror touches occured (yes/no), aggressive mirror touch? = whether any aggressive mirror touches occurred (yes/no).

Table D.3. CNS-specific CO_2 treatment hub genes. For each of these CO_2 treatment hub genes, those genes also identified as a hub gene for one or more behavioural traits in the CNS are indicated in the columns on the right (active time, distance, speed, no. exploratory interactions, exploratory interaction?). The numbers in each column are the gene significance (GS) for the corresponding trait (-1 to 1). Positive GS = positive correlation between gene expression and trait (in red), negative GS = negative correlation between gene expression and trait (in blue). The larger the GS absolute value the more biologically relevant the gene is. Dist. = distance, No. EI = number of exploratory interactions, EI? = whether any exploratory interactions occurred (yes/no).

Gene	Annotation	Putative function	CO_2 treat-ment	Active time	Dist.	Speed	No. EI	EI?
rpl23a	60S ribosomal protein L23a	Component of the large 60S ribosomal subunit.	0.46	0.43	0.49	0.46		
rpl4	60S ribosomal protein L4	Component of the large 60S ribosomal subunit.	0.43	0.55	0.60	0.51		
anb32a	Acidic leucine-rich nuclear phosphoprotein 32 family member A	Multifunctional protein that is involved in the regulation of many processes including tumor suppression, apoptosis, cell cycle progression or transcription. Plays a role in the modulation of histone acetylation and transcription as part of the INHAT (inhibitor of histone acetyltransferases) complex. Plays an essential role in influenza A, B and C viral genome replication and in foamy virus mRNA export from the nucleus.	0.41	0.47	0.56	0.49		
apbb1	amyloid beta A4 precursor protein-binding family B member 1-interacting protein-like isoform X10	Transcription coregulator that can have both coactivator and corepressor functions. Plays a central role in the response to DNA damage by translocating to the nucleus and inducing apoptosis. Involved in hippocampal neurite branching and neuromuscular junction formation, as a result plays a role in spatial memory functioning.	0.47	0.65	0.72	0.64		

Table D.3 continued.

Gene	Annotation	Putative function	CO_2 treatment	Active time	Dist.	Speed	No. EI	EI?
purH	bifunctional purine biosynthesis protein PURH	Involved in step 1 of the subpathway that synthesizes 5-formamido-1-(5-phospho-D-ribosyl)imidazole-4-carboxamide from 5-amino-1-(5-phospho-D-ribosyl)imidazole-4-carboxamide (10-formyl THF route). This subpathway is part of the pathway IMP biosynthesis via de novo pathway, which is itself part of Purine metabolism.	0.41	0.58	0.63	0.64		
daf-36	cholesterol 7-desaturase-like	catalyses the production of 7-dehydrocholesterol (7-DHC or cholesta-5,7-dien-3beta-ol) by inserting a double bond (desaturating) at the C7-C8 single bond of cholesterol. This reaction is the first step in the synthesis of the steroid hormone Delta7-dafachronic acid.	0.45	0.53	0.61	0.55		
col1a1	collagen alpha-1(I) chain-like isoform X4/5	This gene encodes the pro-alpha1 chains of type I collagen whose triple helix comprises two alpha1 chains and one alpha2 chain. Type I is a fibril-forming collagen found in most connective tissues.	0.41	0.51	0.57	0.55		
ncaph	condensin complex subunit 2-like	Regulatory subunit of the condensin complex, a complex required for conversion of interphase chromatin into mitotic-like condense chromosomes. Early in neurogenesis, may play an essential role to ensure accurate mitotic chromosome condensation in neuron stem cells, ultimately affecting neuron pool and cortex size.	0.44	0.49	0.56	0.49		
psf2	DNA replication complex GINS protein PSF2-like	Functions as part of the GINS complex which plays an essential role in the initiation of DNA replication.	0.42	0.45	0.51	0.46		
cdt1	DNA replication factor Cdt1-like	Required for both DNA replication and mitosis.	0.40	0.63	0.69	0.63		
mcm5	DNA replication licensing factor mcm5-like	Acts as component of the MCM2-7 complex (MCM complex) which is the putative replicative helicase essential for ‘once per cell cycle’ DNA replication initiation and elongation in eukaryotic cells.	0.41	0.56	0.64	0.57		

Table D.3 continued.

Gene	Annotation	Putative function	CO_2 treatment	Active time	Dist.	Speed	No. EI	EI?
polr1a	DNA-directed RNA polymerase I subunit RPA1-like	DNA-dependent RNA polymerase catalyses the transcription of DNA into RNA. Largest and catalytic core component of RNA polymerase I which synthesizes ribosomal RNA precursors.	0.46	0.50	0.57	0.50		
stt3a	dolichyl-diphosphooligosaccharide–protein glycosyltransferase subunit STT3A	A catalytic subunit of the N-oligosaccharyltransferase (OST) complex, which functions in the endoplasmic reticulum to transfer glycan chains to asparagine residues of target proteins, the first step in protein N-glycosylation.	0.44	0.52	0.59	0.47		
donson	DONS protein/protein downstream neighbor of son homolog	After the induction of replication stress, required for the stabilization of stalled replication forks, the efficient activation of the intra-S-phase and G/2M cell-cycle checkpoints and the maintenance of genome stability.	0.51	0.46	0.51	0.43		
ttk	dual specificity protein kinase Ttk-like	Phosphorylates proteins on serine, threonine, and tyrosine. Probably associated with cell proliferation. Phosphorylates MAD1L1 to promote mitotic checkpoint signaling. Essential for chromosome alignment, and for the mitotic checkpoint.	0.43	0.65	0.71	0.63		
ttk	dual specificity protein kinase TTK-like	Phosphorylates proteins on serine, threonine, and tyrosine. Probably associated with cell proliferation. Phosphorylates MAD1L1 to promote mitotic checkpoint signaling. Essential for chromosome alignment, and for the mitotic checkpoint	0.42	0.52	0.59	0.41		
ranbp2	E3 SUMO-protein ligase RanBP2-like isoform X1	Component of the nuclear export pathway. Recruits BICD2 to the nuclear envelope and cytoplasmic stacks of nuclear pore complex during G2 phase of cell cycle. Small Ubiquitin-like Modifier (or SUMO) proteins are a family of small proteins that are covalently attached to and detached from other proteins in cells to modify their function. SUMOylation is a post-translational modification involved in various cellular processes.	0.41	0.62	0.69	0.61		

Table D.3 continued.

Gene	Annotation	Putative function	CO_2 treatment	Active time	Dist.	Speed	No. EI	EI?
entpd8	ectonucleoside triphosphate diphosphohydrolase 8 isoform X4	Ectonucleoside NTPDases catalyse the hydrolysis of gamma- and beta-phosphate residues of nucleotides, playing a central role in concentration of extracellular nucleotides. Has activity toward ATP, ADP, UTP and UDP, but not toward AMP.	0.41	0.41	0.48	0.49		
ef-1αO	elongation factor 1-alpha (1) (oocyte form-like)	Promotes the GTP-dependent binding of aminoacyl-tRNA to the A-site of ribosomes during protein biosynthesis.	0.42	0.54	0.59	0.48		
eef1g	elongation factor 1-gamma-like	Subunit of the elongation factor-1 complex, which is responsible for the enzymatic delivery of aminoacyl tRNAs to the ribosome.	0.46	0.52	0.58	0.47		
hspa5	endoplasmic reticulum chaperone BiP/78 kDa glucose-regulated protein	Endoplasmic reticulum chaperone that plays a key role in protein folding and quality control in the endoplasmic reticulum lumen. Acts as a key repressor of the ERN1/IRE1-mediated unfolded protein response. Acts as a receptor for various viruses.	0.40	0.59	0.65	0.55		
elk3	ETS domain-containing protein Elk-3-like isoform X1	May be a negative regulator of transcription, but can activate transcription when coexpressed with Ras, Src or Mos.	0.55	0.43	0.51	0.50		
eif3b	eukaryotic translation initiation factor 3 subunit B-like	RNA-binding component of the eukaryotic translation initiation factor 3 (eIF-3) complex, which is required for several steps in the initiation of protein synthesis. The eIF-3 complex specifically targets and initiates translation of a subset of mRNAs involved in cell proliferation, including cell cycling, differentiation and apoptosis.	0.47	0.47	0.55	0.41		

Table D.3 continued.

Gene	Annotation	Putative function	CO_2 treat-ment	Active time	Dist.	Speed	No. EI	EI?
spt16	FACT complex subunit SPT16-like	Component of the FACT complex, a general chromatin factor that acts to reorganise nucleosomes. The FACT complex is involved in multiple processes that require DNA as a template such as mRNA elongation, DNA replication and DNA repair. During transcription elongation the FACT complex acts as a histone chaperone that both destabilizes and restores nucleosomal structure.	0.41	0.46	0.53	0.47		
foxm1	Forkhead box protein M1	Transcriptional factor regulating the expression of cell cycle genes essential for DNA replication and mitosis. Plays a role in the control of cell proliferation. Plays also a role in DNA breaks repair participating in the DNA damage checkpoint response.	0.51	0.40	0.49	0.45		
foxm1	Forkhead box protein M1	Transcriptional factor regulating the expression of cell cycle genes essential for DNA replication and mitosis. Plays a role in the control of cell proliferation. Plays also a role in DNA breaks repair participating in the DNA damage checkpoint response.	0.44	0.46	0.52	0.45		
ccnb3	G2/mitotic-specific cyclin-B3-like	Cyclins are positive regulatory subunits of the cyclin-dependent kinases (CDKs), and thereby play an essential role in the control of the cell cycle, notably via their destruction during cell division.	0.40	0.48	0.56	0.52		
ashh1 / 2 / 3 / 4 / mes-4 / setd2	Histone-lysine N-methyltransferase ASHH1/2/3/4/Mes-4/SETD2	Histone-modifying enzymes that catalyse the transfer of one, two, or three methyl groups to lysine of histone proteins.	0.58	0.62	0.68	0.64		
incenp	inner centromere protein A isoform X1	Component of the chromosomal passenger complex (CPC), a complex that acts as a key regulator of mitosis. The CPC complex has essential functions at the centromere in ensuring correct chromosome alignment and segregation and is required for chromatin-induced microtubule stabilization and spindle assembly.	0.41	0.54	0.60	0.55		

Table D.3 continued.

Gene	Annotation	Putative function	CO_2 treat-ment	Active time	Dist.	Speed	No. EI	EI?
itga9	integrin alpha-9	Integrin alpha-9/beta-1 (ITGA9:ITGB1) is a receptor for VCAM1, cytotactin and osteopontin.[Vcam = cell-cell recognition, role in immune response. Cytotactin = mediates glia-neuron adhesion *in vitro* and may mediate cell migration. Osteopontin = extracellular structural protein]	0.42	0.46	0.53	0.50		
klf10	Krueppel-like factor 10 isoform X2	Plays a role in the regulation of the circadian clock. Regulates the circadian expression of genes involved in lipogenesis, gluconeogenesis, and glycolysis in the liver. Represses the expression of PCK2, a rate-limiting step enzyme of gluconeogenesis. May play a role in the cell cycle regulation.	0.47	0.69	0.72	0.51		
melk	maternal embryonic leucine zipper kinase-like isoform X1	Serine/threonine-protein kinase involved in various processes such as cell cycle regulation, self-renewal of stem cells, apoptosis and splicing regulation. Acts as a regulator of cell cycle, notably by mediating phosphorylation of CDC25B, promoting localisation of CDC25B to the centrosome and the spindle poles during mitosis. Plays a key role in cell proliferation. Required for proliferation of embryonic and postnatal multipotent neural progenitors.	0.42	0.50	0.58	0.49		
mtbp	mdm2-binding protein-like	Inhibits cell migration *in vitro* and suppresses the invasive behavior of tumor cells. Inhibits autoubiquitination of MDM2, thereby enhancing MDM2 stability. This promotes MDM2-mediated ubiquitination of p53/TP53 and its subsequent degradation.	0.44	0.54	0.59	0.52		
slc25a32	mitochondrial folate transporter/carrier	Transports folate across the inner membranes of mitochondria. Can also transport FAD across the mitochondrial inner membrane.	0.54	0.56	0.62	0.54		

Table D.3 continued.

Gene	Annotation	Putative function	CO_2 treat-ment	Active time	Dist.	Speed	No. EI	EI?
bub1	mitotic checkpoint serine/threonine-protein kinase BUB1-like isoform X1	Serine/threonine-protein kinase that performs 2 crucial functions during mitosis: it is essential for spindle-assembly checkpoint signaling and for correct chromosome alignment.	0.48	0.54	0.61	0.54		
abhd12	monoacylglycerol lipase ABHD12-like	Lysophosphatidylserine (LPS) lipase that mediates the hydrolysis of lysophosphatidylserine, a class of signaling lipids that regulates immunological and neurological processes. Represents a major lysophosphatidylserine lipase in the brain, thereby playing a key role in the central nervous system.This gene encodes an enzyme that catalyses the hydrolysis of 2-arachidonoyl glycerol (2-AG), the main endocannabinoid lipid transmitter that acts on cannabinoid receptors, CB1 and CB2. The endocannabinoid system is involved in a wide range of physiological processes, including neurotransmission, mood, appetite, pain appreciation, addiction behavior, and inflammation.	0.42	0.53	0.57	0.52		
myph	myophilin	Identified in muscles of parasitic worms.	0.45	0.45	0.53	0.51		
myph	myophilin-like	Identified in muscles of parasitic worms.	0.45	0.52	0.60	0.60		
zip	myosin heavy chain, non-muscle isoform X1/3/4/5	Non-muscle myosin appears to be responsible for cellularisation. Required for morphogenesis and	0.43	0.55	0.63	0.56		
myh9/10	non-muscle myosin II heavy chain	cytokinesis. Cellular myosin that appears to play a role in cytokinesis, cell shape, and specialized functions such as secretion and capping. During cell spreading, plays an important role in cytoskeleton reorganisation, focal contacts formation (in the central part but not the margins of spreading cells), and lamellipodial extension.						
zip	myosin heavy chain, non-muscle isoform X1/4	Non-muscle myosin appears to be responsible for cellularisation. Required for morphogenesis and cytokinesis.	0.41	0.49	0.57	0.50		

Table D.3 continued.

Gene	Annotation	Putative function	CO_2 treatment	Active time	Dist.	Speed	No. EI	EI?
zip	myosin heavy chain, embryonic smooth muscle isoform-like myosin heavy chain, non-muscle-like isoform X2/3	Non-muscle myosin appears to be responsible for cellularisation. Required for morphogenesis and cytokinesis.	0.44	0.58	0.65	0.57		
naca	nascent polypeptide-associated complex subunit alpha, muscle-specific form	Cardiac- and muscle-specific transcription factor. May act to regulate the expression of genes involved in the development of myotubes. Plays a critical role in ventricular cardiomyocyte expansion and regulates postnatal skeletal muscle growth and regeneration. Involved in the organised assembly of thick and thin filaments of myofibril sarcomeres.	0.45	0.53	0.61	0.53		
nup155	nuclear pore complex protein Nup155	Essential component of nuclear pore complex. Nucleoporins may be involved both in binding and translocating proteins during nucleocytoplasmic transport. [Nuclear pore = regulates the transportation of molecules between the nucleus and the cytoplasm].	0.46	0.64	0.70	0.66		
nup205	nuclear pore complex protein Nup205	Plays a role in the nuclear pore complex assembly and/or maintenance.	0.43	0.41	0.50	0.45		
nop58	nucleolar protein 58	Required for 60S ribosomal subunit biogenesis.	0.48	0.57	0.64	0.59		
phf24	PHD finger protein 24-like	Codes for GINIP, a key modulator of peripherally evoked GABAB-receptors signaling.	0.41	0.59	0.66	0.62		
piwil1	piwi-like protein 1	Endoribonuclease that plays a central role in postnatal germ cells by repressing transposable elements and preventing their mobilisation, which is essential for the germline integrity. Directly binds methylated piRNAs. Acts as an endoribonuclease that cleaves transposon messenger RNAs. piRNAs are probably involved in other processes during meiosis such as translation regulation.	0.45	0.51	0.60	0.50		

Table D.3 continued.

Gene	Annotation	Putative function	CO_2 treat-ment	Active time	Dist.	Speed	No. EI	EI?
ddx4	probable ATP-dependent RNA helicase DDX4 isoform X2	ATP-dependent RNA helicase required during spermatogenesis . Required to repress transposable elements and preventing their mobilisation, which is essential for the germline integrity. Acts via the piRNA metabolic process, which mediates the repression of transposable elements during meiosis by forming complexes composed of piRNAs and Piwi proteins and governs the methylation and subsequent repression of transposons.	0.41	0.58	0.65	0.61		
dbf4	protein DBF4 homolog A-like	Regulatory subunit for CDC7 which activates its kinase activity thereby playing a central role in DNA replication and cell proliferation. Required for progression of S phase. Involved in regulating the initiation of DNA replication during cell cycle.	0.41	0.51	0.57	0.43		
pdia3	protein disulphide-isomerase A3-like	Catalyses the rearrangement of -S-S- bonds in proteins.Protein of the endoplasmic reticulum that interacts with lectin chaperones calreticulin and calnexin to modulate folding of newly synthesized glycoproteins. This protein also functions as a molecular chaperone that prevents the formation of protein aggregates.	0.43	0.55	0.59	0.41		
pdia4	protein disulphide-isomerase A4	Member of the disulphide isomerase (PDI) family of endoplasmic reticulum (ER) proteins that catalyse protein folding and thiol-disulphide interchange reactions. This protein, when bound to cyclophilin B, enhances the rate of immunoglobulin G intermolecular disulphide bonding and antibody assembly.	0.41	0.50	0.56	0.49		
pdia5	protein disulphide-isomerase A5-like	Member of the disulphide isomerase (PDI) family of endoplasmic reticulum (ER) proteins that catalyse protein folding and thiol-disulphide interchange reactions.	0.50	0.55	0.62	0.50		

Table D.3 continued.

Gene	Annotation	Putative function	CO_2 treatment	Active time	Dist.	Speed	No. EI	EI?
dnaaf2	protein kintoun-like	Required for cytoplasmic pre-assembly of axonemal dyneins, thereby playing a central role in motility in cilia and flagella.	0.43	0.55	0.63	0.57		
rac1	ras-related C3 botulinum toxin substrate 1	Plasma membrane-associated small GTPase which cycles between active GTP-bound and inactive GDP-bound states. In its active state, binds to a variety of effector proteins to regulate cellular responses such as secretory processes, phagocytosis of apoptotic cells, epithelial cell polarization, neurons adhesion, migration and differentiation, and growth-factor induced formation of membrane ruffles. In neurons, is involved in dendritic spine formation and synaptic plasticity. In hippocampal neurons, involved in spine morphogenesis and synapse formation. In synapses, seems to mediate the regulation of F-actin cluster formation performed by SHANK3. Plays a crucial role in regulating GABA(A) receptor synaptic stability and hence GABAergic inhibitory synaptic transmission.	0.42	0.55	0.62	0.55		
ptprc	receptor-type tyrosine-protein phosphatase C isoform X1	Protein tyrosine-protein phosphatase required for T-cell activation through the antigen receptor.	0.41	0.53	0.59	0.46		
ptprc	receptor-type tyrosine-protein phosphatase C isoform X1	Protein tyrosine-protein phosphatase required for T-cell activation through the antigen receptor.	0.47	0.56	0.62	0.53		
ptpr	Receptor-type tyrosine-protein phosphatase mu/F/H/S/eta/gamma/O/delta	RPTPs are a family of integral cell surface proteins that possess intracellular PTP activity, and extracellular domains that have sequence homology to cell adhesion molecules. Protein tyrosine phosphorylation is a major mechanism regulating cellular signaling that affects fundamental cellular events including metabolism, proliferation, adhesion, differentiation, migration and development.	0.42	0.55	0.61	0.57		
rtkn	rhotekin-like isoform X2	Mediates Rho signaling to activate NF-kappa-B.	0.40	0.47	0.56	0.54		

Table D.3 continued.

Gene	Annotation	Putative function	CO_2 treat-ment	Active time	Dist.	Speed	No. EI	EI?
nat10	RNA cytidine acetyltransferase	RNA cytidine acetyltransferase that catalyses the formation of N4-acetylcytidine (ac4C) modification on mRNAs, 18S rRNA and tRNAs, enhancing mRNA stability and translation. In addition to RNA acetyltransferase activity, also able to acetylate lysine residues of proteins, such as histones, microtubules, p53/TP53 and MDM2, *in vitro*. The relevance of the protein lysine acetyltransferase activity is however unsure *in vivo*. Involved in the regulation of centrosome duplication by acetylating CENATAC during mitosis, promoting SASS6 proteasome degradation.	0.43	0.47	0.55	0.53		
shmt1	serine hydroxymethyltransferase, cytosolic-like	Interconversion of serine and glycine.	0.41	0.55	0.60	0.55		
srrt	serrate RNA effector molecule homolog isoform X1	Acts as a mediator between the cap-binding complex (CBC) and the primary microRNAs (miRNAs) processing machinery during cell proliferation. Involved in cell cycle progression at S phase. Plays a role in RNA-mediated gene silencing (RNAi) by miRNAs. Independently of its activity on miRNAs, necessary and sufficient to promote neural stem cell self-renewal.	0.52	0.45	0.52	0.47		
snd1	staphylococcal nuclease domain-containing protein 1-like	Endonuclease that mediates miRNA decay of both protein-free and AGO2-loaded miRNAs. As part of its function in miRNA decay, regulates mRNAs involved in G1-to-S phase transition.	0.42	0.54	0.62	0.52		
smc4	structural maintenance of chromosomes protein 4-like	Central component of the condensin complex, a complex required for conversion of interphase chromatin into mitotic-like condense chromosomes.	0.59	0.41	0.50	0.52		
smc4	structural maintenance of chromosomes protein 4-like	Central component of the condensin complex, a complex required for conversion of interphase chromatin into mitotic-like condense chromosomes.	0.48	0.44	0.51	0.43		

Table D.3 continued.

Gene	Annotation	Putative function	CO_2 treat-ment	Active time	Dist.	Speed	No. EI	EI?
tbc1d1 / tbc1d4	TBC1 domain family member 1 isoform X1 / TBC1 domain family member 4-like	May act as a GTPase-activating protein for Rab family protein(s). May play a role in the cell cycle and differentiation of various tissues. Involved in the trafficking and translocation of GLUT4-containing vesicles and insulin-stimulated glucose uptake into cells.	0.55	0.54	0.61	0.54		
tbc1d1 / tbc1d4	TBC1 domain family member 1 isoform X1 / TBC1 domain family member 4-like	May act as a GTPase-activating protein for Rab family protein(s). May play a role in the cell cycle and differentiation of various tissues. Involved in the trafficking and translocation of GLUT4-containing vesicles and insulin-stimulated glucose uptake into cells.	0.49	0.45	0.52	0.44		
tbc1d10a	TBC1 domain family member 10A-like	Acts as GTPase-activating protein for RAB27A, but not for RAB2A, RAB3A, nor RAB4A.	0.43	0.57	0.64	0.68		
tbc1d22b	TBC1 domain family member 22B-like isoform X2	May act as a GTPase-activating protein for Rab family protein(s).	0.46	0.49	0.57	0.49		
tk1	Thymidine kinase, cytosolic	Two forms have been identified in animal cells, one in cytosol and one in mitochondria. Activity of the cytosolic enzyme is high in proliferating cells and peaks during the S-phase of the cell cycle; it is very low in resting cells.	0.41	0.44	0.51	0.49		
tfap4	transcription factor AP-4-like	Transcription factor that activates both viral and cellular genes by binding to the symmetrical DNA sequence 5'-CAGCTG-3'.	0.41	0.42	0.50	0.42		

Table D.3 continued.

Gene	Annotation	Putative function	CO_2 treat-ment	Active time	Dist.	Speed	No. EI	EI?
tgfb1i1	transforming growth factor beta-1-induced transcript 1 protein isoform X5	Functions as a molecular adapter coordinating multiple protein-protein interactions at the focal adhesion complex and in the nucleus. Links various intracellular signaling modules to plasma membrane receptors and regulates the Wnt and TGFB signaling pathways. In the nucleus, functions as a nuclear receptor coactivator regulating glucocorticoid, androgen, mineralocorticoid and progesterone receptor transcriptional activity. May play a role in the processes of cell growth, proliferation, migration, differentiation and senescence.	0.41	0.53	0.60	0.50		
ssr1	translocon-associated protein subunit alpha-like	TRAP proteins are part of a complex whose function is to bind calcium to the ER membrane and thereby regulate the retention of ER resident proteins. May function as a membrane-bound chaperone facilitating folding of translocated proteins.	0.47	0.49	0.55	0.43		
tm6sf1	transmembrane 6 superfamily member 1-like	May function as sterol isomerase.	0.54	0.49	0.56	0.53		
tmem214-b	transmembrane protein 214-B-like	Critical mediator, in cooperation with CASP4, of endoplasmic reticulum-stress induced apoptosis. Required for the activation of CASP4 following endoplasmic reticulum stress.	0.43	0.49	0.56	0.46		
pus3	tRNA pseudouridine(38/39) synthase-like	Formation of pseudouridine at position 39 in the anticodon stem and loop of transfer RNAs.	0.45	0.50	0.57	0.51		
snrpa	U1 small nuclear ribonucleoprotein A	Component of the spliceosomal U1 snRNP, which is essential for recognition of the pre-mRNA 5' splice-site and the subsequent assembly of the spliceosome.	0.47	0.56	0.61	0.54		

Table D.3 continued.

Gene	Annotation	Putative function	CO_2 treatment	Active time	Dist.	Speed	No. EI	EI?
vcl	vinculin isoform X11	Actin filament (F-actin)-binding protein involved in cell-matrix adhesion and cell-cell adhesion. Regulates cell-surface E-cadherin expression and potentiates mechanosensing by the E-cadherin complex. May also play important roles in cell morphology and locomotion.	0.46	0.66	0.72	0.58		
rpl7l	60S ribosomal protein L7-like	Component of the large 60S ribosomal subunit.	0.45	0.41	0.47			
ap15	apoptosis inhibitor 5-like	Antiapoptotic factor that may have a role in protein assembly. Negatively regulates ACIN1. By binding to ACIN1, it suppresses ACIN1 cleavage from CASP3 and ACIN1-mediated DNA fragmentation. Also known to efficiently suppress E2F1-induced apoptosis.	0.40	0.43	0.50			
adgrb3	brain-specific angiogenesis inhibitor 3	This p53-target gene encodes a brain-specific angiogenesis inhibitor [inhibits formation of new blood vessels]. Receptor that plays a role in the regulation of synaptogenesis and dendritic spine formation at least partly via interaction with ELMO1 and RAC1 activity.	0.45	0.41	0.48			
cstf1	cleavage stimulation factor subunit 1-like	One of the multiple factors required for polyadenylation and 3'-end cleavage of mammalian pre-mRNAs. May be responsible for the interaction of CSTF with other factors to form a stable complex on the pre-mRNA.	0.42	0.47	0.51			
rpn1	dolichyl-diphosphooligosaccharide–protein glycosyltransferase subunit 1	Forms part of the regulatory subunit of the 26S proteasome and may mediate binding of ubiquitin-like domains to this proteasome. Subunit of the oligosaccharyl transferase (OST) complex that catalyses the first step in protein N-glycosylation. N-glycosylation occurs cotranslationally and the complex associates with the Sec61 complex at the channel-forming translocon complex that mediates protein translocation across the endoplasmic reticulum (ER).	0.44	0.46	0.52			

Table D.3 continued.

Gene	Annotation	Putative function	CO_2 treat-ment	Active time	Dist.	Speed	No. EI	EI?
rpn2	dolichyl-diphosphooligosaccharide–protein glycosyltransferase subunit 2	Subunit of the oligosaccharyl transferase (OST) complex that catalyses the first step in protein N-glycosylation. N-glycosylation occurs cotranslationally and the complex associates with the Sec61 complex at the channel-forming translocon complex that mediates protein translocation across the endoplasmic reticulum (ER).	0.43	0.43	0.49			
eif3d	eukaryotic translation initiation factor 3 subunit D	mRNA cap-binding component of the eukaryotic translation initiation factor 3 (eIF-3) complex, a complex required for several steps in the initiation of protein synthesis of a specialized repertoire of mRNAs.	0.43	0.46	0.51			
itga4	integrin alpha-4	Integrins are heterodimeric integral membrane glycoproteins composed of an alpha chain and a beta chain that mediate cell-cell and cell-matrix adhesion. Receptor for fibronectin [is involved in cell adhesion, growth, migration, and differentiation, wound healing], VCAM1 [cell-cell recognition in immune responses], MADCAM1 [cell adhesion molecule - direct leukocytes into mucosal and inflamed tissues]. It may also participate in cytolytic T-cell interactions with target cells.	0.41	0.42	0.47			
mest	mesoderm-specific transcript homolog protein	Member of the alpha/beta hydrolase superfamily. May play a role in development.	0.42	0.42	0.47			
ganab	neutral alpha-glucosidase AB-like isoform X1alpha 1,3-glucosidase	Alpha subunit of glucosidase II and a member of the glycosyl hydrolase 31 family of proteins. Glucosidase II enzyme plays a role in protein folding and quality control by cleaving glucose residues from immature glycoproteins in the endoplasmic reticulum.	0.42	0.41	0.47			
nup160	nuclear pore complex protein Nup160-like	Functions as a component of the nuclear pore complex (NPC). Involved in poly(A)+ RNA transport.	0.48	0.44	0.51			

Table D.3 continued.

Gene	Annotation	Putative function	CO_2 treat-ment	Active time	Dist.	Speed	No. EI	EI?
bptf	nucleosome-remodeling factor subunit BPTF/NURF301-like isoform X1	Regulatory subunit of the ATP-dependent NURF-1 and NURF-5 ISWI chromatin remodeling complexes, which form ordered nucleosome arrays on chromatin and facilitate access to DNA during DNA-templated processes such as DNA replication, transcription, and repair. Within the NURF-1 ISWI chromatin-remodeling complex, binds to the promoters of En1 and En2 to positively regulate their expression and promote brain development. Histone-binding protein which binds to H3 tails trimethylated on 'Lys-4' (H3K4me3), which mark transcription start sites of active genes. May also regulate transcription through direct binding to DNA or transcription factors.	0.45	0.45	0.53			
ppib	peptidyl-prolyl cis-trans isomerase B	PPIase that catalyses the cis-trans isomerization of proline imidic peptide bonds in oligopeptides and may therefore assist protein folding.	0.41	0.40	0.46			
pa2g4	proliferation-associated protein 2G4-like	Seems be involved in growth regulation. Acts as a corepressor of the androgen receptor. Associates with 28S, 18S and 5.8S mature rRNAs, several rRNA precursors and probably U3 small nucleolar RNA. May be involved in regulation of intermediate and late steps of rRNA processing. May be involved in ribosome assembly. Mediates cap-independent translation of specific viral IRESs (internal ribosomal entry site). Regulates cell proliferation, differentiation, and survival.	0.43	0.46	0.53			

Table D.3 continued.

Gene	Annotation	Putative function	CO_2 treatment	Active time	Dist.	Speed	No. EI	EI?
ecd	protein ecdysoneless homolog	Regulator of p53/TP53 stability and function. Inhibits MDM2-mediated degradation of p53/TP53 possibly by cooperating in part with TXNIP. May be involved in transcriptional regulation. May be a transcriptional activator required for the expression of glycolytic genes. Involved in regulation of cell cycle progression. May play a role in regulation of pre-mRNA splicing.	0.45	0.47	0.53			
slc4a11	sodium bicarbonate transporter-like protein 11/plasminogen activator inhibitor 1 RNA-binding protein isoform X2	Multifunctional transporter with an impact in cell morphology and differentiation. At early stages of stem cell differentiation, participates in synergy with ITGA5-ITGB1 and ITGAV-ITGB3 integrins and BMPR1A to promote cell adhesion and contractility. Regulates the oxidative stress response in corneal endothelium by enhancing antioxidant defenses and protecting cells from reactive oxygen species.	0.43	0.46	0.53			
tf	transferrin-like protein	Transferrins bind to and mediate transport of iron in the blood. Part of the iron withholding strategy of the innate immune response in molluscs.	0.47	0.47	0.53			
tmed2	transmembrane emp24 domain-containing protein 2-like	Involved in vesicular protein trafficking. Involved in trafficking of G protein-coupled receptors (GPCRs). Regulates F2RL1, OPRM1 and P2RY4 exocytic trafficking from the Golgi to the plasma membrane thus contributing to receptor resensitization. Facilitates CASR maturation and stabilization in the early secretory pathway and increases CASR plasma membrane targeting. Proposed to be involved in organisation of intracellular membranes such as the maintenance of the Golgi apparatus. May also play a role in the biosynthesis of secreted cargo such as eventual processing.	0.46	0.45	0.50			

Table D.3 continued.

Gene	Annotation	Putative function	CO_2 treat-ment	Active time	Dist.	Speed	No. EI	EI?
arpc5	actin-related protein 2/3 complex subunit 5-like	Component of the Arp2/3 complex, a multiprotein complex that mediates actin polymerization. The Arp2/3 complex mediates the formation of branched actin networks in the cytoplasm, providing the force for cell motility, and promotes actin polymerization in the nucleus, thereby regulating gene transcription and repair of damaged DNA.	0.53		0.45	0.41		
ttc3	E3 ubiquitin-protein ligase TTC3	E3 ubiquitin-protein ligase which mediates the ubiquitination and subsequent degradation of phosphorylated Akt (AKT1, AKT2 and AKT3) in the nucleus. [AKT proteins regulate a wide variety of cellular functions including cell proliferation, survival, metabolism, and angiogenesis]. Regulates neuronal differentiation by regulating actin remodeling and Golgi organisation via a signaling cascade involving RHOA, CIT and ROCK. Inhibits cell proliferation.	0.57		0.41	0.40		
ehrf1	E3 ubiquitin-protein ligase UHRF1-like	Multidomain protein that acts as a key epigenetic regulator by bridging DNA methylation and chromatin modification. Plays a role in DNA repair.	0.50		0.47	0.54		
elk3	ETS domain-containing protein Elk-3-like isoform X1	May be a negative regulator of transcription, but can activate transcription when coexpressed with Ras, Src or Mos. Forms a ternary complex with the serum response factor and the ETS and SRF motifs of the Fos serum response element.	0.54		0.49	0.44		
exosc10	exosome component 10-like	Putative catalytic component of the RNA exosome complex which has 3'->5' exoribonuclease activity and participates in a multitude of cellular RNA processing and degradation events.	0.44		0.49	0.49		

Table D.3 continued.

Gene	Annotation	Putative function	CO_2 treatment	Active time	Dist.	Speed	No. EI	EI?
glyat	glycine N-acyltransferase-like	Mitochondrial acyltransferase which transfers an acyl group to the N-terminus of glycine and glutamine. Can conjugate numerous substrates to form a variety of N-acylglycines, with a preference for benzoyl-CoA over phenylacetyl-CoA as acyl donors.	0.54		0.44	0.41		
anln	anillin isoform X2	Actin-binding protein that plays a role in cell growth and migration, and in cytokinesis.	0.45		0.41			
bub3	mitotic checkpoint protein BUB3-like	Has a dual function in spindle-assembly checkpoint signaling and in promoting the establishment of correct kinetochore-microtubule (K-MT) attachments. Promotes the formation of stable end-on bipolar attachments. Necessary for kinetochore localisation of BUB1.	0.45		0.42			
prpf40a	pre-mRNA-processing factor 40 homolog A-like isoform X1	Binds to WASL/N-WASP and suppresses its translocation from the nucleus to the cytoplasm, thereby inhibiting its cytoplasmic function. Plays a role in the regulation of cell morphology and cytoskeletal organisation. Required in the control of cell shape and migration. May play a role in cytokinesis. May be involved in pre-mRNA splicing.	0.46		0.43			
slit3	slit homolog 3 protein isoform X1/3	May act as molecular guidance cue in cellular migration, and function may be mediated by interaction with roundabout homolog receptors.	0.49		0.43			
cblb	E3 ubiquitin-protein ligase CBL-B-like isoform X2	E3 ubiquitin-protein ligase which accepts ubiquitin from specific E2 ubiquitin-conjugating enzymes, and transfers it to substrates, generally promoting their degradation by the proteasome. Negatively regulates TCR (T-cell receptor), BCR (B-cell receptor) and FCER1 (high affinity immunoglobulin epsilon receptor) signal transduction pathways.	0.51			0.44		

Table D.3 continued.

Gene	Annotation	Putative function	CO_2 treat-ment	Active time	Dist.	Speed	No. EI	EI?
myl9	myosin regulatory light polypeptide 9 (isoform X2)	Myosin regulatory subunit that plays an important role in regulation of both smooth muscle and nonmuscle cell contractile activity via its phosphorylation. Implicated in cytokinesis, receptor capping, and cell locomotion.	0.45			0.42		
tubg1	tubulin gamma-1 chain	Tubulin is the major constituent of microtubules. The gamma chain is found at microtubule organising centers (MTOC) such as the spindle poles or the centrosome. Pericentriolar matrix component that regulates alpha/beta chain minus-end nucleation, centrosome duplication and spindle formation.	0.46			0.41		
cdk10	cyclin-dependent kinase 10	A protein kinase that plays pivotal roles in controlling a range of fundamental cellular processes including cell proliferation, neurogenesis, development, ciliogenesis and actin cytoskeleton organisation.	0.48				-0.48	
trub2/pus2	mitochondrial mRNA pseudouridine synthase Trub2-like/probable tRNA pseudouridine synthase 2	Minor enzyme contributing to the isomerization of uridine to pseudouridine (pseudouridylation) of specific mitochondrial mRNAs (mt-mRNAs) such as COXI and COXIII mt-mRNAs. As a component of a functional protein-RNA module, consisting of RCC1L, NGRN, RPUSD3, RPUSD4, TRUB2, FASTKD2 and 16S mitochondrial ribosomal RNA (16S mt-rRNA), controls 16S mt-rRNA abundance and is required for intra-mitochondrial translation. Formation of pseudouridine at positions 27 and 28 in the anticodon stem and loop of transfer RNAs; at positions 34 and 36 of intron-containing precursor tRNA(Ile) and at position 35 in the intron-containing tRNA(Tyr).	0.53				-0.52	

Table D.3 continued.

Gene	Annotation	Putative function	CO_2 treat-ment	Active time	Dist.	Speed	No. EI	EI?
snrnp200	U5 small nuclear ribonucleoprotein 200 kDa helicase	Plays role in pre-mRNA splicing as core component of precatalytic, catalytic and postcatalytic spliceosomal complexes. Involved in spliceosome assembly, activation and disassembly. Mediates changes in the dynamic network of RNA-RNA interactions in the spliceosome.	0.43				-0.44	
rpl29	60S ribosomal protein L29	Component of the large 60S ribosomal subunit.	0.57					
ankle2	Ankyrin repeat and LEM domain-containing protein 2	Involved in mitotic nuclear envelope reassembly. Involved in brain development.	0.42					
mcm5	DNA replication licensing factor mcm5-like	Acts as component of the MCM2-7 complex (MCM complex) which is the putative replicative helicase essential for 'once per cell cycle' DNA replication initiation and elongation in eukaryotic cells.	0.44					
eef2k	eukaryotic elongation factor 2 kinase-like	Threonine kinase that regulates protein synthesis by controlling the rate of peptide chain elongation.	0.58					
ran	GTP-binding nuclear protein Ran	GTPase involved in nucleocytoplasmic transport, participating both to the import and the export from the nucleus of proteins and RNAsRAN (GTP-bound form) triggers microtubule assembly at mitotic chromosomes and is required for normal mitotic spindle assembly and chromosome segregation. Required for normal progress through mitosis. The complex with BIRC5/survivin plays a role in mitotic spindle formation.	0.57					
hs3st5	heparan sulfate glucosamine 3-O-sulfotransferase 5	Catalyses the rate limiting step in the biosynthesis of heparan sulfate (HSact). This modification is a crucial step in the biosynthesis of anticoagulant heparan sulfate. The substrate-specific O-sulfation generates an enzyme-modified heparan sulfate which acts as a binding receptor to Herpes simplex virus-1 (HSV-1) and permits its entry.	0.44					

Table D.3 continued.

Gene	Annotation	Putative function	CO_2 treatment	Active time	Dist.	Speed	No. EI	EI?
	major egg antigen	In blood fluke.	0.41					
slc25a32	Mitochondrial folate transporter/carrier	Transports folate across the inner membranes of mitochondria. Can also transport FAD across the mitochondrial inner membrane.	0.44					
mpnd	MPN domain-containing protein	Probable protease. Recognizes and binds m6A DNA, leading to its degradation.	0.48					
orc1	origin recognition complex subunit 1-like isoform X1	Component of the origin recognition complex (ORC) that binds origins of replication. ORC is required to assemble the pre-replication complex necessary to initiate DNA replication.	0.55					
psap	proactivator polypeptide-like/prosaposin-like isoform X1/2	May activate the lysosomal degradation of sphingolipids [Sphingolipids are a class of lipids containing a backbone of sphingoid bases, play important roles in signal transduction and cell recognition]. Behaves as a myelinotrophic and neurotrophic factor.	0.71					
dhtkd1	probable 2-oxoglutarate dehydrogenase E1 component DHKTD1, mitochondrial	The 2-oxoglutarate dehydrogenase complex catalyses the overall conversion of 2-oxoglutarate to succinyl-CoA and CO_2. [succinyl-CoA = an important intermediate in the citric acid cycle/Krebs cycle] [2-oxoglutarate = also called, α-ketoglutarate. It is the keto acid produced by deamination of glutamate, and is an intermediate in the citric acid cycle/Krebs cycle].	0.41					
psma5	proteasome subunit alpha type-5	Component of the 20S core proteasome complex involved in the proteolytic degradation of most intracellular proteins. Associated with two 19S regulatory particles, forms the 26S proteasome which plays a key role in the maintenance of protein homeostasis by removing misfolded or damaged proteins that could impair cellular functions, and by removing proteins whose functions are no longer required.	0.45					

Table D.3 continued.

Gene	Annotation	Putative function	CO_2 treat-ment	Active time	Dist.	Speed	No. EI	EI?
ppp1r37	protein phosphatase 1 regulatory subunit 37-like isoform X1/2	Inhibits phosphatase activity of protein phosphatase 1 (PP1) complexes.	0.43					
rbm25	RNA-binding protein 25	RNA-binding protein that acts as a regulator of alternative pre-mRNA splicing. Involved in apoptotic cell death through the regulation of the apoptotic factor BCL2L1 isoform expression.	0.40					
rbm17	splicing factor 45-like	Splice factor that binds to the single-stranded 3'AG at the exon/intron border and promotes its utilization in the second catalytic step. Involved in the regulation of alternative splicing and the utilization of cryptic splice sites.	0.50					
st7	suppressor of tumorigenicity 7 protein homolog isoform X1/3	May act as a tumor suppressor.	0.45					
st7	suppressor of tumorigenicity 7 protein homolog isoform X3	May act as a tumor suppressor.	0.60					
taf6l	TAF6-like RNA polymerase II p300/CBP-associated factor-associated factor 65 kDa subunit 6L	Functions as a component of the PCAF complex, which is capable of efficiently acetylating histones in a nucleosomal context. With TAF5L, acts as an epigenetic regulator essential for somatic reprogramming.	0.50					
e2f5	transcription factor E2F5-like	Transcriptional activator that binds to E2F sites, these sites are present in the promoter of many genes whose products are involved in cell proliferation. May mediate growth factor-initiated signal transduction. It is likely involved in the early responses of resting cells to growth factor stimulation. Specifically required for multiciliate cell differentiation.	0.56					

Table D.3 continued.

Gene	Annotation	Putative function	CO_2 treat-ment	Active time	Dist.	Speed	No. EI	EI?
tmcc1 /tmcc2	Transmembrane and coiled-coil domains protein 1/2	Endoplasmic reticulum membrane protein that promotes endoplasmic reticulum-associated endosome fission. Endosome membrane fission of early and late endosomes is essential to separate regions destined for lysosomal degradation from carriers to be recycled to the plasma membrane.	0.44					
rps27a	ubiquitin-40S ribosomal protein S27a/RS27A protein	Polyubiquitin chains, when attached to a target protein, have different functions depending on the Lys residue of the ubiquitin that is linked, including DNA repair, ERAD, cell-cycle regulation, lysosomal degradation, kinase modification, protein degradation via the proteasome, endocytosis, DNA-damage responses as well as in signaling processes. Component of the 40S subunit of the ribosome.	0.47					
c20orf27	UPF0687 protein C20orf27 homolog	Uncharacterised.	0.51					
vps11	vacuolar protein sorting-associated protein 11 homolog	Plays a role in vesicle-mediated protein trafficking to lysosomal compartments including the endocytic membrane transport and autophagic pathways.	0.48					
vhl	von Hippel-Lindau disease tumor suppressor-like	Involved in the ubiquitination and subsequent proteasomal degradation via the von Hippel-Lindau ubiquitination complex. Involved in transcriptional repression.	0.44					
wdr75	WD repeat-containing protein 75	Ribosome biogenesis factor. Involved in nucleolar processing of pre-18S ribosomal RNA. Required for optimal pre-ribosomal RNA transcription by RNA polymerase I.	0.41					
bcar3	breast cancer anti-estrogen resistance protein 3 homolog isoform X10	Acts as an adapter protein downstream of several growth factor receptors to promote cell proliferation, migration, and redistribution of actin fibers.	-0.42				0.46	

Table D.3 continued.

Gene	Annotation	Putative function	CO_2 treatment	Active time	Dist.	Speed	No. EI	EI?
derl1	derlin-1-like	Component of endoplasmic reticulum-associated protein degradation (ERAD) pathway. Derlin-1 is located in the membrane of the endoplasmic reticulum (ER) and is involved in moving misfolded proteins into the cytosol where they are ubiquitinated and degraded by the proteasome. Also involved in endoplasmic reticulum stress-induced pre-emptive quality control.	-0.44				0.47	
psap	proactivator polypeptide-like/prosaposin-like isoform X1/2	May activate the lysosomal degradation of sphingolipids [Sphingolipids are a class of lipids containing a backbone of sphingoid bases, play important roles in signal transduction and cell recognition]. Behaves as a myelinotrophic and neurotrophic factor.	-0.47				0.44	
snrnp200	U5 small nuclear ribonucleoprotein 200 kDa helicase-like	Plays role in pre-mRNA splicing as core component of precatalytic, catalytic and postcatalytic spliceosomal complexes. Involved in spliceosome assembly, activation and disassembly. Mediates changes in the dynamic network of RNA-RNA interactions in the spliceosome.	-0.65				0.49	
derl1	derlin-1-like isoform X1	Component of endoplasmic reticulum-associated protein degradation (ERAD) pathway. Derlin-1 is located in the membrane of the endoplasmic reticulum (ER) and is involved in moving misfolded proteins into the cytosol where they are ubiquitinated and degraded by the proteasome. Also involved in endoplasmic reticulum stress-induced pre-emptive quality control.	-0.57					0.47
dph2	2-(3-amino-3-carboxypropyl)histidine synthase subunit 2-like	Required for the first step in the synthesis of diphthamide, a post-translational modification of histidine which occurs in translation elongation factor 2 (EEF2).	-0.51	-0.43				

Table D.3 continued.

Gene	Annotation	Putative function	CO_2 treatment	Active time	Dist.	Speed	No. EI	EI?
abcd2	ATP-binding cassette sub-family D member 2-like	ATP-dependent transporter of the ATP-binding cassette (ABC) family involved in the transport of very long chain fatty acid (VLCFA)-CoA from the cytosol to the peroxisome lumen. May play a role in regulation of VLCFAs and energy metabolism namely, in the degradation and biosynthesis of fatty acids by beta-oxidation.	-0.42	-0.45				
btg1	BTG1 protein	Member of an anti-proliferative gene family that regulates cell growth and differentiation. Expression of this gene is highest in the G0/G1 phases of the cell cycle and downregulated when cells progressed through G1. Interacts with several nuclear receptors, and functions as a coactivator of cell differentiation.	-0.44	-0.42				
calm	Calmodulin	Calmodulin is a calcium binding protein that plays a role in signaling pathways, cell cycle progression and proliferation.	-0.46	-0.48				
nit1	deaminated glutathione amidase-like	catalyses the hydrolysis of the amide bond in N-(4-oxoglutarate)-L-cysteinylglycine (deaminated glutathione), a metabolite repair reaction to dispose of the harmful deaminated glutathione. Plays a role in cell growth and apoptosis: loss of expression promotes cell growth, resistance to DNA damage stress. It is also a negative regulator of primary T-cells.	-0.44	-0.48				

Table D.3 continued.

Gene	Annotation	Putative function	CO_2 treatment	Active time	Dist.	Speed	No. EI	EI?
dgkq	diacylglycerol kinase theta-like isoform X1	Diacylglycerol kinase that converts diacylglycerol/DAG into phosphatidic acid/phosphatidate/PA and regulates the respective levels of these two bioactive lipids. Thereby, acts as a central switch between the signaling pathways activated by these second messengers with different cellular targets and opposite effects in numerous biological processes. Also functions downstream of the nerve growth factor signaling pathway being specifically activated in the nucleus by the growth factor. Through its diacylglycerol activity also regulates synaptic vesicle endocytosis.	-0.48	-0.42				
dag	dystroglycan-like	The dystroglycan complex is involved in a number of processes including laminin and basement membrane assembly, sarcolemmal stability, cell survival, peripheral nerve myelination, nodal structure, cell migration, and epithelial polarization.	-0.41	-0.44				
ing3	inhibitor of growth protein 3-like	Component of the NuA4 histone acetyltransferase (HAT) complex which is involved in transcriptional activation of select genes principally by acetylation of nucleosomal histones H4 and H2A. NuA4 may also play a direct role in DNA repair when directly recruited to sites of DNA damage.	-0.41	-0.48				
ing3	inhibitor of growth protein 3-like	Component of the NuA4 histone acetyltransferase (HAT) complex which is involved in transcriptional activation of select genes principally by acetylation of nucleosomal histones H4 and H2A. NuA4 may also play a direct role in DNA repair when directly recruited to sites of DNA damage.	-0.41	-0.49				
mfge8	lactadherin-like isoform X1	Contributes to phagocytic removal of apoptotic cells in many tissues.	-0.43	-0.49				

Table D.3 continued.

Gene	Annotation	Putative function	CO_2 treat-ment	Active time	Dist.	Speed	No. EI	EI?
dhtkd1	probable 2-oxoglutarate dehydrogenase E1 component DHKTD1, mitochondrial	The 2-oxoglutarate dehydrogenase complex catalyses the overall conversion of 2-oxoglutarate to succinyl-CoA and CO_2. [succinyl-CoA = an important intermediate in the citric acid cycle/Krebs cycle] [2-oxoglutarate = also called, α-ketoglutarate. It is the keto acid produced by deamination of glutamate, and is an intermediate in the citric acid cycle/Krebs cycle]	-0.44	-0.42				
abhd13	protein ABHD13-like	Uncharacterised. The α/β-hydrolase domain (ABHD) proteins which are characterized with beta strands connected by alpha helices in common belong to α/β-hydrolase (ABH) superfamily including esterases, lipases, proteases, peroxidases, dehalogenases, and epoxide hydrolases.	-0.43	-0.41				
lin37	protein lin-37 homolog	Uncharacterised.	-0.42	-0.47				
pcdh1	protocadherin-1 isoform X1	May be involved in cell-cell interaction processes and in cell adhesion.	-0.41	-0.51				
f52c9.6	putative uncharacterized transposon-derived protein F52C9.6	Uncharacterised.	-0.53	-0.43				
f52c9.6	putative uncharacterized transposon-derived protein F52C9.6	Uncharacterised.	-0.63	-0.42				
stk10	serine/threonine-protein kinase 10-like isoform X2	Serine/threonine-protein kinase involved in regulation of lymphocyte migration. Acts as a negative regulator of MAP3K1/MEKK1. May also act as a cell cycle regulator by acting as a polo kinase kinase.	-0.46	-0.48				
srap	serine-rich adhesin for platelets-like	In bacteria, mediates binding to human platelets, possibly through a receptor-ligand interaction. Probably associated with virulence in endovascular infection.	-0.46	-0.49				

Table D.3 continued.

Gene	Annotation	Putative function	CO_2 treat-ment	Active time	Dist.	Speed	No. EI	EI?
sh3bp5	SH3 domain-binding protein 5-like	Functions as guanine nucleotide exchange factor (GEF) with specificity for RAB11A and RAB25. Inhibits the auto- and transphosphorylation activity of BTK. Plays a negative regulatory role in BTK-related cytoplasmic signaling in B-cells. May be involved in BCR-induced apoptotic cell death.	-0.42	-0.56				
slc20a1	sodium-dependent phosphate transporter 1-A-like isoform X1 / 1-B	Sodium-phosphate symporter which plays a fundamental housekeeping role in phosphate transport. May function as a retroviral receptor as it confers human cells susceptibility to infection to various viruses.	-0.42	-0.41				
aldh5a1	succinate-semialdehyde dehydrogenase, mitochondrial isoform X2	Involved in the final degradation step of the inhibitory neurotransmitter gamma-aminobutyric acid (GABA).	-0.52	-0.48				
taf6l	TAF6-like RNA polymerase II p300/CBP-associated factor-associated factor 65 kDa subunit 6L	Functions as a component of the PCAF complex. The PCAF complex is capable of efficiently acetylating histones in a nucleosomal context. With TAF5L, acts as an epigenetic regulator essential for somatic reprogramming.	-0.44	-0.43				
scrt2	transcriptional repressor scratch 2-like	May be involved in transcriptional regulation.	-0.43	-0.55				
scrt2	transcriptional repressor scratch 2-like	May be involved in transcriptional regulation.	-0.45	-0.46				
tmcc1 /tmcc2	Transmembrane and coiled-coil domains protein 1/2	Endoplasmic reticulum membrane protein that promotes endoplasmic reticulum-associated endosome fission. Endosome membrane fission of early and late endosomes is essential to separate regions destined for lysosomal degradation from carriers to be recycled to the plasma membrane.	-0.44	-0.40				
	universal stress protein A-like protein isoform X5	Uncharacterised.	-0.59	-0.45				

Table D.3 continued.

Gene	Annotation	Putative function	CO_2 treatment	Active time	Dist.	Speed	No. EI	EI?
	universal stress protein A-like protein isoform X5	Uncharacterised.	-0.63	-0.41				
futsch	microtubule-associated protein futsch	During embryogenesis, necessary for dendritic and axonal organisation and growth at the neuromuscular junction through the regulation of the synaptic microtubule cytoskeleton. Stabilises microtubule hairpin loops in synaptic boutons at the neuromuscular synapse. Rearrangement of these microtubule-based loops may be a critical component of the process of bouton division and for subsequent nerve-terminal growth and branching. Together with Ringer, required for neuromuscular junction (NMJ) bouton growth by regulating synaptic microtubules.	-0.46		-0.40			
smim29	small integral membrane protein 29-like isoform X1	Uncharacterised.	-0.45		-0.41			
gga	ADP-ribosylation factor-binding protein GGA	Plays a role in protein sorting and trafficking between the trans-Golgi network (TGN) and endosomes. Mediates export of the GPCR receptor ADRA2B to the cell surface. Required for targeting PKD1:PKD2 complex from the trans-Golgi network to the cilium membrane.	-0.42					
ctnnal1	alpha-catulin isoform X1	May modulate the Rho pathway signaling by providing a scaffold for the Lbc Rho guanine nucleotide exchange factor (ARHGEF1). [Rho = family of GTPases (small signalling G proteins) regulate many aspects of intracellular actin dynamics. Play a role in organelle development, cytoskeletal dynamics, cell movement, and other common cellular functions].	-0.50					
rbr3	cell wall protein RBR3 isoform X3	GPI-anchored cell wall protein involved in cell wall organisation, hyphal growth, as well as in host-fungal interaction and virulence.	-0.53					

Table D.3 continued.

Gene	Annotation	Putative function	CO_2 treatment	Active time	Dist.	Speed	No. EI	EI?
klhl2	kelch-like protein 2	Component of a cullin-RING-based BCR (BTB-CUL3-RBX1) E3 ubiquitin-protein ligase complex that mediates the ubiquitination of target proteins, such as NPTXR, leading most often to their proteasomal degradation. Responsible for degradative ubiquitination of the WNK kinases WNK1, WNK3 and WNK4. Plays a role in the reorganisation of the actin cytoskeleton. Promotes growth of cell projections in oligodendrocyte precursors.	-0.45					
klhl2	kelch-like protein 2	Component of a cullin-RING-based BCR (BTB-CUL3-RBX1) E3 ubiquitin-protein ligase complex that mediates the ubiquitination of target proteins, such as NPTXR, leading most often to their proteasomal degradation. Responsible for degradative ubiquitination of the WNK kinases WNK1, WNK3 and WNK4. Plays a role in the reorganisation of the actin cytoskeleton. Promotes growth of cell projections in oligodendrocyte precursors.	-0.41					
ppp1r37	protein phosphatase 1 regulatory subunit 37-like isoform X1	Inhibits phosphatase activity of protein phosphatase 1 (PP1) complexes.	-0.45					
vps11	vacuolar protein sorting-associated protein 11 homolog	Plays a role in vesicle-mediated protein trafficking to lysosomal compartments including the endocytic membrane transport and autophagic pathways.	-0.42					
hivep1	zinc finger protein 40 isoform X1	This protein specifically binds to the DNA sequence 5'-GGGACTTTCC-3' which is found in the enhancer elements of numerous viral promoters such as those of SV40, CMV, or HIV-1. It may act in T-cell activation. Involved in activating HIV-1 gene expression.	-0.46					
znf704	zinc finger protein 704-like	Transcription factor which binds to RE2 sequence elements in the MYOD1 enhancer.	-0.41					
10 unannotated genes: positive correlation with CO_2 treatment and all three activity traits								

Table D.3 continued.

Gene	Annotation	Putative function	CO_2 treatment	Active time	Dist.	Speed	No. EI	EI?
1 unannotated hub gene: positive correlation with CO_2 treatment and speed								
1 unannotated hub gene: positive correlation with CO_2 treatment, negative correlation with active time and no. soft mirror touches								
2 unannotated hub genes: positive correlation with CO_2 treatment, negative correlation with number of soft mirror touches								
3 unannotated hub genes: positive correlation with CO_2 treatment								
7 unannotated hub genes: negative correlation with CO_2 treatment and active time								
3 unannotated hub genes: negative correlation with CO_2 treatment and distance								
9 unannotated hub genes: negative correlation with CO_2 treatment								

Table D.4. List of function groups for genes identified as CNS-specific hub genes shared by CO_2 treatment and one or more activity traits.

Function group	Hub genes shared by CO_2 treatment and one or more activity traits: Positive correlation	Hub genes shared by CO_2 treatment and one or more activity traits: Negative correlation
Cell cycle		
G1 phase	*cdt1*	
G1 to S phase transition	*snd1*	
Centrosome duplication	*tubg1, nat10*	
DNA replication	*psf2, cdt1, mcm5, dbf4, spt16, foxm1, bptf*	
G2 phase	*ranbp2*	
G/2M cell-cycle checkpoints	*donson*	
Mitosis	*ncaph, smc4, ttk, incenp, bub1, foxm1, cdt1*	
Spindle assembly checkpoint signalling	*bub3*	
Cytokinesis	*zip, myh9/10, myl9, anln, prpf40a*	
Cell cycle regulators	*foxm1, eif3b, ccnb3, melk, ttk, bub1, dbf4, anb32a, klf10, ecd*	*stk10*
Cell proliferation	*ttk, eif3b, foxm1, melk, dbf4, srrt, tk1, tgfb1i1, pa2g4, ttc3, ptpr*	*btg1, calm*
Cell cycle-related apoptosis	*anb32a, eif3b, melk*	
Other neurogenesis-related		
Cell migration	*arpc5, anln, myl9, slit3, mbtp, prpf40a*	*dag*
Cell adhesion	*itga4, itga9, slc4a11, pcdh1, vcl, rac1, ptpr, pa2g4*	*pcdh1*
Cell differentiation	*eif3b, rac1, ptpr, tbc1d1, tgfb1i1, itga4, pa2g4, slc4a11*	*btg1*
Neuronal differentiation	*ttc3, rac1*	
Neural stem cell self-renewal	*srrt*	
Neural progenitor proliferation	*melk*	
Neurogenesis	*ncaph, adgrb3*	
Somatic reprogramming		*taf6l*
Dendrite spine formation	*adgrb3, rac1*	
Neurite outgrowth and branching	*apbb1, ptpr*	*futsch*
Synaptogenesis	*adgrb3*	

Table D.4 continued.

Function group	Hub genes shared by CO_2 treatment and one or more activity traits: Positive correlation	Hub genes shared by CO_2 treatment and one or more activity traits: Negative correlation
Peripheral nerve myelination		*dag*
Protein synthesis and protein turnover		
Amino acids	*shmt1, glyat*	
Nucleotides	*entpd8, purH*	
Transcription	*polr1a, spt16, bptf, arpc5*	
RNA splicing	*melk, snrpa, ecd, prpf40a*	
RNA processing	*cstf1, exosc10*	
RNA modification	*nat10, pa2g4*	
tRNA	*eef1g, pus3*	
Translation	*eif3b, eif3d, eef1g*	
Ribosome	*rpl23a, rpl4, rpl7l, rps27a, nop58*	
Post-translation modification	*ranbp2*	*dph2*
Protein folding and quality control	*hspa5, pdia3, pdia4, pdia5, ssr1, ganab, ppib*	
Protein trafficking	*stt3a, tmed2, rpn2, rpn1, nup160, nup155, nup205*	
E3 ubiquitin ligase	*ttc3, cblb*	
Proteasome	*rpn1*	
Lysosomal degradation		*tmcc1/2*
Cellular Stress Response		
Apoptosis (other)	*rtkn*	
Apoptosis (response to DNA damage/ER stress)	*apbb1, tmem214-b*	
DNA damage response / DNA repair	*apbb1, spt16, foxm1, bptf, arpc5*	*nit1, ing3*
Oxidative stress response	*slc4a11*	
Unfolded protein response	*hspa5*	
Neurotranmsission		
GABAergic neurotransmission	*phf24, rac1*	*aldh5a1*
Endocannabinoid signalling	*abhd12*	
GPCR trafficking	*tmed2*	
Synaptic microtubule skeleton		*futsch*
Synaptic vesicle endocytosis		*dgkq*

Table D.4 continued.

Function group	Hub genes shared by CO_2 treatment and one or more activity traits: Positive correlation	Hub genes shared by CO_2 treatment and one or more activity traits: Negative correlation
Epigenetic regulation		
Histone modification (acetylation, methylation)	*anb32a, ashh1/2/3/4/mes-4/setd2, nat10, pa2g4*	*ing3, taf6l*
Immune system		
B cells	*cblb*	*sh3bp5*
Cell adhesion in immune response	*itga4, itga9, rac1, ptpr*	
Immunological process regulation	*abhd12*	
Innate immune response	*tf*	
T cell	*ptprc, itga4, cblb*	
Viral binding/receptor	*hspa5, ptprc*	*slc20a1*
Viral replication	*anb32a*	
Energy Production		
Fatty acid metabolism		*abcd2*
Glucose metabolism and transport	*klf10, tbc1d1, tbc1d4, ecd*	
Others		
Angiogenesis	*adgrb3, ttc3*	
Circadian clock regulation	*klf10*	
Folate transport	*slc25a32*	
Motility in cilia and flagella	*dnaaf2*	
Spatial memory	*apbb1*	